

**PALACKÝ UNIVERSITY OLMOUC**

Faculty of Science

Department of Biochemistry



**The role of cytokinins in the response of barley  
and wheat to abiotic stress**

**Ph.D. Thesis**

Author: Cintia Florencia Marchetti, M.Sc.  
Study program: P1416 Biochemistry  
Study branch: Biochemistry  
Study mode: Full-time  
Supervisor: Ing. Nuria De Diego Sanchez, Ph.D.  
Submitted:

I hereby declare that this Ph.D. thesis has been written solely by me. All the sources used in this thesis are cited and listed in the "References" section. All published results included in this work are approved by co-authors.

Olomouc, .....

.....

## Bibliografická identifikace

Jméno a příjmení autora	Cintia Marchetti
Název práce	Role cytokininů v odpovědi na abiotický stres u ječmene a pšenice
Typ práce	Disertační
Pracoviště	Oddělení molekulární biologie, Centrum regionu Haná pro biotechnologický a zemědělský výzkum, Přírodovědecká fakulta, Univerzita Palackého v Olomouci
Vedoucí práce	Ing. Nuria De Diego Sanchez, Ph.D.
Rok obhajoby práce	2019

### Abstrakt

Abiotický stres má negativní dopad na celosvětovou zemědělskou produkci a snižuje finální výnos plodin. Vodní deficit a sluneční záření patří mezi hlavní faktory ovlivňující výnos plodin. Cytokininy (CK) jsou známé, ve spolupráci s dalšími fytohormony, svou účastí v odpovědi na abiotický stres u rostlin, přestože je způsob regulace tolerance rostlin na stres stále neobjasněný. Předkládaná práce se zaměřuje na studium role cytokininů jakožto regulátorů odpovědi na stres u rostlin těchto dvou hlavních stresových faktorů – senescence a vodní stres. K tomuto účelu byly použity dvě zemědělsky významné plodiny, a to ječmen (*Hordeum vulgare* cv. Golden Promised) a pšenice (*Triticum aestivum* cv. Inta Oasis), u kterých byl studován stres vyvolaný stíněním a ječmen, u kterého byl sledován vodní stres a následná regenerace těchto rostlin. V první části práce byl vyhodnocen dopad změny kvality světelného spektra na cytokininový metabolismus u ječmene a pšenice. Navíc byly charakterizovány

transgenní rostliny ječmene s umlčným genem cytokinin oxidasy/dehydrogenasy (CKX), hlavním enzymem nevratně degradující CK. Pro objasnění, zda CK regulují toleranci vodního stresu a kapacitu regenerace u ječmene, bylo vybráno šest nezávislých transgenních linií s umlčnými *HvCKX2.2* a *HvCKX9* geny. Výsledky práce ukazují, že CK jsou důležité hormony, které regulují oba typy stresu a že udržení hladiny endogenních CK (hlavně ve formě volné báze) byly klíčové pro oddálení stresem indukovaných negativních efektů u rostlin. Konkrétně je ukázáno, že jedním z hlavních faktorů udržujících hladinu CK byla regulace degradace CK. U stresu vyvolaného stíněním se objevila výrazná nadregulace genu *CKX1* v senescenčních listech ječmene a pšenice. Podobně, vodou stresované rostliny vykazovaly zvýšenou expresi *HvCKX1*, a to hlavně u nejvíce sensitivních linií. Oproti *CKX1*, nadregulace genu *CKX3* souvisela s nižší degradací chlorofylu u stínem indukované senescence a vyšší tolerance na vodní stres v pšenici a ječmeni. Závěrem je navrženo, že mezi *CKX* isoformami regulujícími odpověď na abiotický stres u ječmene a pšenice existují rozdílné a konzervativní role. Odpověď na vodní stres a regenerační kapacita nesouvisí pouze s CK. Komplexní interakce s dalšími rostlinnými hormony a metabolity souvisejícími se stresem jako aminokyseliny a polyaminy byly také pozorovány. Věříme, že změna CK homeostáze skrze podregulaci genů *CKX* v rostlinách vedla ke vhodnému nástroji pro studium odpovědi rostlin na stres vyvolaný stíněním a vodní deficit a/nebo interakce mezi primárním a sekundárním metabolismem regulujícím stresovou odpověď a regeneraci u rostlin.

Klíčová slova

modré světlo; metabolismus cytokininů; cytokinin oxidasa / dehydrogenasa; exprese genu; senescence; zastínění; *Triticum aestivum*; *Hordeum vulgare*; RGB imaging; fluorescence chlorofylu; indoorové fenotypování; aminokyseliny; polyaminy; antioxidační enzymy

Počet stran	279
Počet příloh	4
Jazyk	Anglický

## Bibliographical identification

Author's first name and surname	Cintia Marchetti
Title	The role of cytokinins in the response of barley and wheat to abiotic stress
Type of thesis	Ph.D.
Workplace	Department of Molecular Biology, Centre of the Region of Haná for Biotechnological and Agricultural Research, Faculty of Science, Palacký University Olomouc
Supervisor	Ing. Nuria De Diego Sanchez, Ph.D.
Year of presentation	2019

### Abstract

Abiotic stress impacts negatively on agriculture production worldwide and diminish the final yield of crops. Among all constraints, water deficit and solar radiation are main determinant of crop production. Cytokinins (CKs) are known to be involved in the abiotic stress responses of plants, in a complex crosstalk with other phytohormones, although their role regulating plant stress tolerance remains unknown. The presented thesis was focused on the study of the role that CKs are playing as regulators of the plant stress response to these two major stressors, senescence and water stress. For this purpose, we focused in two crops with agronomical interest, barley (*Hordeum vulgare* cv. Golden Promised) and wheat (*Triticum aestivum* cv. Inta Oasis). In the first part, we evaluated the effect of changes in light spectral quality by shading-induced stress on CK metabolism in barley and wheat. Besides, we also characterized transgenic barley plants with silenced genes encoding cytokinin

oxidase/dehydrogenase (CKX), the main enzyme irreversibly degrading CKs. Then, to clarify whether CKs regulate water stress tolerance and recovery capacity in barley, six independent transgenic lines with silenced *HvCKX2.2* and *HvCKX9* genes were selected. As results, we showed that CKs are relevant hormones regulating both types of stress and that the maintenance of the endogenous CKs (especially the base forms) was crucial for delaying the stress-induced negative effects in the plants. Concretely, we showed that one of the main factors conditioning the CK content was the regulation of CK degradation. Under shade-induced stress there was a marked up-regulation of the *CKX1* gene in senescing leaves of barley and wheat occurred. Similarly, water stressed plants also increased the expression of *HvCKX1*, especially in the most sensitive lines. Opposite to *CKX1*, the upregulation of the *CKX3* gene was related to a lower Chl degradation under shade-induced senescence and higher waters stress tolerance in wheat and barley, respectively. Altogether, we suggest that differential and conservative roles exist between the *CKX* isoforms regulating the abiotic stress response in barley and wheat. The water stress response and recovery capacity was not only related to CKs. A complex crosstalk with other plant hormones and stress-related metabolites such as amino acids and polyamines was also observed. We believed that the alteration of the CK homeostasis through the down-regulation of *CKX* genes in plants resulted in a good tool to study the plant response to shading-induced stress and water deficit, and/or the crosstalk between the primary and secondary metabolism regulating plant stress response and recovery.

#### Keywords

blue light; cytokinin metabolism;  
cytokinin oxidase/dehydrogenase; gene  
expression; leaf senescence; shading  
stress; *Triticum aestivum*; *Hordeum  
vulgare*; red, green, blue (RGB) imaging;  
chlorophyll fluorescence; indoor

phenotyping; amino acids; polyamines;  
antioxidative enzymes

Number of pages 279

Number of appendices 4

Language English





*"In conclusion, it appears that nothing can be more improving to a young naturalist, than a journey in distant countries."*

*Charles Darwin, Voyage of the Beagle*

To Petr

## Acknowledgements

---

My deepest gratitude belongs to my supervisors: Petr Galuszka and Nuria De Diego Sanchez. I want to thank Petr for putting his trust in me, for his unconditional support and for being a beautiful person. I would like to express my sincere gratitude to Nuria for taking the responsibility of my direction without doubts, for her patience, for encouraging me every day and for transmitting me her unlimited passion for science. It is a pleasure for me every time we discuss science, thank you!

I would like also to acknowledge all the people who made possible the International Cooperation Program between the Ministry of Science, Technology and Productive Innovation of Argentina (MINCyT, Project ARC/14/13) and the Ministry of Education, Youth and Sports of the Czech Republic (MEYS, Grant N° 7AMB15AR011; NPU-I, Grant N° LO1204). Without this possibility, I would have never come to Czech Republic and decided to study here Ph.D.

I want to thank to all my colleagues at the University, especially at the Department of Molecular Biology but also those at the Department of Chemical Biology and Genetics, who support me and encouraged me in my research. I would particularly like to thank Katarína Holubová for her help and suggestions at the beginning of my studies, and to Ivo Frébort, Véronique Bergougnoux and Lukáš Spíchal for their willingness to support me to finish Ph.D. during this difficult last year. My special thanks go to Věra Chytilová and Kateřina Janošíková for their unconditional help with plant material harvest and technical support. I also wish to express my sincere gratitude to my supervisor of Master Thesis in Argentina Fabio Causin, with whom I continued collaborating during my Ph.D. Thank you very much for your guidance and time to discuss science with me, even when the distance sometimes makes it very complicated.

I want to express my feelings of gratitude to all the friends I met here in Czech Republic, inside and outside the academic environment, who embellished these last five years of my life. First, I would like to acknowledge Kristýna Hromadová, for being an incredible friend and the best teacher of Czech culture. Without all we have experienced together, I would have never love Czech Republic as I do. My heartfelt thanks also to: Agáta and Karol, Honza and Venca, Thu, Honza H., Peťka, Zuzi, Srni, Claudia, Katka J., Káťa H., Auguste and Justinas, Yuli, Denisa and whole family,

Estrellita, Pepi, Kaja, Lydia, Iva, Alba, Káťa and Vítá and Evi. You all are beautiful and I will always keep you in my heart!

Finally, I would like to deeply thank my family for all the encouragement and support. Thanks to my parents Diana and Edgardo, to my brother Maximiliano and to my grandparents: Raquel, Juanito, Pepe and Elsa; and, to my boyfriend Pablo. Even when you all knew that I would be long time far away from home, you supported me and accepted my decision to come to study to Czech Republic and follow my dreams.



## Contents

Index of tables and figures.....	1
Tables .....	1
Figures .....	3
Abbreviations .....	14
CHAPTER I: General Introduction .....	16
I. I. Coping with a sessile lifestyle: a stressing plant tale .....	17
I. II. The different kinds of stressors and stress constraints .....	18
I. III. Light as a stress factor .....	19
I. IV. Water stress responses .....	19
I. V. Stress-induced senescence: a common denominator .....	21
I. VI. Cross-signalling of phytohormones in the regulation of shading and water stress responses .....	22
I. VII. Barley and wheat .....	23
I. VIII. Objectives.....	25
CHAPTER II: The role of cytokinins in light-mediated senescence in barley and wheat .....	26
II. I. Introduction.....	27
II. II. Materials and methods .....	30
II. II .I. Plant growth and experimental procedure .....	30
II. II. II. Determination of chlorophyll content and protein concentration .....	33
II. II. III. Cytokinin content measurements .....	33
II. II. IV. Measurement of CKX activity .....	33
II. II. V. Phylogenetic tree construction and identification of wheat orthologues for genes of interest.....	34
II. II. VI. Analysis of gene expression by qPCR .....	36
II. II. VII. Western Blot analysis .....	38
II. II. VIII. Data analysis.....	38
II. III. Results .....	39
A. <b>Experiment 1</b> - Shade-induced senescence in wheat leaves.....	39

<b>B. Experiment 2-</b> Regulatory aspects of shade-induced senescence in barley leaves. ....	51
II. IV. Discussion.....	54
II. V. Conclusion.....	60
CHAPTER III: A novel image-based screening method to study water deficit response and recovery of barley populations using canopy dynamics phenotyping.....	61
III. I. Introduction.....	62
III. II. Materials and Methods.....	64
III. II. I. Plant material and growth conditions.....	64
III. II. II. Non-invasive plant phenotyping.....	64
III. II. III. The Assay Workflow.....	67
III. II. IV. Manual parameters.....	69
III. II. V. Statistical analysis and data representation.....	71
III. III. Results.....	72
III. III. I. PHENOTYPING METHOD- Screening of barley population using simple RGB imaging.....	72
III. III. II. VALIDATION AND REPRODUCIBILITY OF THE PHENOTYPING METHOD.....	81
III. III. III. DATA ANALYSIS- Multivariate statistical analysis for understanding the physiological basis of the image-derived traits and water stress response in barley populations.....	90
III. IV. Discussion.....	96
III. V. Conclusion.....	99
CHAPTER IV: Dissecting the cytokinin-mediated tolerance of plants to water stress using an integrative approach combining phenotyping and metabolomics.....	101
IV. I. Introduction.....	102
IV. II. Materials and Methods.....	104
IV. II. I. Preparation of silencing lines.....	104
IV. II. II. Non-invasive plant phenotyping.....	112
IV. II. III. Manual parameters.....	113
IV. III. Results.....	115
IV. III. I. Generation and selection of transgenic barley plants with silenced HvCKXs genes.....	115



IV. III. II. Phenotyping of barley populations with altered CK homeostasis under water deficit and subsequent rewatering .....	120
IV. IV. Discussion .....	149
IV. V. Conclusion.....	152
CHAPTER V: GENERAL DISCUSSION .....	153
REFERENCES .....	156
SUPPLEMENTS I.....	179
SUPPLEMENTS II.....	180
SUPPLEMENTS III.....	181
SUPPLEMENTS IV .....	182

## Index of tables and figures

---

### Tables

<b>Table II.1.</b> Primer sequences used for real time PCR expression analysis of wheat and barley.....	37
<b>Table II.2.</b> Content of different CK metabolites in excised wheat leaves (pmol gDW <sup>-1</sup> ), at different times of exposure to the shading treatments with neutral (N), blue (B), or green (G) light filters (mean ± SE, n=3). < LOD: below the limit of detection. Different letters mean significant differences among treatments according Tukey HSD test after ANOVA.....	41
<b>Table II.3.</b> Chlorophyll content (%) compared to t0 in excised wheat leaves exposed during 100 h to the green filter (G), in the absence or presence of 2.5 µM of the indicated CKs, which were added at 52 h after the beginning of shading. A group of leaves exposed during 52 h to filter G were changed to filter B without addition of CKs (treatment GB). Data are means ± SE (n= 10). Data with different letters differ at $P \leq 0.05$ .....	44
<b>Table II.4.</b> Chlorophyll content (%) compared to t0 and CKX activity, in excised wheat leaves exposed during 100 h to the neutral (N), blue (B) or green (G) light filters, or during 52 h to filter B and then 48 h to filter G (treatment BG). Where indicated, 10.0 µM INCYDE was supplied to the external solution from either 24 or 52 h after the beginning of the shading treatments. Data are mean ± SE (n=10 for chlorophyll records and n= 4 for CKX analyses). Data with different letters differ at $P \leq 0.05$ .....	46
<b>Table III.1.</b> Scheme of the three performed experiments.....	66
<b>Table III.2.</b> Dynamics of canopy height of barley seedlings grown under water stress conditions. Fold changes ( $\log_2$ ) of the canopy height (pixels) of seedlings grown under stressed conditions for 12 days (endpoint day 15) compared with their respective controls, from five independent trays. Asterisks and ns indicate the level of significance between stressed and non-stressed plants according to ANOVA (n = 50); * $P \leq 0.05$ ; ** $P \leq 0.01$ ; *** $P \leq 0.001$ ; ns, not significant.....	77
<b>Table III.3.</b> Traits related to water deficit and recovery. Traits were extracted from the linear regression of the canopy height in two randomly selected trays. Day is the day when treated and not treated plants are different; Max is the maximal canopy height reached in the stressed plants under drought; min is the minimal canopy height at the end of the drought period; Slope of the	

linear curve from the canopy height in the drought period; MaxR is the maximal canopy height reached in the stressed plants after rewatering; and SlopeR of the linear curve from the canopy height in the rewatering period.....78

**Table III.4.** Statistical analysis of several morphological and physiological traits measured in barley seedlings at the end of the water stress period and after rewatering using two-way ANOVA (Tray and Treatment). \*  $P \leq 0.05$ ; \*\*  $P \leq 0.01$ ; \*\*\*  $P \leq 0.001$ .....85

**Table III.5.** Statistical analysis of free AAs and PAs ( $\mu\text{mol mg}^{-1}$  DW) measured in barley seedlings at the end of the water stress period and after rewatering using one-way ANOVA. \*  $P \leq 0.05$ ; \*\*  $P \leq 0.01$ ; \*\*\*  $P \leq 0.001$ .....88

**Table IV.1.** Primers used in the PCR analysis for confirmation of the presence and orientation of the silencing cassettes.....110

**Table IV.2.** Primer combination used and expected size for each of the sense and antisense components of the silencing cassette.....110

**Table IV.3.** Traits related to water deficit and recovery in wild type, (a) RNAi:HvCKX2.2 and (b) RNAi:HvCKX9. Traits were extracted from the contracted line of the canopy height. Day is the day when treated and not treated plants are separated; Max is the maximal canopy height reached in the stressed plants under water stress and Slope of the line from the canopy height in the water stress period; MaxR is the maximal canopy height reached in the stressed plants after rewatering; and SlopeR of the linear curve from the canopy height in the rewatering period.....122

**Table IV.4.** Content of different CK metabolites in in barley seedlings at the end of the stress period. Different letters mean significant differences among treatments according Tukey HSD test after ANOVA.....134

**Table IV.5.** Content of different CK metabolites in in barley seedlings after 4 days of rewatering. Different letters mean significant differences among treatments according Tukey HSD test after ANOVA.....135

**Table IV.6** Content of ABA and AUXs in barley seedlings (wild type and 3 transgenic lines) at the end of the stress period. Different letters mean significant differences among treatments according Tukey HSD test after ANOVA.....137

**Table IV.7.** Content of ABA and AUXs in barley seedlings (wild type and 3 transgenic lines) after 4 days of rewatering. Different letters mean significant differences among treatments according Tukey HSD test after ANOVA.....137

**Table IV.8.** Content of free PAs in barley seedlings (wild type and 3 transgenic lines) at the end of the water stress period. Different letters mean significant differences among treatments according Tukey HSD test after ANOVA.....140

**Table IV.9.** Content of free PAs in barley seedlings (wild type and 3 transgenic lines) after 4 days of rewatering. Different letters mean significant differences among treatments according Tukey HSD test after ANOVA.....140

**Table IV.10.** Content of AAs in barley seedlings (wild type and 3 transgenic lines) at the end of the water stress period. Different letters mean significant differences among treatments according Tukey HSD test after ANOVA.....141

**Table IV.11.** Content of AAs in barley seedlings (wild type and 3 transgenic lines) after 4 days of rewatering. Different letters mean significant differences among treatments according Tukey HSD test after ANOVA.....141

**Figures**

**Figure I.1.** Scheme of the phase sequences and responses induced in plants by stress exposure (adapted from Lichtenthaler, 1998).....18

**Figure. I.2.** The effect of water stress in crops and target traits for improvement (Adapted from Barnabás et al. (2008).....20

**Figure II.1.** Blue light suppresses the interaction of CIB1 with specific regions of the SAG chromatin, regulating leaf senescence. The scheme shows CRY2a-mediated blue light suppression of the CIB1-dependent activation of leaf senescence. PHR, photolyase homologous region; CCE, CRY C-terminal extension. Adapted from Meng et al. (2013).....27

**Figure II.2.** (a) Percent light transmission spectra of the Lee filters used for the blue (B), green (G) and red (R) light treatments (according to the manufacturer) and illustrative images of the boxes

used for the assay performed in the Experiment 1 with (b) wheat and in the Experiment 2 with (c) barley leaves.....32

**Figure II.3.** Phylogenetic trees for (a) *TaCIB1*, (b) *TaHKs* and (c) and *TaHY5*. The trees are drawn to scale, with branch lengths measured in the number of substitutions per site. The percentage of replicate trees in which the associated taxa clustered together in the bootstrap test (1000 replicates) is shown next to the branches. Along with wheat sequences, family members from *Arabidopsis thaliana* and the soybean *Glyma11g12450* gene (homologous to *AtCIB1*) were used for the construction of the *TaCIB1* phylogenetic tree; sequences of histidine kinases implicated in CK perception in *A. thaliana* and *Zea mays* were used for the construction of the *TaHKs* tree; the proteins OsbZIP01 and OsbZIP18 from rice, identified as the closest orthologous of *A. thaliana* bZIP transcription factors HY5, and the HY5 homolog (HYH) in monocots, were used for the construction of the *TaHY5* phylogenetic tree.....35

**Figure II.4.** (a) Change in the percent chlorophyll content in detached wheat leaves at different times after exposure to the neutral (N), blue (B) or green (G) filters. Asterisks indicate the existence of significant differences for “shading treatment” effect, at a given sampling date. (b) Chlorophyll content in detached wheat leaves at different times after exposure to the following shading treatments: 92 h neutral filter (N), 92 h blue filter (B), 92 h green filter (G), 30 h G + 62 h B (GB 30 h), or 54 h G + 38 h B (GB 54 h). Data are means  $\pm$  SE (a: n= 8; b: n= 4). Asterisks indicate significant differences between treatment G and the remaining shading treatments.....40

**Figure II.5.** Expression profile of two senescence markers in detached wheat leaves at different times after exposure to the blue or green filters, according to the following treatments: 92 h blue filter (B), 92 h green filter (G), 30 h G + 62 h B (GB 30 h), or 54 h G + 38 h B (GB 54 h). Asterisks indicate significant differences for the expression level of both markers between treatment G and the remaining treatments, at a given sampling date.....40

**Figure II.6.** Total CK content (a), cZ-type of CKs (b), O-glucosides (c) and cZOG (d), in detached wheat leaves at different times after exposure to the neutral (N), blue (B) or green (G) filters. Data are means  $\pm$  SE (n= 3). Asterisks indicate the existence of significant differences for “shading treatment” effect, at a given sampling date.....42

**Figure II.7.** CKX specific activity in detached wheat leaves, at different times after exposure to the neutral (N), blue (B) or green (G) filters. Data are means  $\pm$  SE (n= 3). Asterisks indicate significant differences for “shading treatment” effect, at a given sampling date.....45

**Figure II.8.** Expression profile of *TaCKX1* (a) and *TaCKX3* (b) in detached wheat leaves, at different times after exposure to the neutral (N), blue (B) or green (G) filters. Data are means  $\pm$  SE (n= 3). Asterisks indicate significant differences for “shading treatment” effect, at a given sampling date. Gene expression was relativized to 0 h= 1 (orange dashed line).....45

**Figure II.9.** Expression profile of *TaZOG1* (a), *TaZOG2* (b) and *TaGLU1-3* (c), in detached wheat leaves at different times after exposure to the neutral (N), blue (B) or green (G) filters. Data are means  $\pm$  SE (n= 3). Asterisks indicate the existence of significant differences for “shading treatment” effect, at a given sampling date. Gene expression was relativized to 0 h= 1 (orange dashed line).....48

**Figure II.10.** Expression profile of the CK receptors *TaHK3* (a) and *TaHK4* (b) in detached wheat leaves at different times after exposure to the neutral (N), blue (B) or green (G) filters. Data are means  $\pm$  SE (n= 3). Asterisks indicate the existence of significant differences for “shading treatment” effect, at a given sampling date. Gene expression was relativized to 0 h= 1 (orange dashed line).....48

**Figure II.11.** Expression profile of *TaHY5* gene, in detached wheat leaves at different times after exposure to the neutral (N), blue (B) or green (G) filters. Data are means  $\pm$  SE (n= 3). Asterisks indicate the existence of significant differences for “shading treatment” effect, at a given sampling date. Gene expression was relativized to 0 h= 1 (orange dashed line).....49

**Figure II.12.** The correlation between CKX activity (pkat mg<sup>-1</sup> protein) (a) and the expression of *TaCKX1* (b) with the chlorophyll content (%) in detached wheat leaves at different times after exposure to the neutral (N), green (G) or blue (B) filters. The regression curves and significances are shown. \*  $P \leq 0.05$ ; \*\*\* $P \leq 0.001$ .....50

**Figure II.13.** The correlation between the expression of *TaHY5* and (a) the chlorophyll content (%), (b) the CKX activity (pkat mg<sup>-1</sup> protein) and (c) the cytokinins content (pmol g<sup>-1</sup> DW) in detached wheat leaves at different times after exposure to the neutral (N), green (G) or blue (B) filters. The regression curves and significances are shown. \*  $P \leq 0.05$ ; \*\*\* $P \leq 0.001$ .....51

**Figure II.14.** Change in the chlorophyll content (%) in detached barley leaves at different times after exposure to the neutral (N), blue (B) or green (G) filters. Asterisks indicate significant differences for “shading treatment” effect, at a given sampling date.....52

**Figure II.15.** (a) CKX specific activity, (b) expression profile of *HvCKX1* gene and (c) Western Blot analysis of CKX1 protein and (d) Coomassie staining of proteins separated by SDS-PAGE, in detached barley leaves after 120 h of exposure to the neutral (N), blue (B), green (G) or red (R) filters. In (a) and (b), data are means  $\pm$  SE (n= 3). Asterisks indicate significant differences for “shading treatment” effect. Gene expression was relativized to  $t_0 = 1$  (orange dashed line). Lines and values on the right side at (d) represent the molecular weights given by Pre-Stained Protein Ladder.....52

**Figure II.16.** Correlation between CKX activity (pkat mg<sup>-1</sup> protein) and the chlorophyll content (%) in detached barley leaves at different times after exposure to the neutral (N), blue (B), green (G) or red (R) filters. The regression curves and significances are shown. \* $P \leq 0.05$ .....53

**Figure II.17.** Chlorophyll content in detached wild type and transgenic barley leaves at different times after exposure to the (a) neutral (N), (b) blue (B), (c) green (G) or (d) red (R) filters. Asterisks indicate the existence of significant differences for “shading treatment” effect, at a given sampling date. Data are means  $\pm$  SD (n= 8).....54

**Figure II.18.** Summary of the parameters altered in detached wheat leaves exposed to the blue (B) filter at different time points of the experiments.....59

**Figure II.19.** Summary of the parameters altered in detached wheat leaves exposed to the green (G) filter at different time points of the experiments.....59

**Figure III.1.** Scheme of the protocol used for non-invasive phenotyping of barley seedlings growing under water stress conditions. (a) Barley seeds were germinated on filter paper and 50 seedlings of similar radicle size were transplanted into soil in standardized PlantScreen™ measuring trays. (b) The trays were transferred to an XYZ PlantScreen™ chamber with a conveyor system for automatic image acquisition. (c) The canopy height was analysed using an in-house software routine implemented in MatLab R2015, and the data were evaluated by multivariate statistical analyses using R version 3.5.1.....65

**Figure III.2.** Analysis of the reproducibility of canopy height estimation in barley seedlings from two independent experiments. (a) The reproducibility of projected canopy height dynamics (in pixels) in barley seedlings (n = 100) grown under control conditions in December 2017 and July 2018. (b) The correlation between canopy height and fresh aerial biomass (FW,g) determined for replicates measured at day 16 and day 19 in barley seedlings from the two independent experiments. The regression curve and significance calculated from the three independent trays is shown. \*\*\* $P \leq 0.001$ .....73

**Figure III.3.** Analysis of reproducibility of canopy height estimation in barley seedling under water deficit conditions within experimental replicates. Changes in canopy height (in pixels) of stressed (D, discontinuous lines) and non-stressed (W, continuous lines) barley seedlings from five independent trays grown for 12 days (with the endpoint at day 15) (n=50).....74

**Figure III.4.** Dynamics of soil moisture and projected canopy height in barley seedlings growing under water stress conditions with subsequent rewatering. (a) Changes in substrate water content (%) of non-stressed (W, continuous lines) and stressed (D, discontinuous lines) barley seedlings (n = 50) from three independent trays (Barley1, 2 and 3) grown for 13 days under water deficit conditions (with the endpoint at day 16) and subsequently rewatered for 4 days (with the endpoint at day 19). The watering regime consisted in an initial 100% field capacity (FC) after sowing and subsequent constant 80% FC for W variants, and irrigation interruption from day 3 to day 16 for the D variants and posterior rewatering for 4 days. Blue arrows represent the watering regime and red arrow the stop of the irrigation moment in the D variant. (b) Changes in projected canopy height (in pixels) and (c) side view images of the D and W variants from the three independent replicates along the experiment.....76

**Figure III.5.** Linear curve of the projected canopy height and the extracted traits. (a) The average canopy height, regression curve and significance calculated from three independent trays (with 50 plants each) growing under water deficit conditions for 13 days (with the endpoint at day 16) and with subsequent rewatering for 4 days (with the endpoint at day 19). (b) Max is the maximum and Min the minimum canopy height reached by the stressed plants from replicate 1 or 2 (n = 50) under water deficit conditions, and the slope of the linear model curve is shown. (c) MaxR is



the maximum canopy height from replicate 1 or 2 (n = 50) attained after 4 days of rewatering, and the slope of the line (SlopeR) is also shown in the equation.....78

**Figure III.6.** Imaging of chlorophyll fluorescence ( $\Phi_{Po}$  and  $\Phi_{PII}$ ) in barley seedlings under well-water, water stress, and rewatering. Stressed and non-stressed plants labelled as D (left) and W (right), respectively.....79

**Figure III.7.** Variation in chlorophyll parameters in barley seedlings grown under water stress conditions and after subsequent rewatering. Chlorophyll fluorescence parameters from three independent trays (1, 2 and 3) (n = 50) and the average values. D and W variants are represented by discontinuous and continuous lines, respectively. Statistical analyses were performed via ANOVA. Asterisks indicate the significance level relative to the control variant; \*  $P \leq 0.05$ ; \*\*  $P \leq 0.01$ ; \*\*\*  $P \leq 0.001$ ; ns, not significant.....80

**Figure III.8.** Developmental stages of barley seedlings grown under (a) water stress and (b) after subsequent rewatering. Developmental stages of leaves in stressed (D) and non-stressed (W) plants from two independent trays (1 and 2) at the end of the water stress period (n = 8) (a) and after rewatering (n=5) (b).....83

**Figure III.9.** Morphometric and physiological changes in barley seedlings under water stress conditions and after subsequent rewatering. (a) Aerial biomass (FW,g), (b) leaf length (cm) and (c) width (cm) of the last fully expanded (FE) leaf, (d) the ratio between length and width, (e) the relative water content (%), (f) the index of the chlorophyll content, and the activity of the antioxidative enzymes (g) guaiacol peroxidase (POX), (h) catalase (CAT) and (i) ascorbate peroxidase (APX), in stressed (D, colour bars) and non-stressed (W, black bars) barley seedlings from two independent trays at the end of the water stress period (n=8) and after subsequent rewatering (n=5). Asterisks and ns indicate the significance level relative to the control replicate; \*  $P \leq 0.05$ ; \*\*  $P \leq 0.01$ ; \*\*\*  $P \leq 0.001$ ; ns, not significant. Three independent pools containing 5 plants each were used for the quantification of the antioxidant enzyme activity. Different letters mean significant differences according to Tukey HSD test after ANOVA.....84

**Figure III.10.** Metabolic profiles of barley seedlings under water deficit and after subsequent rewatering. Fold changes (presented as log<sub>2</sub> ratio) in the content (pmol mg<sup>-1</sup> DW) of free polyamines (PAs) and amino acids (AAs) between stressed (D) and non-stressed (W) barley

seedlings (three independent pools containing 5 plants from two independent trays, n= 6) at the end of the stress period (red bars) and after subsequent rewatering (gray bars).....87

**Figure III.11.** Multivariate statistical analyses of the traits in barley seedlings related to the water stress response and subsequent rewatering. (a) Principal component analysis (PCA) (b) contribution of the loadings to each PCA (Dim) and (c) a correlation matrix of 45 traits obtained from two different trays of barley seedlings at the end of the water stress period and after subsequent rewatering.....91

**Figure III.12.** Scree plot representing the percentage of explained variance of the model of each PCA (Dimension) performed in R3.5.1.....92

**Figure III.13.** Scatter plots of the correlation between canopy height, slope, morphometric parameters, RWC (%), chl and fluoresce related traits undertaken in R3.5.1.....94

**Figure III.14.** Scatter plots of the correlation between canopy height, slope, the activity of CAT, POX and APX, and some AAs undertaken in R3.5.1.....94

**Figure III.15.** Scatter plots of the correlation between canopy height, slope and some AAs and PAS undertaken in R3.5.1.....95

**Figure III.16.** Scatter plots of the correlation between the activity of CAT, POX and APX, Pro, OH-Pro, GABA, Arg, Glu, Cit and PAS undertaken in R3.5.1.....95

**Figure IV.1.** Target sequence used for the design of the silencing cassette of *HvCKX2.2* (*MLOC\_81291* or *HORVU3Hr1G027430*). The blue arrow indicates the restriction site for Sall and the red arrow the one corresponding to NotI.....104

**Figure IV.2.** Target sequence used for the design of the silencing cassette of *HvCKX9* (*MLOC\_11021* or *HORVU1Hr1G057860*). The green arrow indicates the restriction site for Dral and the orange arrow the one corresponding to XhoI.....105

**Figure IV.3.** Map of the vector pBract207. Arrows denotes the gene and promoter orientation.....106

**Figure IV.4.** Map of the final vectors (a) *HvCKX2.2*-RNAi and (b) *HvCKX9*-RNAi. Arrows denotes the gene and promoter orientation.....107

**Figure IV.5.** Example of PCR screening for the presence of sense (a) and antisense (b) components of HvCKX2.2:RNAi silencing cassette. Lines contain the products obtained by PCR amplification using genomic DNA as a template extracted from selected 6 plants from T0 generation. DNA extracted from plants regenerated from non-transformed embryos was used as negative control (NC) and 5 ng of plasmid pBract207::HvCKX2.2 as positive control (PC). 5  $\mu$ L of GeneRuler™ 1 kb Plus DNA Ladder was used as marker.....116

**Figure. IV.6.** Example of PCR screening for the presence of sense (a) and antisense (b) components of HvCKX9:RNAi silencing cassette. Lines contain products obtained by PCR amplification using genomic DNA as a template extracted from selected 6 plants from T0 generation. DNA extracted from plants regenerated from non-transformed embryos was used as negative control (NC) and 5 ng of plasmid pBract207::HvCKX9as positive control (PC). 5  $\mu$ L of GeneRuler™ 1 kb Plus DNA Ladder was used as marker.....116

**Figure IV.7.** Example of Southern Blot autoradiography from (a) HvCKX2.2:RNAi line 2.9 and (b) HvCKX9:RNAi line 7.3.....117

**Figure IV.8.** Expression analysis of (a) *HvCKX2.2* in RNAi:HvCKX2.2 lines 1.2 and 2.9; and (b) *HvCKX9* in RNAi:HvCKX9 lines 1.8 and 7.3, at different developmental stages (BBCH).....118

**Figure IV.9.** Yield parameters evaluated in silencing lines grown under greenhouse conditions. (a) and (b) dry biomass; (c) and (d) total tillers per plant; (f) and (g) grains per plant; and (h) and (i) total grain weight (TGW) of wild type and transgenic barley lines grown individually under e. greenhouse conditions. RNAi:HvCKX2.2 lines are represented in green, RNAi:HvCKX9 in blue and wild type values in red. Letters indicate the significant differences according to the multiple comparison test performed after the non-parametric test Kruskal–Wallis.....119

**Figure IV.10.** Wild type and transgenic barley plants inside the growth chamber coupled with the Plant Screen™ System.....120

**Figure IV.11.** Dynamics projected canopy height in wild type and transgenic barley seedlings growing under water stress conditions with subsequent rewatering. (a) Changes in projected canopy height (in pixels) and (b) side view images of the D (left) and W (right) treatment along

the experiment. Discontinuous and continuous lines in the figures on the left side represent D and W variants, respectively.....121

**Figure IV.12.** Line of the projected canopy height and the correspondent equation (discontinuous yellow and red line for water and water stress treatment, respectively) in wild type (red lines) and RNAi:HvCKX2.2 lines (green lines). Discontinuous and continuous lines represent D and W variants, respectively.....123

**Figure. IV.13.** Line of the projected canopy height and the correspondent equation (discontinuous yellow and red line for water and water stress treatment, respectively) in wild type (red lines) and RNAi:HvCKX9 lines (blue lines). Discontinuous and continuous lines represent D and W variants, respectively.....124

**Figure IV.14.** Variation in fluorescence related parameters in wild type and transgenic barley seedlings grown under water stress conditions and after subsequent rewatering. Chlorophyll fluorescence parameters (n = 50) and the average values. RNAi:HvCKX2.2 lines are represented in green, RNAi:HvCKX9 in blue and wild type values in red. Discontinuous and continuous lines represent D and W variants, respectively. Asterisks indicate the significance level relative to the control variant according to ANOVA; \*  $P \leq 0.05$ ; \*\*  $P \leq 0.01$ ; \*\*\*  $P \leq 0.001$ ; ns, not significant....125

**Figure IV.15.** Variation in the electron transport rate (ETR) in barley seedlings grown under water stress conditions and after subsequent rewatering. ETR from three independent biological replicates (1, 2 and 3) (n = 50) and the average values. (a) RNAi:HvCKX2.2 lines are represented in green, (b) RNAi:HvCKX9 in blue and wild type values in red. Discontinuous and continuous lines represent D and W variants, respectively. Statistical analyses were performed via ANOVA. Asterisks indicate the significance level relative to the control variant; \*  $P \leq 0.05$ ; \*\*  $P \leq 0.01$ ; \*\*\*  $P \leq 0.001$ ; ns, not significant.....126

**Figure IV.16.** Developmental stages of leaves from wild type and transgenic barley seedlings under water stress and after subsequent rewatering. Developmental stages of leaves from five independent plants (a, b) of wild type or transgenic lines under stressed (D) and non-stressed (W) conditions at the end of the water stress period (n = 8) and (c, d) after rewatering (n=5).....128

**Figure IV.17.** Changes (a, b) in aerial biomass (FW, g) and (c, d) relative water content (RWC, %) in barley seedlings under water stress conditions and after subsequent rewatering. Five independent plants of wild type or from transgenic lines were used as biological replicates per genotype and variant (W-well-watered and D-water stress), and the average values and SE at the end of the water stress period and after 4 days of rewatering are presented. RNAi:HvCKX2.2 lines are represented in green, RNAi:HvCKX9 in blue and wild type values in red. Bars with wide upward diagonal lines indicate water-stressed treatment (D). Different letters mean significant differences among treatments according Tukey HSD test after ANOVA.....129

**Figure IV.18.** (a) Osmotic potential ( $\Psi_{\pi}$ , MPa) and (b) correlation between  $\Psi_{\pi}$  vs. the decrease in RWC (%) in wild type and transgenic barley plants after the water stress period and after rewatering. Bars (a) and symbols (b) with wide upward diagonal lines indicate water-stressed treatment (D), whereas filled bars or symbols represent well-water variants.....130

**Figure IV.19.** Expression profile of *HvCKX* genes in wild type and transgenic barley lines under water stress conditions. RNAi:HvCKX2.2 lines are represented in green, RNAi:HvCKX9 in blue and wild type values in red. Gene expression was relativized to the respective wild type. Asterisks indicate the significance level relative to the control variant according to ANOVA; \*  $P \leq 0.05$ ; \*\*  $P \leq 0.01$ ; \*\*\*  $P \leq 0.001$ ; ns, not significant.....131

**Figure IV.20.** Expression profile of *HvCKX* genes in wild type and transgenic barley lines after 4 days of rewatering. RNAi:HvCKX2.2 lines are represented in green, RNAi:HvCKX9 in blue and wild type values in red. Gene expression was relativized to the respective wild type. Asterisks indicate the significance level relative to the control variant according to ANOVA; \*  $P \leq 0.05$ ; \*\*  $P \leq 0.01$ ; \*\*\*  $P \leq 0.001$ ; ns, not significant.....132

**Figure IV.21.** Profile of cytokinins (CKs) in barley seedlings (wild type and 3 transgenic lines) at the end of the water deficit period (left) and after 4 days of rewatering (right). Fold changes (presented as  $\log_2$  ratio) in the content (pmol  $\text{mg}^{-1}$  FW of CKs between stressed (D) and non-stressed (W) barley genotypes).....136

**Figure IV.22.** Profile of indole-3-acetic acid (IAA), ox-IAA and total auxin content in barley seedlings (wild type and 3 transgenic lines) at the end of the water stress period (left) and after

4 days of rewatering (right). Fold changes (presented as  $\log_2$  ratio) in the content of IAA, ox-IAA and total AUX between stressed (D) and non-stressed (W) barley genotypes.....138

**Figure IV.23.** Profile of the ratio between IAA and free CKs in barley seedlings (wild type and 3 transgenic lines) at the end of the water stress period (upper part) and after 4 days of rewatering (lower part). Fold changes in the content (presented as  $\log_2$  ratio) ratio of this metabolites between stressed (D) and non-stressed (W) barley seedlings from two independent biological replicates (n=5) for each genotype.....138

**Figure IV.24.** Profile of free PAs in barley seedlings (wild type and 3 transgenic lines) (a) at the end of the water stress period and (b) after 4 days of rewatering. Fold changes (presented as  $\log_2$  ratio) in the content of free PAs between stressed (D) and non-stressed (W) barley genotypes.

**Figure IV.25.** Profile of free AAs in barley seedlings (wild type and 3 transgenic lines) (a) at the end of the water stress period and (b) after 4 days of rewatering. Fold changes (presented as  $\log_2$  ratio) in the content of free AAs between stressed (D) and non-stressed (W) genotypes.....139

**Figure IV.26.** Principal component (PC) analysis of the traits in barley seedlings (wild type and 3 transgenic lines) at the end of the water stress period. (a) Principal component analysis (Dim1 and Dim2), (b) scree plot with the percentage of explained variance of the model for each PC (Dim) and (c) a contribution matrix of the loadings to each PC (Dim). Red ellipses indicated the groups according to PC2.....144

**Figure IV.27.** Principal component (PC) analysis of the traits in barley seedlings (wild type and 3 transgenic lines) after 4 days of rewatering. (a) Principal component analysis (Dim1 and Dim2), (b) scree plot with the percentage of explained variance of the model for each PC (Dim) and (c) a contribution matrix of the loadings to each PC (Dim).....145

**Figure IV.28.** Correlation analysis of some traits in barley seedlings (wild type and 3 transgenic lines) at the end of the water stress period. Scatter plots of the most correlated traits presented in Fig.IV.26 undertaken in R 3.5.1.....147

**Figure IV.29.** Correlation analysis of some traits in barley seedlings (wild type and 3 transgenic lines) after 4 days of rewatering. Scatter plots of the most correlated traits presented in Fig.IV.27 undertaken in R 3.5.1.....148

## Abbreviations

---

AA: amino acid	cZOGs: cZ-O-glucosyltransferases
ABA: abscisic acid	DAP: 1,3-diaminopropane / DAP: day(s) after pollination
Ala: L-alanine	DCPIP: 2,6-dichlorophenolindophenol
ANOVA: analysis of variance	DHZ: dihydrozeatin (N <sup>6</sup> -(4-hydroxy-3-methylbutyl) adenine)
APX: ascorbate peroxidase	DNA: deoxyribonucleic acid
Arg: L-arginine	DW: dry weight
ARR: response regulator from <i>Arabidopsis thaliana</i>	ETR: apparent photosynthetic electron transport rate
Asn: L-asparagine	FC: field capacity
Asp: L-aspartic acid	FR: far-red irradiation
AUX: auxin	FW: fresh weight
B: blue treatment	G: green treatment
BAP: benzyl-amino purine	GABA: $\gamma$ -aminobutyric acid
BL: blue light	gdna: genomic DNA
bp: base pair	Gln: L-glutamine
Cad: cadaverine	Glu: L-glutamic acid
CAT: catalase	Gly: L-glycine
cDNA: complementary DNA	His: L-histidine
chl: chlorophyll	HK: histidine kinase receptor
CIB1: cryptochrome-interacting basic helix-loop-helix transcription factor 1	HP: histidine-phosphotransferases
CIM: callus induction media	HY5: LONG HYPOCOTYL 5
Cit: L-citrulline	IAA: indole-3-acetic acid
CKs: cytokinins	Ile: L-ileucine
CKX: cytokinin oxidase/dehydrogenase	INCYDE: inhibitor of cytokinin degradation
CRY: cryptochrome	iP: isopentenyl-adenine
CRY2: cryptochrome 2	Leu: L-leucine
cZ: cis-zeatin	

LOV: light–oxygen–voltage domain photoreceptors  
 Met: *L*-methionine  
 mRNA: messenger RNA  
 N: neutral treatment  
 OH-Pro: *L*- hydroxiproline  
 PA: polyamines  
 Phe: *L*-phenylalanine  
 PMSF: phenylmethanesulfonyl fluoride  
 POX: guaiacol peroxidase  
 PPDF: photosynthetically photon flux density  
 Pro: *L*-proline  
 PSI: photosystem I  
 PSII: photosystem II  
 Put: putrescine  
 PVPP: polyvinylpolypyrrolidone  
 $qP$ : coefficient of photochemical quenching  
 qPCR: Real-Time polymerase chain reaction  
 R: red irradiation  
 RGB: red, green, blue  
 RNA: ribonucleic acid  
 RNAi: RNA interference  
 ROS: reactive oxygen species  
 RR: response regulator, regulatory proteins of CK response  
 RWC: relative water content  
 SAG: senescence-associated genes  
 Ser: *L*-serine  
 Spd: spermidine  
 Spm: spermine  
 TCA: Trichloroacetic acid  
 TQ-S: triple quadrupole mass spectrometer  
 Trp: *L*-tryptophan  
 TW: weight at full turgor  
 Tyr: *L*-tyrosine  
 Tyra: tyramine  
*tZ*: *trans*-zeatin  
 UDP: uracilo-difosfato  
 UGT: UDP-glucosyltransferase  
 UPLC: ultra-high performance liquid chromatography  
 ZOG: zeatin-*O*-glucosyltransferase  
 $\Phi_{(f,D)}$ : quantum yield of the constitutive non-regulatory dissipation  
 $\Phi_{NPQ}$ : total regulatory non-photochemical quenching  
 $\Phi_P$ : actual quantum yield of PSII for light-adapted state  
 $\Phi_{Po}$ : maximal quantum yield of PSII for a dark-adapted state  
 $\Phi_{PSII}$ : maximum quantum yield of PSII for light-adapted state



# **CHAPTER I: General Introduction**

## **I. I. Coping with a sessile lifestyle: a stressing plant tale**

Being restricted by their sessile nature, plants have developed complex mechanisms to fine-tune the perception of the environmental cues in order to flexibly adjust their metabolism, growth and development to continuously changing scenarios (Lichtenthaler, 1996). Plants can follow variations on environmental conditions without any negative impact on their physiology rates. Nevertheless, there are occasions where these fluctuations exceed the tolerance threshold of the plant and a mere homeostatic adjustment is not enough to withstand. Then, they are in presence of a stressing condition, which reduces physiological rates below the maximum possible expressed under optimal conditions (Lambers et al., 1998). In this context, adaptation and acclimation mechanisms must be displayed to minimize the damage, otherwise plant survival and productivity will be compromised (Lichtenthaler, 1996). Four different phases can be recognized in the dynamic process of plant's stress responses (Fig. I.1). At the beginning of the stress, an alarm reaction takes place, characterized by a deviation of the physiological standard conditions leading to a decline of the vitality of the plant. At this point, the catabolic processes begin to exceed the anabolic ones. The minimum of resistance possible that the plant can stand will depend on the mechanisms of defence to stress that it has available. If the stress continues, a stage of resistance will begin. Plants will tend to adapt to the stress, activating the repair processes to reach a new physiological optimum (maximum of resistance) by hardening. If the stress endures, with a high intensity, a stage of exhaustion is reached and there is an overcharge of the adaptation capacity, which leads to chronic disease or death. Nevertheless, if the stressor is removed and the plant damage is not too severe, a partial or full regeneration of the physiological function can be reached.

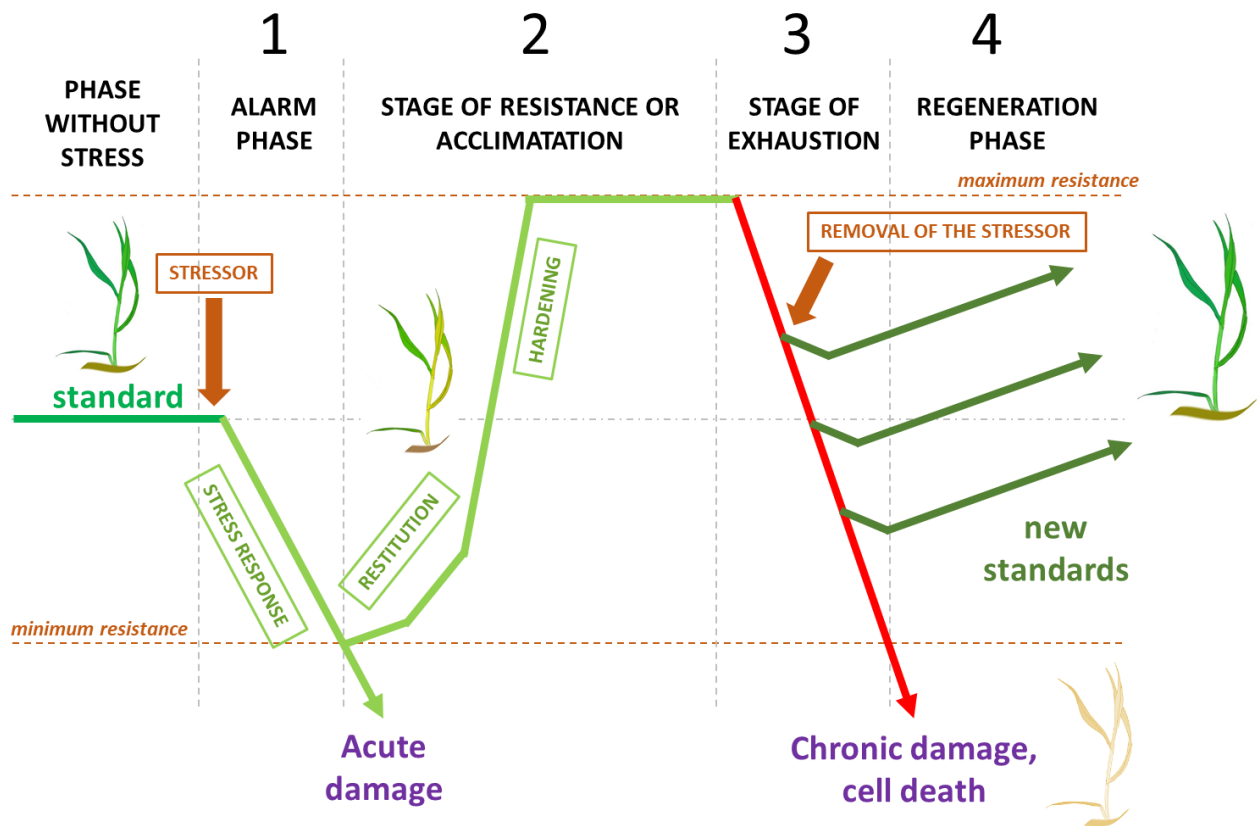


**Figure I.1.** Scheme of the phase sequences and responses induced in plants by stress exposure (adapted from Lichtenthaler, 1998).

## I. II. The different kinds of stressors and stress constraints

Not all stress scenarios are equivalent because the severity, the frequency, the duration and timing of the perturbation can vary, and with it the impact on the plant. The stress response will also depend on the stage of development of the plant, the type of tissue or organ affected, the plant species and the genotype (Bray, 2000). Stress factors can be classified in biotic or abiotic depending if they result from living organisms or from non-living factors. Abiotic stress like drought, salinity, extreme temperatures, deficiency of nutrients, light intensity, chemical toxicity, impact negatively on agriculture production worldwide and diminish the final yield of crops. Among all constraints, water deficit is a major limiting factor in the plant production

(Boyer, 1982), whereas solar radiation is considered the main determinant of crop yield (Hay et al., 2006). A deeper understanding of the physiological basis of the response to these two types of constraints can be crucial to overcome the uncertain future climate change scenarios that threaten global food security and demand (Dai, 2011; Griffiths and Parry, 2002).

### **I. III. Light as a stress factor**

Light is one of the main environmental factors that regulate plant growth and development. In conditions of high irradiation or continuous illumination, plants are in danger of absorbing more light energy than they can use for photosynthesis and other metabolic processes. If so, they generate an excess of excitation energy (Mullineaux and Karpinski, 2002) that can cause photo-oxidative damage and accelerate foliar senescence (Biswal and Biswal, 1984). Besides, changes in the quality and/or intensity of light caused by shading can also induce senescence (Brouwer et al., 2012). This occurs when plants grow under a dense canopy because the presence of the pigments in the leaves generate gradients of light between the top and bottom of the foliage (Tsuchisaka and Theologis, 2004). It remains unclear whether, in this conditions, senescence is triggered by the alteration in C balance, because plants cannot reach the compensation point due to the low amount of light received; or if it is caused by the drop of N and CK content in the xylem caused by stomata closure and decreased transpiration (Brouwer et al., 2012).

### **I. IV. Water stress responses**

The water status of the plants affects their phenology and physiology. Water stress is triggered by insufficient water supply and/or high transpiration rate and it causes decrease in growth, stomatal conductance of plants, photosynthesis and includes the turgor loss of the cell (Hsiao, 1973; Lawlor and Cornic, 2002; Pospíšilová et al., 2000). The limitations in CO<sub>2</sub> absorption due to the fall of the stomata conductance leads to a lower nitrogen uptake, ultimately affecting the C and N metabolism. The decrease in CO<sub>2</sub> availability also limits the electron flux and normal functioning of the photosynthetic system, generating an excess of excitation energy and oxidative damage (Lawlor and Cornic, 2002). Plant strategies to cope with this general imbalance

include the synthesis of compatible solutes: metabolites and proteins, also called osmolites, that lower the osmotic potential and retain water by maintaining positive turgor pressure. The accumulation of some of these compounds also contributes to the stabilization of sub-cellular structures and the activation of defence mechanisms against oxidative stress (Minocha et al., 2014). These osmolites are usually low molecular weight compounds as carbohydrates, amino acids (AA), polyamines (PA) and organic acids (Yancey, 2001).

Seed germination and seedling establishment during the vegetative growth period of plants are severely affected by water stress (Blum, 1996; Volaire, 2003). If they survive, the tolerance to the stress will anyway influence the partitioning of photosynthates to harvested parts, this is the reason why many scientific studies focus on the above-grown tissue development during water scarcity. Nevertheless, water stress has also serious negative impacts on the reproductive development of crops, which is initiated in the transition from vegetative shoot apical meristem to the inflorescence primordia (Fig. I.2). The most susceptible phase to water deficit is during the meiotic-stages, but also floral initiation and differentiation, fertilization, and seed development can be affected. Some of the consequences can be for instance ovule abortion, pollen sterility, failure of pollination, spikelet death and zygotic abortion (Barnabás et al., 2008; Saini and Westgate, 1999).

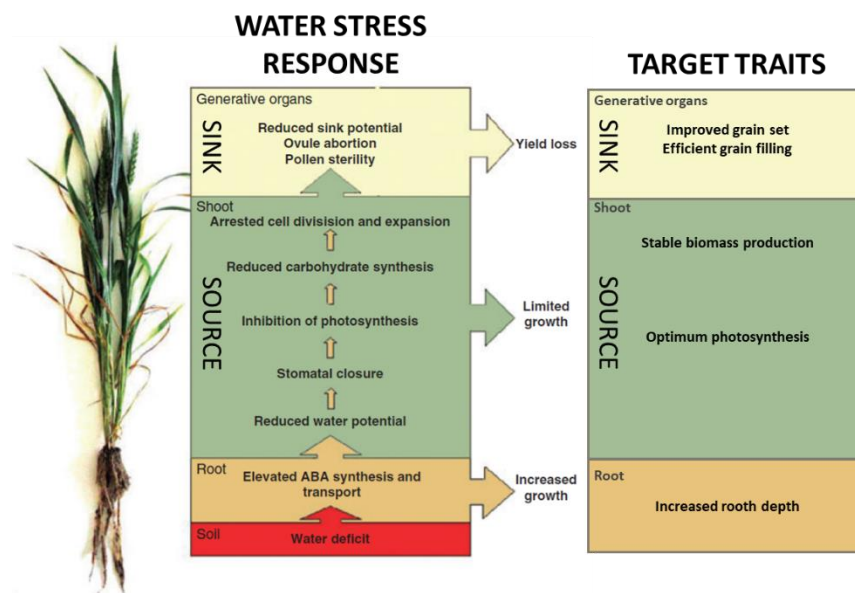


**Figure. I.2.** The effect of water stress in crops and target traits for improvement (Adapted from Barnabás et al. (2008)).

Thus for, breeding strategies for crop improvement need to focus not only on traits associated with water stress tolerance but also those which improve the yield stability more than high productivity (Athar and Ashraf, 2009). The complexity of these traits in combination with the urgency to improve crops for future more adverse climate change scenarios intensify the necessity of better and faster selections. In this sense, breeders can take advantage of the recent developments in large scale, fast and non-destructive imaging technologies that allow the identification of traits related to stress tolerance that simplify the study and selection of interesting phenotypes (Awlia et al., 2016).

### **I. V. Stress-induced senescence: a common denominator**

Senescence is a physiologically controlled process during which the leaves show progressive changes in their morphology, metabolism and gene expression (Lim et al., 2007). It is associated with the cessation of photosynthesis, the disintegration of chloroplasts, the loss of chlorophyll (chl), the degradation of leaf proteins and the translocation of amino acids (Buchanan-Wollaston, 1997). Leaf senescence plays an important role in the efficient use of nutrients, since it is a period of massive mobilization of nitrogen, carbon and minerals from mature leaves to other parts of the plant (Buchanan-Wollaston, 1997; Kajimura et al., 2010). It can be seen as a recycling program at the organism level (Quirino et al., 2000). In cereals, most of the protein content in the grain depends on the N remobilization from the vegetative parts during the senescence phase (Buchanan-Wollaston, 1997). Although in cereals reproduction is mainly triggering this process, other factor can initiate and/or modulate the rate of senescence both in the vegetative stages and during flowering. Moreover, senescence can be regulated by numerous internal and external factors. The phytohormones, such as cytokinins (CK), ethylene, auxins (AUX), jasmonic acid, abscisic acid (ABA) and salicylic acid (Love et al., 2008); as well as the reproductive stage of the plant and its age are crucial internal regulators. Among the external ones, there is evidence that UV-B radiation, ozone, nutrient limitation, extreme temperatures, drought, shading and the attack of pathogens can promote premature senescence.

## I. VI. Cross-signalling of phytohormones in the regulation of shading and water stress responses

Cytokinins (CKs) are phytohormones that promote cell division and differentiation (Mok and Mok, 2001) and affect several life processes throughout the growth and development of plants (Gajdosová et al., 2011). Natural CKs are, mainly, adenine derivatives substituted in the N<sup>6</sup>, and can be divided into two main groups, depending on the substituent: the isoprenoid CKs and aromatic CKs, less abundant (Zalabák et al., 2013). Both groups can be presented as free bases or also conjugated with sugars and amino acids. In the leaves of the Poaceae family (e.g. *Zea mays*, *Avena sativa*, *Triticum aestivum*, *Dactylis glomerata*, *Agropyron repens*, and *Phragmites australis*) the *cis*-zeatin derivatives are the main presented forms (Gajdosová et al., 2011).

Numerous studies have shown that, in plants, CKs exert a marked retardant effect of leaf senescence (Gan and Amasino, 1997; Lim et al., 2007 and the references cited therein), so the reduction of their endogenous levels is one of the main events associated with the development of senescence. In wheat, a strong drop in the endogenous level of *iP* is one of the first events associated with loss of chl and proteins during the development of senescence under N deprivation (Criado et al., 2007). A similar response has been observed in cut leaves when exposed to shade in the absence of blue light (Causin et al., 2009). On the other hand, in the absence of blue light, the rate of senescence of shaded leaves is significantly delayed when they are incubated in the presence of benzylaminopurine (BAP) (Causin et al., 2006). These results suggest that the homeostasis of CKs plays an important role in regulating the rate of senescence in wheat leaves exposed to stress conditions.

CK are also involved in the tolerance to many other types of abiotic stresses. In particular, under water stress conditions, the endogenous CK levels drop in the plants. Strategies to manipulate CKs homeostasis for increasing CK content in transgenic plants via the overexpression of the biosynthetic gene for isopentenyl transferase (IPT; EC 2.5.1.27), enhanced the photosynthetic capacity of plants, delayed senescence, and improved the grain yield under water stress conditions (Gan and Amasino, 1995; Ghanem et al., 2011; Merewitz et al., 2011; Rivero et

al., 2010, 2007; Zhang et al., 2010). Other approaches to improve water stress tolerance in crops through CKs involved the manipulation of enzymes responsible for their irreversible degradation: cytokinin oxidase dehydrogenase (CKX; EC 1.5.99.12). Due to CKs are negative regulators of root growth (von Wirén et al., 2018), the overexpression of CKX causes a CK-deficient phenotype that positive affect the root system and improves the tolerance to water deficient conditions (Pospíšilová et al., 2016; von Wirén et al., 2018). Another interesting feature of CKX has been described in rice, in which a reduction of CKX2 gene expression increased the amount of CK in the inflorescence meristems and enhanced grain yield (Ashikari et al., 2005). A similar effect has been reported in barley plants with down-regulated HvCKX1 expression through RNAi-based silencing (Holubová et al., 2018; Zalewski et al., 2010). Altogether, the possibility for enhancing drought tolerance and plant productivity makes CKX an interesting target for crop improvement under stress conditions.

The response to abiotic stress in the plants are the result of the crosstalk between several phytohormones (Peleg and Blumwald, 2011). For instance, the reduced growth caused by water deficit is generally result of attenuated auxin (AUX) signalling. Abscisic acid (ABA) is the main responsible controlling stomata closure. However, CK and the AUX indole-3-acetic acid (IAA) have been described to be antagonistic of ABA regulating this function (Tran et al., 2007). New evidences suggest that other phytohormones like ethylene (ET), brassinosteroids (BR), jasmonate (JA), salicylic acid (SA), and nitric oxide (NO) are also involved (Acharya and Assmann, 2009). Similarly, leaf senescence is also regulated by the crosstalk of CK and ABA, ET and JA and SA (Kim et al., 2011).

## **I. VII. Barley and wheat**

Since their domestication from the Fertile Crescent region of the Near East, around 10,000 years ago (Badr et al., 2012), barley (*Hordeum vulgare*) and bread wheat (*Triticum aestivum*) still represent major players in global agricultural production nowadays (Schnurbusch, 2019). Barley is the fourth most cultivated cereal worldwide (FAO STAT 2018) and it is used for animal feed and the production of alcoholic beverages. On the contrary, wheat is the principal food grain source for humanity. Both species belong to the Triticeae tribe, although they are quite



different in several aspects. Barley has a diploid genome, with a size of 5.1 gigabases (Gb) and each haploid genome with seven chromosomes. Instead, bread wheat is an allohexaploid, with a genome size estimated at approximately 17 Gb and 21 chromosomes. The complexity in bread wheat is given by the fact that its genome is result of the hybridisation events between the progenitors *Triticum urartu*, *Aegilops speltoides* and *Aegilops tauschii* (Appels et al., 2018).

With respect of the growing conditions, both crops are annual grasses and among them can be found winter or spring varieties, according to the season when they are planted. Winter varieties require a period of vernalization to initiate flowering. However, barley has a high degree of genetic variability and genetic plasticity of yield stability for stress (Kishor et al., 2014). In particular, the spring cultivar Golden Promise, obtained by gamma-ray irradiation of the cultivar Maythorpe (Forster et al., 1994) is of particular interest because it is highly transformable (Harwood, 2012) and its genome is sequenced (Mascher et al., 2017). These characteristics, added to the advantage that it is a self-pollinated plant which lowers the risk of gene flow (Ritala et al., 2002), make from barley an excellent model for genetic studies of Triticeae.

## I. VIII. Objectives

The main aim of this thesis was to understand the genetic and physiological basis of the role of CKs in the response to abiotic stresses in two crops of economic importance. To achieve this goal we separated the main aim in the following partial objectives:

- Objective n°1: To determine the role of CK in light-mediated senescence in barley (*Hordeum vulgare* cv. Golden Promised) and wheat (*Triticum aestivum* cv. Inta Oasis).
- Objective n°2: To develop a rapid, simple and non-invasive phenotyping method for studying water stress response and recovery in barley (an important model for the Triticeae) that allows the identification of traits related to stress tolerance.
- Objective n°3: To characterize the behaviour of CK homeostasis altered transgenic barleys when they are exposed to water stress conditions for the selection of interesting lines with improved stress tolerance and recovery capacity.

## **CHAPTER II: The role of cytokinins in light-mediated senescence in barley and wheat**

Marchetti, C. F., Škrabišová, M., Galuszka, P., Novák, O., & Causin, H. F. (2018). Blue light suppression alters cytokinin homeostasis in wheat leaves senescing under shading stress. *Plant Physiology and Biochemistry*, *130*, 647-657.

## II. I. Introduction

Leaves beneath a dense canopy experience a marked reduction of the photon flux as well as the red (660 nm) and blue (400-450 nm) wavelengths due to the spectral properties of the photosynthetic pigments, and it has been shown that changes in either light intensity or spectral quality can induce leaf senescence in an independent way (revised in Causin & Barneix, 2007). In wheat leaves exposed to shading under different light filters, blue light (BL) suppression plays a central role in the induction of chl and protein loss (Causin et al., 2009; Causin and Barneix, 2007). This effect was shown to be largely independent of differences in either net photosynthetic rate or carbohydrate content among shading treatments (revised in Causin & Barneix, 2007). Diverse classes of flavin-based photoreceptors that mediate the effects of BL have been described, including cryptochromes, phototropins and members of the zeirupe family. Meng et al. (2013) demonstrated that cryptochrome 2 (CRY2) suppress leaf senescence in soybean leaves through a blue-light dependent interaction with the cryptochrome-interacting basic helix-loop-helix transcription factor 1 (CIB1), which is an activator of senescence-associated genes (SAG) (Fig. II.1). In *A. thaliana*, CIB1 is degraded by the 26S proteasome in the absence of blue light (BL)

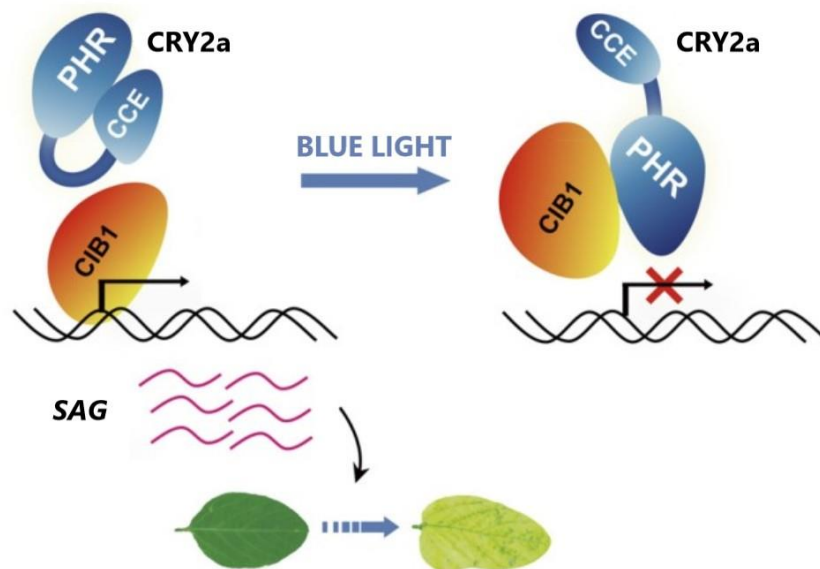


**Figure II.1.** Blue light suppresses the interaction of CIB1 with specific regions of the SAG chromatin, regulating leaf senescence. The scheme shows CRY2a-mediated blue light suppression of the CIB1-dependent activation of leaf senescence. PHR, photolyase homologous region; CCE, CRY C-terminal extension. Adapted from Meng et al. (2013).

(Liu et al., 2013). However, not CRY2 but two light–oxygen–voltage (LOV) domain photoreceptors, ZEITLUPE and LOV KELCH PROTEIN 2, are required for the suppression of the degradation of CIB1 by BL in this species, indicating that BL-regulation of this transcription factor may involve distinct mechanisms. There is a lack of information on whether genes homologous to *CIB1* are present in wheat and, if so, whether they are under the control of BL-mediated signals.

Even though the pathway of the light signal perception and transduction remains to be elucidated, previous studies suggest that the alteration of key components of the oxidative metabolism together with changes in the homeostasis of cytokinins (CKs) may be involved in the regulation of shade-induced senescence in wheat (Causin et al., 2009; Causin and Barneix, 2007). CKs are a major class of phytohormones whose role as retardants of leaf senescence under different stress conditions has been widely documented (e.g. Wang et al., 2016 and references therein). While *cis*-zeatin (*cZ*) has been generally regarded as a CK with little or no activity, isopentenyl-adenine (*iP*) and *trans*-zeatin (*tZ*) (and their ribosides) are usually considered as the main bioactive forms (Sakakibara, 2006). CKs are perceived by the two-component histidyl-aspartyl signalling system. At first, the CK molecule is recognized by a transmembrane histidine kinase (HK) receptor. Three CK-binding HK receptors have been characterized in *Arabidopsis* (AHK2, AKH3 and CRE1/AHK4), and their homologues have been identified in different plant species (e.g. Lomin et al., 2011; Nishimura et al., 2004). In the next step, the signal is transmitted to the regulatory proteins of CK response (RRs) by specific histidine-phosphotransferases (HPs). Kim et al., (2006) showed that AHK3 (but not the other CK receptors), mediates the control of leaf longevity through phosphorylation of ARR2 in *Arabidopsis*. Nevertheless, leaf senescence was not significantly affected in *arr2* knockout plants, suggesting that either other ARR2s and/or signalling components may be involved in the control of CK-mediated leaf longevity.

The homeostasis of CKs can be modulated by several mechanisms, including the degradation or the inactivation of their active forms. CK catabolism is mainly attributed to the activity of cytokinin oxidase/dehydrogenase (CKX, EC: 1.5.99.12), which catalyses the irreversible degradation of active CKs (Schmülling et al., 2003). Several putative members of the *CKX* gene family have been identified, and their relative expression profiles characterized in different

organs and developmental stages of wheat and related crops (e.g. Galuszka et al., 2004; Song et al., 2012, and references therein). CKX activity is usually low in non-senescent leaves, and both the activity as well as the gene expression of several *CKX* members increases under different stress conditions (Vaseva-Gemisheva et al., 2005; Vyroubalová et al., 2009). The *in vitro* activity of CKX was shown to be enhanced in detached apical parts of the first foliage leaves of barley kept in the dark (Conrad et al., 2007; Schlüter et al., 2011). This increment was greatly stimulated when the leaf segments were incubated in the presence of white light, presumably due to an increase of the enzyme expression. It is not known whether changes in light spectral quality can also affect CK degradation and/or *CKX* expression in leaves exposed to shading stress.

The purine moiety of CKs can be modified by ribosylation, phosphoribosylation and glucosylation, all of which affects the final pool of the active hormone. The most common way of CK inactivation involves *N*- or *O*-glycosylation. This deactivation is catalysed by uracilo-difosfato (UDP)-glucosyltransferase (UGT, EC 2.4.1.X), being UDP-glucose the donor of sugar moieties. While *N*<sup>7</sup>- and *N*<sup>9</sup>-glucosides are regarded as the final products of irreversible inactivation (Sakakibara, 2006), *O*-glucosides are considered as a storage form of CKs since they can be converted back to their free forms through the action of  $\beta$ -glucosidase (EC 3.2.1.21, Brzobohaty et al., 1993). Genes encoding for *cZ*-*O*-glucosyltransferases (*cZOGs*) have been identified in different plant species. In cereals, *cZOGs* preferentially catalyse *O*-glycosylation of *cZ* and *cZ*-riboside rather than *tZ* and *tZ*-riboside (Kudo et al., 2012, and references therein). Interestingly, some transgenic rice plants over-expressing the *cZOG1* and *cZOG2* genes exhibit delay of leaf senescence, indicating that *O*-glycosylation of *cZ* (-riboside) might be involved in the regulation of this process (Kudo et al., 2012).

In *A. thaliana*, both BL and CKs have been shown to induce certain photomorphogenetic responses by increasing the levels of the transcription factor LONG HYPOCOTYL 5 (*HY5*) through independent mechanisms, suggesting that this protein is a point of convergence between cryptochrome and CK signalling pathways (Vandenbussche et al., 2007). Moreover, indirect evidence suggests that the repression of *HY5* expression might contribute to the control of some processes associated to dark induced senescence in individual leaves (Keech et al., 2010). However, little is known about the *HY5* gene members in wheat, and it has not been investigated

to what extent the expression of this transcription factor is affected by different light environments in leaves senescing under shading conditions.

In this chapter it was studied whether changes in light spectral quality affects the level of CK metabolites and CKX activity, together with the expression profile of several genes involved in CK signalling and metabolism, in excised wheat leaves exposed to shading stress under specific light filters. The effect of the exogenous CK addition, the pharmacological inhibition of CK degradation, as well as changes in the expression profile of wheat cryptochromes and genes homologous to *CIB1* and *HY5* were also investigated. Moreover, to determine whether the mode of regulation observed for shade-induced leaf senescence in wheat is unique for this species or common to other monocotyledonous plants, an additional study was performed in barley leaves. The senescence pattern of wild type (wt) and transgenic barley plants with altered CK homeostasis were evaluated. Taken together, the results obtained indicate that the suppression of blue wavelengths during shading down-regulates the level of free CKs and alters the expression profile of several genes responsible for the maintenance of CK-homeostasis in shaded leaves of wheat. However, barley leaves are also affected by the change in the ratio of red and infrared light (R: FR), so the mode of response seem to be dependent of each species. The involvement of cryptochromes and *HY5* as putative components of the BL signal perception and transduction pathway in wheat is also discussed.

## II. II. Materials and methods

### II. II .I. Plant growth and experimental procedure

Two different set of experiments were performed. With the set **Experiment 1** we studied spring wheat (*Triticum aestivum* L., cv. INTA Oasis). In the set **Experiment 2** we analysed wt spring barley (*Hordeum vulgare* cv. Golden Promise) and two independent transgenic lines, named line 1.8 and 7.3, with silenced *HvCKX9* gene (please refer to Chapter IV for a detailed description of these lines). In all experiments, the seeds were surface sterilized (12 min in 10% H<sub>2</sub>O<sub>2</sub>), germinated on wet tissue paper and planted in plastic pots containing a mixture of sand: vermiculite (2:1), in a greenhouse at natural photoperiod. The pots were periodically irrigated

with tap water and, after six to seven days from sowing, fertilized twice a week with a modified Hoagland's solution (Causin et al., 2009). To study the effect of light spectral quality on the senescence rate, leaf segments (9 cm length) from the third or fourth fully expanded leaves of 30 day-old plants (BBCH code for cereals number 16) were placed inside plastic boxes containing bi-distilled water, whose lids were covered with Lee filters (blue #075, green #089 or red #026, hereafter referred as treatment B, G or R, respectively). For the **Experiment 1** performed with wheat leaves, only B and G treatments were applied because G and R treatment have similar effects on the senescence pattern (see Causin et al., 2006). Conversely, all types of filters were used in the **Experiment 2** for the study of senescence of wt and transgenic barley leaves. Blue and green filters supplied a similar proportion of red (R = 660 nm) to far-red (FR = 730 nm) irradiation but differed in the percent transmission of BL (450 to 480 nm): treatment B = 70% to 55% transmission, respectively; treatment G < 1% transmission in the indicated range. The red filter supplied a higher red to far-red ratio (six times that of B or G treatment) with a < 1% transmission of BL (see Causin et al., 2015 and Fig. II.2a) for a detailed description of the filters. Boxes with a neutral (N) white filter were used as controls. Photosynthetically photon flux density (PPFD) ranged from 20 (G filter) to 28 (N filter)  $\mu\text{mol m}^{-2} \text{s}^{-1}$ . Three replicates, containing four or five leaf segments each, were used per sampling date and treatments combination, depending on the experimental trial. Soon after excision, leaf segments were superficially sterilized (5 min) with 2% (v/v) commercial NaOCl ( $50 \text{ g Cl I}^{-1}$ ) and carefully rinsed with sterilized water. Part were immediately sampled (t0 point) and the remaining placed in the different treatments (Fig. II.2b and c). Leaf excision facilitates the implementation of pharmacological treatments as well as the simultaneous processing of a large number of experimental units; and even though it induces the development of senescence symptoms, it did not substantially alter the senescence pattern caused by the light filters when applied on intact leaves (Causin and Barneix, 2007). Incubations were performed in a chamber supplied with equal number of white (SYLVANIA F27W T8/LD/54) and red light enriched (SYLVANIA GroLux F30W T12) fluorescent tubes. The conditions in the chamber were 16 : 8 h light : dark photoperiod,  $24 \pm 2 \text{ }^\circ\text{C}$  and  $14 \pm 2 \text{ }^\circ\text{C}$  day and night, respectively. Measurements of R and FR irradiation and PPFD were performed, respectively, with a SKR 110 Red/ Far-red (660/730 nm) sensor (Skye-Probetech, USA) and a LI-190 quantum sensor (LI-COR,



Lincoln, NE, USA) attached to a CAVA-RAD data logger (Cavadevices, Argentina). It should be noted that, because FR irradiation is very low as compared to R light under the fluorescent tubes, the R: FR ratio was higher than 3.0 in all the treatments. Leaves were sampled at different time intervals, briefly rinsed in distilled water, blotted dry, fractioned, and kept at  $-75\text{ }^{\circ}\text{C}$  for further analyses. When indicated, the same procedure was performed with samples of leaves immediately detached prior to the beginning of shading treatments ( $t_0$ ). All the experiments were repeated at least twice. Whenever possible, data from different experiments were averaged, otherwise data from a representative trial are presented. Finally, in the **Experiment 1**, wheat excised leaves were treated with the adenine derivate 2-chloro-6-(3-methoxyphenylamino)-purine ("INCYDE", inhibitor of cytokinin degradation, Zatloukal et al., 2008) or with different CKs which were added in the floating solution. Five  $\text{nl ml}^{-1}$  Tween20 were also supplied in order to increase tissue contact with the medium.

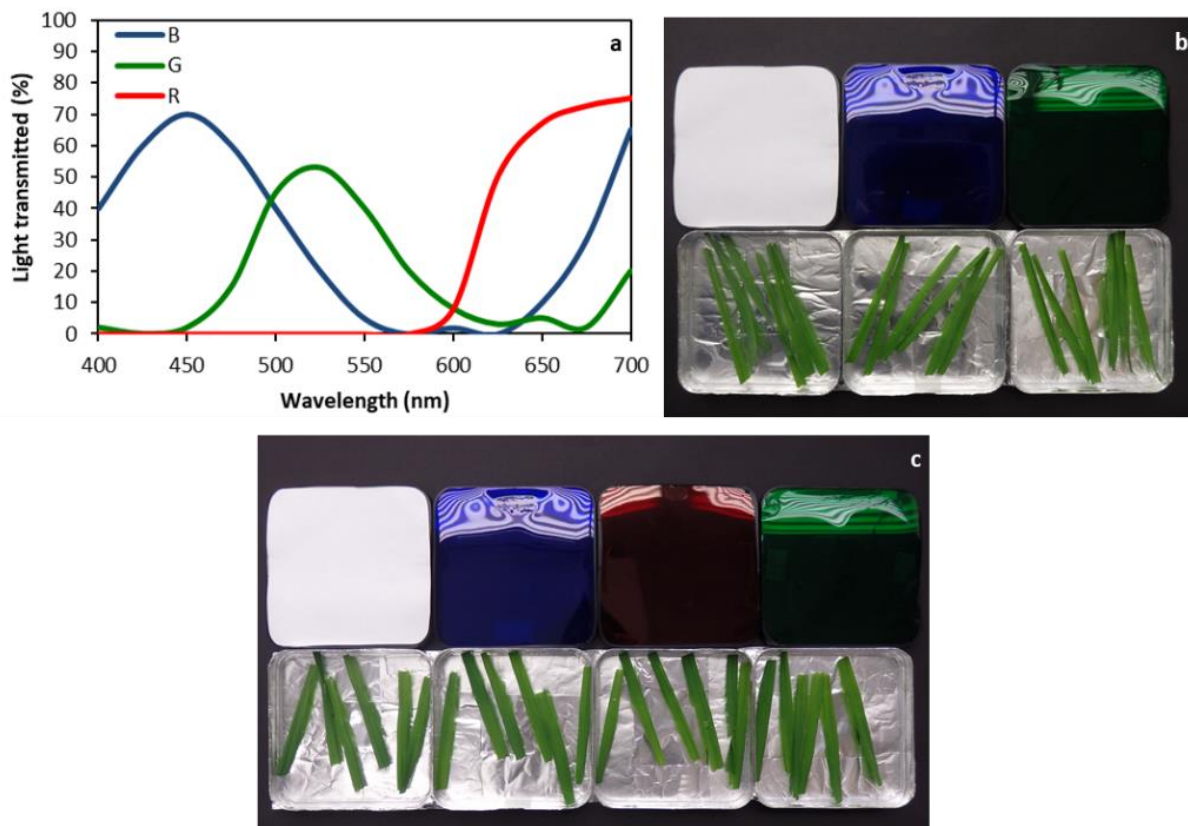


**Figure II.2.** (a) Percent light transmission spectra of the Lee filters used for the blue (B), green (G) and red (R) light treatments (according to the manufacturer) and illustrative images of the boxes used for the assay performed in the Experiment 1 with (b) wheat and in the Experiment 2 with (c) barley leaves.

## II. II. II. Determination of chlorophyll content and protein concentration

Chl content index was measured in wheat and barley leaves using a Chl Content Meter CCM-300 (Opti-Sciences, USA). A total of six measurements per leaf segment and treatment was performed.

Total protein content in the crude extracts was determined according to Bradford (1976), using bovine serum albumin as a standard.

## II. II. III. Cytokinin content measurements

For the **Experiment 1**, the content of different CK metabolites were determined. Lyophilized leaf samples (5 mg) were extracted in 1 ml of modified Bielecki buffer (60% MeOH, 10% HCOOH and 30% H<sub>2</sub>O) and purified using two solid phase extraction columns, the octadecylsilica-based column (C18, 500 mg of sorbent, Applied Separations) and the Oasis MCX column (30 mg/1 ml, Waters), according to the method described by Dobrev and Kamínek (2002), including modifications described by Antoniadis et al. (2015). The quantification of endogenous content of CKs was performed by ultra-high performance liquid chromatography (AcquityUPLC™; Waters) coupled to a Xevo™ TQ-S (Waters) triple quadrupole mass spectrometer using stable isotope-labelled internal standards (0.25 pmol of CK bases, ribosides, *N*-glucosides; 0.5 pmol of CK *O*-glucosides and nucleotides per sample added) as a reference. Three independent biological replicates were performed.

## II. II. IV. Measurement of CKX activity

In each experiment, excised leaves from wheat or barley were homogenized in liquid nitrogen and 200 mg of grounded material was extracted with 0.6ml of 0.2 M Tris/acetate buffer (pH 8.0), containing 0.3% (v/v) Triton X-100 and 1.0 mM phenylmethanesulfonyl fluoride (PMSF), in the presence of polyvinylpolypyrrolidone (PVPP). Cell debris was removed by centrifugation at maximum speed for 20 min at 4 °C. The supernatant was used for the enzymatic activity determination by the end-point assay with 4-aminophenol (Frébort et al., 2002). The reaction

mixture of 0.6 ml final volume contained 0.1 ml of the protein extract, 200  $\mu$ M of *i*P as substrate and 0.5 mM of 2,6-dichlorophenolindophenol (DCPIP) as electron donor, in 200 mM Mcllvaine buffer (citric acid/disodium hydrogen phosphate, pH 6.8). For blank of reaction, *i*P was replaced with dimethyl sulfoxide (solvent); and for every independent enzymatic extract, two technical duplicates were conducted. After overnight incubation at 37 °C, 0.3 ml 40% (w/v) trichloroacetic acid (TCA) was added to the mixture, followed by centrifugation for 5 min at 12,000 *g*. Finally, 0.2 ml 4-aminophenol [2% (w/v) solution in 6% (w/v) TCA] was added and the absorbance at 352 nm was measured to detect the Schiff base of the aldehyde originated from CK side chain and 4-aminophenol reaction, which has a molar absorption coefficient of  $\epsilon_{352} = 15.2 \text{ mM}^{-1} \text{ cm}^{-1}$  (Frébort et al., 2002).

## II. II. V. Phylogenetic tree construction and identification of wheat orthologues for genes of interest

In order to identify putative *CIB1*, *HKs* and *HY5* sequences in wheat and design primers for qPCR analysis in the **Experiment 1**, the annotated genes from the same family members in other related species were used as query for BLASTn search against the partial wheat genome sequence in EnsemblPlants database (<https://plants.ensembl.org/index.html>). Protein sequences from all hits with e-value  $\leq 1e^{-40}$  were aligned with the respective orthologues using the CLUSTAL W program in BioEdit and the unrooted phylogenetic trees were generated in MEGA 6 program (Fig. II.3), using the Neighbour-Joining (NJ) algorithm with 1000 bootstrap replicates. For each gene, the closest wheat orthologues were identified and in most of the cases several members clustered together, most probably corresponding to three copies of the same target gene in the hexaploid wheat genome. When possible, qPCR primers were designed on the identical region of the sequences, to amplify all the copies of each gene. For the remaining genes studied, primers were designed according to data published elsewhere (Table II.1).

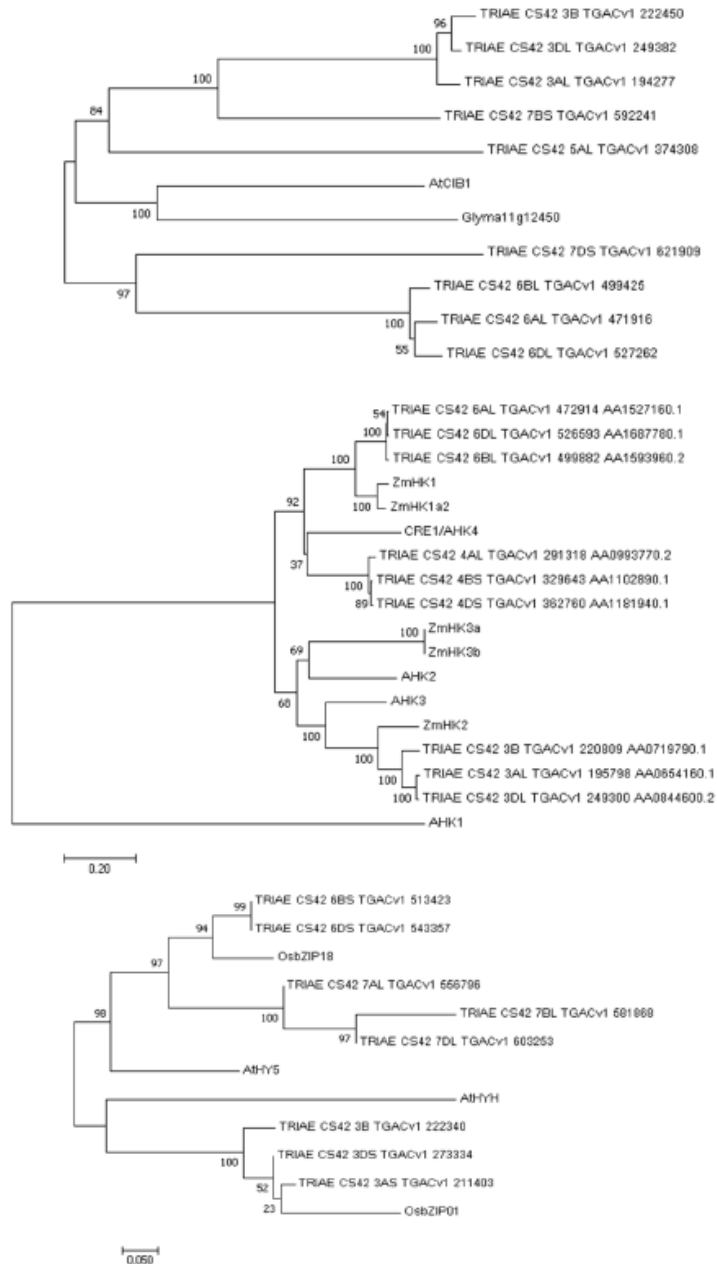


**Figure II.3.** Phylogenetic trees for (a) *TaCIB1*, (b) *TaHKs* and (c) and *TaHY5*. The trees are drawn to scale, with branch lengths measured in the number of substitutions per site. The percentage of replicate trees in which the associated taxa clustered together in the bootstrap test (1000 replicates) is shown next to the branches. Along with wheat sequences, family members from *Arabidopsis thaliana* and the soybean *Glyma11g12450* gene (homologous to *AtCIB1*) were used for the construction of the *TaCIB1* phylogenetic tree; sequences of histidine kinases implicated in CK perception in *A. thaliana* and *Zea mays* were used for the construction of the *TaHKs* tree; the proteins *OsbZIP01* and *OsbZIP18* from rice, identified as the closest orthologous of *A. thaliana* bZIP transcription factors HY5, and the HY5 homolog (HYH) in monocots, were used for the construction of the *TaHY5* phylogenetic tree.

## II. II. VI. Analysis of gene expression by qPCR

Isolation of total RNA from 100 mg of frozen leaves was performed using TRIzol Reagent (Thermo Fisher Scientific), according to the manufacturer's protocol. RNA concentration was determined using a NanoDrop™ Lite Spectrophotometer (Thermo Fisher Scientific). To eliminate traces of genomic DNA, RNA was treated with TURBO DNA-free™ kit (Thermo Fisher Scientific). 2 µg of the purified RNA was used for cDNA synthesis in a reverse transcription reaction containing oligo (dT) primers (Sigma-Aldrich) and RevertAid H Minus Reverse Transcriptase (Thermo Fisher Scientific). Quantitative real-time PCR reactions contained properly diluted cDNA, 300 nM primers and gb SG PCR Master Mix, supplemented with 100 nM ROX passive reference dye (Generi Biotech). The program consisted of an initial denaturation of 2 min at 95 °C, followed by 40 cycles of 15 s at 95 °C and 60 s at 60 °C, performed on a ViiA™ 7 Real-Time PCR System (Applied Biosystems). In order to confirm the specificity of amplification, each run was completed with a melting curve and the resulted amplicons were analysed on 2% agarose gel stained with ethidium bromide, in presence of a 50 base pair (bp) DNA ladder (New England BioLabs) for size determination and visualized using Gel Doc EZ system (Bio-Rad). Changes in the relative mRNA abundance were calculated using the comparative  $2^{-\Delta\Delta C_t}$  according to (Pfaffl, 2001), using t0 as the reference sample. The qPCR efficiency of amplification was 90-110% for all the primers used (data not shown). *TaEF2* and *TaGADPH* were chosen as internal control genes in the **Experiment 1** and *HvEF2* and *HvACT* in the **Experiment 2**. Three biological and two technical replicates were analysed per each condition tested. Fold changes in gene expression were calculated after data normalization for multiple internal controls following the procedures suggested by Vandesompele et al. (2002). All primers used are listed in the Table II. 1. Due to the high similarity in the sequences of *TaEF2* and *HvEF2*, as well as *TaCKX1* and *HvCKX1*, the same set of primers were used for both species.

**Table II.1.** Primer sequences used for real time PCR expression analysis of wheat and barley.

Gene name	Primer sequence (5' to 3' end direction)	
	Fw	Rev
<i>TaEF2</i>	CCGCACTGTCATGAGCAAGT	GGGCGAGCTTCCATGTAAG
<i>TaGAPDH</i>	TTAGACTTGCGAAGCCAGCA	AAATGCCCTTGAGGTTTCCC
<i>TaCKX1</i>	TGTGGACAGTAACACAGCAGTTTAAC	CCGTGCCACCTACTATCAAATTT
<i>TaCKX3</i>	CGTGGCTCAACCTCTTCGTC	GTTGGGTCCCCTTGCTC
<i>TaCKX4</i>	TGCTGTCTCGGCTGAGATACATACAG	TGACGTCCTGTTGCCACTTTG
<i>TaCKX10</i>	GGTAAGGTGGATAAGAGTTCTCTACTT	ATCTGAGTTGAGATAGTAGTGCATGGA
<i>TaCKX11</i>	AGCAACGTCCTGCAGCTCCAA	GAGCTGCGGATGGAGTGCTCA
<i>TaGlu1c</i>	ACCAATAACAAGCCAGCCGTGAC	CGACGAGTTCACAAGGAACACGA
<i>TacZOG1</i>	TCATCTGGGTATTGCGCGAG	CTCAGAGAGCAGCTTGTCGT
<i>TacZOG2</i>	CCAGGTGATCGACAAAATGCC	CGGCATCAAAGGCAAATCAG
<i>TaRR4</i>	AGGAGGTGGGCGTGAATTTGA	TGCGACTTGAGCTTCTTCATGTCA
<i>TaHK3</i>	TTAAAACTGGAGATCGATGGA	GGTGGGATGGTGTACCAAGAA
<i>TaHK4</i>	CCCATCTGGTGTCTTCGTTAT	AGTTGCAAGGAAGTACTGACTTA
<i>TaHY5</i>	GCTGGAGGCGAAGGTGAAG	CGGTGGTGTTCAGTATCTGTCT
<i>TaCIB1</i>	GACGCCGCCTCTCAGGTT	TGCCCCATGTCCATCTGAA
<i>TaCRY2</i>	TCCGATATCAAGGAAAAGATCCA	GAGTGCACTTCGACTGAAGATGA
<i>HvACT</i>	TGTTGACCTCAAAGGAAGCTATT	GGTGCAAGACCTGCTGTTGA

## II. II. VII. Western Blot analysis

For the **Experiment 2**, barley leaves were grounded by mortar and pestle using liquid nitrogen and proteins extracted using a buffer containing 50 mM Tris, 150 mM NaCl, 20 mM MgSO<sub>4</sub>·7H<sub>2</sub>O, 2 mM Na<sub>2</sub>EDTA, 1 mM PMSF, 1 mM DTT and 1% Triton-X-100 (pH=7.7), in a ratio 1:3. For removal of phenolic compounds, 20 mg of PVPP were added during the extraction. Cell debris was removed by centrifugation at 20,000 *g* for 25 min at 4 °C. The protein content was measured according to Bradford (1976). 30 µg of the extracted proteins were subjected to electrophoretic separation in a denaturing 10% SDS-polyacrylamide gel during 15 min at 100V and 60 min at 180 V. The resolved proteins were transferred onto 0.45 µm polyvinylidene fluoride membrane (GE Healthcare Life Sciences, Austria), during 1 h at 100 V using a buffer consisting of 25 mM Tris and 192 mM Glycine in 20% methanol (pH 8.3). Later, the membrane was blocked over-night with 5% powdered milk in blocking buffer containing: 0.02 M Tris, 0.5 M NaCl and 5% (w/v) milk, (pH 7.5). The immunoblot analysis of CKX1 was performed using a rabbit polyclonal antibody (ratio 1:1000) raised against ZmCKX1 (Bilyeu et al., 2001). The secondary antibody used was a goat anti-rabbit IgG horseradish peroxidase conjugate (Merk, Germany) (ratio 1:25000). For detection of the immunoreactive proteins, the membrane was covered with 1 ml of ECL Clarity (Bio-Rad) substrate for 2 min, foil-wrapped, and visualized using ChemiDoc™ MP Imaging System with Image Lab™ Software (BioRad, USA). For homogenising the blot signal per well, the same amount of proteins was loaded and a Coomassie (R-250) staining was performed in gels loaded with the same samples and volumes to those used for the immunoblot.

## II. II. VIII. Data analysis

For chl, CK content and CKX activity data, a conventional two-way ANOVA test (STATISTICA 7, Stat Soft Inc., Tulsa, OK, USA), was performed. When necessary, data transformation was used to meet ANOVA assumptions. Depending on the experimental design, the model included “sampling date” and “light filter”, or “light filter” and “incubation media”, as fixed factors. Post-hoc comparisons for significant main effects or interaction terms were performed using the Tukey HSD test. Significant differences were considered at  $*P \leq 0.05$ .

Normalized qPCR data were analysed for each sampling date and shading treatment separately using the non-parametric Kruskal-Wallis ANOVA, with “light filter” or “sampling date”, respectively, as fixed factors. Where appropriate, multiple comparisons of mean ranks were used to determine the significant differences among treatments.

## II. III. Results

### A. Experiment 1 - Shade-induced senescence in wheat leaves.

II. III. I. The homeostasis of CKs is altered during senescence progression under the different shading treatments in wheat

As previously reported, chl degradation rate in excised leaves exposed to shading increases when BL transmittance is suppressed (i.e. treatment G), while in leaves from treatment B it follows an almost identical trend to the neutral control (Fig. II.4a). Moreover, BL contributes to yellowing retardation yet when supplied at 30 or 54 h after the leaves had been exposed to the green filter (Fig. II.4b). This senescence-retardant effect of BL is corroborated by the expression profile of the two senescence markers analysed (Fig. II.5, see also Causin et al., 2015). The content of CK increased as senescence progressed in all the treatments (Fig. II.6a), being *cZ*-type the major contributor to the total pool of CKs (Fig. II.6 b). *O*-glucosides were the most abundant CK metabolite in senescing leaves (Fig. II.6c), mostly represented by *cZOG* (Fig. II.6d). For instance, at the end of the experimental period the content of *O*-glucosides was between 300 and 470 pmol g<sup>-1</sup> DW, among which 54% to 62% corresponded to *cZOG* and 37% to 45% to *cZROG*. In all cases, the increment in CK content was higher in absence of BL (Fig. II.6a-d). Regarding the bases, two distinct trends were observed. On the one hand, the content of *tZ* and *cZ* decreased in all shading treatments during the first 78 h. It is noteworthy that although no differences among treatments were found at 24 h after the beginning of shading, the decrement of both free CKs thereafter was on average significantly higher in leaves exposed to the G filter (Table II.2, ANOVA for “light filter” and “sampling date” main effects  $P \leq 0.01$  for both traits). On the other hand, while the content of *iP* also tended to decrease as senescence progressed in treatment G,



it oscillated around the initial value in treatments N and B (Table II.2). Nevertheless, due to the variation found in tissue *iP* levels, significant differences were only detected at the last sampling date between treatments N and G.

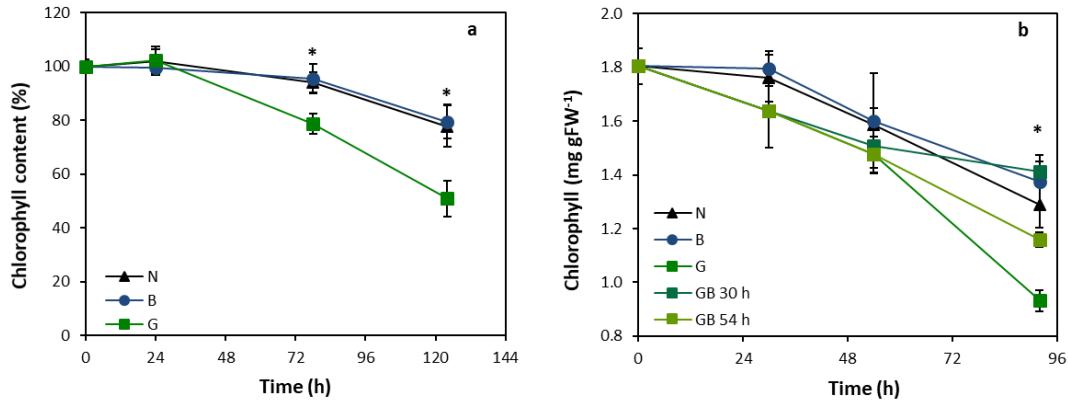


**Figure II.4.** (a) Change in the percent chlorophyll content in detached wheat leaves at different times after exposure to the neutral (N), blue (B) or green (G) filters. Asterisks indicate the existence of significant differences for “shading treatment” effect, at a given sampling date. (b) Chlorophyll content in detached wheat leaves at different times after exposure to the following shading treatments: 92 h neutral filter (N), 92 h blue filter (B), 92 h green filter (G), 30 h G + 62 h B (GB 30 h), or 54 h G + 38 h B (GB 54 h). Data are means  $\pm$  SE (a:  $n = 8$ ; b:  $n = 4$ ). Asterisks indicate significant differences between treatment G and the remaining shading treatments.

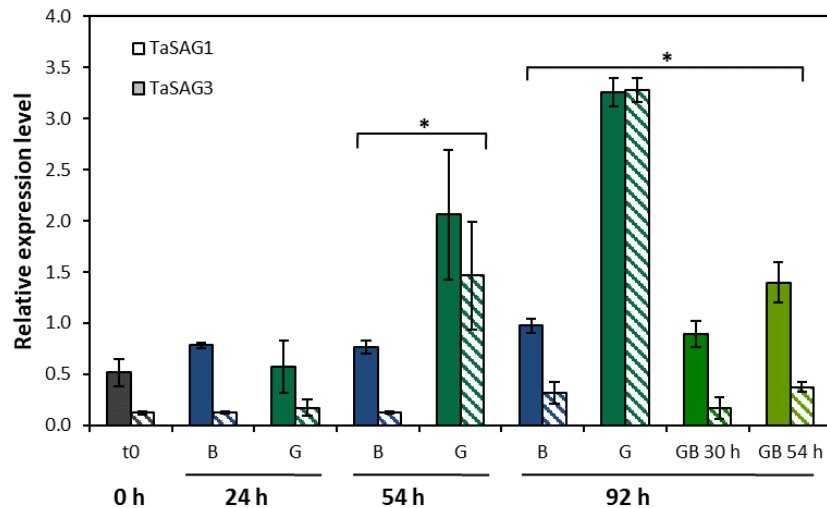


**Figure II.5.** Expression profile of two senescence markers in detached wheat leaves at different times after exposure to the blue or green filters, according to the following treatments: 92 h blue filter (B), 92 h green filter (G), 30 h G + 62 h B (GB 30 h), or 54 h G + 38 h B (GB 54 h). Asterisks indicate significant differences for the expression level of both markers between treatment G and the remaining treatments, at a given sampling date.

Contrary to expected, the content of precursors (CK-ribotides and the riboside forms) did not follow similar trends than those found for free CKs. While the level of CK-ribosides slightly increased at the end of the experimental period in leaves exposed to filter B, a sharp increase was observed at 78 h in leaves from the remaining treatments (Table II.2). Then, only in treatment G the content of CK-ribosides fell to similar levels to those found in treatment B. *Cis*-zeatin riboside (cZR) was the most prevalent metabolite among CK-ribosides (Table II.2). The content of CK-ribotides did not significantly change during the first 78 h, but peaked at 124 h in all the treatments, with values more than eight, ten, and twelve folds higher than t0 in treatment B, N, and G, respectively (Table II.2). Isopentenyladenosine-5'-monophosphate (iPR5MP) was the most prevalent form of CK-ribotides (Table II.2).

The content of most of the conjugated forms, involved in storage (*O*-glucosides) and deactivation (*N*-glucosides), was considerably higher than those found for active CKs (free bases and ribosides). The *O*-glucosides were mostly represented by those of cZ and its riboside, meanwhile the *N*-glucosides by *N*<sup>9</sup>-glucosides of tZ and iP (Table II.2). As observed for the CK-ribotides and -ribosides, the level of *O*-glucosides tended to increase as senescence progressed (Table II.2). Notably, this effect was statistically significant only for leaves from treatment G, which more than doubled the initial amount of CK-*O*-glucosides at the end of the experimental period. On the contrary, the content of *N*-glucosides did not follow a consistent trend and oscillated around 34% of the initial value, depending on the treatment and sampling date considered (Table II.2). At 124 h, significant differences for the content of CK *N*-glucosides were found only between treatments N and B.

To evaluate the effect of different free CK bases on leaf senescence rate when BL is suppressed, changes in chl content were analysed at 100 h after exposure to the G filter, either in the absence or presence of 2.5 µM iP, tZ, cZ, BAP or the B filter (as a control), which were applied at 52 h from the beginning of the experiment. As shown in Table II.3, only the addition of BAP or tZ significantly delayed leaf senescence when compared to treatment G. Interestingly, the effect was like that exerted by exposure to filter B in the absence of exogenously applied CKs (see Table II.3, treatment GB).

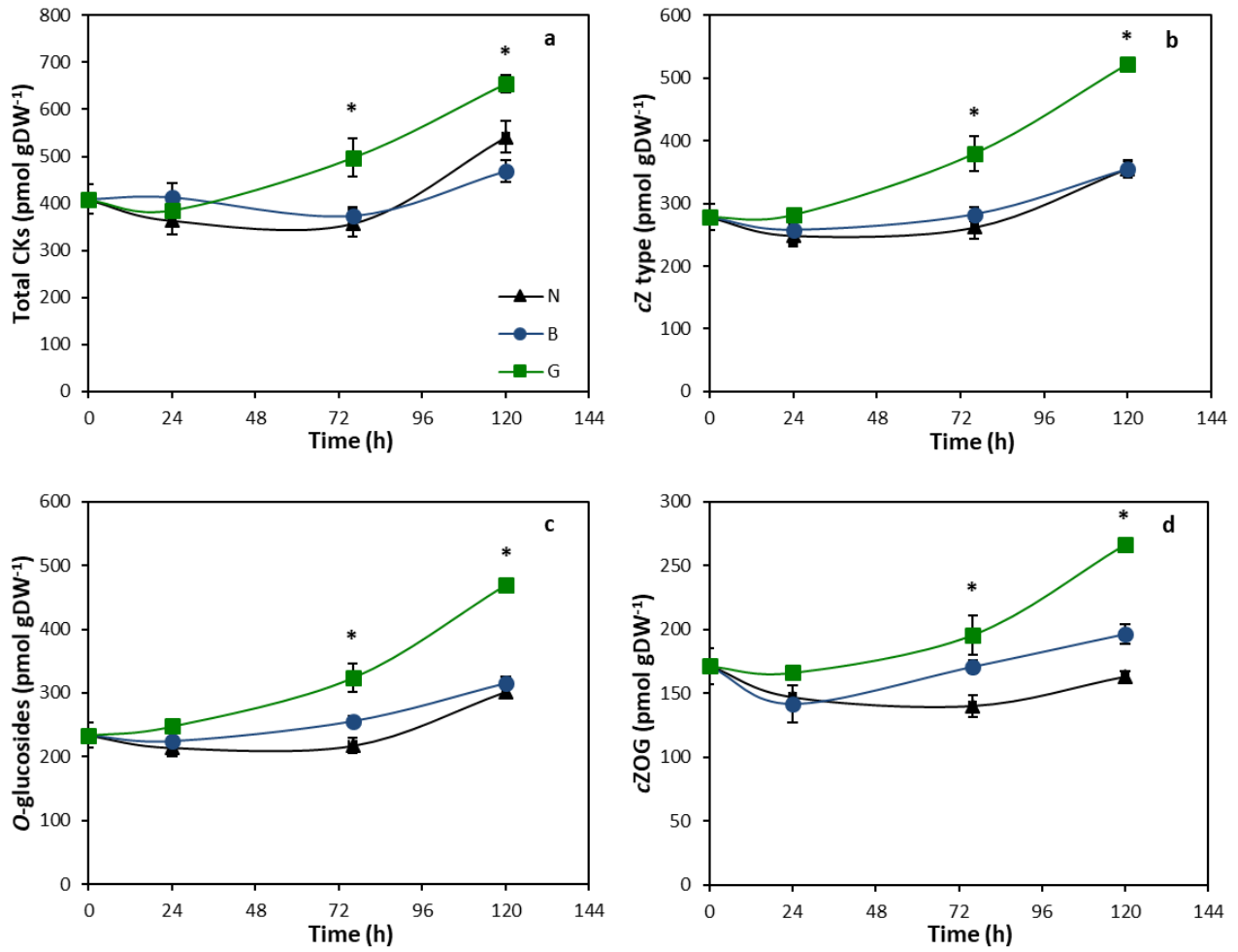


**Figure II.6.** Total CK content (a), *cZ*-type of CKs (b), *O*-glucosides (c) and *cZOG* (d), in detached wheat leaves at different times after exposure to the neutral (N), blue (B) or green (G) filters. Data are means  $\pm$  SE ( $n=3$ ). Asterisks indicate the existence of significant differences for “shading treatment” effect, at a given sampling date.

**Table II.2.** Content of different CK metabolites in excised wheat leaves (pmol gDW<sup>-1</sup>), at different times of exposure to the shading treatments with neutral (N), blue (B), or green (G) light filters (mean ± SE, n=3). < LOD: below the limit of detection. Different letters mean significant differences among treatments according Tukey HSD test after ANOVA.

	To	24 hs				78 hs			124 hs		
		N	G	B		N	G	A 76 hs	N	G	B
pmol/g DW	average ± SE	average ± SE	average ± SE	average ± SE	average ± SE	average ± SE	average ± SE	average ± SE	average ± SE	average ± SE	average ± SE
<b>cZRMP</b>	< LOD	< LOD	< LOD	< LOD	< LOD	< LOD	< LOD	5.54 <sup>a</sup> ± 0.22	12.88 <sup>a</sup> ± 1.49	6.03 <sup>a</sup> ± 0.81	
<b>iPRMP</b>	< LOD	< LOD	< LOD	< LOD	1.45 <sup>a</sup> ± 0.25	< LOD	1.66 <sup>a</sup> ± 0.14	5.36 <sup>b</sup> ± 0.61	< LOD	2.21 <sup>a</sup> ± 0.19	
<b>Ribotides</b>	< LOD	< LOD	< LOD	< LOD	1.45 <sup>a</sup> ± 0.25	< LOD	1.66 <sup>a</sup> ± 0.14	10.90 <sup>a</sup> ± 0.84	12.88 <sup>a</sup> ± 1.49	8.24 <sup>a</sup> ± 1.00	
<b>tZR</b>	0.29 <sup>a</sup> ± 0.03	0.23 <sup>a</sup> ± 0.01	0.18 <sup>a</sup> ± 0.01	0.18 <sup>a</sup> ± 0.01	0.47 <sup>ab</sup> ± 0.09	0.67 <sup>b</sup> ± 0.07	0.30 <sup>a</sup> ± 0.03	0.59 <sup>b</sup> ± 0.03	0.29 <sup>a</sup> ± 0.01	0.36 <sup>a</sup> ± 0.05	
<b>cZR</b>	15.56 <sup>a</sup> ± 0.44	14.11 <sup>a</sup> ± 1.57	16.47 <sup>a</sup> ± 0.70	12.40 <sup>a</sup> ± 0.98	27.71 <sup>ab</sup> ± 4.77	44.91 <sup>b</sup> ± 5.17	11.42 <sup>a</sup> ± 1.24	35.30 <sup>b</sup> ± 3.01	29.15 <sup>ab</sup> ± 0.97	20.94 <sup>a</sup> ± 1.31	
<b>iPR</b>	6.55 <sup>a</sup> ± 0.40	7.82 <sup>a</sup> ± 0.83	6.37 <sup>a</sup> ± 0.33	9.48 <sup>a</sup> ± 0.79	15.32 <sup>a</sup> ± 1.75	13.67 <sup>a</sup> ± 0.72	9.98 <sup>a</sup> ± 0.79	16.14 <sup>c</sup> ± 0.68	7.42 <sup>a</sup> ± 0.23	10.58 <sup>b</sup> ± 0.27	
<b>DHZR</b>	0.33 <sup>a</sup> ± 0.02	0.33 <sup>a</sup> ± 0.06	0.29 <sup>a</sup> ± 0.01	0.28 <sup>a</sup> ± 0.01	0.58 <sup>ab</sup> ± 0.12	0.76 <sup>b</sup> ± 0.07	0.19 <sup>a</sup> ± 0.03	0.59 <sup>b</sup> ± 0.05	0.43 <sup>ab</sup> ± 0.00	0.33 <sup>a</sup> ± 0.04	
<b>Ribosides</b>	22.73 <sup>a</sup> ± 0.89	22.49 <sup>a</sup> ± 2.47	23.32 <sup>a</sup> ± 1.06	22.34 <sup>a</sup> ± 1.79	44.09 <sup>ab</sup> ± 6.73	60.01 <sup>b</sup> ± 6.03	21.89 <sup>a</sup> ± 2.10	52.63 <sup>b</sup> ± 3.77	37.30 <sup>a</sup> ± 1.21	32.21 <sup>a</sup> ± 1.67	
<b>tZ</b>	4.93 <sup>a</sup> ± 0.30	3.16 <sup>a</sup> ± 0.21	2.91 <sup>a</sup> ± 0.22	3.26 <sup>a</sup> ± 0.26	2.31 <sup>a</sup> ± 0.18	1.64 <sup>a</sup> ± 0.14	2.62 <sup>a</sup> ± 0.24	2.49 <sup>a</sup> ± 0.20	1.40 <sup>a</sup> ± 0.01	2.05 <sup>a</sup> ± 0.30	
<b>cZ</b>	26.39 <sup>a</sup> ± 1.06	18.00 <sup>a</sup> ± 1.23	15.74 <sup>a</sup> ± 0.42	16.86 <sup>a</sup> ± 0.62	15.93 <sup>a</sup> ± 1.71	9.06 <sup>a</sup> ± 0.57	13.96 <sup>a</sup> ± 1.74	11.57 <sup>a</sup> ± 1.11	8.46 <sup>a</sup> ± 0.12	11.44 <sup>a</sup> ± 1.74	
<b>iP</b>	9.57 <sup>a</sup> ± 0.67	17.79 <sup>a</sup> ± 2.56	9.81 <sup>a</sup> ± 0.28	12.60 <sup>a</sup> ± 1.40	7.40 <sup>a</sup> ± 0.88	7.09 <sup>a</sup> ± 1.29	5.55 <sup>a</sup> ± 0.95	13.86 <sup>b</sup> ± 2.07	5.28 <sup>a</sup> ± 0.31	6.41 <sup>a</sup> ± 0.70	
<b>DHZ</b>	< LOD	< LOD	< LOD	< LOD	< LOD	< LOD	0.20 <sup>a</sup> ± 0.01	< LOD	0.23 <sup>a</sup> ± 0.03	0.22 <sup>a</sup> ± 0.01	
<b>Free Bases</b>	40.89 <sup>a</sup> ± 2.03	38.95 <sup>a</sup> ± 4.00	28.45 <sup>a</sup> ± 0.91	32.72 <sup>a</sup> ± 2.27	25.63 <sup>a</sup> ± 2.77	17.78 <sup>a</sup> ± 2.00	22.33 <sup>a</sup> ± 2.94	27.92 <sup>b</sup> ± 3.38	15.37 <sup>a</sup> ± 0.47	20.12 <sup>a</sup> ± 2.76	
<b>tZ7G</b>	0.03 <sup>a</sup> ± 0.00	0.03 <sup>a</sup> ± 0.00	0.02 <sup>a</sup> ± 0.00	0.03 <sup>a</sup> ± 0.00	0.05 <sup>b</sup> ± 0.00	0.04 <sup>ab</sup> ± 0.00	0.02 <sup>a</sup> ± 0.00	0.06 <sup>c</sup> ± 0.00	0.01 <sup>a</sup> ± 0.00	0.03 <sup>b</sup> ± 0.00	
<b>tZ9G</b>	100.87 <sup>a</sup> ± 8.62	78.09 <sup>a</sup> ± 7.62	78.52 <sup>a</sup> ± 2.62	111.10 <sup>b</sup> ± 3.11	25.93 <sup>a</sup> ± 4.17	66.69 <sup>b</sup> ± 10.29	45.83 <sup>ab</sup> ± 4.91	28.14 <sup>a</sup> ± 1.52	67.84 <sup>b</sup> ± 2.97	39.50 <sup>a</sup> ± 4.43	
<b>cZ9G</b>	4.47 <sup>a</sup> ± 0.47	4.08 <sup>a</sup> ± 0.39	4.12 <sup>a</sup> ± 0.20	5.86 <sup>a</sup> ± 0.53	2.16 <sup>a</sup> ± 0.21	4.18 <sup>b</sup> ± 0.36	3.16 <sup>ab</sup> ± 0.17	3.14 <sup>a</sup> ± 0.27	4.67 <sup>b</sup> ± 0.16	2.87 <sup>a</sup> ± 0.06	
<b>iP9G</b>	5.59 <sup>a</sup> ± 0.12	5.61 <sup>a</sup> ± 0.02	3.51 <sup>a</sup> ± 0.53	15.71 <sup>a</sup> ± 1.70	40.53 <sup>b</sup> ± 2.69	24.75 <sup>a</sup> ± 0.71	22.43 <sup>a</sup> ± 0.50	116.33 <sup>b</sup> ± 14.98	47.38 <sup>a</sup> ± 2.36	48.88 <sup>a</sup> ± 4.25	
<b>DHZ9G</b>	0.09 <sup>a</sup> ± 0.02	0.20 <sup>a</sup> ± 0.04	0.21 <sup>a</sup> ± 0.04	0.14 <sup>a</sup> ± 0.02	0.15 <sup>a</sup> ± 0.03	0.21 <sup>a</sup> ± 0.03	0.11 <sup>a</sup> ± 0.01	0.35 <sup>b</sup> ± 0.01	0.27 <sup>ab</sup> ± 0.04	0.18 <sup>a</sup> ± 0.01	
<b>N-glucosides</b>	111.05 <sup>a</sup> ± 9.23	88.00 <sup>a</sup> ± 8.08	86.39 <sup>a</sup> ± 3.39	132.84 <sup>b</sup> ± 5.36	68.83 <sup>a</sup> ± 7.10	95.87 <sup>a</sup> ± 11.40	71.54 <sup>a</sup> ± 5.60	148.02 <sup>a</sup> ± 16.78	120.17 <sup>a</sup> ± 5.54	91.45 <sup>a</sup> ± 8.76	
<b>tZOG</b>	2.09 <sup>a</sup> ± 0.13	1.12 <sup>a</sup> ± 0.05	1.72 <sup>b</sup> ± 0.08	1.14 <sup>a</sup> ± 0.14	0.50 <sup>a</sup> ± 0.15	1.09 <sup>a</sup> ± 0.11	1.10 <sup>a</sup> ± 0.15	0.86 <sup>a</sup> ± 0.10	1.19 <sup>a</sup> ± 0.07	0.88 <sup>a</sup> ± 0.14	
<b>tZROG</b>	< LOD	0.43 <sup>a</sup> ± 0.05	0.63 <sup>a</sup> ± 0.08	0.40 <sup>a</sup> ± 0.08	0.67 <sup>a</sup> ± 0.10	1.51 <sup>b</sup> ± 0.13	0.61 <sup>a</sup> ± 0.11	1.46 <sup>a</sup> ± 0.12	1.40 <sup>a</sup> ± 0.26	1.04 <sup>a</sup> ± 0.20	
<b>cZOG</b>	171.15 <sup>a</sup> ± 14.28	146.58 <sup>a</sup> ± 9.15	166.12 <sup>a</sup> ± 2.00	141.69 <sup>a</sup> ± 14.75	139.80 <sup>a</sup> ± 8.52	195.59 <sup>a</sup> ± 15.27	170.73 <sup>a</sup> ± 5.00	162.67 <sup>a</sup> ± 4.43	266.25 <sup>c</sup> ± 4.92	196.28 <sup>b</sup> ± 7.33	
<b>cZROG</b>	60.46 <sup>a</sup> ± 4.93	66.17 <sup>a</sup> ± 5.34	79.33 <sup>a</sup> ± 2.11	81.19 <sup>a</sup> ± 6.10	76.40 <sup>a</sup> ± 3.78	125.37 <sup>b</sup> ± 6.39	83.44 <sup>a</sup> ± 3.09	137.21 <sup>a</sup> ± 4.65	200.00 <sup>b</sup> ± 4.25	117.42 <sup>a</sup> ± 1.50	
<b>DHZOG</b>	0.10 <sup>a</sup> ± 0.00	0.09 <sup>a</sup> ± 0.01	0.09 <sup>a</sup> ± 0.00	0.08 <sup>a</sup> ± 0.00	0.21 <sup>a</sup> ± 0.11	0.11 <sup>a</sup> ± 0.01	0.09 <sup>a</sup> ± 0.00	0.16 <sup>a</sup> ± 0.01	0.12 <sup>a</sup> ± 0.01	0.12 <sup>a</sup> ± 0.01	
<b>O-glucosides</b>	233.80 <sup>a</sup> ± 19.33	214.39 <sup>a</sup> ± 14.61	247.89 <sup>a</sup> ± 4.27	224.49 <sup>a</sup> ± 21.08	217.58 <sup>a</sup> ± 12.66	323.68 <sup>b</sup> ± 21.92	255.97 <sup>ab</sup> ± 8.35	302.36 <sup>a</sup> ± 9.32	468.95 <sup>b</sup> ± 9.50	315.75 <sup>a</sup> ± 9.17	
<b>tZ-type</b>	108.22 <sup>a</sup> ± 9.07	83.04 <sup>a</sup> ± 7.95	83.99 <sup>a</sup> ± 3.01	116.11 <sup>b</sup> ± 3.60	29.94 <sup>a</sup> ± 4.69	71.65 <sup>b</sup> ± 10.75	50.48 <sup>ab</sup> ± 5.44	33.60 <sup>a</sup> ± 1.98	72.12 <sup>b</sup> ± 3.32	43.86 <sup>a</sup> ± 5.12	
<b>cZ-type</b>	278.03 <sup>a</sup> ± 21.18	248.95 <sup>a</sup> ± 17.68	281.78 <sup>a</sup> ± 5.43	257.99 <sup>a</sup> ± 22.98	262.00 <sup>a</sup> ± 18.99	379.10 <sup>b</sup> ± 27.76	282.70 <sup>a</sup> ± 11.25	355.43 <sup>a</sup> ± 13.71	521.41 <sup>b</sup> ± 11.91	354.99 <sup>a</sup> ± 12.75	
<b>iP-type</b>	21.71 <sup>a</sup> ± 1.19	31.22 <sup>a</sup> ± 3.40	19.68 <sup>a</sup> ± 1.14	37.79 <sup>a</sup> ± 3.89	64.70 <sup>b</sup> ± 5.57	45.51 <sup>a</sup> ± 2.72	39.62 <sup>a</sup> ± 2.39	151.68 <sup>b</sup> ± 18.34	60.08 <sup>a</sup> ± 2.90	68.08 <sup>a</sup> ± 5.42	
<b>DHZ-type</b>	0.52 <sup>a</sup> ± 0.04	0.62 <sup>a</sup> ± 0.11	0.59 <sup>a</sup> ± 0.05	0.50 <sup>a</sup> ± 0.03	0.94 <sup>a</sup> ± 0.25	1.08 <sup>a</sup> ± 0.12	0.59 <sup>a</sup> ± 0.06	1.11 <sup>a</sup> ± 0.07	1.06 <sup>a</sup> ± 0.08	0.85 <sup>a</sup> ± 0.07	
<b>TOTAL CKs</b>	408.48 <sup>a</sup> ± 31.48	363.83 <sup>a</sup> ± 29.15	386.05 <sup>a</sup> ± 9.63	412.39 <sup>a</sup> ± 30.51	357.58 <sup>a</sup> ± 29.50	497.34 <sup>b</sup> ± 41.35	373.39 <sup>a</sup> ± 19.14	541.83 <sup>b</sup> ± 34.09	654.67 <sup>c</sup> ± 18.21	467.77 <sup>a</sup> ± 23.35	

**Table II.3.** Chlorophyll content (%) compared to t0 in excised wheat leaves exposed during 100 h to the green filter (G), in the absence or presence of 2.5  $\mu$ M of the indicated CKs, which were added at 52 h after the beginning of shading. A group of leaves exposed during 52 h to filter G were changed to filter B without addition of CKs (treatment GB). Data are means  $\pm$  SE (n= 10). Data with different letters differ at  $P \leq 0.05$ .

Treatment	Chlorophyll (%)
G	37.85 $\pm$ 5.60 <sup>a</sup>
GB	67.81 $\pm$ 4.08 <sup>b</sup>
G + iP	41.90 $\pm$ 4.89 <sup>a</sup>
G + tZ	61.45 $\pm$ 4.09 <sup>b</sup>
G + cZ	38.02 $\pm$ 3.81 <sup>a</sup>
G + BAP	62.55 $\pm$ 4.60 <sup>b</sup>

### II. III. II. The turnover of CKs differs among shading treatments in wheat senescing leaves

To test whether changes in the levels of active CKs were related to the alteration of their degradation, inactivation and/or reactivation rates, the effect of the shading treatments on CKX activity, as well as on the expression pattern of genes involved in the regulation of CK homeostasis were analysed. CKX activity was very low at the beginning of the assay, but increased as senescence progressed, particularly in leaves exposed to the G filter (Fig. II.7).

Among the genes belonging to the *CKX* family analysed, *TaCKX1* was found to be by far the most up-regulated. As for CKX activity, the expression of *TaCKX1* was initially very low but markedly increased after about 54 h of exposure to the shading treatments. This effect was noticeable in leaves from treatment G, where its expression was several folds higher than the remaining treatments towards the end of the experimental period (Fig. II.8a). From the remaining *TaCKX* family members, only *TaCKX3*, *TaCKX4*, *TaCKX10* and *TaCKX11* showed detectable transcript levels. Among them, only *TaCKX3* showed a consistent up-regulation under certain treatments. In fact, while no major differences across time were detected in leaves from treatment G, its expression increased about five times (treatment B) and three times (treatment N) after 54 and 92 h from the beginning of the shading treatments, respectively (Fig. II.8b). Then

the transcript content decreased in both conditions to similar levels than those found in treatment G. As opposed to *TaCKX1*, the expression of *TaCKX4* and *TaCKX10* markedly decreased in all treatments during the first 52 h, and their transcript levels remained low until the end of the experimental period (SUPPLEMENTS II, Fig. 2D, E). Finally, the mRNA levels of *TaCKX11* did not show major changes across time in any of the shading treatments (SUPPLEMENTS II, Fig. 2F).

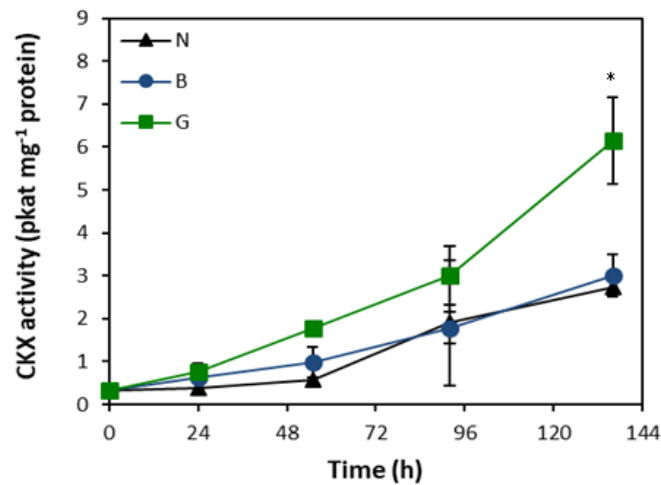


**Figure II.7.** CKX specific activity in detached wheat leaves, at different times after exposure to the neutral (N), blue (B) or green (G) filters. Data are means  $\pm$  SE (n=3). Asterisks indicate significant differences for “shading treatment” effect, at a given sampling date.

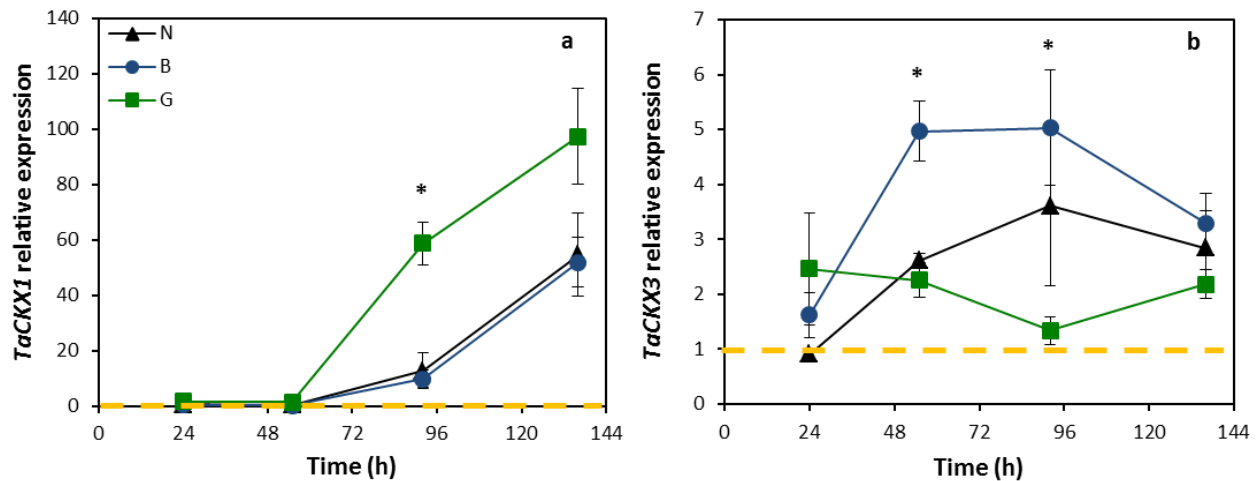


**Figure II.8.** Expression profile of *TaCKX1* (a) and *TaCKX3* (b) in detached wheat leaves, at different times after exposure to the neutral (N), blue (B) or green (G) filters. Data are means  $\pm$  SE (n=3). Asterisks indicate significant differences for “shading treatment” effect, at a given sampling date. Gene expression was relativized to 0 h= 1 (orange dashed line).

To further explore the role of CK degradation in the shade-induced senescence in wheat, we tested whether the inhibition of CKX activity with INCYDE delayed leaf senescence in leaves exposed to filter G. Based on published data (e.g. Zatloukal et al., 2008) a concentration of 10  $\mu$ M INCYDE was chosen, which was supplied from 24 or 52 h after the beginning of shading. Another treatment was also included, where leaves exposed during 52 h to filter B were changed to filter G (hereafter referred as treatment BG), with or without application of the inhibitor at the time of changing. Treatments N and B without inhibitor were run for comparison. In all cases, leaves were sampled after 100 h for the evaluation of chl content and CKX activity. As shown in Table II.4, the presence of INCYDE delayed chl degradation in filter G to a similar extent than in the B or N treatments when supplied after 24 h, which coincided with a significant reduction of CKX activity. The effect of INCYDE on both CKX activity and chl degradation rate was less evident when it was supplied after 52 h, except in the case of leaves previously exposed to filter B (Table II.4, compare treatments BG with or without the inhibitor). Altogether these results suggest that, in the experimental model used, the inhibitor is effective to the extent that it is added well in advance of the increase in CKX activity, and that the down-regulation of CK degradation is an important component of the senescence delaying effect exerted by blue light.

**Table II.4.** Chlorophyll content (%) compared to t0 and CKX activity, in excised wheat leaves exposed during 100 h to the neutral (N), blue (B) or green (G) light filters, or during 52 h to filter B and then 48 h to filter G (treatment BG). Where indicated, 10.0  $\mu$ M INCYDE was supplied to the external solution from either 24 or 52 h after the beginning of the shading treatments. Data are mean  $\pm$  SE (n=10 for chlorophyll records and n= 4 for CKX analyses). Data with different letters differ at  $P \leq 0.05$ .

Treatment	Chlorophyll (%)	CKX (pkat mg <sup>-1</sup> protein)
N	81.50 $\pm$ 5.94 <sup>a</sup>	0.597 $\pm$ 0.091 <sup>a</sup>
B	77.88 $\pm$ 3.73 <sup>a</sup>	0.612 $\pm$ 0.066 <sup>a</sup>
G	43.71 $\pm$ 5.25 <sup>c</sup>	1.743 $\pm$ 0.084 <sup>c</sup>
BG	53.34 $\pm$ 5.84 <sup>c</sup>	0.983 $\pm$ 0.098 <sup>b</sup>
G + INCYDE (24 h)	79.94 $\pm$ 6.16 <sup>a</sup>	0.970 $\pm$ 0.089 <sup>b</sup>
G + INCYDE (52 h)	52.82 $\pm$ 5.71 <sup>c</sup>	1.754 $\pm$ 0.106 <sup>c</sup>
BG + INCYDE (52 h)	64.84 $\pm$ 6.49 <sup>b</sup>	0.871 $\pm$ 0.099 <sup>b</sup>

II. III. III. Genes involved in CK inactivation and reactivation are differentially expressed depending on the light spectral quality of the shading environment

Another metabolic pathway responsible for the down-regulation of active CKs involves glucosylation mediated by the family of the zeatin *O*-glucosyltransferase (ZOG) enzyme. Given that the content of CK-*O*-glucosides increased with time in our experimental conditions and, particularly in the absence of BL, the expression profiles of *TaZOG1* and *TaZOG2* were studied. The expression of *TaZOG1* was markedly down regulated at 24 h after the initiation of the shading treatments (Fig. II.9a). Then it increased with time, though at a consistently higher rate in leaves from treatment G than B. Leaves from treatment N showed an intermediate behaviour (Fig. II.9a). As for *TaZOG1*, the expression of *TaZOG2* fell down at 24 h after leaf excision, which was followed by significant increments at 54 h (treatment G) and 92 h (treatments B and N) (Fig. II.9b). Subsequently, while the expression of the gene decreased in the two latter treatments, the up-regulation persisted in treatment G until the end of the experimental period.

To find out whether the rate of CK reactivation was also affected, the relative expression of *TaGLU* genes (encoding for  $\beta$ -glucosidase) was monitored. From all *TaGLU* family members, only *TaGLU1-3* (Song et al., 2012) was detected in our experimental conditions. In leaves from treatment B, the expression of this gene was markedly up-regulated at 54 h and it maintained around two folds higher than the initial levels until the end of the experimental period (Fig. II.9 c). On the contrary, the level of the transcript slightly decreased at 24 h in treatments G and N. Thereupon, it steadily increased with time in both cases, although at an initially slower rate as compared to filter B.

II. III. IV. Changes in the light spectral quality during shading affect some key components of the CK-signalling pathway

To investigate whether the effect of the light filters on the senescence rate involves the alteration of the CK signal reception, we analysed the expression profile of putative CK- receptors in wheat (hereafter referred as *TaHKs*). Once identified the closest orthologues to the genes *HvHK3* and *HvHK4* (SUPPLEMENTS II, Sup. material Fig. 3S) it was possible to analyse their



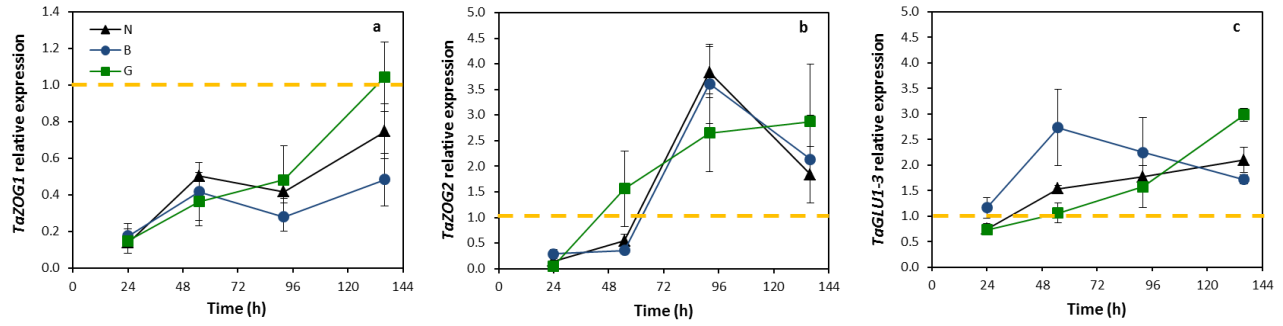


**Figure II.9.** Expression profile of *TaZOG1* (a), *TaZOG2* (b) and *TaGLU1-3* (c), in detached wheat leaves at different times after exposure to the neutral (N), blue (B) or green (G) filters. Data are means  $\pm$  SE ( $n=3$ ). Asterisks indicate the existence of significant differences for “shading treatment” effect, at a given sampling date. Gene expression was relativized to 0 h = 1 (orange dashed line).

expression patterns. *TaHK3* was slightly down-regulated at 24 h after the beginning of the shading treatments, but then its expression increased to the initial levels, though at a faster rate in leaves from treatment G than in treatments B and N (Fig. II.10 a). The levels of *TaHK4* mRNA also markedly dropped during the beginning of the experiment, but, as opposed to *TaHK3*, its initial expression was never recovered, and at 54 h it tended to be lower in treatment G than in treatments B and N (Fig. II.10b).

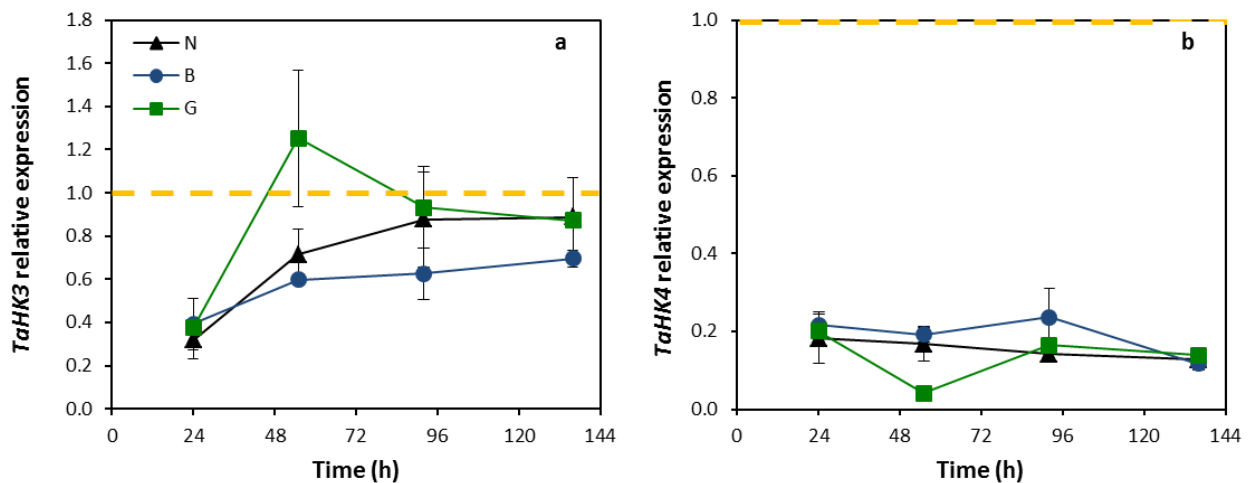


**Figure II.10.** Expression profile of the CK receptors *TaHK3* (a) and *TaHK4* (b) in detached wheat leaves at different times after exposure to the neutral (N), blue (B) or green (G) filters. Data are means  $\pm$  SE ( $n=3$ ). Asterisks indicate the existence of significant differences for “shading treatment” effect, at a given sampling date. Gene expression was relativized to 0 h = 1 (orange dashed line).

II. III. V. The expression profile of genes involved in blue-light signalling pathway is differentially affected by the shading treatments

As for other genes tested, the expression of *TaCRY2* markedly decreased during the first 24 h but increased thereafter until reaching the initial levels (SUPPLEMENTS II, Fig. 5A). Surprisingly, at 92 h the *TaCRY2* transcript level was significantly higher in treatment G than B.

Although the transcript levels of *TaCIB1* also declined at 24 h after the beginning of the shading treatments, its expression rapidly increased and showed a peak at 55 h (treatment G) and at 96 h (treatments B and N) (SUPPLEMENTS II, Fig. 5B). Despite the average *TaCIB1* levels in treatment G doubled those of treatment N at 55 h, the difference was not statistically significant.

The expression of *TaHY5* sharply increased in all treatments after 54 h. Nevertheless, the highest and significant increment was in leaves from treatment B, where it almost doubled and tripled compared to N and G, respectively (Fig. II.11).

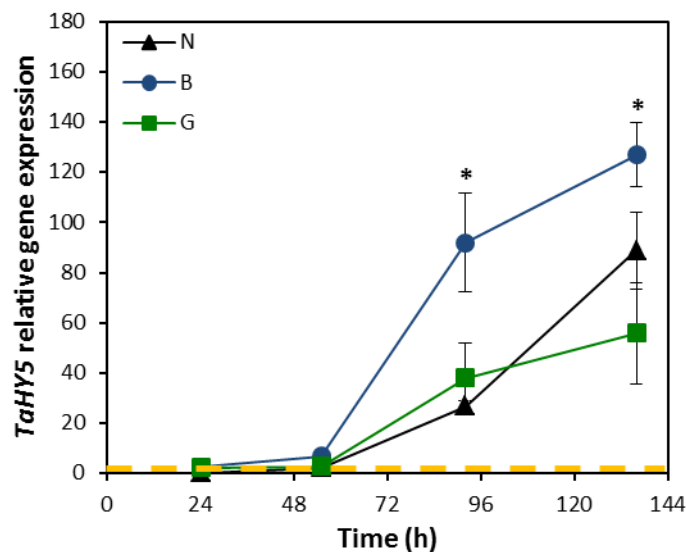


**Figure II.11.** Expression profile of *TaHY5* gene, in detached wheat leaves at different times after exposure to the neutral (N), blue (B) or green (G) filters. Data are means  $\pm$  SE ( $n=3$ ). Asterisks indicate the existence of significant differences for “shading treatment” effect, at a given sampling date. Gene expression was relativized to 0 h= 1 (orange dashed line).

## II. III. VI. Correlation analysis in wheat

The decrement in the percentage of chlorophyll observed in wheat leaves senescing under shading stress was inversely correlated with an increase in the CKX activity and with the expression of *TaCKX1*, independently of the type of light filter applied (Fig. II.12a and b), pointing out that the response of CKX activity was mainly due to *TaCKX1* in our experimental conditions and conserved for all the treatments. However, when the expression of *TaHY5* gene was evaluated, we could see that although it presented a negative correlation with the chl content, the intensity was dependent of the type of filter used (Fig. II.13a). Thus, leaves treated with B filter showed the highest *TaHY5* expression and lower chl degradation, whereas G treated leaves showed the lowest chl content and gene expression. Interestingly, the relation between the expression of *TaHY5* gene and the CKX activity (Fig. II.13b) and the CK content of the leaves (Fig. II.13c) showed totally opposite profile compared to that of the chl degradation. These results suggested that the degradation of CKs and the main CK metabolites involved in the senescence processes could be regulating the expression of *TaHY5* or vice versa.

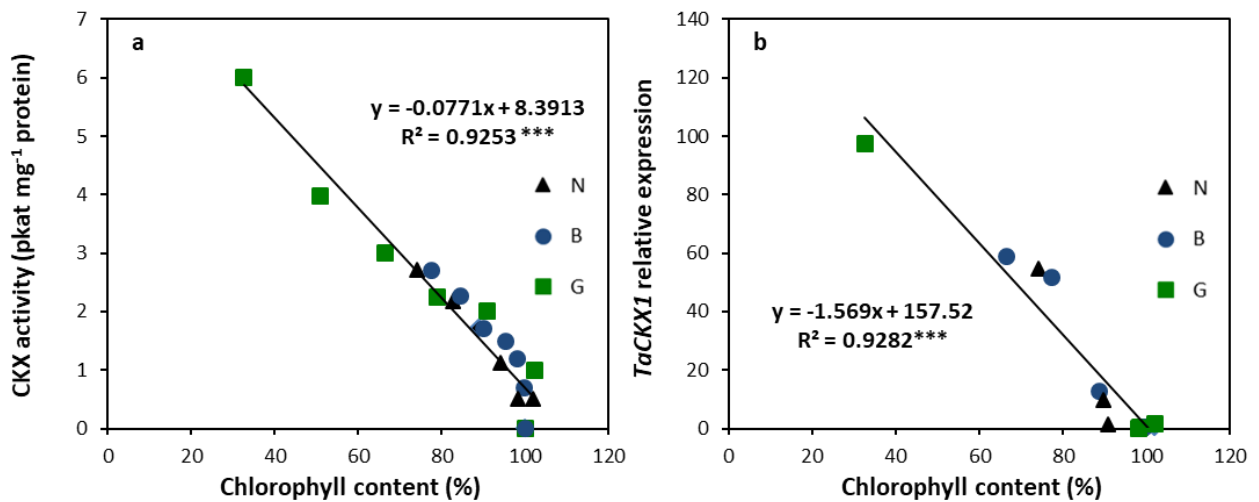


**Figure II.12.** The correlation between CKX activity (pkat mg<sup>-1</sup> protein) (a) and the expression of *TaCKX1* (b) with the chlorophyll content (%) in detached wheat leaves at different times after exposure to the neutral (N), green (G) or blue (B) filters. The regression curves and significances are shown. \*  $P \leq 0.05$ ; \*\*\* $P \leq 0.001$ .

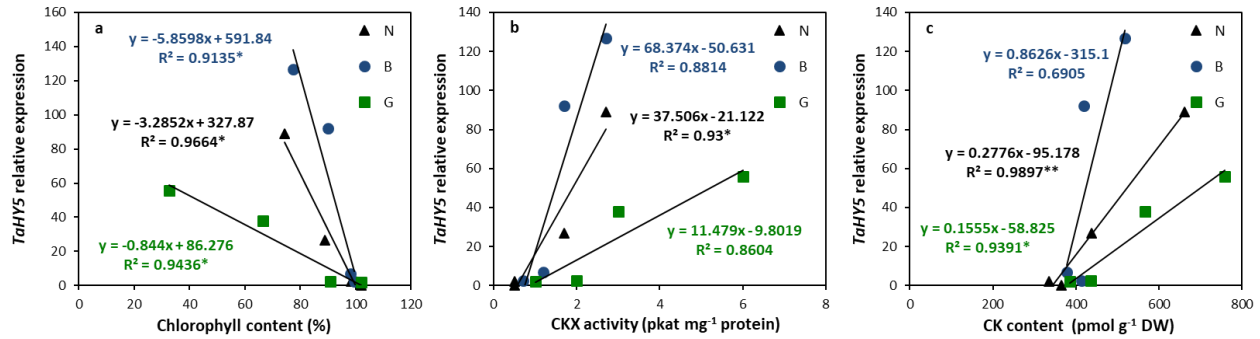


**Figure II.13.** The correlation between the expression of *TaHY5* and (a) the chlorophyll content (%), (b) the CKX activity (pkat mg<sup>-1</sup> protein) and (c) the cytokinins content (pmol g<sup>-1</sup> DW) in detached wheat leaves at different times after exposure to the neutral (N), green (G) or blue (B) filters. The regression curves and significances are shown. \*  $P \leq 0.05$ ; \*\* $P \leq 0.001$ .

## B. Experiment 2- Regulatory aspects of shade-induced senescence in barley leaves.

II. III. VII. BL suppression and changes in the R/FR ratio alter the pattern of leaf senescence in the barley cultivar Golden Promise

When the shading induced leaf senescence of barley was studied, we observed that barley senescing leaves followed similar trends in chl degradation as wheat under the N, B and G filter (Fig. II.14). However, in the case of barley there was an abrupt acceleration of the senescence rate when the R/FR ratio was also altered (i. e. treatment R).

To analyse if the different shading treatments on barley leaves caused a similar effect on CK degradation observed for wheat leaves, we measured several parameters after 120 h of the application of treatments. There was a clear effect of the filters (Fig. II.15). Only barley leaves exposed to the R filter showed significantly higher CKX activity compared to N (Fig. II.15a). Moreover, the expression profile of *HvCKX1*, the closest orthologue to *TaCKX1* (the most up-regulated gene in our experimental conditions in wheat), was also significantly upregulated in R treated leaves (Fig. II.15b). To monitor if those differences in CKX activity and *HvCKX1* expression among the R and the rest treatments correlated with differences in the levels of CKX1 protein, a Western Blot analysis was performed. The levels of detected CKX1 protein were higher in leaves

senescing under the G and R filter compared to those under the N and B, but no differences were observed among the G and R filter (Fig. II.15c and d).

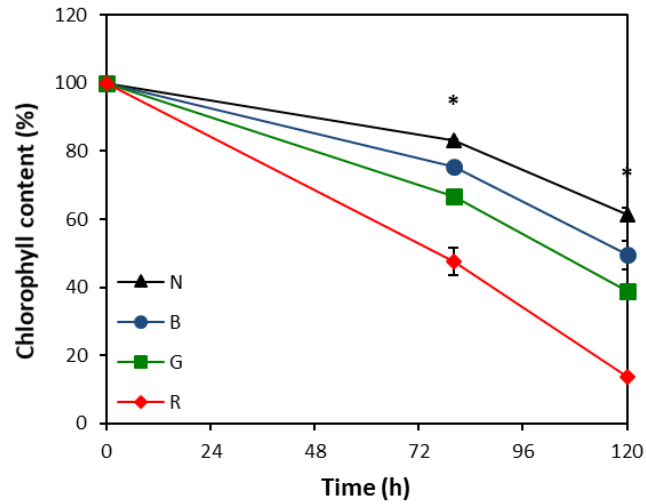


**Figure II.14.** Change in the chlorophyll content (%) in detached barley leaves at different times after exposure to the neutral (N), blue (B) or green (G) filters. Asterisks indicate significant differences for “shading treatment” effect, at a given sampling date.

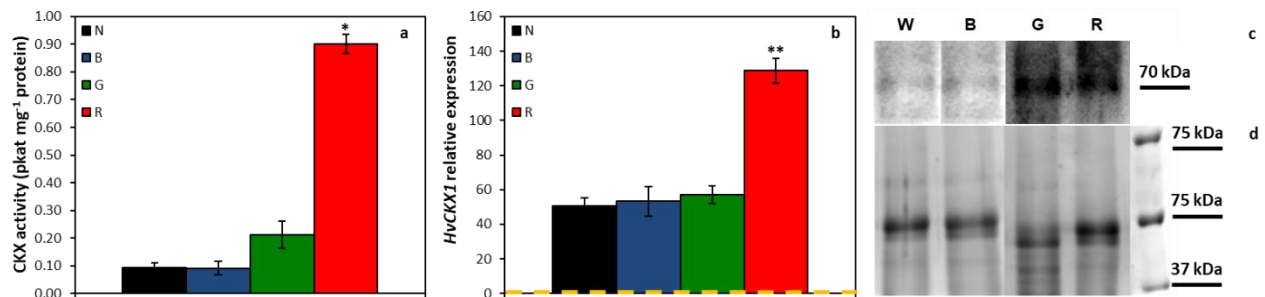


**Figure II.15.** (a) CKX specific activity, (b) expression profile of *HvCKX1* gene and (c) Western Blot analysis of CKX1 protein and (d) Coomassie staining of proteins separated by SDS-PAGE, in detached barley leaves after 120 h of exposure to the neutral (N), blue (B), green (G) or red (R) filters. In (a) and (b), data are means  $\pm$  SE ( $n=3$ ). Asterisks indicate significant differences for “shading treatment” effect. Gene expression was relativized to 1 (orange dashed line). Lines and values on the right side at (d) represent the molecular weights given by Pre-Stained Protein Ladder.

## II. III. VIII. Correlation analysis in barley

For further evaluation of the treatment effect in shading induced barley leaf senescence, we performed a correlation analysis between the CKX activity and the Chl content, as it was previously done in wheat (Fig. II.12a). In this case, we observed a clear effect of the light quality, with two separated groups, one including the treatments N and B, and another one including the treatments G and R (Fig. II.16).

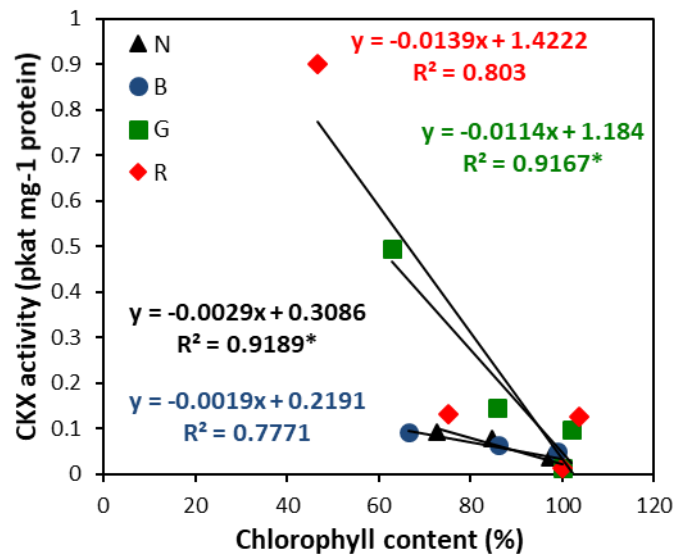


**Figure II.16.** Correlation between CKX activity (pkat mg<sup>-1</sup> protein) and the chlorophyll content (%) in detached barley leaves at different times after exposure to the neutral (N), blue (B), green (G) or red (R) filters. The regression curves and significances are shown. \* $P \leq 0.05$ .

## II. III. IX. Leaves from lines with altered CK homeostasis present alterations in the shade-induced senescence pattern compared to wt

Finally, to corroborate the role of CKX regulating shading induced barley leaf senescence and the influence of the light quality, we treated leaves from wt and transgenic lines with altered CK homeostasis with the same filters. For this purpose, we used two independent transgenic lines with silenced *HvCKX9* gene, a gene which is highly expressed in the developmental stage of leaves

used for our experimental set up (Mrízořa et al., 2013). There were significant differences in the rate of chl degradation in transgenic plants compared to wt (Fig. II.17). Concretely, the line 1.8 presented significantly slower senescence rate under the G (Fig. II.17c) and R treatments (Fig. II.17d). These results pointed to the CKX activity, and hence the Chl degradation is affected by the light quality at least in barley variety Golden Promise.

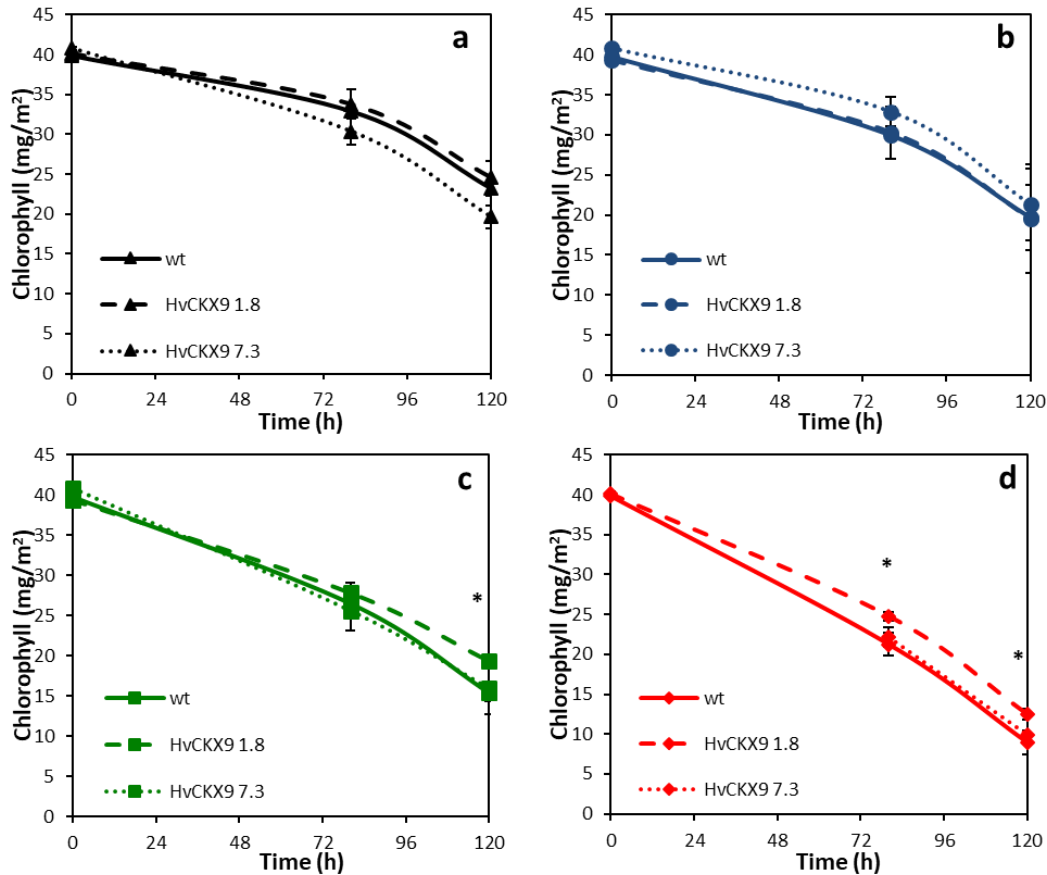


**Figure II.17.** Chlorophyll content in detached wild type and transgenic barley leaves at different times after exposure to the (a) neutral (N), (b) blue (B), (c) green (G) or (d) red (R) filters. Asterisks indicate the existence of significant differences for “shading treatment” effect, at a given sampling date. Data are means  $\pm$  SD (n = 8).

## II. IV. Discussion

Light quality regulates shade-induced leaf senescence in barley and wheat. BL is an important ambient cue involved in the regulatory pathway of shade-induced senescence in the

spring wheat cultivar INTA Oasis (Fig. II.4). Similar results have been obtained in other cultivars of this crop (Causin et al., 2009, 2006). Contrarily, in the spring barley cv. Golden Promise the shading-induced leaf senescence is rather mediated by R/RF ratio than by BL (Fig. II.14). Interestingly, the involvement of the CKs regulating leaf senescence was corroborated. For instance, the concentration of free CKs (but particularly *tZ* and *cZ*) in excised leaves of wheat decreases soon after exposure to the shading treatments. Remarkably, when BL transmission is not suppressed, a significantly higher endogenous level of *cZ* and *tZ* is maintained, which points out a possible role for these active forms in the control of senescence symptoms. However, no significant differences in the endogenous levels of *iP* existed between leaves from treatments B and G, despite having marked differences in their senescence rates. Besides, the exogenous addition of *iP* was not able to emulate the senescence delaying effect of filter B in leaves previously exposed to filter G, suggesting that this CK form are not be directly involved in the regulation of this process. On the contrary, the exogenous *tZ* supply was almost as effective as BL in down-regulating the senescence rate in leaves exposed to filter G (Table II.3). This result pointed at the maintenance of higher endogenous *tZ* levels as a contributor to the senescence-delaying effect by BL. With regards to *cZ*, a recent review performed by (Schäfer et al., 2015) summarized a series of studies that investigate its role in regulating plant development and defense responses to pathogen and herbivore attack, and highlighted their potential role as 'novel' stress-response markers. Moreover, data reported by (Kudo et al., 2012) suggest that *cZ* has physiological effects on growth and development of rice plants, and may act as an important regulator of the senescence rate in this species. Hluska et al. (2016) reported that when *cZ* was exogenously supplied to intact 7-d-old maize seedlings, a great proportion was immobilized as *O*-glucoside, even though a significant increase of *tZ* was also induced. These changes, however, were mostly evident in root tissue, while in the shoot the trends were less profound. Hence, despite *cZ* addition did not alter the senescence rate in our experimental model, further investigation is needed to assess its potential contribution to the control of this developmental process.

Different processes seem to have contributed to decrease the content of free CKs in shading-induced senescence leaves. One of the main factors could be the up-regulation of CK



degradation, although its relevance would be greater once senescence is triggered rather than at the beginning of it. As corroboration, the highest expression of both *TaCKK1* and *HvCKK1* was observed after more than 120 h of shading-induced senescence (Fig. II.7, II.8a and II.15). The marked up-regulation of the *CKX1* gene in senescing leaves of barley and wheat has been documented elsewhere (Conrad et al., 2007; Song et al., 2012) and its behaviour resembles that of typical senescence associated genes. It should be noted, however, that the acceleration of the senescence rate did not necessarily correlate with an up-regulation of all *CKX* members. In fact, while the expression of *TaCKX4* and *TaCKX11* did not show major differences among shading conditions, a higher increase in the transcript levels of *TaCKX3* was observed in those leaves of wheat exposed to filter B as compared to the remaining treatments (e.g. Fig. II.8b). Moreover, *TaCKX10* mRNA levels decreased as the time exposure to shading increased. In maize leaves it has been also reported that *ZmCKX10* expression is high in young leaves but markedly decreases in senescent tissues (Smehilová et al., 2009), which is consistent with our findings. In barley, the reduction of *HvCKX9* expression in the transgenic lines also modified the senescence profile, delaying senescence especially in G and R treated leaves (Fig. II.17). It is possible that the difference in the pattern of expression among *CKX* genes is associated to alterations in the levels of the preferred substrates of the respective enzymes, and/or to their particular sub-cellular localization (Smehilová et al., 2009). Whatever the case, their role in the maintenance of CK homeostasis is far from being understood, since the regulation of gene expression of different *CKXs* is not only tissue- and developmentally- dependent, but also inter- and intra- species and the stressful conditions considered (Song et al., 2012; Vyroubalová et al., 2009).

The formation of CK-*O*-glucosides, whose concentration increased with time, had probably an important role in the inactivation of free CKs at least in wheat cv. INTA Oasis. From the two *TaZOG* genes analysed, only *TaZOG2* showed a consistent up-regulation compared to the initial (t0) levels. Interestingly, the increment of *TaZOG2* transcript amount was first evident in leaves exposed to treatment G (Fig. II.9b). This is in agreement with previous reports indicating that CK inactivation through *O*-glucosylation plays an important role in the development of senescence symptoms in different plant species (Koeslin-Findeklee et al., 2015; Rubia et al., 2014; Šmehilová et al., 2016; Taverner et al., 1999). However, to our knowledge, this is the first report

showing that the expression pattern of *ZOG* genes may differ depending on the spectral quality of the light environment in wheat leaves senescing under shading stress. *O*-glucosides are regarded as reversible storage forms of CKs given that they can be reversibly converted to active forms by the action of  $\beta$ -glucosidase (Sakakibara, 2006). Interestingly, the expression of *TaGLU1-3* was up-regulated at a faster rate in leaves shaded under the B than the G filter, which may have also contributed to maintain higher levels of free CKs (Fig. II.9c).

Surprisingly, the concentration of CK-ribotides as well as CK-ribosides increased as senescence progressed, particularly in wheat leaves exposed to the G filter. Again, *cZ* derivatives were the most abundant among these glycosylated forms (see Table II.2). While CK-ribotides are inactive, *cZR* was shown to have a relatively high biological activity when compared to its free base (Gajdosová et al., 2011). Nevertheless, the observed increment was not enough to compensate the negative effect of BL suppression on the senescence rate. Since we used excised leaves, the increment of these CK-forms cannot be attributed to an enhanced translocation from other organs. Similarly, given that the expression of *IPT* genes in wheat leaves decreases as senescence progresses (e.g. Song et al., 2012), it is unlikely that their increment was due to the up-regulation of CK-synthesis pathways. Rather, it is possible that, as for *O*-glucosylation, a stimulation of the conversion of free bases to their respective ribosides/ribotides was the main process responsible of their accumulation. Alternatively, *tRNA* degradation (which is expected to increase in senescent leaves) might also have contributed to enhance the level of *cZ* derivatives (Sakakibara, 2006; Vyroubalová et al., 2009). Whichever the mechanism, it is clear that the accumulation of conjugated forms of CKs favours the senescence progresses in excised wheat leaves exposed to shading stress. Finally, it should be mentioned that changes in the translocation rate of different CKs might contribute to the alteration of CK homeostasis in attached leaves. Even though this process could not be explored in our experimental system, there is evidence that CK transport might also be under the control of light cues (e.g. Roman et al., 2016).

Given that the action of growth regulators does not only depend on their endogenous concentration but also on the presence and activity of proper receptors, we analysed the expression profile of some components of the CK-reception system in our experimental

conditions. The expression level of *TaHK3* decreased during the first 24 h after the beginning of the shading treatments, in coincidence with the marked decrement of some free CKs, but gradually recovered to the initial levels thereafter. This increment, however, occurred at an initially faster rate in leaves exposed to the G filter, even though their senescence was accelerated. Kim et al. (2006) reported that a gain-of-function mutation in the *Arabidopsis* CK-receptor AHK3 increased the sensitivity to endogenous CKs and delayed leaf senescence, while the opposite effect occurred when the expression of this receptor was suppressed. Interestingly, the AHK3 receptor has a strong preference of *tZ*-type CKs as compared to *iP* type CKs (Lomin et al., 2012). Hence, despite a faster up-regulation of *TaHK3* might have helped to enhance the perception of CK signals in treatment G, either its contribution was not enough to prevent the development of senescent symptoms, or other CK receptor/s and/or signalling components are involved in the regulation of senescence by light spectral quality in wheat. In this sense, it is interesting to note the marked down-regulation observed for *TaHK4*, an effect that was enhanced in the absence of BL at 52 h after the beginning of the shading treatments.

There is evidence that in soybean plants the activation of the BL receptor CRY2a down-regulates the transcription activity of the senescence-promoting transcription factor CIB1, through direct protein-protein interaction (Meng et al., 2013). Apparently, the decrement in free CIB1 content did not involve changes in its mRNA levels. As for soybean plants, we did not find major differences in the expression pattern of the wheat *TaCIB1* homologue among shading treatments, which supports the evidence that its regulation by light cues would not occur at the transcriptional level. Additionally, green light has been shown to suppress certain BL-mediated responses by reducing the semi-reduced state of the FAD chromophore (i.e. FADH\*) of active CRY (Liu et al., 2011). Given the available information and considering the lack of correlation observed between senescence rate and the expression patterns of *TaCIB1* and *TaCRY2*, further research involving the analysis of protein-protein interactions is needed to better assess their regulatory role in our experimental model.

Contrary to *TaCIB1*, in wheat leaves the expression profile of *TaHY5* was significantly affected by the light spectral quality of the shading treatment. While the involvement of this bZIP protein in photomorphogenic responses has been extensively studied, the information regarding

its role in the regulation of leaf senescence is scarce, and in some aspects contradictory. In fact, in *A. thaliana* leaves exposed to darkness HY5 is degraded via the 26S proteasome pathway, an effect that has been associated to the induction of senescence symptoms (Keech et al., 2010). On the contrary, the accumulation of HY5 due to its interaction with active phytochrome B was shown to positively regulate programmed cell death in *Arabidopsis* leaves exposed to excess red light (Chai et al., 2015). Another study showed that HY5 and CKs are required for the expression of key chlorophyll biosynthesis genes in roots (Kobayashi et al., 2012). In rice, *HY5* also functions as an activator of genes for chlorophyll and carotenoid accumulation upon BL light signalling (Mohanty et al., 2016). Our data show that the expression of *TaHY5* increased as senescence progressed in all shading conditions, but the rate of accumulation of the transcript was higher under BL and, hence, inversely correlated with the development of senescence symptoms. Thus, HY5 could have dual role promoting the pigment synthesis in tissues under control conditions and delaying their degradation under shading-induced senescence. Another putative explanation is that either the activity or the stability of the protein is negatively regulated by other BL-altered components. Indeed, a complex regulation of HY5 functioning and /or turnover might be expected when considering that it is a point of convergence between multiple hormonal and light signalling pathways (Gangappa and Botto, 2016).

24 H	48 H	72 H	120 H
↑ <i>N</i> -glucosides	-	-	↓ <i>iP</i> , ribosides
	↑ <i>CKX3</i> , ↓ <i>CKX4</i>	↑ <i>CKX3</i>	-
	↑ <i>GLU</i>	↑ <i>Hy5</i>	↑ <i>Hy5</i>

**Figure II.18.** Summary of the parameters altered in detached wheat leaves exposed to the blue (B) filter at different time points of the experiments.

24 H	48 H	72 H	120 H
-	-	↓ Chl	↓↓ Chl
	-	↓ <i>tZ</i> , <i>cZ</i>	↓ <i>tZ</i> , <i>iP</i> , ribosides
	↑ <i>O</i> -glucosides	↑ <i>O</i> -glucosides	↑↑ <i>O</i> -glucosides
	↓ <i>CKX4</i>	↑ <i>CKX1</i>	↑↑ <i>CKX1</i>
	↑ CKX activity		↑ CKX activity
	↑ <i>TaHK3</i> , ↓ <i>TaHK4</i>	↑ <i>CRY2</i>	<i>ZOG1</i>

**Figure II.19.** Summary of the parameters altered in detached wheat leaves exposed to the green (G) filter at different time points of the experiments.

## II. V. Conclusion

The present results demonstrate that changes in light spectral quality alters CK homeostasis as well as the expression of several genes involved in their metabolism, in wheat and barley exposed to shading stress. In wheat, the depletion of *tZ* rather than *cZ* or *iP* seems to have a predominant role in senescence acceleration. The analysis of gene expression profiles suggests that BL in wheat and also R/FR ration in barley would contribute to delay the development of senescence symptoms through the retardation of both CK-degradation and CK-inactivation, as well as a faster up-regulation of some  $\beta$ -glucosidase isoforms that may restore active CKs. However, the shade-induced CK-degradation and hence senescence through CKX activity can be a conservative plant response independent or dependent of the light quality according plant species. Besides, the marked changes observed in the mRNA levels of *TaHY5* seem a promising cue to deepen the study of its role in the regulation of leaf senescence in other wheat varieties and plant species. Further studies are needed to understand how the light quality and CKs interplay the shading-induced leaf senescence and to define whether this process is inter- or intra species.

# **CHAPTER III: A novel image-based screening method to study water deficit response and recovery of barley populations using canopy dynamics phenotyping**

Marchetti, C. F.\*, Ugena L.\*, Humplík J. F., Polák M., Podlešáková K., Fürst T., De Diego N. and Spíchal, L. (2019). A novel image-based screening method to study water deficit response and recovery of barley populations using canopy dynamics phenotyping. *Frontiers in Plant Science*, submitted in December 2018 and UNDER MAYOR REVISIONS.

\*These authors contributed equally to this work.

### III. I. Introduction

Abiotic stresses, in particular water deficit, constrain the global production of crops, affecting both the vegetative and reproductive phases of development (Wang et al., 2003). Not all water stress scenarios are equivalent, however, because the severity, frequency, duration and timing of the stress can vary, and with them the impact on the plant (Chen et al., 2014). A robust and reliable analysis of phenotypic traits is therefore essential for each context, to shed light on the basic tolerance mechanisms and develop strategies for breeding crops that are more tolerant to adverse environments.

Barley is the fourth most cultivated crop world-wide (<http://www.fao.org/faostat/en/#data/QC>). As a diploid organism, it is considered a suitable model for studying the more complex polyploid species belonging to the Triticeae tribe. Under water stress conditions, barley displays reduced growth and adaptations of other physiological parameters, such as chlorophyll content, net photosynthetic rate and water content (Ahmed et al., 2013; Saade et al., 2018). However, the mechanisms that confer water stress tolerance and recovery capacity in this crop species are still not fully understood.

Plant phenotyping platforms provide the potential for automated, fast scoring of several traits related to stress tolerance over a time-course, using non-invasive sensors (Awlia et al., 2016; Chen et al., 2014; De Diego et al., 2017; Granier et al., 2006; Humplík et al., 2015b). Until now, published indoor protocols have been based on the response of individual plants often restricted by pot growth, whereas in the field plant growth results in a canopy (Araus and Cairns, 2014). Nevertheless, in the field the plant growth is seasonally dependent, often reducing the number of possible experiments to one per year, whereas indoor phenotyping allows continuous repetition of experiments. Furthermore, screening for specific tolerance traits under controlled conditions is often necessary to manage the complexity of interactions between genotype and environment on the phenotype (Ghanem et al., 2015). The specific metric being monitored therefore needs to be defined and its relationship with the physiological trait of interest has to be resolved and validated. The plant phenotype is also determined by complex genome × environment × management interactions: the sum of the complex interactions between

metabolic pathways and intracellular regulatory networks are reflected in internal, physiological and biochemical phenotypes (Großkinsky et al., 2015). Thus, a characterization limited only to a detailed description of a set of image-based traits remains incomplete for understanding plant responses to water stress. An integration of data from phenomics with other ‘-omics’ (e.g. metabolomics and genomics) may help dissect the plant response and clarify the key traits involved in the mechanisms of stress tolerance and acclimation. As example, the combination of phenomics with metabolomics can help to identify metabolites that are mainly accumulated under water stress conditions. Particularly, some metabolites such as polyamines and some amino acids involved in glutamate metabolism like  $\gamma$ -amino butyric acid (GABA) and L-proline (Pro) play essential role regulating stress tolerance like compatible solutes contributing to osmotic potential, mediators of antioxidant responses or signal molecules (De Diego et al., 2013; Podlešáková et al., 2019). Concretely, GABA, Pro and L-arginine (Arg) have been described as metabolites involved in plant recovery and hardening under drought stress conditions (De Diego et al., 2015).

The objective of this part of the thesis was to develop a non-destructive method for studying the water stress tolerance and recovery on a population of barley based on image analysis of canopy height using a simple red, green, blue (RGB) camera. To introduce the method we used barley cultivar Golden Promise as a good representative of the varieties with agronomical interest due to its semi-dwarf with low lodging problems (Thomas et al., 1984) and stress tolerance (Forster et al., 2000). Moreover, we focused on profiling the primary and secondary metabolites, amino acids and polyamines, which play a dual role as tolerance indicators and signal molecules (Muscolo et al., 2015; Urano et al., 2010) to study further the involvement of these molecules regulating plant water stress response and recovery capacity. We show that, in combination with other -omic approaches such as metabolomics, followed by multivariate statistical methods, the experimental procedures for studying stress response can be made more efficient. The result is a simple and highly reproducible method for studying the stress response and recovery in barley populations, which is applicable for breeding programmes to select and characterize potentially successful varieties.



## III. II. Materials and Methods

### III. II. I. Plant material and growth conditions

Barley (*Hordeum vulgare*) cultivar Golden Promise was used for the study. Seeds were surface-sterilized by soaking in 70% ethanol for 30 s, and then washed three times with sterilized water, and immediately after that with a 4% solution of sodium hypochlorite for 4 min followed by an additional four washes with sterilized water. The sterile seeds were placed on wet tissue paper inside square plastic plates (120 mm × 120 mm) and maintained for 2 days at 4 °C in the dark for imbibition, as schematized in Fig. III.1. The plates were then transferred into a growth-chamber, under controlled conditions of a 22 °C, 16 : 8 h, light : dark cycle with a photosynthetically active radiation (PAR) light intensity of 120  $\mu\text{mol photons m}^{-2} \text{s}^{-1}$  for 2 days, to induce germination (Fig. III.1).

### III. II. II. Non-invasive plant phenotyping

#### III. II. II. I. Phenotyping platform, experimental setup and assay conditions

To develop the barley screening method, firstly we performed and analysed reproducibility of two independent assays using well-watered conditions (1st experiment- December 2017 and 2nd experiment- June- 2018; Table III.1). After that, we performed a final experiment to evaluate the growth of barley seedling population under water deficit (3rd experiment- Table III.1). In all experiments, the barley seedlings were planted in plastic containers (32 cm × 19.5 cm × 10 cm, with a volume of 4 l) filled with 2.8 kg of a 2:1 mixture of substrate (Substrate 2; Klasmann-Deilmann GmbH, Geeste, Germany) and sand. A total of 50 seedlings per container was sown, distributed in five rows containing 10 plants each, with a final density of 1000 plants  $\text{m}^{-2}$  (Fig. III.1). Two containers with 50 seedlings each were then placed together in a standard PlantScreen™ measuring tray (Photon Systems Instruments, Brno, Czech Republic).

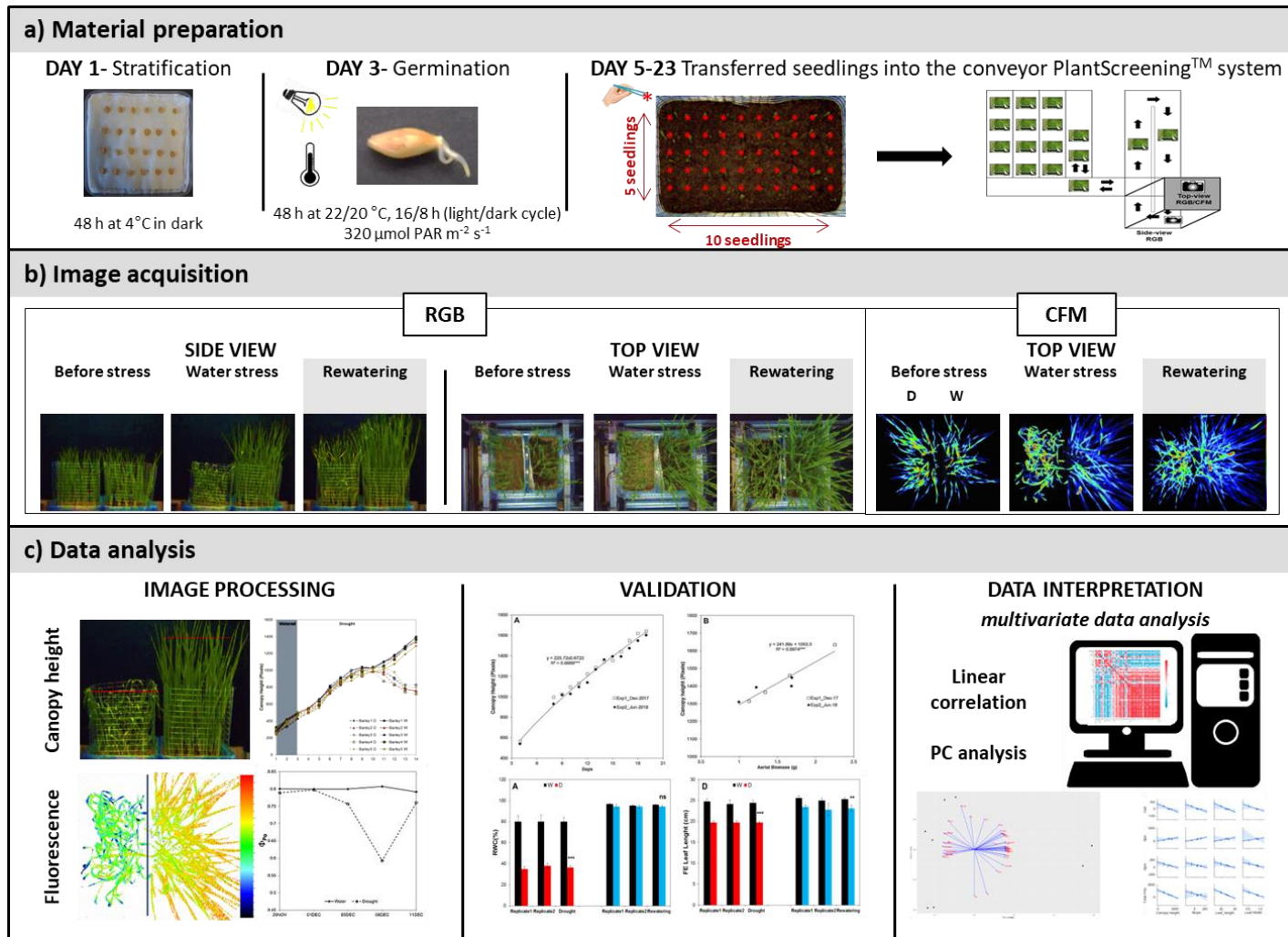


**Figure III.1.** Scheme of the protocol used for non-invasive phenotyping of barley seedlings growing under water stress conditions. (a) Barley seeds were germinated on filter paper and 50 seedlings of similar radicle size were transplanted into soil in standardized PlantScreen™ measuring trays. (b) The trays were transferred to an XYZ PlantScreen™ chamber with a conveyor system for automatic image acquisition. (c) The canopy height was analysed using an in-house software routine implemented in MatLab R2015, and the data were evaluated by multivariate statistical analyses using R version 3.5.1.

**Table III.1.** Scheme of the three performed experiments.

EXPERIMENT	DATE	CONDITIONS
1st	December 2017	control
2nd	June 2018	water stress
3rd	July 2018	

For the image analysis, the tray with two containers housing 50 plants each was transferred onto an OloPhen platform ([http://www.plant-phenotyping.org/db\\_infrastructure#/tool/57](http://www.plant-phenotyping.org/db_infrastructure#/tool/57)). In the water deficit experiment a metal mesh was installed for better separation of the leaves from the variants [well-watered (W) and water stress-drought (D)] in each container (Fig. III.1). The trays were located into the PlantScreen™ conveyor system installed in a growth chamber with a controlled environment and LED lighting (Photon Systems Instruments). The growth conditions were set to simulate a long day, with a regime of 22 °C : 20 °C in a 16 : 8 h light : dark cycle, a PAR irradiance of 320  $\mu\text{mol photons m}^{-2} \text{s}^{-1}$  and a relative humidity of 40%.

### III. II. II. II. Imaging acquisition

The PlantScreen™ system is equipped with a top-view and side-view RGB camera and top-view FluorCam (Fig. III.1). The RGB and FluorCam images were stored in a database server. The images were then evaluated. The side-view RGB images were analysed using an in-house software routine implemented in MatLab R2015 that was developed and validated by the authors of this study. The application can be used without charge by obtaining a licence from Palacký University, by emailing Tomáš Füst ([tomas.furst@upol.cz](mailto:tomas.furst@upol.cz)) and agreeing not to use the application for commercial purposes.

To provide a comparative view, we analysed chl fluorescence-related parameters throughout the experiments using a top-view FluorCam. A standard protocol was used for the measurement of Chl fluorescence quenching using the Chl fluorescence imaging (CFIM) part of the PlantScreen™ platform using the same protocol described by Humplík et al. (2015). Image

data were processed and chl fluorescence parameters were calculated using software FluorCam 7 (Photon Systems Instruments). Thus, it was estimated: (a) the maximum quantum yield of photosystem II (PSII) photochemistry for a dark-adapted state,  $\Phi_{P_0}$ ; (b) the actual quantum yield of PSII photochemistry for a light-adapted state,  $\Phi_P$ ; (c) the quantum yield of constitutive non-light induced (basal or dark) dissipation processes consisting of chl (Chl) fluorescence emission and heat dissipation,  $\Phi_{f,D}$ , quantum yield of regulatory light-induced non-photochemical quenching,  $\Phi_{NPQ}$ . It is worth mentioning that  $\Phi_P + \Phi_{f,D} + \Phi_{NPQ} = 1$ , and  $\Phi_P = qP \Phi_{PSII}$ , where  $qP = ((F_M' - F(t)) / (F_M' - F_0'))$  is the coefficient of photochemical quenching, which estimates a fraction of the so-called open PSII reaction centres, and that  $\Phi_{PSII} = ((F_M' - F_0') / F_M')$  is the maximal quantum yield of the PSII photochemistry for a light-adapted state.

### III. II. II. III. Watering regime

In each container the substrate water content (%) was calculated as follow: the substrate was weighted and then watered to full capacity and the top was covered with plastic bags for reducing evaporation losses. When the water stopped draining from the container (cca. 10 h later), the weight was again measured. The substrate was then dried for 48 h at 105 °C until complete dryness and the weight was determined. The three weights of the substrate water moisture status were used for calculating the gravimetric water content ( $\theta_g$ ) and substrate maximum water holding capacity. All containers were watered with tap water (average conductivity c. 56 mS m<sup>-1</sup>) at 100% of field capacity after sowing. Then, the control plants were irrigated every second day to maintain 80% of field capacity until the end of the experiment. In the 3rd experiment, the irrigation was stopped in the water stress variant when the plants presented the first fully expanded leaf. When the substrate water content decreased to 65% (Day 15), the water limited variants were rewatered at full water capacity (100%).

### III. II. III. The assay workflow

To study water deficit and recovery in barley populations we established the protocol schematized in Fig. III.1. The protocol takes a total of 3 weeks, including seed germination (2

days), seedling growth under water stress conditions (16 days) and subsequent rewatering (4 days). After imbibition, a total of 50 germinated seeds was transferred to plastic containers (Fig. III.1). The selection of germinated seeds at a similar developmental stage (radicle length) is an important to reduce within-population variability. Two randomly selected containers were then placed in standardized trays and transported within the PlantScreen™ on conveyor belts. Automated RGB imaging from two optical projections (top and side view) was performed every day for the next 19 days. The daily RGB measurement of 16 trays (1600 seedlings) took 20 min in total. When the top-view fluorescence intensity measurement was included (every third day), the total process time increased to 4 h. The PlantScreen™ Analyzer software processed the raw data automatically. Raw data were automatically stored in PlantScreen™ database from where they were subsequently exported for further image processing and analysis.

Side view imaging allowed separation of the plants from the background and the differentiation between the left and right containers using a pre-defined vertical line in the image based on the metal mesh installed between them (Fig. III.1). To define and evaluate the canopy height in each container (or variant) automatically, the green mask of the plant was found using a thresholding algorithm. A line was then placed above the upper most pixel of the mask. The line was gradually lowered (each step by one pixel) and the following criterion evaluated for each possible position of the line:

$$\text{crit} = A / B$$

where A is the number of pixels on a line that also belong to the mask and B is the length of the line (in pixels). Thus, the criterion represents the fraction of the line that intersects the mask. Once this fraction exceeded a user-defined threshold, the process was stopped and the position of the line recorded. This position was then used as a proxy for canopy height.

### III. II. IV. Manual parameters

#### III. II. IV. I. Biometric parameters

The aerial biomass of the seedlings was determined from the fresh weight (FW, g) by cutting the shoots 1 cm above ground level from eight or five plants per replicate and variant at the end of the water stress period and after 4 days of rewatering, respectively. The developmental stage of each plant at the same time points, according to the BBCH scale (Earth Observation and Research Branch Team, 2011), and the size (length and width) of the youngest and fully expanded leaf were also evaluated.

#### III. II. IV. II. Plant water status

The relative water content (RWC, %) was measured in five individual plants per variant and replicate. The measurement was performed using 2 cm from the middle part of the last youngest mature leaf collected at the end of the water stress period and after rewatering. RWC was calculated using the following equation:  $RWC (\%) = (FW - DW) / (TW - DW) \times 100$ , where FW is the fresh weight at harvesting time, TW is the total weight as total turgor estimated after 24 h of imbibition, and DW is the dry weight after 48 h at 85 °C.

#### III. II. IV. III. Chlorophyll content

The index of relative chl content or 'greenness' of leaves was measured in vivo using a portable SPAD-502 Plus chl meter (Konica Minolta Inc.). Six measurements were taken in the last youngest mature leaf in five individual plants per replicate and variant at the end of the water stress period and after rewatering.

#### III. II. IV. IV Antioxidant enzymes

For the enzymatic analysis, three groups of five plants per replicate and variant after water stress and rewatering were collected and immediately frozen in liquid nitrogen. Before

extraction, the plants were grounded by mortar and pestle using liquid nitrogen. The resulting pool from each replicate and variant was divided into three analytical replicates for quantification of antioxidant activity. 100 mg of grounded material was homogenized at a ratio of 1:5 with extraction buffer [50 mM Tris (pH 7.6), containing 2 mM magnesium sulphate, 1 mM ethylenediaminetetraacetic acid (EDTA), 1 mM ascorbic acid, 1 mM PMSF and 0.5% (v/v) Triton X-100] in the presence of PVPP. After centrifugation at 19,000 *g* for 20 min at 4 °C, the supernatant was collected and centrifuged under the same conditions for an additional 10 min. The content of proteins in the crude extract was evaluated using the method described by Bradford (1976). Catalase (CAT) activity ( $\mu\text{mol min}^{-1} \text{mg}^{-1}$  total protein) was measured according to Aebi (1984). Briefly, the decrease in absorbance at 240 nm of a reaction mixture consisting of 25  $\mu\text{l}$  enzymatic extract in a final volume of 1 ml reaction mixture containing 50 mM potassium phosphate (pH 7.0) and 25 mM  $\text{H}_2\text{O}_2$  was measured. The molar extinction coefficient of  $38 \text{ M}^{-1} \text{cm}^{-1}$  was used to calculate CAT activity.

Ascorbate peroxidase (APX) and guaiacol peroxidase (POX) activity was determined according to Prochazkova et al. (2001). APX activity was deduced from the decrease in ascorbate concentration, seen as a decline in the optical density at 290 nm. A value for the activity was calculated using an extinction coefficient of  $2.8 \text{ mM}^{-1} \text{cm}^{-1}$  for the ascorbate during 30 s. The assay was performed in a final volume of 1 ml containing 50 mM potassium phosphate (pH 7.0), 1.7 mM  $\text{H}_2\text{O}_2$ , 0.3 mM ascorbic acid and 85  $\mu\text{l}$  enzymatic extract. POX activity was determined from the increase in formation of tetra-guaiacol, seen as an increase in the optical density at 470 nm. The activity was calculated using an extinction coefficient  $26.6 \text{ mM}^{-1} \text{cm}^{-1}$  during 30 s. The assay was carried out using a reaction mixture consisting of 4  $\mu\text{l}$  extract, 150 mM potassium phosphate (pH 6.1), 8 mM guaiacol and 2.2 mM  $\text{H}_2\text{O}_2$ .

### III. II. IV. V. Metabolite quantification

For the AA analysis, three groups of five individual plants per replicate and variant were collected after water stress and rewatering. All individuals from each group were pooled together using liquid nitrogen. 5 mg FW of aforementioned grounded plant material was measured and

extracted. The extraction procedure was performed using an AccQTag Ultra derivatization kit (©Waters). All extracted samples were analysed using an ACQUITY UPLC® System and a XevoTM 122 TQ-S triple quadrupole mass spectrometer (©Waters) according to the annotation note of Waters Corporation (Milford, MA, USA) (Gray and Plumb, 2016). Calibration curves were constructed for each component analysed using internal standards:  $\gamma$ -aminobutyric acid (GABA), L-alanine (Ala), L-arginine (Arg), L-asparagine (Asn), L-aspartic acid (Asp), L-citrulline (Cit), L-glutamine (Gln), L-glutamic acid (Glu), L-glycine (Gly), L-histidine (His), L-ileucine (Ile), L-leucine (Leu), L-methionine (Met), L-phenylalanine (Phe), L-proline (Pro), L-serine (Ser), L-tryptophan (Trp) and L-tyrosine (Tyr), and the deuterium-labelled compounds L-glutamic acid-2,3,3,4,4-d<sub>5</sub>,  $\gamma$ -aminobutyric acid-2,2,3,3,4,4-d<sub>6</sub> and DL-leucine-2,3,3,4,5,5,5',5',5'-d<sub>10</sub>, all purchased from ©Sigma-Aldrich Inc. (Germany).

For PAs determination 10 mg FW of the remaining material used for the AAs was extracted and quantified as described by Malec et al., 2017, using the same equipment as for the analysis of free AAs. The final quantification was performed using the internal standards cadaverine (Cad), 1,3-diaminopropane (DAP), putrescine (Put), spermidine (Spd), spermine (Spm) and tyramine (Tyra), all purchased from ©Sigma-Aldrich Inc., were added to each sample to construct the calibration curve. The concentration of AAs and PAs per dry weight (DW) was then using the absolute water content of the plants.

### III. II. V. Statistical analysis and data representation

To assess the differences between the variants of each non-invasive trait extracted from the image analysis, the non-parametric Kruskal Wallis one-way analysis of variance (ANOVA) by racks was performed. For the validation of the method and to evaluate the influence of a tray position and the effect of the treatment (well-watered or water limited variant) in the morphological and physiological measurements at a particular time-point, the two-way ANOVA was used. Different letters mean significant differences between variants. One-way ANOVA was used to analyse significant differences between the metabolites differed between the variants. Represented values annotated with ns indicate non-significant differences and means annotated



with asterisks indicate significant differences (\*  $P \leq 0.05$ ; \*\*  $P \leq 0.01$ ; \*\*\*  $P \leq 0.001$ ). Tukey HSD test was used for multiple comparison after ANOVA. All the analysis were performed in R 3.5.1 software using *multcomp* package.

For multidimensional analyses, a principal component analysis (PCA) was carried out using the packages *factoextra*, *corrplot*, *PerformanceAnalytics* and *ggpubr*, and the results were displayed in a biplot. The Pearson's linear correlation coefficients between all pairs of studied variables and the significance were also represented in the correlation matrix and scatter plots.

### III. III. Results

#### III. III. I. Phenotyping method- Screening of barley population using simple RGB imaging

A. Experiment 1 and 2- Analysis of projected canopy height in barley population at control conditions

Applying the aforementioned approach, the side-view RGB images of the barley seedling canopy from two independent experiments (**Experiment 1** in December 2017 and **Experiment 2** in June 2018) were analysed (Table III.1). Two randomly distributed trays containing 50 plants each were used per experiment. The reproducibility of the bioassay was corroborated, as the canopy height from both experiments presented the same trend line (Fig. III.2a).

A manual assessment of plants was then performed to complement and validate the traits derived from the automated plant imaging and image analysis, including the functionality of the hardware and software components. The aerial biomass in fresh weight (FW, g) from five seedlings randomly selected from the two different trays of each experiment was determined manually at days 16 and 19. A Pearson correlation-based comparison between the canopy height (pixels, from 50 plants) and the aerial biomass (the average of the five measured plants) revealed a highly significant correlation, with an  $R^2$  of 0.90 ( $P \leq 0.001$ ) (Fig. III. 2b). This result provided clear evidence of the reliability of the method for analysing shoot growth in the population of barley cv. Golden Promise.

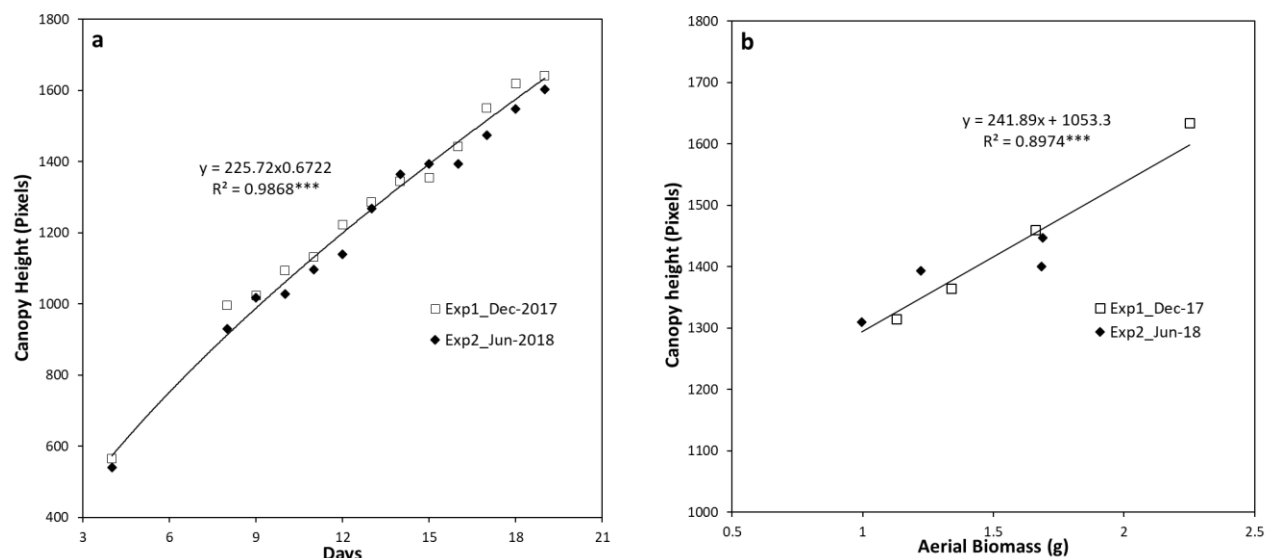


**Figure III.2.** Analysis of the reproducibility of canopy height estimation in barley seedlings from two independent experiments. (a) The reproducibility of projected canopy height dynamics (in pixels) in barley seedlings ( $n = 100$ ) grown under control conditions in December 2017 and July 2018. (b) The correlation between canopy height and fresh aerial biomass (FW,g) determined for replicates measured at day 16 and day 19 in barley seedlings from the two independent experiments. The regression curve and significance calculated from the three independent trays is shown.  $***P \leq 0.001$ .

### B-Experiment 3- Analysis of projected canopy height in barley population under water deficit and subsequent rewatering

For studying water stress response and recovery capacity in barley at a population level, we performed a final **Experiment 3** (Table III.1). In this case, the projected canopy height of five randomly distributed trays containing two plastic containers; a water-stressed variant (D, left) and a well-watered variant (W, right) with 50 plants each each (with a final number of 500 barley seedlings), was recorded over the time-course of 15 days (Fig. III.1 and 3). Three biological replicates with five plants ( $3 \times 5 = 15$  plants) were taken from two randomly selected trays in each variant (D and W) and then, they were used for validation and reproducibility of the method. The three remaining trays were collected at the end of the rewatering period. First of all, we determined the substrate water content of all the trays during the experiment. The first 6 days

the substrate water content of the irrigated and non-irrigated variants was very similar, with no differences between treatments (Fig. III.4a). At day 9, the substrate water content of non-irrigated variants started to decrease with significant differences compared to W variants ( $P \leq 0.05$ ). At the day 15 the substrate water content of the D variant reached 65%. In this point, the containers with the D variant were rewatered to 100% full capacity (Fig. III.4a).

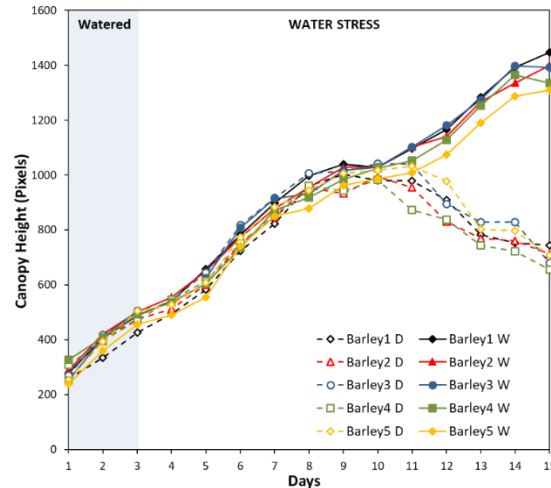


**Figure III.3.** Analysis of reproducibility of canopy height estimation in barley seedling under water deficit conditions within experimental replicates. Changes in canopy height (in pixels) of stressed (D, discontinuous lines) and non-stressed (W, continuous lines) barley seedlings from five independent trays grown for 12 days (with the endpoint at day 15) ( $n=50$ ).

The automated RGB imaging yielded curves with the same pattern for the five independent trays until the end of the water deficit period (Fig. III.3) and for three trays through the whole experiment (Fig. III.4b y c). For the first 7 days after water withdrawal, the stressed plants retained projected canopy height kinetics similar to the well-watered plants, but they were significantly reduced from day 11 to day 15 (Fig. III.4b and Table III.2). After rewatering, the D variant from each independent tray similarly recovered the projected canopy height but the values were still significantly smaller than the W variants (Fig. III.4b and Table III.2). From the obtained dynamic changes in the projected canopy height of the barley seedling population, we created a model curve different for the stressed and non-stressed variants, as represented in Fig. III.5a. From each curve, we extracted several traits, such as the maximum canopy height on the

days when watered and non-watered curves separated (Max), water loss as the slope of the line obtained for the reduction in canopy height, the minimum canopy for the water stress period (Min), the water recovery capacity as the slope of the line obtained for the increase of canopy height after rewatering, and the maximum canopy height of the water-stressed variant after rewatering (MaxR). As an example of the potential use of our bioassay, we calculated the slope of the line for the water deficit period and after rewatering from the two trays selected for the posterior manual measurements (Fig. III.5b, c). In all linear curves, a highly significant correlation ( $R^2 > 0.90$ ;  $P \leq 0.001$ ) was obtained for both growth conditions. Together with the slopes, the Max, Min and MaxR are shown in Table III.3; similar values were obtained in both replicates for these traits. These results confirmed the reproducibility of the method, which was later validated using destructive parameters.

Our phenotyping system is also equipped with a FluorCam unit for the analysis of chl fluorescence parameters (Fig. III.6). In our study, it was clear that water deficit significantly changed all the chl fluorescence parameters, albeit with different dynamics and intensity (Fig. III.7). Some parameters responded quickly and had already changed by day 11, e.g.  $\Phi_{Po}$  and  $qP$  had decreased, and  $\Phi_{(f,D)}$  had increased. Other parameters, such as decreasing  $\Phi_{PSII}$  and  $\Phi_P$ , and increasing  $\Phi_{NPQ}$ , had occurred by day 16 as late stress response parameters (Fig. III.7). After rewatering, the stressed variants recovered to control values for  $qP$  and  $\Phi_P$ . However,  $\Phi_{Po}$ ,  $\Phi_{PSII}$ ,  $\Phi_{(f,D)}$  and  $\Phi_{NPQ}$  maintained significant differences compared with the well-watered plants (Fig. III.7). The results indicated that these parameters were potential indicators for evaluating the recovery capacity of plants, at least in barley.

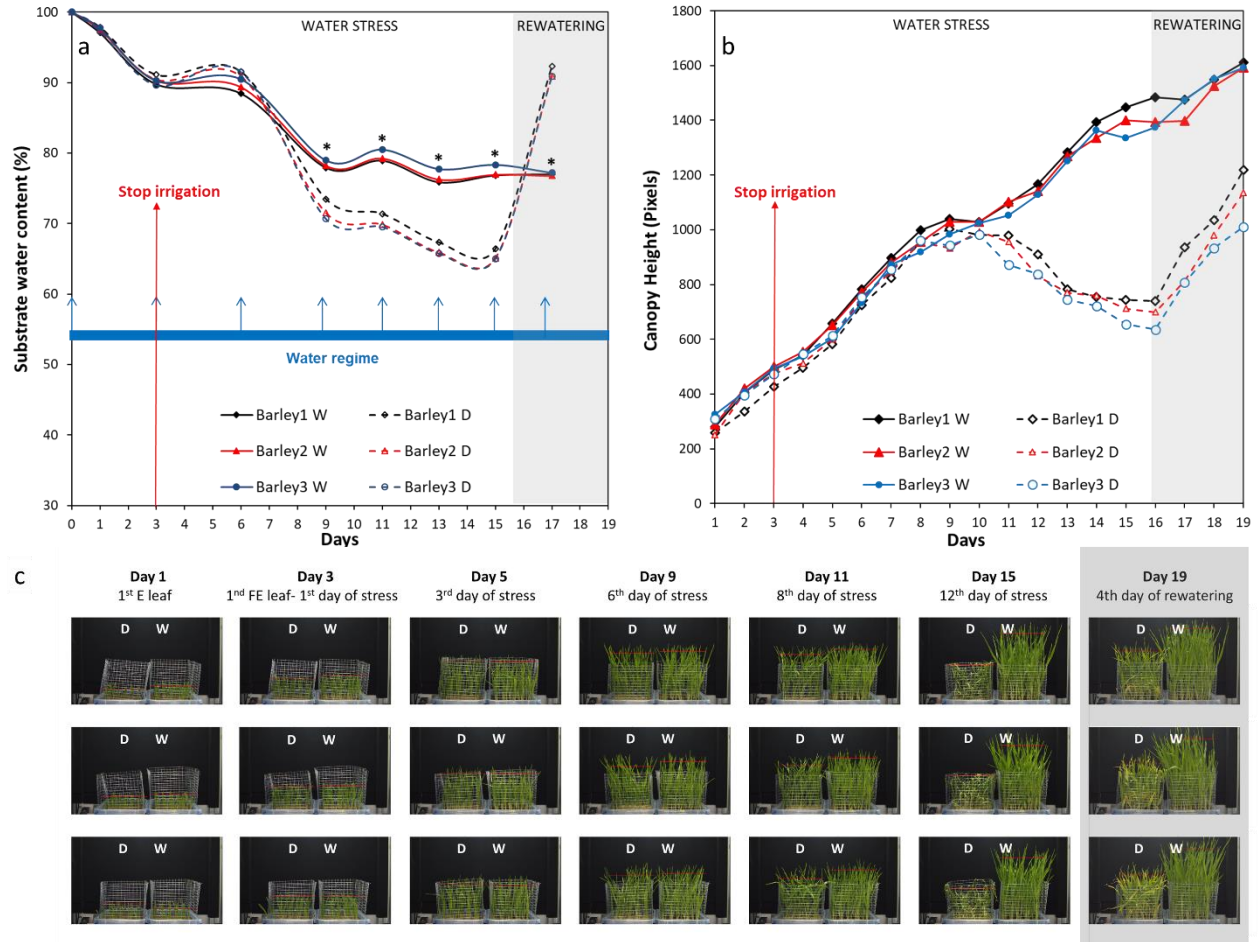


**Figure III.4.** Dynamics of soil moisture and projected canopy height in barley seedlings growing under water stress conditions with subsequent rewatering. (a) Changes in substrate water content (%) of non-stressed (W, continuous lines) and stressed (D, discontinuous lines) barley seedlings ( $n = 50$ ) from three independent trays (Barley1, 2 and 3) grown for 13 days under water deficit conditions (with the endpoint at day 16) and subsequently rewatered for 4 days (with the endpoint at day 19). The watering regime consisted in an initial 100% field capacity (FC) after sowing and subsequent constant 80% FC for W variants, and irrigation interruption from day 3 to day 16 for the D variants and posterior rewatering for 4 days. Blue arrows represent the watering regime and red arrow the stop of the irrigation moment in the D variant. (b) Changes in projected canopy height (in pixels) and (c) side view images of the D and W variants from the three independent replicates along the experiment.

**Table III.2.** Dynamics of canopy height of barley seedlings grown under water stress conditions. Fold changes ( $\log_2$ ) of the canopy height (pixels) of seedlings grown under stressed conditions for 12 days (endpoint day 15) compared with their respective controls, from five independent trays. Asterisks and ns indicate the level of significance between stressed and non-stressed plants according to ANOVA ( $n = 50$ ); \*  $P \leq 0.05$ ; \*\*  $P \leq 0.01$ ; \*\*\*  $P \leq 0.001$ ; ns, not significant.

Replicate	Day 1	Day 2	Day 3	Day 4	Day 5	Day 6	Day 7	Day 8	Day 9	Day 10	Day 11	Day 12	Day 13	Day 14	Day 15	Day 16	Day 17	Day 18	Day 19	
Barley R1	-0.12	-0.28	-0.20	-0.13	-0.18	-0.11	-0.13	-0.06	-0.05	-0.07	-0.16	-0.36	-0.72	-0.89	-0.96	-1.00	-0.66	-0.58	-0.40	
Barley R2	-0.20	-0.05	-0.08	-0.12	-0.12	-0.04	-0.05	0.00	-0.14	-0.05	-0.21	-0.46	-0.72	-0.81	-0.98	-1.00	-0.78	-0.64	-0.49	
Barley R3	-0.08	-0.04	-0.06	0.02	0.02	0.04	-0.03	0.06	-0.06	-0.06	-0.27	-0.43	-0.75	-0.92	-1.03	-1.11	-0.87	-0.73	-0.65	
<b>Average</b>	<b>-0.13</b>	<b>-0.12</b>	<b>-0.11</b>	<b>-0.07</b>	<b>-0.09</b>	<b>-0.04</b>	<b>-0.07</b>	<b>0.00</b>	<b>-0.08</b>	<b>-0.06</b>	<b>-0.21</b>	<b>-0.41</b>	<b>-0.73</b>	<b>-0.87</b>	<b>-0.99</b>	<b>-1.04</b>	<b>-0.77</b>	<b>-0.65</b>	<b>-0.51</b>	
<i>Significanc</i>																				
<i>e</i>	ns	ns	ns	ns	ns	ns	ns	ns	ns	ns	*	*	*	*	*	*	*	*	*	*

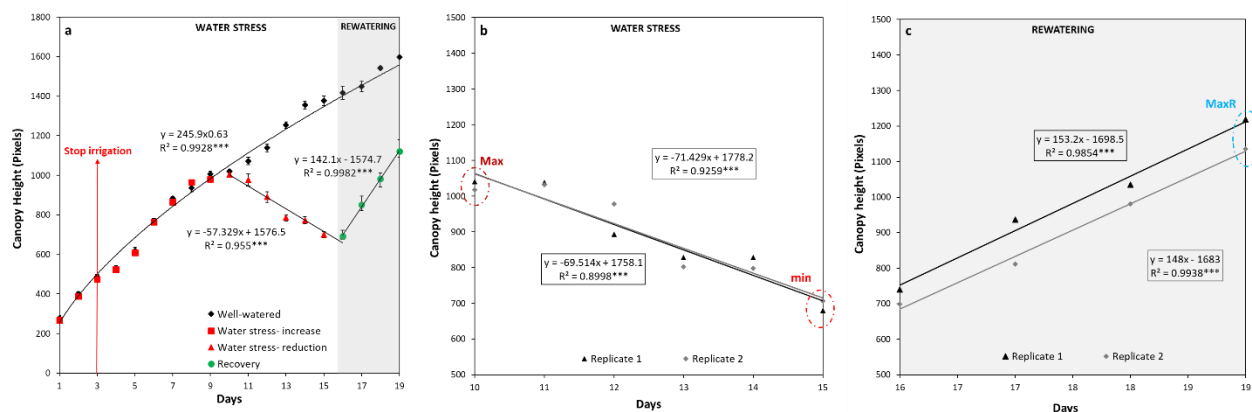


**Figure III.5.** Linear curve of the projected canopy height and the extracted traits. (a) The average canopy height, regression curve and significance calculated from three independent trays (with 50 plants each) growing under water deficit conditions for 13 days (with the endpoint at day 16) and with subsequent rewatering for 4 days (with the endpoint at day 19). (b) Max is the maximum and Min the minimum canopy height reached by the stressed plants from replicate 1 or 2 ( $n = 50$ ) under water deficit conditions, and the slope of the linear model curve is shown. (c) MaxR is the maximum canopy height from replicate 1 or 2 ( $n = 50$ ) attained after 4 days of rewatering, and the slope of the line (SlopeR) is also shown in the equation.

**Table III.3.** Traits related to water deficit and recovery. Traits were extracted from the linear regression of the canopy height in two days randomly selected trays. Day is the day when treated and not treated plants are different; Max is the maximal canopy height reached in the stressed plants under drought; min is the minimal canopy height at the end of the drought period; Slope of the linear curve from the canopy height in the drought period; MaxR is the maximal canopy height reached in the stressed plants after rewatering; and SlopeR of the linear curve from the canopy height in the rewatering period.

	Water stress				Rewatering	
	Day	Max	min	Slope	MaxR	SlopeR
Tray 1	8	1041	680	-69.514	1218	153.2
Tray 2	8	1018	707	-71.429	1136	148

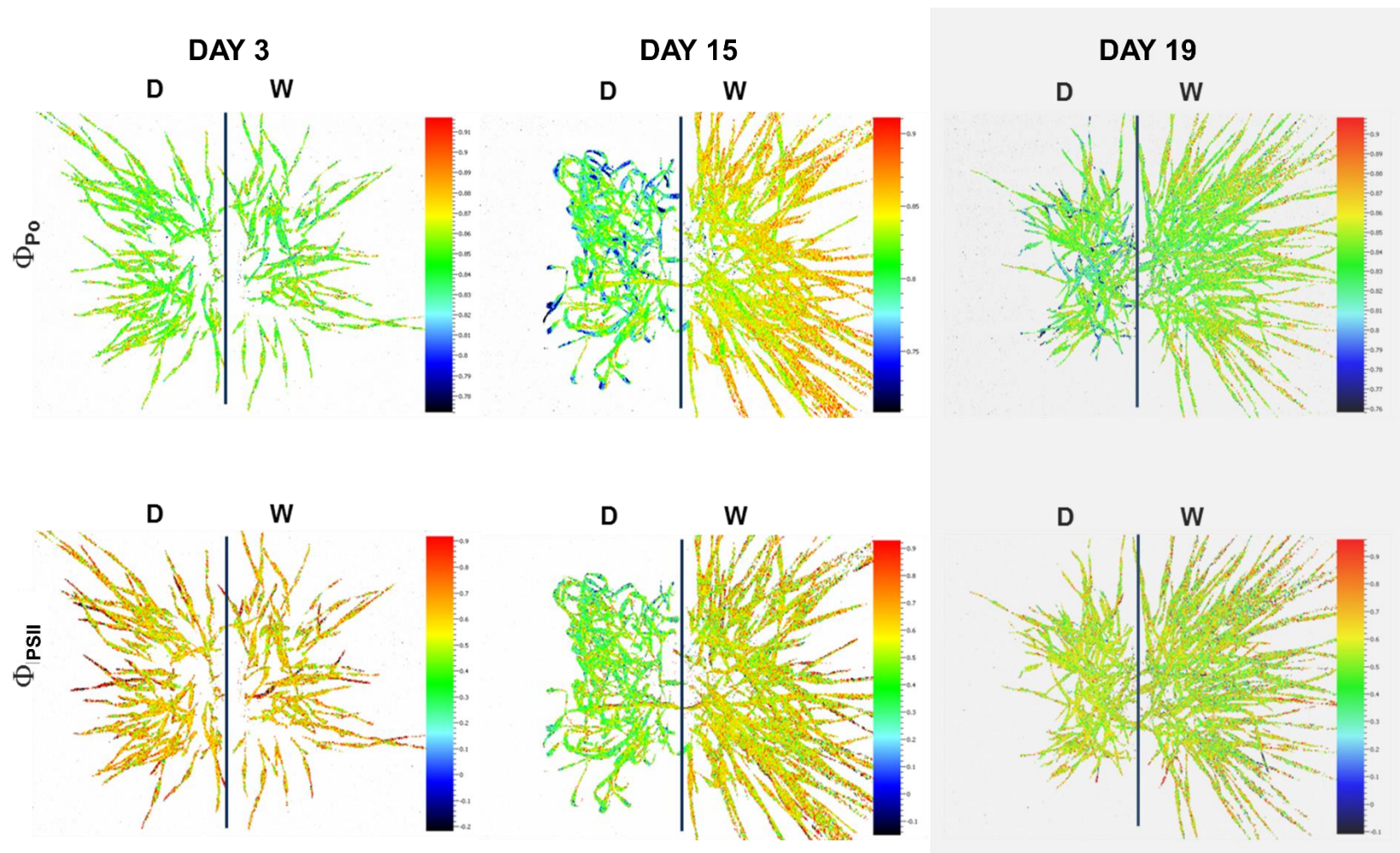


**Figure III.6.** Imaging of chlorophyll fluorescence ( $\Phi_{Po}$  and  $\Phi_{PSII}$ ) in barley seedlings under well-water, water stress, and rewatering. Stressed and non-stressed plants labelled as D (left) and W (right), respectively.



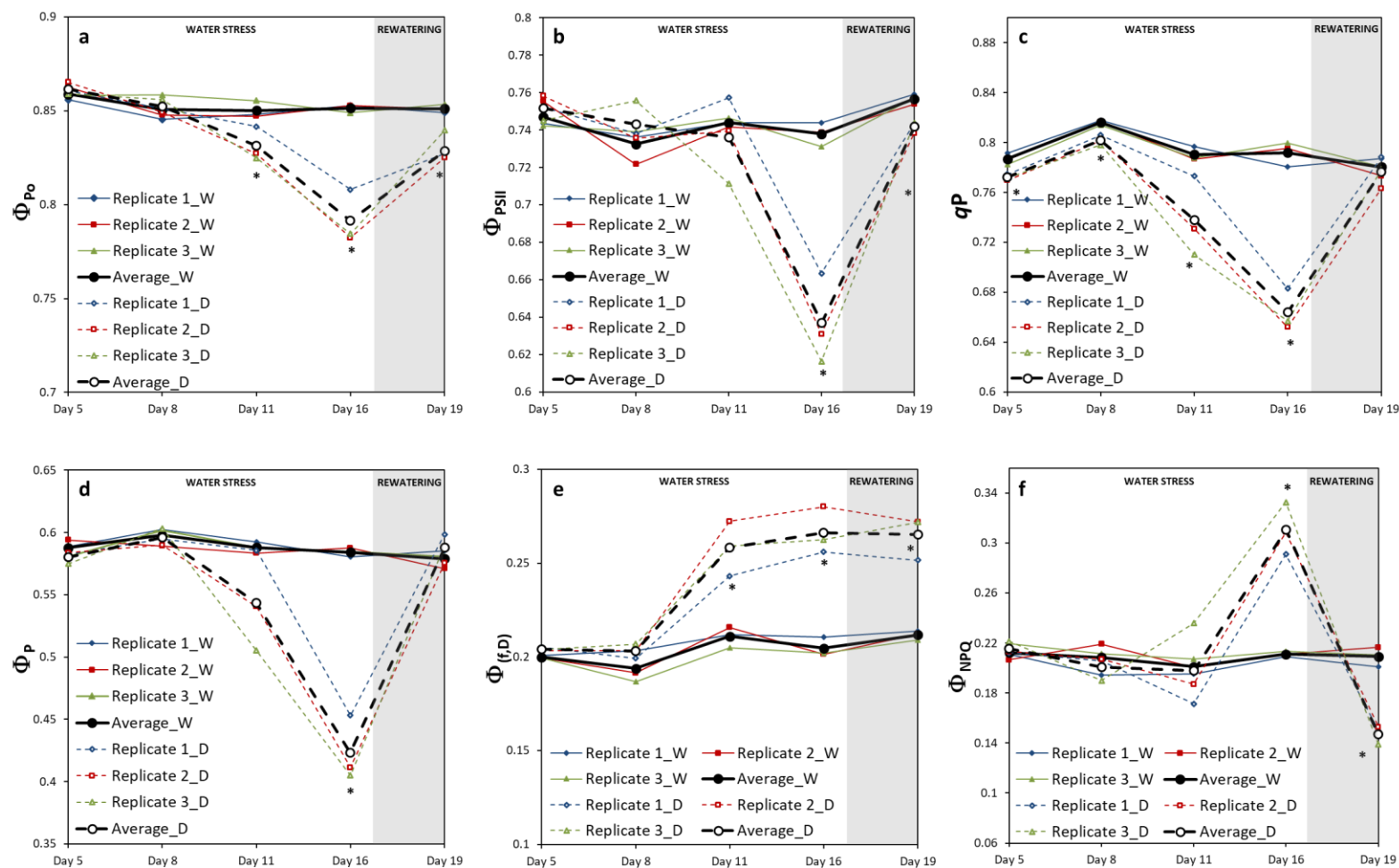


**Figure III.7.** Variation in chlorophyll parameters in barley seedlings grown under water stress conditions and after subsequent rewatering. Chlorophyll fluorescence parameters from three independent trays (1, 2 and 3) ( $n = 50$ ) and the average values. D and W variants are represented by discontinuous and continuous lines, respectively. Statistical analyses were performed via ANOVA. Asterisks indicate the significance level relative to the control variant; \*  $P \leq 0.05$ ; \*\*  $P \leq 0.01$ ; \*\*\*  $P \leq 0.001$ ; ns, not significant.

### III. III. II. Validation and reproducibility of the phenotyping method

A-The reproducibility of morphometric and physiological parameters between biological replicates and trays confirmed the reliability of the method

We performed a manual evaluation of several morphological and physiological parameters in two independent trays to integrate and validate our results obtained by imaged-based measurements. Firstly, we evaluated the developmental stage of the plant population by analysing the last emerging leaf in eight and five randomly selected plants per variant at the end of the water period and rewatering, respectively (Fig. III.8). We observed differences among variants (treated and non-treated) and not between biological trays. Whereas in the watered control at day 16 the fifth leaf had appeared, the stressed plants were still expanding the third leaf at this point of the assay (Fig. III.8a). After rewatering, the differences were reduced to one leaf less, with the fourth and fifth leaf in expansion for stressed and non-stressed plants, respectively (Fig. III.8b).

In the case of the aerial biomass (FW, g), full expanded (FE) leaf length and width (cm) and the ratio between length and width, eight plants per variant and tray were individually collected at the end the water stress period and after rewatering, respectively (Fig. III.9a-c). In almost all the cases, the changes were due to the treatment and not because of the tray position effect (Table III.4). Regarding biomass, the seedlings from the D variant were significantly smaller than the W plants in both trays (Fig. III.9a). After recovery, D plants were still only half the weight of the well-watered variants (Fig. III.9a). When the length and width of the last fully expanded leaf were evaluated, we observed that the seedlings from the same variant showed the same profile for both traits (Fig. III.9b and c); the length and width were significantly reduced under water stress conditions. After rewatering only the width recovered to control values (Fig. III.9b), affecting the length/width ratio (Fig. III.9d).

There was also no effect of the tray recorded for the RWC and total chlorophyll (chl) content between the trays (Table III.4). The water deficit treatment caused a c. 50% decrease in plant RWC, and rewatering returned the plant water status to 95% in only 4 days (day 19) (Fig. III.9e). Chl content showed a similar pattern (Fig. III.9f). The values were significantly lower in

stressed plants than in the controls, indicating that the Chl content and N status of the plants were significantly affected by water stress conditions but were recovered after 4 days of rewatering (Fig. III.9f). Altogether, the high reproducibility of the individual biometric and physiological parameters among the assay replicates corroborated the reproducibility of the method for studying water deficit and recovery capacity in barley.

Altogether, the high reproducibility of the individual biometric and physiological parameters among the trays corroborated the reproducibility of the method for studying water deficit and recovery capacity at least in barley cv. Golden Promise.

B- The reproducibility of the antioxidative response between replicates also validated the method for study water deficit and recovery in barley population

It is well known that plants activate their antioxidative machinery as a response to stress. Hence, we quantified the activity of the three antioxidant enzymes CAT, POX and APX (Fig. III.9g–i). The same profile was observed between trays as stress response and subsequent recovery (Fig. III.9g–i, Table III.4). Interestingly, only CAT and POX increased significantly in the stressed variants, and then recovered to control values after rewatering (Fig. III.9g and h). In contrast, APX kept increasing during the recovery period, resulting in values four times higher in the stressed seedlings than in the controls (Fig. III.9i). These results indicated that each type of antioxidant enzyme plays a different role in the barley cv. Golden Promise stress response.

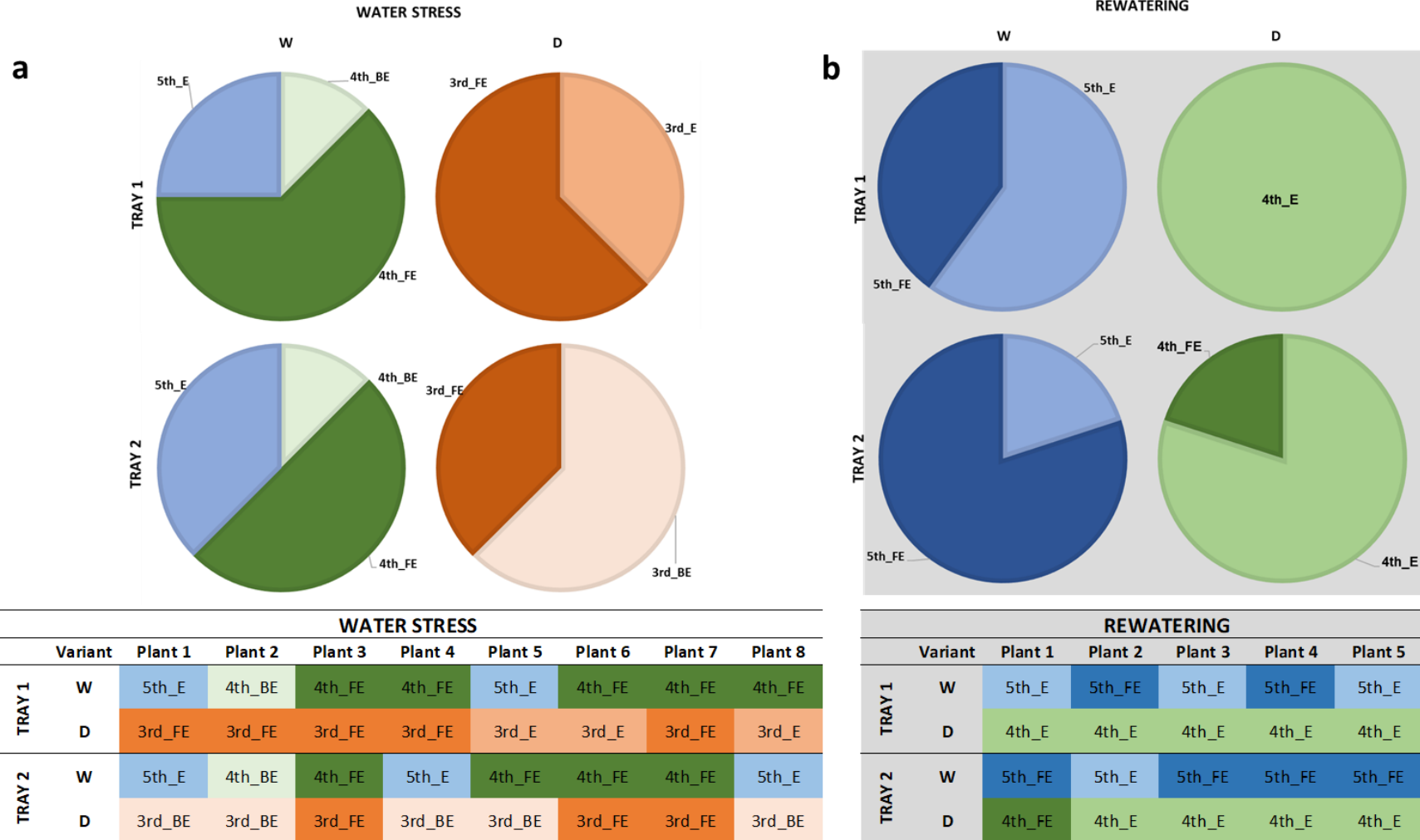


**Figure III.8.** Developmental stages of barley seedlings grown under (a) water stress and (b) after subsequent rewatering. Developmental stages of leaves in stressed (D) and non-stressed (W) plants from two independent trays (1 and 2) at the end of the water stress period (n = 8) (a) and after rewatering (n=5) (b).

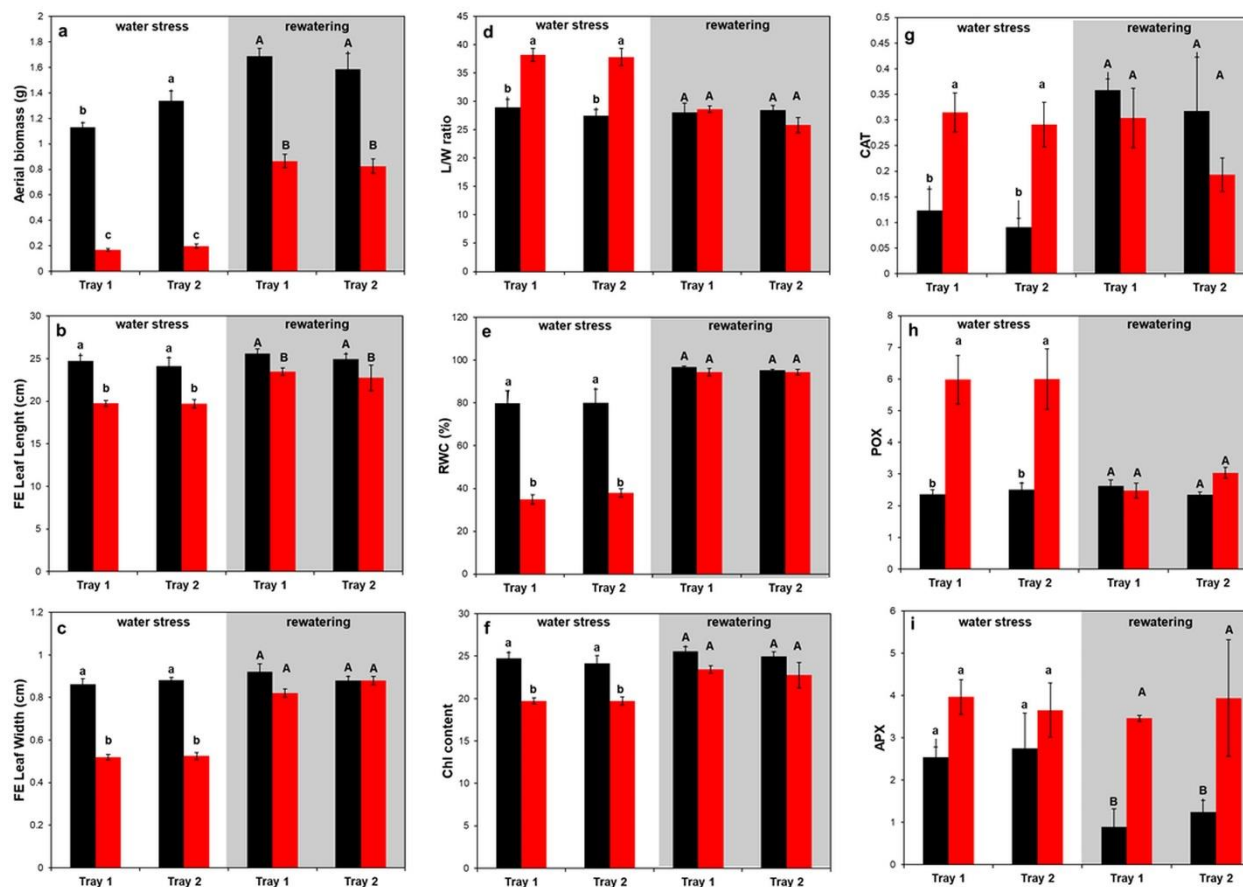


**Figure III.9.** Morphometric and physiological changes in barley seedlings under water stress conditions and after subsequent rewatering. (a) Aerial biomass (FW,g), (b) leaf length (cm) and (c) width (cm) of the last fully expanded (FE) leaf, (d) the ratio between length and width, (e) the relative water content (%), (f) the index of the chlorophyll content, and the activity of the antioxidative enzymes (g) guaiacol peroxidase (POX), (h) catalase (CAT) and (i) ascorbate peroxidase (APX), in stressed (D, colour bars) and non-stressed (W, black bars) barley seedlings from two independent trays at the end of the water stress period (n=8) and after subsequent rewatering (n=5). Asterisks and ns indicate the significance level relative to the control replicate; \*  $P \leq 0.05$ ; \*\*  $P \leq 0.01$ ; \*\*\*  $P \leq 0.001$ ; ns, not significant. Three independent pools containing 5 plants each were used for the quantification of the antioxidant enzyme activity. Different letters mean significant differences according to Tukey HSD test after ANOVA.

**Table III.4.** Statistical analysis of several morphological and physiological traits measured in barley seedlings at the end of the water stress period and after rewatering using two-way ANOVA (Tray and Treatment). \*  $P \leq 0.05$ ; \*\*  $P \leq 0.01$ ; \*\*\*  $P \leq 0.001$ .

	WATER STRESS						REWATERING					
	Df	Sum Sq	Mean Sq	F value	Pr(>F)		Df	Sum Sq	Mean Sq	F value	Pr(>F)	
Biomass	TRAY	1	0.063	0.063	8.505	0.0069 **	TRAY	1	0.003	0.003	0.142	0.712
	Treatment	1	8.333	8.333	1122.907	<2e-16 ***	Treatment	1	3.547	3.547	194.408	2.27e-10 ***
	TRAY:Treatment	1	0.029	0.029	3.923	0.0575	TRAY:Treatment	1	0.002	0.002	0.088	0.771
	Residuals	28	0.208	0.007			Residuals	16	0.292	0.018		
Leaf Length	TRAY	1	0.78	0.78	0.228	0.637	TRAY	1	2.24	2.244	0.583	0.456
	Treatment	1	178.60	178.60	52.062	7.46e-08 ***	Treatment	1	23.54	23.544	6.112	0.025 *
	TRAY:Treatment	1	0.60	0.60	0.176	0.678	TRAY:Treatment	1	0.00	0.005	0.001	0.973
	Residuals	28	96.06	3.43			Residuals	16	61.64	3.852		
Leaf Width	TRAY	1	0.0013	0.0013	0.479	0.495	TRAY	1	0.0005	0.00050	0.154	0.7001
	Treatment	1	0.9800	0.9800	375.248	<2e-16 ***	Treatment	1	0.0125	0.01250	3.846	0.0675
	TRAY:Treatment	1	0.0003	0.0003	0.120	0.732	TRAY:Treatment	1	0.0125	0.01250	3.846	0.0675
	Residuals	28	0.0731	0.0026			Residuals	16	0.0520	0.00325		
Ratio L/W	TRAY	1	7.5	7.5	0.555	0.463	TRAY	1	7.78	7.778	1.148	0.300
	Treatment	1	769.0	769.0	57.022	3.17e-08 ***	Treatment	1	5.22	5.225	0.771	0.393
	TRAY:Treatment	1	2.4	2.4	0.180	0.675	TRAY:Treatment	1	12.76	12.756	1.883	0.189
	Residuals	28	377.6	13.5			Residuals	16	108.41	6.775		
Chl	TRAY	1	1.02	1.015	0.257	0.6161	TRAY	1	4.05	4.050	1.400	0.254
	Treatment	1	29.45	29.453	7.459	0.0108 *	Treatment	1	1.06	1.058	0.366	0.554
	TRAY:Treatment	1	0.20	0.195	0.049	0.8256	TRAY:Treatment	1	3.70	3.698	1.279	0.275
	Residuals	28	110.56	3.948			Residuals	16	46.27	2.892		
RWC	TRAY	1	8	8	0.538	0.474	TRAY	1	40.4	40.42	1.414	0.252
	Treatment	1	16318	16318	1146.045	2.55e-16 ***	Treatment	1	1.5	1.46	0.051	0.824
	TRAY:Treatment	1	16	16	1.138	0.302	TRAY:Treatment	1	39.2	39.22	1.372	0.259
	Residuals	16	228	14			Residuals	16	457.3	28.58		
CAT	TRAY	1	0.00239	0.00239	0.599	0.461063	TRAY	1	0.01703	0.017028	1.433	0.266
	Treatment	1	0.11435	0.11435	28.646	0.000684 ***	Treatment	1	0.02372	0.023716	1.996	0.195
	TRAY:Treatment	1	0.00007	0.00007	0.016	0.901389	TRAY:Treatment	1	0.00369	0.003695	0.311	0.592
	Residuals	8	0.03194	0.00399			Residuals	8	0.09506	0.011882		
POX	TRAY	1	0.02	0.02	0.019	0.894008	TRAY	1	0.0590	0.0590	0.596	0.4623
	Treatment	1	37.82	37.82	32.020	0.000477 ***	Treatment	1	0.2248	0.2248	2.272	0.1701
	TRAY:Treatment	1	0.01	0.01	0.012	0.915079	TRAY:Treatment	1	0.5467	0.5467	5.525	0.0466 *
	Residuals	8	9.45	1.18			Residuals	8	0.7916	0.0989		
APX	TRAY	1	0.009	0.009	0.009	0.9263	TRAY	1	0.523	0.523	0.321	0.58648
	Treatment	1	4.080	4.080	4.074	0.0783	Treatment	1	20.834	20.834	12.789	0.00723 **
	TRAY:Treatment	1	0.197	0.197	0.196	0.6695	TRAY:Treatment	1	0.012	0.012	0.007	0.93400
	Residuals	8	8.012	1.002			Residuals	8	13.032	1.629		

### C- Different free AAs and PAs regulated plant stress response and recovery

Free PA and AA are typical metabolites involved in the plant water stress response (Fig. III.10). As expected, both groups of metabolites accumulated significantly under stress, and the profile of the fold change between treated and non-treated plants was similar (Fig. III.10).

Water deficit induced a significant accumulation of AAs ( $\text{pmol mg}^{-1}$  DW) (Fig. III.10 and Table III.5), with the highest increases in Pro and OH-Pro. After rewatering, many of the AA kept significantly higher in the stressed plants than in the controls, except for Arg and GABA did not showed significant differences between treatments ((Fig. III.10). Interestingly, at this time-point the accumulation of Cit in stressed plants was 11.7-fold ( $\log_2 = 3.55$ ) higher compared to the control levels (Fig. III.10).

For the PAs, quantification of Cad was only possible in the water-stressed plants (with an average of 9.73 and 7.85  $\text{pmol mg}^{-1}$  DW for tray 1 and 2, respectively); in the well-watered and the stressed variants after rewatering it was under the limits of detection. Tyra and DAP were the most accumulated compounds and Spd was the only PA that did not change in stressed plants compared to the non-stressed ones (Fig. III. 10 and Table III.5). After rewatering, water stressed plants kept higher content of Tyra and DAP compared to the well-watered plants, Spd accumulated to higher levels, whereas no significant differences between variants were found in the case of Put and Spm (Fig. III.10 and Table III.5). Based on these results, we could classify the metabolites into two groups, a water stress-related compounds (e.g. Pro, OH-Pro, Tyra, DAP and Cad) and a group involved in the recovery of the plants after rewatering (e.g. Cit and Spd).

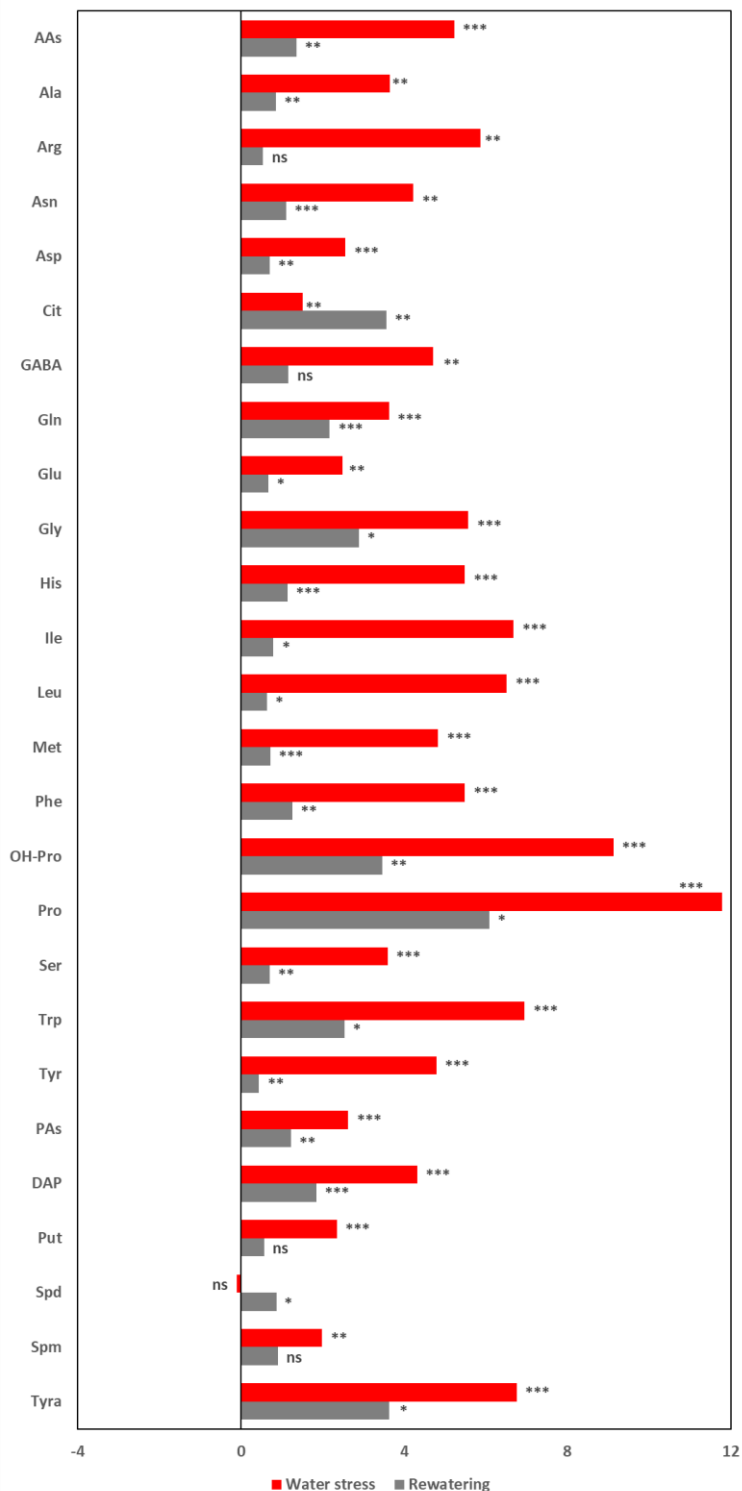


**Figure III.10.** Metabolic profiles of barley seedlings under water deficit and after subsequent rewatering. Fold changes (presented as log<sub>2</sub> ratio) in the content (pmol mg<sup>-1</sup> DW) of free polyamines (PAs) and amino acids (AAs) between stressed (D) and non-stressed (W) barley seedlings (three independent pools containing 5 plants from two independent trays, n = 6) at the end of the stress period (red bars) and after subsequent rewatering (gray bars).



**Table III.5.** Statistical analysis of free AAs and PAs (pmol mg<sup>-1</sup> DW) measured in barley seedlings at the end of the water stress period and after rewatering using one-way ANOVA. \*  $P \leq 0.05$ ; \*\*  $P \leq 0.01$ ; \*\*\*  $P \leq 0.001$ .

	WATER STRESS					REWATERING								
Aaa	Df	Sum Sq	Mean Sq	F value	Pr(>F)	Df	Sum Sq	Mean Sq	F value	Pr(>F)				
Ala	Treat	1	3.444	3.444	46.23	0.00244	**	Treat	1	0.05929	0.05929	57.86	0.0016	**
	Residuals	4	0.298	0.074				Residuals	4	0.00410	0.00102			
Arg	Df	Sum Sq	Mean Sq	F value	Pr(>F)	Df	Sum Sq	Mean Sq	F value	Pr(>F)				
	Treat	1	0.5545	0.5545	44.01	0.00268	**	Treat	1	0.0001913	1.913e-04	2.557	0.185	
Asn	Residuals	4	0.0504	0.0126			Residuals	4	0.0002994	7.485e-05				
	Df	Sum Sq	Mean Sq	F value	Pr(>F)	Df	Sum Sq	Mean Sq	F value	Pr(>F)				
Asp	Treat	1	18.289	18.289	58.88	0.00155	**	Treat	1	0.1205	0.12052	193.1	0.000155	***
	Residuals	4	1.242	0.311			Residuals	4	0.0025	0.00062				
Cit	Df	Sum Sq	Mean Sq	F value	Pr(>F)	Df	Sum Sq	Mean Sq	F value	Pr(>F)				
	Treat	1	41.54	41.54	87.08	0.000734	***	Treat	1	1.1986	1.1986	33.68	0.00438	**
GABA	Residuals	4	1.91	0.48			Residuals	4	0.1423	0.0356				
	Df	Sum Sq	Mean Sq	F value	Pr(>F)	Df	Sum Sq	Mean Sq	F value	Pr(>F)				
Gln	Treat	1	5.102e-05	5.102e-05	28.65	0.00587	**	Treat	1	0.0003207	0.0003207	65.41	0.00127	**
	Residuals	4	7.120e-06	1.780e-06			Residuals	4	0.0000196	0.0000049				
Glu	Df	Sum Sq	Mean Sq	F value	Pr(>F)	Df	Sum Sq	Mean Sq	F value	Pr(>F)				
	Treat	1	0.9506	0.9506	25.35	0.00731	**	Treat	1	0.02496	0.024964	6.389	0.0648	
Gly	Residuals	4	0.1500	0.0375			Residuals	4	0.01563	0.003907				
	Df	Sum Sq	Mean Sq	F value	Pr(>F)	Df	Sum Sq	Mean Sq	F value	Pr(>F)				
His	Treat	1	14.696	14.696	712.8	1.17e-05	***	Treat	1	2.1068	2.1068	187.9	0.000164	***
	Residuals	4	0.082	0.021			Residuals	4	0.0449	0.0112				
Ile	Df	Sum Sq	Mean Sq	F value	Pr(>F)	Df	Sum Sq	Mean Sq	F value	Pr(>F)				
	Treat	1	33.67	33.67	64.78	0.00129	**	Treat	1	0.9953	0.9953	16.94	0.0147	*
Leu	Residuals	4	2.08	0.52			Residuals	4	0.2350	0.0588				
	Df	Sum Sq	Mean Sq	F value	Pr(>F)	Df	Sum Sq	Mean Sq	F value	Pr(>F)				
Met	Treat	1	0.005175	0.005175	13.88	0.0204	*	Treat	1	0.005175	0.005175	13.88	0.0204	*
	Residuals	4	0.001492	0.000373			Residuals	4	0.001492	0.000373				
Phe	Df	Sum Sq	Mean Sq	F value	Pr(>F)	Df	Sum Sq	Mean Sq	F value	Pr(>F)				
	Treat	1	1.343	1.3431	358.5	4.58e-05	***	Treat	1	0.003950	0.003950	114	0.000436	***
Pro	Residuals	4	0.015	0.0037			Residuals	4	0.000139	0.000035				
	Df	Sum Sq	Mean Sq	F value	Pr(>F)	Df	Sum Sq	Mean Sq	F value	Pr(>F)				
Ser	Treat	1	2.1271	2.1271	333.5	5.29e-05	***	Treat	1	0.0008674	0.0008674	14.67	0.0186	*
	Residuals	4	0.0255	0.0064			Residuals	4	0.0002366	0.0000591				
Thr	Df	Sum Sq	Mean Sq	F value	Pr(>F)	Df	Sum Sq	Mean Sq	F value	Pr(>F)				
	Treat	1	1.0025	1.0025	369.7	4.31e-05	***	Treat	1	0.0003770	3.77e-04	14.24	0.0195	*
Val	Residuals	4	0.0108	0.0027			Residuals	4	0.0001059	2.65e-05				
	Df	Sum Sq	Mean Sq	F value	Pr(>F)	Df	Sum Sq	Mean Sq	F value	Pr(>F)				
Tyr	Treat	1	0.015151	0.015151	705.5	1.19e-05	***	Treat	1	3.074e-05	3.074e-05	237.7	0.000103	***
	Residuals	4	0.000086	0.000021			Residuals	4	5.170e-07	1.290e-07				

Phe	Df	Sum Sq	Mean Sq	F value	Pr(>F)	Df	Sum Sq	Mean Sq	F value	Pr(>F)		
	Treat	1	0.3306	0.3306	83805	8.54e-10 ***	Treat	1	0.0011638	0.0011638	28.12	0.00608 **
	Residuals	4	0.0000	0.0000			Residuals	4	0.0001656	0.0000414		
OH-Pro	Df	Sum Sq	Mean Sq	F value	Pr(>F)	Df	Sum Sq	Mean Sq	F value	Pr(>F)		
	Treat	1	0.0007348	0.0007348	166.4	0.000208 ***	Treat	1	9.210e-07	9.21e-07	26.39	0.00681 **
	Residuals	4	0.0000177	0.0000044			Residuals	4	1.396e-07	3.49e-08		
Pro	Df	Sum Sq	Mean Sq	F value	Pr(>F)	Df	Sum Sq	Mean Sq	F value	Pr(>F)		
	Treat	1	11410	11410	289.4	7e-05 ***	Treat	1	11.947	11.947	8.653	0.0423 *
	Residuals	4	158	39			Residuals	4	5.522	1.381		
Ser	Df	Sum Sq	Mean Sq	F value	Pr(>F)	Df	Sum Sq	Mean Sq	F value	Pr(>F)		
	Treat	1	15.890	15.890	234.6	0.000106 ***	Treat	1	0.12556	0.1256	26.69	0.00667 **
	Residuals	4	0.271	0.068			Residuals	4	0.01882	0.0047		
Trp	Df	Sum Sq	Mean Sq	F value	Pr(>F)	Df	Sum Sq	Mean Sq	F value	Pr(>F)		
	Treat	1	1.3558	1.3558	12212	4.02e-08 ***	Treat	1	0.013065	0.013065	16.39	0.0155 *
	Residuals	4	0.0004	0.0001			Residuals	4	0.003188	0.000797		
Tyr	Df	Sum Sq	Mean Sq	F value	Pr(>F)	Df	Sum Sq	Mean Sq	F value	Pr(>F)		
	Treat	1	0.4327	0.4327	30796	6.33e-09 ***	Treat	1	0.0004264	0.0004264	25.59	0.00718 **
	Residuals	4	0.0001	0.00003			Residuals	4	0.0000666	0.0000167		
AAs	Df	Sum Sq	Mean Sq	F value	Pr(>F)	Df	Sum Sq	Mean Sq	F value	Pr(>F)		
	Treat	1	19930	19930	227.9	0.000112 ***	Treat	1	72.15	72.15	26.54	0.00674 **
	Residuals	4	350	87			Residuals	4	10.87	2.72		
Cad	Df	Sum Sq	Mean Sq	F value	Pr(>F)							
	Treat	1	115.79	115.79	262.2	8.51e-05 ***						
	Residuals	4	1.77	0.44								
DAP	Df	Sum Sq	Mean Sq	F value	Pr(>F)	Df	Sum Sq	Mean Sq	F value	Pr(>F)		
	Treat	1	178.03	178.03	11682	4.39e-08 ***	Treat	1	8.214	8.214	147.3	0.000264 ***
	Residuals	4	0.06	0.02			Residuals	4	0.223	0.056		
Put	Df	Sum Sq	Mean Sq	F value	Pr(>F)	Df	Sum Sq	Mean Sq	F value	Pr(>F)		
	Treat	1	328.2	328.2	2220	1.21e-06 ***	Treat	1	3.988	3.988	4.684	0.0964 .
	Residuals	4	0.6	0.1			Residuals	4	3.406	0.851		
Spd	Df	Sum Sq	Mean Sq	F value	Pr(>F)	Df	Sum Sq	Mean Sq	F value	Pr(>F)		
	Treat	1	1.492	1.492	0.956	0.384	Treat	1	160.45	160.45	9.114	0.0392 *
	Residuals	4	6.244	1.561			Residuals	4	70.42	17.61		
Spm	Df	Sum Sq	Mean Sq	F value	Pr(>F)	Df	Sum Sq	Mean Sq	F value	Pr(>F)		
	Treat	1	475.4	475.4	22.8	0.00881 **	Treat	1	9.838	9.838	3.868	0.121
	Residuals	4	83.4	20.9			Residuals	4	10.172	2.543		
Tyra	Df	Sum Sq	Mean Sq	F value	Pr(>F)	Df	Sum Sq	Mean Sq	F value	Pr(>F)		
	Treat	1	11955	11955	135.8	0.00031 ***	Treat	1	179.92	179.92	16.99	0.0146 *
	Residuals	4	352	88			Residuals	4	42.36	10.59		
PAs	Df	Sum Sq	Mean Sq	F value	Pr(>F)	Df	Sum Sq	Mean Sq	F value	Pr(>F)		
	Treat	1	26044	26044	134.6	0.000315 ***	Treat	1	1161.4	1161.4	73.11	0.00103 **
	Residuals	4	774	193			Residuals	4	63.5	15.9		

### III. III. III. Data analysis- Multivariate statistical analysis for understanding the physiological basis of the image-derived traits and water stress response in barley populations

To integrate all parameters measured and confirm the reliability of the traits derived from our method based on the canopy height of barley populations, we performed a PCA in which trays 1 and 2 were evaluated for two different growth regimens, water-stressed (D) and well-watered (W) plants, at two time-points, at the end of the stress period or after 4 days of rewatering (RD and RW, respectively). To facilitate visualization, the results were projected onto a biplot representing the scores (variants) and the loadings (analysed traits) (Fig. III.11a). The first two principal components (PC1 and PC2), which together captured 89.9% of the variance, explained the experimental model almost completely (Fig. III.12). We could see that the trays with the same variant and time-point were closely located. PC1 accounted for 79.9% of the total variation, and included almost all the traits and metabolites, except chl, qP,  $\Phi_{(f,D)}$  ( $\Phi_{f,D}$ ), APX, CAT, Cit and Spd. The accumulation of metabolites was positively correlated with the water deficit conditions (D) (Fig. III.11a). In contrast, they showed a negative correlation with the controls from the water stress and rewatering period, which were positively correlated with the canopy height, slope, development,  $\Phi_{Po}$  ( $\Phi_{Po}$ ),  $\Phi_{PSII}$  ( $\Phi_{PSII}$ ),  $\Phi_P$  ( $\Phi_P$ ), biomass, leaf length and width and RWC. PC2 captured an additional 11.5% of the total variance, and was positively dominated by CAT, Cit and Spd in the rewatered trays (RD) (Fig. III.11a and b). This analysis demonstrated the reproducibility of the measurements performed, as the independent trays were grouped together in all analysed situations. In addition, the separation of the loadings allowed us to identify possible traits related to water stress and rewatering responses in the barley cultivar used in this study.

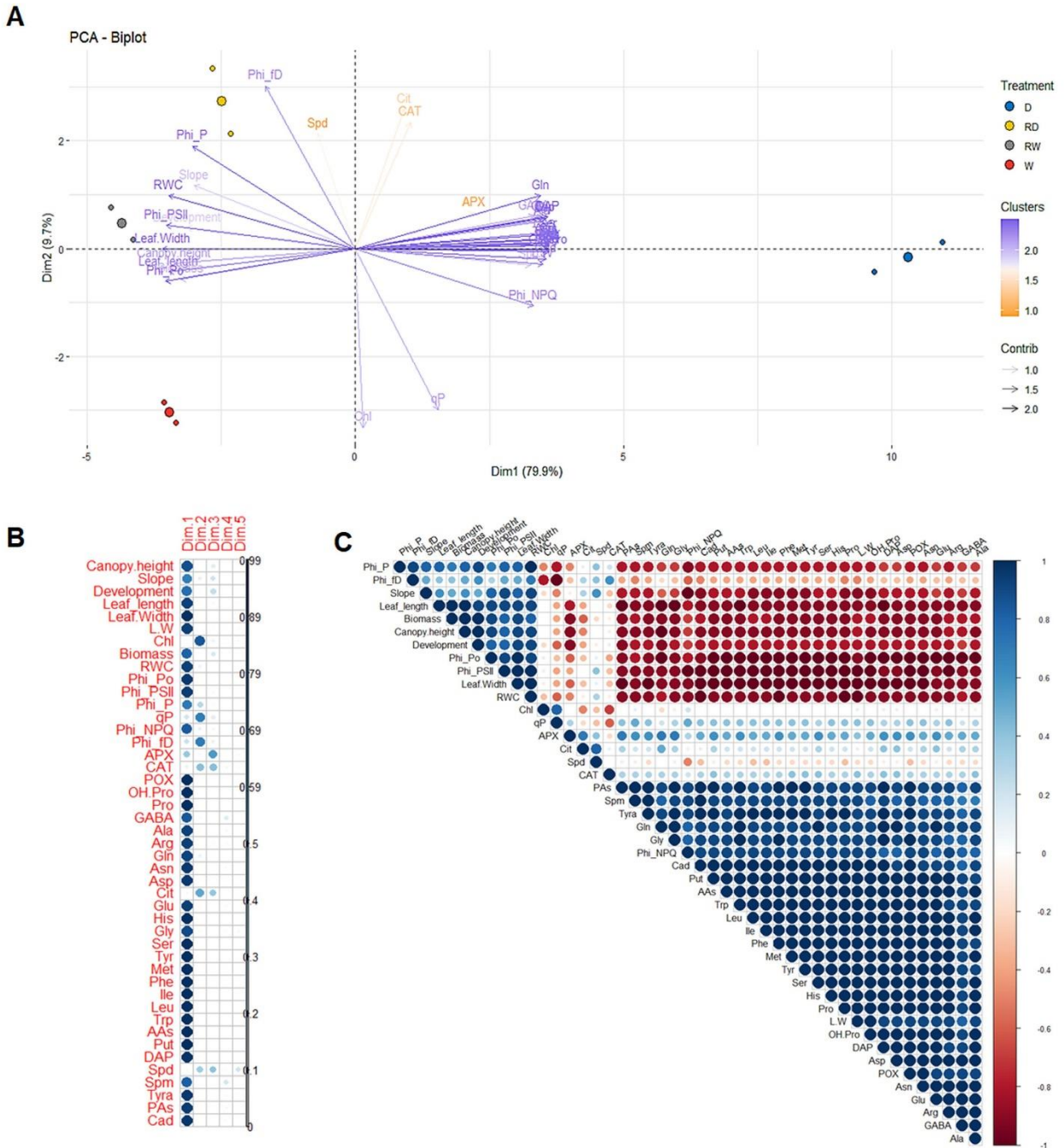


**Figure III.11.** Multivariate statistical analyses of the traits in barley seedlings related to the water stress response and subsequent rewatering. (a) Principal component analysis (PCA) (b) contribution of the loadings to each PCA (Dim) and (c) a correlation matrix of 45 traits obtained from two different trays of barley seedlings at the end of the water stress period and after subsequent rewatering.

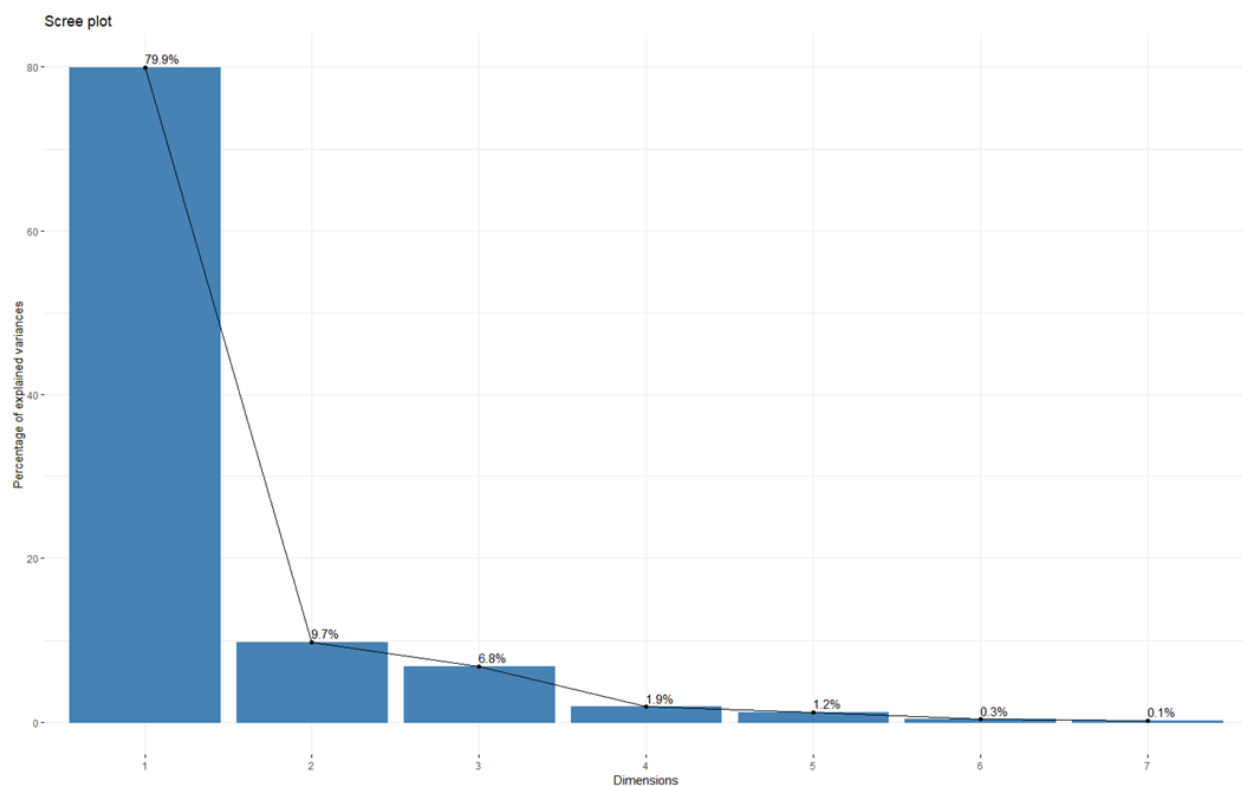


**Figure III.12.** Scree plot representing the percentage of explained variance of the model of each PCA (Dimension) performed in R3.5.1.

Finally, to reduce the number of possible traits observed in the PCA, we performed a linear correlation across all traits. The outcome helped us to (a) validate our non-invasive method with other traditionally invasive parameters and metabolites and (b) determine the collinearity among traits for identifying the most representative traits of the water deficit response. For better visualization of the results, we created a correlation matrix and two scatter plots (Fig. III.11c and 13-16). The correlation matrix was constructed based on Pearson correlation coefficients, which is represented by circles with different intensity colours and sizes, blue (positive) or red (negative) (Fig. III.11c). Similarly, we prepared four scatter plot matrices from the most correlated traits that included sloped linear regressions, Pearson correlation coefficients and significance (Fig. III.13-16). We found that canopy height had the strongest positive correlation with aerial biomass and leaf length, with an  $r$  of 0.99 and 0.98 ( $P^{***} \leq 0.001$ ), respectively (Fig. 11c and 13). The correlation of canopy height versus RWC was also positive ( $r = 0.88$ ,  $P^{**} \leq 0.01$ ), showing that this non-invasive parameter integrated both the growth and

water status of the plants. Canopy height was positively correlated with  $\Phi_{Po}$ ,  $\Phi_{PSII}$  and  $\Phi_P$ , and negatively with  $\Phi_{NPQ}$ , APX and POX, several AAs and PAs, except for Cit and Spd (Fig. III. 11c and 13-15). Interestingly, these two compounds showed a very different response compared to the rest of the metabolites and presented a significant correlation each other ( $r = 0.77$ ,  $P^* \leq 0.05$ ) (Fig. III.16). Besides, Cit showed linear correlation with the antioxidant enzyme APX ( $r = 0.72$ ,  $P^* \leq 0.05$ ). Another phenotype-derived trait, the slope of the curves, did not show any linear correlation with the morphometric traits related to canopy height, and was directly correlated with  $\Phi_{PSII}$  ( $r = 0.92$ ,  $P^{**} \leq 0.01$ ) and inversely with  $\Phi_{NPQ}$  ( $r = 0.97$ ,  $P^{***} \leq 0.01$ ) (Fig. III.14). These results suggested that the slope or plant water turgor was influenced by the light intensity and showed that the side-view traits of canopy height and slope provided additional useful information for studying and understanding the water stress response of barley populations. Altogether, we showed that the use of canopy height and its derived traits are a good approach to analysing the growth and water status of barley populations and, in combination with other markers such as the fluorescence parameter  $qP$  and the content of Cad and Cit, it could provide enough information for understanding the water stress response and recovery capacity in barley plants from the cultivar Golden Promise.

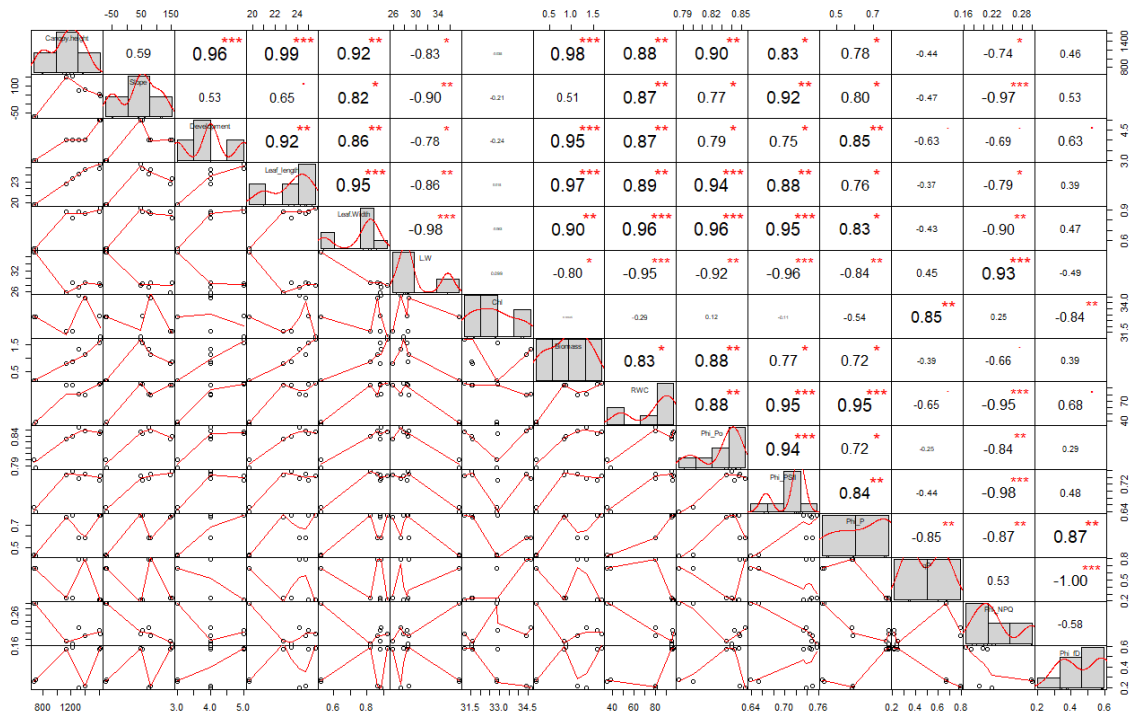


Figure III.13. Scatter plots of the correlation between canopy height, slope, morphometric parameters, RWC (%), chl and fluoresce related traits undertaken in R3.5.1.

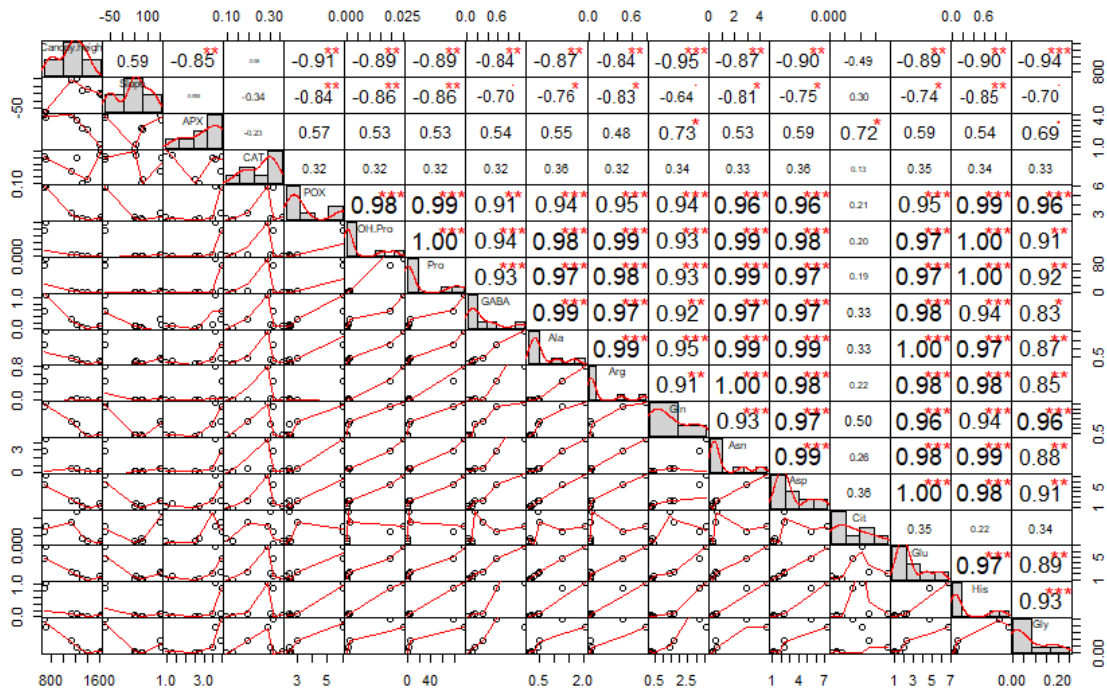


Figure III.14. Scatter plots of the correlation between canopy height, slope, the activity of CAT, POX and APX, and some AAs undertaken in R3.5.1.

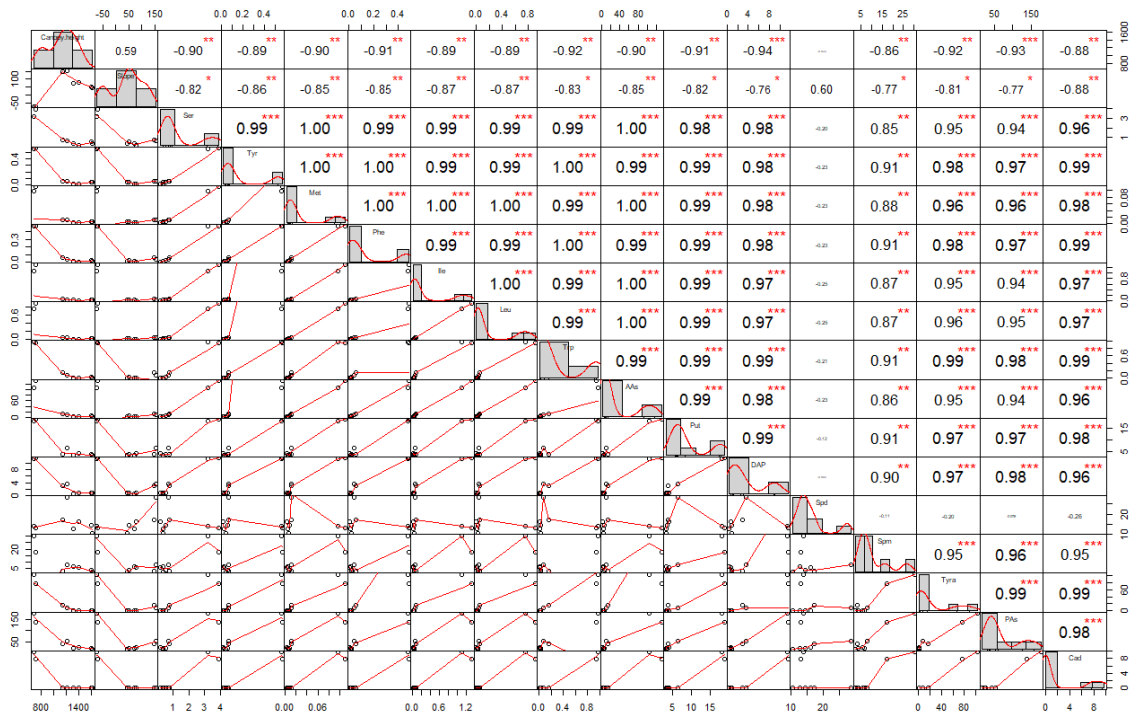


Figure III.15. Scatter plots of the correlation between canopy height, slope and some AAs and PAS undertaken in R3.5.1.

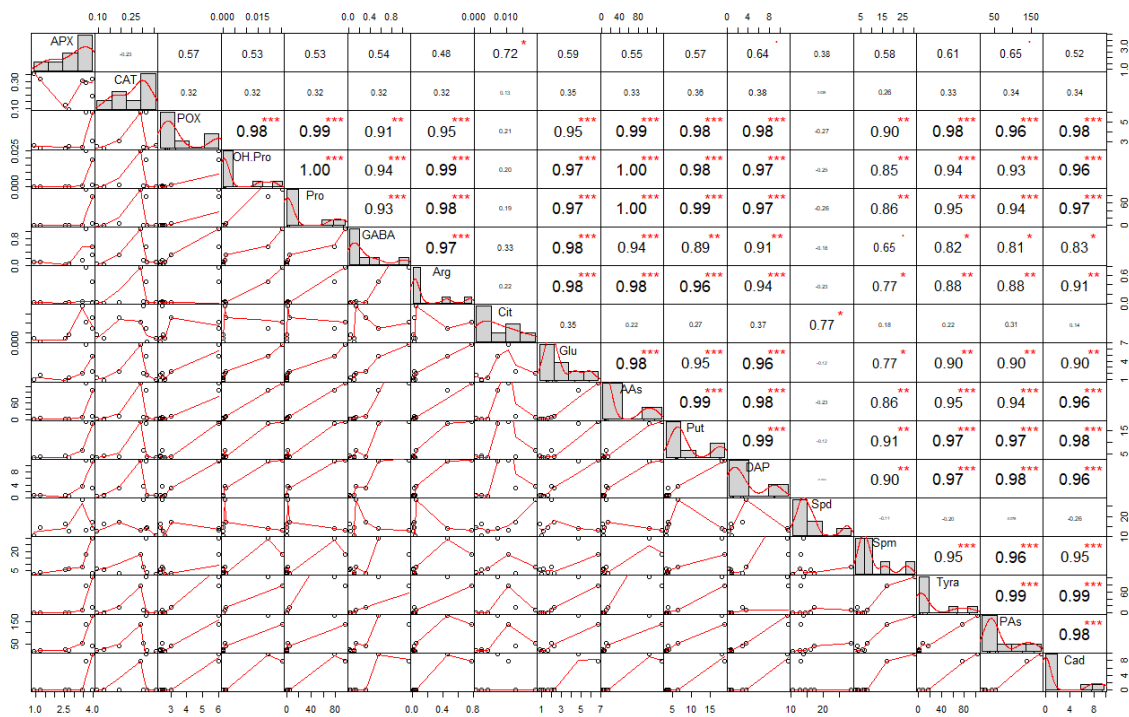


Figure III.16. Scatter plots of the correlation between the activity of CAT, POX and APX, Pro, OH-Pro, GABA, Arg, Glu, Cit and PAS undertaken in R3.5.1.



### III. IV. Discussion

Indoor phenotyping methods enable the evaluation of various traits from a large number of plants in a fast and non-invasive manner. Routinely, experiments are performed in controlled conditions mimicking environmental conditions. However, an effective translation of indoor simulations to what plants experience in the field is not straight-forward because of the complexity and variability of the field conditions, which complicate data analysis and interpretation (Araus and Cairns, 2014). As reviewed by Poorter et al. (2016), it is necessary to develop new protocols that can adjust growth conditions to be closer to field conditions. A common problem is the use of high relative humidity (RH) in protocols for studying water deficit (Junker et al., 2015; Nosalewicz et al., 2016), whereas in the field water stress is frequently associated with low RH values. We have optimized our method for studying water deficit in barley at a RH of 40%, which is closer to real conditions and thus accelerates the stress response. Another limitation in the translation from the laboratory to the field is the method of growing the plants in different spatial conditions. Indoor phenotyping traditionally analyses the plant growth in individual pots (Cabrera-Bosquet et al., 2016; Honsdorf et al., 2014; Poorter et al., 2016), whereas in the field plants grow to form a canopy, competing with neighbours for above- and below-ground resources. To form the canopy, in our method we planted 50 barley seedlings in the same plastic container (Fig. III.1), reaching a final density of 1000 plants  $\text{m}^{-2}$  instead of the 20–50 plants  $\text{m}^{-2}$  normally used in indoor phenotyping (Poorter et al., 2016). When plants are grown in individual pots, image analysis allows to dissect plants as individuals, because they are not masking each other (Chen et al., 2014; Honsdorf et al., 2014). Plants grown in a dense canopy overlap the leaves making almost impossible to extract projections of single plants. We overcame this by analysis of whole canopies instead of individuals. Using side-view RGB images and developing a software routine we can estimate the projected canopy height of the barley population (Figs III.1 and 5). This provided indirect information about several invasive parameters, such as biomass, leaf length and width and RWC (Fig. III.11 and 13-15), which are important manually measurements for studying barley populations in water stress conditions. Chen et al. (2014) previously described a similar phenotyping setup with a water stress phase

followed by a re-watering phase. They also showed that the plant height was highly correlated with the destructive measured shoot biomass. However, they evaluated single plants and used very sophisticated and expensive sensors such as FluorCam and NIR. To our knowledge, our indoor phenotyping approach is the first that uses projected canopy height in populations, representing overall growth conditions that are more similar to those that plants experience in the field, especially when compared to single pot-single plant studies. Besides, we also showed that from each obtained canopy height curve is possible to extract more traits such as the slope of the obtained line for the water stress and recovery period (Fig. III.5 and Table III.3). In addition, a simple and cheap RGB camera is enough to analyse the population canopy height, making this phenotyping method adaptable to other commercial or home-built systems.

The reliability and repeatability of the method was validated by two independent experiments under control conditions (Fig. III.2), and under water deficit with subsequent rewatering in randomly distributed trays (Fig. III.3 and 4), showing similar behaviours for 45 analysed traits and metabolites (Fig. III.4-11). Regarding fluorescence-related traits (Fig. III.7), water stress reduced the total Chl content in barley seedlings (Fig. III.9f) and the maximum quantum yield in the dark- and light-adapted stages  $\Phi_{P_0}$  and  $\Phi_{PSII}$ , and increased the regulatory and non-regulatory dissipation processes reflected in  $\Phi_{NPQ}$  and  $\Phi_{f,D}$  respectively to ameliorate photoinhibition and protect the photosynthetic apparatus (Xu et al., 1999). Similar observations have been reported in many studies of the water stress response of barley (Filek et al., 2015; Li et al., 2006). However, we observed that whereas some parameters changed in parallel with the projected canopy height, others changed at a later stage. For example, the decrease in  $\Phi_{PSII}$  happened at the end of the water stress period (Fig. III.7b), as observed by Berger et al. (2010), disabling it as a possible marker of early water stress response in barley. However,  $qP$  was a fast response fluorescence parameter (reduced from day 5) (Fig. III.7c) and positively correlated to Chl (Fig. III.13). Optimal utilization of photochemical energy in carbon metabolism is characterised by high  $qP$  values. When light absorption exceeded the requirement by carbon metabolism, the  $qP$  declines. Thus, it serves as a good indicator of “light stress” (Gallé and Flexas, 2010). However, the fluctuations of this parameter has been described as cultivar dependent at least in wheat (X. Wang et al., 2016). Altogether, these results suggested that under our growth conditions the

water stressed plants might suffer photoinhibition and that  $qP$  could be a good trait for estimating the photosynthetic status of barley plants during water stress conditions and subsequent recovery.

Water deficit increases the production of reactive oxygen species (ROS) in plants that stimulate antioxidant enzymes to counteract the oxidative damage and detoxify ROS. Similarly, in our work the barley seedlings increased the antioxidant enzyme activity of CAT and POX in stressed plants compared with the controls (Fig. III.9g and h). However, APX only increased significantly after the rewatering. It has been described that APX enhanced tolerance under water deficit in many plant species, but the increased expression of APXs varied in different developmental stages, among species and type of stress (reviewed by Pandey et al., 2017). Another study demonstrated that a simple pre-treatment with a stressor can induce an increase in the activity of this enzyme, protecting the plants against future stress events, process traditionally called hardening (Hsu and Kao, 2007). These assumptions suggested that the high APX activity in the stressed plants after recovery could be related to the developmental stage (4th leaf, Fig. III.5) and/or a fast mechanism to reduce ROS.

Another strategy of plants to cope with water stress is the synthesis and/or accumulation of compatible solutes (e.g. amino acids), which can be involved in ROS scavenging and/or perform as signal molecules (Urano et al., 2010). As revealed by metabolite profiling, most of the AAs accumulated in barley under water stress conditions (Fig. III.10), especially Pro and OH-Pro. Pro was described in 1972 (Singh et al., 1972) as a useful marker for screening the physiological status of plants grown under water deficit conditions. In our work, even when the rewatered plants recovered their RWC, they maintained both Pro and OH-Pro levels above the control values (Fig. III.10). This was already described in barley (Reddy et al., 2004), as well as in other species (De Diego et al., 2013; Zhang et al., 2018). It is worth mentioning that Cit was the only AA that kept increased levels after rewatering (Fig. III.10). Although there are only few works reporting the possible role of Cit in the plant stress response, Akashi et al. (2001) demonstrated that Cit was more effective hydroxyl radical scavenger than other compatible solutes such as Pro or Mannitol and it can effectively protect DNA and enzymes from oxidative injuries. Thus, Cit could accelerate

the recovery of the stressed plants by reducing the stress-induced oxidative damage, being an interesting metabolite for evaluating acclimation to water stress in barley (Fig. III.10).

Regarding PAs, although Put, Spd and Spm are usually accumulated under stress conditions (Podlešáková et al., 2019). However, in our study Cad, DAP and Tyra were the major contributors to the water stress response and recovery in barley (Fig. III.10). In fact, DAP and Tyra remained at higher levels in the stressed plants even after rewatering. The conversion of Spd to DAP is a stress response that can control ROS (Bitrián et al., 2012; Liu et al., 2015). DAP accumulation during water deficit and recovery could also be a mechanism for modulating membrane electrical and ion transportation properties and for controlling stomata closure, counteracting the action of ABA (Jammes et al., 2014). Cad is synthesized by an independent pathway through lysine catabolism, and its accumulation has been reported in other species under stress conditions (Jancewicz et al., 2016). Although the role of Cad in the stress response is still unclear, it has been recently shown that Cad displays anti-senescence activity (Tomar et al., 2013), suggesting that it is another important ROS-modulating compound and possible plant growth regulator (Jancewicz et al., 2016). Concerning Tyra, there are few studies showing its accumulation in plants under stress (Aziz et al., 1999; Lehmann and Pollmann, 2009). Aziz et al., 1998 have shown that Tyra can regulate Pro production. In our study by highly significant correlation ( $P^{***} \leq 0.001$ ) existed between Put, DAP, Tyra or Cad and Pro (Fig. III.16), result that supported the existence of a relevant crosstalk between PAs and Pro regulating plant stress response (Podlešáková et al., 2019). In addition, the results obtained in correlation matrix suggested that quantification of either PAs or AAs might be enough to characterize the level of stress in this barley genotype under water stress and recovery.

### **III. V. Conclusion**

In conclusion, we have designed, optimized and validated a non-invasive image-based method for automated high-throughput screening of potential water stress tolerance phenotypes using projected canopy height in barley. Using multivariate statistical methods we have also identified new metabolites involved in stress response and recovery using a highly

tolerant cultivar. As shown here, projected canopy height is sensitive trait that truly reflects other studied morphological and physiological parameters and metabolites. It represents very informative, simple and robust trait that does not require expensive sensor and hence is suitable to be used in low-cost systems using single RGB imaging. It can be also seen as easy-to-understand and self-speaking trait, since the reduction of plant growth and loss of turgor are traditionally traits to characterize the water stress response of the plants. Besides, we demonstrated that the simple analysis of canopy height combined with quantification of AAs or PAs bring enough data to define the plant stress strategy. For this reason, our method can be used to study the mechanisms involved in the water deficit response and recovery capacity of crops such as barley. We believe that it has high potential to be integrated into breeding programmes for fast screening and identification of stress-tolerant genotypes under different individual or combined stresses and/or the identification and testing of priming agents with potential to mitigate the adverse stress effects.

**CHAPTER IV: Dissecting the cytokinin-  
mediated tolerance of plants to water stress  
using an integrative approach combining  
phenotyping and metabolomics**

## IV. I. Introduction

The reduction in water availability, due to the increase in the frequency and severity of extreme climatic events (Dai, 2013), threatens the agricultural production worldwide. Water deficit impacts negatively in crop physiology and productivity. For that, the selection and cultivation of water stress-tolerant lines is essential. Besides, the study of the physiological basis of the stress tolerance mechanisms in the high tolerance genotypes is needed for a better understanding of these biological processes to ensure food production in a sustainable manner. The timing and characteristics of the episodes of water deficit during the crop cycle may have different yield penalties. Many studies have focused on the effects of water scarcity during the early stages of vegetative development because at this point crucial processes are occurring, for instance seedling establishment and later on the change of the identity of the shoot meristem to the inflorescence meristem (Saini and Westgate, 1999) and barley is not an exception. However, being barley one of the crops with the highest tolerance to salt stress, water deficit and high temperature at late sowing can cause negative impacts on the spike development, plant growth and grain yield (Hossain et al., 2012).

All the developmental stages of the plants are orchestrated by several phytohormones, which crosstalk and activate signals to regulate a broad number of physiological responses. In particular, the role of cytokinins (CKs) in many biological processes including the regulation of sink/source relationships (Roitsch and Ehneß, 2000; Werner et al., 2008), nutrient uptake (Criado et al., 2009; Sakakibara, 2006), leaf senescence (Jordi et al., 2000; Marchetti et al., 2018; W. W. Wang et al., 2016) and response to abiotic stress (Bielach et al., 2017) has been well documented. In the latter, the modification of CK homeostasis through either upregulation of their synthesis or downregulation of their degradation has shown positive effects on water stress tolerance and recovery capacity in several species (Rivero et al., 2007; Zhang et al., 2010) including crops such as rice (Peleg et al., 2011), maize (Décima Oneto et al., 2016) and barley (Pospíšilová et al., 2016). Many of these approaches are based on the delay of the stress-induced senescence by increasing the endogenous CK content in the plant. One of the explanation can be due to the positive influence of CKs in the photosynthetic performance of the plants and the modification of the

sink/source relationships (Peleg and Blumwald, 2011), which allow the extension of the vegetative period of growth. However, what are CK related mechanisms for delaying plant senescence and those that confer plant water stress tolerance and recovery remain still unclear. Besides, as CK is a negative regulator of root growth and branching, many studies have also focused on strategies to decrease CK content in roots to modify root morphology, S:R ratio or total biomass (Pospíšilová et al., 2016; von Wirén et al., 2018). These authors have pointed out the crucial role of cytokinin oxidase/dehydrogenase (CKX), as being the main enzyme responsible for the irreversible degradation of CKs, and hence a key regulator in the final pool of active hormone. Barley genome includes eleven CKX genes with time and tissue-specific expression, among which *HvCKX2.2* and *HvCKX9* are highly expressed during the reproductive organ formation and the latest stages of leaf development, respectively (Mrízořa et al., 2013).

However, the water stress response of the plants is not only regulated by CKs. Rather than the single action of a particular hormone, the total outcome of the stress response is given by the balance and crosstalk among CKs and the rest of the phytohormones (Peleg and Blumwald, 2011). Water stressed plants are characterized by an increase in the abscisic acid (ABA)/CK ratio due to the increase in ABA biosynthesis and reduction of CKs (Pospíšilová et al., 2005), but also changes in the levels of auxins (AUXs) (Salopek-Sondi et al., 2017).

CKs as sink/source regulator have been described to modify the C and N metabolism, and for that the amino acid content of the plant (Saiz-Fernández et al., 2017; Sakakibara et al., 2006). Besides, the amino acid glutamine has been identified as modulator of CKs pathway (Kamada-Nobusada et al., 2013; Sakakibara, 2006). It has been also described that the accumulation of several amino acids, especially those one related to glutamate metabolism including Gln, is another strategy that the plants use as defence against the stress and for a following recovery (Saiz-Fernandez et al. 2017, De Diego et al. 2013, 2015). However, how the CKs and the amino acid metabolism are linked to regulate water stress response is still unknown.

The objective of this chapter was to evaluate the role of CK in the water stress tolerance response in barley. For this purpose, we analysed the effect of the down-regulation of two different isoforms of CKX on barley plants growing under well-watered or water deficit conditions. Six independent transgenic lines with silenced *HvCKX2.2* and *HvCKX9* genes, prepared



using RNAi-based silencing technique, with the same yield as wild type (wt) (see M&M section) were evaluated. We applied the method optimized in the chapter III to identify the different behaviours of the lines to water stress and recovery. We also studied the relationship between CKs and other plant hormones; AUXs and ABA, and several molecules involved in the Glu metabolism, including polyamines, to go deeper in the knowledge whether CKs and their metabolism crosstalk with them for regulating plant stress response and recovery in barley.

## IV. II. Materials and Methods



### IV. II. I. Preparation of silencing lines

#### IV. II. I. I. Construction of RNAi interference vectors for silencing *HvCKX2.2* or *HvCKX9* genes

Two constructs generating hairpin RNA structures (hpRNA) were prepared to silence either *HvCKX2.2* (HORVU3Hr1G027430) or *HvCKX9* (HORVU1Hr1G057860) gene. For both cases, the target sequence was designed in the 5' end of the open reading frame (ORF) and 3'untranslated region (3'UTR) of the gene. We selected the 3'UTR region to avoid silencing of other *HvCKXs* genes. For *HvCKX2.2*-RNAi construct preparation, we synthesized the target sequence (196 bp) bordered by the *Sall* and *NotI* restriction sites on the 5'end and 3'end respectively (Fig. IV.1). In the case of *HvCKX9*-RNAi, the fragment of the gene (244 bp) was bordered by *DraI* and *XhoI* restriction sites on the 5'end and 3'end respectively (Fig. IV.2).

```
5'- g tcgacGCCGACCAGGCCGGGTGGGAGAAGAAGCACTTCGGTCCGGCCAAGTGGGCCAGGTTCGT
GGAGCGGAAGAGGAAGTATGACCCAAGGCGATTCTGTCCCGTGGTCAGAGAATTTTCACCTCCCCGCT
GGCTTGATCACGAAGTTAATCGATTGGCCCCGAGTCCCCGACCTAGCTACTAGAGAA/CTAGAGAGGG
Agc ggccgcg - 3'
```

**Figure IV.1.** Target sequence used for the design of the silencing cassette of *HvCKX2.2* (*MLOC\_81291* or *HORVU3Hr1G027430*). The blue arrow indicates the restriction site for *Sall* and the red arrow the one corresponding to *NotI*.

5' - ttt  aaaGGTGGGACGCATTTCAACAGAGGAAAAACACCTATGACCCCCTGGCAATCCTAGCTCCAGGA  
 CAGAAAATATTTCAAAAGAAACCAGCATCACTACCCTTGTCTCGTTACAGTACCTACTGtaaAAAATATA  
 TATGTGGAGCAATATGTCTATGTTAGTATGGAAGTATAGTCGCTTTGCAAAAGATAACGAACTGCAGCG  
 TGAAGAACACTGTACAGAGTAGTGACTATTAGTAGTGGTGATcc  tcgagg - 3'

**Figure IV.2.** Target sequence used for the design of the silencing cassette of *HvCKX9* (*MLOC\_11021* or *HORVU1Hr1G057860*). The green arrow indicates the restriction site for DraI and the orange arrow the one corresponding to XhoI.

Firstly, the specific synthesized fragment was assembled into the high-copy number vector pMA (GeneArt, Thermo Fischer Scientific, Waltham, United States). Then, it was subcloned into the Gateway™ Entry Vector pENTR1A, through the specific restriction sites presented in each of the synthesized fragments (Sall and NotI for *HvCKX2.2* and DraI and XhoI for *HvCKX9*).

Finally, the resulting entry clone was used to transfer two copies of the target gene in the antisense and sense directions at the 5' and 3' ends of the Gateway™ Destination Vector pBract207 (Fig. IV.3, provided by John Innes Centre, Norwich, United Kingdom), downstream of the maize ubiquitin-1 promoter via Gateway LR recombination reaction (Invitrogen, Carlsbad, CA, United States). The final silencing cassettes contain the Hygromycin (hyg) phosphotransferase (hpt) gene (conferring hyg resistance) driven by the Cauliflower mosaic virus (CaMV) 35S promoter at the left border (LB); and the terminator of the nopaline synthase (nos) gene adjacent to the right border (RB) (Fig. IV.4).

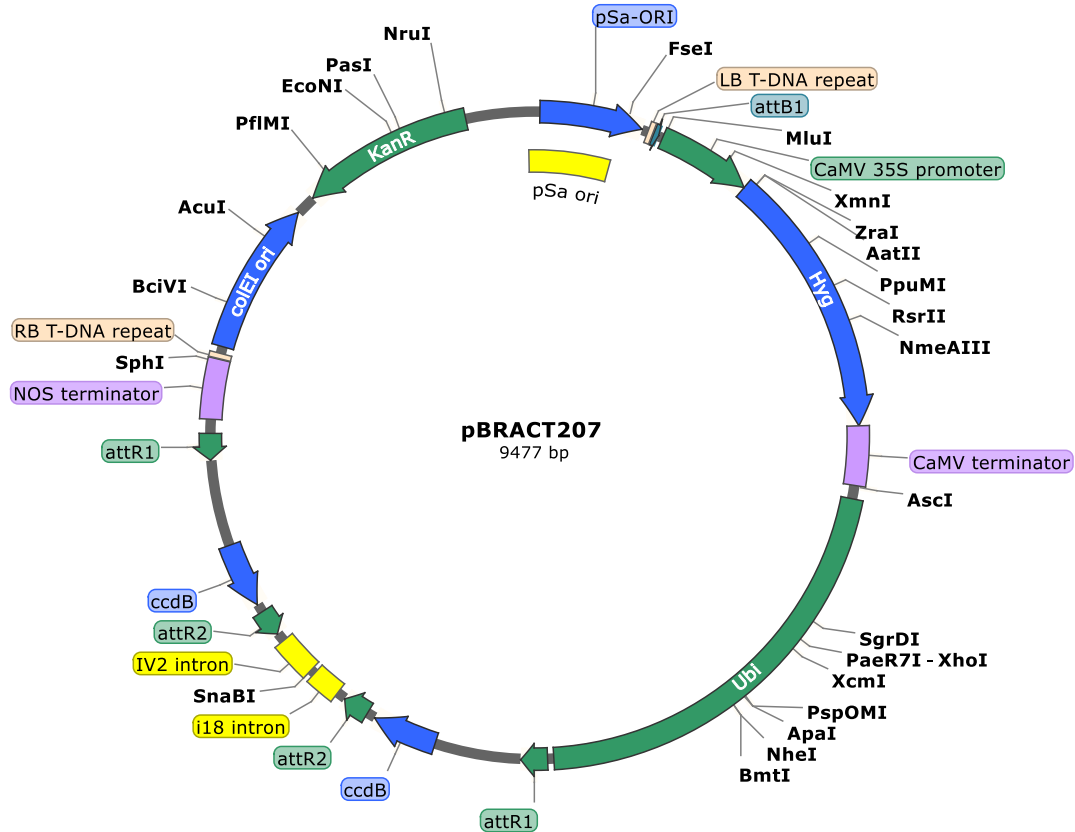


**Figure IV.3.** Map of the vector pBract207. Arrows denotes the gene and promoter orientation.

The resulting plasmids were named HvCKX2.2-RNAi and HvCKX9-RNAi. Both vectors were sequenced (SeqMe, Czechia) to confirm the right orientation of both copies of the targeted gene and then electrotransformed into *Agrobacterium tumefaciens* strain AGL1 together with the helper vector pSoup. *A. tumefaciens*. containing the final construct was mixed with glycerol in ratio 1:1 (50% solution, v/v) and stored at  $-80^{\circ}\text{C}$ .

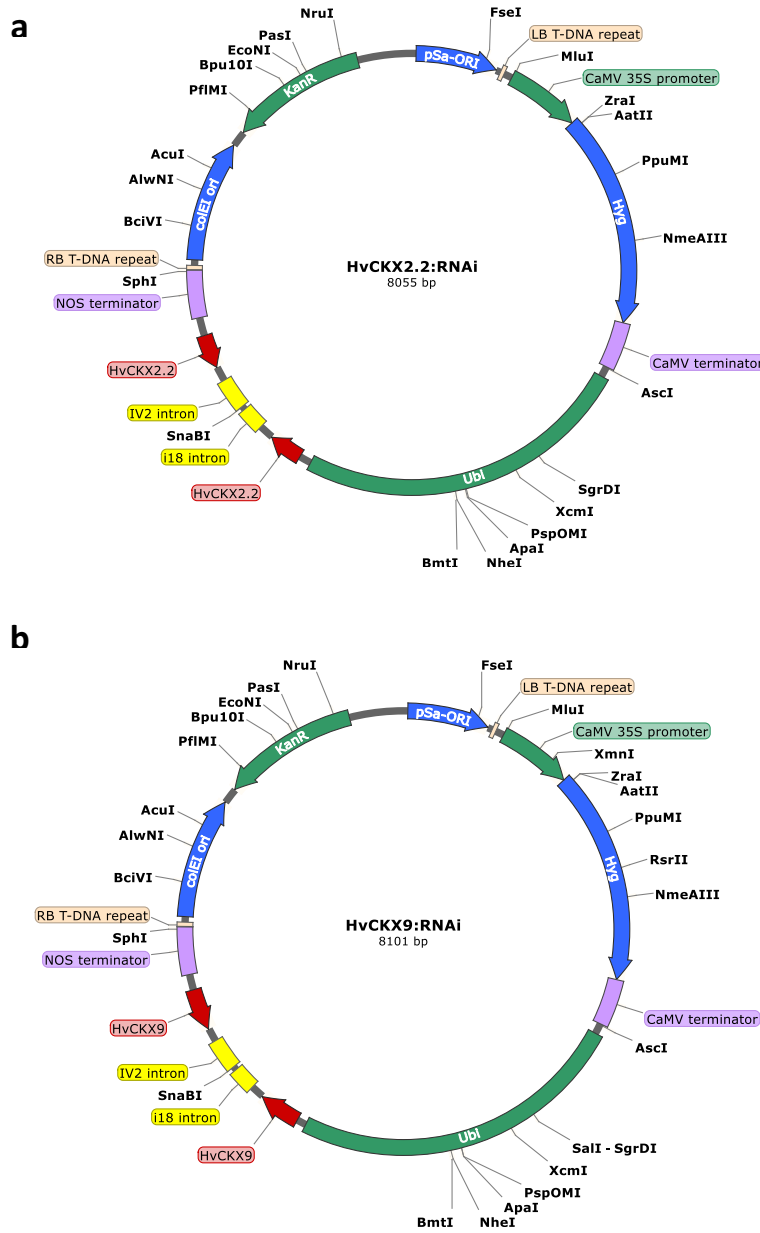


**Figure IV.4.** Map of the final vectors (a) HvCKX2.2-RNAi and (b) HvCKX9-RNAi. Arrows denotes the gene and promoter orientation.

#### IV. II. I. II. Growth conditions of the donor plants used for transformation

Plants of the spring barley (*Hordeum vulgare* L.) cultivar Golden Promise were germinated on 2L pots filled with a mixture of 94% peat mix substrate (Gramoflor GmbH & Co. KG, Germany)

and 6% perlite (Perlit Ltd., Czech Republic). Plants were cultivated in a growth-chamber set to simulate a long day, with a regime of 18:16 °C, 16: 8 h, light: dark photoperiod, and a relative humidity (RH) of 60%. The light source was a combination of low-pressure mercury discharge lamps and sodium lamps providing a photosynthetically active radiation (PAR)/ light intensity of ca. 300  $\mu\text{mol photons m}^{-2} \text{s}^{-1}$ . Plants were fertilized with 6 g of YaraMila Complex (YARA Agri Czech Republic, Czech Republic) containing: 12% N (5% nitrate), 11%  $\text{P}_2\text{O}_5$ , 18%  $\text{K}_2\text{O}$ , 2.7%  $\text{MgO}$ , 20%  $\text{SO}_3$ , 0.015% B, 0.2% Fe, 0.02% Mn and 0.02% Zn.

#### IV. II. I. III. *Agrobacterium* - mediated transformation of barley immature embryos

Transgenic barley plants were prepared according to Harwood et al. (2009) using *A. tum.*-mediated transformation of immature embryos. Briefly, barley spikes were collected when they were still immature and the diameter of the embryo was 1.5–2 mm. The seeds were surface-sterilized, the immature embryos isolated from the seeds and the axis removed. The embryos were then placed scutellum side up on callus induction medium (CIM) overnight at 26 °C. After that, they were inoculated with 400  $\mu\text{l}$  of *A. tumefaciens*. suspension bearing the desired vector (HvCKX2.2-RNAi, Fig. IV.4a or HvCKX9-RNAi, Fig. IV.4b) and then placed scutellum side down on the CIM mentioned, but in this case supplemented also with 200  $\mu\text{mol l}^{-1}$  acetosyringone. They remain in darkness for 3 days at 26 °C and after that they were transferred to CIM containing 150  $\text{mg l}^{-1}$  Timentin® and 50  $\text{mg l}^{-1}$  hyg (Roche). The embryos were transferred to the same fresh media every two weeks and then and always kept in darkness. Once the calluses were formed, they were transferred to a transition media supplemented with 5  $\text{mg l}^{-1}$  2, 4-dichlorophenoxyacetic acid, 1  $\text{mg l}^{-1}$  BAP, and 50  $\text{mg l}^{-1}$  hyg and placed into a growth chamber set to simulate a long day, with a regime of 24/22 °C, 16/8 h light: dark photoperiod and a light intensity of 80  $\mu\text{mol m}^{-2} \text{s}^{-1}$ . After two weeks in this grown conditions, they were transferred to regeneration media containing 50  $\text{mg l}^{-1}$  hyg and placed into a growth chamber with the setup and a light intensity of 160  $\mu\text{mol m}^{-2} \text{s}^{-1}$ . Those calluses that developed shoots were finally transferred to CIM containing 50  $\text{mg l}^{-1}$  hyg and kept in the same aforementioned light conditions until they developed proper root system. The obtained transformants were placed into soaked

jiffy pellets (A/S Jiffy Products, Norway) and acclimatized using the same conditions as during the regeneration phase. After additional two weeks, they were planted into soil, at the same conditions mentioned for the growth of wt donor plants.

All obtained transgenic lines were screened for the presence of sense and antisense components of the silencing cassette in T0, T1, and T2 generation. For this purpose, gDNA was extracted from barley leaves according to Edwards et al. (1991) and both copies of the silencing cassettes were amplified using GoTaq polymerase (Promega) with specific primers (Table IV.1). The PCR conditions were 95 °C for 2 min; then 30 cycles of 95 °C for 30 s, 65/59 °C for 30/45 s (sense/antisense), 72 °C for 1 min, followed by final extension of 72°C for 10 min. The products were assessed by agarose gel electrophoresis. The 1 kb Plus DNA marker was used for determination of the amplicon size (Thermo Fischer Scientific, Waltham, MA, United States). Products of a 422 bp and 259 bp indicated the presence of sense and antisense component of the silencing cassette of *HvCKX2.2* and 207 bp and 485 bp of *HvCKX9* (see Table IV.2).

To determine the inheritance of the RNAi construct and the phenotype, transgenic lines were allowed to self-pollinate, and segregation analyses were performed in the T1 and T2 generations by means of PCR.

#### IV. II. I. IV. Assessment of DNA Ploidy

Flow cytometry was used for the determination of the DNA ploidy levels of the obtained transformants, by evaluation of the relative fluorescence intensities of PI-stained nuclei. The extraction of nuclei and the analysis of data was performed as described by Holubová et al. (2018).

#### IV. II. I. V. Copy number determination: Southern Blot analysis

We also determined the number of T-DNA insertions in the silencing lines by DNA Southern hybridization, using genomic DNA extracted for the wt and transgenic barley lines. Leaves from 10 days old seedlings were grinded in liquid nitrogen and 0.2 g was

**Table IV.1.** Primers used in the PCR analysis for confirmation of the presence and orientation of the silencing cassettes.

Primer name	Sequence 5' to 3'
Ubi1_Fw sense	TGCTCACCTGTTGTTTGGTGTTAC
IV2_Fw antisense	GTAAGTTCTGCTTCTACCTTTGAT
<i>HvCKX2.2</i> stread_Fw antisense	AGGTTCGTGGAGCGGAAGAGGAA
<i>HvCKX2.2</i> stread_Rv sense	CAATCGATTA ACTTCGTGATCAAG
<i>HvCKX9</i> stread_Fw antisense	ACCTATGACCCCTGGCAATCCTA
<i>HvCKX9</i> stread_Rv sense	GTAGGTA CTGTAACGAGGACAAGGGTAG

**Table IV.2.** Primer combination used and expected size for each of the sense and antisense components of the silencing cassette.

	SET 1 <i>HvCKX9</i>	SET 2 <i>HvCKX9</i>	SET1 <i>HvCKX2.2</i>	SET2 <i>HvCKX2.2</i>
PRIMER	SC2stread_Fw	Ubi1_Fw	SC8stread_Fw	Ubi1_Fw
PRIMER	IV2_Fw	SC2stread_Rv	IV2_Fw	SC8stread_Rv
SIZE PRODUCT (bp)	207	485	422	259

extracted with 800  $\mu$ l of extraction buffer containing 0.1 M Tris-HCl (pH 8.0), 10 mM EDTA, 0.1 M NaCl and 1% (v/v) Sarkosyl. Samples were vortexed, mixed with 800  $\mu$ l phenol-chloroform-isoamyl alcohol (25:24:1) and again vortexed. After a centrifugation 3 min at 2,800  $g$  and 4 °C, the aqueous phase was collected and the DNA was precipitated by the addition of 0.1 vol of 3M sodium acetate (pH 5.2) and 1 vol of isopropanol. Samples were centrifuged for another 10 min at 19,000  $g$  and 4 °C and the pellet washed with 1 vol of 70% (v/v) ethanol followed by centrifugation for 5 min at 19,000  $g$  and 4 °C. The pellet was air dried and then resuspended in 100  $\mu$ l of TE buffer (pH 8.0) containing 40  $\mu$ g  $\mu$ l<sup>-1</sup> of RNase A (TopBio, Czech Republic). gDNA samples were incubated for 1 h at 37 °C. 30  $\mu$ g of plant genomic DNA from transgenic lines and non-transformed plants (negative control) was digested at 37 °C for 12 h with XhoI (enzyme that had unique restriction sites in the corresponding T-DNA region). As a positive control, 80 pg of

the plasmid DNA corresponding to each silencing vector were restricted with the same enzyme for 1 h and used as positive controls. Genomic DNA from regenerated in vitro wt, non-transformed, was also used as a second negative control. The digested DNA was separated by size via gel electrophoresis on 0.8% (w/v) agarose in Tris Buffer EDTA (TBE Buffer). After denaturation, the DNA was then blot-transferred to a nylon membrane (type B, Merck, Germany) and then exposed to hpt gene-specific DIG-labelled probe (PCR DIG Probe Synthesis Kit; Roche, Germany) prepared accordingly to the manufacturer's protocol. To visualize the hybridized probes we used an anti-digoxigenin antibody (anti-digoxigenin-AP, Fab fragments; Roche, Germany) conjugated to alkaline phosphatase and we detected with the CSPD ready-to-use substrate solution (Roche, Germany) and the Lumi-Film chemiluminescent detection films (Roche Diagnostics GmbH, Germany).

To verify the results obtained by Southern Blot analysis, the same selected transgenic lines were submitted to copy number analysis with the iDNA Genetics service (<http://www.idnagenetics.com>; Norwich, United Kingdom).

#### IV. II. I. VI. Real-time quantitative PCR analyses

For the qPCR analysis, RNA extraction and cDNA synthesis were performed as described previously in the chapter II section II. IV. Quantitative real-time PCR reactions contained properly diluted cDNA, 300 nM primers, 250 nM of specific 5' end 6-carboxyfluorescein (FAM) dye and 3' end 5(6)-carboxytetramethylrhodamine (TAMRA) quencher, and the TaqMan gb Easy Master Mix, supplemented with 100 nM ROX passive reference dye (Generi Biotech). The primers and probes used for the evaluation of the expression of CKX family members are the same as described by Holubová et al. (2018). The program consisted of an initial denaturation of 2 min at 95 °C, followed by 40 cycles of 15 s at 95 °C and 60 s at 60 °C, performed on a ViiA™ 7 Real-Time PCR System (Applied Biosystems). Changes in the relative mRNA abundance were calculated using the comparative  $2^{-\Delta\Delta Ct}$  according to (Pfaffl, 2001), being t0 the reference sample. The qPCR efficiency and the fold changes in gene expression were also calculated as described in chapter II, section II. II. VI.



#### IV. II. I. VII. Yield parameters

For yield determination, 30 plants from each genotype were cultivated individually in 2L pots filled with a mixture of 94% peat mix substrate (Gramoflor GmbH & Co. KG, Vechta, Germany) and 6% perlite (LBK PERLIT Ltd., Czech Republic). Plants were cultivated under controlled greenhouse conditions at 15/ 12 °C, 16: 8 h, light: dark photoperiod, 30-40% HR. The transgenic lines and the WT plants were harvested and the following yield-related traits were evaluated: number of tillers per plant, number of spikes per plant, number of grains per spike, number of filled grains per plant, weight of grains per plant, thousand grains weight (TGW) were determined.

#### IV. II. II. Non-invasive plant phenotyping

##### IV. II. II. I. Plant material, growth conditions, experimental setup and assay conditions

Barley seeds from wt and transgenic lines were surface-sterilized and germinated as described in chapter III, section III. II. I. and then the assay was set up as indicated in the section III. II. II. I.

##### IV. II. II. II. Imaging acquisition

Plant Screen™ System was used to determine RGB- side view and FluorCam Top view derived traits as described in chapter III, section III. II. II. II. Different Traits such as canopy height and slope of the line, and fluoresce derived parameters were thus determined for all the genotypes. Moreover, we calculated the electron transport rate (ETR) as:

$$\text{ETR} (\mu\text{mol e}^- \text{m}^{-2} \text{s}^{-1}) = \Phi_{\text{PSII}} \times \text{PPDF} \times 0.84 \times 0.5$$

where,

PPDF was 320  $\mu\text{mol photons m}^{-2} \text{s}^{-1}$ , 0.84 represents the average value of incident photons absorbed by the photosynthetic pigments of the leaf, and 0.5 accounts for the fraction

of excitation energy absorbed by the two photosystems if there is an equal distribution of photons.

#### IV. II. II. III. Watering regime

The substrate water content (%) was calculated in each container. For this purpose, the water capacity of the used substrate was determined as also described in section III. II. II. III. All containers were watered with tap water (average conductivity c. 56 mS m<sup>-1</sup>) at 100% of field capacity after sowing. Then, the control plants were irrigated every second day to maintain 80% of field capacity until the end of the experiment. The irrigation was stopped in the water stress variant when the plants presented the first fully expanded leaf. When the substrate water content decreased to 65%, the rewatering was performed at full water capacity (100%).

#### IV. II. III. Manual parameters

##### IV. II. III. I. Biometric parameters

The aerial biomass and the developmental stage of barley seedlings, as well as the size of the youngest and fully expanded leaf were determined as described in chapter III, section III. II. IV. I. A total of five plants per genotype and variant were evaluated, at the end of the water stress period and after 4 days of rewatering.

##### IV. II. III. II. Plant water status

The relative water content (RWC, %) was measured in five individual plants per variant and genotype, at the end of the water stress period and after rewatering, as described previously in chapter III, section III. II. IV. II.

#### IV. II. III. III. Osmotic potential

The osmotic potential ( $\Psi_n$ ) (MPa) was measured in five plants per variant, after water stress and rewatering. One leaf segment (of cca. 150 mg) per plant and treatment was cut and immediately frozen in liquid nitrogen. The frozen sample was placed in a 0.6 ml Eppendorf tube located into a 1.5 ml microcentrifuge tubes and allowed to thaw. The sap was extracted by centrifugation at 15,000 *g* for 20 min, and then collected for measurement. After the conditioning of the extracts at 25 °C for 15 min, the osmolarity was determined by freezing point osmometry using a 3320 Single-Sample Micro Osmometer (Advanced Instruments, USA). The  $\Psi_n$  was calculated by Van't Hoff equation:

$$\Psi_n = -R \times T \times c_s$$

where,

R is the gas constant, T the sample temperature (K), and  $c_s$  the solute concentration (mol  $\text{kg}^{-1}$ ).

#### IV. II. III. IV. Chlorophyll content

The index of relative chl content of leaves was measured as described in chapter III, section III. II. IV. III. The last youngest mature leaf of five individual plants per genotype and treatment was measured, at the end of the water stress period and after rewatering.

IV. II. III. V. Metabolite quantification: AAs, PAs and phytohormones content determination.

For the quantification of metabolites, three independent groups consisting of five individual plants were collected per genotype and treatment after the water stress period and rewatering. The samples was immediately frozen in liquid nitrogen and then grounded by mortar and pestle using liquid nitrogen. The resulting pool from each variant was divided into three analytical replicates for quantification of all the following parameters.

For the AA and PAs analysis, 5 mg and 10 mg FW respectively of each pool were extracted and analysed according to the methodology described in the chapter III, section III. II. IV. V.

For the analysis of the different group of phytohormones: ABA, AUX and CKs, the same aforementioned pools were used. 5 mg of FW were extracted using ice-cold modified Bielecki buffer (methanol/water/formic acid, 15/4/1, v/v/v) containing isotope-labeled CK internal standards (0.5 pmol of CK bases, ribosides, *N*-glucosides, 1 pmol of CK *O*-glucosides and nucleotides). The extract was then purified using the same two SPE columns (C18 and MCX) as described in chapter II, section II. II. III.

The level of AUXs and ABA were determined using the method described by Floková et al. (2014). Briefly, the metabolites were extracted in phosphate buffer with stable isotope-labelled internal standards (10 pmol of each labelled metabolite). After centrifugation, the supernatant was immediately purified on a MAX column and evaporated to dryness prior to chromatographic analysis.

The quantification of all purified samples was performed using an ACQUITY UPLC® System and a Xevo™ 122 TQ-S triple quadrupole mass spectrometer (Waters). All phytohormones were quantified using multiple monitoring mode (MRM), targeting selected precursor ions and the corresponding product ions. The stable isotope-labelled internal standards were used as references.

## **IV. III. Results**

### **IV. III. I. Generation and selection of transgenic barley plants with silenced *HvCKXs* genes**

In order to study the effect of the down-regulation of cytokinin oxidase dehydrogenase, and the concomitant increase in cytokinin content on water stress and recovery, we evaluated two *CKX* genes, *HvCKX2.2* and *HvCKX9*, with different tissue-specific expression, the reproductive organ formation and the latest stages of leaf development, respectively. Several independent transgenic barley lines were obtained from the *A. tumefaciens* -mediated transformation of immature embryos. After the ploidy evaluation, tetraploid plants were identified and excluded,

and only diploid plants were considered. The selected transgenic plants were evaluated for the presence of the sense and antisense copy of the inverted repeats by PCR (Fig. IV.5 and 6). Only plants with both copies were selected for further analysis. Three independent transgenic lines for each silencing were propagated (self-fertilized), and they were PCR identified in each generation as described above. For the silencing of *HvCKX2.2*, the selected lines were called as 1.2, 2.9 and 19. In the case of *HvCKX9* silencing, the lines were identified as 1.8, 7.3 and 6.2. The stability of the silencing was evaluated by transgene expression on consecutive generations (data not shown).

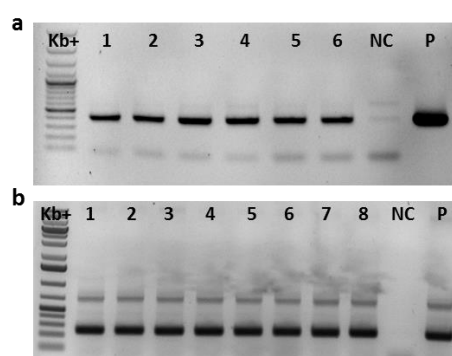


**Figure IV.5.** Example of PCR screening for the presence of sense (a) and antisense (b) components of *HvCKX2.2*:RNAi silencing cassette. Lines contain the products obtained by PCR amplification using genomic DNA as a template extracted from selected 6 plants from T<sub>0</sub> generation. DNA extracted from plants regenerated from non-transformed embryos was used as negative control (NC) and 5 ng of plasmid pBract207::*HvCKX2.2* as positive control (PC). 5  $\mu$ L of GeneRuler™ 1 kb Plus DNA Ladder was used as marker.

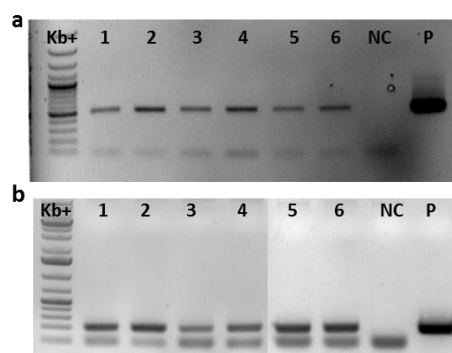


**Figure. IV.6.** Example of PCR screening for the presence of sense (a) and antisense (b) components of *HvCKX9*:RNAi silencing cassette. Lines contain products obtained by PCR amplification using genomic DNA as a template extracted from selected 6 plants from T<sub>0</sub> generation. DNA extracted from plants regenerated from non-transformed embryos was used as negative control (NC) and 5 ng of plasmid pBract207::*HvCKX9* as positive control (PC). 5  $\mu$ L of GeneRuler™ 1 kb Plus DNA Ladder was used as marker.

To determine the integration copy number, three representative plants from each independent line were evaluated on Southern Blot (Fig. IV.7). Moreover, for testing the stability of the transgene integration, the analysis was repeated in two subsequent generations. All transgenic lines presented different number of integrations. The lines 1.2, 2.9 and 19 from the silencing of *HvCKX2.2* gene presented at least 1, 10 and 4 integrations, respectively. The lines 1.8, 7.3 and 6.2 from the silencing of *HvCKX9* gene presented at least four, two and three integrations, respectively.

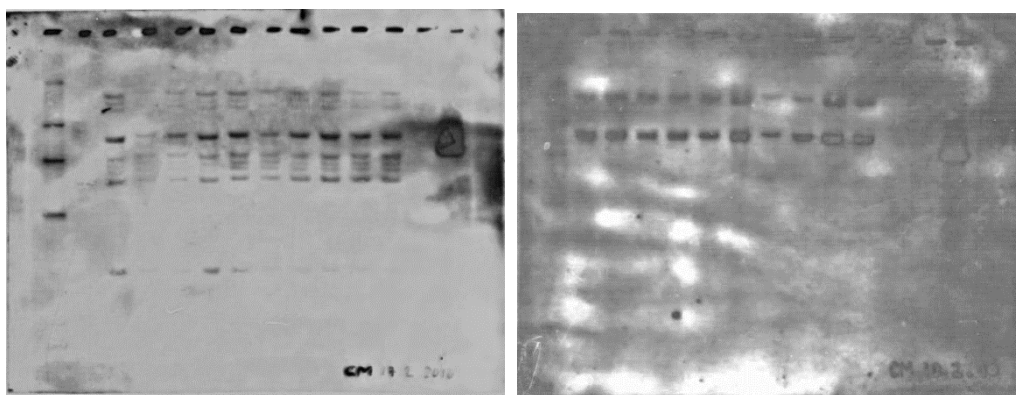


**Figure IV.7.** Example of Southern Blot autoradiography from (a) *HvCKX2.2*:RNAi line 2.9 and (b) *HvCKX9*:RNAi line 7.3.

The expression profile of the genes of interest (GOI) was evaluated in eight biological replicates from two independent transgenic lines of each silencing gene along the plant development. In the *HvCKX2.2*-RNAi lines, a decrement of *HvCKX2.2* transcript level was observed only in leaves at the first stages of development (BBCH 11, 21 and 37). In *HvCKX9*-RNAi lines, a significant reduction of the *HvCKX9* expression was observed in almost all the analysed developmental stages. After a second round of transformation, one extra line per silencing was obtained but the the gene expression pattern of these two new lines was evaluated directly in the conditions of the experiments for water stress response.

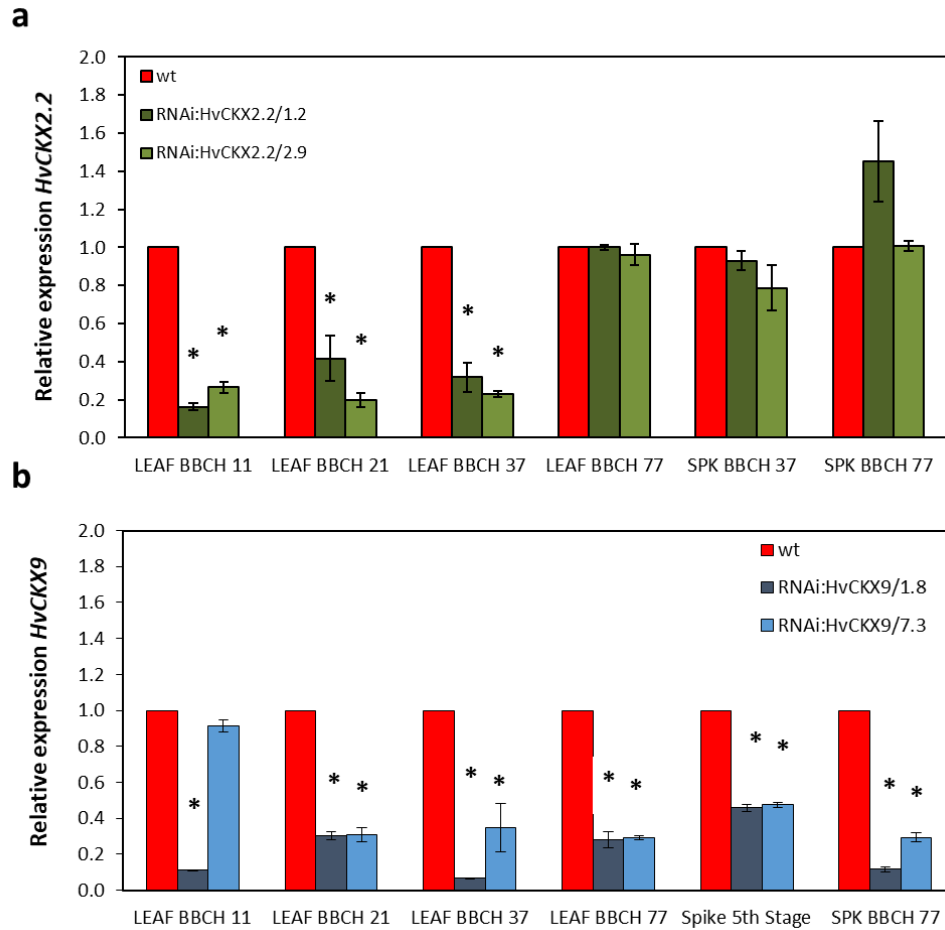


**Figure IV.8.** Expression analysis of (a) *HvCKX2.2* in RNAi:*HvCKX2.2* lines 1.2 and 2.9; and (b) *HvCKX9* in RNAi:*HvCKX9* lines 1.8 and 7.3, at different developmental stages (BBCH) and organs (leaves: LEAF; spikes: SPK).

For better selection of the obtained transgenic lines, we evaluated the final yield and compared with the wt plants. The barley plants were grown until production in a greenhouse under controlled conditions (Fig. IV.9). As results, the line19 from RNAi:*HvCKX2.2*, and the lines 1.8 and 6.2 in RNAi:*HvCKX9* significantly increased the total biomass of plants (FW, g) compared to wt. This increase in biomass was not reflected in changes in the final number of grains per plant or the TGW. There were no significant differences in the final productivity of transgenic plants compared to wt, only the line 7.3 from RNAi:*HvCKX9* had a significant increase in the TGW. Altogether, the transgenic lines did not reduced the productivity compared to wt, so we consider them suitable to be tested in our next experiments.

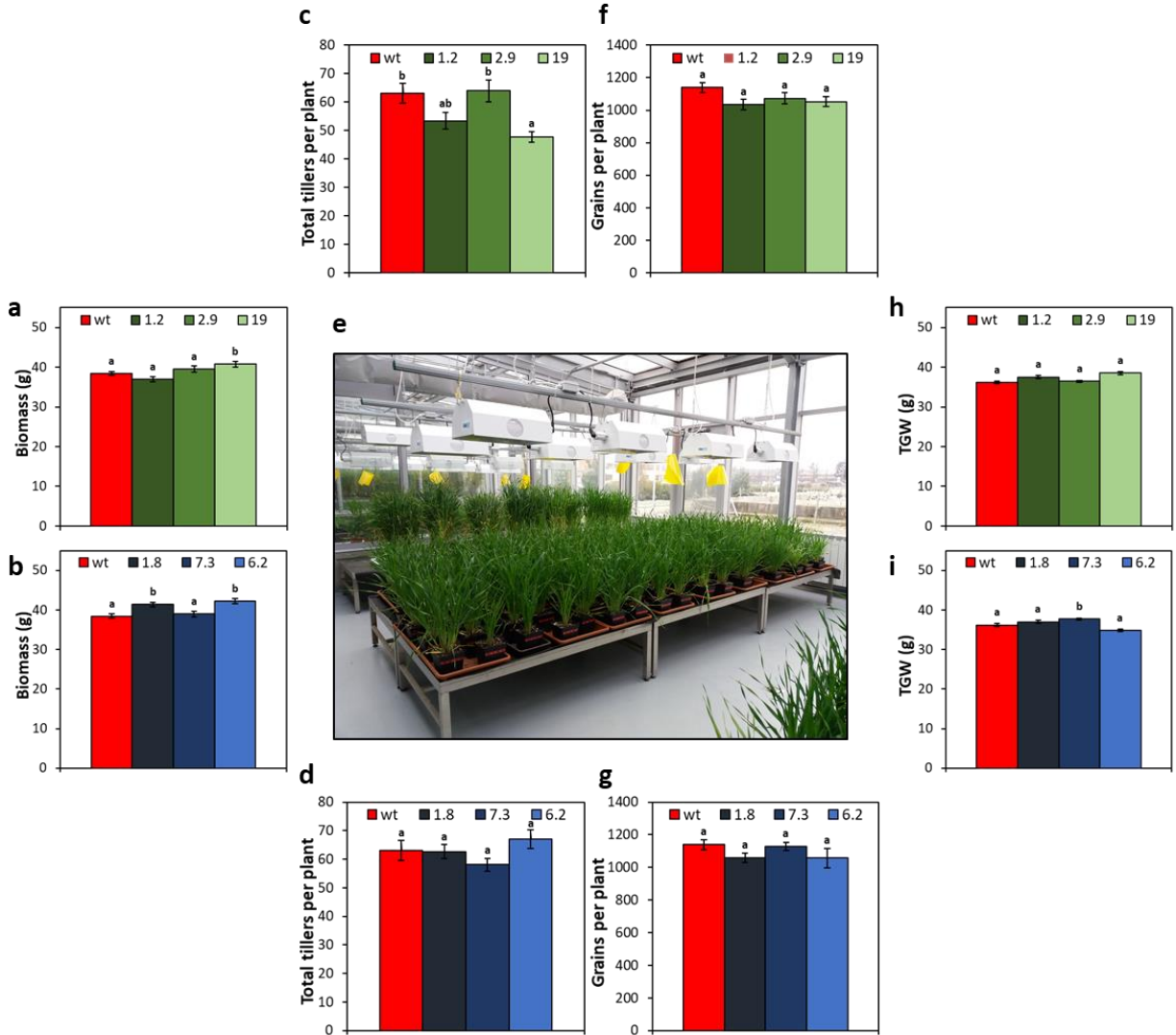


**Figure IV.9.** Yield parameters evaluated in silencing lines grown under greenhouse conditions. (a) and (b) dry biomass; (c) and (d) total tillers per plant; (f) and (g) grains per plant; and (h) and (i) total grain weight (TGW) of wild type and transgenic barley lines grown individually under e. greenhouse conditions. RNAi:HvCKX2.2 lines are represented in green, RNAi:HvCKX9 in blue and wild type values in red. Letters indicate the significant differences according to the multiple comparison test performed after the non-parametric test Kruskal–Wallis.



#### IV. III. II. Phenotyping of barley populations with altered CK homeostasis under water deficit and subsequent rewatering

To study the role of CK during the water stress response and recovery capacity in barley we used the method described in the chapter III to phenotype our generated transgenic lines. The projected canopy height was evaluated in two trays per genotype, each tray containing a water-stressed variant (D) and a well-watered variant (W) with 50 plants each, using the PlantScreen™ phenotyping platform (Photons Systems Instruments, Czech Republic) (Fig IV.10 and 11).



**Figure IV.10.** Wild type and transgenic barley plants inside the growth chamber coupled with the Plant Screen™ System.

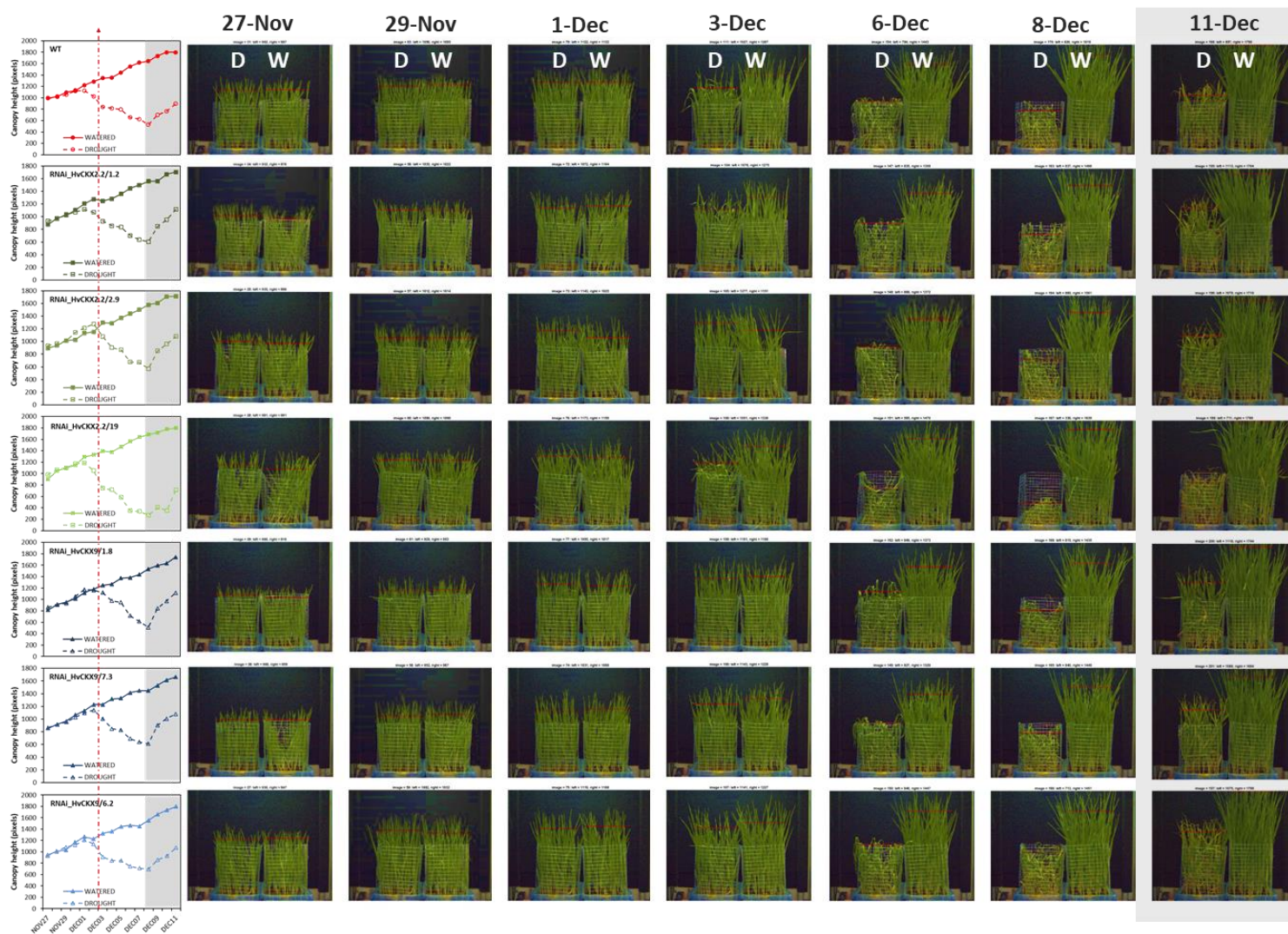


**Figure IV.11.** Dynamics projected canopy height in wild type and transgenic barley seedlings growing under water stress conditions with subsequent rewatering. (a) Changes in projected canopy height (in pixels) and (b) side view images of the D (left) and W (right) treatment along the experiment. Discontinuous and continuous lines in the figures on the left side represent D and W variants, respectively.

During the beginning of the stress period, no differences were observed in the projected canopy height kinetics between wt and transgenic plants. Between NOV 29 and DEC 01, W and D variants started to separate, and this event was genotype-dependent. For instance, some lines (e.g. RNAi:HvCKX9 6.2) stop growing early than wt, meanwhile others prolonged the growing period up to DEC02 (two additional days) (e.g. RNAi:HvCKX2.2 2.9 and e.g. RNAi:HvCKX9 1.8) (Fig. IV.11). After rewatering, the recovery of the canopy height was also genotype-dependent (Fig. IV.11). With the traits extracted from the model constructed curves from the projected canopy height (Fig. IV.12, 13 and Table IV.3) we could identify those lines with a better performance during the water stress period, and those with a better performance during the recovery. For example, after rewatering RNAi:HvCKX9 1.8 had the highest SlopeR value (rehydration) and MaxR.

**Table IV.3.** Traits related to water deficit and recovery in wild type, (a) RNAi:HvCKX2.2 and (b) RNAi:HvCKX9. Traits were extracted from the contracted line of the canopy height. Day is the day when treated and not treated plants are separated; Max is the maximal canopy height reached in the stressed plants under water stress and Slope of the line from the canopy height in the water stress period; MaxR is the maximal canopy height reached in the stressed plants after rewatering; and SlopeR of the linear curve from the canopy height in the rewatering period.

**a.**

Line	Treatment	WATER STRESS			REWATERING	
		Day	Slope	Max	SlopeR	MaxR
RNAi_HvCKX2.2/1.2	W	NOV30	50.7	1557	54.8	1704
	D		-76.5	606	162.5	1113
RNAi_HvCKX2.2/2.9	W	NOV30	64.2	1577	50.1	1710
	D		-104.4	572	162.8	1079
RNAi_HvCKX2.2/19	W	DEC01	58.3	1685	40.0	1799
	D		-134.5	271	126.5	711
WT	W	DEC01	63.1	1642	53.4	1799
	D		-80.4	529	117.0	897

**b.**

Line	Treatment	WATER STRESS			REWATERING	
		Day	Slope	Max	SlopeR	MaxR
RNAi_HvCKX9/1.8	W	NOV30	56.2	1536	65.9	1744
	D		-102.7	509	195.9	1118
RNAi_HvCKX9/7.3	W	NOV30	46.2	1448	73.2	1664
	D		-81.7	612	150.8	1080
RNAi_HvCKX9/6.2	W	NOV29	43.6	1554	81.0	1799
	D		-74.0	696	120.9	1075
WT	W	DEC01	63.1	1642	53.4	1799
	D		-80.4	529	117.0	897

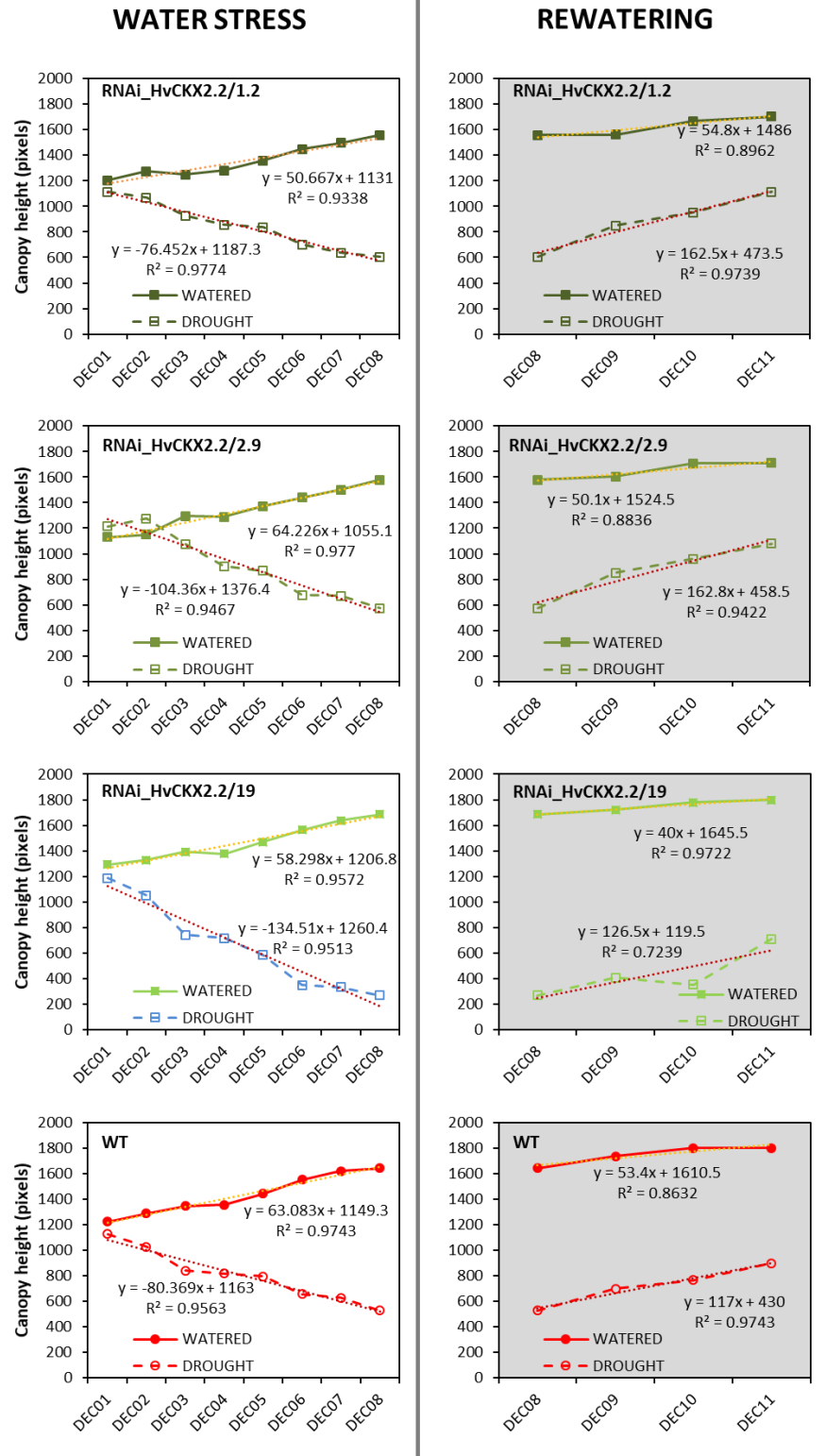


**Figure IV.12.** Line of the projected canopy height and the correspondent equation (discontinuous yellow and red line for water and water stress treatment, respectively) in wild type (red lines) and RNAi:HvCKX2.2 lines (green lines). Discontinuous and continuous lines represent D and W variants, respectively.

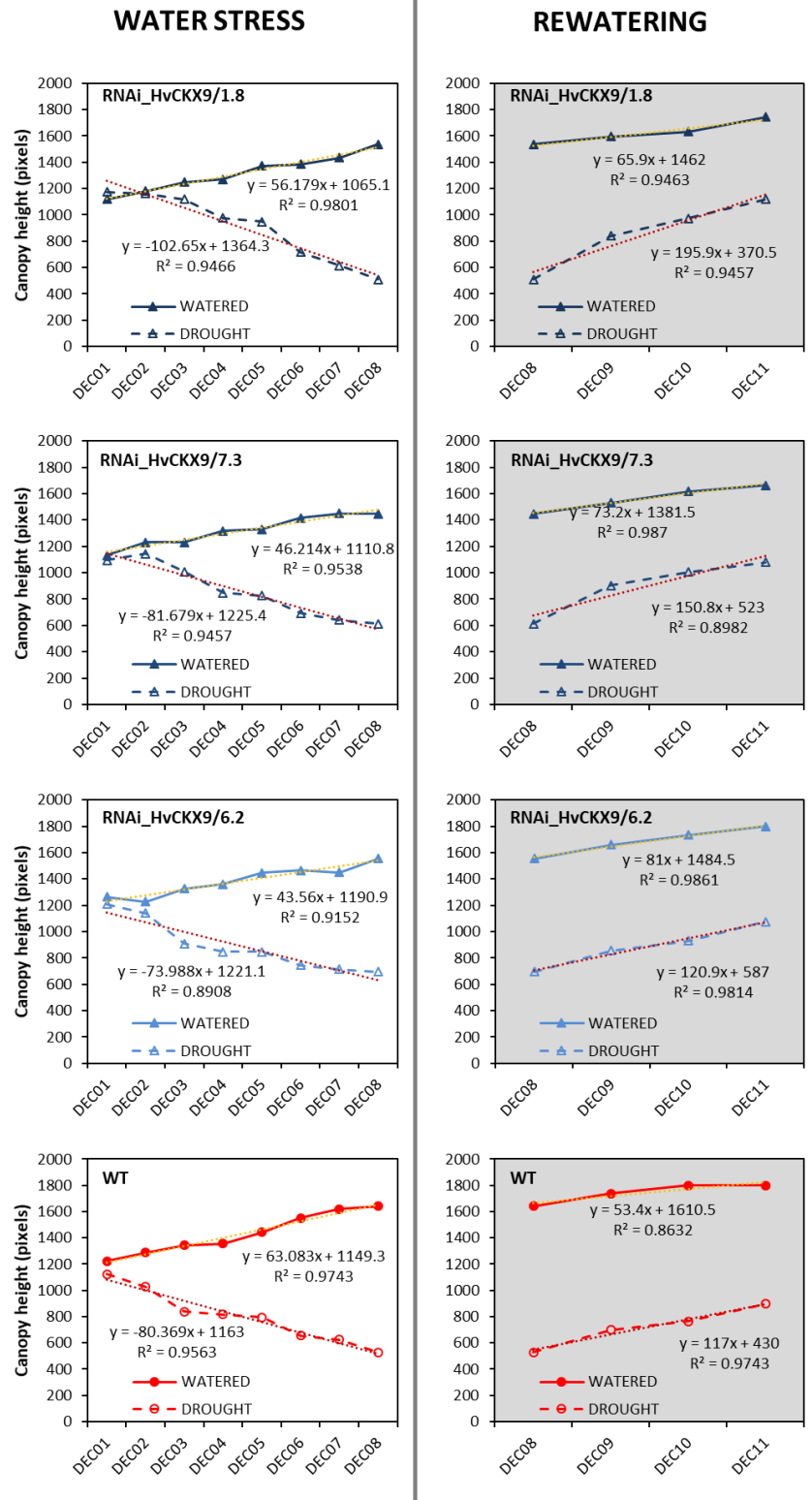


**Figure. IV.13.** Line of the projected canopy height and the correspondent equation (discontinuous yellow and red line for water and water stress treatment, respectively) in wild type (red lines) and RNAi:HvCKX9 lines (blue lines). Discontinuous and continuous lines represent D and W variants, respectively.

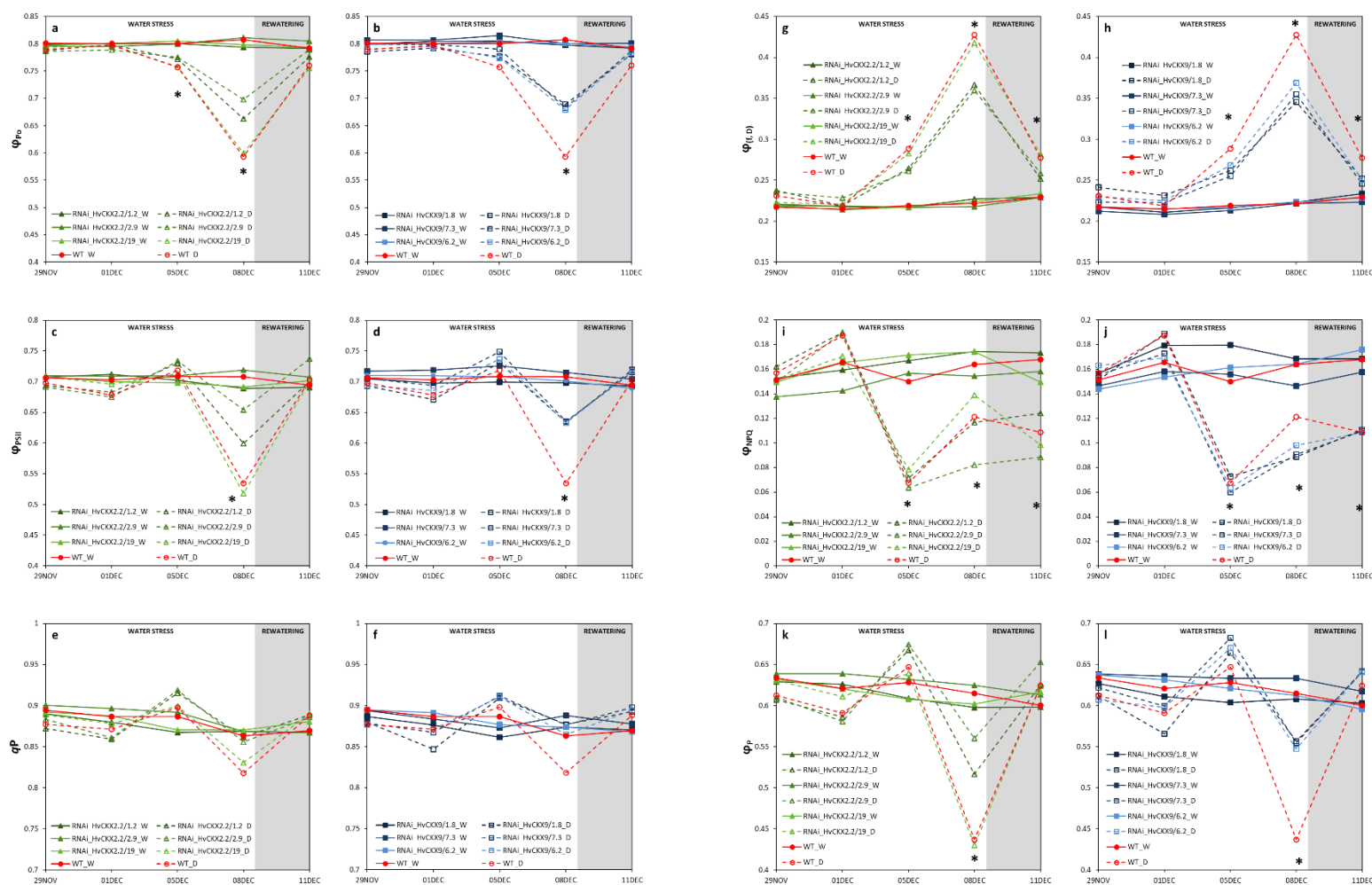


**Figure IV.14.** Variation in fluorescence related parameters in wild type and transgenic barley seedlings grown under water stress conditions and after subsequent rewatering. Chlorophyll fluorescence parameters ( $n = 50$ ) and the average values. RNAi:HvCKX2.2 lines are represented in green, RNAi:HvCKX9 in blue and wild type values in red. Discontinuous and continuous lines represent D and W variants, respectively. Asterisks indicate the significance level relative to the control variant according to ANOVA; \*  $P \leq 0.05$ ; \*\*  $P \leq 0.01$ ; \*\*\*  $P \leq 0.001$ ; ns, not significant.

All transgenic lines with the silenced *HvCKX9* gene presented similar dynamics of chl fluorescence parameters, but not for the lines with silenced *HvCKX2.2* gene. At the end of the water deficit period (day 8DEC), all RNAi:*HvCKX9* had higher  $\Phi_{Po}$ ,  $qP$ ,  $\Phi_{PSII}$  and  $\Phi_P$  but lower intensity of  $\Phi_{(f,D)}$  and  $\Phi_{NPQ}$  than wt. After rewatering, all stressed lines and wt recovered their control values except for  $\Phi_{NPQ}$ , which kept lower values compared with the well-watered plants (Fig. IV.14). We also calculated the ETR of all the lines. At 5DEC, all plants under water stress tend to increase the ETR values, but 3 days later the values dropped down. Interestingly, all RNAi:*HvCKX9* presented the same ETR changes and maintained higher levels of ETR than the wt plants at the end of the water stress period (Fig. IV.15).

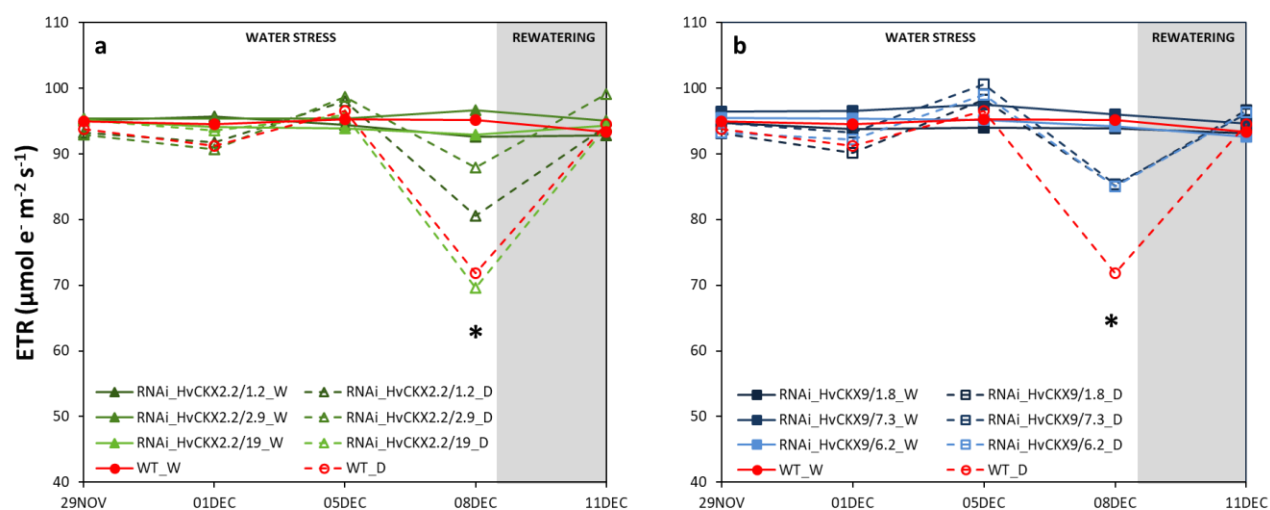


**Figure IV.15.** Variation in the electron transport rate (ETR) in barley seedlings grown under water stress conditions and after subsequent rewatering. ETR from three independent biological replicates (1, 2 and 3) ( $n = 50$ ) and the average values. (a) RNAi:*HvCKX2.2* lines are represented in green, (b) RNAi:*HvCKX9* in blue and wild type values in red. Discontinuous and continuous lines represent D and W variants, respectively. Statistical analyses were performed via ANOVA. Asterisks indicate the significance level relative to the control variant; \*  $P \leq 0.05$ ; \*\*  $P \leq 0.01$ ; \*\*\*  $P \leq 0.001$ ; ns, not significant.

Water deficiency delayed the leaf expansion in a genotype-dependent manner. At the end of the stress period (8DEC), the stressed variants had the 3<sup>rd</sup> leaf fully expanded and the 4<sup>th</sup> one in expansion, except in the lines 1.8 and 6.2 that had already expanded the fourth leaf. However, all well-watered plants were already developing the 5<sup>th</sup> leaf (Fig. IV.16). After four days

of rewatering, well-watered and water stressed plants maintained different developmental stages. Regarding the rewatered plants, the differences between the wt and transgenic lines in the water stress variant were more visible, all transgenic barley lines were expanding the 5<sup>th</sup> leaf but wt was still developing the 4<sup>th</sup> one (Fig. IV.16).

The aerial biomass (FW, g) was also affected in all stressed plants (Fig. IV. 17a and b). All water stressed seedlings decreased c.a. three times of the control values. After recovery, the stressed plants were still only half the weight of the well-watered variants.

All lines and wt did not differ in the RWC at DEC8 (Fig. IV.17c y d). However, a significant decreased in RWC was observed in the water stressed plants compared to their respective well-watered variant. Only the lines 2.9 from the silenced *HvCKX2.2* gene and 1.8 and 6.2 from *HvCKX9* had significantly higher RWC than the wt under water stress conditions. After the recovery period, all genotypes from the water stress treatment returned to a similar plant water status than WT, with exception of the lines 19 from *HvCKX2.2*.

Due to the homogeneity of lines from the silenced *HvCKX9* gene responding to water stress in the previously evaluated traits, we decided to go deeper in the study whether the silencing of this gene is affecting plant water stress response and recovery. For this aim, the traits presented below were only performed in these lines.

The values of osmotic potential varied among genotypes (Fig. IV.18). The transgenic lines 1.8 and 6.2 had less negative osmotic potential than wt and the line 7.3 at the end of water stress conditions. After the rewatering period, all stressed plants reduced the differences compared to each control, but only the line 1.8 did not show significant differences (Fig. IV. 18).



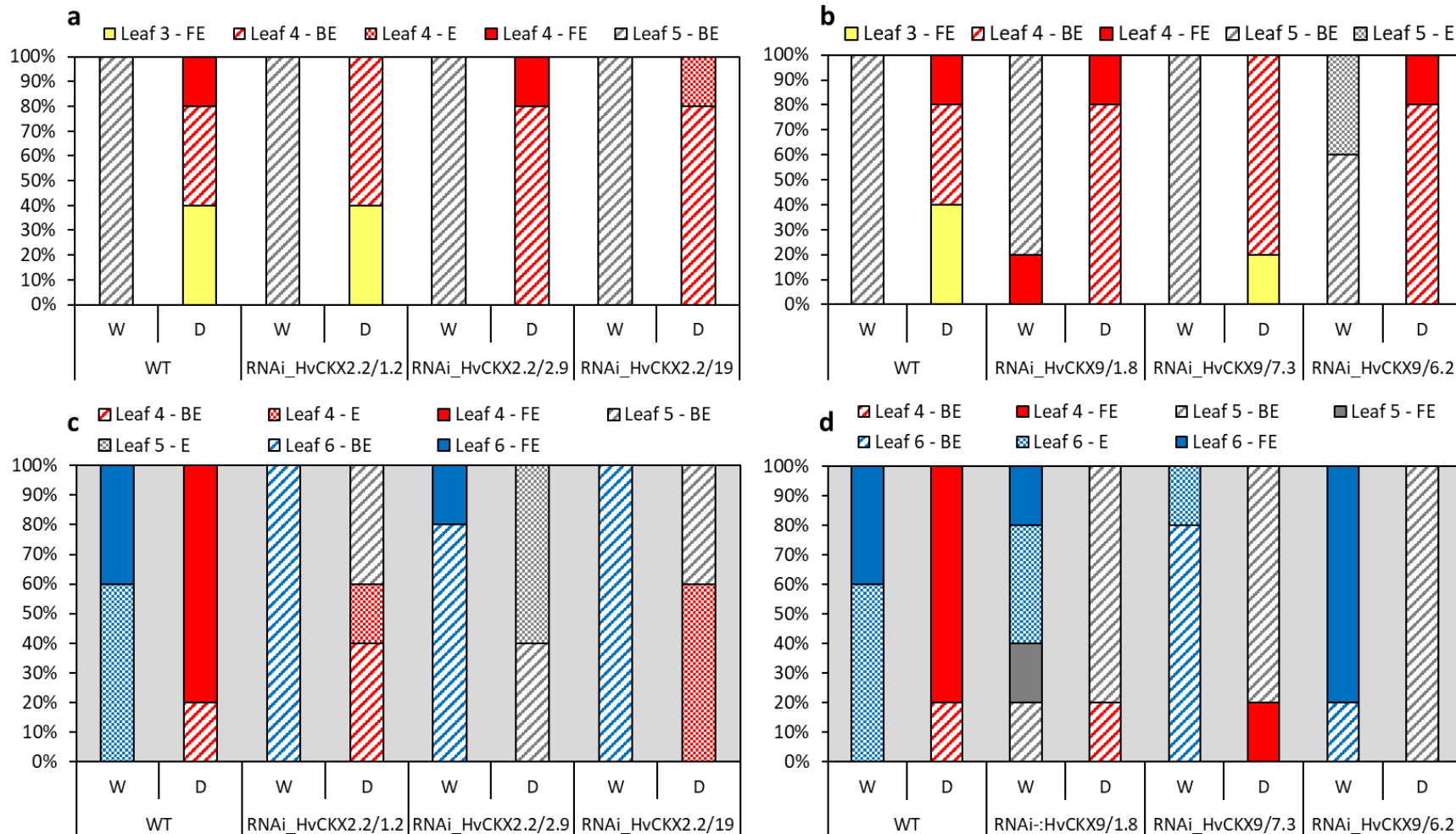


**Figure IV.16.** Developmental stages of leaves from wild type and transgenic barley seedlings under water stress and after subsequent rewatering. Developmental stages of leaves from five independent plants (a, b) of wild type or transgenic lines under stressed (D) and non-stressed (W) conditions at the end of the water stress period (n = 8) and (c, d) after rewatering (n=5).

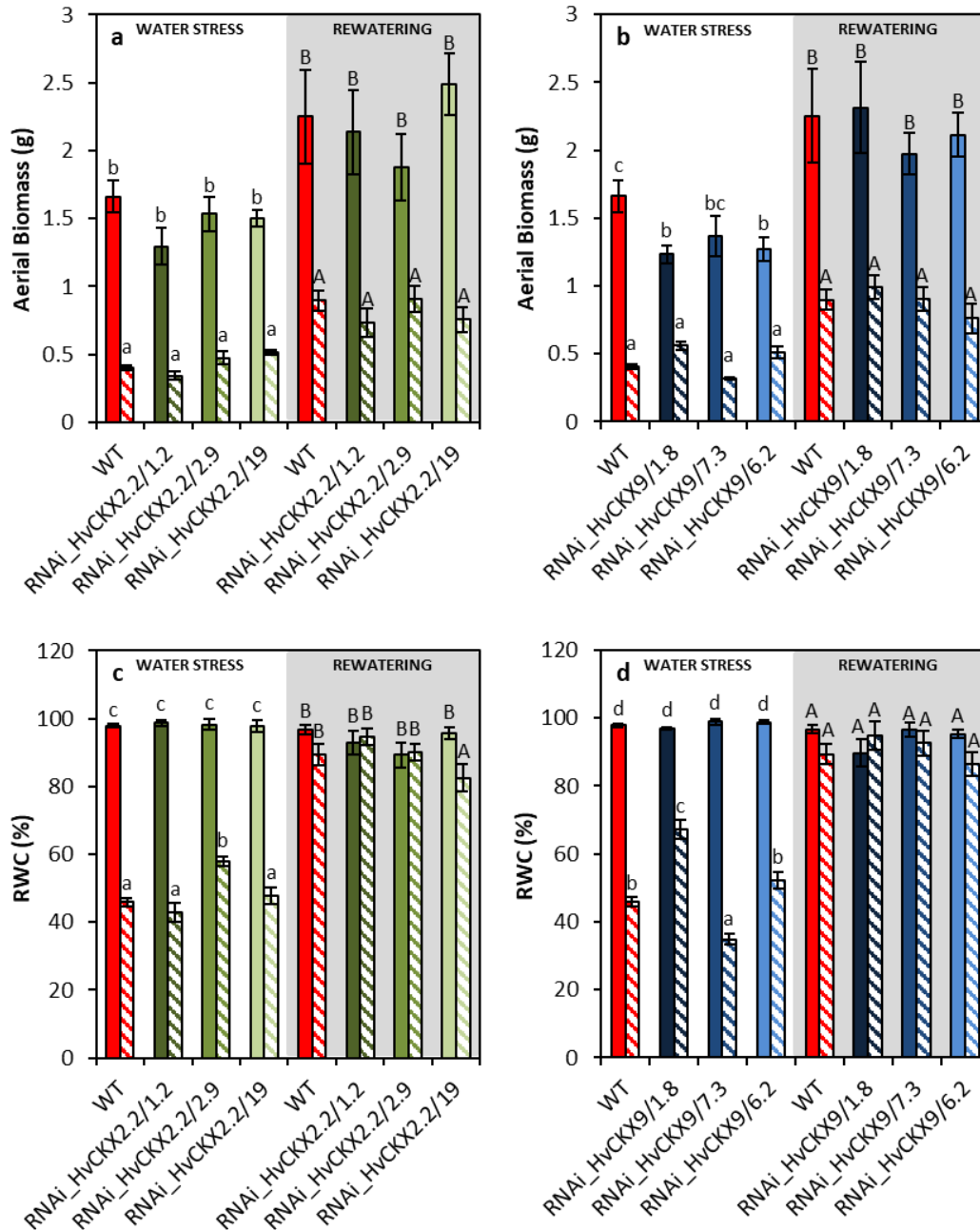


**Figure IV.17.** Changes (a, b) in aerial biomass (FW, g) and (c, d) relative water content (RWC, %) in barley seedlings under water stress conditions and after subsequent rewatering. Five independent plants of wild type or from transgenic lines were used as biological replicates per genotype and variant (W-well-watered and D-water stress), and the average values and SE at the end of the water stress period and after 4 days of rewatering are presented. RNAi:HvCKX2.2 lines are represented in green, RNAi:HvCKX9 in blue and wild type values in red. Bars with wide upward diagonal lines indicate water-stressed treatment (D). Different letters mean significant differences among treatments according Tukey HSD test after ANOVA.

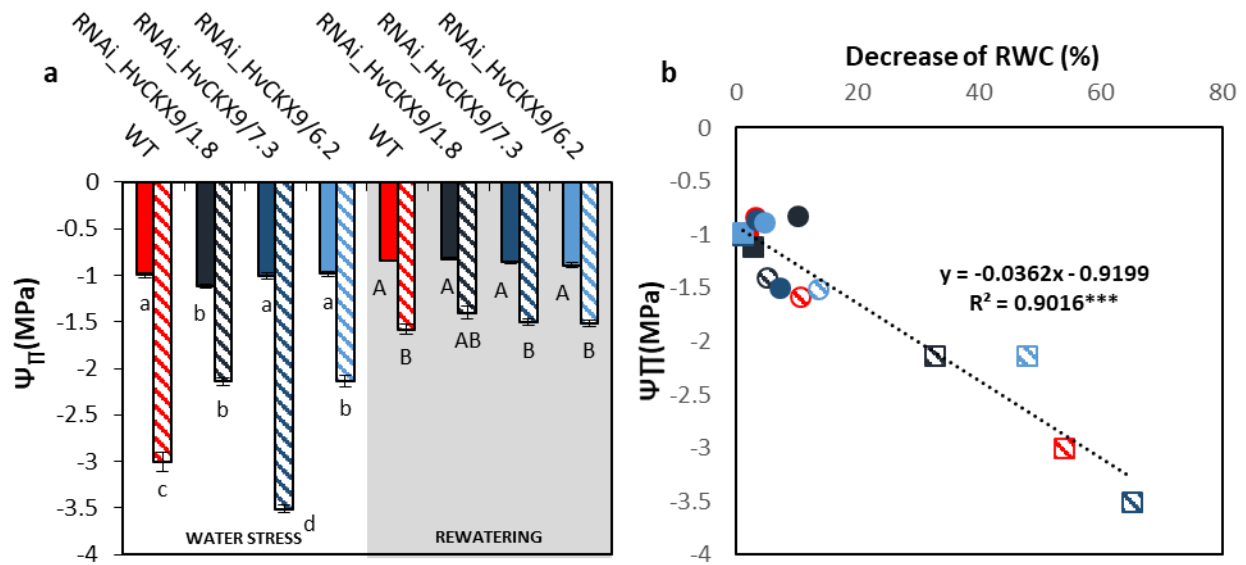


**Figure IV.18.** (a) Osmotic potential ( $\Psi_{\pi}$ , MPa) and (b) correlation between  $\Psi_{\pi}$  vs. the decrease in RWC (%) in wild type and transgenic barley plants after the water stress period and after rewatering. Bars (a) and symbols (b) with wide upward diagonal lines indicate water-stressed treatment (D), whereas filled bars or symbols represent well-water variants.

To determine the possible changes in the expression of the targeted genes under water stress conditions and rewatering, qPCR was performed and the expression of all members of *CKX* family members was evaluated. At the end of the water stress conditions, no detectable levels of *HvCKX2.2* were observed in RNAi:*HvCKX2.2* transgenic lines and a significant decrease in the expression of *HvCKX9* in RNAi:*HvCKX9* (Fig. IV.19). The most tolerant RNAi:*HvCKX9* lines (RNAi:*HvCKX9*/1.8 and RNAi:*HvCKX9*/6.2) presented higher levels of expression of *HvCKX3* and *HvCKX5* genes. After 4 days of rewatering, the RNAi:*HvCKX2.2* lines lost the silencing effect, evidenced by higher levels of *HvCKX2.2* mRNA compared to wt plants. Nevertheless, the lines 1.8 and 6.2 maintained lower levels of expression of the corresponding silenced gene and all lines accumulated higher mRNA from *HvCKX3* and *HvCKX2.2* after rewatering and lower of *HvCKX4* compared to wt plants (Fig. IV.20).

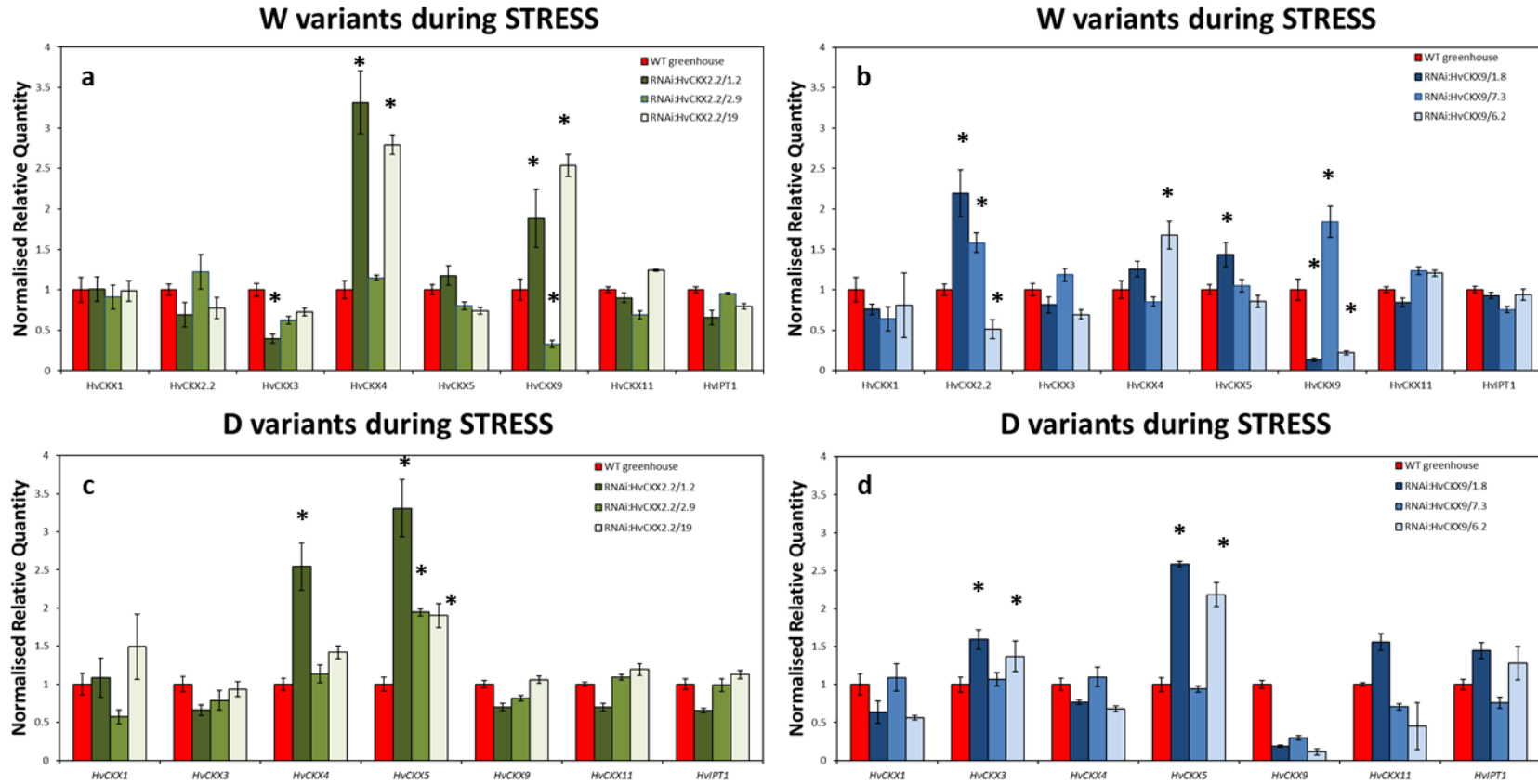


**Figure IV.19.** Expression profile of *HvCKX* genes in wild type and transgenic barley lines under water stress conditions. RNAi:*HvCKX*2.2 lines are represented in green, RNAi:*HvCKX*9 in blue and wild type values in red. Gene expression was relativized to the respective wild type. Asterisks indicate the significance level relative to the control variant according to ANOVA; \*  $P \leq 0.05$ ; \*\*  $P \leq 0.01$ ; \*\*\*  $P \leq 0.001$ ; ns, not significant.

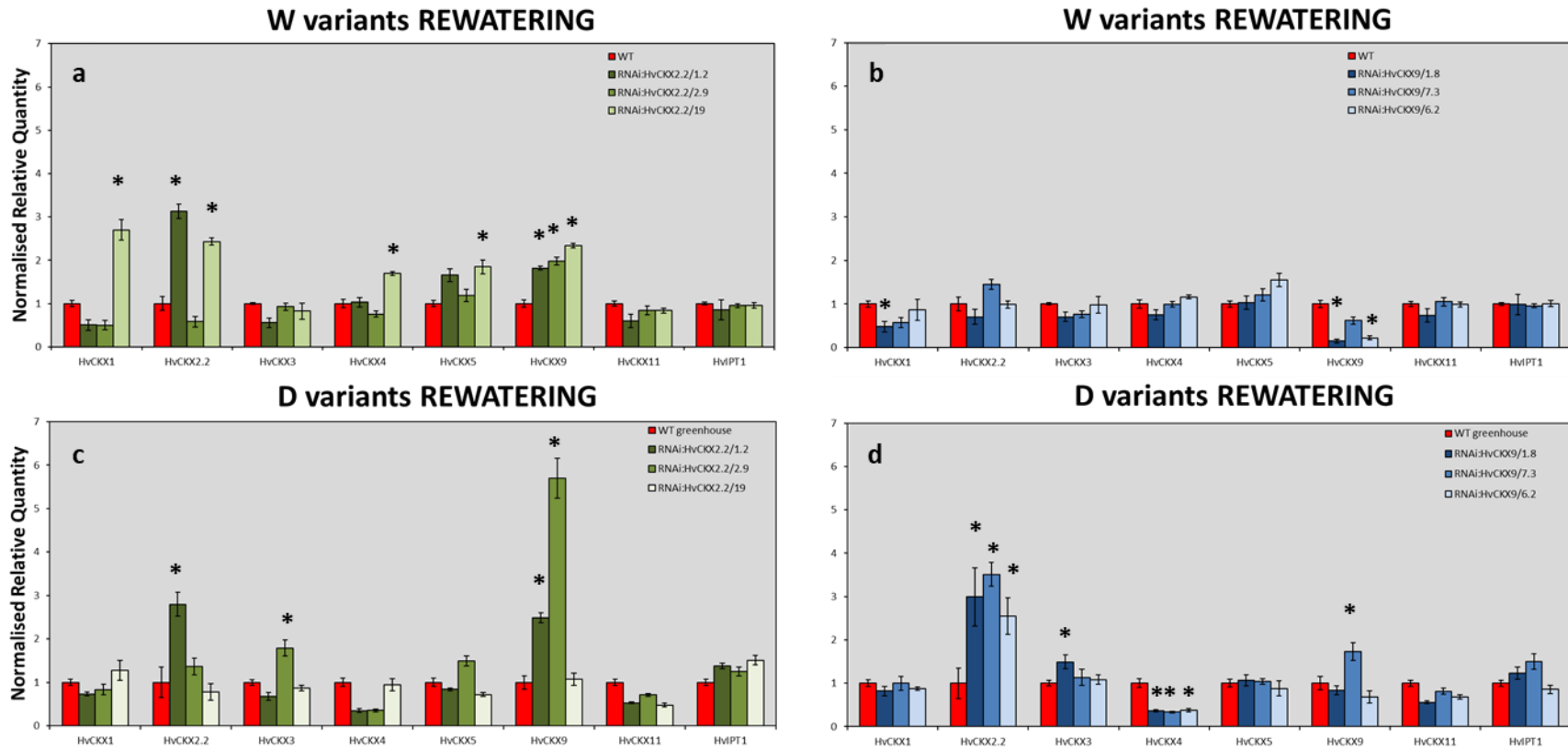


**Figure IV.20.** Expression profile of *HvCKX* genes in wild type and transgenic barley lines after 4 days of rewatering. RNAi:*HvCKX2.2* lines are represented in green, RNAi:*HvCKX9* in blue and wild type values in red. Gene expression was relativized to the respective wild type. Asterisks indicate the significance level relative to the control variant according to ANOVA; \*  $P \leq 0.05$ ; \*\*  $P \leq 0.01$ ; \*\*\*  $P \leq 0.001$ ; ns, not significant.

It is well known that water stress alters the hormonal homeostasis of plants. All barley lines altered their endogenous content of CKs, AUXs and ABA, but the values varied among lines. At the end of the water stress period, all stressed plants reduced the synthesis of CKs (reduction of ribotides) compared to well-watered plants, especially significant reduction of the CKs *tZ*- and *cZ*-type occurred. However, in the RNAi:HvCKX9 lines the levels of the base form *tZ* were maintained whereas the wt significantly reduced them compared to its control (Table IV.4 and Fig. IV.21). After 4 days of rewatering, all the genotypes significantly accumulated *tZ*, and the differences were higher in the case of the transgenic lines, especially for RNAi:HvCKX9 lines 1.8 and 7.3 (Table IV.5 and Fig. IV.21). This result pointed out that *tZ* would be involved in the recovery capacity of the barley plants after a water limited period.

Water stress induced the accumulation of ABA in all genotypes (Table IV.6). All water stressed plants also increased the total amount of AUXs, and this increment was mainly due to ox-IAA-glc. Only ox-IAA varied between wt and transgenic lines. The latter did not increase the levels whereas wt doubled them. Regarding the free AUX form, IAA was only significantly accumulated in the line 7.3, which did not show very good performance under water stress conditions (Table IV.6 and Fig. IV.22).

After the rewatering, the level of ABA kept upper in the D variant compared to controls (Table IV.7). The stressed plants also increased the levels of IAA, especially in the case of wt with 3.5 times more than in its control. Nevertheless, the line 1.8 did not show significant differences in IAA among variants. Finally, only the water stressed wt significantly reduced the content of ox-IAA-glc compared to control (Table IV.7 and Fig. IV.22).

We also determined the changes in the AUX-CK ratios, particularly among their free forms. At the end of the stress period, the IAA/BASES ratio of wt water stressed plants doubled the values of the well-watered plants. However, the lines 1.8 and 7.3 decreased the ratio (Fig. IV.23). Interestingly, after 4 days of rewatering, meanwhile the wt and the line 6.2 kept increased values of the ratio compared to their respective controls, the lines 1.8 and 7.3 recovered the control numbers (Fig. IV.23).

**Table IV.4.** Content of different CK metabolites in in barley seedlings at the end of the stress period. Different letters mean significant differences among treatments according Tukey HSD test after ANOVA.

	wild-type				HvCKX9 line 1.8				HvCKX9 line 7.3				HvCKX9 line 6.2			
	W		D		W		D		W		D		W		D	
pmol/g	average	SE	average	SE	average	SE	average	SE	average	SE	average	SE	average	SE	average	SE
tZRMP	6.09 <sup>ab</sup>	± 0.43	< LOD		6.77 <sup>b</sup>	± 0.42	< LOD		6.50 <sup>ab</sup>	± 0.34	< LOD		5.21 <sup>a</sup>	± 0.58	< LOD	
cZRMP	3.78 <sup>ab</sup>	± 0.59	< LOD		4.36	± 1.11	< LOD		5.37 <sup>b</sup>	± 0.58	< LOD		4.88 <sup>ab</sup>	± 0.44	< LOD	
iPRMP	10.98 <sup>abc</sup>	± 0.49	10.57 <sup>abc</sup>	± 0.68	16.90 <sup>e</sup>	± 0.57	13.13 <sup>cd</sup>	± 0.93	15.14 <sup>de</sup>	± 0.79	8.85 <sup>a</sup>	± 0.57	12.21 <sup>bc</sup>	± 0.47	9.37 <sup>ab</sup>	± 0.19
DHZRMP	1.70 <sup>ab</sup>	± 0.33	4.15 <sup>bc</sup>	± 0.27	3.45 <sup>abc</sup>	± 0.99	5.59 <sup>c</sup>	± 0.66	3.72 <sup>abc</sup>	± 0.76	5.70 <sup>c</sup>	± 0.60	1.14 <sup>a</sup>	± 0.22	4.90 <sup>c</sup>	± 0.32
Ribotides	22.56 <sup>bc</sup>	± 1.84	14.71 <sup>a</sup>	± 0.95	31.48	± 0.67	18.71 <sup>ab</sup>	± 1.59	30.73 <sup>d</sup>	± 2.47	14.55 <sup>a</sup>	± 1.16	23.44 <sup>c</sup>	± 1.71	14.27 <sup>a</sup>	± 0.51
tZR	0.46	± 0.05	0.12	± 0.02	0.63	± 0.10	0.11	± 0.02	0.42	± 0.09	0.04	± 0.01	0.42	± 0.08	0.18	± 0.01
cZR	0.52 <sup>abc</sup>	± 0.01	0.41 <sup>a</sup>	± 0.06	0.31 <sup>a</sup>	± 0.04	0.36 <sup>a</sup>	± 0.04	0.46 <sup>ab</sup>	± 0.02	0.91 <sup>bc</sup>	± 0.21	0.96 <sup>c</sup>	± 0.19	0.53 <sup>abc</sup>	± 0.07
iPR	0.85 <sup>a</sup>	± 0.07	1.84 <sup>cd</sup>	± 0.08	1.97 <sup>d</sup>	± 0.20	1.63 <sup>bcd</sup>	± 0.07	1.14 <sup>ab</sup>	± 0.07	1.03 <sup>ab</sup>	± 0.09	1.26 <sup>abc</sup>	± 0.26	1.87 <sup>cd</sup>	± 0.12
DHZR	0.15 <sup>a</sup>	± 0.02	0.12 <sup>a</sup>	± 0.01	0.12 <sup>a</sup>	± 0.01	0.12 <sup>a</sup>	± 0.01	0.14 <sup>a</sup>	± 0.01	0.12 <sup>a</sup>	± 0.02	0.13 <sup>a</sup>	± 0.02	0.12 <sup>a</sup>	± 0.01
Ribosides	1.99 <sup>a</sup>	± 0.15	2.49 <sup>ab</sup>	± 0.17	3.03 <sup>b</sup>	± 0.28	2.23 <sup>ab</sup>	± 0.14	2.16 <sup>ab</sup>	± 0.20	2.10 <sup>ab</sup>	± 0.32	2.78 <sup>ab</sup>	± 0.56	2.69 <sup>ab</sup>	± 0.21
tZ	23.68 <sup>b</sup>	± 3.13	11.89 <sup>a</sup>	± 1.00	18.26 <sup>ab</sup>	± 0.41	16.49 <sup>ab</sup>	± 1.17	17.77 <sup>ab</sup>	± 2.53	13.56 <sup>a</sup>	± 0.55	15.07 <sup>a</sup>	± 1.35	17.58 <sup>ab</sup>	± 1.18
cZ	276.47 <sup>a</sup>	± 49.00	158.05 <sup>a</sup>	± 14.03	158.61 <sup>a</sup>	± 32.96	207.75 <sup>a</sup>	± 10.54	202.46 <sup>a</sup>	± 48.04	189.57 <sup>a</sup>	± 9.62	227.75 <sup>a</sup>	± 27.83	191.39 <sup>a</sup>	± 7.93
iP	21.99 <sup>a</sup>	± 5.46	17.31 <sup>a</sup>	± 0.47	26.79 <sup>a</sup>	± 3.46	24.97 <sup>a</sup>	± 2.51	18.17 <sup>a</sup>	± 2.31	17.60 <sup>a</sup>	± 1.82	20.85 <sup>a</sup>	± 2.67	27.69 <sup>a</sup>	± 4.91
Free Bases	322.14 <sup>a</sup>	± 57.59	187.25 <sup>a</sup>	± 15.51	203.67 <sup>a</sup>	± 31.68	249.21 <sup>a</sup>	± 14.22	238.39 <sup>a</sup>	± 52.88	220.72 <sup>a</sup>	± 11.99	263.67 <sup>a</sup>	± 31.85	236.66 <sup>a</sup>	± 14.02
tZ9G	48.36 <sup>bc</sup>	± 2.74	28.33 <sup>a</sup>	± 1.52	49.79 <sup>bc</sup>	± 2.23	35.71 <sup>ab</sup>	± 2.00	59.38 <sup>c</sup>	± 5.37	26.86 <sup>a</sup>	± 2.01	82.61 <sup>d</sup>	± 7.11	34.32 <sup>ab</sup>	± 1.72
cZ9G	0.96 <sup>abc</sup>	± 0.10	0.93 <sup>ab</sup>	± 0.04	1.18 <sup>bcd</sup>	± 0.09	1.36 <sup>cd</sup>	± 0.08	1.07 <sup>abcd</sup>	± 0.14	0.70 <sup>a</sup>	± 0.07	1.39 <sup>d</sup>	± 0.11	0.89 <sup>ab</sup>	± 0.05
iP9G	1.99 <sup>a</sup>	± 0.10	3.46 <sup>cd</sup>	± 0.13	2.68 <sup>abc</sup>	± 0.16	4.38 <sup>e</sup>	± 0.23	2.15 <sup>ab</sup>	± 0.15	2.58 <sup>ab</sup>	± 0.22	2.83 <sup>bc</sup>	± 0.20	3.79 <sup>de</sup>	± 0.21
DHZ9G	0.06 <sup>a</sup>	± 0.01	0.05 <sup>a</sup>	± 0.01	0.05 <sup>a</sup>	± 0.01	0.08 <sup>a</sup>	± 0.01	0.05 <sup>a</sup>	± 0.01	0.04 <sup>a</sup>	± 0.01	0.05 <sup>a</sup>	± 0.01	0.05 <sup>a</sup>	± 0.00
N-glucosides	51.36 <sup>bc</sup>	± 2.95	33.08 <sup>a</sup>	± 1.70	53.70 <sup>bc</sup>	± 2.21	41.52 <sup>ab</sup>	± 2.32	62.64 <sup>c</sup>	± 5.67	30.18 <sup>a</sup>	± 2.31	86.88 <sup>d</sup>	± 7.44	39.06 <sup>ab</sup>	± 1.99
tZOG	2.44 <sup>ab</sup>	± 0.15	1.96 <sup>ab</sup>	± 0.13	2.74 <sup>b</sup>	± 0.17	2.01 <sup>ab</sup>	± 0.12	2.52 <sup>ab</sup>	± 0.20	1.80 <sup>a</sup>	± 0.24	2.79 <sup>b</sup>	± 0.12	2.56 <sup>ab</sup>	± 0.27
tZROG	0.09 <sup>a</sup>	± 0.01	0.10	± 0.02	0.09 <sup>a</sup>	± 0.01	0.04	± 0.01	0.04 <sup>a</sup>	± 0.01	0.05	± 0.00	0.06 <sup>a</sup>	± 0.01	0.06	± 0.01
cZOG	203.25	± 5.91	261.81	± 0.01	207.59	± 8.23	242.72	± 0.01	189.37	± 9.92	232.96	± 0.01	214.00	± 10.71	270.05	± 0.01
cZROG	9.77	± 0.11	14.71	± 0.00	9.00	± 0.19	12.85	± 0.00	8.83	± 0.40	13.92	± 0.00	9.28	± 0.61	11.51	± 0.00
O-glucosides	215.55	± 6.19	278.58	± 0.14	219.42	± 7.98	257.62	± 0.13	200.76	± 10.54	248.73	± 0.24	226.13	± 11.44	284.19	± 0.29
tZ-type	81.12 <sup>b</sup>	± 6.51	42.40 <sup>a</sup>	± 2.67	78.28 <sup>b</sup>	± 2.55	54.36 <sup>a</sup>	± 3.30	86.62 <sup>bc</sup>	± 8.53	42.32 <sup>a</sup>	± 2.80	106.17 <sup>c</sup>	± 9.26	54.70 <sup>a</sup>	± 3.18
cZ-type	494.76 <sup>a</sup>	± 55.72	435.91 <sup>a</sup>	± 14.14	381.05	± 34.22	465.04 <sup>a</sup>	± 10.67	407.55 <sup>a</sup>	± 59.11	438.06 <sup>a</sup>	± 9.91	458.25 <sup>a</sup>	± 39.88	474.37 <sup>a</sup>	± 8.06
iP-type	35.82 <sup>a</sup>	± 6.13	33.18 <sup>a</sup>	± 1.36	48.34 <sup>a</sup>	± 3.95	44.12 <sup>a</sup>	± 3.75	36.59 <sup>a</sup>	± 3.33	30.06 <sup>a</sup>	± 2.69	37.15 <sup>a</sup>	± 3.60	42.72 <sup>a</sup>	± 5.44
DHZ-type	1.92 <sup>ab</sup>	± 0.35	4.32 <sup>bc</sup>	± 0.30	3.62 <sup>abc</sup>	± 0.99	5.78 <sup>c</sup>	± 0.67	3.91 <sup>abc</sup>	± 0.78	5.86 <sup>c</sup>	± 0.62	1.33 <sup>a</sup>	± 0.24	5.09 <sup>c</sup>	± 0.33
TOTAL CKs	613.62 <sup>a</sup>	± 68.71	515.80 <sup>a</sup>	± 18.47	511.29	± 33.96	569.29 <sup>a</sup>	± 18.40	534.67 <sup>a</sup>	± 71.75	516.30 <sup>a</sup>	± 16.03	602.89 <sup>a</sup>	± 52.99	576.86 <sup>a</sup>	± 17.02

**Table IV.5.** Content of different CK metabolites in in barley seedlings after 4 days of rewatering. Different letters mean significant differences among treatments according Tukey HSD test after ANOVA.

	wild-type				HvCKX9 line 1.8				HvCKX9 line 7.3				HvCKX9 line 6.2			
	RW		RD		RW		RD		RW		RD		RW		RD	
pmol/g	average	± SE	average	± SE	average	± SE	average	± SE	average	± SE	average	± SE	average	± SE	average	± SE
tZRMP	3.86 <sup>ab</sup>	± 0.86	3.13 <sup>a</sup>	± 0.35	2.60 <sup>a</sup>	± 0.21	6.42 <sup>b</sup>	± 0.56	4.03 <sup>ab</sup>	± 0.48	5.33 <sup>ab</sup>	± 0.35	3.45 <sup>a</sup>	± 0.26	4.98 <sup>ab</sup>	± 0.65
cZRMP	4.36 <sup>a</sup>	± 0.76	5.55 <sup>a</sup>	± 0.75	3.86 <sup>a</sup>	± 0.41	4.29 <sup>a</sup>	± 0.34	4.95 <sup>a</sup>	± 0.70	4.53 <sup>a</sup>	± 0.74	3.62 <sup>a</sup>	± 0.47	3.85 <sup>a</sup>	± 0.36
iPRMP	13.06 <sup>ab</sup>	± 0.48	11.42 <sup>a</sup>	± 0.36	11.61 <sup>a</sup>	± 0.93	16.13 <sup>c</sup>	± 0.24	16.08 <sup>c</sup>	± 0.26	14.98 <sup>bc</sup>	± 0.30	14.06 <sup>bc</sup>	± 0.58	14.65 <sup>bc</sup>	± 0.45
DHZRMP	1.74 <sup>a</sup>	± 0.18	1.70	± 0.28	2.69	± 0.79	1.87 <sup>a</sup>	± 0.28	1.26	± 0.09	1.42 <sup>a</sup>	± 0.16	1.51	± 0.41	1.80 <sup>a</sup>	± 0.21
Ribotides	23.03	± 2.33	21.80	± 1.46	20.77	± 2.34	28.71	± 1.43	26.32	± 1.43	26.26	± 1.57	22.04	± 1.31	25.28	± 1.66
tZR	0.10 <sup>a</sup>	± 0.01	0.13 <sup>a</sup>	± 0.01	0.12 <sup>a</sup>	± 0.04	0.36 <sup>a</sup>	± 0.06	0.24 <sup>a</sup>	± 0.03	0.32 <sup>a</sup>	± 0.02	0.21 <sup>a</sup>	± 0.04	0.33 <sup>a</sup>	± 0.05
cZR	0.45	± 0.03	3.18	± 0.35	0.60	± 0.06	1.08	± 0.11	0.67	± 0.12	1.58	± 0.08	1.11	± 0.23	2.11	± 0.21
iPR	1.54 <sup>a</sup>	± 0.15	1.71 <sup>a</sup>	± 0.14	0.68 <sup>a</sup>	± 0.06	1.15 <sup>a</sup>	± 0.14	2.79 <sup>a</sup>	± 0.50	1.62 <sup>a</sup>	± 0.14	1.92 <sup>a</sup>	± 0.23	1.60 <sup>a</sup>	± 0.05
DHZR	0.12 <sup>a</sup>	± 0.02	0.16 <sup>a</sup>	± 0.01	0.13 <sup>a</sup>	± 0.01	0.13 <sup>a</sup>	± 0.01	0.15 <sup>a</sup>	± 0.02	0.16 <sup>a</sup>	± 0.01	0.13 <sup>a</sup>	± 0.01	0.17 <sup>a</sup>	± 0.02
Ribosides	2.21	± 0.22	5.18	± 0.51	1.52	± 0.18	2.72	± 0.33	3.86	± 0.66	3.68	± 0.25	3.37	± 0.51	4.21	± 0.33
tZ	11.60 <sup>ab</sup>	± 1.63	20.75 <sup>c</sup>	± 1.43	5.52 <sup>a</sup>	± 0.31	35.00 <sup>d</sup>	± 2.15	8.26 <sup>ab</sup>	± 1.08	34.16 <sup>d</sup>	± 0.71	12.46 <sup>b</sup>	± 1.92	29.27 <sup>d</sup>	± 1.52
cZ	368.98	± 21.88	383.61	± 37.25	238.84	± 28.66	422.71	± 27.69	251.09	± 18.59	486.60	± 55.13	389.18	± 66.22	382.84	± 39.22
iP	33.39 <sup>a</sup>	± 3.53	17.61 <sup>a</sup>	± 2.35	22.77 <sup>a</sup>	± 0.78	23.68 <sup>a</sup>	± 3.14	32.83	± 7.64	20.23 <sup>a</sup>	± 1.18	43.50 <sup>a</sup>	± 8.39	21.14 <sup>a</sup>	± 3.05
Free Bases	413.98	± 27.04	421.96	± 41.02	267.12	± 29.75	481.39	± 32.97	292.18	± 27.31	540.99	± 57.02	445.15	± 76.53	433.25	± 43.79
tZ9G	25.69 <sup>a</sup>	± 2.46	30.09 <sup>a</sup>	± 2.46	35.38 <sup>a</sup>	± 3.77	48.71 <sup>a</sup>	± 8.16	39.07 <sup>a</sup>	± 6.93	39.75 <sup>a</sup>	± 4.35	48.88 <sup>a</sup>	± 13.03	46.95 <sup>a</sup>	± 5.82
cZ9G	0.81 <sup>ab</sup>	± 0.05	0.57 <sup>a</sup>	± 0.06	0.56 <sup>a</sup>	± 0.12	0.55 <sup>a</sup>	± 0.12	0.58 <sup>a</sup>	± 0.08	0.46 <sup>a</sup>	± 0.06	1.03 <sup>b</sup>	± 0.15	0.46 <sup>a</sup>	± 0.04
iP9G	2.12 <sup>ab</sup>	± 0.13	1.90 <sup>a</sup>	± 0.15	2.22 <sup>ab</sup>	± 0.13	2.11 <sup>ab</sup>	± 0.24	2.14 <sup>ab</sup>	± 0.23	1.93 <sup>a</sup>	± 0.13	3.34 <sup>b</sup>	± 0.71	2.03 <sup>ab</sup>	± 0.18
DHZ9G	0.05 <sup>a</sup>	± 0.01	0.05 <sup>a</sup>	± 0.00	0.07 <sup>a</sup>	± 0.01	0.05 <sup>a</sup>	± 0.01	0.06 <sup>a</sup>	± 0.01	0.06 <sup>a</sup>	± 0.01	0.09 <sup>a</sup>	± 0.02	0.06 <sup>a</sup>	± 0.01
N-glucosides	28.67 <sup>a</sup>	± 2.65	32.62 <sup>a</sup>	± 2.68	38.23 <sup>a</sup>	± 4.04	51.43 <sup>a</sup>	± 8.52	41.85 <sup>a</sup>	± 7.24	42.21 <sup>a</sup>	± 4.56	53.33 <sup>a</sup>	± 13.91	49.49 <sup>a</sup>	± 6.05
tZOG	1.87 <sup>ab</sup>	± 0.20	1.46 <sup>a</sup>	± 0.21	1.72 <sup>a</sup>	± 0.34	2.81 <sup>b</sup>	± 0.26	1.72 <sup>a</sup>	± 0.21	1.87 <sup>ab</sup>	± 0.29	1.91 <sup>ab</sup>	± 0.22	2.52 <sup>ab</sup>	± 0.11
tZROG	0.05 <sup>a</sup>	± 0.01	0.06 <sup>a</sup>	± 0.01	0.07 <sup>a</sup>	± 0.01	0.13 <sup>a</sup>	± 0.02	0.10 <sup>a</sup>	± 0.02	0.09 <sup>a</sup>	± 0.02	0.08 <sup>a</sup>	± 0.01	0.08 <sup>a</sup>	± 0.01
cZOG	246.70 <sup>ab</sup>	± 11.40	214.99 <sup>a</sup>	± 25.09	255.52 <sup>ab</sup>	± 23.36	212.42 <sup>a</sup>	± 3.56	259.65 <sup>ab</sup>	± 7.81	212.12 <sup>a</sup>	± 3.98	292.71 <sup>b</sup>	± 22.19	211.37 <sup>a</sup>	± 5.31
cZROG	18.75	± 1.40	11.51	± 1.35	18.30	± 1.41	10.50	± 0.39	21.91	± 4.39	10.08	± 0.11	14.92	± 0.33	10.30	± 0.16
O-glucosides	267.36 <sup>ab</sup>	± 13.01	228.02 <sup>a</sup>	± 26.67	275.62 <sup>ab</sup>	± 25.11	225.86 <sup>a</sup>	± 4.24	283.38 <sup>ab</sup>	± 12.43	224.16 <sup>a</sup>	± 4.40	309.61 <sup>b</sup>	± 22.75	224.27 <sup>a</sup>	± 5.59
tZ-type	43.17	± 5.17	55.62	± 4.48	45.41	± 4.67	93.44	± 11.21	53.42	± 8.74	81.52	± 5.74	66.99	± 15.47	84.13	± 8.17
cZ-type	640.04 <sup>a</sup>	± 35.53	619.41 <sup>a</sup>	± 64.85	517.68 <sup>a</sup>	± 54.02	651.55 <sup>a</sup>	± 32.22	538.85 <sup>a</sup>	± 31.68	715.38 <sup>a</sup>	± 60.10	702.56 <sup>a</sup>	± 89.59	610.93 <sup>a</sup>	± 45.30
iP-type	50.12 <sup>a</sup>	± 4.29	32.64 <sup>a</sup>	± 2.99	37.27 <sup>a</sup>	± 1.91	43.07 <sup>a</sup>	± 3.76	53.84	± 8.63	38.77 <sup>a</sup>	± 1.76	62.82 <sup>a</sup>	± 9.91	39.42 <sup>a</sup>	± 3.72
DHZ-type	1.92 <sup>a</sup>	± 0.26	1.92	± 0.02	2.89	± 0.17	2.05 <sup>a</sup>	± 0.38	1.47	± 0.02	1.64 <sup>a</sup>	± 0.23	1.73	± 0.03	2.03 <sup>a</sup>	± 0.23
TOTAL CKs	735.25 <sup>ab</sup>	± 45.25	709.58	± 72.35	603.26	± 60.77	790.11 <sup>ab</sup>	± 47.57	647.59	± 49.08	837.30 <sup>b</sup>	± 67.84	834.10	± 115.01	736.51 <sup>ab</sup>	± 57.43



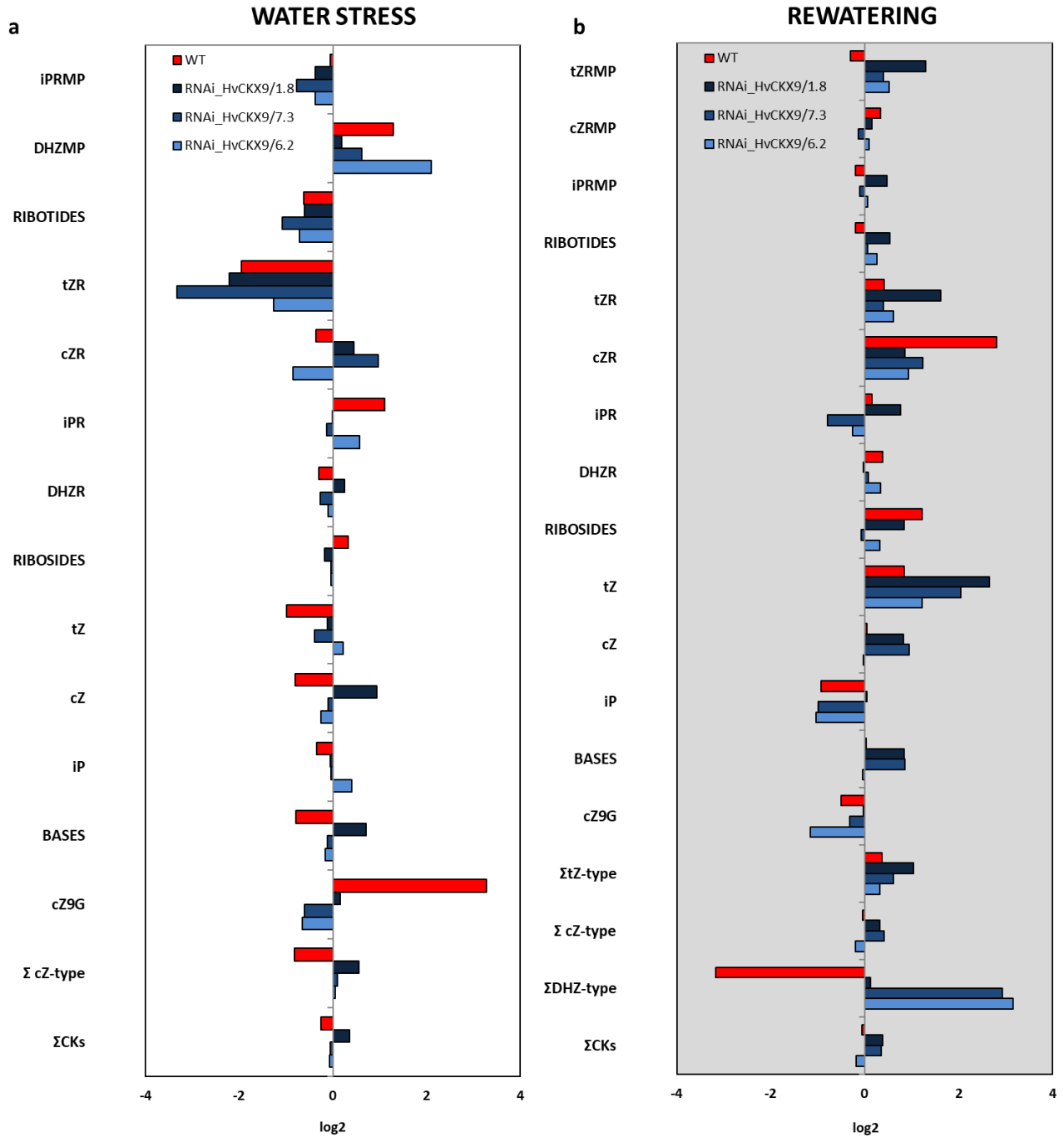


**Figure IV.21.** Profile of cytokinins (CKs) in barely seedlings (wild type and 3 transgenic lines) at the (a) end of the water deficit period and (b) after 4 days of rewatering. Fold changes (presented as log<sub>2</sub> ratio) in the content (pmol mg<sup>-1</sup> FW of CKs between stressed (D) and non-stressed (W) barley genotypes).

**Table IV.6** Content of ABA and AUXs in barley seedlings (wild type and 3 transgenic lines) at the end of the stress period. Different letters mean significant differences among treatments according Tukey HSD test after ANOVA.

	wild-type				HvCKX9 line 1.8				HvCKX9 line 7.3				HvCKX9 line 6.2			
	W		D		W		D		W		D		W		D	
pmol/g	average	SE	average	SE	average	SE	average	SE	average	SE	average	SE	average	SE	average	SE
<b>ABA</b>	4.76 <sup>a</sup>	± 0.19	530.71 <sup>c</sup>	± 12.16	5.24 <sup>a</sup>	± 0.35	606.90 <sup>d</sup>	± 12.95	4.31 <sup>a</sup>	± 0.23	684.62 <sup>e</sup>	± 25.47	5.02 <sup>a</sup>	± 0.17	430.79 <sup>b</sup>	± 5.59
<b>IAA</b>	621.23 <sup>b</sup>	± 17.32	695.77 <sup>b</sup>	± 34.77	637.08 <sup>b</sup>	± 17.28	615.41 <sup>b</sup>	± 34.00	637.33 <sup>b</sup>	± 11.59	1043.90 <sup>c</sup>	± 36.67	591.84 <sup>ab</sup>	± 29.92	477.36 <sup>a</sup>	± 18.16
<b>ox-IAA</b>	264.86 <sup>a</sup>	± 24.31	601.76 <sup>b</sup>	± 121.62	261.65 <sup>a</sup>	± 31.29	345.97 <sup>ab</sup>	± 64.26	288.85 <sup>a</sup>	± 62.10	323.30 <sup>a</sup>	± 16.25	312.86 <sup>a</sup>	± 14.55	339.00 <sup>ab</sup>	± 59.27
<b>IAA-glc</b>	< LOD		5576.75 <sup>a</sup>	± 406.73	< LOD		7695.90 <sup>b</sup>	± 344.38	< LOD		4804.37 <sup>a</sup>	± 397.92	< LOD		8852.92 <sup>b</sup>	± 504.15
<b>ox-IAA-glc</b>	475.64 <sup>a</sup>	± 24.88	2015.28 <sup>b</sup>	± 90.52	352.12 <sup>a</sup>	± 57.24	1703.70 <sup>b</sup>	± 199.26	359.87 <sup>a</sup>	± 38.84	1527.50 <sup>b</sup>	± 138.04	474.07 <sup>a</sup>	± 86.23	1473.69 <sup>b</sup>	± 222.85
<b>TOTAL AUXs</b>	1361.72 <sup>a</sup>	± 66.51	8889.56 <sup>bc</sup>	± 653.64	1250.85 <sup>a</sup>	± 105.80	10360.99 <sup>c</sup>	± 641.91	1286.05 <sup>a</sup>	± 112.54	7699.08 <sup>b</sup>	± 588.88	1378.77 <sup>a</sup>	± 130.69	11142.97 <sup>c</sup>	± 804.44

**Table IV.7.** Content of ABA and AUXs in barley seedlings (wild type and 3 transgenic lines) after 4 days of rewatering. Different letters mean significant differences among treatments according Tukey HSD test after ANOVA.

	wild-type				HvCKX9 line 1.8				HvCKX9 line 7.3				HvCKX9 line 6.2			
	RW		RD		RW		RD		RW		RD		RW		RD	
pmol/g	average	SE	average	SE	average	SE	average	SE	average	SE	average	SE	average	SE	average	SE
<b>ABA</b>	11.23 <sup>a</sup>	± 0.87	51.55 <sup>c</sup>	± 1.53	8.57 <sup>a</sup>	± 0.38	43.80 <sup>bc</sup>	± 6.65	10.27 <sup>a</sup>	± 0.95	34.72 <sup>b</sup>	± 1.19	10.30 <sup>a</sup>	± 0.73	36.12 <sup>b</sup>	± 2.26
<b>IAA</b>	695.20 <sup>ab</sup>	± 6.36	2487.92 <sup>d</sup>	± 186.60	722.04 <sup>ab</sup>	± 4.97	1068.42 <sup>bc</sup>	± 57.08	722.40 <sup>ab</sup>	± 5.55	1387.32 <sup>c</sup>	± 172.44	604.25 <sup>a</sup>	± 5.74	1457.66 <sup>c</sup>	± 24.76
<b>ox-IAA</b>	785.00 <sup>a</sup>	± 108.28	9133.19 <sup>b</sup>	± 1954.43	700.86 <sup>a</sup>	± 59.21	1656.87 <sup>a</sup>	± 182.07	814.62 <sup>a</sup>	± 81.12	2340.60 <sup>a</sup>	± 158.14	616.80 <sup>a</sup>	± 43.70	3109.98 <sup>a</sup>	± 210.58
<b>IAA-glc</b>	11758.25 <sup>bc</sup>	± 1965.86	4869.28 <sup>a</sup>	± 294.53	11803.05 <sup>bc</sup>	± 1350.20	4090.76 <sup>a</sup>	± 370.35	12675.58 <sup>c</sup>	± 1122.17	6182.42 <sup>ab</sup>	± 1187.07	12948.57 <sup>c</sup>	± 2705.35	4751.95 <sup>a</sup>	± 529.90
<b>ox-IAA-glc</b>	754.39 <sup>b</sup>	± 154.13	234.19 <sup>a</sup>	± 73.73	507.72 <sup>ab</sup>	± 37.76	492.77 <sup>ab</sup>	± 88.08	759.43 <sup>b</sup>	± 88.50	446.08 <sup>ab</sup>	± 109.31	643.31 <sup>b</sup>	± 89.32	414.83 <sup>ab</sup>	± 91.41
<b>TOTAL AUXs</b>	13992.83 <sup>ab</sup>	± 2234.63	16724.57 <sup>b</sup>	± 2509.30	13733.67 <sup>ab</sup>	± 1452.14	7308.82 <sup>a</sup>	± 697.58	14972.02 <sup>b</sup>	± 1297.35	10356.42 <sup>ab</sup>	± 1626.95	14812.94 <sup>b</sup>	± 2844.11	9734.43 <sup>ab</sup>	± 856.66

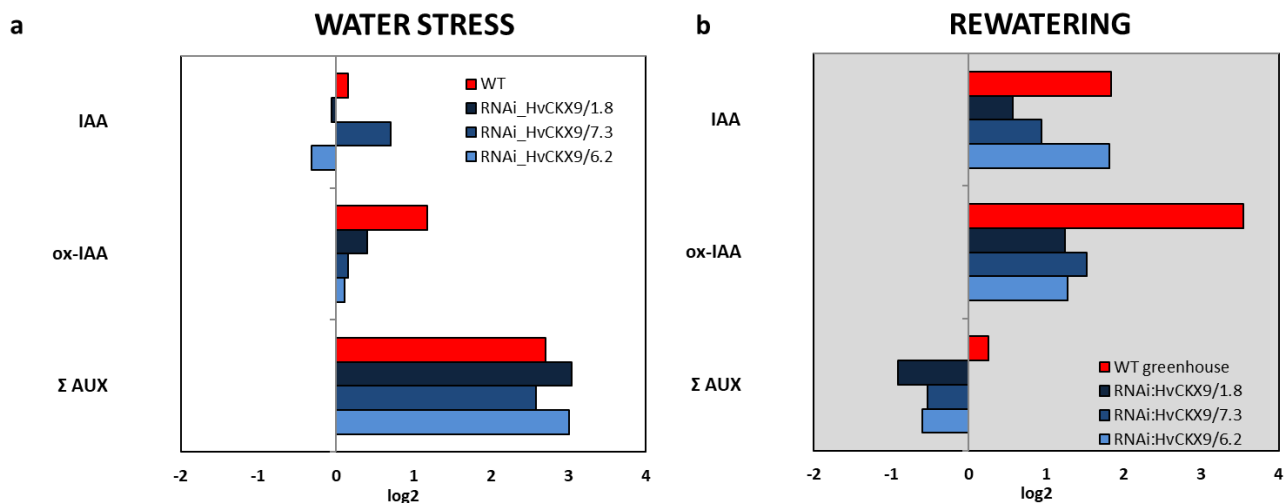


**Figure IV.22.** Profile of indole-3-acetic acid (IAA), ox-IAA and total auxin content in barley seedlings (wild type and 3 transgenic lines) at the end of the water stress period (left) and after 4 days of rewatering (right). Fold changes (presented as log<sub>2</sub> ratio) in the content of IAA, ox-IAA and total AUX between stressed (D) and non-stressed (W) barley genotypes.

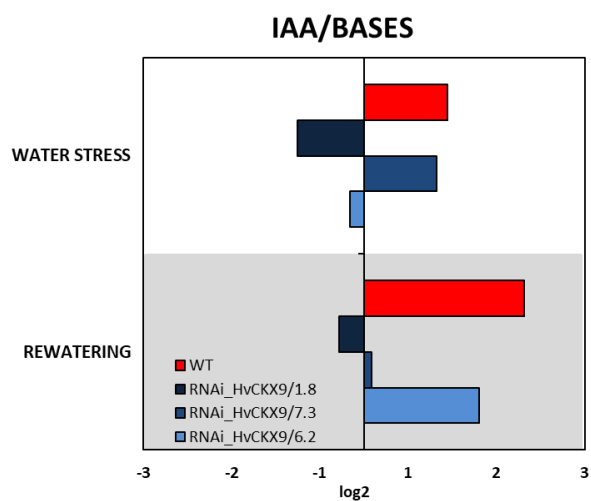


**Figure IV.23.** Profile of the ratio between IAA and free CKs in barley seedlings (wild type and 3 transgenic lines) at the end of the water stress period (upper part) and after 4 days of rewatering (lower part). Fold changes in the content (presented as log<sub>2</sub> ratio) ratio of this metabolites between stressed (D) and non-stressed (W) barley seedlings from two independent biological replicates (n=5) for each genotype.

The content of free PAs and AAs was also quantified. As showed in the previous chapter, most of these metabolites were accumulated as response to the stress. Only the AA Gln and the PA Spd dropped down in the D variants compared to the well-watered variant (Table IV.8 and 10,

Fig. IV.24a and 25a). Cad was only accumulated in the stressed variants under water-limited conditions but it was under the detection limits for the rest of the situations. No differences in Put and Spd were observed in the wt between non-stressed and stressed plants, whereas the stressed plants from all transgenic lines significantly accumulated Put. a higher increase in the level of Spm than wt but a lower decrease in Spd content after the stress period. The wt plants and the silenced line 7.3 presented high levels of Cad at the end of the water stress period, whereas a lower content was observed in the plants from the 1.8 and 6.2 lines (Table IV.9). After 4 days of rewatering, the water stressed plants from the silenced lines significantly reduced the content of Put, but not for wt (Table IV.9, Fig. IV.24b). Regarding AAs, as reported in Chapter III Pro was the most accumulated AA with the in all genotypes at the end of the water stress period (Table IV.10). The water stressed plants from all transgenic lines had lower accumulated levels of Asn, Asp, Glu but higher of Gln than wt plants (Table IV.10, Fig. IV.25a). After 4 days of rewatering, the content of total AAs was reduced in the stressed plants but were still significantly higher than the values of their controls. However, the stressed plants from the transgenic lines had less content of AAs than those from the wt, especially in the lines 1.8 and 7.3 that showed the faster recovery. This reduction was due to the recovery of the Tyr, Ile and Leu observed in these two lines (Table IV.11 and Fig. IV.25b).

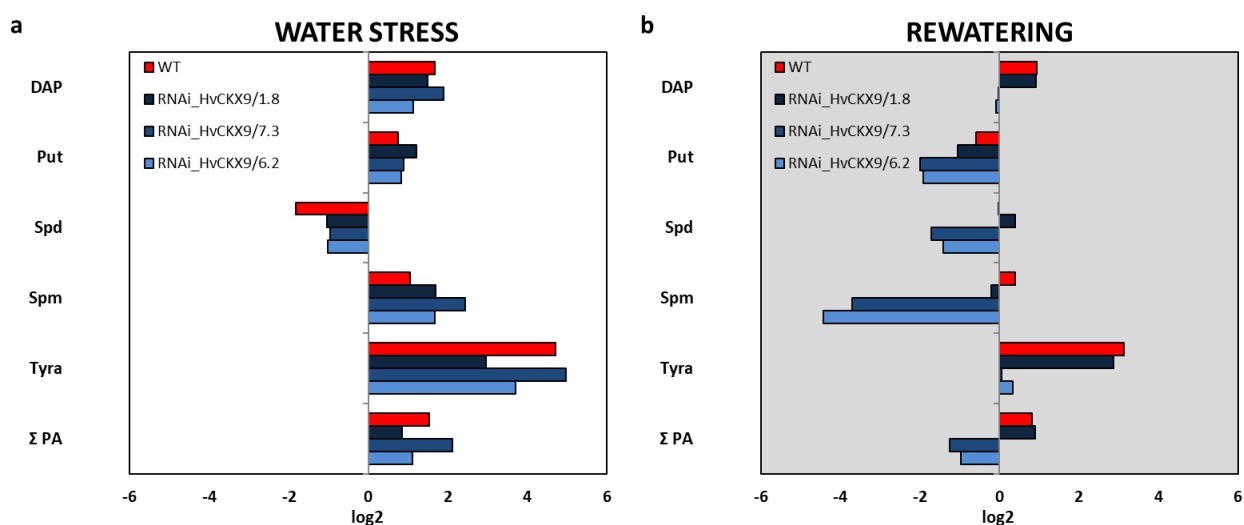


**Figure IV.24.** Profile of free PAs in barley seedlings (wild type and 3 transgenic lines) (a) at the end of the water stress period and (b) after 4 days of rewatering. Fold changes (presented as log<sub>2</sub> ratio) in the content of free PAs between stressed (D) and non-stressed (W) barley genotypes.

**Table IV.8.** Content of free PAs in barley seedlings (wild type and 3 transgenic lines) at the end of the water stress period. Different letters mean significant differences among treatments according Tukey HSD test after ANOVA.

	wild-type		HvCKX9 line 1.8		HvCKX9 line 7.3		HvCKX9 line 6.2	
	W	D	W	D	W	D	W	D
pmol/mg	average ± SE	average ± SE	average ± SE	average ± SE	average ± SE	average ± SE	average ± SE	average ± SE
<b>Cad</b>	< LOD	10.56 <sup>b</sup> ± 1.75	< LOD	1.48 <sup>a</sup> ± 0.43	< LOD	20.34 <sup>c</sup> ± 3.00	< LOD	2.20 <sup>a</sup> ± 1.19
<b>DAP</b>	17.80 <sup>ab</sup> ± 2.64	56.52 <sup>d</sup> ± 7.56	11.81 <sup>a</sup> ± 2.40	33.02 <sup>bc</sup> ± 2.05	18.40 <sup>ab</sup> ± 0.40	68.37 <sup>d</sup> ± 2.17	17.50 <sup>ab</sup> ± 1.54	38.27 <sup>c</sup> ± 2.59
<b>Put</b>	31.23 <sup>abcd</sup> ± 4.63	52.37 <sup>de</sup> ± 8.87	29.89 <sup>abc</sup> ± 5.45	69.03 <sup>e</sup> ± 1.00	27.42 <sup>a</sup> ± 0.81	50.71 <sup>bcde</sup> ± 2.41	29.06 <sup>ab</sup> ± 2.14	51.19 <sup>cde</sup> ± 4.01
<b>Spd</b>	128.28 <sup>b</sup> ± 24.40	36.30 <sup>a</sup> ± 4.19	96.01 <sup>a</sup> ± 30.36	46.29 <sup>a</sup> ± 6.68	96.15 <sup>a</sup> ± 14.42	49.19 <sup>a</sup> ± 1.47	105.42 <sup>a</sup> ± 21.55	51.66 <sup>a</sup> ± 5.07
<b>Spm</b>	2.28 <sup>cd</sup> ± 0.21	4.69 <sup>e</sup> ± 0.16	0.66 <sup>a</sup> ± 0.59	2.13 <sup>bcd</sup> ± 0.18	1.43 <sup>abc</sup> ± 0.14	7.75 <sup>f</sup> ± 0.01	0.88 <sup>ab</sup> ± 0.30	2.79 <sup>d</sup> ± 0.27
<b>Tyra</b>	15.69 <sup>a</sup> ± 0.94	411.01 <sup>d</sup> ± 46.63	16.56 <sup>a</sup> ± 2.46	128.54 <sup>b</sup> ± 16.00	16.63 <sup>a</sup> ± 1.34	518.57 <sup>e</sup> ± 6.79	16.99 <sup>a</sup> ± 1.16	220.75 <sup>c</sup> ± 15.22
<b>TOTAL PAs</b>	195.28 <sup>ab</sup> ± 32.81	571.46 <sup>c</sup> ± 69.17	154.94 <sup>a</sup> ± 41.25	280.49 <sup>ab</sup> ± 26.34	160.03 <sup>a</sup> ± 17.12	714.92 <sup>c</sup> ± 15.85	169.85 <sup>a</sup> ± 26.69	366.86 <sup>b</sup> ± 28.35

**Table IV.9.** Content of free PAs in barley seedlings (wild type and 3 transgenic lines) after 4 days of rewatering. Different letters mean significant differences among treatments according Tukey HSD test after ANOVA.

	wild-type		HvCKX9 line 1.8		HvCKX9 line 7.3		HvCKX9 line 6.2	
	RW	RD	RW	RD	RW	RD	RW	RD
pmol/mg	average ± SE	average ± SE	average ± SE	average ± SE	average ± SE	average ± SE	average ± SE	average ± SE
<b>Cad</b>	< LOD	< LOD	< LOD	< LOD	< LOD	< LOD	< LOD	< LOD
<b>DAP</b>	11.82 <sup>a</sup> ± 1.76	22.61 <sup>a</sup> ± 2.62	10.68 <sup>a</sup> ± 1.00	20.14 <sup>a</sup> ± 5.50	11.53 <sup>a</sup> ± 1.32	11.33 <sup>a</sup> ± 2.54	13.72 <sup>a</sup> ± 1.97	13.04 <sup>a</sup> ± 0.46
<b>Put</b>	37.91 <sup>bc</sup> ± 3.21	25.37 <sup>ab</sup> ± 3.13	37.25 <sup>bc</sup> ± 3.36	17.96 <sup>a</sup> ± 5.29	40.27 <sup>bc</sup> ± 3.53	10.06 <sup>a</sup> ± 2.54	47.12 <sup>c</sup> ± 6.27	12.54 <sup>a</sup> ± 0.30
<b>Spd</b>	109.64 <sup>a</sup> ± 17.15	108.88 <sup>a</sup> ± 21.03	99.09 <sup>a</sup> ± 6.02	131.26 <sup>a</sup> ± 43.21	132.05 <sup>a</sup> ± 26.36	40.40 <sup>a</sup> ± 4.81	145.53 <sup>a</sup> ± 38.74	54.67 <sup>a</sup> ± 3.64
<b>Spm</b>	2.92 <sup>abc</sup> ± 0.06	3.85 <sup>c</sup> ± 0.78	3.74 <sup>c</sup> ± 0.85	3.25 <sup>bc</sup> ± 1.10	3.89 <sup>c</sup> ± 0.10	0.30 <sup>ab</sup> ± 0.20	3.36 <sup>bc</sup> ± 0.70	0.16 <sup>a</sup> ± 0.09
<b>Tyra</b>	18.40 <sup>a</sup> ± 2.07	160.76 <sup>a</sup> ± 83.55	20.52 <sup>a</sup> ± 3.24	149.57 <sup>a</sup> ± 53.36	27.88 <sup>a</sup> ± 8.80	28.89 <sup>a</sup> ± 4.70	35.83 <sup>a</sup> ± 8.60	45.37 <sup>a</sup> ± 14.10
<b>TOTAL PAs</b>	180.69 <sup>a</sup> ± 24.25	321.47 <sup>a</sup> ± 111.11	171.28 <sup>a</sup> ± 14.48	322.18 <sup>a</sup> ± 108.47	215.62 <sup>a</sup> ± 40.11	90.98 <sup>a</sup> ± 14.79	245.56 <sup>a</sup> ± 56.28	125.78 <sup>a</sup> ± 18.59

**Table IV.10.** Content of AAs in barley seedlings (wild type and 3 transgenic lines) at the end of the water stress period. Different letters mean significant differences among treatments according Tukey HSD test after ANOVA.

pmol/mg	wild-type_W		wild-type_D		HvCKX9 line 1.8_W		HvCKX9 line 1.8_D		HvCKX9 line 7.3_W		HvCKX9 line 7.3_D		HvCKX9 line 6.2_W		HvCKX9 line 6.2_D	
	average	± SE	average	± SE	average	± SE	average	± SE	average	± SE	average	± SE	average	± SE	average	± SE
Ala	1.93 <sup>ab</sup>	± 0.14	3.53 <sup>c</sup>	± 0.09	1.95 <sup>ab</sup>	± 0.14	2.77 <sup>bc</sup>	± 0.05	2.66 <sup>bc</sup>	± 0.19	2.35 <sup>ab</sup>	± 0.02	1.33 <sup>a</sup>	± 0.05	2.44 <sup>abc</sup>	± 0.33
Arg	0.26 <sup>a</sup>	± 0.03	1.86 <sup>c</sup>	± 0.06	0.23 <sup>a</sup>	± 0.02	1.88 <sup>c</sup>	± 0.04	0.24 <sup>a</sup>	± 0.03	1.56 <sup>bc</sup>	± 0.15	0.37 <sup>a</sup>	± 0.02	1.26 <sup>b</sup>	± 0.15
Asn	1.29 <sup>a</sup>	± 0.08	9.86 <sup>b</sup>	± 0.40	2.08 <sup>a</sup>	± 0.15	10.74 <sup>b</sup>	± 0.40	1.71 <sup>a</sup>	± 0.20	8.41 <sup>b</sup>	± 0.15	1.97 <sup>a</sup>	± 0.05	7.60 <sup>b</sup>	± 1.22
Asp	8.16 <sup>ab</sup>	± 0.64	10.92 <sup>b</sup>	± 0.14	9.02 <sup>ab</sup>	± 0.63	9.87 <sup>ab</sup>	± 0.07	9.47 <sup>ab</sup>	± 0.64	8.62 <sup>ab</sup>	± 0.10	6.59 <sup>a</sup>	± 0.10	8.22 <sup>ab</sup>	± 1.10
GABA	0.24 <sup>ab</sup>	± 0.04	1.21 <sup>cd</sup>	± 0.06	0.19 <sup>a</sup>	± 0.01	0.81 <sup>a</sup>	± 0.02	0.35 <sup>abc</sup>	± 0.03	1.09 <sup>b</sup>	± 0.03	0.25 <sup>ab</sup>	± 0.01	1.41 <sup>d</sup>	± 0.34
Gln	7.69 <sup>bc</sup>	± 0.58	5.90 <sup>abc</sup>	± 0.16	8.30 <sup>bc</sup>	± 0.58	5.10 <sup>ab</sup>	± 0.16	9.02 <sup>c</sup>	± 0.86	6.19 <sup>abc</sup>	± 0.16	7.07 <sup>ab</sup>	± 0.24	3.68 <sup>a</sup>	± 0.60
Glu	7.17 <sup>a</sup>	± 0.53	14.49 <sup>c</sup>	± 0.33	7.90 <sup>a</sup>	± 0.45	13.25 <sup>bc</sup>	± 0.11	9.06 <sup>ab</sup>	± 0.75	9.56 <sup>ab</sup>	± 0.24	6.52 <sup>a</sup>	± 0.17	10.29 <sup>abc</sup>	± 1.46
Gly	0.18 <sup>a</sup>	± 0.01	0.55 <sup>b</sup>	± 0.01	0.61 <sup>b</sup>	± 0.04	0.49 <sup>b</sup>	± 0.01	0.14 <sup>a</sup>	± 0.01	0.60 <sup>b</sup>	± 0.03	0.07 <sup>a</sup>	± 0.00	0.16 <sup>a</sup>	± 0.03
Ile	0.17 <sup>a</sup>	± 0.02	2.35 <sup>d</sup>	± 0.01	0.18 <sup>a</sup>	± 0.01	1.89 <sup>c</sup>	± 0.02	0.19 <sup>a</sup>	± 0.02	2.49 <sup>d</sup>	± 0.01	0.20 <sup>a</sup>	± 0.01	1.11 <sup>b</sup>	± 0.16
Leu	0.10 <sup>a</sup>	± 0.01	1.07 <sup>c</sup>	± 0.02	0.09 <sup>a</sup>	± 0.01	0.96 <sup>c</sup>	± 0.01	0.10 <sup>a</sup>	± 0.01	1.09 <sup>c</sup>	± 0.01	0.14 <sup>a</sup>	± 0.01	0.60 <sup>b</sup>	± 0.09
Phe	0.07 <sup>a</sup>	± 0.00	0.45 <sup>c</sup>	± 0.01	0.08 <sup>a</sup>	± 0.01	0.27 <sup>b</sup>	± 0.00	0.08 <sup>a</sup>	± 0.01	0.60 <sup>d</sup>	± 0.03	0.07 <sup>a</sup>	± 0.00	0.16 <sup>a</sup>	± 0.02
Pro	0.16 <sup>a</sup>	± 0.01	98.87 <sup>c</sup>	± 0.89	0.19 <sup>a</sup>	± 0.03	43.39 <sup>b</sup>	± 0.43	0.19 <sup>a</sup>	± 0.03	106.81 <sup>c</sup>	± 1.21	0.20 <sup>a</sup>	± 0.02	35.98 <sup>b</sup>	± 4.99
Ser	8.17 <sup>a</sup>	± 0.57	15.55 <sup>c</sup>	± 0.34	9.77 <sup>ab</sup>	± 0.72	14.22 <sup>bc</sup>	± 0.20	9.39 <sup>ab</sup>	± 0.61	14.08 <sup>bc</sup>	± 0.65	5.88 <sup>a</sup>	± 0.23	9.69 <sup>ab</sup>	± 1.56
Thr	1.46 <sup>a</sup>	± 0.11	5.15 <sup>c</sup>	± 0.06	1.61 <sup>a</sup>	± 0.13	4.59 <sup>bc</sup>	± 0.06	1.91 <sup>a</sup>	± 0.11	4.11 <sup>bc</sup>	± 0.15	1.20 <sup>a</sup>	± 0.05	3.44 <sup>b</sup>	± 0.51
Trp	0.05 <sup>ab</sup>	± 0.00	0.72 <sup>d</sup>	± 0.03	0.05 <sup>ab</sup>	± 0.00	0.36 <sup>c</sup>	± 0.01	0.08 <sup>ab</sup>	± 0.01	1.08 <sup>e</sup>	± 0.05	0.04 <sup>a</sup>	± 0.00	0.23 <sup>bc</sup>	± 0.04
Tyr	0.21 <sup>a</sup>	± 0.01	0.85 <sup>c</sup>	± 0.05	0.21 <sup>a</sup>	± 0.02	0.71 <sup>bc</sup>	± 0.06	0.25 <sup>a</sup>	± 0.02	0.84 <sup>c</sup>	± 0.06	0.24 <sup>a</sup>	± 0.02	0.46 <sup>ab</sup>	± 0.06
Val	0.42 <sup>a</sup>	± 0.03	3.39 <sup>d</sup>	± 0.03	0.43 <sup>a</sup>	± 0.03	2.52 <sup>c</sup>	± 0.01	0.48 <sup>a</sup>	± 0.04	3.70 <sup>d</sup>	± 0.05	0.43 <sup>a</sup>	± 0.01	1.70 <sup>b</sup>	± 0.26
<b>TOTAL AAs</b>	<b>37.74<sup>a</sup></b>	<b>± 2.81</b>	<b>176.71<sup>c</sup></b>	<b>± 2.69</b>	<b>42.90<sup>a</sup></b>	<b>± 2.98</b>	<b>113.81<sup>b</sup></b>	<b>± 1.65</b>	<b>45.31<sup>a</sup></b>	<b>± 3.56</b>	<b>173.19<sup>c</sup></b>	<b>± 3.11</b>	<b>32.57<sup>a</sup></b>	<b>± 0.97</b>	<b>88.43<sup>b</sup></b>	<b>± 12.92</b>

**Table IV.11.** Content of AAs in barley seedlings (wild type and 3 transgenic lines) after 4 days of rewatering. Different letters mean significant differences among treatments according Tukey HSD test after ANOVA.

pmol/mg	wild-type_W		wild-type_D		HvCKX9 line 1.8_W		HvCKX9 line 1.8_D		HvCKX9 line 7.3_W		HvCKX9 line 7.3_D		HvCKX9 line 6.2_W		HvCKX9 line 6.2_D	
	average	± SE	average	± SE	average	± SE	average	± SE	average	± SE	average	± SE	average	± SE	average	± SE
Ala	1.45 <sup>a</sup>	± 0.11	2.53 <sup>ab</sup>	± 0.07	1.27 <sup>a</sup>	± 0.12	2.81 <sup>b</sup>	± 0.07	1.48 <sup>a</sup>	± 0.12	1.51 <sup>a</sup>	± 0.08	1.41 <sup>a</sup>	± 0.13	3.13 <sup>b</sup>	± 0.42
Arg	0.59 <sup>c</sup>	± 0.05	0.27 <sup>ab</sup>	± 0.02	0.62 <sup>c</sup>	± 0.05	0.36 <sup>abc</sup>	± 0.02	0.38 <sup>bc</sup>	± 0.04	0.07 <sup>a</sup>	± 0.03	0.49 <sup>bc</sup>	± 0.04	0.37 <sup>b</sup>	± 0.05
Asn	2.34 <sup>a</sup>	± 0.28	6.26 <sup>b</sup>	± 0.26	2.35 <sup>a</sup>	± 0.20	4.37 <sup>ab</sup>	± 0.13	2.06 <sup>a</sup>	± 0.19	2.23 <sup>a</sup>	± 0.18	2.32 <sup>a</sup>	± 0.13	6.47 <sup>b</sup>	± 0.94
Asp	6.47 <sup>a</sup>	± 0.37	10.52 <sup>ab</sup>	± 0.21	6.37 <sup>a</sup>	± 0.66	14.09 <sup>b</sup>	± 0.21	6.89 <sup>a</sup>	± 0.57	7.78 <sup>a</sup>	± 0.36	6.29 <sup>a</sup>	± 0.64	13.89 <sup>b</sup>	± 1.63
GABA	0.87 <sup>a</sup>	± 0.03	2.79 <sup>b</sup>	± 0.09	0.56 <sup>a</sup>	± 0.06	0.98 <sup>a</sup>	± 0.03	0.97 <sup>a</sup>	± 0.11	0.82 <sup>a</sup>	± 0.03	0.80 <sup>a</sup>	± 0.09	1.97 <sup>b</sup>	± 0.28
Gln	2.92 <sup>a</sup>	± 0.31	9.67 <sup>bc</sup>	± 0.27	2.78 <sup>a</sup>	± 0.22	13.44 <sup>c</sup>	± 0.34	2.56 <sup>a</sup>	± 0.24	6.07 <sup>ab</sup>	± 0.43	3.20 <sup>a</sup>	± 0.19	14.11 <sup>c</sup>	± 2.16
Glu	5.99 <sup>ab</sup>	± 0.42	7.99 <sup>abc</sup>	± 0.23	6.13 <sup>ab</sup>	± 0.61	11.03 <sup>c</sup>	± 0.16	7.17 <sup>abc</sup>	± 0.70	6.17 <sup>a</sup>	± 0.40	5.89 <sup>a</sup>	± 0.56	10.81 <sup>bc</sup>	± 1.45
Gly	0.07 <sup>a</sup>	± 0.01	0.23 <sup>bc</sup>	± 0.01	0.07 <sup>a</sup>	± 0.01	0.23 <sup>bc</sup>	± 0.01	0.07 <sup>a</sup>	± 0.01	0.12 <sup>ab</sup>	± 0.01	0.07 <sup>a</sup>	± 0.01	0.29 <sup>c</sup>	± 0.05
Ile	0.23 <sup>a</sup>	± 0.02	0.95 <sup>c</sup>	± 0.02	0.25 <sup>a</sup>	± 0.03	0.38 <sup>a</sup>	± 0.01	0.24 <sup>a</sup>	± 0.02	0.24 <sup>a</sup>	± 0.02	0.20 <sup>a</sup>	± 0.02	0.61 <sup>b</sup>	± 0.07
Leu	0.17 <sup>ab</sup>	± 0.01	0.32 <sup>c</sup>	± 0.01	0.16 <sup>ab</sup>	± 0.02	0.20 <sup>abc</sup>	± 0.00	0.18 <sup>ab</sup>	± 0.02	0.11 <sup>a</sup>	± 0.01	0.14 <sup>a</sup>	± 0.01	0.30 <sup>bc</sup>	± 0.04
Phe	0.09 <sup>a</sup>	± 0.01	0.51 <sup>c</sup>	± 0.02	0.08 <sup>a</sup>	± 0.01	0.17 <sup>ab</sup>	± 0.00	0.11 <sup>a</sup>	± 0.01	0.11 <sup>a</sup>	± 0.01	0.07 <sup>a</sup>	± 0.00	0.28 <sup>bc</sup>	± 0.04
Pro	0.13 <sup>a</sup>	± 0.02	44.20 <sup>d</sup>	± 0.95	0.24 <sup>a</sup>	± 0.02	7.39 <sup>b</sup>	± 0.11	0.19 <sup>a</sup>	± 0.03	8.47 <sup>b</sup>	± 0.36	0.14 <sup>a</sup>	± 0.01	22.69 <sup>c</sup>	± 2.50
Ser	5.67 <sup>a</sup>	± 0.49	8.73 <sup>ab</sup>	± 0.34	5.55 <sup>a</sup>	± 0.61	9.99 <sup>ab</sup>	± 0.14	6.34 <sup>ab</sup>	± 0.74	5.35 <sup>a</sup>	± 0.40	5.59 <sup>a</sup>	± 0.51	11.05 <sup>b</sup>	± 1.64
Thr	1.43 <sup>a</sup>	± 0.13	1.86 <sup>a</sup>	± 0.09	1.32 <sup>a</sup>	± 0.18	2.13 <sup>a</sup>	± 0.04	1.48 <sup>a</sup>	± 0.17	1.22 <sup>a</sup>	± 0.08	1.27 <sup>a</sup>	± 0.13	2.37 <sup>a</sup>	± 0.34
Trp	0.07 <sup>a</sup>	± 0.01	0.69 <sup>b</sup>	± 0.02	0.07 <sup>a</sup>	± 0.01	0.26 <sup>a</sup>	± 0.02	0.06 <sup>a</sup>	± 0.01	0.22 <sup>a</sup>	± 0.02	0.05 <sup>a</sup>	± 0.00	0.49 <sup>b</sup>	± 0.07
Tyr	0.24 <sup>a</sup>	± 0.03	0.60 <sup>b</sup>	± 0.02	0.29 <sup>a</sup>	± 0.04	0.31 <sup>a</sup>	± 0.03	0.29 <sup>a</sup>	± 0.05	0.19 <sup>a</sup>	± 0.01	0.21 <sup>a</sup>	± 0.01	0.40 <sup>ab</sup>	± 0.07
Val	0.39 <sup>a</sup>	± 0.03	1.75 <sup>b</sup>	± 0.06	0.42 <sup>a</sup>	± 0.05	0.85 <sup>a</sup>	± 0.00	0.41 <sup>a</sup>	± 0.05	0.53 <sup>a</sup>	± 0.03	0.38 <sup>a</sup>	± 0.04	1.43 <sup>b</sup>	± 0.19
<b>TOTAL AAs</b>	<b>29.09<sup>a</sup></b>	<b>± 2.32</b>	<b>99.86<sup>c</sup></b>	<b>± 2.69</b>	<b>28.54<sup>a</sup></b>	<b>± 2.87</b>	<b>68.98<sup>bc</sup></b>	<b>± 1.31</b>	<b>30.87<sup>a</sup></b>	<b>± 3.07</b>	<b>41.20<sup>ab</sup></b>	<b>± 2.45</b>	<b>28.54<sup>a</sup></b>	<b>± 2.51</b>	<b>90.65<sup>c</sup></b>	<b>± 11.93</b>

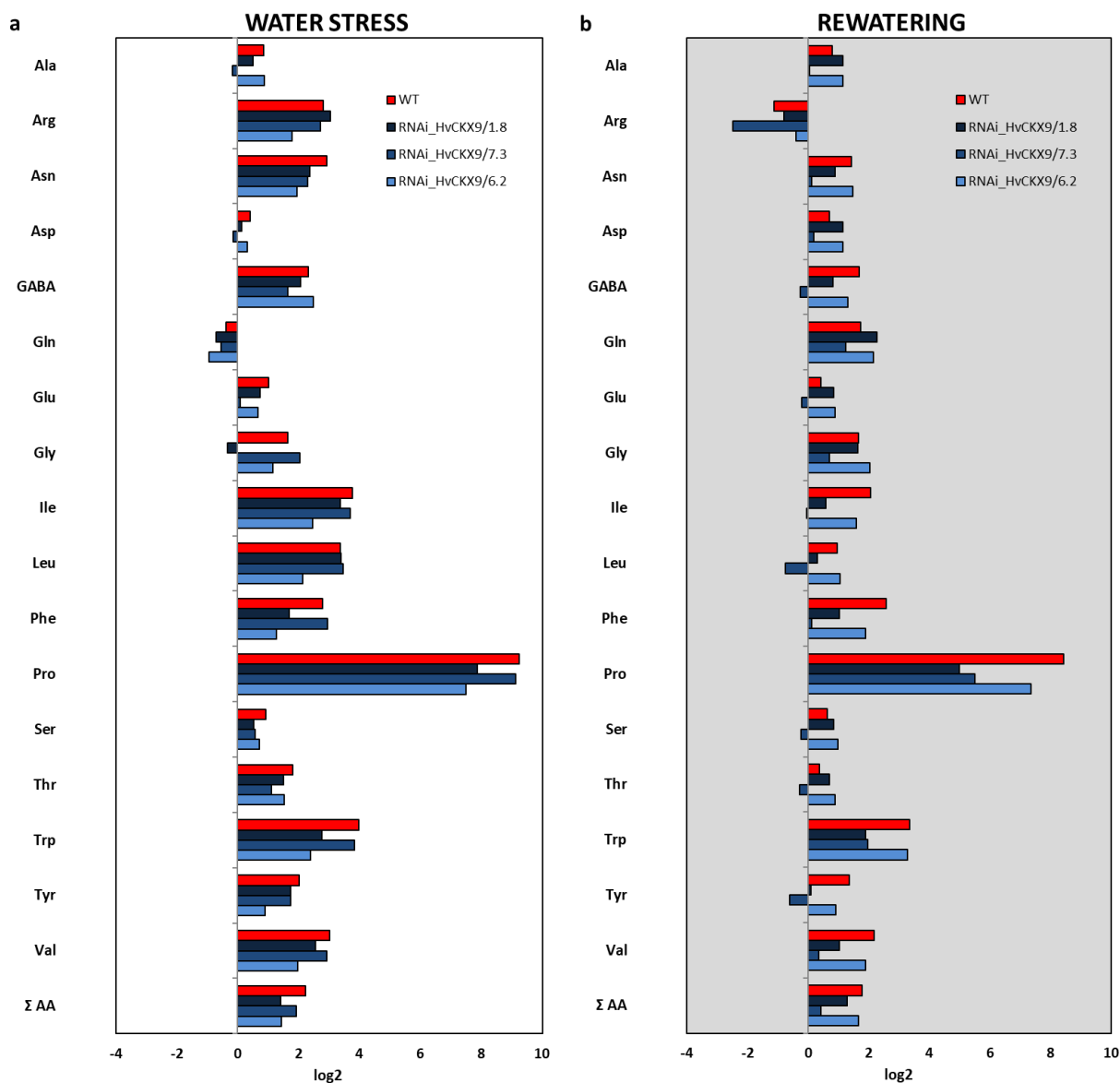


**Figure IV.25.** Profile of free AAs in barley seedlings (wild type and 3 transgenic lines) (a) at the end of the water stress period and (b) after 4 days of rewatering. Fold changes (presented as log<sub>2</sub> ratio) in the content of free AAs between stressed (D) and non-stressed (W) genotypes.

To understand the mechanism that conferred higher waters stress tolerance and recovery capacity to the selected transgenic lines we carried out two principal component (PC or dimension) analyses, in which the plants were evaluated for two different growth regimens, water-stressed (D) and well-watered (W) plants, at two time-points one at the end of the water stress period and the second one after 4 days of rewatering (RD and RW, respectively). To

facilitate visualization, the results were projected onto a biplot representing the scores (lines and treatment) and the loadings (analysed traits and quantified metabolites). At the end of the water stress period, the first two PCs together captured 71.5% of the variance (Fig. IV.26a and b). PC1 (Dim1) that accounted for 62.6% of the total variation, separated the D and W variants. The D lines were positively correlated with almost all quantified metabolites except for Gln, Spd and some type of CKs, such as *tZ*- and *cZ*-type, which correlated to the well-watered genotype (Fig. IV.26a and c). The W variants also showed positive correlation with the expression of *HvCKX2.2*, the canopy height, slope, biomass, BBCH and some florescence related parameters such as  $\Phi_{Po}$  and ETR. The PC2 (Dim2) that captured an additional 12.5% of the total variance and divided the D variants in two groups (red ellipses, Fig. IV.21a); the two lines RNAi:HvCKX9/1.8 and RNAi:HvCKX9/6.2 that delayed the symptoms of stress, and RNAi:HvCKX9/7.3 that stopped faster the growth (less canopy height) (Fig. IV.26a). The lines RNAi:HvCKX9/1.8 and RNAi:HvCKX9/6.2 were positively correlated with *iP*-type CKs and the expression of *HvCKX3* and *HvCKX5* genes but inversely related to the expression of *HvCKX1*, the IAA and the polyamines Cad and Spm.

Similar distribution of the variants was obtained in the PC analysis for the rewatering period (Fig. IV.27). The PC1 and 2 (Dim1 and Dim2) together captured also 68.7% of the variance of the model. Again, the PC1 only separated the well-watered plants from the water stressed ones. However, in the PC2, the transgenic lines separated from the stressed wt and among them. The lines that showed a faster recovery after the water limited period RNAi:HvCKX9/1.8 and RNAi:HvCKX9/7.3 positively correlated with the CKs *tZ*-type, ribotides and *N*-glucosides, the expression of the genes *HvCKX2.2* and in less extend with the expression of *HvCKX3*, the slope and the photosynthetic parameters *tZ*,  $\Phi_{PSII}$  and ETR. Contrarily, the stressed plants from the wt showed a positive correlation with some stress related metabolites such as GABA and Pro, the AAs Tyr, Ile and Leu, the total AUXs, ox-IAA, some *cZ*-type metabolites such as *cZRMP* and *cZR*, and the expression of the genes *HvCKX4* and *HvCKX11* (Fig. IV.27).



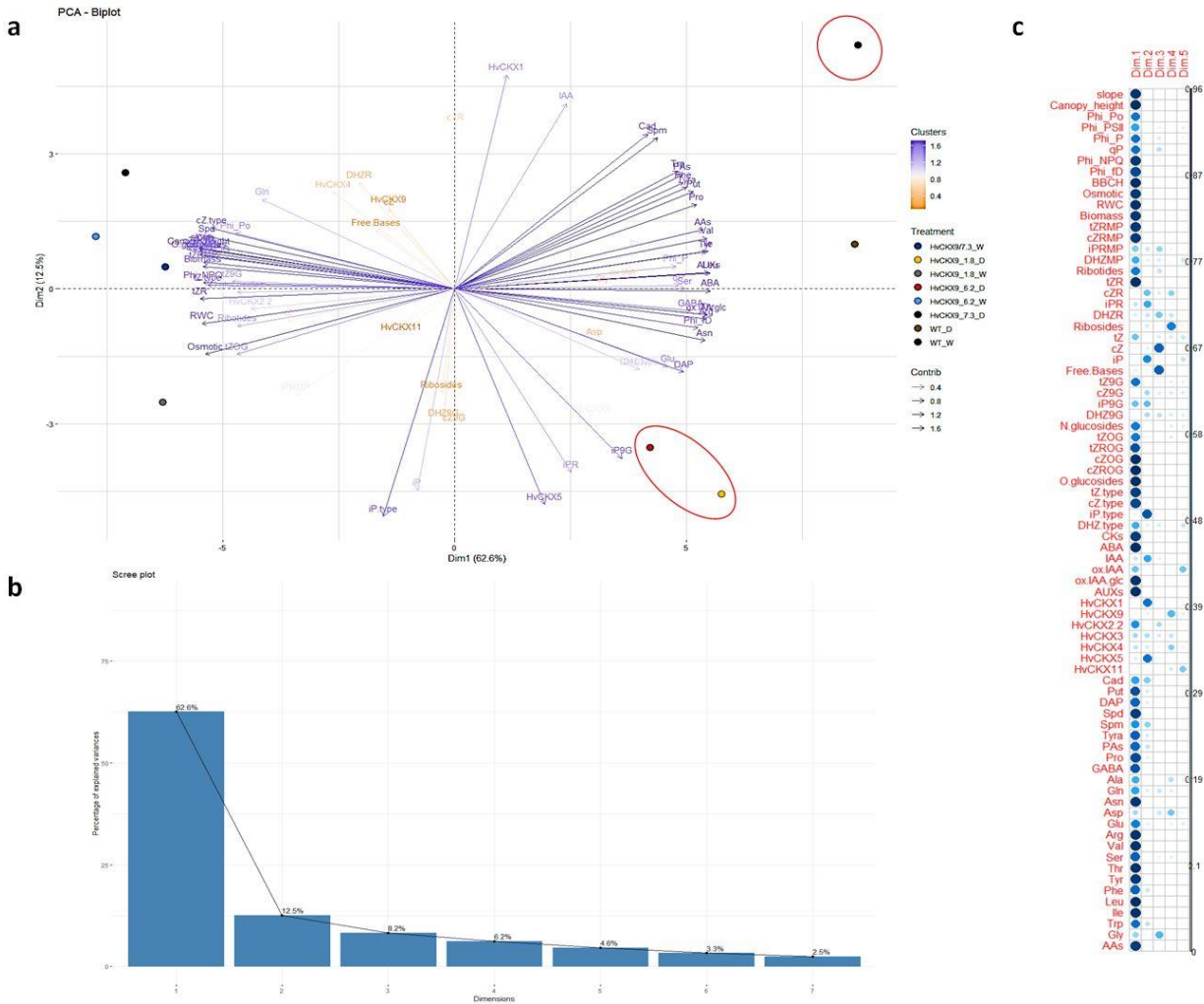


**Figure IV.26.** Principal component (PC) analysis of the traits in barley seedlings (wild type and 3 transgenic lines) at the end of the water stress period. (a) Principal component analysis (Dim1 and Dim2), (b) scree plot with the percentage of explained variance of the model for each PC (Dim) and (c) a contribution matrix of the loadings to each PC (Dim). Red ellipses indicated the groups according to PC2.

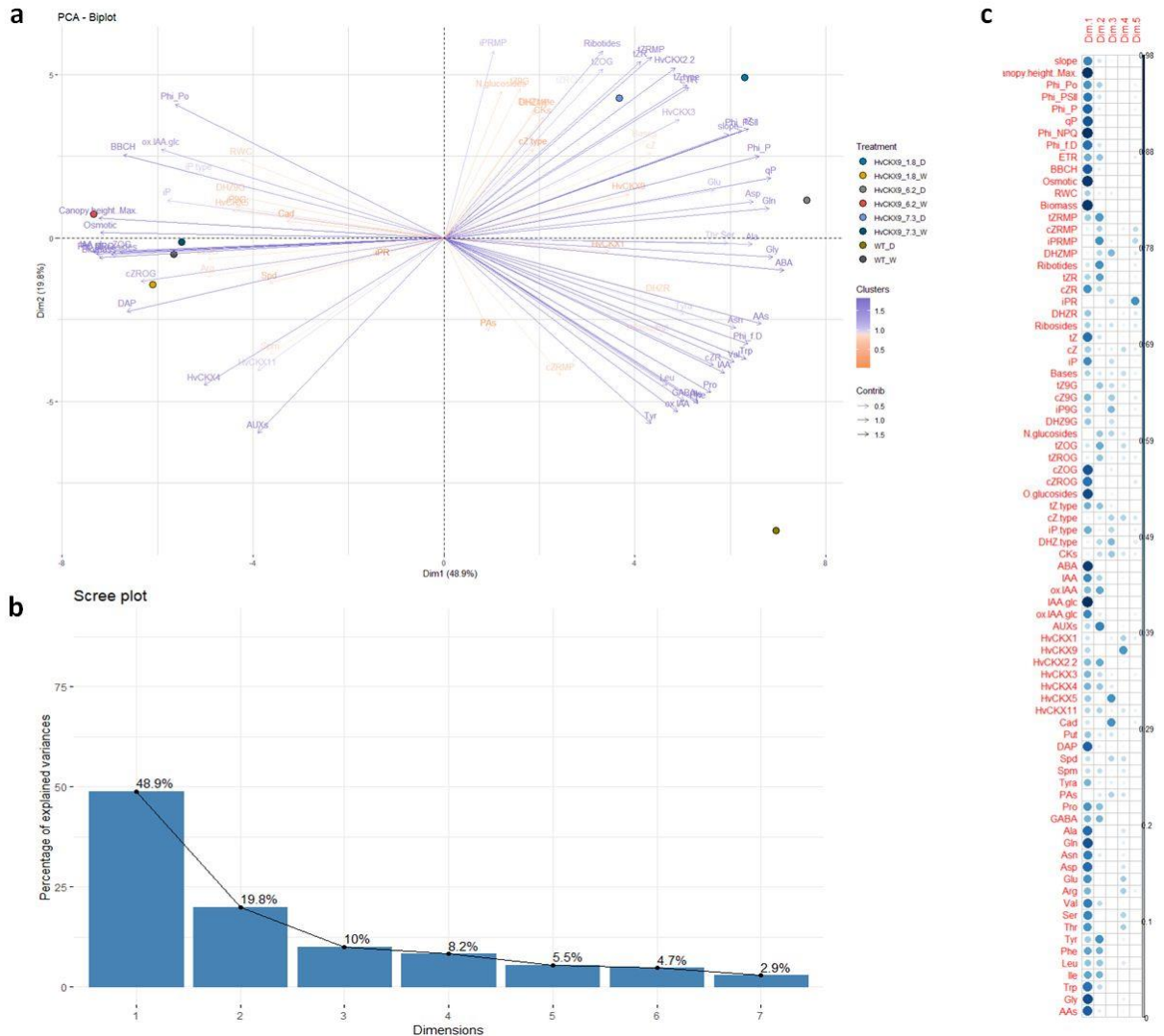


**Figure IV.27.** Principal component (PC) analysis of the traits in barley seedlings (wild type and 3 transgenic lines) after 4 days of rewatering. (a) Principal component analysis (Dim1 and Dim2), (b) scree plot with the percentage of explained variance of the model for each PC (Dim) and (c) a contribution matrix of the loadings to each PC (Dim).

Finally, to go further in the understanding whether CKs regulate the stress response in barley, we performed a linear correlation between the canopy height, slope, and the changes in the content of active CK forms, ABA, IAA and the variations of the CKX expression at the end of the water stress period and after 4 days of rewatering. The results were represented in two scatter plot, were the Pearson correlation and the significance were also included (Fig. IV.28 and 29). At the end of the water stress period, we observed that the canopy height and slope of the plants were positively correlated with the expression of *HvCKX2.2* ( $r= 0.80, P^* \leq 0.05$  and  $r= 0.83, P^* \leq 0.05$ , respectively). The changes in the expression of this gene also showed a significantly negative correlation with ABA levels ( $r= -0.81, P^* \leq 0.05$ ). At the same time, ABA negatively correlated with the canopy height and slope ( $r= -0.97, P^{***} \leq 0.001$  and  $r= -0.98, P^{***} \leq 0.001$ , respectively), pointing out the existence of a close relationship between these four trait regulating plants stress response in barley. Strong correlation was also found between the content of *iP* and the changes in the *HvCKX5* expression ( $r= 0.76, P^* \leq 0.05$ ) (Fig. IV.28). The expression of *HvCKX5* and *HvCKX3* were significantly correlated ( $r= 0.81, P^* \leq 0.05$ ) under water stress conditions.

Significant correlation was also obtained between the expression of *HvCKX5* and the levels of *iP* in the plants after 4 days of rewatering (Fig. IV.24). Similarly, the slope and the expression of *HvCKX2.2* and *HvCKX3* were also correlated ( $r= 0.83, P^* \leq 0.05$ ), and these two genes with *tZ* ( $r= 0.90, P^{**} \leq 0.01$  and  $r= 0.87, P^{**} \leq 0.01$ , respectively). However, *HvCKX4* showed totally opposite results with negative correlation with the slope and the *tZ* levels ( $r= 0.75, P^* \leq 0.05$  and  $r= 0.81, P^* \leq 0.05$ , respectively). At the same time, the slope and canopy height had opposite behaviour and showed positive and negative correlation with ABA and *tZ*, respectively. Altogether, it is clear that the changes in the CKX expression and the homeostasis between the different types of phytohormones play different roles for the plants water stress response and the recovery capacity.

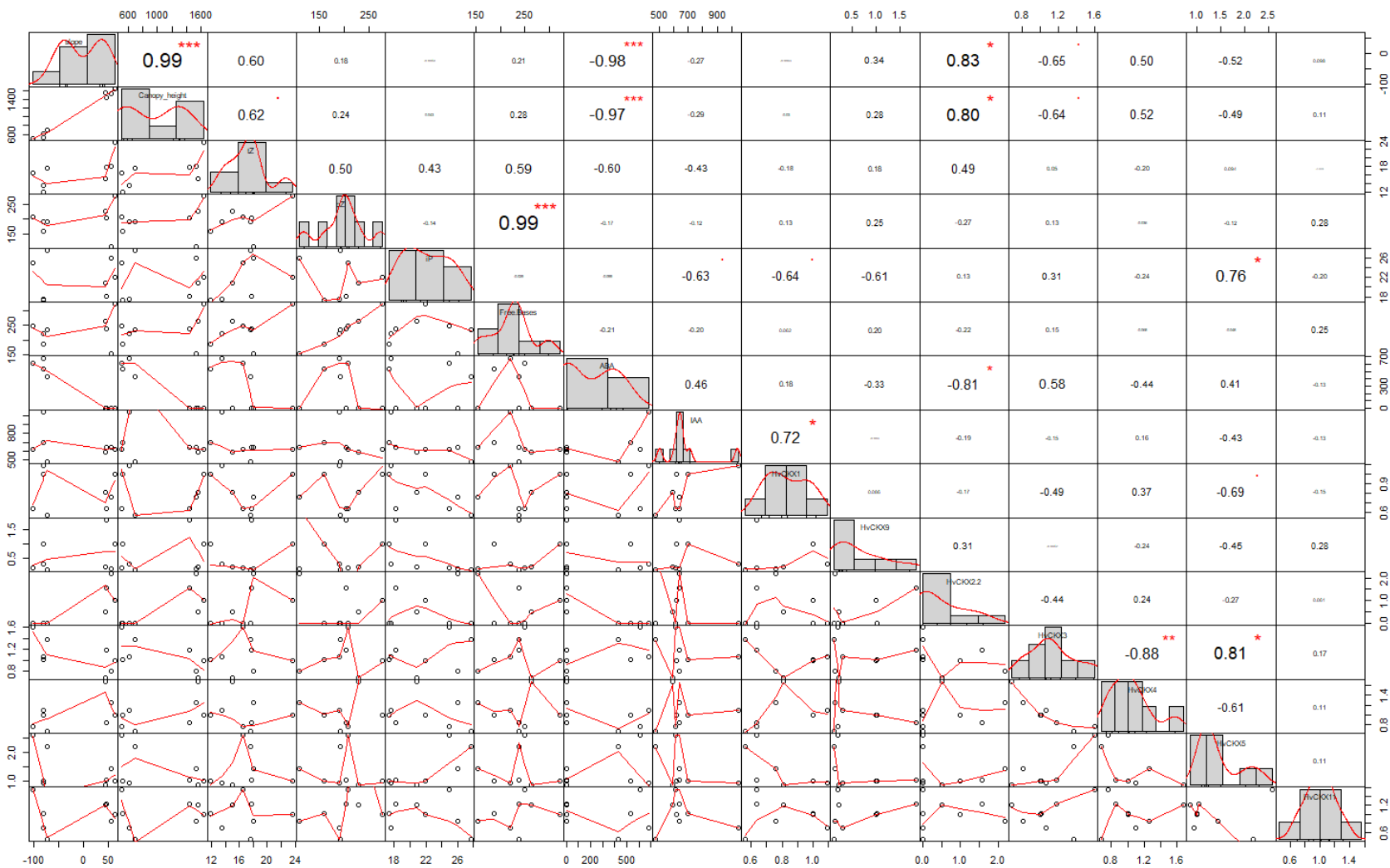


**Figure IV.28.** Correlation analysis of some traits in barley seedlings (wild type and 3 transgenic lines) at the end of the water stress period. Scatter plots of the most correlated traits presented in Fig.IV.26 undertaken in R 3.5.1.

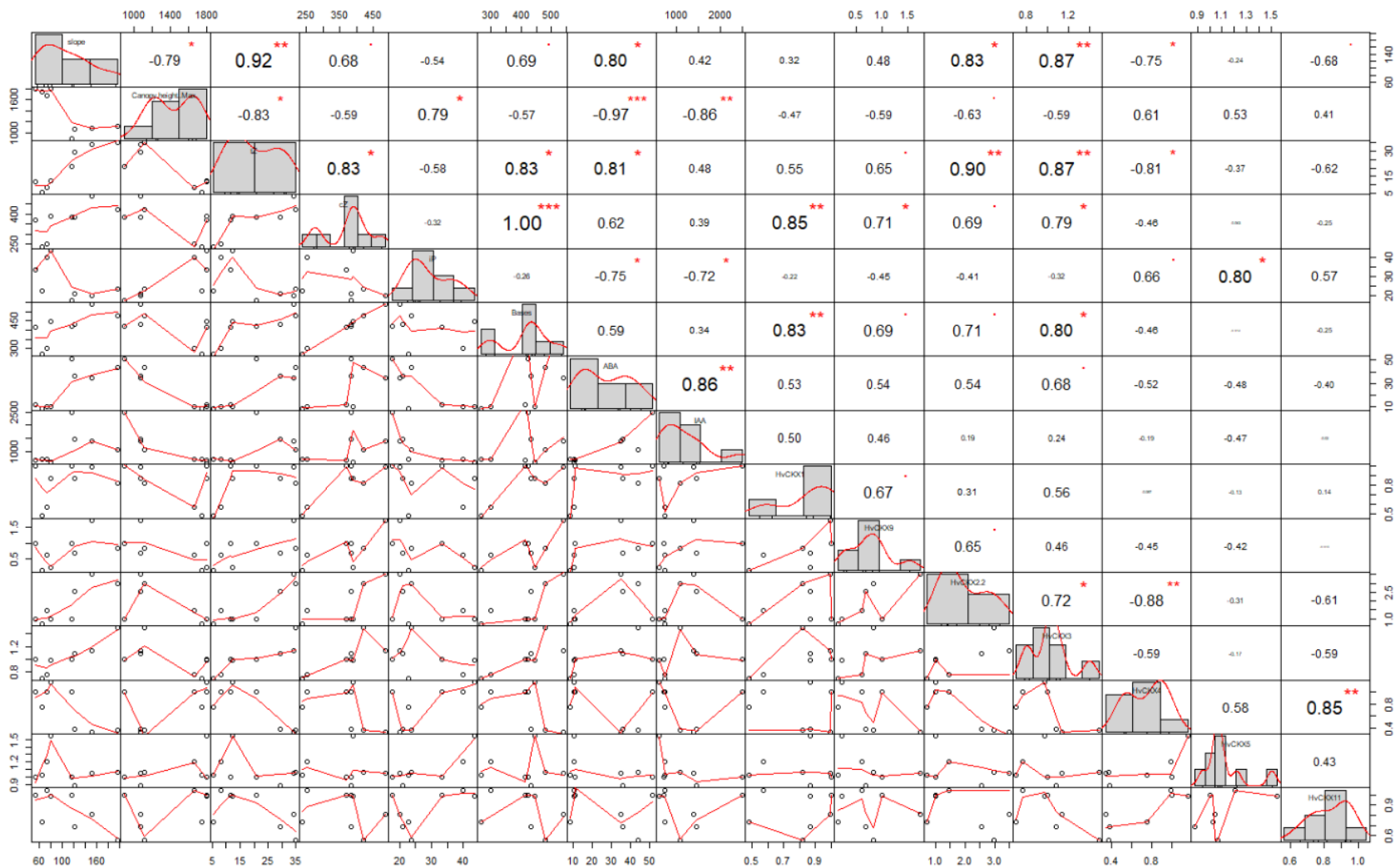


**Figure IV.29.** Correlation analysis of some traits in barley seedlings (wild type and 3 transgenic lines) after 4 days of rewatering. Scatter plots of the most correlated traits presented in Fig.IV.27 undertaken in R 3.5.1.

## IV. IV. Discussion

Water deficit is one of the main constraints limiting the crop production. Understanding the physiological bases of the water stress response of crops can help the breeders to improve crop management and production in many adverse climatic change scenarios. The goal of this chapter was to understand whether CKs regulate the plant stress response under limited water availability and the recovery after the stress in barley, as model plant and due to its agronomical interest. We performed a comparative study between wt and RNAi transgenic lines with silenced *CKX* genes. We focused on CK metabolism because the manipulation of endogenous levels of CK have been showed to improve water stress tolerance (Peleg and Blumwald, 2011; Pospíšilová et al., 2016; Rivero et al., 2007; von Wirén et al., 2018). It is well-known that plants are submitted to water deficit conditions, in general they reduced their endogenous CK content (Nishiyama et al., 2011; Todaka et al., 2017). Different approaches to alter the CK homeostasis in plants have been reported, either by overexpression biosynthetic (*IPT*) (Peleg and Blumwald, 2011; Rivero et al., 2009) or degradation (*CKX*) genes (Pospíšilová et al., 2016; Prerostova et al., 2018; von Wirén et al., 2018), leading to up- or down-regulation of the final pool of this hormone, respectively. In both cases, they showed that the alteration in the CK homeostasis has positive effects in the tolerance to water deficit. This is due to CK influences in many biological processes such as photosynthesis (Cortleven and Schmölling, 2015) or regulating the antioxidant response of the plant (Zavaleta-Mancera et al., 2007), among others.

We produced six RNAi transgenic lines, three for each silencing of *HvCKX2.2* and *HvCKX9* gene. The decrease expression of the targeted genes was confirmed in all transgenic barley lines in several developmental stages. Both silencing cassettes were functional, although the silencing of *HvCKX9* gene was more efficient, being the silencing effective in all stages analyzed. For the study, a total of 6 transgenic lines (3 lines per silencing) were selected so they have the same yield as the wt plants (Fig. IV.9). When the lines were grown under limited water availability the lines showed different phenotype than wt, with more homogeneous phenotype between the different RNAi:*HvCKX9* transgenic lines (Fig... IV. 11 y 14). The lack of homogeneity in the response to water stress among the different independent lines with silenced *HvCKX2.2* could be

caused by several factors such as number of integrations, position of the insertion as well as changes in expression of the silencing cassette along the development of the plants, as reviewed by Kooter et al. (1999), Matzke and Matzke (1998) and Wakimoto (1998).

We performed a deeper study of the three selected transgenic lines RNAi:HvCKX9 and different response to water stress were obtained classified in three groups; genotypes with water stress tolerance (RNAi:HvCKX9/6.2), genotypes with high capacity of recovery (RNAi:HvCKX9/7.3), or both (RNAi:HvCKX9/1.8). Under water stress conditions, the improved tolerance in RNAi:HvCKX9/1.8 and RNAi:HvCKX9/6.2 was in parallel with a higher accumulation of transcripts for *HvCKX3* and *HvCKX5*. The gene *HvCKX5* has been reported to improve nitrogen use efficiency (Han et al., 2016). Besides, in our study the expression of *HvCKX5* was only positively correlated to the *iP* content ( $R= 0.76$ ,  $P^*\leq 0.05$ ) (Fig. IV.28), and according to the PC analysis both traits related to the two more tolerant lines (Fig. IV.26). The base *iP* together with *tZ* have been also described to regulate nitrogen uptake in maize (Lacuesta et al., 2018). In addition, a strong positive correlation existed between the expression profile of *HvCKX3* and *HvCKX5* ( $R= 0.81$ ,  $P^*\leq 0.05$ ) (Fig. IV.28). The expression of *TaCKX3*, a close orthologue of *HvCKX3* was also described to be induced by water and salt stress (Ma et al., 2010). Altogether, we suggested that the water stress tolerance in barley is related to a higher nitrogen use efficiency regulated by *HvCKX5* and probably *HvCKX3*, together with a lower reduction of the *iP*-type CKs.

After rewatering, all stressed plants increased their CK content. Increased levels of CKs have been already reported to influence positively the recovery (Prerostova et al., 2018), but our results suggest that this must be due to the accumulation of particular CKs and specific *CKX* expression profile. Thus, after 4 days of recovery, the genes *HvCKX2.2* and again *HvCKX3* were highly expressed in the most tolerant varieties (Fig. IV.29). In both cases, the variations in the expression profile were positively correlated with the *tZ* content. Opposite to our results Prerostova et al. (2018) reported that the up-regulation of *HvCKX2* reduced the endogenous levels of *tZ* in the plants. This contradiction could be due to the plant species studied and also the way in which the stress is applied.

The water stress response of the plants involves a complex crosstalk with other plant hormone and metabolites. As example, ABA acts antagonistically to CK and both phytohormones

tightly regulate each other. It was reported that ABA regulate CK metabolism (Vysotskaya et al., 2009) and also that CK receptors are negative regulators of ABA signaling pathway (Tran et al., 2007). In our work, it was clear that ABA regulated canopy height and slope and hence the growth of our barley plants in the two studied situations at the end of the water stress period and after 4 days of rewatering (Fig. IV.28 and 29). However, all the stressed plants accumulated ABA, and the differences among genotypes did not allow the separation between the identified plant stress strategies.

The changes in the content of AUXs, however, varied among lines. For example, more IAA was positively correlated with the more sensitive lines at the end of the stress period (Fig. IV. 28). Many controversial results existed about the accumulation or reduction of IAA levels in plant under water stress conditions. For example, IAA has been reported to be accumulated at least in *Arabidopsis* and pine (De Diego et al., 2013; Prerostova et al., 2018). The IAA accumulation could be a physiological strategy that plants used to induce leaf epinasty (De Diego et al., 2013). Thus, the leaf curvature contributes to reduce the light capture area, and hence leaf photodamage. As corroboration, in our work, the stressed seedlings from the wt plants showed more reduced the chlorophyll fluorescence parameter than the *HvCKX9* lines. In addition, they also showed the highest accumulation of Pro under stress conditions and after rewatering. The AA Pro is considered a compatible solute contributing to the osmotic response of the plant, antioxidant and that also acts as signal molecule (Podlešáková et al., 2019). However, in our study was more an indicator of stress than a tolerance marker so after rewatering it was maintained at high concentration in those genotypes with worse recovery capacity. Finally, it is worth mentioning that Gln used to be accumulated in plant under water stress conditions (Fig. III.10). However, the stressed plants from the transgenic lines did not change the Gln levels compared to their respective controls (Fig. IV.25 y Table IV.10). This AA has been also reported to regulate CK biosynthesis (Sakakibara et al., 2006). Altogether, there is a clear overlapping of activated functions between closely related metabolites that act as signal molecules, including CKs, AAs and also PAs.

PAs are also considered plant growth regulators that have a crucial role like antioxidants, contributors to the plant osmotic adjustment and as signal molecules (Liu et al., 2015; Minocha



et al., 2014). In our experimental conditions, the modification in CK homeostasis affected the PA content. Particularly, higher tolerance to stress was negatively correlated with the accumulation of Cad and Spm, being the last one also accumulated together with Put in plants with lower recovery capacity (Fig. IV.24 and Table 9). However, the exogenous application of PAs has been proved to a good approach to mitigate the stress adverse effects status (Ebeed et al., 2017; Ugena et al., 2018). This must be because the plants stress tolerance is due to the homeostasis of many different metabolic pathway in which not only the synthesis but also the catabolism define the plant stress response and tolerance.

## IV. V. Conclusion

We performed a detailed phenotypic characterization of barley lines with altered CK content to dissect and interpret the metabolic readjustments during CK- mediated water stress tolerance and recovery. Three type of responses were identified, i.e.: sensitive, tolerant and/or high recovery capacity. The RNAi:*HvCKX9* transgenic lines showed better stress tolerance and recovery capacity compared to wt plant. They presented a higher canopy height and water related parameters, and more efficient fluorescence. Besides, they accumulated more *iP*-type CK but less IAA, Cad and Spm, and showed a higher expression of *HvCKX3* and *HvCKX5*. The faster recovery was related to a higher canopy height and expression of *HvCKX3* and *HvCKX2.2* and more *tZ*-type CKs. As summary, the modification of the CK levels in barley could be an effective biotechnological approach to improve plant performance under water stress. Further studies should be performed using *HvCKX3* or *HvCKX5* as candidate genes for improve barley stress tolerance.

## **CHAPTER V: GENERAL DISCUSSION**

The presented thesis focused on the study of the role that CKs are playing as regulators of the plant stress response to two of the major stressors such as shade and water deficit. The study was performed in two crops with agronomical interest, barley and wheat, for the shading-induced stress and barley for the water stress.

All results showed that CKs are relevant hormones regulating plant to shading-induced and water stress response. In both cases, the maintenance of the endogenous CKs (especially the base forms) was crucial for delaying the stress-induced negative effects in the plants. Concretely, we showed that one of the main factors conditioning the CK content was the regulation of CK degradation. Under shading-induced stress a marked up-regulation of the *CKX1* gene in senescing leaves of barley and wheat occurred (Chapter II). Similarly, water stressed plants also increased the expression of *HvCKX1*, especially in the most sensitive lines (Chapter III). Silencing of the *HvCKX1* gene decreases the cytokinin oxidase/dehydrogenase level in barley and leads to higher plant productivity (Zalewski et al., 2010). However, the involvements of the different CKX isoform regulating plant stress response is still unclear.

Opposite to *CKX1*, the upregulation of the *CKX3* gene has been related to a lower Chl degradation under shading-induced stress and higher water stress tolerance in wheat and barley, respectively. In agreement with our results, previous published study showed that the expression of *TaCKX3*, a close orthologue of *HvCKX3* was also described to be induced by water and salt stress (Ma et al., 2010). The expression of this gene was also closely related to *HvCKX5*, which at the same time correlated with the *iP* content of the plants ( $R=0.76$ ,  $P^*\leq 0.05$ ) (Fig. IV.28). The higher values of all these traits were obtained in the most tolerant lines (Fig. IV.26). The CK base *iP* together with *tZ* have been also described to regulate nitrogen uptake in maize (Lacuesta et al., 2018). Altogether, the results suggested that the water stress tolerance of barley depends of the crosstalk between CK and N metabolism, and hence the nitrogen use efficiency of the plants. In addition, the transgenic *HvCKX9* lines were more efficient capturing the light. It can be due to their capacity to delay the senescence under stress, as we observed in the Chapter II.

The recovery capacity after a water-limited period varied among lines. In this regard, a higher expression of *HvCKX2.2* and *HvCKX3* improved the recovery capacity of the barley plants. These plants have also higher levels of *tZ*-type CKs. Prerostova et al. (2018) also reported that

after re-watering, the growth rate acceleration in *Arabidopsis* was accompanied by high levels of *tZ*. However, they also reported that the up-regulation of *HvCKX2* reduced the endogenous levels of *tZ* in the plants. Opposite results were obtained in our work whereas the *HvCKX2* was positively correlated with *tZ* levels at least after the rewatering. In Barley, two *HvCKX2*, *HvCKX2.1* and *HvCKX2.2*, have been characterized and identified (Zalewski et al., 2014). It could happen that both isoforms differentially respond to the growth conditions and including among lines.

The water stress response and recovery capacity was not only related to CKs. A complex crosstalk with other plant hormones and stress-related metabolites such as AAs and PAs was also observed. As example, our results showed that Pro and PA pathway is highly affected in the transgenic lines. However, the exogenous addition of these compounds has been also reported to modify the hormone homeostasis of the plants (reviewed by Podlešáková et al., 2019). Thus, there is a clear overlapping of function between these compounds regulating plant stress response

As summary, the changes in plant homeostasis condition the performance of the plant under different growth conditions, especially under stress. Thus, the alteration of the CK homeostasis through the down-regulation of *CKX* genes in plants resulted in a good tool to study the plant response to shading-induced stress and water deficit. Besides, as we showed in this thesis additional information can be obtained about the crosstalk between the primary and secondary metabolism regulating plant stress response and recovery.

## **REFERENCES**

- Acharya, B.R., Assmann, S.M., 2009. Hormone interactions in stomatal function. *Plant Mol. Biol.* 69, 451–462. <https://doi.org/10.1007/s11103-008-9427-0>
- Aebi, H., 1984. Catalase in vitro. *Methods Enzymol.* 105, 121–126.
- Ahmed, I.M., Dai, H., Zheng, W., Cao, F., Zhang, G., Sun, D., Wu, F., 2013. Genotypic differences in physiological characteristics in the tolerance to drought and salinity combined stress between Tibetan wild and cultivated barley. *Plant Physiol. Biochem.* 63, 49–60. <https://doi.org/10.1016/j.plaphy.2012.11.004>
- Akashi, K., Miyake, C., Yokota, A., 2001. Citrulline, a novel compatible solute in drought-tolerant wild watermelon leaves, is an efficient hydroxyl radical scavenger. *FEBS Lett.* 508, 438–442. [https://doi.org/10.1016/S0014-5793\(01\)03123-4](https://doi.org/10.1016/S0014-5793(01)03123-4)
- Antoniadi, I., Plačková, L., Simonovik, B., Doležal, K., Turnbull, C., Ljung, K., Novák, O., 2015. Cell-type-specific cytokinin distribution within the arabidopsis primary root apex. *Plant Cell* 27, 1955–1967. <https://doi.org/10.1105/tpc.15.00176>
- Appels, R., Eversole, K., Feuillet, C., Keller, B., Rogers, J., Stein, N., Pozniak, C.J., Choulet, F., Distelfeld, A., Poland, J., Ronen, G., Barad, O., Baruch, K., Keeble-Gagnère, G., Mascher, M., Ben-Zvi, G., Josselin, A.A., Himmelbach, A., Balfourier, F., Gutierrez-Gonzalez, J., Hayden, M., Koh, C.S., Muehlbauer, G., Pasam, R.K., Paux, E., Rigault, P., Tibbits, J., Tiwari, V., Spannagl, M., Lang, D., Gundlach, H., Haberer, G., Mayer, K.F.X., Ormanbekova, D., Prade, V., Wicker, T., Swarbreck, D., Rimbart, H., Felder, M., Guilhot, N., Kaithakottil, G., Keilwagen, J., Leroy, P., Lux, T., Twardziok, S., Venturini, L., Juhasz, A., Abrouk, M., Fischer, I., Uauy, C., Borrill, P., Ramirez-Gonzalez, R.H., Arnaud, D., Chalabi, S., Chalhoub, B., Cory, A., Datla, R., Davey, M.W., Jacobs, J., Robinson, S.J., Steuernagel, B., Van Ex, F., Wulff, B.B.H., Benhamed, M., Bendahmane, A., Concia, L., Latrasse, D., Alaux, M., Bartoš, J., Bellec, A., Berges, H., Doležal, J., Frenkel, Z., Gill, B., Korol, A., Letellier, T., Olsen, O.A., Šimková, H., Singh, K., Valárik, M., Van Der Vossen, E., Vautrin, S., Weining, S., Fahima, T., Glikson, V., Raats, D., Toegelová, H., Vrána, J., Sourdille, P., Darrier, B., Barabaschi, D., Cattivelli, L., Hernandez, P., Galvez, S., Budak, H., Jones, J.D.G., Witek, K., Yu, G., Small, I., Melonek, J., Zhou, R., Belova, T., Kanyuka, K., King, R., Nilsen, K., Walkowiak, S., Cuthbert, R., Knox, R., Wiebe, K., Xiang, D., Rohde, A., Golds, T., Čížková, J., Akpinar, B.A., Biyiklioglu, S., Gao, L., N'Daiye, A., Číhalíková, J., Kubaláková, M., Šafář, J., Alfama, F., Adam-Blondon, A.F., Flores, R., Guerche, C., Loaec, M., Quesneville, H., Sharpe, A.G., Condie, J., Ens, J., Maclachlan, R., Tan, Y., Alberti, A., Aury, J.M., Barbe, V., Couloux, A., Cruaud, C., Labadie, K., Mangenot, S., Wincker, P., Kaur, G., Luo, M., Sehgal, S., Chhuneja, P., Gupta, O.P., Jindal, S., Kaur, P., Malik, P., Sharma, P., Yadav, B., Singh, N.K., Khurana, J.P., Chaudhary, C., Khurana, P., Kumar, V.,

- Mahato, A., Mathur, S., Sevanthi, A., Sharma, N., Tomar, R.S., Holušová, K., Plíhal, O., Clark, M.D., Heavens, D., Kettleborough, G., Wright, J., Balcárková, B., Hu, Y., Ravin, N., Skryabin, K., Beletsky, A., Kadnikov, V., Mardanov, A., Nesterov, M., Rakitin, A., Sergeeva, E., Kanamori, H., Katagiri, S., Kobayashi, F., Nasuda, S., Tanaka, T., Wu, J., Cattonaro, F., Jiumeng, M., Kugler, K., Pfeifer, M., Sandve, S., Xun, X., Zhan, B., Batley, J., Bayer, P.E., Edwards, D., Hayashi, S., Tulpová, Z., Visendi, P., Cui, L., Du, X., Feng, K., Nie, X., Tong, W., Wang, L., 2018. Shifting the limits in wheat research and breeding using a fully annotated reference genome. *Science* 361, eaar7191. <https://doi.org/10.1126/science.aar7191>
- Araus, J.L., Cairns, J.E., 2014. Field high-throughput phenotyping: The new crop breeding frontier. *Trends Plant Sci.* 19, 52–61. <https://doi.org/10.1016/j.tplants.2013.09.008>
- Ashikari, M., Sakakibara, H., Lin, S.Y., Yamamoto, T., Takashi, T., Nishimura, A., Angeles, E.R., Qian, Q., Kitano, H., Matsuoka, M., 2005. Cytokinin Oxidase Regulates Rice Grain Production *Science* 309, 741-5. <https://doi.org/10.1126/science.1113373>.
- Athar, H., Ashraf, M., 2009. Salinity and water stress 44. <https://doi.org/10.1007/978-1-4020-9065-3>
- Awlia, M., Nigro, A., Fajkus, J., Schmoeckel, S.M., Negrão, S., Santelia, D., Trtílek, M., Tester, M., Julkowska, M.M., Panzarová, K., 2016. High-throughput non-destructive phenotyping of traits that contribute to salinity tolerance in *Arabidopsis thaliana*. *Front. Plant Sci.* 7, 1–15. <https://doi.org/10.3389/fpls.2016.01414>
- Aziz, A., Martin-Tanguy, J., Larher, F., 1999. Salt stress-induced proline accumulation and changes in tyramine and polyamine levels are linked to ionic adjustment in tomato leaf discs. *Plant Sci.* 145, 83–91. [https://doi.org/10.1016/S0168-9452\(99\)00071-0](https://doi.org/10.1016/S0168-9452(99)00071-0)
- Aziz, A., Martin-Tanguy, J., Larher, F., 1998. Stress-induced changes in polyamine and tyramine levels can regulate proline accumulation in tomato leaf discs treated with sodium chloride. *Physiol. Plant.* 104, 195-202. <https://doi.org/10.1034/j.1399-3054.1998.1040207.x>
- Badr, A., Salamini, F., M, K., Pozzi, C., Effgen, S., Rohde, W., Ibrahim, H.H., Rabey, H. El, Sch, R., 2012. On the origin and domestication history of barley (*Hordeum vulgare*). *Mol. Biol. Evol.* 17, 499–510. <https://doi.org/10.1093/oxfordjournals.molbev.a026330>
- Barnabás, B., Jäger, K., Fehér, A., 2008. The effect of drought and heat stress on reproductive processes in cereals. *Plant, Cell Environ.* 31, 11–38. <https://doi.org/10.1111/j.1365-3040.2007.01727.x>
- Berger, B., Parent, B., Tester, M., 2010. High-throughput shoot imaging to study drought responses. *J. Exp. Bot.* 61, 3519–3528. <https://doi.org/10.1093/jxb/erq201>
- Bielach, A., Hrtyan, M., Tognetti, V.B., 2017. Plants under stress: Involvement of auxin and cytokinin. *Int.*

- J. Mol. Sci. 4, E1427. <https://doi.org/10.3390/ijms18071427>
- Bilyeu, K.D., Cole, J.L., Laskey, J.G., Riekhof, W.R., Esparza, T.J., Kramer, M.D., Morris, R.O., 2001. Molecular and biochemical characterization of a cytokinin oxidase from maize. *Plant Physiol.* 125, 378–86. <https://doi.org/10.1104/pp.125.1.378>
- Biswal, U.C., Biswal, B., 1984. Photocontrol of leaf senescence. *Photochem. Photobiol.* 39, 875–879. <https://doi.org/10.1111/j.1751-1097.1984.tb08874.x>
- Bitrián, M., Zarza, X., Altabella, T., Tiburcio, A.F., Alcázar, R., 2012. Polyamines under abiotic stress: Metabolic crossroads and hormonal crosstalks in plants. *Metabolites* 2, 516–528. <https://doi.org/10.3390/metabo2030516>
- Blum, A., 1996. Crop responses to drought and the interpretation of adaptation. *Plant Growth Regul.* 20, 135–148. <https://doi.org/10.1007/BF00024010>
- Boyer, J.S., 1982. Plant productivity and environment. *Science.* 218, 443-8.
- Bradford, M.M., 1976. A rapid and sensitive method for the quantitation of microgram quantities of protein utilizing the principle of protein-dye binding. *Anal. Biochem.* 72, 248–54. [https://doi.org/10.1016/0003-2697\(76\)90527-3](https://doi.org/10.1016/0003-2697(76)90527-3)
- Bray, E.A., 2000. Response to abiotic stress. *Biochem. Mol. Biol. plants.* In: Gruissem, W. and Jones, R., Eds., American Society of Plant Physiologists, 1158–1203.
- Brouwer, B., Ziolkowska, A., Bagard, M., Keech, O., Gardeström, P., 2012. The impact of light intensity on shade-induced leaf senescence. *Plant, Cell Environ.* 35, 1084–1098. <https://doi.org/10.1111/j.1365-3040.2011.02474.x>
- Brzobohaty, B., Moore, I., Kristoffersen, P., Bako, L., Campos, N., Schell, J., Palme, K., 1993. Release of active cytokinin by a (beta)-glucosidase localize. *Science* 262(5136):1051-4.
- Buchanan-Wollaston, V., 1997. The molecular biology of leaf senescence. *J. Exp. Bot.* 48, 181–199. <https://doi.org/10.1093/jxb/48.2.181>
- Cabrera-Bosquet, L., Fournier, C., Bricchet, N., Welcker, C., Suard, B., Tardieu, F., 2016. High-throughput estimation of incident light, light interception and radiation-use efficiency of thousands of plants in a phenotyping platform. *New Phytol.* 212, 269–281. <https://doi.org/10.1111/nph.14027>
- Causin, H.F., Barneix, A.J., 2007. The Role of oxidative metabolism in the regulation of leaf senescence by the light environment. *Int. J. Plant Dev. Biol.* 1, 239-244.
- Causin, H.F., Jauregui, R.N., Barneix, A.J., 2006. The effect of light spectral quality on leaf senescence and oxidative stress in wheat. *Plant Sci.* 171, 24–33. <https://doi.org/10.1016/j.plantsci.2006.02.009>
- Causin, H.F., Roberts, I.N., Criado, M. V., Gallego, S.M., Pena, L.B., Ríos, M.D.C., Barneix, A.J., 2009.



- Changes in hydrogen peroxide homeostasis and cytokinin levels contribute to the regulation of shade-induced senescence in wheat leaves. *Plant Sci.* 177, 698–704. <https://doi.org/10.1016/j.plantsci.2009.08.014>
- Causin, H.F.F., Marchetti, C.F.F., Pena, L.B.B., Gallego, S.M.M., Barneix, A.J.J., 2015. Down-regulation of catalase activity contributes to senescence induction in wheat leaves exposed to shading stress. *Biol. Plant.* 59, 154–162. <https://doi.org/10.1007/s10535-014-0480-z>
- Chai, T., Zhou, J., Liu, J., Xing, D., 2015. LSD1 and HY5 antagonistically regulate red light induced-programmed cell death in Arabidopsis. *Front. Plant Sci.* 6, 1–13. <https://doi.org/10.3389/fpls.2015.00292>
- Chen, D., Neumann, K., Friedel, S., Kilian, B., Chen, M., Altmann, T., Klukas, C., 2014. Dissecting the phenotypic components of crop plant growth and drought responses based on high-throughput image analysis. *Plant Cell* 26(12):4636-55. <https://doi.org/10.1105/tpc.114.129601>
- Conrad, K., Motyka, V., Schlüter, T., 2007. Increase in activity, glycosylation and expression of cytokinin oxidase/dehydrogenase during the senescence of barley leaf segments in the dark. *Physiol. Plant.* 130, 572–579. <https://doi.org/10.1111/j.1399-3054.2007.00914.x>
- Cortleven, A., Schmölling, T., 2015. Regulation of chloroplast development and function by cytokinin. *J. Exp. Bot.* 66, 4999–5013. <https://doi.org/10.1093/jxb/erv132>
- Criado, M.V., Roberts, I.N., Echeverria, M., Barneix, A.J., 2007. Plant growth regulators and induction of leaf senescence in nitrogen-deprived wheat plants. *J. Plant Growth Regul.* 26, 301–307. <https://doi.org/10.1007/s00344-007-9016-5>
- Criado, M. V, Caputo, C., Roberts, I.N., Castro, M.A., Barneix, A.J., 2009. Cytokinin-induced changes of nitrogen remobilization and chloroplast ultrastructure in wheat (*Triticum aestivum*). *Jl Plant Physiol.* 166, 1775–1785. <https://doi.org/10.1016/j.jplph.2009.05.007>
- Dai, A., 2013. Increasing drought under global warming in observations and models. *Nat. Clim. Chang.* 3, 52–58. <https://doi.org/10.1038/nclimate1633>
- Dai, A., 2011. Drought under global warming: A review. *Wiley Interdiscip. Rev. Clim. Chang.* 2, 45–65. <https://doi.org/10.1002/wcc.81>
- De Diego, N., Fürst, T., Humplík, J.F., Ugena, L., Podlešáková, K., Spíchal, L., 2017. An automated method for high-throughput screening of arabidopsis rosette growth in multi-well plates and its validation in stress conditions. *Front. Plant Sci.* 8, 1–16. <https://doi.org/10.3389/fpls.2017.01702>
- De Diego, N., Sampedro, M.C., Barrio, R.J., Saiz-Fernández, I., Moncaleán, P., Lacuesta, M., 2013. Solute accumulation and elastic modulus changes in six radiata pine breeds exposed to drought. *Tree*

- Physiol. 33, 69–80. <https://doi.org/10.1093/treephys/tps125>
- Décima Oneto, C., Otegui, M.E., Baroli, I., Beznec, A., Faccio, P., Bossio, E., Blumwald, E., Lewi, D., 2016. Water deficit stress tolerance in maize conferred by expression of an isopentenyltransferase (IPT) gene driven by a stress- and maturation-induced promoter. *J. Biotechnol.* 220, 66–77. <https://doi.org/10.1016/j.jbiotec.2016.01.014>
- Dobrev, P.I., Kamínek, M., 2002. Fast and efficient separation of cytokinins from auxin and abscisic acid and their purification using mixed-mode solid-phase extraction. *J. Chromatogr. A* 950, 21–29. [https://doi.org/10.1016/S0021-9673\(02\)00024-9](https://doi.org/10.1016/S0021-9673(02)00024-9)
- Earth Observation and Research Branch Team, 2011. Crop Identification and BBCH Staging Manual: SMAP-12 Field Campaign.
- Ebeed, H.T., Hassan, N.M., Aljarani, A.M., 2017. Exogenous applications of polyamines modulate drought responses in wheat through osmolytes accumulation, increasing free polyamine levels and regulation of polyamine biosynthetic genes. *Plant Physiol. Biochem.* 118, 438–448. <https://doi.org/10.1016/j.plaphy.2017.07.014>
- Filek, M., Labanowska, M., Kościelniak, J., Biesaga-Kościelniak, J., Kurdziel, M., Szarejko, I., Hartikainen, H., 2015. Characterization of barley leaf tolerance to drought stress by chlorophyll fluorescence and electron paramagnetic resonance studies. *J. Agron. Crop Sci.* 201, 228–240. <https://doi.org/10.1111/jac.12063>
- Floková, K., Tarkowská, D., Miersch, O., Strnad, M., Wasternack, C., Novák, O., 2014. UHPLC-MS/MS based target profiling of stress-induced phytohormones. *Phytochemistry* 105, 147–157. <https://doi.org/10.1016/j.phytochem.2014.05.015>
- Forster, B.P., Ellis, R.P., Thomas, W.T.B., Newton, A.C., Tuberosa, R., This, D., El-Enein, R.A., Bahri, M.H., Ben Salem, M., 2000. The development and application of molecular markers for abiotic stress tolerance in barley. *J. Exp. Bot.* 51, 19–27. <https://doi.org/10.1093/jxb/51.342.19>
- Forster, B.P., Pakniyat, H., Macaulay, M., Matheson, W., Phillips, M.S., Thomas, W.T.B., Powell, W., 1994. Variation in the leaf sodium content of the *Hordeum vulgare* (Barley) cultivar maythorpe and its derived mutant cv. Golden promise. *Heredity (Edinb.)* 73, 249–253. <https://doi.org/10.1038/hdy.1994.130>
- Frébort, I., Sebelá, M., Galuszka, P., Werner, T., Schmölling, T., Pec, P., 2002. Cytokinin oxidase/cytokinin dehydrogenase assay: optimized procedures and applications. *Anal. Biochem.* 306, 1–7. <https://doi.org/10.1006/abio.2002.5670>
- Gajdosová, S., Spíchal, L., Kamínek, M., Hoyerová, K., Novák, O., Dobrev, P.I., Galuszka, P., Klíma, P.,

- Gaudinová, A., Zizková, E., Hanus, J., Dancák, M., Trávníček, B., Pesek, B., Krupicka, M., Vanková, R., Strnad, M., Motyka, V., 2011. Distribution, biological activities, metabolism, and the conceivable function of cis-zeatin-type cytokinins in plants. *J. Exp. Bot.* 62, 2827–40. <https://doi.org/10.1093/jxb/erq457>
- Gallé, A., Flexas, J., 2010. Gas-exchange and chlorophyll fluorescence measurements in grapevine leaves in the field, in: Delrot, S., Medrano, H., Or, E., Bavaresco, L., Grando, S. (Eds.), *Methodologies and Results in Grapevine Research*. Springer Netherlands, Dordrecht, pp. 107–121. [https://doi.org/10.1007/978-90-481-9283-0\\_8](https://doi.org/10.1007/978-90-481-9283-0_8)
- Galuszka, P., Frébortová, J., Werner, T.T., Yamada, M., Strnad, M., Schmölling, T., Frébort, I., 2004. Cytokinin oxidase/dehydrogenase genes in barley and wheat: cloning and heterologous expression. *Eur. J. Biochem.* 271, 3990–4002. <https://doi.org/10.1111/j.1432-1033.2004.04334.x>
- Gan, S., Amasino, R.M., 1997. Making sense of senescence (Molecular genetic regulation and manipulation of leaf senescence). *Plant Physiol.* 113, 313–319.
- Gan, S., Amasino, R.M., 1995. Inhibition of leaf senescence by autoregulated production of cytokinin. *Science* 270:1986–8. <https://doi.org/10.1126/science.270.5244.1986>
- Gangappa, S.N., Botto, J.F., 2016. The Multifaceted roles of HY5 in plant growth and development. *Mol. Plant* 9, 1353–1365. <https://doi.org/10.1016/j.molp.2016.07.002>
- Ghanem, M.E., Albacete, A., Smigocki, A.C., Frébort, I., Pospíšilová, H., Martínez-Andújar, C., Acosta, M., Sánchez-Bravo, J., Lutts, S., Dodd, I.C., Pérez-Alfocea, F., 2011. Root-synthesized cytokinins improve shoot growth and fruit yield in salinized tomato (*Solanum lycopersicum* L.) plants. *J. Exp. Bot.* 62, 125–140. <https://doi.org/10.1093/jxb/erq266>
- Ghanem, M.E., Marrou, H., Sinclair, T.R., 2015. Physiological phenotyping of plants for crop improvement. *Trends Plant Sci.* 20, 139–144. <https://doi.org/10.1016/j.tplants.2014.11.006>
- Granier, C., Aguirrezabal, L., Chenu, K., Cookson, S.J., Cookson, S.J., Dauzat, M., Dauzat, M., Hamard, P., Hamard, P., Thioux, J., Thioux, J., Bouchier-combaud, S., Bouchier-combaud, S., Lebaudy, A., Lebaudy, A., Muller, B., Muller, B., Simonneau, T., Simonneau, T., 2006. PHENOPSIS, an automated platform for reproducible phenotyping of plant responses to soil water in *Arabidopsis thaliana* permitted the identification of an accession with low sensitivity to soil water deficit. *New Phytol.* 169, 623–635. <https://doi.org/10.1111/j.1469-8137.2005.01609.x>
- Gray, N., Plumb, R., 2016. A validated assay for the quantification of amino acids in mammalian urine. *Waters* 1–8.
- Griffiths, H., Parry, M.A.J., 2002. Plant responses to water stress. *Ann. Bot.* 89, 801–802.

- <https://doi.org/10.1093/aob/mcf159>
- Großkinsky, D.K., Svendsgaard, J., Christensen, S., Roitsch, T., 2015. Plant phenomics and the need for physiological phenotyping across scales to narrow the genotype-to-phenotype knowledge gap. *J. Exp. Bot.* 66, 5429–5440. <https://doi.org/10.1093/jxb/erv345>
- Han, M., Wong, J., Su, T., Beatty, P.H., Good, A.G., 2016. Identification of nitrogen use efficiency genes in barley: searching for QTLs controlling complex physiological traits. *Front. Plant Sci.* 7, 1–17. <https://doi.org/10.3389/fpls.2016.01587>
- Harwood, W.A., 2012. Advances and remaining challenges in the transformation of barley and wheat. *J. Exp. Bot.* 63, 1791–1798. <https://doi.org/10.1093/jxb/err380>
- Harwood, W.A., Bartlett, J.G., Alves, S.C., Perry, M., Smedley, M.A., Leyland, N., Snape, J.W., 2009. Transgenic Wheat, Barley and Oats 478, 137–147. <https://doi.org/10.1007/978-1-59745-379-0>
- Hay, R.K.M., Porter, J.R., others, 2006. *The physiology of crop yield*. Blackwell Publishing.
- Hluska, T., Dobrev, P.I., Tarkowská, D., Frébortová, J., Zalabák, D., Kopečný, D., Plíhal, O., Kokáš, F., Briozzo, P., Zatloukal, M., Motyka, V., Galuszka, P., 2016. Cytokinin metabolism in maize: Novel evidence of cytokinin abundance, interconversions and formation of a new trans-zeatin metabolic product with a weak anticytokinin activity. *Plant Sci.* 247, 127–137. <https://doi.org/10.1016/j.plantsci.2016.03.014>
- Holubová, K., Hensel, G., Vojta, P., Tarkowski, P., Bergougnoux, V., Galuszka, P., 2018. Modification of barley plant productivity through regulation of cytokinin content by Reverse-Genetics Approaches. *Front. Plant Sci.* 9, 1–18. <https://doi.org/10.3389/fpls.2018.01676>
- Honsdorf, N., March, T.J., Berger, B., Tester, M., Pillen, K., 2014. High-throughput phenotyping to detect drought tolerance QTL in wild barley introgression lines. *PLoS One* 9. <https://doi.org/10.1371/journal.pone.0097047>
- Hossain, A., Teixeira da Silva, J.A., Lozovskaya, M.V., Zvolinsky, V.P., 2012. High temperature combined with drought affect rainfed spring wheat and barley in South-Eastern Russia: I. Phenology and growth. *Saudi J. Biol. Sci.* 19, 473–487. <https://doi.org/10.1016/j.sjbs.2012.07.005>
- Hsiao, T.C., 1973. Plant responses to water stress. *Annu. Rev. Plant Physiol.* 24, 519–570. <https://doi.org/10.1146/annurev.pp.24.060173.002511>
- Hsu, Y.T., Kao, C.H., 2007. Heat shock-mediated H<sub>2</sub>O<sub>2</sub> accumulation and protection against Cd toxicity in rice seedlings. *Plant Soil* 300, 137–147. <https://doi.org/10.1007/s11104-007-9396-0>
- Humlík, J.F., Lazár, D., Fürst, T., Husicková, A., Hýbl, M., Spíchal, L., 2015a. Automated integrative high-throughput phenotyping of plant shoots: A case study of the cold-tolerance of pea (*Pisum sativum*)

- L.). *Plant Methods* 11, 20. <https://doi.org/10.1186/s13007-015-0063-9>
- Humplík, J.F., Lazár, D., Husičková, A., Spíchal, L., 2015b. Automated phenotyping of plant shoots using imaging methods for analysis of plant stress responses - A review. *Plant Methods* 11, 29. <https://doi.org/10.1186/s13007-015-0072-8>
- Jammes, F., Leonhardt, N., Tran, D., Bousserouel, H., Véry, A.A., Renou, J.P., Vavasseur, A., Kwak, J.M., Sentenac, H., Bouteau, F., Leung, J., 2014. Acetylated 1,3-diaminopropane antagonizes abscisic acid-mediated stomatal closing in *Arabidopsis*. *Plant J.* 79, 322–333. <https://doi.org/10.1111/tpj.12564>
- Jancewicz, A.L., Gibbs, N.M., Masson, P.H., 2016. Cadaverine's functional role in plant development and environmental response. *Front. Plant Sci.* 7, 1–8. <https://doi.org/10.3389/fpls.2016.00870>
- Jordi, W., Schapendonk, A., Davelaar, E., Stoopen, G.M., Pot, C.S., De Visser, R., Van Rhijn, J.A., Gan, S., Amasino, R.M., 2000. Increased cytokinin levels in transgenic P(SAG12)-IPT tobacco plants have large direct and indirect effects on leaf senescence, photosynthesis and N partitioning. *Plant, Cell Environ.* 23, 279–289. <https://doi.org/10.1046/j.1365-3040.2000.00544.x>
- Junker, A., Muraya, M.M., Weigelt-Fischer, K., Arana-Ceballos, F., Klukas, C., Melchinger, A.E., Meyer, R.C., Riewe, D., Altmann, T., 2015. Optimizing experimental procedures for quantitative evaluation of crop plant performance in high throughput phenotyping systems. *Front. Plant Sci.* 5, 1–21. <https://doi.org/10.3389/fpls.2014.00770>
- Kajimura, T., Mizuno, N., Takumi, S., 2010. Utility of leaf senescence-associated gene homologs as developmental markers in common wheat. *Plant Physiol. Biochem.* 48, 851–9. <https://doi.org/10.1016/j.plaphy.2010.08.014>
- Kamada-Nobusada, T., Makita, N., Kojima, M., Sakakibara, H., 2013. Nitrogen-dependent regulation of de novo cytokinin biosynthesis in rice: The role of glutamine metabolism as an additional signal. *Plant Cell Physiol.* 54, 1881–1893. <https://doi.org/10.1093/pcp/pct127>
- Keech, O., Pesquet, E., Gutierrez, L., Ahad, A., Bellini, C., Smith, S.M., Gardestrom, P., 2010. Leaf senescence is accompanied by an early disruption of the microtubule network in *Arabidopsis*. *Plant Physiol.* 154, 1710–1720. <https://doi.org/10.1104/pp.110.163402>
- Kim, H.J., Ryu, H., Hong, S.H., Woo, H.R., Lim, P.O., Lee, I.C., Sheen, J., Nam, H.G., Hwang, I., 2006. Cytokinin-mediated control of leaf longevity by AHK3 through phosphorylation of ARR2 in *Arabidopsis*. *Proc. Natl. Acad. Sci. U. S. A.* 103, 814–819. <https://doi.org/10.1073/pnas.0505150103>
- Kim, J.H., Chung, K.M., Woo, H.R., 2011. Three positive regulators of leaf senescence in *Arabidopsis*, ORE1, ORE3 and ORE9, play roles in crosstalk among multiple hormone-mediated senescence pathways. *Genes and Genomics* 33, 373–381. <https://doi.org/10.1007/s13258-011-0044-y>

- Kishor, P.B.K., Rajesh, K., Reddy, P.S., Seiler, C., Sreenivasulu, N., 2014. Drought stress tolerance mechanisms in barley and its relevance to cereals, in: *Biotechnological Approaches to Barley Improvement*. Springer, pp. 161–179.
- Kobayashi, K., Baba, S., Obayashi, T., Sato, M., Toyooka, K., Keranen, M., Aro, E.-M., Fukaki, H., Ohta, H., Sugimoto, K., Masuda, T., 2012. Regulation of root greening by light and auxin/cytokinin signaling in *Arabidopsis*. *Plant Cell* 24, 1081–1095. <https://doi.org/10.1105/tpc.111.092254>
- Koeslin-Findeklee, F., Becker, M.A., Van Der Graaff, E., Roitsch, T., Horst, W.J., 2015. Differences between winter oilseed rape (*Brassica napus* L.) cultivars in nitrogen starvation-induced leaf senescence are governed by leaf-inherent rather than root-derived signals. *J. Exp. Bot.* 66, 3669–3681. <https://doi.org/10.1093/jxb/erv170>
- Kooter, J.M., Matzke, M.A., Meyer, P., 1999. Listening to the silent genes: transgene silencing, gene regulation and pathogen control. *Trends Plant Sci.* 4, 340–347.
- Kudo, T., Makita, N., Kojima, M., Tokunaga, H., Sakakibara, H., 2012. Cytokinin activity of cis-zeatin and phenotypic alterations induced by overexpression of putative cis-zeatin-O-glucosyltransferase in Rice. *Plant Physiol.* 160, 319–331. <https://doi.org/10.1104/pp.112.196733>
- Lacuesta, M., Saiz-Fernández, I., Podlešáková, K., Miranda-Apodaca, J., Novák, O., Doležal, K., De Diego, N., 2018. The trans and cis zeatin isomers play different roles in regulating growth inhibition induced by high nitrate concentrations in maize. *Plant Growth Regul.* 85, 199–209. <https://doi.org/10.1007/s10725-018-0383-7>
- Lambers, H., Chapin, F.S., Pons, T.L., 1998. *Plant physiological ecology*. Nov. York.
- Lawlor, D.W., Cornic, G., 2002. Photosynthetic carbon assimilation and associated metabolism in relation to water deficits in higher plants. *Plant, Cell Environ.* 25, 275–294. <https://doi.org/10.1046/j.0016-8025.2001.00814.x>
- Lehmann, T., Pollmann, S., 2009. Gene expression and characterization of a stress-induced tyrosine decarboxylase from *Arabidopsis thaliana*. *FEBS Lett.* 583, 1895–1900. <https://doi.org/10.1016/j.febslet.2009.05.017>
- Li, R., Guo, P., Baum, M., Grando, S., Ceccarelli, S., 2006. Evaluation of chlorophyll content and fluorescence parameters as indicators of drought tolerance in barley. *Agric. Sci. China* 5, 751–757. [https://doi.org/10.1016/S1671-2927\(06\)60120-X](https://doi.org/10.1016/S1671-2927(06)60120-X)
- Lichtenthaler, H.K., 1998. The stress concept in plants: An introduction, in: *Annals of the New York Academy of Sciences*. <https://doi.org/10.1111/j.1749-6632.1998.tb08993.x>
- Lichtenthaler, H.K., 1996. *Vegetation stress: an introduction to the stress concept in plants*. *J. Plant*

- Physiol. 148, 4–14. [https://doi.org/10.1016/S0176-1617\(96\)80287-2](https://doi.org/10.1016/S0176-1617(96)80287-2)
- Lim, P.O., Kim, H.J., Nam, H.G., 2007. Leaf senescence. *Annu. Rev. Plant Biol.* 58, 115–36. <https://doi.org/10.1146/annurev.arplant.57.032905.105316>
- Liu, H., Liu, B., Zhao, C., Pepper, M., Lin, C., 2011. The action mechanisms of plant cryptochromes. *Trends Plant Sci.* 16, 684–691. <https://doi.org/10.1016/j.tplants.2011.09.002>
- Liu, H., Wang, Q., Liu, Y., Zhao, X., Imaizumi, T., Somers, D.E., Tobin, E.M., Lin, C., 2013. Arabidopsis CRY2 and ZTL mediate blue-light regulation of the transcription factor CIB1 by distinct mechanisms. *Proc. Natl. Acad. Sci. U. S. A.* 110, 17582–7. <https://doi.org/10.1073/pnas.1308987110>
- Liu, J.-H., Wang, W., Wu, H., Gong, X., Moriguchi, T., 2015. Polyamines function in stress tolerance: from synthesis to regulation. *Front. Plant Sci.* 6, 1–10. <https://doi.org/10.3389/fpls.2015.00827>
- Lomin, S.N., Krivosheev, D.M., Steklov, M.Y., Osolodkin, D.I., Romanov, G.A., 2012. Receptor properties and features of cytokinin signaling. *Acta Naturae* 4, 31–45.
- Lomin, S.N., Yonekura-Sakakibara, K., Romanov, G.A., Sakakibara, H., 2011. Ligand-binding properties and subcellular localization of maize cytokinin receptors. *J. Exp. Bot.* 62, 5149–5159. <https://doi.org/10.1093/jxb/err220>
- Love, A.J., Milner, J.J., Sadanandom, A., 2008. Timing is everything: regulatory overlap in plant cell death. *Trends Plant Sci.* 13, 589–95. <https://doi.org/10.1016/j.tplants.2008.08.006>
- Ma, X., Feng, D.-S., Wang, H.-G., Li, X.-F., Kong, L.-R., 2010. Cloning and expression analysis of wheat cytokinin oxidase/dehydrogenase gene TaCKX3. *Plant Mol. Biol. Report.* 29, 98–105. <https://doi.org/10.1007/s11105-010-0209-x>
- Malec, P.A., Oteri, M., Inferrera, V., Cacciola, F., Mondello, L., Kennedy, R.T., 2017. Determination of amines and phenolic acids in wine with benzoyl chloride derivatization and liquid chromatography-mass spectrometry. *J. Chromatogr. A.* <https://doi.org/10.1016/j.chroma.2017.07.061>
- Marchetti, C.F., Škrabišová, M., Galuszka, P., Novák, O., Causin, H.F., 2018. Blue light suppression alters cytokinin homeostasis in wheat leaves senescing under shading stress. *Plant Physiol. Biochem.* 130. <https://doi.org/10.1016/j.plaphy.2018.08.005>
- Mascher, M., Gundlach, H., Himmelbach, A., Beier, S., Twardziok, S.O., Wicker, T., Radchuk, V., Dockter, C., Hedley, P.E., Russell, J., Bayer, M., Ramsay, L., Liu, H., Haberer, G., Zhang, X.Q., Zhang, Q., Barrero, R.A., Li, L., Taudien, S., Groth, M., Felder, M., Hastie, A., Šimková, H., Stanková, H., Vrána, J., Chan, S., Munõz-Amatriaín, M., Ounit, R., Wanamaker, S., Bolser, D., Colmsee, C., Schmutzer, T., Aliyeva-Schnorr, L., Grasso, S., Tanskanen, J., Chailyan, A., Sampath, D., Heavens, D., Clissold, L., Cao, S., Chapman, B., Dai, F., Han, Y., Li, H., Li, X., Lin, C., McCooke, J.K., Tan, C., Wang, P., Wang, S., Yin, S.,

- Zhou, G., Poland, J.A., Bellgard, M.I., Borisjuk, L., Houben, A., Doleael, J., Ayling, S., Lonardi, S., Kersey, P., Langridge, P., Muehlbauer, G.J., Clark, M.D., Caccamo, M., Schulman, A.H., Mayer, K.F.X., Platzer, M., Close, T.J., Scholz, U., Hansson, M., Zhang, G., Braumann, I., Spannagl, M., Li, C., Waugh, R., Stein, N., 2017. A chromosome conformation capture ordered sequence of the barley genome. *Nature* 544, 427–433. <https://doi.org/10.1038/nature22043>
- Matzke, A.J.M., Matzke, M.A., 1998. Position effects and epigenetic silencing of plant transgenes. *Curr. Opin. Plant Biol.* 1, 142–148. [https://doi.org/10.1016/S1369-5266\(98\)80016-2](https://doi.org/10.1016/S1369-5266(98)80016-2)
- Meng, Y., Li, H., Wang, Q., Liu, B., Lin, C., 2013. Blue light-dependent interaction between cryptochrome2 and CIB1 regulates transcription and leaf senescence in soybean. *Plant Cell* 25, 4405–20. <https://doi.org/10.1105/tpc.113.116590>
- Merewitz, E.B., Gianfagna, T., Huang, B., 2011. Photosynthesis, water use, and root viability under water stress as affected by expression of SAG12-ipt controlling cytokinin synthesis in *Agrostis stolonifera*. *J. Exp. Bot.* 62, 383–395. <https://doi.org/10.1093/jxb/erq285>
- Minocha, R., Majumdar, R., Minocha, S.C., 2014. Polyamines and abiotic stress in plants: a complex relationship1. *Front. Plant Sci.* 5, 1–17. <https://doi.org/10.3389/fpls.2014.00175>
- Mohanty, B., Lakshmanan, M., Lim, S.H., Kim, J.K., Ha, S.H., Lee, D.Y., 2016. Light-specific transcriptional regulation of the accumulation of carotenoids and phenolic compounds in rice leaves. *Plant Signal. Behav.* 11, 1–4. <https://doi.org/10.1080/15592324.2016.1184808>
- Mok, D.D.W.S., Mok, M.M.C., 2001. Cytokinin metabolism and action. *Annu. Rev. Plant Biol.* 52, 89–118.
- Mrázová, K., Jiskrová, E., Vyroubalová, Š., Novák, O., Ohnoutková, L., Pospíšilová, H., Frebort, I., Harwood, W. a., Galuszka, P., 2013. Overexpression of cytokinin dehydrogenase genes in barley (*Hordeum vulgare* cv. Golden Promise) fundamentally affects morphology and fertility. *PLoS One* 8, 1–13. <https://doi.org/10.1371/journal.pone.0079029>
- Mullineaux, P., Karpinski, S., 2002. Signal transduction in response to excess light: getting out of the chloroplast. *Curr. Opin. Plant Biol.* 5, 43–8. [https://doi.org/10.1016/S1369-5266\(01\)00226-6](https://doi.org/10.1016/S1369-5266(01)00226-6)
- Muscolo, A., Junker, A., Klukas, C., Weigelt-Fischer, K., Riewe, D., Altmann, T., 2015. Phenotypic and metabolic responses to drought and salinity of four contrasting lentil accessions. *J. Exp. Bot.* 66, 5467–5480. <https://doi.org/10.1093/jxb/erv208>
- Nishimura, C., Ohashi, Y., Sato, S., Kato, T., Tabata, S., Ueguchi, C., 2004. Histidine kinase homologs that act as cytokinin receptors possess overlapping functions in the regulation of shoot and root growth in *Arabidopsis*. *Plant Cell* 16, 1365–1377. <https://doi.org/10.1105/tpc.021477>
- Nishiyama, R., Watanabe, Y., Fujita, Y., Le, D.T., Kojima, M., Werner, T., Vankova, R., Yamaguchi-Shinozaki,



- K., Shinozaki, K., Kakimoto, T., Sakakibara, H., Schmölling, T., Tran, L.-S.P., 2011. Analysis of cytokinin mutants and regulation of cytokinin metabolic genes reveals important regulatory roles of cytokinins in drought, salt and abscisic acid responses, and abscisic acid biosynthesis. *Plant Cell* 23, 2169–2183. <https://doi.org/10.1105/tpc.111.087395>
- Nosalewicz, A., Siecińska, J., Śmiech, M., Nosalewicz, M., Wiącek, D., Pecio, A., Wach, D., 2016. Transgenerational effects of temporal drought stress on spring barley morphology and functioning. *Environ. Exp. Bot.* 131, 120–127. <https://doi.org/10.1016/j.envexpbot.2016.07.006>
- Pandey, S., Fartyal, D., Agarwal, A., Shukla, T., James, D., Kaul, T., Negi, Y.K., Arora, S., Reddy, M.K., 2017. Abiotic stress tolerance in plants: myriad roles of ascorbate peroxidase. *Front. Plant Sci.* 8, 1–13. <https://doi.org/10.3389/fpls.2017.00581>
- Peleg, Z., Blumwald, E., 2011. Hormone balance and abiotic stress tolerance in crop plants. *Curr. Opin. Plant Biol.* 14, 290–295. <https://doi.org/10.1016/j.pbi.2011.02.001>
- Peleg, Z., Reguera, M., Tumimbang, E., Walia, H., Blumwald, E., 2011. Cytokinin-mediated source/sink modifications improve drought tolerance and increase grain yield in rice under water-stress. *Plant Biotechnol. J.* 9, 747–758. <https://doi.org/10.1111/j.1467-7652.2010.00584.x>
- Pfaffl, M.W., 2001. A new mathematical model for relative quantification in real-time RT-PCR. *Nucleic Acids Res.* 29, e45. <https://doi.org/10.1093/nar/29.9.e45>
- Podlešáková, K., Ugena, L., Spíchal, L., Doležal, K., De Diego, N., 2019. Phytohormones and polyamines regulate plant stress responses by altering GABA pathway. *N. Biotechnol.* 25;48:53-65. <https://doi.org/10.1016/j.nbt.2018.07.003>
- Poorter, H., Fiorani, F., Pieruschka, R., Wojciechowski, T., van der Putten, W.H., Kleyer, M., Schurr, U., Postma, J., 2016. Pampered inside, pestered outside? Differences and similarities between plants growing in controlled conditions and in the field. *New Phytol.* 212, 838–855. <https://doi.org/10.1111/nph.14243>
- Pospíšilová, H., Jiskrová, E., Vojta, P., Mrízová, K., Kokáš, F., Čudejková, M.M., Bergougnoux, V., Plíhal, O., Klimešová, J., Novák, O., Dzurová, L., Frébort, I., Galuszka, P., 2016. Transgenic barley overexpressing a cytokinin dehydrogenase gene shows greater tolerance to drought stress. *N. Biotechnol.* 33, 692–705. <https://doi.org/10.1016/j.nbt.2015.12.005>
- Pospíšilová, J., Synková, H., Rulcová, J., 2000. Cytokinins and water stress. *Biol. Plant.* 43, 321–328. <https://doi.org/10.1023/A:1026754404857>
- Pospíšilová, J., Vágner, M., Malbeck, J., Trávníčková, A., Bařková, P., 2005. Interactions between abscisic acid and cytokinins during water stress and subsequent rehydration. *Biol. Plant.* 49, 533–540.

- <https://doi.org/10.1007/s10535-005-0047-0>
- Prerostova, S., Dobrev, P.I., Gaudinova, A., Knirsch, V., Körber, N., Pieruschka, R., Fiorani, F., Brzobohatý, B., černý, M., Spichal, L., Humplik, J., Vanek, T., Schurr, U., Vankova, R., 2018. Cytokinins: their impact on molecular and growth responses to drought stress and recovery in arabidopsis. *Front. Plant Sci.* 9, 1–14. <https://doi.org/10.3389/fpls.2018.00655>
- Prochazkova, D., Sairam, R.K., Srivastava, G.C., Singh, D.V., 2001. Oxidative stress and antioxidant activity as the basis of senescence in maize leaves. *Plant Sci.* 161, 765–771. [https://doi.org/10.1016/S0168-9452\(01\)00462-9](https://doi.org/10.1016/S0168-9452(01)00462-9)
- Quirino, B.F., Noh, Y.S., Himelblau, E., Amasino, R.M., 2000. Molecular aspects of leaf senescence. *Trends Plant Sci.* 5, 278–82. [https://doi.org/10.1016/S1360-1385\(00\)01655-1](https://doi.org/10.1016/S1360-1385(00)01655-1)
- Reddy, A.R., Chaitanya, K.V., Vivekanandan, M., 2004. Drought-induced responses of photosynthesis and antioxidant metabolism in higher plants. *J. Plant Physiol.* 161, 1189–1202. <https://doi.org/10.1016/j.jplph.2004.01.013>
- Ritala, A., Nuutila, A.M., Aikasalo, R., Kauppinen, V., Tammissola, J., 2002. Measuring gene flow in the cultivation of transgenic barley. *Crop Sci.* 42, 278–285. <https://doi.org/10.2135/cropsci2002.0278>
- Rivero, R.M., Gimeno, J., Van Deynze, A., Walia, H., Blumwald, E., 2010. Enhanced cytokinin synthesis in tobacco plants expressing PSARK::IPT prevents the degradation of photosynthetic protein complexes during drought. *Plant Cell Physiol.* 51, 1929–1941. <https://doi.org/10.1093/pcp/pcq143>
- Rivero, R.M., Kojima, M., Gepstein, A., Sakakibara, H., Mittler, R., Gepstein, S., Blumwald, E., 2007. Delayed leaf senescence induces extreme drought tolerance in a flowering plant. *Proc. Natl. Acad. Sci. U. S. A.* 104, 19631–19636. <https://doi.org/10.1073/pnas.0709453104>
- Rivero, R.M., Shulaev, V., Blumwald, E., 2009. Cytokinin-dependent photorespiration and the protection of photosynthesis during water deficit. *Plant Physiol.* 150, 1530–1540. <https://doi.org/10.1104/pp.109.139378>
- Roitsch, T., Ehneß, R., 2000. Regulation of source / sink relations by cytokinins. *Plant Growth Regul.* 32, 359. <https://doi.org/10.1023/A:1010781500705>
- Roman, H., Girault, T., Barbier, F., Péron, T., Brouard, N., Pěňčík, A., Novák, O., Vian, A., Sakr, S., Lothier, J., Le Gourrierc, J., Leduc, N., 2016. Cytokinins Are Initial Targets of Light in the Control of Bud Outgrowth. *Plant Physiol.* 172, 489–509. <https://doi.org/10.1104/pp.16.00530>
- Rubia, L., Rangan, L., Choudhury, R.R., Kamínek, M., Dobrev, P., Malbeck, J., Fowler, M., Slater, A., Scott, N., Bennett, J., Peng, S., Khush, G.S., Elliott, M., 2014. Changes in the chlorophyll content and cytokinin levels in the top three leaves of new plant type rice during grain filling. *J. Plant Growth*

- Regul. 33, 66–76. <https://doi.org/10.1007/s00344-013-9374-0>
- Saade, S., Negrão, S., Plett, D., Garnett, T., Tester, M., 2018. The barley genome, compendium of plant genomes. Springer International Publishing, Cham. <https://doi.org/10.1007/978-3-319-92528-8>
- Saini, H.S., Westgate, M.E., 1999. Reproductive development in grain crops during drought. *Adv. Agron.* 68, 59–96. [https://doi.org/10.1016/S0065-2113\(08\)60843-3](https://doi.org/10.1016/S0065-2113(08)60843-3)
- Saiz-Fernández, I., De Diego, N., Brzobohaty, B., Muñoz-Rueda, A., Lacuesta, M., 2017. The imbalance between C and N metabolism during high nitrate supply inhibits photosynthesis and overall growth in maize (*Zea mays* L.). *Plant Physiol. Biochem.* 120, 213–222. <https://doi.org/10.1016/j.plaphy.2017.10.006>
- Sakakibara, H., 2006. Cytokinins: activity, biosynthesis, and translocation. *Annu. Rev. Plant Biol.* 57, 431–49. <https://doi.org/10.1146/annurev.arplant.57.032905.105231>
- Sakakibara, H., Takei, K., Hirose, N., 2006. Interactions between nitrogen and cytokinin in the regulation of metabolism and development. *Trends Plant Sci.* 11, 440–448. <https://doi.org/10.1016/j.tplants.2006.07.004>
- Salopek-Sondi, B., Pavlović, I., Smolko, A., Šamec, D., 2017. Auxin as a mediator of abiotic stress responses. *Mech. Plant Horm. Signal. under Stress* 1–36. <https://doi.org/10.1002/9781118889022.ch1>
- Schäfer, M., Brütting, C., Meza-Canales, I.D., Großkinsky, D.K., Vankova, R., Baldwin, I.T., Meldau, S., 2015. The role of cis-zeatin-type cytokinins in plant growth regulation and mediating responses to environmental interactions. *J. Exp. Bot.* 66, 4873–4884. <https://doi.org/10.1093/jxb/erv214>
- Schlüter, T., Leide, J., Conrad, K., 2011. Light promotes an increase of cytokinin oxidase/dehydrogenase activity during senescence of barley leaf segments. *J. Plant Physiol.* 168, 694–8. <https://doi.org/10.1016/j.jplph.2010.10.004>
- Schmülling, T., Werner, T., Riefler, M., Krupková, E., Bartrina y Manns, I., 2003. Structure and function of cytokinin oxidase/dehydrogenase genes of maize, rice, arabidopsis and other species. *J. Plant Res.* 116, 241–52. <https://doi.org/10.1007/s10265-003-0096-4>
- Schnurbusch, T., 2019. Wheat and barley biology: towards new frontiers. *J. Integr. Plant Biol.* 61, 198–203. <https://doi.org/10.1111/jipb.12782>
- Singh, T.N., Aspinall, D., Paleg, L.G., 1972. Proline accumulation and varietal adaptability to drought in Barley: a potential metabolic measure of drought resistance. *Nature* 236, 188–189. <https://doi.org/10.1038/newbio236188a0>
- Šmehilová, M., Dobrušková, J., Novák, O., Takáč, T., Galuszka, P., 2016. Cytokinin-specific glycosyltransferases possess different roles in cytokinin homeostasis maintenance. *Front. Plant Sci.*

- 7, 1264. <https://doi.org/doi:10.3389/fpls.2016.01264>
- Smehilová, M., Galuszka, P., Bilyeu, K.D., Jaworek, P., Kowalska, M., Sebela, M., Sedlářová, M., English, J.T., Frébort, I., 2009. Subcellular localization and biochemical comparison of cytosolic and secreted cytokinin dehydrogenase enzymes from maize. *J. Exp. Bot.* 60, 2701–12. <https://doi.org/10.1093/jxb/erp126>
- Song, J., Jiang, L., Jameson, P.E., 2012. Co-ordinate regulation of cytokinin gene family members during flag leaf and reproductive development in wheat. *BMC Plant Biol.* 12, 78. <https://doi.org/10.1186/1471-2229-12-78>
- Taverner, E., Letham, D.S., Wang, J., Cornish, E., Willcocks, D.A., 1999. Influence of ethylene on cytokinin metabolism in relation to *Petunia* corolla senescence. *Phytochemistry* 51, 341–347. [https://doi.org/10.1016/S0031-9422\(98\)00757-2](https://doi.org/10.1016/S0031-9422(98)00757-2)
- Thomas, W.T.B., Powell, W., Wood, W., 1984. The chromosomal location of the dwarfing gene present in the spring barley variety golden promise. *Heredity (Edinb.)* 53, 177–183. <https://doi.org/10.1038/hdy.1984.73>
- Todaka, D., Zhao, Y., Yoshida, T., Kudo, M., Kidokoro, S., Mizoi, J., Kodaira, K.S., Takebayashi, Y., Kojima, M., Sakakibara, H., Toyooka, K., Sato, M., Fernie, A.R., Shinozaki, K., Yamaguchi-Shinozaki, K., 2017. Temporal and spatial changes in gene expression, metabolite accumulation and phytohormone content in rice seedlings grown under drought stress conditions. *Plant J.* 90, 61–78. <https://doi.org/10.1111/tpj.13468>
- Tomar, P.C., Lakra, N., Mishra, S.N., 2013. Cadaverine: A lysine catabolite involved in plant growth and development. *Plant Signal. Behav.* 8. <https://doi.org/10.4161/psb.25850>
- Tran, L.-S.P., Urao, T., Qin, F., Maruyama, K., Kakimoto, T., Shinozaki, K., Yamaguchi-Shinozaki, K., 2007. Functional analysis of AHK1/ATHK1 and cytokinin receptor histidine kinases in response to abscisic acid, drought, and salt stress in *Arabidopsis*. *Proc. Natl. Acad. Sci. U. S. A.* 104, 20623–20628. <https://doi.org/10.1073/pnas.0706547105>
- Tsuchisaka, A., Theologis, A., 2004. Unique and overlapping expression patterns among the *Arabidopsis* 1-amino-cyclopropane-1-carboxylate synthase gene family members. *Plant Physiol.* 136, 2982–3000. <https://doi.org/10.1104/pp.104.049999>
- Ugena, L., Hýlová, A., Podlešáková, K., Humplík, J.F., Doležal, K., Diego, N. De, Spíchal, L., 2018. Characterization of biostimulant mode of action using novel multi-trait high-throughput screening of *Arabidopsis* germination and rosette growth. *Front. Plant Sci.* 9, 1–17. <https://doi.org/10.3389/fpls.2018.01327>

- Urano, K., Kurihara, Y., Seki, M., Shinozaki, K., 2010. "Omics" analyses of regulatory networks in plant abiotic stress responses. *Curr. Opin. Plant Biol.* 13, 132–138. <https://doi.org/10.1016/j.pbi.2009.12.006>
- Vandenbussche, F., Habricot, Y., Condiff, A.S., Maldiney, R., Straeten, D.V.D., Ahmad, M., 2007. HY5 is a point of convergence between cryptochrome and cytokinin signalling pathways in *Arabidopsis thaliana*. *Plant J.* 49, 428–441. <https://doi.org/10.1111/j.1365-313X.2006.02973.x>
- Vandesompele, J., De Preter, K., Pattyn, F., Poppe, B., Van Roy, N., De Paepe, A., Speleman, F., 2002. Accurate normalization of real-time quantitative RT-PCR data by geometric averaging of multiple internal control genes. *3. Genome Biol.* <https://doi.org/10.1186/gb-2002-3-7-research0034>
- Vaseva-Gemisheva, I., Lee, D., Karanov, E., 2005. Response of *Pisum Sativum* cytokinin oxidase/dehydrogenase expression and specific activity to drought stress and herbicide treatments. *Plant Growth Regul.* 46, 199–208. <https://doi.org/10.1007/s10725-005-0143-3>
- Volaire, F., 2003. Seedling survival under drought differs between an annual (*Hordeum vulgare*) and a perennial grass (*Dactylis glomerata*). *New Phytol.* 160, 501–510. <https://doi.org/10.1046/j.1469-8137.2003.00906.x>
- von Wirén, N., Gillandt, S., Eggert, K., Ramireddy, E., Hosseini, S.A., Gnad, H., Schmölling, T., 2018. Root engineering in barley: increasing cytokinin degradation produces a larger root system, mineral enrichment in the shoot and improved drought tolerance. *Plant Physiol.* 177, 1078–1095. <https://doi.org/10.1104/pp.18.00199>
- Vyroubalová, S., Václavíková, K., Turecková, V., Novák, O., Smehilová, M., Hluska, T., Ohnoutková, L., Frébort, I., Galuszka, P., 2009. Characterization of new maize genes putatively involved in cytokinin metabolism and their expression during osmotic stress in relation to cytokinin levels. *Plant Physiol.* 151, 433–447. <https://doi.org/10.1104/pp.109.142489>
- Vysotskaya, L.B., Korobova, A. V., Veselov, S.Y., Dodd, I.C., Kudoyarova, G.R., 2009. ABA mediation of shoot cytokinin oxidase activity: assessing its impacts on cytokinin status and biomass allocation of nutrient-deprived durum wheat. *Funct. Plant Biol.* 36, 66. <https://doi.org/10.1071/fp08187>
- Wakimoto, B.T., 1998. Beyond the nucleosome: Epigenetic aspects of position-effect variegation in *Drosophila*. *Cell* 93, 321–324. [https://doi.org/10.1016/S0092-8674\(00\)81159-9](https://doi.org/10.1016/S0092-8674(00)81159-9)
- Wang, W., Vinocur, B., Altman, A., 2003. Plant responses to drought, salinity and extreme temperatures: Towards genetic engineering for stress tolerance. *Planta* 218, 1–14. <https://doi.org/10.1007/s00425-003-1105-5>
- Wang, W.W., Hao, Q., Tian, F., Li, Q., Wang, W.W., 2016. The stay-green phenotype of wheat mutant *tasg1*

- is associated with altered cytokinin metabolism. *Plant Cell Rep.* 35, 585–599. <https://doi.org/10.1007/s00299-015-1905-7>
- Wang, X., Wang, L., Shangguan, Z., Pandey, S., Fartyal, D., Agarwal, A., Shukla, T., James, D., Kaul, T., Negi, Y.K., Arora, S., Reddy, M.K., Hsu, Y.T., Kao, C.H., 2016. Leaf gas exchange and fluorescence of two winter wheat varieties in response to drought stress and nitrogen supply. *Front. Plant Sci.* 11, 1–13. <https://doi.org/10.1371/journal.pone.0165733>
- Werner, T., Holst, K., Pörs, Y., Guivarc’h, A., Mustroph, A., Chriqui, D., Grimm, B., Schmölling, T., 2008. Cytokinin deficiency causes distinct changes of sink and source parameters in tobacco shoots and roots. *J. Exp. Bot.* 59, 2659–2672. <https://doi.org/10.1093/jxb/ern134>
- Xu, C.C., Jeon, Y.A., Lee, C.H., 1999. Relative contributions of photochemical and non-photochemical routes to excitation energy dissipation in rice and barley illuminated at a chilling temperature. *Physiol. Plant.* 107, 447–453. <https://doi.org/10.1034/j.1399-3054.1999.100411.x>
- Yancey, P.H., 2001. Water Stress, Osmolytes and Proteins. *AMER.ZOOL.* 41, 699–709.
- Zalabák, D., Pospíšilová, H., Šmečilová, M., Mrízová, K., Frébort, I., Galuszka, P., 2013. Genetic engineering of cytokinin metabolism: prospective way to improve agricultural traits of crop plants. *Biotechnol. Adv.* 31, 97–117. <https://doi.org/10.1016/j.biotechadv.2011.12.003>
- Zalewski, W., Galuszka, P., Gasparis, S., Orczyk, W., Nadolska-Orczyk, A., 2010. Silencing of the HvCKX1 gene decreases the cytokinin oxidase/dehydrogenase level in barley and leads to higher plant productivity. *J. Exp. Bot.* 61, 1839–1851. <https://doi.org/10.1093/jxb/erq052>
- Zalewski, W., Gasparis, S., Boczkowska, M., Rajchel, I.K., Kała, M., Orczyk, W., Nadolska-Orczyk, A., 2014. Expression patterns of HvCKX Genes indicate their role in growth and reproductive development of barley. *PLoS One* 9. <https://doi.org/10.1371/journal.pone.0115729>
- Zatloukal, M., Gemrotová, M., Doležal, K., Havlíček, L., Spíchal, L., Strnad, M., 2008. Novel potent inhibitors of *A. thaliana* cytokinin oxidase/dehydrogenase. *Bioorganic Med. Chem.* 16, 9268–9275. <https://doi.org/10.1016/j.bmc.2008.09.008>
- Zavaleta-Mancera, H.A., López-Delgado, H., Loza-Tavera, H., Mora-Herrera, M., Trevilla-García, C., Vargas-Suárez, M., Ougham, H., 2007. Cytokinin promotes catalase and ascorbate peroxidase activities and preserves the chloroplast integrity during dark-senescence. *J. Plant Physiol.* 164, 1572–82. <https://doi.org/10.1016/j.jplph.2007.02.003>
- Zhang, P., Wang, W.Q., Zhang, G.L., Kaminek, M., Dobrev, P., Xu, J., Grissem, W., 2010. Senescence-inducible expression of isopentenyl transferase extends leaf life, increases drought stress resistance and alters cytokinin metabolism in Cassava. *J. Integr. Plant Biol.* 52, 653–669.

<https://doi.org/10.1111/j.1744-7909.2010.00956.x>

Zhang, S. han, Xu, X. feng, Sun, Y. min, Zhang, J. lian, Li, C. zhou, 2018. Influence of drought hardening on the resistance physiology of potato seedlings under drought stress. *J. Integr. Agric.* 17, 336–347.

[https://doi.org/10.1016/S2095-3119\(17\)61758-1](https://doi.org/10.1016/S2095-3119(17)61758-1)

## Curriculum vitae

### Personal data

First name and surname      Cintia Marchetti  
Title                              M.Sc.  
Place and date of birth      Villa Luzuriaga, Argentina, 8th February 1987  
Nationality                      Argentinean  
email                              [cintia.marchetti@upol.cz](mailto:cintia.marchetti@upol.cz)

### Education

09. 2014 - PRESENT

PhD in Biochemistry, Faculty of Science, Palacký University Olomouc, Czech Republic.  
Research topic: The role of cytokinins in the response of barley and wheat to abiotic stress.  
Supervisor: Ing. Nuria De Diego Sanchez, Ph.D.

03.2005 – 08.2014 (Master's degree & Bachelor's degree altogether)

M.Sc. Biology, Faculty of Exact and Natural Sciences, University of Buenos Aires, Argentina.  
Research topic: Regulatory aspects of wheat leaf senescence induced by shade stress.  
Supervisor: Fabio Causin, Ph.D.

### Employment

09.2014 – present

Student research assistant, Department of Molecular Biology, Faculty of Science, Centre of the Region Haná for Biotechnological and Agricultural Research, Palacký University Olomouc.

### Research fellowship

08.07 - 08.10.2016

Department of Biodiversity and Experimental Biology, Faculty of Exact and Natural Sciences,



University of Buenos Aires, Argentina.

Dr. Fabio Causin.

### Teaching

2014-present.

KBC/LABT Basic Course in Laboratory Work, Department of Biochemistry, Faculty of Science, Palacký University in Olomouc, Czech Republic.

### Supervision of students

Supervisor of the student Karel Mitura, Master degree in Biochemistry defended in May 2016. Topic: Regulatory aspects of shade-induced leaf senescence and cytokinin metabolism in *Triticum aestivum* L. (wheat).

### Conference presentations

De Diego N., Marchetti C.F., Ugena L., Humplik J.F., Fürst T., Spíchal L.: Integrated phenotyping of canopy height in crops under drought stress conditions and recovery. 3<sup>rd</sup> INTEGRATED PLANT AND ALGAL PHENOMICS MEETING (IPAP). Prague, Czech Republic (2018).

Marchetti C.F., Kokáš F., Vojta P., Novák O., Bergougnoux V., Galuszka P.: Silencing of two cytokinin dehydrogenase genes in barley alters the fine-tuning of the hormonal homeostasis and modifies plant productivity. International Plant Molecular Biology 2018. Montpellier, France (2018).

Marchetti C.F., Galuszka P., Causin H.F.: Changes in the light spectral quality affects cytokinin homeostasis, regulating the senescence rate in wheat leaves exposed to shading stress. Auxins and Cytokinins in Plant Development International Symposium (ACPD). Prague, Czech Republic (2018).

Marchetti C.F., Kokáš F., Vojta P., Novák O., Bergougnoux V., Galuszka P.: Characterization of barley plants with altered cytokinin metabolism. Green for Good IV, Olomouc, Czech Republic (2017).

Marchetti C.F., Galuszka P., Causin H.F.: Light spectral quality affects the expression

profile of genes involved in cytokinin signalling and homeostasis, in wheat leaves exposed to shading stress. XXXI Argentina Plant Physiology Meeting, Corrientes (2016). Marchetti C.F., Holubobá K., Novák O., Galuszka P.: Transgenic barley plants (*Hordeum vulgare* L. cv. Golden Promise) with altered CK homeostasis. 17th European Congress on Biotechnology, Poland (2016).

Marchetti C.F., Holubobá K., Novák O., Galuszka P.: Characterization of barley plants (*Hordeum vulgare* L. cv. Golden Promise) with silenced expression of *HvCKX2.2* and *HvCKX9* genes. Annual Conference of the German Society of Plant Biotechnology e.V., Germany (2016).

Marchetti C.F., Mrízová K., Galuszka P.: Silencing of *HvCKX2.2* and *HvCKX9* genes in barley plants (*Hordeum vulgare* L. cv. Golden Promise). Green for Good III, Olomouc, Czech Republic (2015). Causin H.F., Marchetti C.F., Servi L., Barneix A. J.: Proteolytic activity and antioxidant metabolism in leaves of knockout GPC mutants of wheat exposed to shading stress. Green for Good III, Olomouc, Czech Republic (2015).

## Publications

Marchetti, C. F.\*, Ugena L. \*, Humplík J. F., Polák M., Podlešáková K., Fürst T., De Diego N. and Spíchal, L. (2019). A novel image-based screening method to study water deficit response and recovery of barley populations using canopy dynamics phenotyping. *Frontiers in Plant Science*, submitted in December 2018 and UNDER MAYOR REVISIONS. \*These authors contributed equally to this work.

Marchetti, C. F., Škrabišová M., Galuszka P., Novák O. and Causin, H. F. (2018). Blue light suppression alters cytokinin homeostasis in wheat leaves senescing under shading stress. *Plant Physiology and Biochemistry*, 130, 647-657.

Vojta P., Kokáš F., Husičková A., Gruz J., Bergougnoux V., Marchetti C. F., Jiskrová E., Ježilová E., Mik V., Ikeda Y. and Galuszka P. (2016). Whole transcriptome analysis of transgenic barley with altered cytokinin homeostasis and increased tolerance to drought stress. *New Biotechnology*, 33 (5 Pt B), 676-91.

Causin, H. F., Marchetti, C. F., Pena, L. B., Gallego, S. M. and Barneix, A. J. (2015). Down-regulation of catalase activity contributes to senescence induction in wheat leaves exposed to shading stress. *Biologia Plantarum*, 59(1), 154-162.

Causin H. F., Roqueiro G., Petrillo E., Láinez V., Pena L. B., Marchetti C. F., Gallego S .M. and Maldonado S. I. (2012). The control of root growth by reactive oxygen species in *Salix nigra* Marsh. seedlings. *Plant Science*, 183, 197–205.

### **Fields of interest**

Plant physiology, plant molecular biology, plant biotechnology, agricultural plant science, senescence, oxidative stress, cytokinin metabolism, hormonal cross-talk, plant stress. Biochemical methods: preparation of proteins extracts, electrophoresis and immunolocalization of proteins by Western Blot, measurement of activity of enzymes connected with antioxidant metabolism. Molecular biology methods: nucleic acids purification, PCR, RT-PCR, qPCR and southern blot. Plant transformation methods: Biolistic and *Agrobacterium*-mediated transformation of barley plants.

# SUPPLEMENTS I

## Research article

Marchetti, C. F.\*, Ugena L.\*, Humplík J. F., Polák M., Podlešáková K., Fürst T., De Diego N. and Spíchal, L. (2019). A novel image-based screening method to study water deficit response and recovery of barley populations using canopy dynamics phenotyping. *Frontiers in Plant Science*, submitted in December 2018 and UNDER MAYOR REVISIONS.

\*These authors contributed equally to this work.

## SUPPLEMENTS II

### Research article

Marchetti, C. F., Škrabišová M., Galuszka P., Novák O. and Causin, H. F. (2018). Blue light suppression alters cytokinin homeostasis in wheat leaves senescing under shading stress. *Plant Physiology and Biochemistry*, 130, 647-657.

# SUPPLEMENTS III

## Research article

Vojta P., Kokáš F., Husičková A., Gruz J., Bergounoux V., Marchetti C. F., Jiskrová E., Ježilová E., Mik V., Ikeda Y. and Galuszka P. (2016). Whole transcriptome analysis of transgenic barley with altered cytokinin homeostasis and increased tolerance to drought stress. *New Biotechnology*, 33 (5 Pt B), 676-91

# SUPPLEMENTS IV

## Research article

Causin, H. F., Marchetti, C. F., Pena, L. B., Gallego, S. M. and Barneix, A. J. (2015). Down-regulation of catalase activity contributes to senescence induction in wheat leaves exposed to shading stress. *Biologia Plantarum*, 59(1), 154-162.

# A novel image-based screening method to study water deficit response and recovery of barley populations using canopy dynamics phenotyping

Cintia F. Marchetti<sup>1</sup>, Lydia Ugena<sup>1</sup>, Jan F. Humplík<sup>1</sup>, Michal Polak<sup>1</sup>, **Kateřina Podleřáková<sup>1</sup>**, Tomáš Fürst<sup>1</sup>, Nuria De Diego<sup>1\*</sup>, Lukas Spichal<sup>1</sup>

<sup>1</sup>Palacký University, Olomouc, Czechia

*Submitted to Journal:*  
Frontiers in Plant Science

*Specialty Section:*  
Plant Breeding

*Article type:*  
Methods Article

*Manuscript ID:*  
445018

*Received on:*  
22 Dec 2018

*Revised on:*  
09 Apr 2019

*Frontiers website link:*  
[www.frontiersin.org](http://www.frontiersin.org)



### *Conflict of interest statement*

The authors declare that the research was conducted in the absence of any commercial or financial relationships that could be construed as a potential conflict of interest

### *Author contribution statement*

CFM, LU, JFH, LS and NDD designed the experiments. CFM and LU performed the experiments. JFH performed the protocol for automated phenotyping, image-processing and image-based data analysis. TF developed the software routine for projected canopy height. MP and NDD performed the statistical analysis of the data, KP and NDD performed the metabolite quantification. NDD and LS supervised the study and formulated the concept of the project. All authors discussed the results. CFM, NDD and LS wrote the manuscript.

### *Keywords*

Amino Acids, Antioxidative enzymes, Canopy height, fluorescence, *Hordeum vulgare*, indoor phenotyping, Polyamines, red, green, blue (RGB) imaging

### *Abstract*

Word count: 313

Plant phenotyping platforms offer automated, fast scoring of traits that simplify the selection of varieties that are more competitive under stress conditions. However, indoor phenotyping methods are frequently based on the analysis of plant growth in individual pots. We present a reproducible indoor phenotyping method for screening young barley populations under water stress conditions and after subsequent rewatering. The method is based on a simple read-out of data using RGB imaging, projected canopy height, as a useful feature for indirectly following the kinetics of growth and water loss in a population of barley. A total of 45 variables including 15 traits and 30 biochemical metabolites measured (morphometric parameters, chlorophyll fluorescence imaging, quantification of stress-related metabolites; amino acids and polyamines, and enzymatic activities) were used to validate the method. We showed that the canopy height correlated with 36 of the 45 analysed parameters. Besides, the study allowed the identification of metabolites related to water stress response and recovery. Specifically, we found that the polyamines cadaverine, 1,3-diaminopropane and tyramine are good indicators of the plant water stress response whereas citrulline (Cit), spermidine (Spd) and the antioxidant enzyme ascorbate peroxidase (APX) were related to recovery in the high tolerant barley cultivar Golden Promise. Concretely, Cit, Spd and APX as high efficient oxygen radical scavengers could help the recovery of plants after the stress, pointing to them as possible mediators of plant stress hardening. In this work, we designed, optimized and validated a non-invasive image-based method for automated screening of potential water stress tolerance genotypes in barley populations. We showed that the projected canopy height is sensitive trait that truly reflects other invasively studied morphological, physiological and metabolic traits and can be easily applicable in low cost systems equipped with a simple RGB camera. We suggest that our approach might contribute to understanding of the plant water stress response and recovery capacity in crops such as barley.

### *Funding statement*

This work was funded by the Ministry of Education, Youth and Sports of the Czech Republic (Grant LO1204 from the National Program of Sustainability), the ERDF project "Plants as a tool for sustainable global development" (No. CZ.02.1.01/0.0/0.0/16\_019/0000827) and the Internal Grant Agency of Palacký University (IGA\_PrF\_2018\_023).

### *Ethics statements*

(Authors are required to state the ethical considerations of their study in the manuscript, including for cases where the study was exempt from ethical approval procedures)

Does the study presented in the manuscript involve human or animal subjects: No

### *Data availability statement*

Generated Statement: All datasets generated for this study are included in the manuscript and the supplementary files.

1 **Title: A novel image-based screening method to study water deficit response and recovery of**  
2 **barley populations using canopy dynamics phenotyping**

3 **Running title: Screening method using canopy height dynamics**

4 Cintia F. Marchetti<sup>1\*</sup>, Lydia Ugena<sup>2\*</sup>, Jan F. Humplík<sup>2</sup>, Michal Polák<sup>2</sup>, Kateřina Podlešáková<sup>2</sup>,  
5 Tomáš Füst<sup>2,3</sup>, Nuria De Diego<sup>2 +</sup> and Lukáš Spíchal<sup>2</sup>

6 <sup>1</sup>Department of Molecular Biology, Centre of the Region of Haná for Biotechnological and  
7 Agricultural Research, Faculty of Science, Palacký University, Šlechtitelů 27, 783 71 Olomouc,  
8 Czech Republic; <sup>2</sup>Department of Chemical Biology and Genetics, Centre of the Region Haná for  
9 Biotechnological and Agricultural Research, Faculty of Science, Palacký University, Šlechtitelů  
10 27, 783 71 Olomouc, Czech Republic; <sup>3</sup>Department of Mathematical Analysis and Applications of  
11 Mathematics, Faculty of Science, Palacký University, Olomouc, Czech Republic

12 E-mail addresses: Cintia F. Marchetti: [cintia.marchetti@upol.cz](mailto:cintia.marchetti@upol.cz); Lydia Ugena:  
13 [lydia.ugena@upol.cz](mailto:lydia.ugena@upol.cz); Jan F. Humplik: [jan.humplik@upol.cz](mailto:jan.humplik@upol.cz); Michal Polák:  
14 [michal.polak@upol.cz](mailto:michal.polak@upol.cz); Kateřina Podlešáková: [katerina.podlesakova@upol.cz](mailto:katerina.podlesakova@upol.cz); Tomáš Füst:  
15 [tomas.furst@upol.cz](mailto:tomas.furst@upol.cz); Lukáš Spíchal: [lukas.spichal@upol.cz](mailto:lukas.spichal@upol.cz)

16

17 **<sup>+</sup>Author for correspondence: Nuria De Diego, Tel: +420585634940, Email: [nuria.de@upol.cz](mailto:nuria.de@upol.cz)**

18 **\*These authors contributed equally to this work.**

## 19 **Keywords**

20 Amino acids, antioxidative enzymes, canopy height, fluorescence, *Hordeum vulgare*, indoor  
21 phenotyping, polyamines, red, green, blue (RGB) imaging.

22

23

## 24 Abstract

25 Plant phenotyping platforms offer automated, fast scoring of traits that simplify the selection of  
26 varieties that are more competitive under stress conditions. However, indoor phenotyping methods  
27 are frequently based on the analysis of plant growth in individual pots. We present a reproducible  
28 indoor phenotyping method for screening young barley populations under water stress conditions  
29 and after subsequent rewatering. The method is based on a simple read-out of data using RGB  
30 imaging, projected canopy height, as a useful feature for indirectly following the kinetics of growth  
31 and water loss in a population of barley. A total of 45 variables including 15 traits and 30  
32 biochemical metabolites measured (morphometric parameters, chlorophyll fluorescence imaging,  
33 quantification of stress-related metabolites; amino acids and polyamines, and enzymatic activities)  
34 were used to validate the method. We showed that the canopy height correlated with 36 of the 45  
35 analysed parameters. Besides, the study allowed the identification of metabolites related to water  
36 stress response and recovery. Specifically, we found that the polyamines cadaverine, 1,3-  
37 diaminopropane and tyramine are good indicators of the plant water stress response whereas  
38 citrulline (Cit), spermidine (Spd) and the antioxidant enzyme ascorbate peroxidase (APX) were  
39 related to recovery in the high tolerant barley cultivar Golden Promise. Concretely, Cit, Spd and  
40 APX as high efficient oxygen radical scavengers could help the recovery of plants after the stress,  
41 pointing to them as possible mediators of plant stress hardening. In this work, we designed,  
42 optimized and validated a non-invasive image-based method for automated screening of potential  
43 water stress tolerance genotypes in barley populations. We showed that the projected canopy  
44 height is sensitive trait that truly reflects other invasively studied morphological, physiological and  
45 metabolic traits and can be easily applicable in low cost systems equipped with a simple RGB  
46 camera. We suggest that our approach might contribute to understanding of the plant water stress  
47 response and recovery capacity in crops such as barley.

## 48 Abbreviations

49 amino acids (AAs);  $\gamma$ -aminobutyric acid (GABA); ascorbate peroxidase (APX); catalase (CAT);  
50 guaiacol peroxidase (POX); 1,3-diaminopropane (DAP); *L*-alanine (Ala); *L*-arginine (Arg); *L*-  
51 asparagine (Asn); *L*-aspartic acid (Asp); *L*-citrulline (Cit); *L*-glutamine (Gln); *L*-glutamic acid  
52 (Glu); *L*-glycine (Gly); *L*-histidine (His); *L*-ileucine (Ile); *L*-leucine (Leu); *L*-methionine (Met); *L*-

53 phenylalanine (Phe); *L*-proline (Pro); *L*-serine (Ser); *L*-tryptophan (Trp); *L*-tyrosine (Tyr);  
54 polyamines (PAs); putrescine (Put); reactive oxygen species (ROS); spermidine (Spd); spermine  
55 (Spm); cadaverine (Cad); red, green, blue (RGB); tyramine (Tyra).

56

## 57 **Introduction**

58 Abiotic stresses, in particular water deficit, constrain the global production of crops, affecting both  
59 the vegetative and reproductive phases of development (Wang et al., 2003). Not all water stress  
60 scenarios are equivalent, however, because the severity, frequency, duration and timing of the  
61 stress can vary, and with them the impact on the plant (Chen et al., 2014). A robust and reliable  
62 analysis of phenotypic traits is therefore essential for each context, to shed light on the basic  
63 tolerance mechanisms and develop strategies for breeding crops that are more tolerant to adverse  
64 environments.

65 Barley is the fourth most cultivated crop world-wide (<http://www.fao.org/faostat/en/#data/QC>).  
66 As a diploid organism, it is considered to be a suitable model for studying the more complex  
67 polyploid species belonging to the *Triticeae* tribe. Under water stress conditions, barley displays  
68 reduced growth and adaptations of other physiological parameters, such as chlorophyll content,  
69 net photosynthetic rate and water content (Ahmed et al., 2013; Saade et al., 2018). However, the  
70 mechanisms that confer water stress tolerance and recovery capacity in this crop species are still  
71 not fully understood.

72 **Plant** phenotyping platforms provide the potential for automated, fast scoring of several traits  
73 related to stress tolerance over a time-course, using non-invasive sensors (Awlia et al., 2016; Chen  
74 et al., 2014; De Diego et al., 2017; Granier et al., 2006; Humplík et al., 2015). Until now, published  
75 indoor protocols have been based on the response of individual plants often restricted by pot  
76 growth, whereas in the field plant growth results in a canopy (Araus and Cairns, 2014).  
77 Nevertheless, in the field the plant growth is seasonally dependent, often reducing the number of  
78 possible experiments to one per year, whereas indoor phenotyping allows continuous repetition of  
79 experiments. Furthermore, screening for specific tolerance traits under controlled conditions is  
80 often necessary to manage the complexity of interactions between genotype and environment on

81 the phenotype (Ghanem et al., 2015). The specific metric being monitored therefore needs to be  
82 defined and its relationship with the physiological trait of interest has to be resolved and validated.  
83 The plant phenotype is also determined by complex genome × environment × management  
84 interactions: the sum of the complex interactions between metabolic pathways and intracellular  
85 regulatory networks are reflected in internal, physiological and biochemical phenotypes  
86 (Großkinsky et al., 2015). Thus, a characterization limited only to a detailed description of a set of  
87 image-based traits remains incomplete for understanding plant responses to drought. An  
88 integration of data from phenomics with other ‘-omics’ (e.g. metabolomics and genomics) may  
89 help dissect the plant response and clarify the key traits involved in the mechanisms of stress  
90 tolerance and acclimation. As example, the combination of phenomics with metabolomics can help  
91 to identify metabolites that are mainly accumulated under water stress conditions. Particularly,  
92 some metabolites such as polyamines and some amino acids involved in glutamate metabolism  
93 like  $\gamma$ -amino butyric acid (GABA) and *L*-proline (Pro) play essential role regulating stress  
94 tolerance like compatible solutes contributing to osmotic potential, mediators of antioxidant  
95 responses or signal molecules (De Diego et al., 2013; Podlešáková et al., 2019). Concretely,  
96 GABA, Pro and *L*-arginine (Arg) have been described as metabolites involved in plant recovery  
97 and hardening under drought stress conditions (De Diego et al., 2015).

98 We present a non-destructive method for studying the water stress tolerance and recovery on a  
99 population of barley based on image analysis of canopy height using a simple red, green, blue  
100 (RGB) camera. To introduce the method we used barley cultivar Golden Promise as a good  
101 representative of the varieties with agronomical interest due to its semi-dwarf with low lodging  
102 problems (Thomas et al., 1984) and stress tolerance (Forster et al., 2000). Moreover, we focused  
103 on profiling the primary and secondary metabolites, amino acids and polyamines, which play a  
104 dual role as tolerance indicators and signal molecules (Muscolo et al., 2015; Urano et al., 2010) to  
105 study further the involvement of these molecules regulating plant water stress response and  
106 recovery capacity. We show that, in combination with other -omic approaches such as  
107 metabolomics, followed by multivariate statistical methods, the experimental procedures for  
108 studying stress response can be made more efficient. The result is a simple and highly reproducible  
109 method for studying the stress response and recovery in barley populations, which is applicable  
110 for breeding programmes to select and characterize potentially successful varieties.

## 111 **Materials and Methods**

### 112 *Plant material and growth conditions*

113 Barley (*Hordeum vulgare*) cultivar Golden Promise was used for the study. Seeds were surface-  
114 sterilized by soaking in 70% ethanol for 30 s, and then washed three times with sterilized water,  
115 and immediately after that with a 4% solution of sodium hypochlorite for 4 min followed by an  
116 additional four washes with sterilized water. The sterile seeds were placed on wet tissue paper  
117 inside square plastic plates (120 mm × 120 mm) and maintained for 2 days at 4°C in the dark for  
118 imbibition, as schematized in Fig. 1. The plates were then transferred into a growth-chamber, under  
119 controlled conditions of a 22°C, 16 : 8 h, light : dark cycle with a photosynthetically active  
120 radiation (PAR) light intensity of 120  $\mu\text{mol photons m}^{-2} \text{ s}^{-1}$  for 2 days, to induce germination (Fig.  
121 1).

### 122 *Non-invasive plant phenotyping*

#### 123 - *Phenotyping platform, experimental setup and assay conditions*

124 To develop the barley screening method, firstly we performed and analysed reproducibility of two  
125 independent assays using well-watered conditions (1<sup>st</sup> experiment- December 2017 and 2<sup>nd</sup>  
126 experiment- June- 2018; Supplementary Table 1). After that, we performed a final experiment to  
127 evaluate the growth of barley seedling population under water deficit (3<sup>rd</sup> experiment-  
128 Supplementary Table 1). In all experiments, the barley seedlings were planted in plastic containers  
129 (32 cm × 19.5 cm × 10 cm, with a volume of 4 l) filled with 2.8 kg of a 2:1 mixture of substrate  
130 (Substrate 2; Klasmann-Deilmann GmbH, Geeste, Germany) and sand. A total of 50 seedlings per  
131 container was sown, distributed in five rows containing 10 plants each, with a final density of 1000  
132 plants  $\text{m}^{-2}$  (Figure 1). Two containers with 50 seedlings each were then placed together in a  
133 standard PlantScreen™ measuring tray (Photon Systems Instruments, Brno, Czech Republic).

134 For the image analysis, the tray with two containers housing 50 plants each was transferred onto  
135 an OloPhen platform ([http://www.plant-phenotyping.org/db\\_infrastructure#/tool/57](http://www.plant-phenotyping.org/db_infrastructure#/tool/57)). In the water  
136 deficit experiment a metal mesh was installed for better separation of the leaves from the variants  
137 [well-watered (W) and water stress-drought (D)] in each container (Figure 1). The trays were  
138 located into the PlantScreen™ conveyor system installed in a growth chamber with a controlled

139 environment and LED lighting (Photon Systems Instruments). The growth conditions were set to  
140 simulate a long day, with a regime of 22°C : 20°C in a 16 : 8 h light : dark cycle, a PAR irradiance  
141 of 320  $\mu\text{mol photons m}^{-2} \text{s}^{-1}$  and a relative humidity of 40%.

142 - *Imaging acquisition*

143 The PlantScreen™ system is equipped with a top-view and side-view RGB camera and top-view  
144 FluorCam (Figure 1). The RGB and FluorCam images were automatically stored in a database  
145 server. The images were then evaluated. The side-view RGB images were analysed using an in-  
146 house software routine implemented in MatLab R2015 that was developed and validated by the  
147 authors of this study. The application can be used without charge by obtaining a licence from  
148 Palacký University, by emailing Tomáš Füst ([tomas.furst@upol.cz](mailto:tomas.furst@upol.cz)) and agreeing not to use the  
149 application for commercial purposes.

150 To provide a comparative view, we analysed chlorophyll fluorescence-related parameters  
151 throughout the experiments using a top-view FluorCam. A standard protocol was used for the  
152 measurement of Chl fluorescence quenching using the Chl fluorescence imaging (CFIM) part of  
153 the PlantScreen™ platform using the same protocol described by Humplík et al. (2015). Image  
154 data were processed and chlorophyll fluorescence parameters were calculated using software  
155 FluorCam 7 (Photon Systems Instruments). Thus, we estimated: (a) the maximum quantum yield  
156 of photosystem II (PSII) photochemistry for a dark-adapted state,  $\Phi_{P_0}$ ; (b) the actual quantum yield  
157 of PSII photochemistry for a light-adapted state,  $\Phi_P$ ; (c) the quantum yield of constitutive non-  
158 light induced (basal or dark) dissipation processes consisting of chlorophyll (Chl) fluorescence  
159 emission and heat dissipation,  $\Phi_{(f,D)}$ , quantum yield of regulatory light-induced non-photochemical  
160 quenching,  $\Phi_{NPQ}$ . It is worth mentioning that  $\Phi_P + \Phi_{(f,D)} + \Phi_{NPQ} = 1$ , and  $\Phi_P = qP \Phi_{PSII}$ , where  $qP$   
161 =  $((F_M' - F(t)) / (F_M' - F_0'))$  is the coefficient of photochemical quenching, which estimates a  
162 fraction of the so-called open PSII reaction centres, and that  $\Phi_{PSII} = ((F_M' - F_0') / F_M')$  is the  
163 maximal quantum yield of the PSII photochemistry for a light-adapted state.

164 - *Watering regime*

165 In each container the substrate water content (%) was calculated as follow; the substrate was  
166 weighted and then watered to full capacity and the top was covered with plastic bags for reducing

167 evaporation losses. When the water stopped draining from the container (c. 10 h later) the weight  
168 was again measured. The substrate was then dried for 48 h at 105°C until complete dryness and  
169 the weight was also determined. The three weights of the substrate water moisture status were used  
170 for calculating the gravimetric water content ( $\theta_g$ ) and substrate maximum water holding capacity.  
171 All containers were watered with tap water (average conductivity c. 56 mS m<sup>-1</sup>) at 100% of field  
172 capacity after sowing. Then, the control plants were irrigated every second day to maintain 80%  
173 of field capacity until the end of the experiment. In the 3<sup>rd</sup> experiment, the irrigation was stopped  
174 in the water stress variant when the plants presented the first fully expanded leaf. When the  
175 substrate water content decreased to 65% (Day 15), the water limited variants were rewatered at  
176 full water capacity (100%).

### 177 *The Assay Workflow*

178 To study water deficit and recovery in barley populations using imaging acquisition approaches  
179 we established the protocol schematized in Figure 1. The protocol takes a total of 3 weeks,  
180 including seed germination (2 days), seedling growth under water stress conditions (16 days) and  
181 subsequent rewatering (4 days). After imbibition, a total of 50 germinated seeds was transferred  
182 to plastic containers (Figure 1). The selection of germinated seeds at a similar developmental stage  
183 (radicle length) is an important to reduce within-population variability. Two randomly selected  
184 containers were then placed in standardized trays and transported within the PlantScreen™ on  
185 conveyor belts. Automated RGB imaging from two optical projections (top- and side-view) was  
186 performed every day for the next 19 days. The daily RGB measurements of 16 trays (1600  
187 seedlings) took 20 min in total. When the top-view fluorescence intensity measurement was  
188 included (every third day), the total process time increased to 4 h. The PlantScreen™ Analyzer  
189 software processed the raw data automatically. Raw data were automatically stored in PlantScreen  
190 database from where they were subsequently exported for further image processing and analysis.

191 Side-view imaging allowed separation of the plants from the background and the differentiation  
192 between the left and right containers using a pre-defined vertical line in the image based on the  
193 metal mesh installed between them (Figure 1). To define and evaluate the canopy height in each  
194 container (or variant) automatically, the green mask of the plant was found using a thresholding  
195 algorithm. A line was then placed above the upper most pixel of the mask. The line was gradually



196 lowered (each step by one pixel) and the following criterion evaluated for each possible position  
197 of the line:

198  $\text{crit} = A / B$

199 where A is the number of pixels on a line that also belong to the mask, and B is the length of the  
200 line (in pixels). Thus, the criterion represents the fraction of the line that intersects the mask. Once  
201 this fraction exceeded a user-defined threshold, the process was stopped and the position of the  
202 line recorded. This position was then used as a proxy for canopy height.

### 203 ***Manual parameters***

#### 204 - *Biometric parameters*

205 The aerial biomass of the seedlings was determined from the fresh weight (FW, g) by cutting the  
206 shoots 1 cm above ground level from eight or five plants per replicate and variant at the end of the  
207 water stress period and after 4 days of rewatering, respectively. The developmental stage of each  
208 plant at the same time points, according to the BBCH scale (Earth Observation and Research  
209 Branch Team, 2011), and the size (length and width) of the youngest and fully expanded leaf were  
210 also evaluated.

#### 211 - *Plant water status*

212 The relative water content (RWC, %) was measured in five individual plants per variant and  
213 replicate. The measurement was performed using 2 cm from the middle part of the last youngest  
214 mature leaf collected at the end of the water stress period and after rewatering. RWC was  
215 calculated using the following equation:  $\text{RWC} (\%) = (\text{FW} - \text{DW}) / (\text{TW} - \text{DW}) \times 100$ , where FW  
216 is the fresh weight at harvesting time, TW is the total weight as total turgor estimated after 24 h of  
217 imbibition, and DW is the dry weight after 48 h at 85°C.

#### 218 - *Chlorophyll content*

219 The index of relative chlorophyll content or ‘greenness’ of leaves was measured *in vivo* using a  
220 portable SPAD-502 Plus chlorophyll meter (Konica Minolta Inc.). Six measurements were taken

221 in the last youngest mature leaf in five individual plants per replicate and variant at the end of the  
222 water stress period and after rewatering.

223 - *Antioxidant enzymes*

224 For the enzymatic analysis, three groups of five plants per replicate and variant after water stress  
225 and rewatering were collected and immediately frozen in liquid nitrogen. Before extraction, the  
226 five plants per each group were grounded by mortar and pestle using liquid nitrogen. The resulting  
227 pool from each replicate and variant was divided into three analytical replicates for quantification  
228 of antioxidant activity. 100 mg of grounded material was homogenized at a ratio of 1:5 with  
229 extraction buffer [50 mM Tris (pH 7.6), containing 2 mM magnesium sulphate, 1 mM  
230 ethylenediaminetetraacetic acid (EDTA), 1 mM ascorbic acid, 1 mM phenylmethylsulfonyl  
231 fluoride and 0.5 % (v/v) Triton X100] in the presence of polyvinylpolypyrrolidone. After  
232 centrifugation at 19,000 g for 20 min at 4°C, the supernatant was collected and centrifuged under  
233 the same conditions for an additional 10 min. The concentration of proteins in the crude extract  
234 was evaluated using the method described by Bradford (Bradford, 1976). Catalase (CAT) activity  
235 ( $\mu\text{mol min}^{-1} \text{mg}^{-1}$  total protein) was measured according to Aebi (1984). Briefly, the decrease in  
236 absorbance at 240 nm of a reaction mixture consisting of 25  $\mu\text{l}$  enzymatic extract in a final volume  
237 of 1 ml reaction mixture containing 50 mM potassium phosphate (pH 7.0) and 25 mM  $\text{H}_2\text{O}_2$  was  
238 measured. The molar extinction coefficient of  $38 \text{ M}^{-1} \text{cm}^{-1}$  was used to calculate CAT activity.

239 Ascorbate peroxidase (APX) and guaiacol peroxidase (POX) activity was determined according  
240 to Prochazková et al. (2001). APX activity was deduced from the decrease in ascorbate  
241 concentration, seen as a decline in the optical density at 290 nm. A value for the activity was  
242 calculated using an extinction coefficient of  $2.8 \text{ mM}^{-1} \text{cm}^{-1}$  for the ascorbate during 30 s. The  
243 assay was performed in a final volume of 1 ml containing 50 mM potassium phosphate (pH 7.0),  
244 1.7 mM  $\text{H}_2\text{O}_2$ , 0.3 mM ascorbic acid and 85  $\mu\text{l}$  enzymatic extract. POX activity was determined  
245 from the increase in formation of tetra-guaiacol, seen as an increase in the optical density at 470  
246 nm. The activity was calculated using an extinction coefficient  $26.6 \text{ mM}^{-1} \text{cm}^{-1}$  during 30 s. The  
247 assay was carried out using a reaction mixture consisting of 4  $\mu\text{l}$  extract, 150 mM potassium  
248 phosphate (pH 6.1), 8 mM guaiacol and 2.2 mM  $\text{H}_2\text{O}_2$ .

250 For the AA analysis, three groups of five individual plants per replicate and variant were collected  
251 after water stress and rewatering. All individuals from each group were pooled together using  
252 liquid nitrogen. 5 mg FW of the pooled material was measured and extracted. The extraction  
253 procedure was performed using a AccQTag Ultra derivatization kit (©Waters). All extracted  
254 samples were analysed using an ACQUITY UPLC® System and a Xevo™ 122 TQ-S triple  
255 quadrupole mass spectrometer (©Waters) according to the annotation note of Waters Corporation  
256 (Milford, MA, USA) (Gray and Plumb, 2016). Calibration curves were constructed for each  
257 component analysed using internal standards:  $\gamma$ -aminobutyric acid (GABA), *L*-alanine (Ala), *L*-  
258 arginine (Arg), *L*-asparagine (Asn), *L*-aspartic acid (Asp), *L*-citrulline (Cit), *L*-glutamine (Gln), *L*-  
259 glutamic acid (Glu), *L*-glycine (Gly), *L*-histidine (His), *L*-ileucine (Ile), *L*-leucine (Leu), *L*-  
260 methionine (Met), *L*-phenylalanine (Phe), *L*-proline (Pro), *L*-serine (Ser), *L*-tryptophan (Trp) and  
261 *L*-tyrosine (Tyr), and the deuterium-labelled compounds *L*-glutamic acid-2,3,3,4,4-d<sub>5</sub>,  $\gamma$ -  
262 aminobutyric acid-2,2,3,3,4,4-d<sub>6</sub> and *DL*-leucine-2,3,3,4,5,5,5',5',5'-d<sub>10</sub>, all purchased from  
263 ©Sigma-Aldrich Inc. (Germany).

264 For PAs determination 10 mg FW of the remaining material used for the AAs was extracted and  
265 quantified as described by Malec et al. (2017), using the same equipment as for the analysis of free  
266 AAs. The final quantification was performed using the internal standards cadaverine (Cad), 1,3-  
267 diaminopropane (DAP), putrescine (Put), spermidine (Spd), spermine (Spm) and tyramine (Tyra),  
268 all purchased from ©Sigma-Aldrich Inc., were added to each sample to construct the calibration  
269 curve. The concentration of AAs and PAs per dry weight (DW) was then using the absolute water  
270 content of the plants.

### 271 *Statistical analysis and data representation*

272 To assess the differences between the variants of each non-invasive trait extracted from the image  
273 analysis, the non-parametric Kruskal Wallis one-way analysis of variance (ANOVA) by raks was  
274 performed. For the validation of the method and to evaluate the influence of a tray position and  
275 the effect of the treatment (well-watered or water limited variant) in the morphological and  
276 physiological measurements at a particular time-point, the two-way ANOVA was used. Different  
277 letters mean significant differences between variants. One-way ANOVA was used to analyse

278 significant differences between the metabolites differed between the variants. Represented values  
279 annotated with ns indicate non-significant differences and means annotated with asterisks indicate  
280 significant differences (\*  $P \leq 0.05$ ; \*\*  $P \leq 0.01$ ; \*\*\*  $P \leq 0.001$ ). Tukey HSD test was used for  
281 multiple comparison after ANOVA. All the analysis were performed in R 3.5.1 software using  
282 *multcomp* package.

283 For multidimensional analyses, a principal component analysis (PCA) was carried out using the  
284 packages *factoextra*, *corrplot*, *PerformanceAnalytics* and *ggpubr*, and the results were displayed  
285 in a biplot. The Pearson's linear correlation coefficients between all pairs of studied variables and  
286 the significance werer also represented in the correlation matrix and scatter plots.

## 287 Results

### 288 ***1- PHENOTYPING METHOD- Screening of barley population using simple RGB imaging***

289 *A- Experiment 1 and 2- Analysis of projected canopy height in barley population at control*  
290 *conditions*

291 Applying the aforementioned approach, the side-view RGB images of the barley seedling canopy  
292 from two independent experiments (**Experiment 1** in December 2017 and **Experiment 2** in June  
293 2018) were analysed (Supplementary Table S1). Two randomly distributed trays containing 50  
294 plants each were used per experiment. The reproducibility of the bioassay was corroborated, as the  
295 canopy height from both experiments presented the same trend line (Figure 2a).

296 A manual assessment of plants was then performed to complement and validate the traits derived  
297 from the automated plant imaging and image analysis, including the functionality of the hardware  
298 and software components. The aerial biomass in fresh weight (FW, g) from five seedlings  
299 randomly selected from the two different trays of each experiment was determined manually at  
300 days 16 and 19. A Pearson correlation-based comparison between the canopy height (pixels, from  
301 50 plants) and the aerial biomass (the average of the five measured plants) revealed a highly  
302 significant correlation, with an  $R^2$  of 0.90 ( $P < 0.001$ ) (Fig. 2b). This result provided clear evidence  
303 of the reliability of the method for analysing shoot growth in the population of barley cv. Golden  
304 Promise.

305 *B-Experiment 3- Analysis of projected canopy height in barley population under water deficit and*  
306 *subsequent rewatering*

307 For studying water stress response and recovery capacity in barley at a population level, we  
308 performed a final **experiment 3** (Supplementary Table **S1**). In this case, the projected canopy  
309 height of five **randomly distributed trays** containing two plastic containers; a water-stressed variant  
310 (D, left) and a well-watered variant (W, right) with 50 plants each (with a final number of 500  
311 barely seedlings), was recorded over the time-course of 15 days (Figure 1 and Supplementary  
312 Figure **S1**). **Three biological replicates with five plants (3 x 5 = 15 plants) were taken from two**  
313 **randomly selected trays in each variant (D and W) and then, they were** used for validation and  
314 reproducibility of the method. **The three remaining trays were collected at the end of the rewatering**  
315 **period**. First of all, we determined the substrate water content **of all the trays during the experiment**.  
316 The first **6** days the substrate water content of the irrigated and non-irrigated variants was very  
317 similar, with no differences between treatments (Figure 3a). **At day 9**, the substrate water content  
318 of non-irrigated variants started to decrease **with significant differences compared to W variants**  
319 **( $P < 0.05$ )**. **At the day 15 the substrate water content of the D variant** reached 65%. **In this point,**  
320 **the containers with the D variant were rewatered to 100% full capacity** (Figure 3a).

321 The automated RGB imaging yielded curves with the same pattern for the **five independent trays**  
322 **until the end of the water deficit period (Supplementary Figure 1) and for** three **trays through the**  
323 **whole experiment** (Figure 3b **and c**). For the first 7 days after water withdrawal, the stressed plants  
324 retained projected canopy height kinetics similar to the well-watered plants, but they were  
325 significantly reduced from day 11 to day 15 (Figure 3b and Supplementary Table **S2**). After  
326 rewatering, the **D** variant from each **independent tray** similarly recovered the projected canopy  
327 height but the values were still significantly smaller than **the W variants** (Figure 3b and  
328 Supplementary Table **S2**). From the obtained dynamic changes in the projected canopy height of  
329 the barley seedling population, we created a model curve different for the stressed and non-stressed  
330 variants, as represented in Figure 4a. From each curve, we extracted several traits; the maximum  
331 canopy height on the days when watered and non-watered curves separated (Max), water loss as  
332 the slope of **line obtained for** the reduction in canopy height, the minimum canopy **height** for the  
333 water stress period (Min), **the** water recovery **capacity** as the slope of the **line obtained for the**  
334 **increase of canopy height after rewatering**, and the maximum canopy height after rewatering

335 (MaxR). As an example of the potential use of our bioassay, we calculated the slope of the line for  
336 the water deficit period and after rewatering from the two trays selected for the posterior manual  
337 measurements (Figure 4b,c). In all linear curves, a highly significant correlation ( $R^2 > 0.90$ ;  $P <$   
338  $0.001$ ) was obtained for both growth conditions. Together with the slopes, the Max, Min and MaxR  
339 are shown in Table 1; similar values were obtained in both replicates for these traits. These results  
340 confirmed the reproducibility of the method, which was later validated using destructive  
341 parameters.

342 Our phenotyping system is also equipped with a FluorCam unit for the analysis of chlorophyll  
343 fluorescence parameters. In our study was clear that water deficit significantly changed all the  
344 chlorophyll fluorescence parameters, albeit with different dynamics and intensity (Figure 5a,b).  
345 Some parameters responded quickly and had already changed by day 11, e.g.  $\Phi_{Po}$  and  $qP$  had  
346 decreased, and  $\Phi_{(f,D)}$  had increased. Other parameters, such as decreasing  $\Phi_{PSII}$  and  $\Phi_P$ , and  
347 increasing  $\Phi_{NPQ}$ , had occurred by day 16 as late stress response parameters (Figure 5b). After  
348 rewatering, the stressed variants recovered to control values for  $qP$  and  $\Phi_P$ . However,  $\Phi_{Po}$ ,  $\Phi_{PSII}$ ,  
349  $\Phi_{(f,D)}$  and  $\Phi_{NPQ}$  maintained significant differences compared with the well-watered plants (Figure  
350 5b). The results indicated that these last four parameters were potential indicators for evaluating  
351 the recovery capacity of plants, at least in barley.

## 352 ***2- VALIDATION AND REPRODUCIBILITY OF THE PHENOTYPING METHOD***

### 353 ***A-The reproducibility of morphometric and physiological parameters between biological*** 354 ***replicates and trays confirmed the reliability of the method***

355 We performed a manual evaluation of several morphological and physiological parameters in two  
356 independent trays to integrate and validate our results obtained by imaged-based measurements.  
357 Firstly, we evaluated the developmental stage of the plant population by analysing the last  
358 emerging leaf in eight and five randomly selected plants per variant at the end of the water period  
359 and rewatering, respectively (Figure 6). We observed differences among variants (treated and non-  
360 treated) and not between trays. Whereas in the watered control at day 16 the fifth leaf had appeared,  
361 the stressed plants were still expanding the third leaf at this point of the assay (Figure 6). After  
362 rewatering, the differences were reduced to one leaf less, with the fourth and fifth leaf in expansion  
363 for stressed and non-stressed plants, respectively (Figure 6).

364 In the case of the aerial biomass (FW, g), full expanded (FE) leaf length and width (cm) and the  
365 ratio between length and width, eight plants per variant and tray were individually collected at the  
366 end the water stress period and after rewatering, respectively (Figure 7a-c). In almost all the cases,  
367 the changes were due to the treatment and not because of the tray position effect (Supplementary  
368 Table S3). Regarding biomass, the seedlings from the D variant were significantly smaller than  
369 the W plants in both trays (Figure 7a). After recovery, D plants were still only half the weight of  
370 the well-watered variants (Figure 7a). When the length and width of the last fully expanded leaf  
371 were evaluated, we observed that the seedlings from the same variant showed the same profile for  
372 both traits (Figure 7b,c); the length and width were significantly reduced under water stress  
373 conditions. After rewatering only the width recovered to control values (Figure 7b), affecting the  
374 length/width ratio (Figure 7d).

375 There was also no effect of the tray recorded for the RWC and total chlorophyll (Chl) content  
376 between the trays (Supplementary Table S3). The water deficit treatment caused a c. 50% decrease  
377 in plant RWC, and rewatering returned the plant water status to 95% in only 4 days (day 19)  
378 (Figure 7e). Total chlorophyll (Chl) content showed a similar pattern (Figure 7f). The values were  
379 significantly lower in stressed plants than in the controls, indicating that the Chl content and N  
380 status of the plants were significantly affected by water stress conditions but were recovered after  
381 4 days of rewatering (Figure 7f).

382 Altogether, the high reproducibility of the individual biometric and physiological parameters  
383 among the trays corroborated the reproducibility of the method for studying water deficit and  
384 recovery capacity at least in barley cv. Golden Promise.

### 385 ***B- The reproducibility of the antioxidative response between trays validated the method for study*** 386 ***water deficit and recovery in barley population***

387 It is well-known that plants activate their antioxidative machinery as a response to stress. Hence,  
388 we quantified the activity of the three antioxidant enzymes CAT, POX and APX (Figure 7g-i).  
389 The same profile was observed between trays as stress response and subsequent recovery (Figure  
390 7g-i, Supplementary Table S3). Interestingly, only CAT and POX increased significantly in the  
391 stressed variants, and then recovered to control values after rewatering (Figure 7g,h). In contrast,  
392 APX kept increasing during the recovery period, resulting in values four times higher in the

393 stressed seedlings than in the controls (Figure 7i). These results indicated that each type of  
394 antioxidant enzyme plays a different role in the barley *cv. Golden Promise* stress response.

### 395 *C- Different free AAs and PAs regulated plant stress response and recovery*

396 Free polyamines (PAs) and amino acids (AAs) are typical metabolites involved in the plant water  
397 stress response (Podlešáková et al., 2019) (Figure 8). As expected, both groups of metabolites  
398 accumulated significantly under stress, and the profile of the fold change between treated and non-  
399 treated plants was similar (Figure 8).

400 Water deficit induced a significant accumulation of AAs (pmol mg<sup>-1</sup> DW) (Figure 8 and  
401 Supplementary Table S4), with the highest increases in Pro and OH-Pro. After rewatering, many  
402 of the AA kept significantly higher in the stressed plants than in the controls, except for Arg and  
403 GABA did not showed significant differences between treatments (Figure 8). Interestingly, at this  
404 time-point the accumulation of Cit in stressed plants was 11.7-fold (log<sub>2</sub>= 3.55) higher compared  
405 to the control levels (Figure 8).

406 For the PAs, quantification of Cad was only possible in the water-stressed plants (with an average  
407 of 9.73 and 7.85 pmol mg<sup>-1</sup> DW for tray 1 and 2, respectively); in the well-watered and the stressed  
408 variants after rewatering it was under the limits of detection. Tyra and DAP were the most  
409 accumulated compounds and Spd was the only PA that did not change in stressed plants compared  
410 to the non-stressed ones (Figure 8 and Supplementary Table S4). After rewatering, water stressed  
411 plants kept higher content of Tyra and DAP compared to the well-watered plants, Spd accumulated  
412 to higher levels, whereas no significant differences between variants were found in the case of Put  
413 and Spm (Figure 8 and Supplementary Table S4). Based on these results, we could classify the  
414 metabolites into two groups, a water stress-related compounds (e.g. Pro, OH-Pro, Tyra, DAP and  
415 Cad) and a group involved in the recovery of the plants after rewatering (e.g. Cit and Spd).

416



417 **3- DATA ANALYSIS- Multivariate statistical analysis for understanding the physiological basis**  
418 **of the image-derived traits and water stress response in barley populations**

419 To integrate all parameters measured and confirm the reliability of the traits derived from our  
420 method based on the canopy height of barley populations, we performed a PCA in which tray 1  
421 and 2 were evaluated for two different growth regimens, water-stressed (D) and well-watered (W)  
422 plants, at two time-points, at the end of the stress period or after 4 days of rewatering (RD and  
423 RW, respectively). To facilitate visualization, the results were projected onto a biplot representing  
424 the scores (variants) and the loadings (analysed traits) (Figure 9a). The first two principal  
425 components (PC1 and PC2), which together captured 89.9% of the variance, explained the  
426 experimental model almost completely (Supplementary Figure S2). We could see that the trays  
427 with the same variant and time-point were closely located. PC1 accounted for 79.9% of the total  
428 variation, and included almost all the traits and metabolites, except Chl,  $qP$ ,  $\Phi_{(f,D)}$  ( $\Phi_{f,D}$ ), APX,  
429 CAT, Cit and Spd. The accumulation of metabolites was positively correlated with the water  
430 deficit conditions (D) (Figure 9a). In contrast, they showed a negative correlation with the controls  
431 from the water stress and rewatering period, which were positively correlated with the canopy  
432 height, slope, development,  $\Phi_{Po}$  ( $\Phi_{Po}$ ),  $\Phi_{PSII}$  ( $\Phi_{PSII}$ ),  $\Phi_P$  ( $\Phi_P$ ), biomass, leaf length and  
433 width and RWC. PC2 captured an additional 9.7% of the total variance, and was positively  
434 dominated by CAT, Cit and Spd in the rewatered trays (RD) (Figure 9a and b). This analysis  
435 demonstrated the reproducibility of the measurements performed, as the independent trays were  
436 grouped together in all analysed situations. In addition, the separation of the loadings allowed us  
437 to identify possible traits related to water stress and rewatering responses in the barley cultivar  
438 used in this study.

439 Finally, to reduce the number of possible traits observed in the PCA, we performed a linear  
440 correlation across all traits. The outcome helped us to (a) validate our non-invasive method with  
441 other traditionally invasive parameters and metabolites and (b) determine the collinearity among  
442 them for identifying the most representative traits of the water deficit response. For better  
443 visualization of the results, we created a correlation matrix and four scatter plots (Figure 9c and  
444 Supplementary Figures S3-S6). The correlation matrix was constructed based on Pearson  
445 correlation coefficients, which is represented by circles with different intensity colours and sizes,  
446 blue (positive) or red (negative) (Figure 9c). Similarly, we prepared four scatter plot matrices from

447 the most correlated traits that included sloped linear regressions, Pearson correlation coefficients  
448 and significance (Supplementary Figure S3-S6). We found that canopy height had the strongest  
449 positive correlation with aerial biomass and leaf length, with an  $r$  of 0.99 and 0.98 ( $P^{***} \leq 0.001$ ),  
450 respectively (Figure 9c and Supplementary Figure S3). The correlation of canopy height versus  
451 RWC was also positive ( $r = 0.88, P^{**} \leq 0.01$ ), showing that this non-invasive parameter integrated  
452 both the growth and water status of the plants. Canopy height was positively correlated with  $\Phi_{Po}$ ,  
453  $\Phi_{PSII}$  and  $\Phi_P$ , and negatively with  $\Phi_{NPQ}$ , APX and POX, several AAs and PAs, except for Cit and  
454 Spd (Figure 9c and Supplementary Figure S3-S5). Interestingly, these two compounds showed a  
455 very different response compared to the rest of the metabolites and presented a significant  
456 correlation each other ( $r = 0.77, P^* \leq 0.05$ ) (Supplementary Figure S6). Besides, Cit showed linear  
457 correlation with the antioxidant enzyme APX ( $r = 0.72, P^* \leq 0.05$ ). Another phenotype-derived  
458 trait, the slope of the curves, did not show any linear correlation with the morphometric traits  
459 related to canopy height, and was directly correlated with  $\Phi_{PSII}$  ( $r = 0.92, P^{**} \leq 0.01$ ) and inversely  
460 with  $\Phi_{NPQ}$  ( $r = 0.97, P^{***} \leq 0.01$ ) (Supplementary Figure S4). These results suggested that the slope  
461 or plant water turgor was influenced by the light intensity and showed that the side-view traits of  
462 canopy height and slope provided additional useful information for studying and understanding  
463 the water stress response of barley populations. Altogether, we showed that the use of canopy  
464 height and its derived traits are a good approach to analysing the growth and water status of barley  
465 populations and, in combination with other traits such as the fluorescence parameter  $qP$  and the  
466 content of Cad and Cit, it could provide enough information for understanding the water stress  
467 response and recovery capacity in barley plants cultivar Golden Promise.

## 468 Discussion

469 Indoor phenotyping methods enable the evaluation of various traits from a large number of plants  
470 in a fast and non-invasive manner. Routinely, experiments are performed in controlled conditions  
471 mimicking environmental conditions. However, an effective translation of indoor simulations to  
472 what plants experience in the field is not straight-forward because of the complexity and variability  
473 of the field conditions, which complicate data analysis and interpretation (Araus and Cairns, 2014).  
474 As reviewed by Poorter et al. (2016), it is necessary to develop new protocols that can adjust  
475 growth conditions to be closer to field conditions. A common problem is the use of high relative

476 humidity (RH) in protocols for studying water deficit (Junker et al., 2015; Nosalewicz et al., 2016),  
477 whereas in the field water stress is frequently associated with low RH values. We have optimized  
478 our method for studying water deficit in barley at a RH of 40%, which is closer to real conditions  
479 and thus accelerates the stress response. Another limitation in the translation from the laboratory  
480 to the field is the method of growing the plants in different spatial conditions. Indoor phenotyping  
481 traditionally analyses the plant growth in individual pots (Cabrera-Bosquet et al., 2016; Honsdorf  
482 et al., 2014; Poorter et al., 2016), whereas in the field plants grow to form a canopy, competing  
483 with neighbours for above- and below-ground resources. To form the canopy, in our method we  
484 planted 50 barley seedlings in the same plastic container (Figure 1), reaching a final density of 1000  
485 plants  $m^{-2}$  instead of the 20–50 plants  $m^{-2}$  normally used in indoor phenotyping (Poorter et al.,  
486 2016). When plants are grown in individual pots, image analysis allows to dissect plants as  
487 individuals, because they are not masking each other (Chen et al., 2014; Honsdorf et al., 2014).  
488 Plants grown in a dense canopy overlap the leaves making almost impossible to extract projections  
489 of single plants. We overcame this by analysis of whole canopies instead of individuals. Using  
490 side-view RGB images and developing a software routine we can estimate the projected canopy  
491 height of the barley population (Figure 1 and 4). This provided indirect information about several  
492 invasive parameters, such as biomass, leaf length and width and RWC (Figure 9 and  
493 supplementary Figures S3-S6), which are important manually measurements for studying barley  
494 populations in water stress conditions. Chen et al. (2014) previously described a similar  
495 phenotyping setup with a water stress phase followed by a re-watering phase. They also showed  
496 that the plant height was highly correlated with the destructive measured shoot biomass. However,  
497 they evaluated single plants and used very sophisticated and expensive sensors such as FluorCam  
498 and NIR. To our knowledge, our indoor phenotyping approach is the first that uses projected  
499 canopy height in populations, representing overall growth conditions that are more similar to those  
500 that plants experience in the field, especially when compared to single pot-single plant studies.  
501 Besides, we also showed that from each obtained canopy height curve is possible to extract more  
502 traits such as the slope of the obtained line for the water stress and recovery period (Figure 4 and  
503 Table 1). In addition, a simple and cheap RGB camera is enough to analyse the population canopy  
504 height, making this phenotyping method adaptable to other commercial or home-built systems.

505 The reliability and repeatability of the method was validated by two independent experiments  
506 under control conditions (Figure 2), and under water deficit with subsequent rewatering in

507 randomly distributed trays (Figure 3 and Supplementary Figure 1), showing similar behaviours for  
508 45 analysed traits and metabolites (Fig. 3-9). Regarding fluorescence-related traits (Figure 5),  
509 water stress reduced the total Chl content in barley seedlings (Figure 7f) and the maximum  
510 quantum yield in the dark- and light-adapted stages  $\Phi_{P_0}$  and  $\Phi_{PSII}$ , and increased the regulatory and  
511 non-regulatory dissipation processes reflected in  $\Phi_{NPQ}$  and  $\Phi_{(f,D)}$  respectively to ameliorate  
512 photoinhibition and protect the photosynthetic apparatus (Xu et al., 1999). Similar observations  
513 have been reported in many studies of the water stress response of barley (Filek et al., 2015; Li et  
514 al., 2006). However, we observed that whereas some parameters changed in parallel with the  
515 projected canopy height, others changed at a later stage. For example, the decrease in  $\Phi_{PSII}$   
516 happened at the end of the water stress period (Figure 5b), as observed by Berger et al. (2010),  
517 disabling it as a possible marker of early water stress response in barley. However,  $qP$  was a fast  
518 response fluorescence parameter (reduced from day 5) (Figure 5b) and positively correlated to Chl  
519 (Supplementary Figure S3). Optimal utilization of photochemical energy in carbon metabolism is  
520 characterised by high  $qP$  values. When light absorption exceeded the requirement by carbon  
521 metabolism, the  $qP$  declines. Thus, it serves as a good indicator of “light stress” (Gallé and Flexas,  
522 2010). However, the fluctuations of this parameter has been described as cultivar dependent at  
523 least in wheat (Wang et al., 2016). Altogether, these results suggested that under our growth  
524 conditions the water stressed plants might suffer photoinhibition and that  $qP$  could be a good trait  
525 for estimating the photosynthetic status of barley plants during water stress conditions and  
526 subsequent recovery.

527 Water deficit increases the production of reactive oxygen species (ROS) in plants that stimulate  
528 antioxidant enzymes to counteract the oxidative damage and detoxify ROS. Similarly, in our work  
529 the barley seedlings increased the antioxidant enzyme activity of CAT and POX in stressed plants  
530 compared with the controls (Figure 7g,h). However, APX only increased significantly after the  
531 rewatering. It has been described that APX enhanced tolerance under water deficit in many plant  
532 species, but the increased expression of APXs varied in different developmental stages, among  
533 species and type of stress (reviewed by Pandey et al., 2017). Another study demonstrated that a  
534 simple pre-treatment with a stressor can induce an increase in the activity of this enzyme,  
535 protecting the plants against future stress events, process traditionally called hardening (Hsu and  
536 Kao, 2007). These assumptions suggested that the high APX activity in the stressed plants after

537 recovery could be related to the developmental stage (4<sup>th</sup> leaf, Figure 4) and/or a fast mechanism  
538 to reduce ROS.

539 Another strategy of plants to cope with drought-induced stress is the synthesis and/or accumulation  
540 of compatible solutes (e.g. amino acids), which can be involved in ROS scavenging and/or perform  
541 as signal molecules (Urano et al., 2010). As revealed by metabolite profiling, most of the AAs  
542 accumulated in barley under water stress conditions (Figure 8a), especially Pro and OH-Pro. Pro  
543 was described in 1972 (Singh et al., 1972) as a useful marker for screening the physiological status  
544 of plants grown under water deficit conditions. In our work, even when the rewatered plants  
545 recovered their RWC, they maintained both Pro and OH-Pro levels above the control values  
546 (Figure 8b). This was already described in barley (Reddy et al., 2004), as well as in other species  
547 (De Diego et al., 2013; Zhang et al., 2018). It is worth mentioning that Cit was the only AA that  
548 kept increased levels after rewatering (Figure 8). Although there are only few works reporting the  
549 possible role of Cit in the plant stress response, Akashi et al. (2001) demonstrated that Cit was  
550 more effective hydroxyl radical scavenger than other compatible solutes such as Pro or Mannitol  
551 and it can effectively protect DNA and enzymes from oxidative injuries. Thus, Cit could accelerate  
552 the recovery of the stressed plants by reducing the stress-induced oxidative damage, being an  
553 interesting metabolite for evaluating acclimation to water stress in barley (Figure 9a).

554 Regarding PAs, Put, Spd and Spm are usually accumulated under stress conditions (Podlešáková  
555 et al., 2019). However, in our study Cad, DAP and Tyra were the major contributors to the water  
556 stress response and recovery in barley (Figure 8). In fact, DAP and Tyra remained at higher levels  
557 in the stressed plants even after rewatering. The conversion of Spd to DAP is a stress response that  
558 can control ROS (Bitrián et al., 2012; Liu et al., 2015). DAP accumulation during water deficit  
559 and recovery could also be a mechanism for modulating membrane electrical and ion  
560 transportation properties and for controlling stomata closure, counteracting the action of ABA  
561 (Jammes et al., 2014). Cad is synthesized by an independent pathway through lysine catabolism,  
562 and its accumulation has been reported in other species under stress conditions (Jancewicz et al.,  
563 2016). Although the role of Cad in the stress response is still unclear, it has been recently shown  
564 that Cad displays anti-senescence activity (Tomar et al., 2013), suggesting that it is another  
565 important ROS-modulating compound and possible plant growth regulator (Jancewicz et al.,  
566 2016). Concerning Tyra, there are few studies showing its accumulation in plants under stress

567 (Aziz et al., 1999; Lehmann and Pollmann, 2009). Aziz et al. (1998) have shown that Tyra can  
568 regulate Pro production. In our study highly significant correlations ( $P^{***} \leq 0.001$ ) existed between  
569 Put, DAP, Tyra or Cad and Pro (Supplementary Figure S6), result that supported the existence of  
570 a relevant crosstalk between PAs and Pro regulating plant stress response (Podlešáková et al.,  
571 2019). In addition, the results obtained in correlation matrix suggested that quantification of either  
572 PAs or AAs might be enough to characterize the level of stress in this barley genotype under water  
573 stress and recovery.

574 In conclusion, we have designed, optimized and validated a non-invasive image-based method for  
575 automated high-throughput screening of potential water stress tolerance phenotypes using  
576 projected canopy height in barley (An additional movie file shows this in more detail [see  
577 Supplementary File 1]). Using multivariate statistical methods we have also identified new  
578 metabolites involved in stress response and recovery using a highly tolerant cultivar. As shown  
579 here, projected canopy height is sensitive trait that truly reflects other studied morphological and  
580 physiological parameters and metabolites. It represents very informative, simple and robust trait  
581 that does not require expensive sensor and hence is suitable to be used in low-cost systems using  
582 single RGB imaging. It can be also seen as easy-to-understand and self-speaking trait, since the  
583 reduction of plant growth and loss of turgor are traditionally traits to characterize the water stress  
584 response of the plants. Besides, we demonstrated that the simple analysis of canopy height  
585 combined with quantification of AAs or PAs bring enough data to define the plant stress strategy .  
586 For this reason, our method can be used to study the mechanisms involved in the water deficit  
587 response and recovery capacity of crops such as barley. We believe that it has high potential to be  
588 integrated into breeding programmes for fast screening and identification of stress-tolerant  
589 genotypes under different individual or combined stresses and/or the identification and testing of  
590 priming agents with potential to mitigate the adverse stress effects.

## 591 **Acknowledgements**

592 This work was funded by the Ministry of Education, Youth and Sports of the Czech Republic  
593 (Grant LO1204 from the National Program of Sustainability), the ERDF project "Plants as a tool  
594 for sustainable global development" (No. CZ.02.1.01/0.0/0.0/16\_019/0000827) and the Internal  
595 Grant Agency of Palacký University (IGA\_PrF\_2018\_023). The authors thank to Dušan Lazár for

596 expert help to optimize the chlorophyll fluorescence imaging protocol and Sees-editing Ltd for  
597 correcting the English.

## 598 **Author Contribution**

599 CFM, LU, JFH, LS and NDD designed the experiments. CFM and LU performed the experiments.  
600 JFH performed the protocol for automated phenotyping, image-processing and image-based data  
601 analysis. TF developed the software routine for projected canopy height. MP and NDD performed  
602 the statistical analysis of the data, KP and NDD performed the metabolite quantification. NDD  
603 and LS supervised the study and formulated the concept of the project. All authors discussed the  
604 results. CFM, NDD and LS wrote the manuscript.

## 605 **References**

606 Aebi, H. (1984). Catalase in Vitro. *Methods Enzymol.* 105, 121–126.

607 Ahmed, I. M., Dai, H., Zheng, W., Cao, F., Zhang, G., Sun, D., et al. (2013). Genotypic  
608 differences in physiological characteristics in the tolerance to drought and salinity combined  
609 stress between Tibetan wild and cultivated barley. *Plant Physiol. Biochem.* 63, 49–60.  
610 doi:10.1016/j.plaphy.2012.11.004.

611 Akashi, K., Miyake, C., and Yokota, A. (2001). Citrulline, a novel compatible solute in drought-  
612 tolerant wild watermelon leaves, is an efficient hydroxyl radical scavenger. *FEBS Lett.* 508,  
613 438–442. doi:10.1016/S0014-5793(01)03123-4.

614 Araus, J. L., and Cairns, J. E. (2014). Field high-throughput phenotyping: The new crop breeding  
615 frontier. *Trends Plant Sci.* 19, 52–61. doi:10.1016/j.tplants.2013.09.008.

616 Awlia, M., Nigro, A., Fajkus, J., Schmoeckel, S. M., Negrão, S., Santelia, D., et al. (2016). High-  
617 throughput non-destructive phenotyping of traits that contribute to salinity tolerance in  
618 *Arabidopsis thaliana*. *Front. Plant Sci.* 7, 1–15. doi:10.3389/fpls.2016.01414.

619 Aziz, A., Martin-Tanguy, J., and Larher, F. (1998). Stress-induced changes in polyamine and  
620 tyramine levels can regulate proline accumulation in tomato leaf discs treated with sodium

621 chloride. *Physiol. Plant.* 104, 195–202. doi:10.1034/j.1399-3054.1998.1040207.x.

622 Aziz, A., Martin-Tanguy, J., and Larher, F. (1999). Salt stress-induced proline accumulation and  
623 changes in tyramine and polyamine levels are linked to ionic adjustment in tomato leaf  
624 discs. *Plant Sci.* 145, 83–91. doi:10.1016/S0168-9452(99)00071-0.

625 Berger, B., Parent, B., and Tester, M. (2010). High-throughput shoot imaging to study drought  
626 responses. *J. Exp. Bot.* 61, 3519–3528. doi:10.1093/jxb/erq201.

627 Bitrián, M., Zarza, X., Altabella, T., Tiburcio, A. F., and Alcázar, R. (2012). Polyamines under  
628 abiotic stress: metabolic crossroads and hormonal crosstalks in plants. *Metabolites* 2, 516–  
629 528. doi:10.3390/metabo2030516.

630 Bradford, M. M. (1976). A rapid and sensitive method for the quantitation of microgram  
631 quantities of protein utilizing the principle of protein-dye binding. *Anal. Biochem.* 72, 248–  
632 254. doi:10.1016/0003-2697(76)90527-3.

633 Cabrera-Bosquet, L., Fournier, C., Brichet, N., Welcker, C., Suard, B., and Tardieu, F. (2016).  
634 High-throughput estimation of incident light, light interception and radiation-use efficiency  
635 of thousands of plants in a phenotyping platform. *New Phytol.* 212, 269–281.  
636 doi:10.1111/nph.14027.

637 Chen, D., Neumann, K., Friedel, S., Kilian, B., Chen, M., Altmann, T., et al. (2014). Dissecting  
638 the phenotypic components of crop plant growth and drought responses based on high-  
639 throughput image analysis. *Plant Cell Online.* doi:10.1105/tpc.114.129601.

640 De Diego, N., Fürst, T., Humplík, J. F., Ugena, L., Podlešáková, K., and Spíchal, L. (2017). An  
641 automated method for high-throughput screening of *Arabidopsis* rosette growth in multi-  
642 well plates and its validation in stress conditions. *Front. Plant Sci.* 8, 1–16.  
643 doi:10.3389/fpls.2017.01702.

644 De Diego, N., Saiz-Fernández, I., Rodríguez, J. L., Pérez-Alfocea, P., Sampedro, M. C., Barrio,  
645 R. J., et al. (2015). Metabolites and hormones are involved in the intraspecific variability of  
646 drought hardening in radiata pine. *J. Plant Physiol.* 188, 64–71.  
647 doi:10.1016/j.jplph.2015.08.006.



648 De Diego, N., Sampedro, M. C., Barrio, R. J., Saiz-Fernandez, I., Moncalean, P., and Lacuesta,  
649 M. (2013). Solute accumulation and elastic modulus changes in six radiata pine breeds  
650 exposed to drought. *Tree Physiol.* 33, 69–80. doi:10.1093/treephys/tps125.

651 Earth Observation and Research Branch Team (2011). Crop Identification and BBCH Staging  
652 Manual: SMAP-12 Field Campaign.

653 Filek, M., Labanowska, M., Kościelniak, J., Biesaga-Kościelniak, J., Kurdziel, M., Szarejko, I.,  
654 et al. (2015). Characterization of barley leaf tolerance to drought stress by chlorophyll  
655 fluorescence and electron paramagnetic resonance studies. *J. Agron. Crop Sci.* 201, 228–  
656 240. doi:10.1111/jac.12063.

657 Forster, B. P., Ellis, R. P., Thomas, W. T. B., Newton, A. C., Tuberosa, R., This, D., et al.  
658 (2000). The development and application of molecular markers for abiotic stress tolerance  
659 in barley. *J. Exp. Bot.* 51, 19–27. doi:10.1093/jxb/51.342.19.

660 Gallé, A., and Flexas, J. (2010). “Gas-Exchange and Chlorophyll Fluorescence Measurements in  
661 Grapevine Leaves in the Field,” in *Methodologies and Results in Grapevine Research*, eds.  
662 S. Delrot, H. Medrano, E. Or, L. Bavaresco, and S. Grando (Dordrecht: Springer  
663 Netherlands), 107–121. doi:10.1007/978-90-481-9283-0\_8.

664 Ghanem, M. E., Marrou, H., and Sinclair, T. R. (2015). Physiological phenotyping of plants for  
665 crop improvement. *Trends Plant Sci.* 20, 139–144. doi:10.1016/j.tplants.2014.11.006.

666 Granier, C., Aguirrezabal, L., Chenu, K., Cookson, S. J., Dautzat, M., Hamard, P., et al. (2006).  
667 PHENOPSIS, an automated platform for reproducible phenotyping of plant responses to  
668 soil water deficit in *Arabidopsis thaliana* permitted the identification of an accession with  
669 low sensitivity to soil water deficit. *New Phytol.* 169, 623–635.

670 Gray, N., and Plumb, R. (2016). A validated assay for the quantification of amino acids in  
671 mammalian urine. *Waters*, 1–8.

672 Großkinsky, D. K., Svensgaard, J., Christensen, S., and Roitsch, T. (2015). Plant phenomics and  
673 the need for physiological phenotyping across scales to narrow the genotype-to-phenotype  
674 knowledge gap. *J. Exp. Bot.* 66, 5429–5440. doi:10.1093/jxb/erv345.

675 Honsdorf, N., March, T. J., Berger, B., Tester, M., and Pillen, K. (2014). High-throughput  
676 phenotyping to detect drought tolerance QTL in wild barley introgression lines. *PLoS One*  
677 9. doi:10.1371/journal.pone.0097047.

678 Hsu, Y. T., and Kao, C. H. (2007). Heat shock-mediated H<sub>2</sub>O<sub>2</sub> accumulation and protection  
679 against Cd toxicity in rice seedlings. *Plant Soil* 300, 137–147. doi:10.1007/s11104-007-  
680 9396-0.

681 Humplík, J. F., Lazár, D., Husičková, A., and Spíchal, L. (2015). Automated phenotyping of  
682 plant shoots using imaging methods for analysis of plant stress responses -- a review. *Plant*  
683 *Methods* 11, 29. doi:10.1186/s13007-015-0072-8.

684 Jammes, F., Leonhardt, N., Tran, D., Bousserouel, H., Véry, A. A., Renou, J. P., et al. (2014).  
685 Acetylated 1,3-diaminopropane antagonizes abscisic acid-mediated stomatal closing in  
686 *Arabidopsis*. *Plant J.* 79, 322–333. doi:10.1111/tpj.12564.

687 Jancewicz, A. L., Gibbs, N. M., and Masson, P. H. (2016). Cadaverine's functional role in plant  
688 development and environmental response. *Front. Plant Sci.* 7, 1–8.  
689 doi:10.3389/fpls.2016.00870.

690 Junker, A., Muraya, M. M., Weigelt-Fischer, K., Arana-Ceballos, F., Klukas, C., Melchinger, A.  
691 E., et al. (2015). Optimizing experimental procedures for quantitative evaluation of crop  
692 plant performance in high throughput phenotyping systems. *Front. Plant Sci.* 5, 1–21.  
693 doi:10.3389/fpls.2014.00770.

694 Lehmann, T., and Pollmann, S. (2009). Gene expression and characterization of a stress-induced  
695 tyrosine decarboxylase from *Arabidopsis thaliana*. *FEBS Lett.* 583, 1895–1900.  
696 doi:10.1016/j.febslet.2009.05.017.

697 Li, R., Guo, P., Baum, M., Grando, S., and Ceccarelli, S. (2006). Evaluation of chlorophyll  
698 content and fluorescence parameters as indicators of drought tolerance in barley. *Agric. Sci.*  
699 *China* 5, 751–757. doi:10.1016/S1671-2927(06)60120-X.

700 Liu, J.-H., Wang, W., Wu, H., Gong, X., and Moriguchi, T. (2015). Polyamines function in stress  
701 tolerance: from synthesis to regulation. *Front. Plant Sci.* 6, 1–10.

702 doi:10.3389/fpls.2015.00827.

703 Malec, P. A., Oteri, M., Inferrera, V., Cacciola, F., Mondello, L., and Kennedy, R. T. (2017).  
704 Determination of amines and phenolic acids in wine with benzoyl chloride derivatization  
705 and liquid chromatography-mass spectrometry. *J. Chromatogr. A*.  
706 doi:10.1016/j.chroma.2017.07.061.

707 Muscolo, A., Junker, A., Klukas, C., Weigelt-Fischer, K., Riewe, D., and Altmann, T. (2015).  
708 Phenotypic and metabolic responses to drought and salinity of four contrasting lentil  
709 accessions. *J. Exp. Bot.* 66, 5467–5480. doi:10.1093/jxb/erv208.

710 Nosalewicz, A., Siecińska, J., Śmiech, M., Nosalewicz, M., Wiącek, D., Pecio, A., et al. (2016).  
711 Transgenerational effects of temporal drought stress on spring barley morphology and  
712 functioning. *Environ. Exp. Bot.* 131, 120–127. doi:10.1016/j.envexpbot.2016.07.006.

713 Pandey, S., Fartyal, D., Agarwal, A., Shukla, T., James, D., Kaul, T., et al. (2017). Abiotic stress  
714 tolerance in plants: myriad roles of ascorbate peroxidase. *Front. Plant Sci.* 8, 1–13.  
715 doi:10.3389/fpls.2017.00581.

716 Podlešáková, K., Ugena, L., Spíchal, L., Doležal, K., and De Diego, N. (2019). Phytohormones  
717 and polyamines regulate plant stress responses by altering GABA pathway. *N. Biotechnol.*  
718 48, 53–65. doi:10.1016/j.nbt.2018.07.003.

719 Poorter, H., Fiorani, F., Pieruschka, R., Wojciechowski, T., van der Putten, W. H., Kleyer, M., et  
720 al. (2016). Pampered inside, pestered outside? Differences and similarities between plants  
721 growing in controlled conditions and in the field. *New Phytol.* 212, 838–855.  
722 doi:10.1111/nph.14243.

723 Prochazkova, D., Sairam, R. K., Srivastava, G. C., and Singh, D. V. (2001). Oxidative stress and  
724 antioxidant activity as the basis of senescence in maize leaves. *Plant Sci.* 161, 765–771.  
725 doi:10.1016/S0168-9452(01)00462-9.

726 Reddy, A. R., Chaitanya, K. V., and Vivekanandan, M. (2004). Drought-induced responses of  
727 photosynthesis and antioxidant metabolism in higher plants. *J. Plant Physiol.* 161, 1189–  
728 1202. doi:10.1016/j.jplph.2004.01.013.

- 729 Saade, S., Negrão, S., Plett, D., Garnett, T., and Tester, M. (2018). *The Barley Genome*. , eds. N.  
730 Stein and G. J. Muehlbauer Cham: Springer International Publishing doi:10.1007/978-3-  
731 319-92528-8.
- 732 Singh, T. N., Aspinall, D., and Paleg, L. G. (1972). Proline accumulation and varietal  
733 adaptability to drought in barley: a potential metabolic measure of drought resistance.  
734 *Nature* 236, 188–189.
- 735 Thomas, W. T. B., Powell, W., and Wood, W. (1984). The chromosomal location of the  
736 dwarfing gene present in the spring barley variety golden promise. *Heredity (Edinb)*. 53,  
737 177–183. doi:10.1038/hdy.1984.73.
- 738 Tomar, P. C., Lakra, N., and Mishra, S. N. (2013). Cadaverine: A lysine catabolite involved in  
739 plant growth and development. *Plant Signal. Behav.* 8. doi:10.4161/psb.25850.
- 740 Urano, K., Kurihara, Y., Seki, M., and Shinozaki, K. (2010). “Omics” analyses of regulatory  
741 networks in plant abiotic stress responses. *Curr. Opin. Plant Biol.* 13, 132–138.  
742 doi:10.1016/j.pbi.2009.12.006.
- 743 Wang, W., Vinocur, B., and Altman, A. (2003). Plant responses to drought, salinity and extreme  
744 temperatures: Towards genetic engineering for stress tolerance. *Planta* 218, 1–14.  
745 doi:10.1007/s00425-003-1105-5.
- 746 Wang, X., Wang, L., and Shanguan, Z. (2016). Leaf gas exchange and fluorescence of two  
747 winter wheat varieties in response to drought stress and nitrogen supply. *PLoS One* 11, 1–  
748 15. doi:10.1371/journal.pone.0165733.
- 749 Xu, C. C., Jeon, Y. A., and Lee, C. H. (1999). Relative contributions of photochemical and non-  
750 photochemical routes to excitation energy dissipation in rice and barley illuminated at a  
751 chilling temperature. *Physiol. Plant.* 107, 447–453. doi:10.1034/j.1399-  
752 3054.1999.100411.x.
- 753 Zhang, S. han, Xu, X. feng, Sun, Y. min, Zhang, J. lian, and Li, C. (2018). Influence of drought  
754 hardening on the resistance physiology of potato seedlings under drought stress. *J. Integr.*  
755 *Agric.* 17, 336–347. doi:10.1016/S2095-3119(17)61758-1.

In review

**Table 1| Traits related to water deficit and recovery.** Traits were extracted from the linear regression of the canopy height in two **randomly selected trays**. **Day** is the day when treated and not treated plants are different; **Max** is the maximal canopy height reached in the stressed plants under drought; **min** is the minimal canopy height at the end of the drought period; **Slope** of the linear curve from the canopy height in the drought period; **MaxR** is the maximal canopy height reached in the stressed plants after rewatering; and **SlopeR** of the linear curve from the canopy height in the rewatering period.

	Water stress				Rewatering	
	Day	Max	min	Slope	MaxR	SlopeR
<b>Tray 1</b>	8	1041	680	-69.514	1218	153.2
<b>Tray 2</b>	8	1018	707	-71.429	1136	148

In review

## FIGURE LEGENDS

**Figure 1| Scheme of the protocol used for non-invasive phenotyping of barley (*Hordeum vulgare*) seedlings growing under water stress conditions.** (a) Barley seeds were germinated on filter paper and 50 seedlings of similar radicle size were transplanted into soil in standardized PlantScreen™ measuring trays. (b) The trays were transferred to an XYZ PlantScreen™ chamber with a conveyor system for automatic image acquisition. (c) The canopy height was analysed using an in-house software routine implemented in MatLab R2015, and the data were evaluated by multivariate statistical analyses using Python version 3.6.5 and R version 3.5.1.

**Figure 2| Analysis of the reproducibility of canopy height estimation in barley (*Hordeum vulgare*) seedlings from two independent experiments.** (a) The reproducibility of projected canopy height dynamics (in pixels) in barley seedlings (n = 100) grown under control conditions in December 2017 and July 2018. (b) The correlation between canopy height and fresh aerial biomass (g) (n = 5) determined for replicates measured at day 16 and day 19 in barley seedlings from the two independent experiments. The regression curve and significance calculated from three independent trays is shown. \*\*\* $P \leq 0.001$ .

**Figure 3| Dynamics of soil moisture and projected canopy height in barley seedlings growing under water stress conditions with subsequent rewatering.** (a) Changes in substrate water content (%) of non-stressed (W, continuous lines) and stressed (D, discontinuous lines) barley seedlings (n = 50) from three independent trays (Barley 1, 2 and 3) grown for 13 days under water deficit conditions (with the endpoint at day 16) and subsequently rewatered for 4 days (with the endpoint at day 19). The watering regime consisted in an initial 100% field capacity (FC) after sowing and subsequent constant 80% FC for W variants, and irrigation interruption from day 3 to day 16 for the D variants and posterior rewatering for 4 days. Blue arrows represent the watering regime and red arrow the stop of the irrigation moment in the D variant. (b) Changes in projected canopy height (in pixels) and (c) side view images of the D and W variants from the three independent replicates along the experiment.

**Figure 4| Linear curve of the projected canopy height and the extracted traits.** (a) The average canopy height, regression curve and significance calculated from three independent trays (with 50 plants each) growing under water deficit conditions for 13 days (with the endpoint at day 16) and with subsequent rewatering for 4 days (with the endpoint at day 19). (b) Max is the maximum and Min the minimum canopy height reached by the stressed plants from replicate 1 or 2 (n = 50) under

water deficit conditions, and the slope of the linear model curve is shown. (c) MaxR is the maximum canopy height from replicate 1 or 2 ( $n = 50$ ) attained after 4 days of rewatering, and the slope of the line (SlopeR) is also shown in the equation.

**Figure 5| Variation in chlorophyll parameters in barley (*Hordeum vulgare*) seedlings grown under water stress conditions and after subsequent rewatering.** (a) Imaging of chlorophyll fluorescence ( $\Phi_{P_0}$  and  $\Phi_{PII}$ ) in barley seedlings under well-water, water stress, and rewatering. Stressed and non-stressed plants labelled as D (left) and W (right), respectively. (b) Chlorophyll fluorescence parameters from three independent trays (Barley 1, 2 and 3) ( $n = 50$ ) and the average values. D and W variants are represented by discontinuous and continuous lines, respectively. Statistical analyses were performed via ANOVA. Asterisks indicate the significance level relative to the control variant; \*  $P \leq 0.05$ ; \*\*  $P \leq 0.01$ ; \*\*\*  $P \leq 0.001$ ; ns, not significant.

**Figure 6| Developmental stages of barley seedlings (*Hordeum vulgare*) under water stress and after subsequent rewatering.** Developmental stages of leaves in stressed (D) and non-stressed (W) plants from two independent trays (1 or 2) at the end of the water stress period ( $n = 8$ ) (a) and after rewatering ( $n=5$ ) (b).

**Figure 7| Morphometric and physiological changes in barley (*Hordeum vulgare*) seedlings under water stress conditions and after subsequent rewatering.** (a) Aerial biomass (FW, g), (b) leaf length (cm) and (c) width (cm) of the last fully expanded (FE) leaf, (d) the ratio between length and width, (e) the relative water content (%), (f) the index of the chlorophyll content, and the activity of the antioxidative enzymes (g) guaiacol peroxidase (POX), (h) catalase (CAT) and (i) ascorbate peroxidase (APX), in stressed (D, colour bars) and non-stressed (W, black bars) barley seedlings from two independent trays at the end of the water stress period ( $n=8$ ) and after subsequent rewatering. ( $n=5$ ). Three independent pools containing 5 plants each were used for the quantification of the antioxidant enzyme activity. Different letters mean significant differences according to Tukey HSD test after ANOVA.

**Figure 8| Metabolic profiles of barley (*Hordeum vulgare*) seedlings under water deficit and after subsequent rewatering.** Fold changes (presented as  $\log_2$  ratio) in the content ( $\text{pmol mg}^{-1}$  DW) of free polyamines (Pas) and amino acids (AAs) between stressed (D) and non-stressed (W) barley seedlings (three independent pools containing 5 plants from two independent trays,  $n= 6$ ) at the end of the stress period (red bars) and after subsequent rewatering (gray bars).

**Figure 9| Multivariate statistical analyses of the traits in barley (*Hordeum vulgare*) seedlings**



**related to the water stress response and subsequent rewatering.** (a) Principal component analysis (PCA) (b) contribution of the loadings to each PCA (Dim) and (c) a correlation matrix of 45 traits obtained from two different trays of barley seedlings at the end of the water stress period and after subsequent rewatering.

## SUPPLEMENTARY MATERIAL

**Supplementary Table S1**| Scheme of the three performed experiments

**Supplementary Table S2**| Dynamics of canopy height of barley (*Hordeum vulgare*) seedlings grown under drought conditions. Fold changes ( $\log_2$ ) of the canopy height (pixels) of seedlings grown under stressed conditions for 12 days (endpoint day 15) compared with their respective controls, from five independent trays. Asterisks and ns indicate the level of significance between stressed and non-stressed plants according to ANOVA ( $n = 50$ ); \*  $P \leq 0.05$ ; \*\*  $P \leq 0.01$ ; \*\*\*  $P \leq 0.001$ ; ns, not significant

**Supplementary Table S3**| Statistical analysis of several traits measured in barley seedlings at the end of the water stress period and after rewatering using two-way ANOVA (Tray and Treatment). \*  $P \leq 0.05$ ; \*\*  $P \leq 0.01$ ; \*\*\*  $P \leq 0.001$

**Supplementary Table S4**| Statistical analysis of free AAs and PAs measured in barley seedlings at the end of the water stress period and after rewatering using one-way ANOVA. \*  $P \leq 0.05$ ; \*\*  $P \leq 0.01$ ; \*\*\*  $P \leq 0.001$

**Supplementary Figure S1**| Analysis of reproducibility of canopy height estimation in barley (*Hordeum vulgare*) seedling under water deficit conditions within experimental replicates. Changes in canopy height (in pixels) of stressed (D, discontinuous lines) or non-stressed (W, continuous lines) barley seedlings ( $n=50$ ) from five independent trays grown for 12 days (with the endpoint at day 15)

**Supplementary Figure S2**| Scree plot representing the percentage of explained variance of the model of each PCA (Dimension) performed in R3.5.1

**Supplementary Figure S3**| Scatter plots of the correlation between canopy height, slope, morphometric parameters, RWC (%), chl and fluoresce related traits undertaken in R3.5.1.

**Supplementary Figure S4** | Scatter plots of the correlation between canopy height, slope, the activity of CAT, POX and APX, and some AAs undertaken in R3.5.1

**Supplementary Figure S5** | Scatter plots of the correlation between canopy height, slope and some AAs and PAS undertaken in R3.5.1

**Supplementary Figure S6** | Scatter plots of the correlation between the activity of CAT, POX and APX, Pro, OH-Pro, GABA, Arg, Glu, Cit and PAS undertaken in R3.5.1

**Supplementary File S1** | Movie file of the projected canopy height in barley seedlings growing under water stress conditions with subsequent rewatering.

In review

Figure 1.JPEG

**a) Material preparation**

**DAY 1- Stratification**



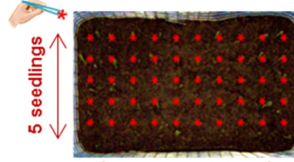
48 h at 4°C in dark

**DAY 3- Germination**



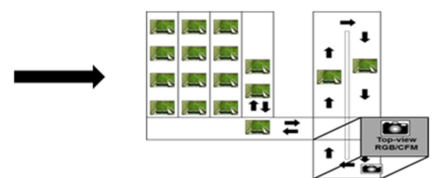
48 h at 22/20 °C, 16/8 h (light/dark cycle)  
320 μmol PAR m<sup>-2</sup> s<sup>-1</sup>

**DAY 5-23 Transferred seedlings into the conveyor PlantScreening™ system**

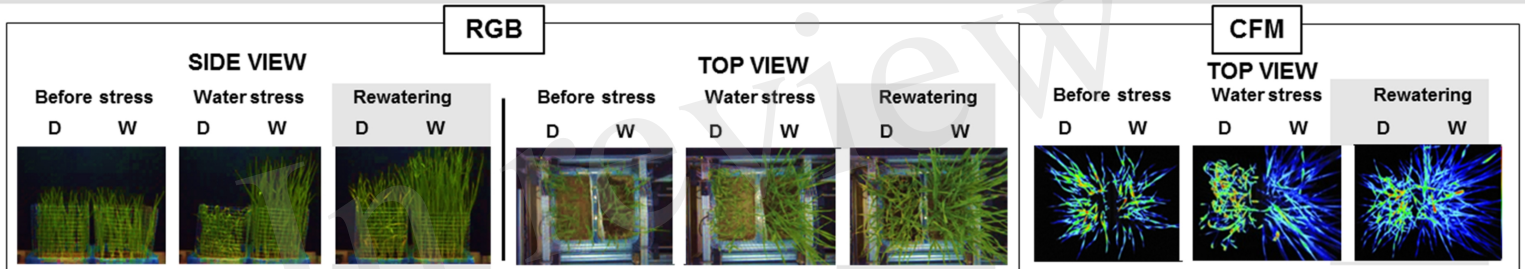


5 seedlings

10 seedlings

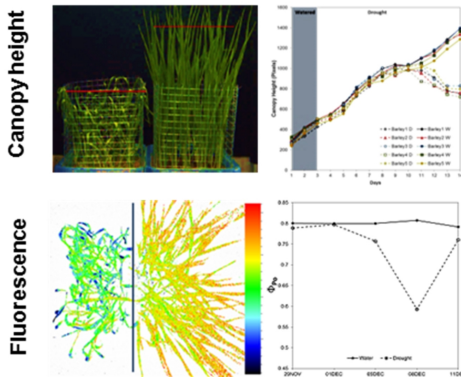


**b) Image acquisition**

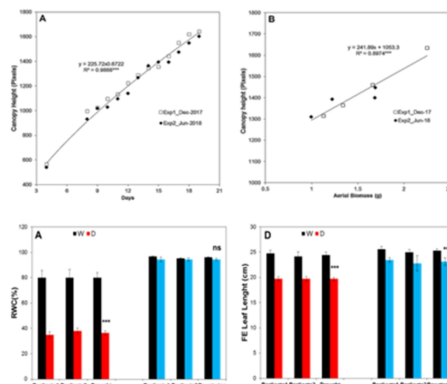


**c) Data analysis**

**IMAGE PROCESSING**



**VALIDATION**



**DATA INTERPRETATION**

*multivariate data analysis*

Linear correlation  
PC analysis

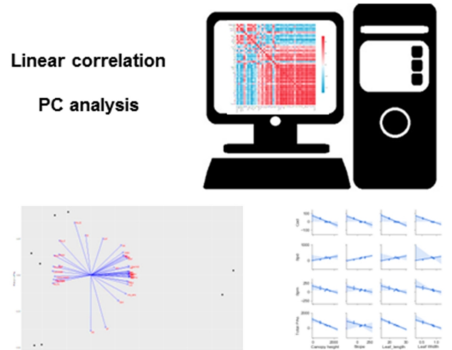


Figure 2.TIF

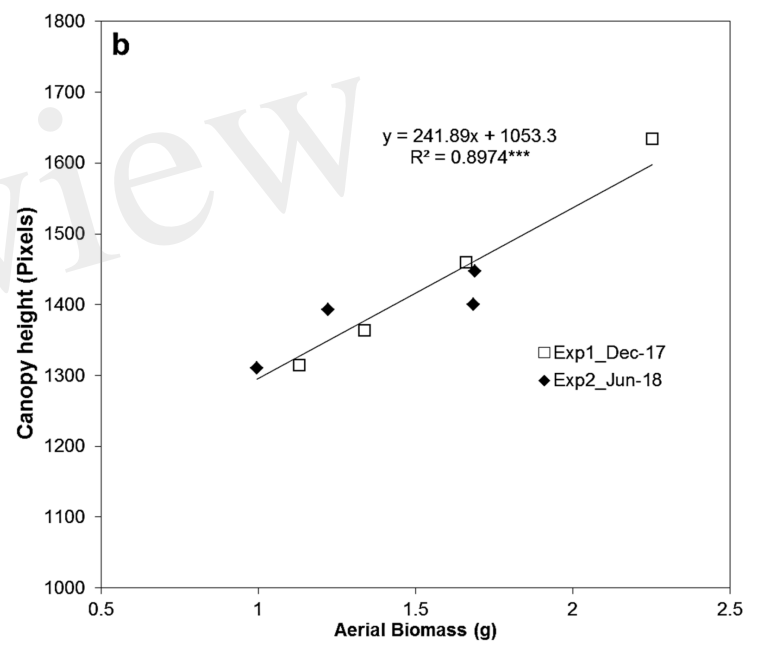
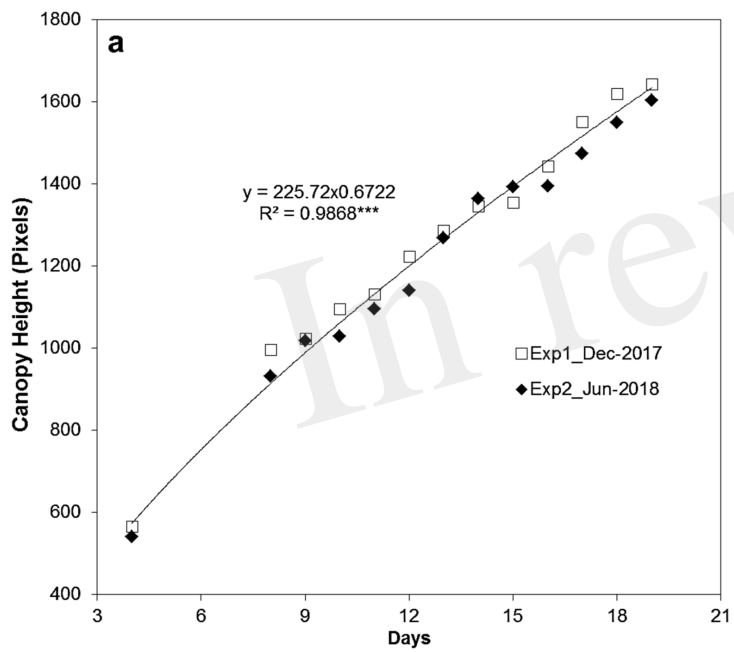


Figure 3.JPEG

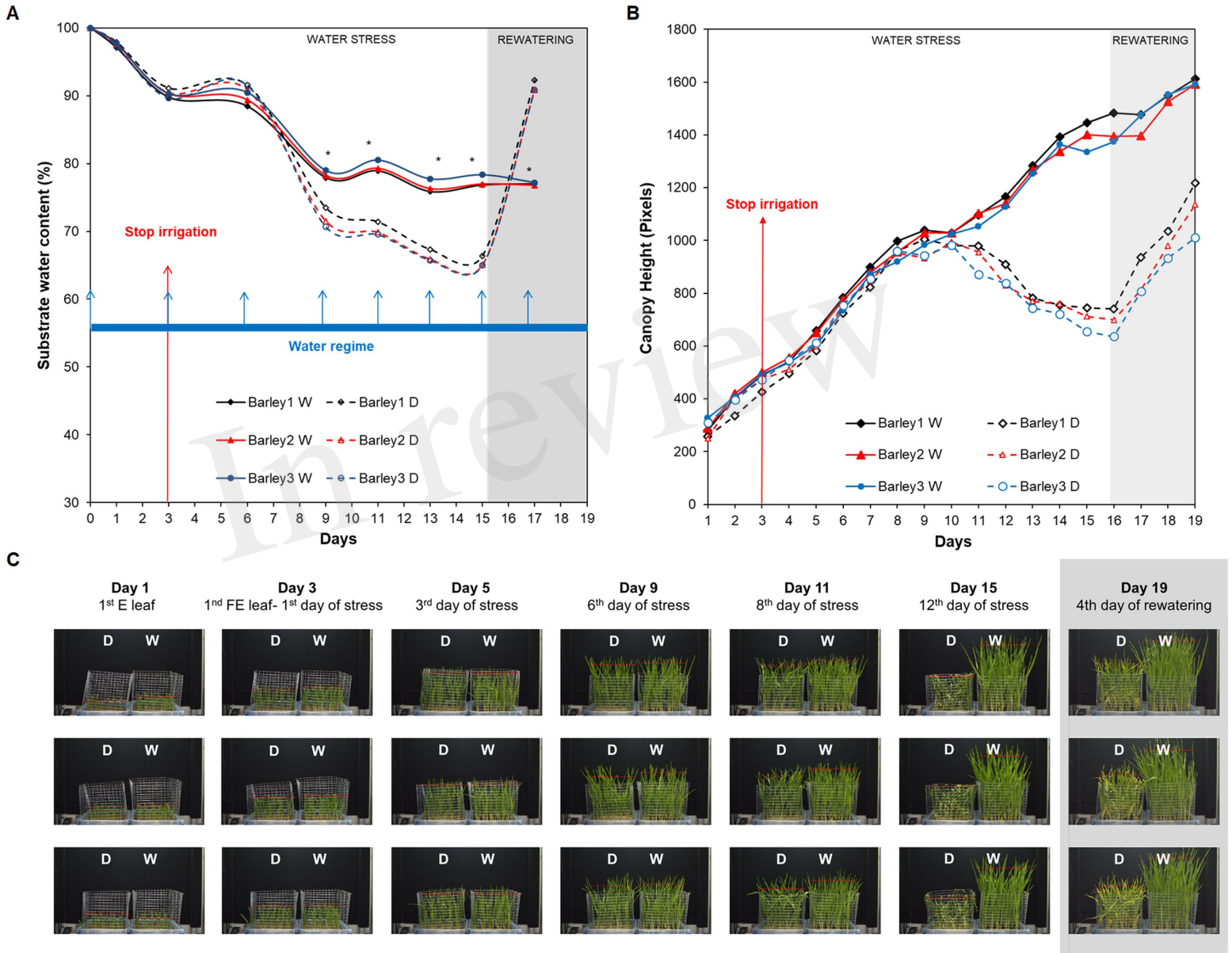


Figure 4.TIF

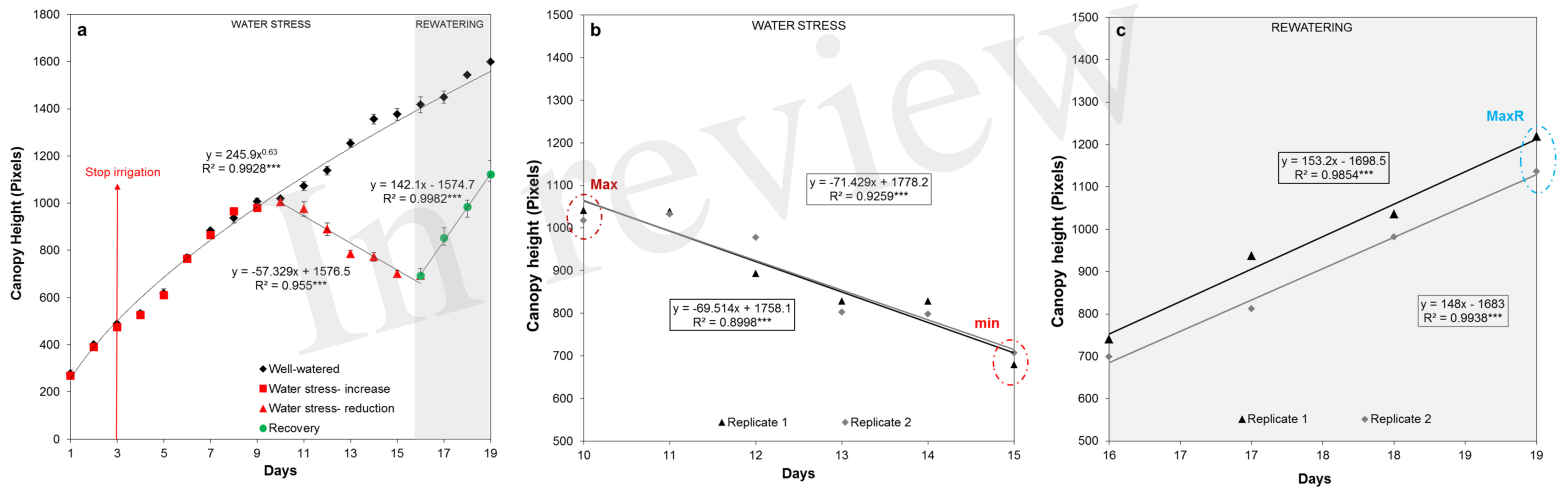


Figure 5.JPEG

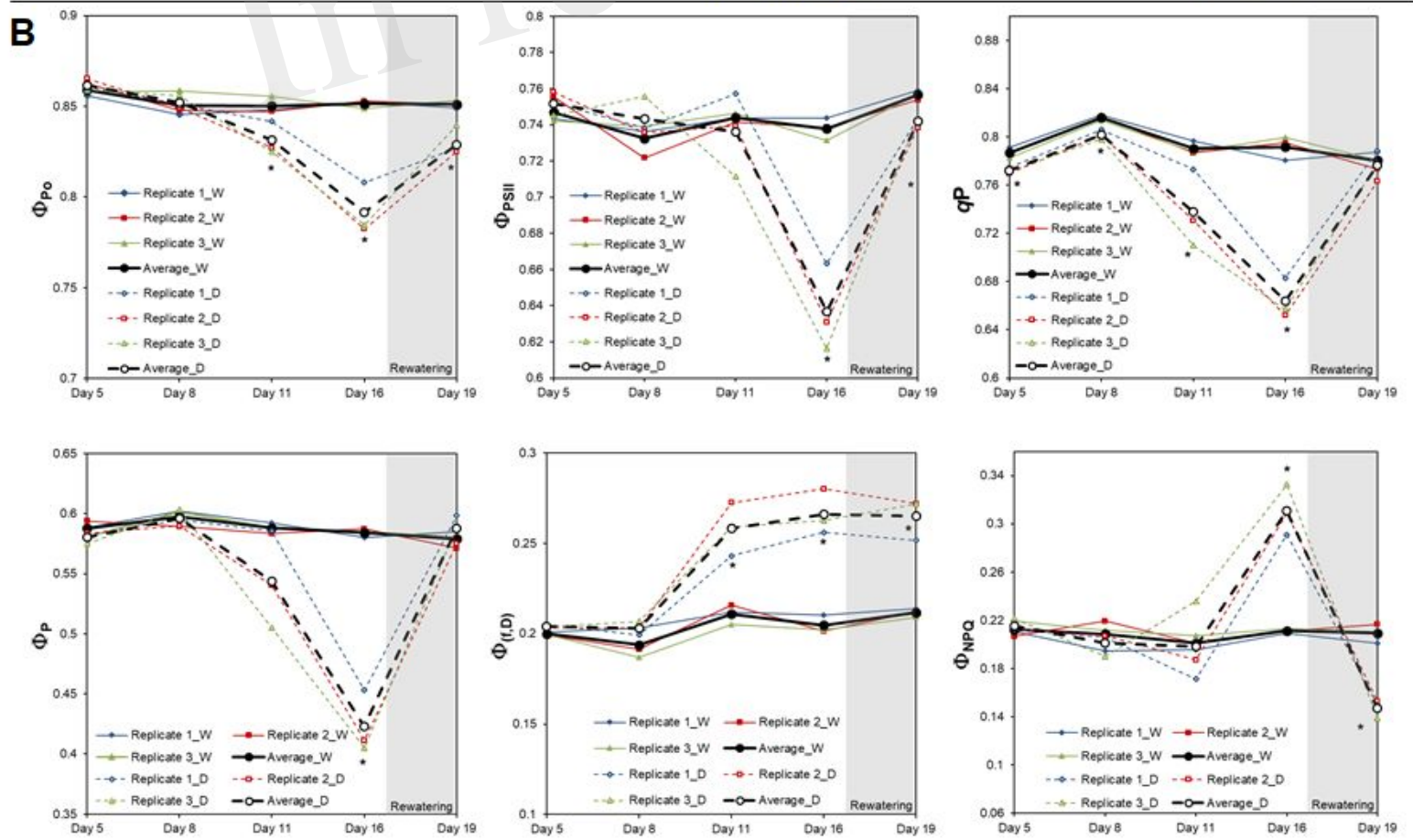
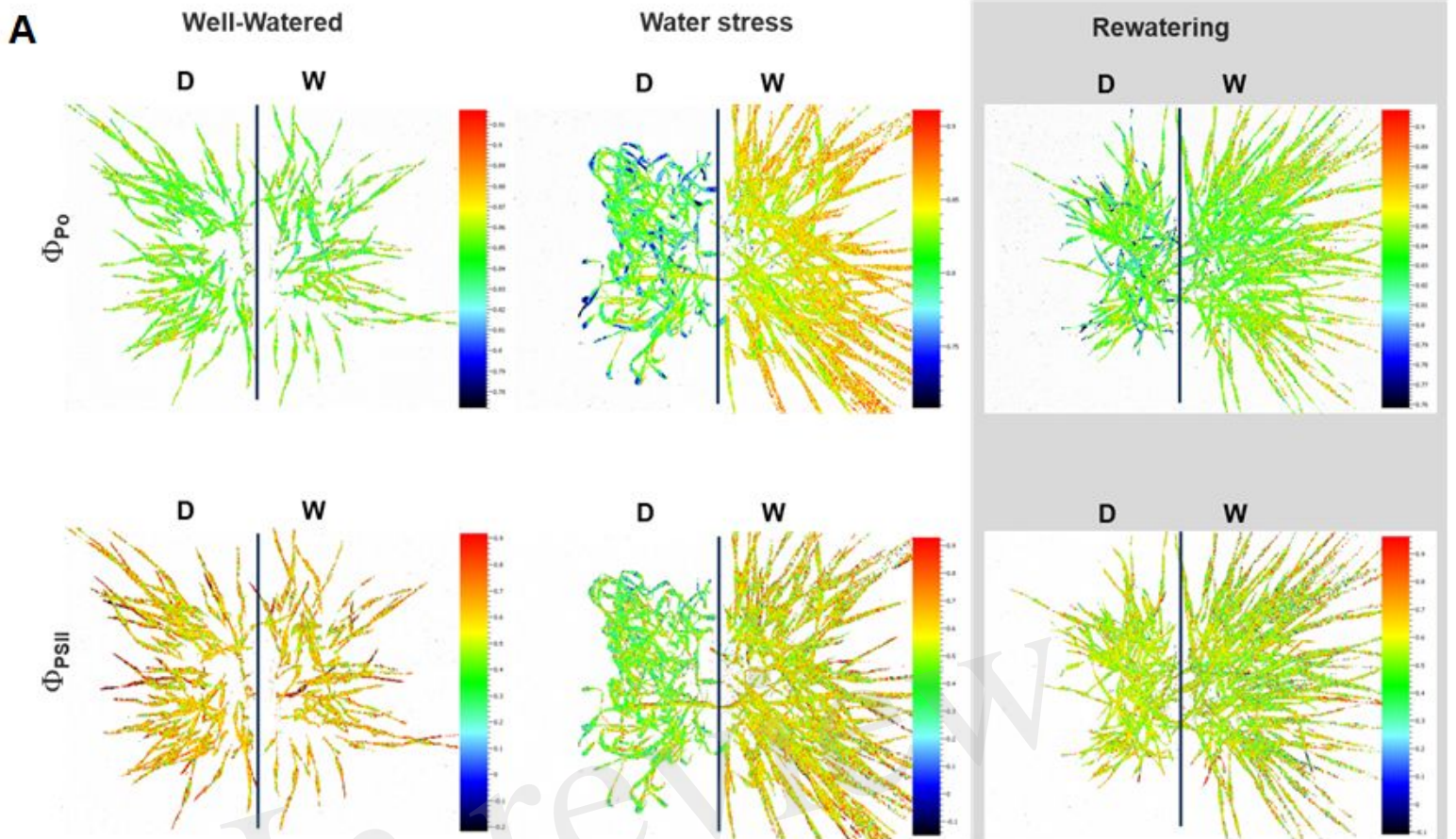
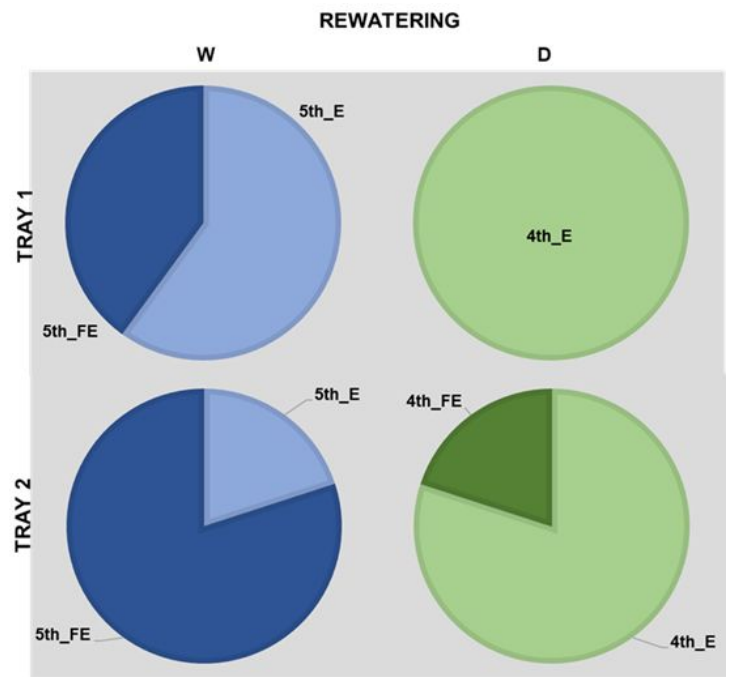
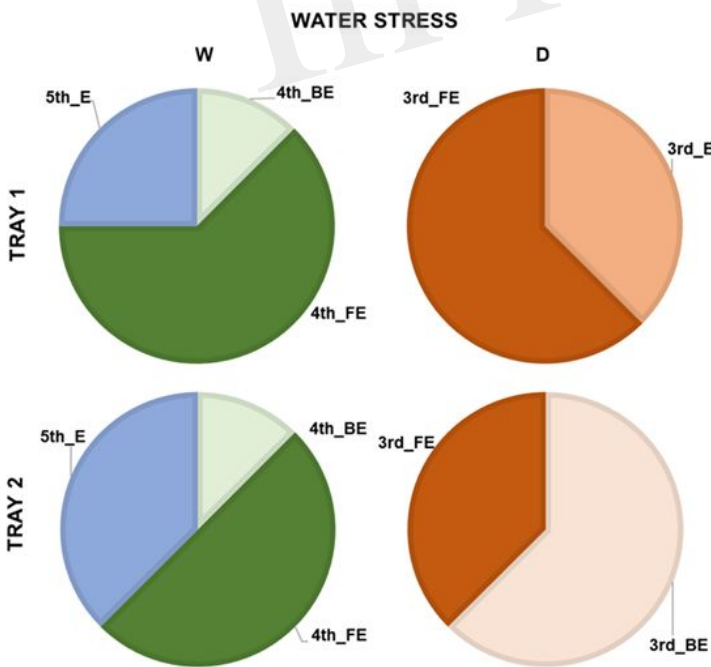


Figure 6.JPEG

In review



		WATER STRESS								
		Variant	Plant 1	Plant 2	Plant 3	Plant 4	Plant 5	Plant 6	Plant 7	Plant 8
TRAY 1	W		5th_E	4th_BE	4th_FE	4th_FE	5th_E	4th_FE	4th_FE	4th_FE
	D		3rd_FE	3rd_FE	3rd_FE	3rd_FE	3rd_E	3rd_E	3rd_FE	3rd_E
TRAY 2	W		5th_E	4th_BE	4th_FE	5th_E	4th_FE	4th_FE	4th_FE	5th_E
	D		3rd_BE	3rd_BE	3rd_FE	3rd_BE	3rd_BE	3rd_FE	3rd_FE	3rd_BE

		REWATERING					
		Variant	Plant 1	Plant 2	Plant 3	Plant 4	Plant 5
TRAY 1	W		5th_E	5th_FE	5th_E	5th_FE	5th_E
	D		4th_E	4th_E	4th_E	4th_E	4th_E
TRAY 2	W		5th_FE	5th_E	5th_FE	5th_FE	5th_FE
	D		4th_FE	4th_E	4th_E	4th_E	4th_E



Figure 7.JPEG

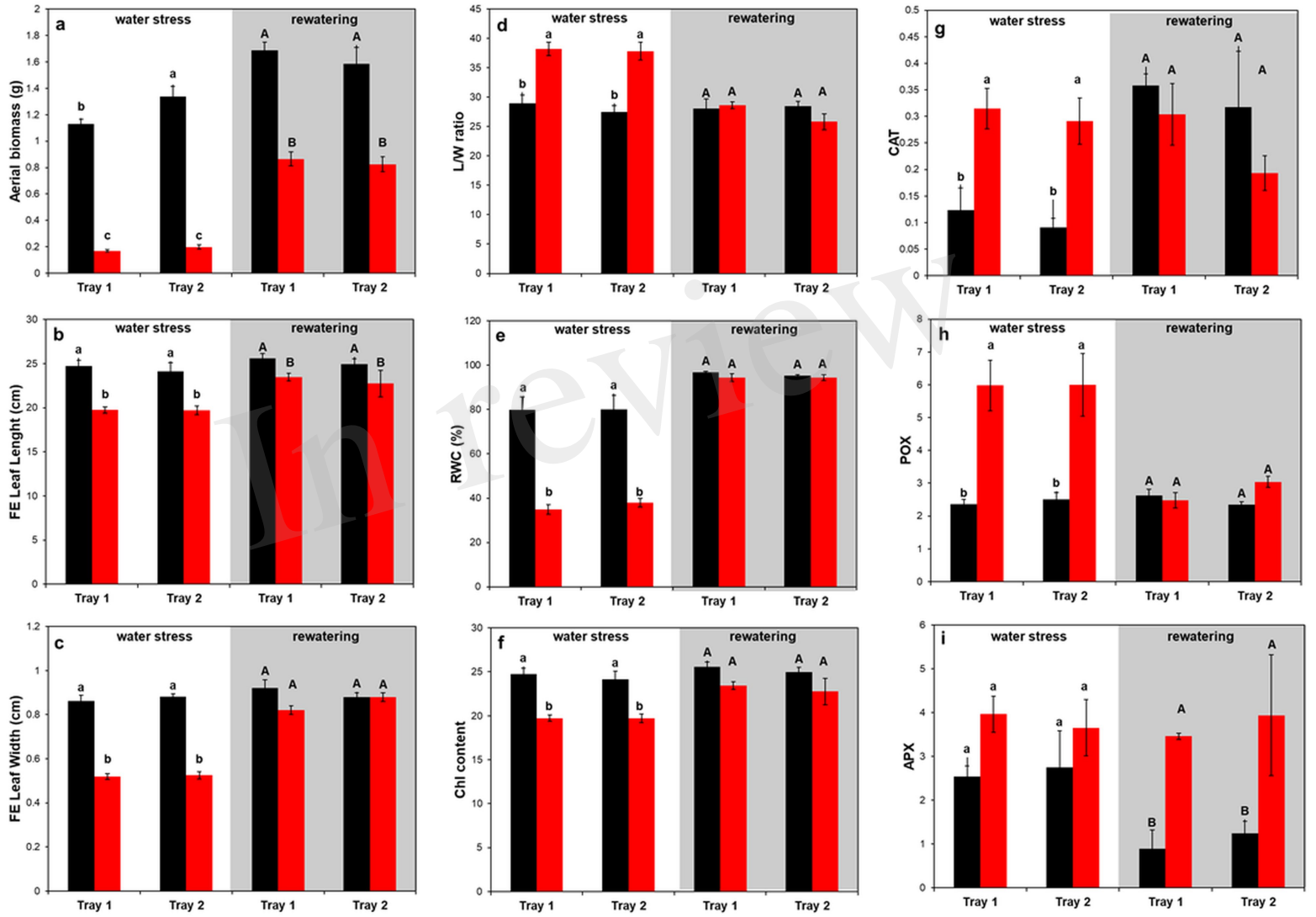


Figure 8.TIF

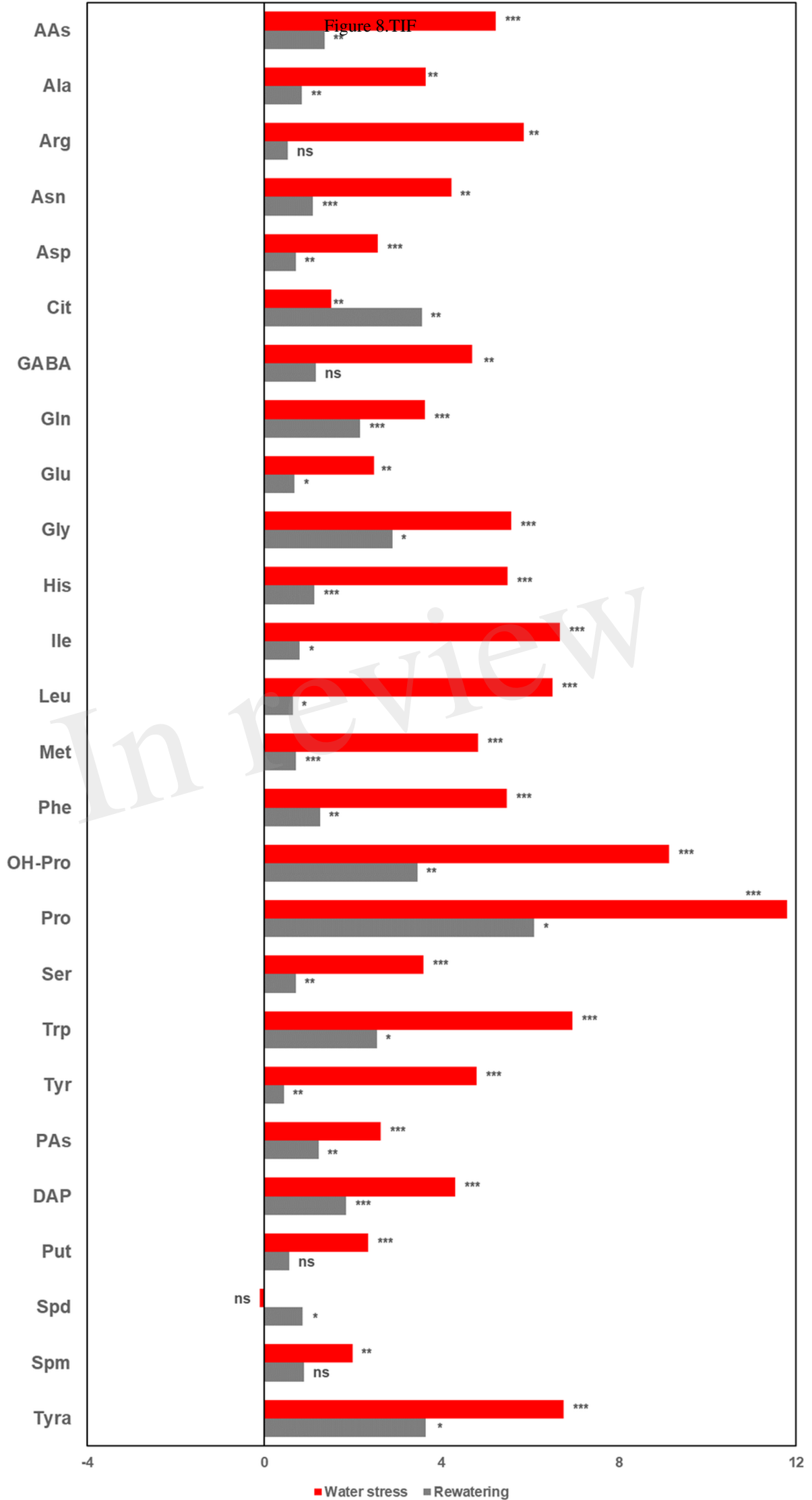
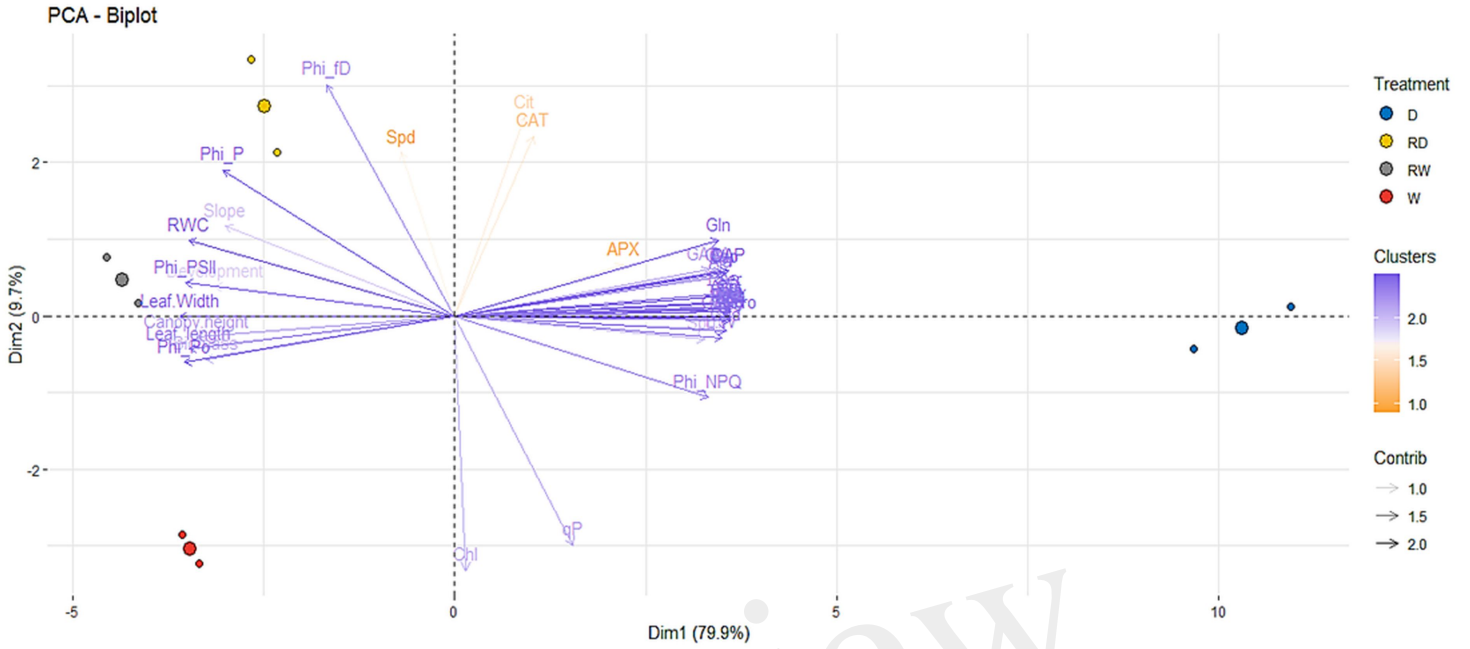
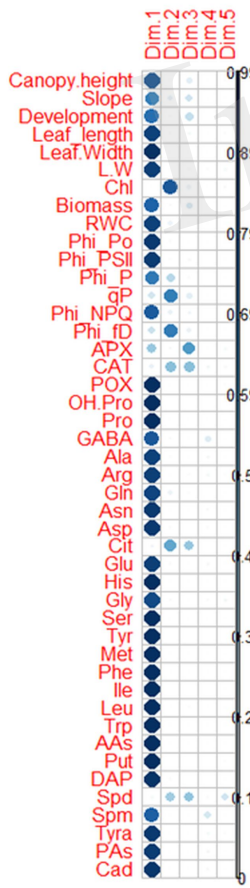


Figure 9.JPEG

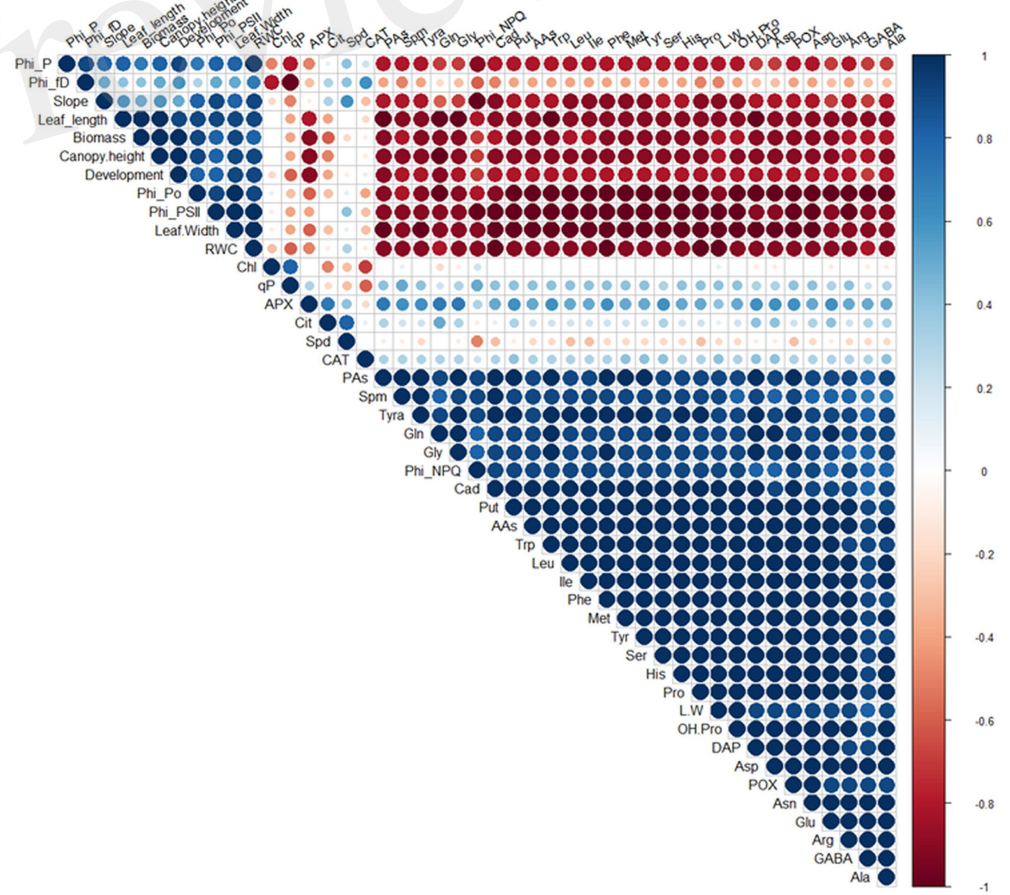
**A**



**B**



**C**





## Research article

# Blue light suppression alters cytokinin homeostasis in wheat leaves senescing under shading stress

Cintia F. Marchetti<sup>a</sup>, Mária Škrabišová<sup>a</sup>, Petr Galuszka<sup>a,†</sup>, Ondřej Novák<sup>b</sup>, Humberto F. Causin<sup>c,\*</sup>

<sup>a</sup> Department of Molecular Biology, Centre of the Region of Haná for Biotechnological and Agricultural Research, Faculty of Science, Palacký University, Šlechtitelů 27, 783 71 Olomouc, Czech Republic

<sup>b</sup> Laboratory of Growth Regulators, Centre of the Region Haná for Biotechnological and Agricultural Research, Faculty of Science, Palacký University & Institute of Experimental Botany, Academy of Sciences of the Czech Republic, Šlechtitelů 27, 783 71 Olomouc, Czech Republic

<sup>c</sup> Institute of Biodiversity, Experimental and Applied Biology (IBBEA), CONICET-UBA, Department of Biodiversity and Experimental Biology (DBBE), University of Buenos Aires, Faculty of Exact and Natural Sciences, Ciudad Universitaria, Pab. II, C1428EGA, C.A.B.A. Argentina

## ARTICLE INFO

## Keywords:

Blue light  
Cytokinin metabolism  
Gene expression  
Leaf senescence  
Shading stress  
*Triticum aestivum*

## ABSTRACT

Blue light (BL) suppression accelerates the senescence rate of wheat (*Triticum aestivum* L.) leaves exposed to shading. In order to study whether this effect involves the alteration of different cytokinin (CK) metabolites, CK-degradation, as well as the expression profile of genes responsible of CK-perception, -inactivation, -reactivation and/or -turnover, leaf segments of 30 day-old plants were placed in boxes containing bi-distilled water and covered with blue (B) or green (G) light filters, which supplied a similar irradiance but differed in the percentage of BL transmitted (G < < B). A neutral (N) filter was used as control. When appropriate, different CK metabolites or an inhibitor of CK-degradation were added in order to alter the endogenous CK levels. A rapid decrement of *trans*-zeatin (*tZ*) and *cis*-zeatin (*cZ*) content was observed after leaf excision, which progressed at a higher rate in treatment G than in the control and B treatments. Senescence progression correlated with an accumulation of glycosylated forms (particularly *cZ*-derivatives), and an increment of CK-degradation, both of which were slowed in the presence of BL. On the contrary, CK-reactivation (analyzed through *TaGLU1-3* expression) was delayed in the absence of BL. When different CK were exogenously supplied, *tZ* was the only natural free base capable to emulate the senescence-retarding effect of BL. Even though the signaling components involved in the regulation of senescence rate and CK-homeostasis by BL remain elusive, our data suggest that changes in the expression profile and/or functioning of the transcription factor HY5 might play an important role.

## 1. Introduction

Leaves beneath a dense canopy experience a marked reduction of the photon flux as well as the red (660 nm) and blue (400–450 nm) wavelengths due to the spectral properties of the photosynthetic pigments, and it has been shown that changes in either light intensity or spectral quality can induce leaf senescence in an independent way (reviewed in Causin and Barneix, 2007). In wheat leaves exposed to shading under different light filters, blue light (BL) suppression plays a central role in the induction of chlorophyll and protein loss (Causin and

Barneix, 2007; Causin et al., 2009). This effect was shown to be largely independent of differences in either net photosynthetic rate or carbohydrate content among shading treatments (reviewed in Causin and Barneix, 2007). Diverse classes of flavin-based photoreceptors that mediate the effects of BL have been described, including cryptochromes, phototropins and members of the zeitelupe family. Meng et al. (2013) demonstrated that cryptochrome 2 (CRY2) suppress leaf senescence in soybean leaves through a blue-light dependent interaction with the cryptochrome-interacting basic helix-loop-helix transcription factor 1 (CIB1), which is an activator of senescence-associated genes. In

**Abbreviations:** BAP, benzyl-amino purine; BL, blue light; CIB, cryptochrome-interacting basic helix-loop-helix transcription factor; CKX, cytokinin oxidase/dehydrogenase; CRY, cryptochrome; CK, cytokinin; *cZ*, *cis*-zeatin; ZOG, zeatin-O-glucosyltransferase; HK, histidine kinase; INCYDE, inhibitor of cytokinin degradation; iP, isopentenyl-adenine; RR, response regulator; TCA, trichloroacetic acid; *tZ*, *trans*-zeatin

\* Corresponding author.

E-mail addresses: [cintia.marchetti@upol.cz](mailto:cintia.marchetti@upol.cz) (C.F. Marchetti), [maria.skrabisova@upol.cz](mailto:maria.skrabisova@upol.cz) (M. Škrabišová), [petr.galuszka@upol.cz](mailto:petr.galuszka@upol.cz) (P. Galuszka), [ondrej.novak@upol.cz](mailto:ondrej.novak@upol.cz) (O. Novák), [causin@bg.fcen.uba.ar](mailto:causin@bg.fcen.uba.ar) (H.F. Causin).

† Deceased 04.06.2018.

<https://doi.org/10.1016/j.plaphy.2018.08.005>

Received 14 May 2018; Received in revised form 19 July 2018; Accepted 6 August 2018

Available online 11 August 2018

0981-9428/ © 2018 Elsevier Masson SAS. All rights reserved.

*A. thaliana*, CIB1 is degraded by the 26S proteasome in the absence of blue light (Liu et al., 2013). However, not CRY2 but two light–oxygen–voltage (LOV) domain photoreceptors, ZEITLUPE and LOV KELCH PROTEIN 2, are required for the suppression of the degradation of CIB1 by BL in this species, indicating that BL-regulation of this transcription factor may involve distinct mechanisms. There is a lack of information on whether genes homologous to *CIB1* are present in wheat and, if so, whether they are under the control of BL-mediated signals.

Even though the pathway of the light signal perception and transduction remains to be elucidated, our previous studies suggest that the alteration of key components of the oxidative metabolism together with changes in the homeostasis of cytokinins (CKs) may be involved in the regulation of shade-induced senescence in wheat (Causin and Barneix, 2007; Causin et al., 2009). CKs are a major class of phytohormones whose role as retardants of leaf senescence under different stress conditions has been widely documented (e.g. Wang et al., 2016 and references therein). While *cis*-zeatin (*cZ*) has been generally regarded as a cytokinin with little or no activity, isopentenyl-adenine (iP) and *trans*-zeatin (*tZ*) (and their ribosides) are usually considered as the main CK-bioactive forms (Sakakibara, 2006). CKs are perceived by the two-component histidyl-aspartyl signaling system. At first, the CK molecule is recognized by a transmembrane histidine kinase (HK) receptor. Three CK-binding HK receptors have been characterized in *Arabidopsis* (AHK2, AKH3 and CRE1/AHK4), and their homologues have been identified in different plant species (e.g. Nishimura et al., 2004; Lomin et al., 2011). In the next step, the signal is transmitted to the regulatory proteins of CK response (RRs) by specific histidine-phosphotransferases (HPs). Kim et al. (2006) showed that AHK3 (but not the other CK receptors), mediates the control of leaf longevity through phosphorylation of ARR2 in *Arabidopsis*. Nevertheless, leaf senescence was not significantly affected in *arr2* knockout plants, suggesting that either other ARR2 and/or signaling components may be involved in the control of CK-mediated leaf longevity.

The homeostasis of CKs can be modulated by several mechanisms, including the degradation or the inactivation of their active forms. CK catabolism is mainly attributed to the activity of cytokinin oxidase/dehydrogenase (CKX, EC: 1.5.99.12), which catalyzes the irreversible degradation of active CKs (Schmülling et al., 2003). Several putative members of the *CKX* gene family have been identified, and their relative expression profiles characterized in different organs and developmental stages of wheat and related crops (e.g. Galuszka et al., 2004; Song et al., 2012, and references therein). CKX activity is usually low in non-senescent leaves, and both the activity as well as the gene expression of several *CKX*-members increases under different stress conditions. The *in vitro* activity of CKX was shown to be enhanced in detached apical parts of the first foliage leaves of barley kept in the dark (Conrad et al., 2007; Schlüter et al., 2011). This increment was greatly stimulated when the leaf segments were incubated in the presence of white light, presumably due to an increase of the enzyme expression. It is not known whether changes in light spectral quality can also affect CK degradation and/or *CKX* expression in leaves exposed to shading stress.

The purine moiety of CKs can be modified by ribosylation, phosphoribosylation and glucosylation, all of which affects the final pool of the active hormone. The most common way of CK inactivation involves *N*- or *O*-glycosylation. This deactivation is catalyzed by UDP-glucosyltransferase (UGT, EC 2.4.1.X), being UDP-glucose the donor of sugar moieties. While *N*<sub>7</sub>- and *N*<sub>9</sub>-glucosides are regarded as the final products of irreversible inactivation (Sakakibara, 2006), *O*-glucosides are considered as a storage form of CKs since they can be converted back to their free forms through the action of  $\beta$ -glucosidase (EC 3.2.1.21). Genes encoding for *cZ*-*O*-glucosyltransferases (*cZOGs*) have been identified in different plant species. In cereals, *cZOGs* preferentially catalyze *O*-glycosylation of *cZ* and *cZ*-riboside rather than *tZ* and *tZ*-riboside (Kudo et al., 2012, and references therein). Interestingly, some transgenic rice plants over-expressing the *cZOG1* and *cZOG2* genes exhibit delay of leaf senescence, indicating that *O*-glycosylation of *cZ*

(-riboside) might be involved in the regulation of this process (Kudo et al., 2012).

In *A. thaliana*, both blue light and cytokinins have been shown to induce certain photomorphogenetic responses by increasing the levels of the transcription factor HY5 through independent mechanisms, suggesting that this protein is a point of convergence between cryptochrome and cytokinin signaling pathways (Vandenbussche et al., 2007). Moreover, indirect evidence suggests that the repression of *HY5* expression might contribute to the control of some processes associated to dark induced senescence in individual leaves (Keech et al., 2010). However, little is known about the *HY5* gene members in wheat, and it has not been investigated to what extent the expression of this transcription factor is affected by different light environments in leaves senescing under shading conditions.

In the present work we studied whether changes in light spectral quality affects the level of CK metabolites and CKX activity, together with the expression profile of several genes involved in CK signaling and metabolism, in wheat leaves exposed to shading stress under specific light filters. The effect of the pharmacological inhibition of CK degradation, exogenous CK addition, as well as changes in the expression profile of wheat cryptochromes and genes homologous to *CIB1* and *HY5* were also investigated. Our results indicate that the suppression of blue wavelengths during shading down-regulates the level of free CKs and alters the expression profile of several genes responsible for the maintenance of CK-homeostasis. The involvement of cryptochromes and *HY5* as putative components of the BL signal perception and transduction pathway is also discussed.

## 2. Materials and methods

### 2.1. Plant growth and experimental procedure

Wheat (*Triticum aestivum* L., cv. INTA Oasis) caryopses were surface sterilized (12 min in 10% H<sub>2</sub>O<sub>2</sub>), germinated on wet tissue paper and planted in plastic pots containing a mixture of sand: vermiculite (2:1), in a greenhouse at natural photoperiod. The pots were periodically irrigated with tap water and, after six to seven days from sowing, fertilized twice a week with a modified Hoagland's solution (Causin et al., 2009). To study the effect of light spectral quality on the senescence rate, leaf segments (9 cm length) from the third or fourth fully expanded leaves of 30 d-old plants were placed inside plastic boxes containing bi-distilled water, whose lids were covered with Lee filters (green #089 or blue #075, hereafter referred as treatment G or B, respectively). Both filters supplied a similar proportion of red (R = 660 nm) to far-red (FR = 730 nm) irradiation, but differed in the percent transmission of BL (450–480 nm): treatment B = 70%–55% transmission, respectively; treatment G < 1% transmission in the indicated range (see Causin et al., 2015, for a detailed description of the filters). Boxes with a neutral (N) white filter were used as controls. Photosynthetically photon flux density (*PPFD*) ranged from 20 (G filter) to 28 (N filter)  $\mu\text{mol m}^{-2} \text{s}^{-1}$ . When indicated, an inhibitor of CK-degradation (INCYDE) or different CKs were included in the floating solution. Five nL mL<sup>-1</sup> Tween 20 were also supplied in order to increase tissue contact with the medium. Leaf excision facilitates the implementation of pharmacological treatments as well as the simultaneous processing of a large number of experimental units; and even though it induces the development of senescence symptoms, it did not substantially alter the senescence pattern caused by the light filters when applied on intact leaves (Causin and Barneix, 2007). Three replicates, containing four or five leaf segments each, were used per sampling date and treatments combination, depending on the experimental trial. Soon after excision, leaf segments were superficially sterilized (5 min) with 2% (v/v) commercial NaOCl (50 g Cl/L) and carefully rinsed with sterilized water. Part were immediately sampled (t0 point) and the remaining placed in the different treatments. Incubations were performed in a chamber supplied with equal number of white

(SYLVANIA F27W T8/LD/54) and red light enriched (SYLVANIA GroLux F30W T12) fluorescent tubes (16 h photoperiod), at  $24 \pm 2^\circ\text{C}$  and  $14 \pm 2^\circ\text{C}$  day and night temperatures, respectively. Measurements of R and FR irradiation and *PPFD* were performed, respectively, with a SKR 110 660/730 nm sensor (Skye-Probetech, USA) and a LI-190 quantum sensor (LI-COR, Lincoln, NE, USA) attached to a CAVA-RAD data logger (Cavadevices, Argentina). It should be noted that, because FR irradiation is very low as compared to R light under the fluorescent tubes, the R: FR ratio was higher than 3.0 in all the treatments. Leaves were sampled at different time intervals, briefly rinsed in distilled water, blotted dry, fractioned, and kept at  $-75^\circ\text{C}$  for further analyses. When indicated, the same procedure was performed with samples of leaves immediately detached prior to the beginning of shading treatments (t0). All the experiments were repeated at least twice. Whenever possible, data from different experiments were averaged, otherwise data from a representative trial are presented.

## 2.2. Determination of chlorophyll content and protein concentration

Chlorophyll content was measured with a CCM-300 Chlorophyll Content Meter (Opti Sciences, USA). The average value of 6 measurements per leaf segment was used for chlorophyll estimations.

Protein concentration in the crude extracts was determined according to Bradford (1976), using bovine serum albumin as a standard.

## 2.3. Cytokinin content measurements

Lyophilized leaf samples (5 mg) were extracted in 1 mL of modified Bielecki buffer (60% MeOH, 10% HCOOH and 30% H<sub>2</sub>O) and purified using two solid phase extraction columns, the octadecylsilica-based column (C18, 500 mg of sorbent, Applied Separations) and the Oasis MCX column (30 mg/1 mL, Waters), according to the method described by Dobrev and Kamínek (2002), including modifications described by Antoniadis et al. (2015). The quantification of endogenous content of CKs was performed by ultra-high performance liquid chromatography (AcquityUPLC™; Waters) coupled to a Xevo™ TQ-S (Waters) triple quadrupole mass spectrometer using stable isotope-labelled internal standards (0.25 pmol of CK bases, ribosides, *N*-glucosides, 0.5 pmol of CK *O*-glucosides and nucleotides per sample added) as a reference. Three independent biological replicates were performed.

## 2.4. Measurement of CKX activity

Samples were homogenized in liquid nitrogen and extracted with 0.2 M Tris/acetate buffer (pH = 8.0) containing 0.3% Triton-X-100 and 1.0 mM phenylmethanesulfonyl fluoride (1:3 w/v ratio), in the presence of polyvinylpyrrolidone (PVPP). Cell debris was removed by centrifugation at maximum speed for 20 min at  $4^\circ\text{C}$ . The supernatant was used for the enzymatic activity determination by the end-point assay with 4-aminophenol (Frébert et al., 2002). The reaction mixture of 0.6 mL final volume contained 100  $\mu\text{L}$  of the protein extract, 200  $\mu\text{M}$  of iP as substrate and 0.5 mM of 2,6-dichlorophenolindophenol (DCPIP) as electron donor, in 200 mM McIlvaine buffer (citric acid/disodium hydrogen phosphate, pH = 6.8). For blank of reaction, iP was replaced with dimethyl sulfoxide (solvent); and for every independent enzymatic extract, two technical duplicates were conducted. After overnight incubation at  $37^\circ\text{C}$ , 0.3 mL 40% TCA was added to the mixture, followed by centrifugation for 5 min at 12,000 g. Finally, 0.2 mL 4-aminophenol (2% solution in 6% TCA) was added and the absorbance at 352 nm was measured to detect the Schiff base of the aldehyde originated from cytokinin side chain and *p*-aminophenol reaction, which has a molar absorption coefficient of  $\epsilon_{352} = 15.2 \text{ mM}^{-1} \text{ cm}^{-1}$  (Frébert et al., 2002).

## 2.5. Phylogenetic tree construction and identification of wheat orthologues for genes of interest

In order to identify putative *CIB1*, *HKs* and *HY5* sequences in wheat and design primers for qPCR analysis, the annotated genes from the same family members in other related species were used as query for BLASTn search against the partial wheat genome sequence in EnsemblPlants database (<https://plants.ensembl.org/index.html>). Protein sequences from all hits with  $e\text{-value} \leq 1e-40$  were aligned with the respective orthologues using the CLUSTAL W program in BioEdit and the unrooted phylogenetic trees were generated in MEGA 6 program (Supplementary Material Fig. S1), using the Neighbor-Joining (NJ) algorithm with 1000 bootstrap replicates.

For each gene, the closest wheat orthologues were identified and in most of the cases several members clustered together, most probably corresponding to three copies of the same target gene in the hexaploid wheat genome. When possible, qPCR primers were designed on the identical region of the sequences, in order to amplify all the copies of each gene. For the remaining genes studied, primers were designed according to data published elsewhere (Supplementary Material Table S1).

## 2.6. Analysis of gene expression by qRT-PCR

Isolation of total RNA from frozen leaves was performed by the use of TRIzol Reagent (Thermo Fisher Scientific), according to the manufacturer's protocol. RNA concentration was determined using a NanoDrop™ Lite Spectrophotometer (Thermo Fisher Scientific). To eliminate traces of genomic DNA, RNA was treated with TURBO DNA-free™ kit (Thermo Fisher Scientific). 2  $\mu\text{g}$  of the purified RNA was used for cDNA synthesis in a reverse transcription reaction containing oligo (dT) primers (Sigma-Aldrich) and RevertAid H Minus Reverse Transcriptase (Thermo Fisher Scientific). Quantitative real-time PCR reactions contained properly diluted cDNA, 300 nM primers and gb SG PCR Master Mix, supplemented with 100 nM ROX passive reference dye (Generi Biotech). The program consisted of an initial denaturation of 2 min at  $95^\circ\text{C}$ , followed by 40 cycles of 15 s at  $95^\circ\text{C}$  and 60 s at  $60^\circ\text{C}$ , performed on a ViiA™ 7 Real-Time PCR System (Applied Biosystems). In order to confirm the specificity of amplification, each run was completed with a melting curve and the resulted amplicons were analyzed on 2% agarose gel stained with ethidium bromide, in presence of a 50 bp DNA ladder (New England Biolabs) for size determination and visualized using Gel Doc EZ system (Bio-Rad). Changes in the relative mRNA abundance were calculated using the comparative  $2^{-\Delta\Delta\text{Ct}}$  according to Pfaffl (2001), using t0 as the reference sample. The qPCR efficiency of amplification was 90–110% for all the primers used (data not shown). *TaEF2* and *TaGADPH* were chosen as internal control genes. Three biological and two technical replicates were analyzed per each condition tested. Fold changes in gene expression were calculated after data normalization for multiple internal controls following the procedures suggested by Vandesompele et al. (2002). All primers used are listed in Supplementary Table 1.

## 2.7. Data analysis

In the case of chlorophyll, cytokinin content and CKX activity data, conventional two-way ANOVA test (STATISTICA 7, Stat Soft Inc., Tulsa, OK, USA), was performed. When necessary, data transformation was used to meet ANOVA assumptions. Depending on the experimental design, the model included “sampling date” and “light filter”, or “light filter” and “incubation media”, as fixed factors. Post-hoc comparisons for significant main effects or interaction terms were performed using the Tukey HSD test. Significant differences were considered at  $p < 0.05$ , unless otherwise stated. Normalized qPCR data were analyzed for each sampling date and each shading treatment separately through the non-parametric Kruskal-Wallis ANOVA, using “light filter”

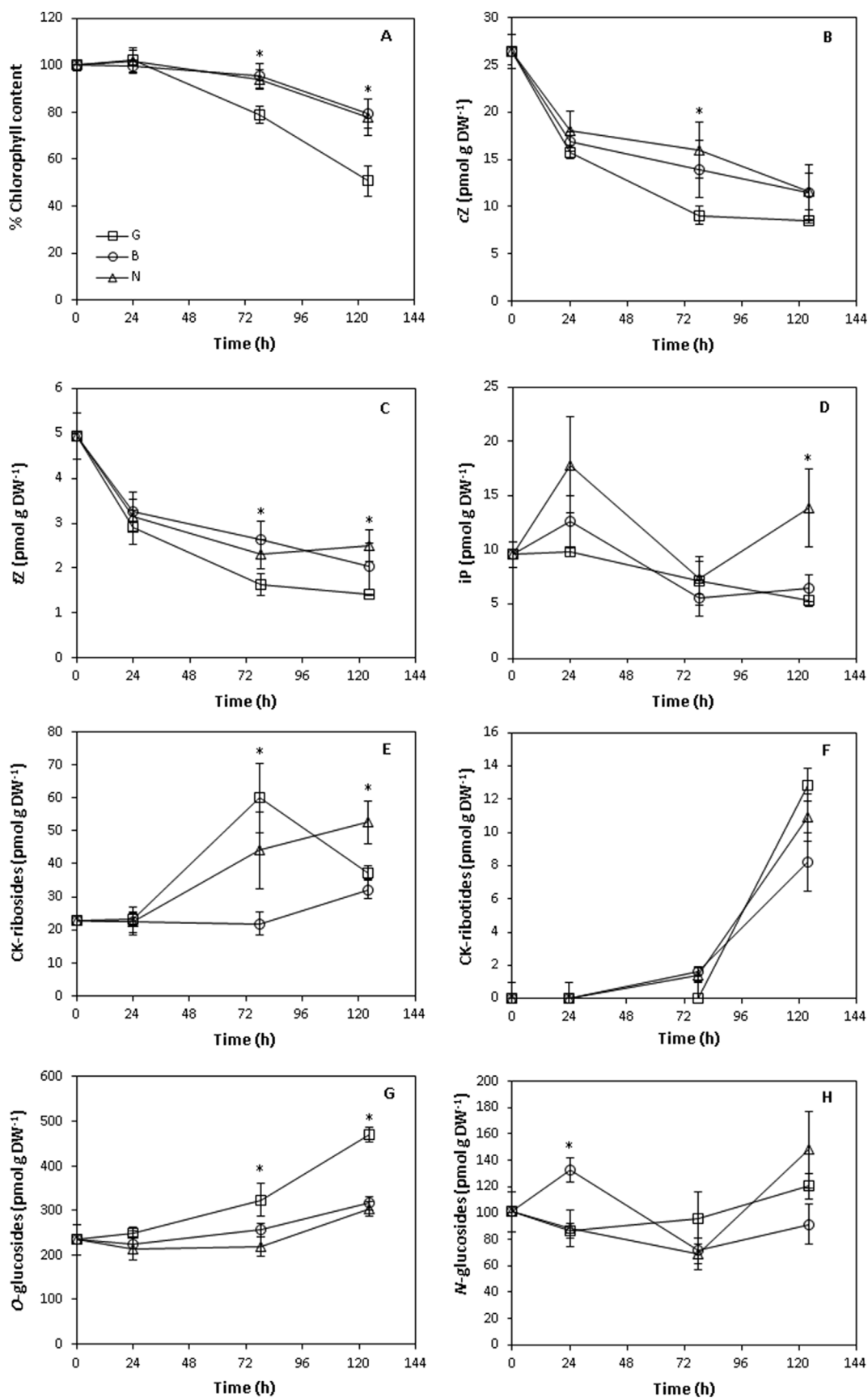


**Fig. 1.** Change in percent chlorophyll content (A), and in the concentration of free CKs (B–D) or CK-conjugates (E–H), in detached wheat leaves at different times after exposure to the neutral (N), green (G) or blue (B) filters. Data are means  $\pm$  SD (A: n = 8; B–H: n = 3). Asterisks indicate the existence of significant differences for “shading treatment” effect, at a given sampling date.

**Table 1**

Percent chlorophyll content with respect to T0 in excised wheat leaves exposed during 100 h to the green filter (G), in the absence or presence of 2.5  $\mu\text{M}$  of the indicated CKs, which were added at 52 h after the beginning of shading. A group of leaves exposed during 52 h to filter G were changed to filter B without addition of CKs (treatment GB). Data are means  $\pm$  SD ( $n = 10$ ). Statistically homogeneous groups are indicated with similar letters.

Treatment	% Chlorophyll
G	37.85 $\pm$ 5.60 <sup>a</sup>
GB	67.81 $\pm$ 4.08 <sup>b</sup>
G + iP	41.90 $\pm$ 4.89 <sup>a</sup>
G + tZ	61.45 $\pm$ 4.09 <sup>b</sup>
G + cZ	38.02 $\pm$ 3.81 <sup>a</sup>
G + BAP	62.55 $\pm$ 4.60 <sup>b</sup>

or “sampling date”, respectively, as fixed factors. Where appropriate, multiple comparisons of mean ranks were used to determine statistically different groups. Considering that non-parametric tests may increase the likelihood of not detecting a significant effect when it truly exists, a given effect was assumed significant at  $p \leq 0.055$ , to avoid excluding a couple of responses that consistently repeated across experimental trials. When indicated, data were considered marginally significant if  $0.055 < p \leq 0.065$ .

### 3. Results

#### 3.1. The homeostasis of CKs is altered during senescence progression under the different shading treatments

As previously reported, chlorophyll degradation rate in excised leaves exposed to shading increases when BL transmittance is suppressed (i.e. treatment G), while in leaves from treatment B it follows an almost identical trend to the neutral control (Fig. 1A). Moreover, BL contributes to yellowing retardation yet when supplied at 30 or 54 h after the leaves had been exposed to the green filter (Supplementary Material Fig. S2). This senescence-retardant effect of BL is corroborated by the expression profile of the two senescence markers analyzed (Supplementary Material Fig. S3, see also Causin et al., 2015).

Regarding the response of free CKs in the presence or absence of BL, two distinct trends were observed. On the one hand, the content of tZ and cZ decreased in all shading treatments during the first 78 h. It is noteworthy that although no differences among treatments were found at 24 h after the beginning of shading, the decrement of both free CKs thereafter was on average significantly higher in leaves exposed to the green filter (Fig. 1B–C, ANOVA for “light filter” and “sampling date” main effects  $p < 0.01$ , for both traits). On the other hand, while the content of iP also tended to decrease as senescence progressed in treatment G, it oscillated around the initial value in treatments N and B (Fig. 1D). Nevertheless, due to the variation found in tissue iP levels, significant differences were only detected at the last sampling date between treatments N and G.

Contrary to expected, the concentration of precursors (i.e. CK-ribotides and CK-ribosides) did not follow similar trends than those found for free CKs. While the level of CK-ribosides slightly increased at the end of the experimental period in leaves exposed to filter B, a sharp increase was observed at 78 h in leaves from the remaining treatments (Fig. 1E). Then, only in treatment G the concentration of CK-ribosides fell to similar levels to those found in treatment B. Cis-zeatin riboside (cZR) was the most prevalent metabolite among CK-ribosides (Supplementary Material Table S2). The concentration of CK-ribotides did not significantly change during the first 78 h, but peaked at 124 h in all the treatments, with values more than eight, ten, and twelve folds

higher than t0 in treatment B, N, and G, respectively (Fig. 1F). Isopentenyladenosine-5'-monophosphate (iPR5MP) was the most prevalent form of CK-ribotides in our experimental conditions (Supplementary Material, Table S2).

The concentration of most of the conjugated forms involved in storage (O-glucosides) and deactivation (N-glucosides), was considerably higher than those found for active CKs (free bases and ribosides). The O-glucosides were mostly represented by those of cZ and its riboside, meanwhile the N-glucosides by N<sub>9</sub>-glucosides of tZ and iP (Supplementary Material Table S2). As observed for the CK-ribotides and -ribosides, the level of O-glucosides tended to increase as senescence progressed (Fig. 1G). Notably, this effect was statistically significant only for leaves from treatment G, which more than doubled the initial amount of CK-O-glucosides at the end of the experimental period. On the contrary, the content of N-glucosides did not follow a consistent trend and oscillated within  $\pm 34\%$  of the initial value, depending on the treatment and sampling date considered (Fig. 1H). At 124 h, significant differences for the content of CK N-glucosides were found only between treatments N and B.

In order to evaluate the effect of different free CK bases on leaf senescence rate when BL is suppressed, changes in chlorophyll content were analyzed at 100 h after exposure to the G filter, either in the absence or presence of 2.5  $\mu\text{M}$  iP, tZ, cZ, BAP or the blue filter (as a control), which were applied at 52 h from the beginning of the experiment. As shown in Table 1, only the addition of BAP or tZ significantly delayed leaf senescence when compared to treatment G. Interestingly, the effect was similar to that exerted by exposure to filter B in the absence of exogenously applied CKs (see Table 1, treatment GB).

#### 3.2. The turnover of CKs differs among shading treatments

To test whether changes in the levels of active CKs were related to the alteration of their degradation, inactivation and/or reactivation rates, a second experiment was performed to analyze the effect of the shading treatments on CKX activity, as well as on the expression pattern of genes involved in the regulation of CK homeostasis.

CKX activity was very low at the beginning of the assay, but increased as senescence progressed, particularly in leaves exposed to the G filter (Fig. 2A).

Among the genes belonging to the CKX family analyzed, *TaCKX1* was found to be by far the most up-regulated. As for CKX activity, the expression of *TaCKX1* was initially very low but markedly increased after about 54 h of exposure to the shading treatments. This effect was noticeable in leaves from treatment G, where its expression was several folds higher than the remaining treatments towards the end of the experimental period (Fig. 2B).

From the remaining *TaCKX* family members, only *TaCKX3*, *TaCKX4*, *TaCKX10* and *TaCKX11* showed detectable transcript levels in our experimental conditions. Among them, only *TaCKX3* showed a consistent up-regulation under certain treatment conditions. In fact, while no major differences across time were detected in leaves from treatment G, its expression increased about five times (treatment B) and three times (treatment N) after 54 and 92 h from the beginning of the shading treatments, respectively (Fig. 2C). Then the transcript content decreased in both conditions to similar levels than those found in treatment G. As opposed to *TaCKX1*, the expression of *TaCKX4* and *TaCKX10* markedly decreased in all treatments during the first 52 h, and their transcript levels remained low until the end of the experimental period (Fig. 2D–E). Finally, the mRNA levels of *TaCKX11* did not show major changes across time in any of the shading treatments (Fig. 2F).

To further explore the role of CK degradation in our experimental model, we decided to test whether the inhibition of CKX activity with the adenine derivative 2-chloro-6-(3-methoxyphenylamino)-purine (“INCYDE”, inhibitor of cytokinin degradation, Zatloukal et al., 2008), delayed leaf senescence in leaves exposed to filter G. Based on



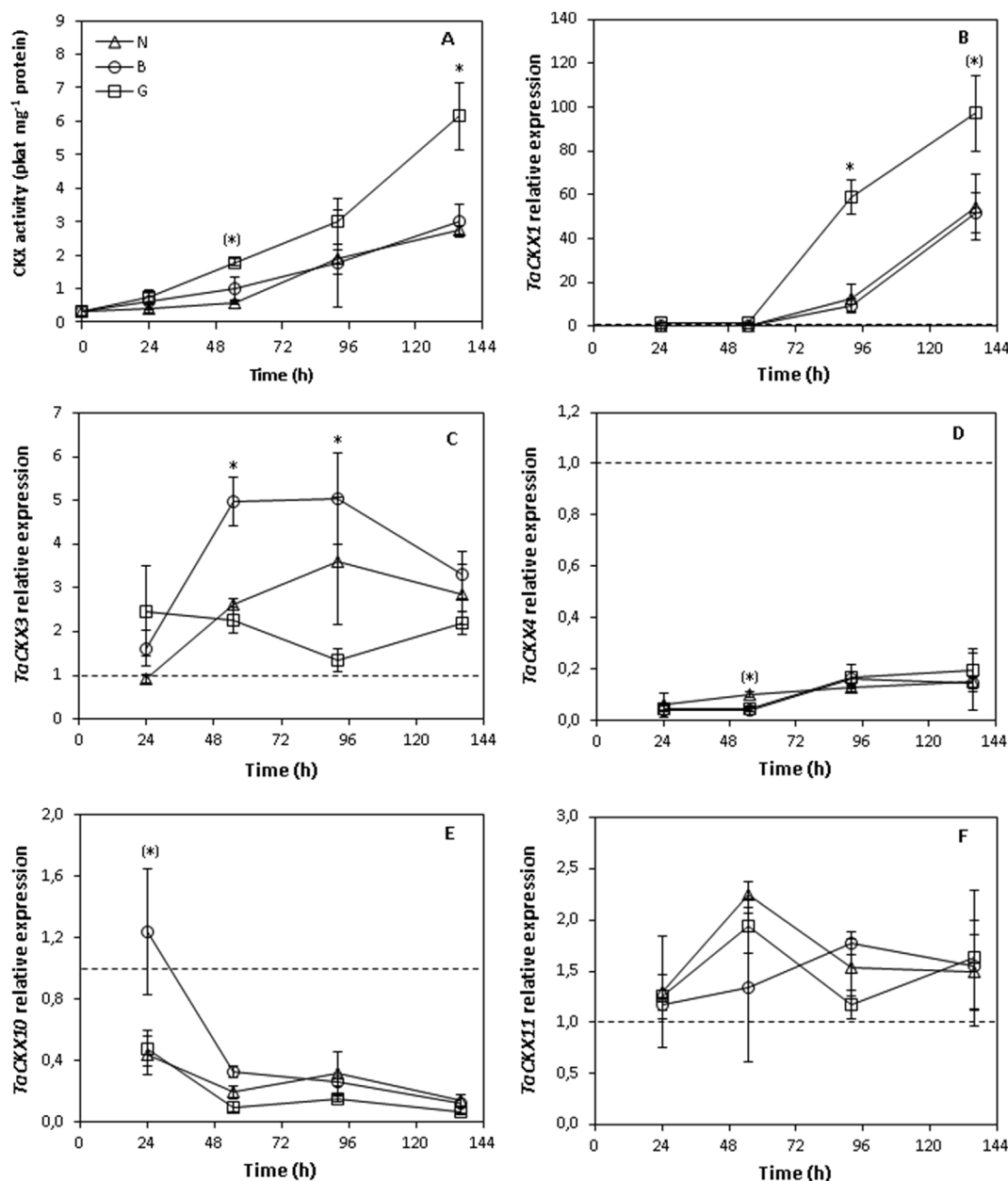


**Fig. 2.** CKX specific activity (A) and expression profile of different *TaCKX* members (B–F) in detached wheat leaves, at different times after exposure to the neutral (N), green (G) or blue (B) filters. Data are means  $\pm$  SD ( $n = 3$ ). Asterisks alone or between brackets indicate the existence of significant or marginally significant differences, respectively, for “shading treatment” effect, at a given sampling date. Gene expression was relativized to 0 h = 1 (dashed line).

**Table 2**

Percentage chlorophyll content with respect to t0 and CKX activity, in excised wheat leaves exposed during 100 h to the neutral (N), blue (B) or green (G) light filters, or during 52 h to filter B and then 48 h to filter G (treatment BG). Where indicated, 10.0  $\mu$ M INCYDE was supplied to the external solution from either 24 or 52 h after the beginning of the shading treatments. Data are mean  $\pm$  SD ( $n = 10$  for chlorophyll records and  $n = 4$  for CKX analyses). Data with different letters differ at  $p < 0.05$ .

Treatment	% Chlorophyll	CKX (pkat mg <sup>-1</sup> protein)
N	81.50 $\pm$ 5.94 <sup>a</sup>	0.597 $\pm$ 0.091 <sup>a</sup>
B	77.88 $\pm$ 3.73 <sup>a</sup>	0.612 $\pm$ 0.066 <sup>a</sup>
G	43.71 $\pm$ 5.25 <sup>c</sup>	1.743 $\pm$ 0.084 <sup>c</sup>
BG	53.34 $\pm$ 5.84 <sup>c</sup>	0.983 $\pm$ 0.098 <sup>b</sup>
G + INCYDE (24 h)	79.94 $\pm$ 6.16 <sup>a</sup>	0.970 $\pm$ 0.089 <sup>b</sup>
G + INCYDE (52 h)	52.82 $\pm$ 5.71 <sup>c</sup>	1.754 $\pm$ 0.106 <sup>c</sup>
BG + INCYDE (52 h)	64.84 $\pm$ 6.49 <sup>b</sup>	0.871 $\pm$ 0.099 <sup>b</sup>

published data (e.g. [Zatloukal et al., 2008](#)) a concentration of 10  $\mu$ M INCYDE was chosen, which was supplied from 24 or 52 h after the beginning of shading. We also included a treatment where leaves exposed during 52 h to filter B were changed to filter G (hereafter referred as treatment BG), with or without application of the inhibitor at the time of changing. Treatments N and B without inhibitor were run for comparison. In all cases, leaves were sampled after 100 h for the evaluation of chlorophyll content and CKX activity. As shown in [Table 2](#), the presence of INCYDE delayed chlorophyll degradation in filter G to a similar extent than in the B or N treatments when supplied after 24 h, which coincided with a significant reduction of CKX activity. The effect of INCYDE on both CKX activity and chlorophyll degradation rate was less evident when it was supplied after 52 h, except in the case of leaves previously exposed to filter B ([Table 2](#), compare treatments BG with or without the inhibitor). Altogether these results suggest that, in our experimental model, the inhibitor is effective to the extent that it is

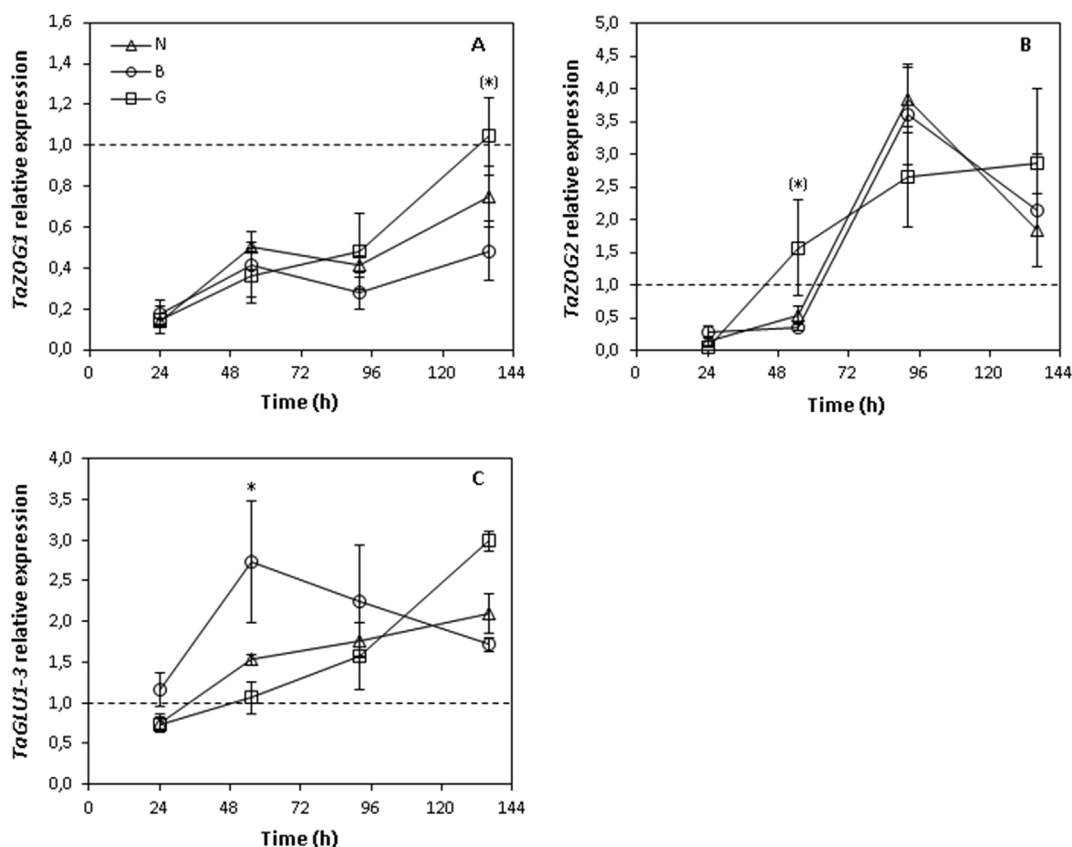


Fig. 3. Expression profile of *TaZOG1* (A), *TaZOG2* (B) and *TaGLU1-3* (C), in detached wheat leaves at different times after exposure to the neutral (N), green (G) or blue (B) filters. Data are means  $\pm$  SD ( $n = 3$ ). Asterisks alone or between brackets indicate the existence of significant or marginally significant differences, respectively, for “shading treatment” effect, at a given sampling date. Gene expression was relativized to 0 h = 1 (dashed line).

added well in advance of the increase in CKX activity, and that the down-regulation of CK degradation is an important component of the senescence delaying effect exerted by blue light.

### 3.3. Genes involved in CK inactivation and reactivation are differentially expressed depending on the light spectral quality of the shading environment

Another metabolic pathway responsible for the down-regulation of active CKs involves glucosylation mediated by the family of the zeatin *O*-glucosyltransferase (ZOG) enzyme. Given that the concentration of CK-*O*-glucosides increased with time in our experimental conditions and, particularly in the absence of BL, the expression profiles of *TaZOG1* and *TaZOG2* were studied. The expression of *TaZOG1* was markedly down regulated at 24 h after the initiation of the shading treatments (Fig. 3A). Then it increased with time, though at a consistently higher rate in leaves from treatment G than B. Leaves from treatment N showed an intermediate behaviour (Fig. 3A). As for *TaZOG1*, there was a fall in the expression of *TaZOG2* at 24 h after leaf excision, which was followed by significant increments at 54 h (treatment G) and 92 h (treatments B and N) (Fig. 3B). Subsequently, while the expression of the gene decreased in the two latter treatments, the up-regulation persisted in treatment G until the end of the experimental period.

In order to find out whether the rate of CK reactivation was also affected, the relative expression of *TaGLU* genes (encoding for  $\beta$ -glucosidase) was monitored. From all *TaGLU* family members, only *TaGLU1-3* (Song et al., 2012) was detected in our experimental conditions. In leaves from treatment B, the expression of this gene was markedly up-regulated at 54 h and it maintained around two folds higher than the initial levels until the end of the experimental period (Fig. 3C). On the contrary, the level of the transcript slightly decreased

at 24 h in treatments G and N. Thereupon, it steadily increased with time in both cases, although at an initially slower rate as compared to filter B.

### 3.4. Changes in the light spectral quality during shading affect some key components of the CK-signaling pathway

To investigate whether the effect of the light filters on the senescence rate involves the alteration of the CK signal reception, we analyzed the expression profile of putative cytokinin-receptors in wheat (hereafter referred as *TaHKs*). We identified the closest orthologues to the genes *HvHK3* and *HvHK4* (Supplementary material Fig. 3S) and analyzed their expression patterns. *TaHK3* was slightly down-regulated at 24 h after the beginning of the shading treatments, but then its expression increased to the initial levels, though at a faster rate in leaves from treatment G than in treatments B and N (Fig. 4A). The levels of *TaHK4* mRNA also markedly dropped during the beginning of the experiment, but, as opposed to *TaHK3*, its initial expression was never recovered, and at 54 h it tended to be lower in treatment G than in treatments B and N (Fig. 4B).

### 3.5. The expression profile of genes involved in blue-light signaling pathway is differentially affected by the shading treatments

As for other genes tested, the expression of *TaCRY2* markedly decreased during the first 24 h, but increased thereafter until reaching the initial levels (Fig. 5A). Surprisingly, at 92 h the *TaCRY2* transcript level was significantly higher in treatment G than B.

Although the transcript levels of *TaCIB1* also declined at 24 h after the beginning of the shading treatments, its expression rapidly increased and showed a peak at 55 h (treatment G) and at 96 h

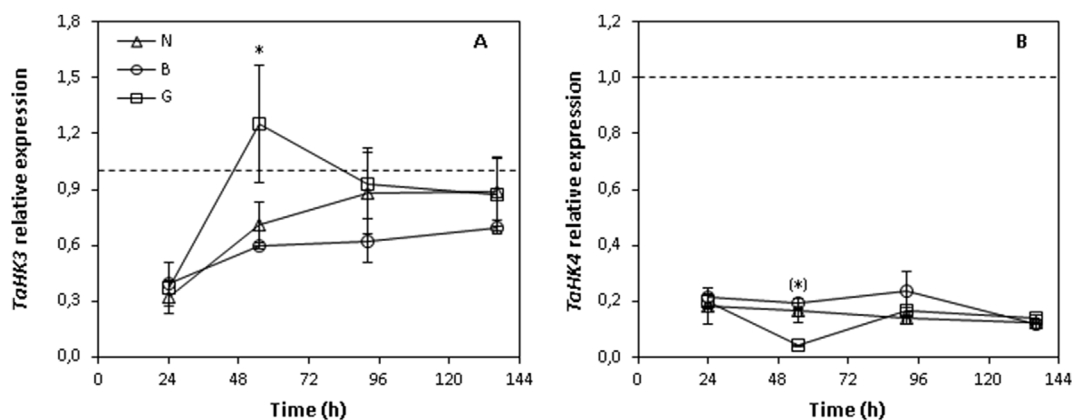


Fig. 4. Expression profile of the CK receptors *TaHK3* (A) and *TaHK4* (B) in detached wheat leaves at different times after exposure to the neutral (N), green (G) or blue (B) filters. Data are means  $\pm$  SD ( $n = 3$ ). Asterisks alone or between brackets indicate the existence of significant or marginally significant differences, respectively, for “shading treatment” effect, at a given sampling date. Gene expression was relativized to 0 h = 1 (dashed line).

(treatments B and N) (Fig. 5B). Despite the average *TaCIB1* levels in treatment G doubled those of treatment N at 55 h, the difference was not statistically significant.

The expression of *TaHY5* sharply increased in all treatments after 54 h, nevertheless the highest and significant increment was in leaves from treatment B, where it almost doubled and tripled that of treatments N and G, respectively (Fig. 5C).

#### 4. Discussion

Blue light is an important ambient cue involved in the regulatory pathway of shade-induced leaf senescence in wheat leaves (Causin and Barneix, 2007). Our present results show that the concentration of free CKs (but particularly *tZ* and *cZ*) in excised leaves decreases soon after exposure to the shading treatments. Remarkably, when BL transmission is not suppressed, a significantly higher endogenous level of *cZ* and *tZ* is maintained, which points out a possible role for these active forms in the control of senescence symptoms. Moreover, in our experimental

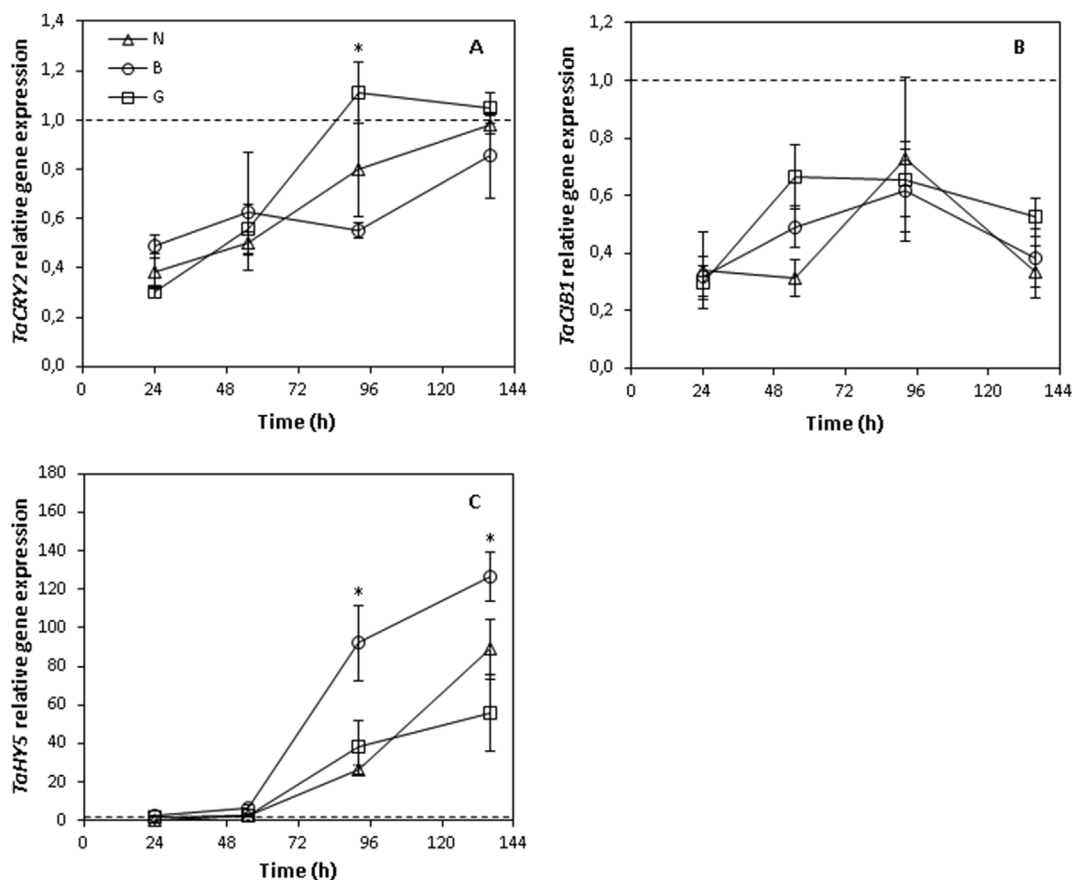


Fig. 5. Expression profile of *TaCRY2* (A), *TaCIB1* (B) and *TaHY5* (C) genes, in detached wheat leaves at different times after exposure to the neutral (N), green (G) or blue (B) filters. Data are means  $\pm$  SD ( $n = 3$ ). Asterisks alone or between brackets indicate the existence of significant or marginally significant differences, respectively, for “shading treatment” effect, at a given sampling date. Gene expression was relativized to 0 h = 1 (dashed line).

conditions, iP addition was not able to emulate the senescence delaying effect of filter B in leaves previously exposed to filter G, suggesting that this CK form would not be directly involved in the regulation of this process. This assumption is also supported by the fact that no significant differences in the endogenous levels of iP were found between leaves from treatments B and G, despite having marked differences in their senescence rates. On the contrary, tZ supply was almost as effective as BL in down-regulating the senescence rate in leaves exposed to filter G (Table 1), suggesting that the maintenance of higher endogenous levels of this form may contribute to the senescence-delaying effect by BL. With regards to cZ, in a recent review, Schäfer et al. (2015) summarize a series of studies that investigate its role in regulating plant development and defense responses to pathogen and herbivore attack, and highlight their potential role as ‘novel’ stress-response markers. Moreover, data reported by Kudo et al. (2012) suggest that cZ has physiological effects on growth and development of rice plants, and may act as an important regulator of the senescence rate in this species. Hluska et al. (2016) reported that when cZ was exogenously supplied to intact 7-d-old maize seedlings, a great proportion was immobilized as O-glucoside, even though a significant increase of tZ was also induced. These changes, however, were mostly evident in root tissue, while in the shoot the trends were less profound. Hence, despite cZ addition did not alter the senescence rate in our experimental model, further investigation is needed to assess its potential contribution to the control of this developmental process.

Different processes seem to have contributed to decrease the content of free CKs in our experimental system. Up-regulation of CK degradation, particularly in the absence of BL, is an important factor, although its relevance would be greater once senescence has been triggered rather than at the beginning of it. This is suggested both by the CKX activity and the *TaCKX1* expression profiles, the latter being by far the most up-regulated of the *TaCKX* family members evaluated. The marked up-regulation of the *CKX1* gene in senescing leaves of barley and wheat has been documented elsewhere (Conrad et al., 2007; Song et al., 2012) and its behaviour resembles that of typical senescence associated genes. It should be noted, however, that the acceleration of the senescence rate in the absence of BL did not necessarily correlate with an up-regulation of all *CKX* members. In fact, while the expression of *TaCKX4* and *TaCKX11* did not show major differences among shading conditions, a higher increase in the transcript levels of *TaCKX3* was observed in leaves exposed to filter B as compared to the remaining treatments (e.g. Fig. 2C). Moreover, *TaCKX10* mRNA levels decreased as the time exposure to shading increased. In maize leaves, *CKX10* expression is high in young leaves but markedly decreases in senescent tissues (Šmehilová et al., 2009), which is consistent with our findings. It is possible that the difference in the pattern of expression among *CKX* genes is associated to alterations in the levels of the preferred substrates of the respective enzymes, and/or to their particular sub-cellular localization (Šmehilová et al., 2009). Whatever the case, their role in the maintenance of CK homeostasis is far from being understood, since the regulation of gene expression of different *CKXs* is not only tissue- and developmentally-dependent, but also varies with the species and the stressful conditions considered (Vyrubalová et al., 2009; Song et al., 2012).

The formation of CK-O-glucosides, whose concentration increased with time, had probably an important role in the inactivation of free CKs under our experimental conditions. From the two *TaZOG* genes analyzed, only *TaZOG2* showed a consistent up-regulation with respect to the initial (t0) levels. Interestingly, the increment of *TaZOG2* transcript amount was first evident in leaves exposed to treatment G (Fig. 3B). This is in agreement with previous reports indicating that CK inactivation through O-glucosylation plays an important role in the development of senescence symptoms in different plant species (Rubia et al., 2014; Koeslin-Findeklee et al., 2015). However, to our knowledge, this is the first report showing that the expression pattern of *ZOG* genes may differ depending on the spectral quality of the light

environment in leaves senescing under shading stress. O-glucosides are regarded as reversible storage forms of CKs given that they can be reversibly converted to active forms by the action of  $\beta$ -glucosidase (Sakakibara, 2006). Interestingly, the expression of *TaGLUI-3* was up-regulated at a faster rate in leaves shaded under the blue than the green filter, which may have also contributed to maintain higher levels of free CKs.

Surprisingly, the concentration of CK-ribotides as well as CK-ribosides increased as senescence progressed, particularly in leaves exposed to the green filter. Again, cZ derivatives were the most abundant among these glycosylated forms (see Supplementary Material Table S2). While CK-ribotides are inactive, cZR was shown to have a relatively high biological activity when compared to its free base (Gajdosová et al., 2011). Nevertheless, the observed increment was not sufficient to compensate the negative effect of BL suppression on the senescence rate. Since we used excised leaves, the increment of these CK-forms cannot be attributed to an enhanced translocation from other organs. Similarly, given that the expression of *IPT* genes in wheat leaves decreases as senescence progresses (e.g. Song et al., 2012), it is unlikely that their increment was due to the up-regulation of CK-synthesis pathways. Rather, it is possible that, as for O-glucosylation, a stimulation of the conversion of free bases to their respective ribosides/ribotides was the main process responsible of their accumulation. Alternatively, tRNA degradation (which is expected to increase in senescent leaves) might also have contributed to enhance the level of cZ derivatives (Sakakibara, 2006; Vyrubalová et al., 2009). Whichever the mechanism, it is clear that the accumulation of conjugated forms of CKs is favored as senescence progresses in excised wheat leaves exposed to shading stress. Finally, it should be mentioned that changes in the translocation rate of different CKs may contribute to the alteration of CK homeostasis in attached leaves. Even though this process could not be explored in our experimental system, there is evidence that CK transport might also be under the control of light cues (e.g. Roman et al., 2016).

Given that the action of growth regulators does not only depend on their endogenous concentration but also on the presence and activity of proper receptors, we analyzed the expression profile of some components of the CK-reception system in our experimental conditions. The expression level of *TaHK3* decreased during the first 24 h after the beginning of the shading treatments, in coincidence with the marked decrement of some free CKs, but gradually recovered to the initial levels thereafter. This increment, however, occurred at an initially faster rate in leaves exposed to the G filter, even though their senescence was accelerated. Kim et al. (2006) reported that a gain-of-function mutation in the *Arabidopsis* CK-receptor AHK3 increased the sensitivity to endogenous CKs and delayed leaf senescence, while the opposite effect occurred when the expression of this receptor was suppressed. Interestingly, the AHK3 receptor is a strong preference of tZ-type CKs as compared to iP type CKs (Lomin et al., 2012). Hence, despite a faster up-regulation of *TaHK3* might have helped to enhance the perception of CK signals in treatment G, either its contribution was not sufficient to prevent the development of senescent symptoms, or other CK receptor/s and/or signaling components are involved in the regulation of senescence by light spectral quality in wheat. In this sense it is interesting to note the marked down-regulation observed for *TaHK4*, an effect that was enhanced in the absence of BL at 52 h after the beginning of the shading treatments.

There is evidence that in soybean plants the activation of the BL receptor CRY2a down-regulates the transcription activity of the senescence-promoting transcription factor CIB1, through direct protein-protein interaction (Meng et al., 2013). Apparently, the decrement in free CIB1 content did not involve changes in its mRNA levels. As for soybean plants, we did not find major differences in the expression pattern of the wheat *TaCIB1* homologue among shading treatments, which supports the evidence that its regulation by light cues would not occur at the transcriptional level. Additionally, green light has been shown to

suppress certain BL-mediated responses by reducing the semi-reduced state of the FAD chromophore (i.e. FADH\*) of active CRY (Liu et al., 2011). Given the available information and considering the lack of correlation observed between senescence rate and the expression patterns of *TaCIB1* and *TaCRY2*, further research involving the analysis of protein-protein interactions is needed to better assess their regulatory role in our experimental model.

Contrary to *TaCIB1*, the expression profile of *TaHY5* was significantly affected by the light spectral quality of the shading treatment. While the involvement of this bZIP protein in photomorphogenic responses has been extensively studied, the information regarding its role in the regulation of leaf senescence is scarce, and in some aspects contradictory. In fact, in *A. thaliana* leaves exposed to darkness HY5 is degraded via the 26S proteasome pathway, an effect that has been associated to the induction of senescence symptoms (Keech et al., 2010). On the contrary, the accumulation of HY5 due to its interaction with active phytochrome B was shown to positively regulate programmed cell death in *Arabidopsis* leaves exposed to excess red light (Chai et al., 2015). In agreement with the latter assumption, our data show that the expression of *TaHY5* increased as senescence progressed in all shading conditions, but the rate of accumulation of the transcript was higher under BL and, hence, inversely correlated with the development of senescence symptoms. A putative explanation is that either the activity or the stability of the protein is negatively regulated by other BL-altered components. Indeed, a complex regulation of HY5 functioning and/or turnover might be expected when considering that it is a point of convergence between multiple hormonal and light signaling pathways.

## 5. Conclusion

The present results demonstrate that changes in light spectral quality, and particularly BL suppression, alters CK homeostasis as well as the expression of several genes involved in their metabolism, in wheat leaves exposed to shading stress. The depletion of *tZ* rather than *cZ* or *iP* seems to have a predominant role in senescence acceleration. The analysis of gene expression profiles suggest that BL would contribute to delay the development of senescence symptoms through the retardation of both CK-degradation and CK-inactivation, as well as a faster up-regulation of some  $\beta$ -glucosidase isoforms that may restore active CKs. While the factors directly involved in the light signal perception and transduction are still elusive, the marked changes observed in the mRNA levels of *TaHY5* seem a promising cue to deepen the study of its role as well as that of BL receptors like cryptochrome in the regulation of this process.

## Contribution

Cintia Marchetti is a former graduate student of Dr. Causin's lab at the University of Buenos Aires, and is currently a PhD student at Palacký University. She was one of the main responsible of the development of the different experiments and, particularly, the analysis of CKX activity and gene expression profiles. The present work was performed as part of the research activities that both labs are developing, in the frame of an International Collaboration Program (please see “acknowledgements”). Dr. Maria Škrabišová is the coordinator of the Czech counterpart at Dr. Galuszka's lab and, together with Dr. Causin (who is the coordinator of the Argentine counterpart) and Dr. Galuszka, collaborated with the experimental design, technical training as well as the analysis of data and results discussion. Ondřej Novák contribution was essential for the determination and analysis of the different CK metabolites.

## Acknowledgements

The authors are thankful to Dr. Lukáš Spíchal for providing the INCYDE, Mgr. Josef Vrabka and the former master student Karel Mítura

for collaborating with some of the qPCR analyses. This work was partially financed by the University of Buenos Aires (project UBACyT 20020130200256BA) and by the International Cooperation Program between the Ministry of Science, Technology and Productive Innovation of Argentina (MINCYT, Project ARC/14/13) and the Ministry of Education, Youth and Sports of the Czech Republic (MEYS, Grant N° 7AMB15AR011; NPU-I, Grant N° LO1204).

## Appendix A. Supplementary data

Supplementary data related to this article can be found at <https://doi.org/10.1016/j.plaphy.2018.08.005>.

## References

- Antoniadi, I., Plačková, L., Simonovik, B., Doležal, K., Turnbull, C., Ljung, K., Novák, O., 2015. Cell-type specific cytokinin distribution within the Arabidopsis primary root apex. *Plant Cell* 27, 1955–1967.
- Bradford, M.M., 1976. A rapid and sensitive method for the quantitation of microgram quantities of protein utilizing the principle of protein-dye binding. *Anal. Biochem.* 72, 248–254.
- Causin, H.F., Barneix, A.J., 2007. The role of oxidative metabolism in the regulation of leaf senescence by the light environment. *Int. J. Plant Dev. Biol.* 1, 239–244.
- Causin, H.F., Roberts, I.N., Criado, M.V., Gallego, S.M., Pena, L.B., Ríos, M., del, C., Barneix, A.J., 2009. Changes in hydrogen peroxide homeostasis and cytokinin levels contribute to the regulation of shade-induced senescence in wheat leaves. *Plant Sci.* 177, 698–704.
- Causin, H.F., Marchetti, C.F., Pena, L.B., Gallego, S.M., Barneix, A.J., 2015. Down-regulation of catalase activity contributes to senescence induction in wheat leaves exposed to shading stress. *Biol. Plant.* 59, 154–162.
- Chai, T., Zhou, J., Liu, J., Xing, D., 2015. LSD1 and HY5 antagonistically regulate red light induced-programmed cell death in Arabidopsis. *Front. Plant Sci.* 6, 292. <https://doi.org/10.3389/fpls.2015.00292>.
- Conrad, K., Motyka, V., Schlüter, T., 2007. Increase in activity, glycosylation and expression of cytokinin oxidase/dehydrogenase during the senescence of barley leaf segments in the dark. *Physiol. Plantarum* 130, 572–579.
- Dobrev, P.I., Kamínek, M., 2002. Fast and efficient separation of cytokinins from auxin and abscisic acid and their purification using mixed-mode solidphase extraction. *J. Chromatogr. A* 950, 21–29.
- Frébert, I., Sébela, M., Galuszka, P., Werner, T., Schülling, T., Peč, P., 2002. Cytokinin oxidase/cytokinin dehydrogenase assay: optimized procedures and applications. *Anal. Biochem.* 306, 1–7.
- Gajdosová, S., Spíchal, L., Kamínek, M., Hoyerová, K., Novák, O., Dobrev, P.I., Galuszka, P., Klíma, P., Gaudinová, A., Zizková, E., Hanus, J., Dancák, M., Trávníček, B., Pesek, B., Krupicka, M., Vanková, R., Strnad, M., Motyka, V., 2011. Distribution, biological activities, metabolism, and the conceivable function of cis-zeatin-type cytokinins in plants. *J. Exp. Bot.* 62, 2827–2840.
- Galuszka, P., Frébertová, J., Werner, T., Yamada, M., Strnad, M., Schülling, T., Frébert, I., 2004. Cytokinin oxidase/dehydrogenase genes in barley and wheat: cloning and heterologous expression. *Eur. J. Biochem.* 271, 3990–4002.
- Hluska, T., Dobrev, P.I., Tarkowskác, D., Frébertová, J., Zalabák, D., Kopečný, D., Plíhal, O., Kokáš, F., Briozzo, P., Zatloukal, M., Motyka, V., Galuszka, P., 2016. Cytokinin metabolism in maize: novel evidence of cytokinin abundance, interconversions and formation of a new *trans*-zeatin metabolic product with a weak anticytokinin activity. *Plant Sci.* 247, 127–137.
- Keech, O., Pesquet, E., Gutierrez, L., Ahad, A.I., Bellini, C., Smith, S.M., Gardeström, P., 2010. Leaf senescence is accompanied by an early disruption of the microtubule network in Arabidopsis. *Plant Physiol.* 154, 1710–1720.
- Kim, H.J., Ryu, H., Hong, S.H., Woo, H.R., Lim, P.O., Lee, I.C., Sheen, J., Nam, H.G., Hwang, I., 2006. Cytokinin-mediated control of leaf longevity by AHK3 through phosphorylation of ARR2 in Arabidopsis. *P. Natl. Acad. Sci. USA* 103, 814–819.
- Koeslin-Findeklee, F., Becker, M.A., van der Graaff, E., Roitsch, T., Horst, W.J., 2015. Differences between winter oilseed rape (*Brassica napus* L.) cultivars in nitrogen starvation-induced leaf senescence are governed by leaf-inherent rather than root-derived signals. *J. Exp. Bot.* 66, 3669–3681.
- Kudo, T., Makita, N., Kojima, M., Tokunaga, H., Sakakibara, H., 2012. Cytokinin activity of cis-zeatin and phenotypic alterations induced by overexpression of putative cis-zeatin-O-glucosyltransferase in rice. *Plant Physiol.* 160, 319–331.
- Liu, H., Liu, B., Zhao, C., Pepper, M., Lin, C., 2011. The action mechanisms of plant cryptochromes. *Trends Plant Sci.* 16, 684–691.
- Liu, H., Wang, Q., Liu, Y., Zhao, X., Imaizumi, T., Somers, D.E., Tobin, E.M., Lin, C., 2013. Arabidopsis CRY2 and ZTL mediate blue-light regulation of the transcription factor CIB1 by distinct mechanisms. *P. Natl. Acad. Sci. USA* 110, 17582–17587.
- Lomin, S.N., Yonekura-Sakakibara, K., Romanov, G.A., Sakakibara, H., 2011. Ligand-binding properties and subcellular localization of maize cytokinin receptors. *J. Exp. Bot.* 62, 5149–5159.
- Lomin, S.N., Krivosheev, D.M., Steklov, M.Y., Osolodkin, D.I., Romanov, G.A., 2012. Receptor properties and features of cytokinin signaling. *Acta Naturae* 4, 31–45.
- Meng, Y., Li, H., Wang, Q., Liu, B., Lin, C., 2013. Blue light-dependent interaction between cryptochrome2 and CIB1 regulates transcription and leaf senescence in soybean. *Plant Cell* 25, 4405–4420.

- Nishimura, C., Ohashi, Y., Sato, S., Kato, T., Tabata, S., Ueguchi, C., 2004. Histidine kinase homologs that act as cytokinin receptors possess overlapping functions in the regulation of shoot and root growth in *Arabidopsis*. *Plant Cell* 16, 1365–1377.
- Pfaffl, M.W., 2001. A new mathematical model for relative quantification in real-time RT-PCR. *Nucleic Acids Res.* 29, e45.
- Roman, H., Girault, T., Barbier, F., Péron, T., Brouard, N., Pěnčík, A., Novák, O., Vian, A., Sakr, S., Lothier, J., Le Gourrierec, J. Leduc N., 2016. Cytokinins are initial targets of light in the control of bud outgrowth. *Plant Physiol. (Wash. D C)* 172, 489–509.
- Rubia, L., Rangan, L., Choudhury, R.R., Kamínek, M., Dobrev, P., Malbeck, J., Fowler, M., Slater, A., Scott, N., Bennett, J., Peng, S., Khush, G.S., Elliott, M., 2014. Changes in the chlorophyll content and cytokinin levels in the top three leaves of new plant type rice during grain filling. *J. Plant Growth Regul.* 33, 66–76.
- Sakakibara, H., 2006. CYTOKININS: activity, biosynthesis, and translocation. *Annu. Rev. Plant Biol.* 57, 431–449.
- Schäfer, M., Brütting, C., Meza-Canales, I.D., Groškinsky, D.K., Vankova, R., Baldwin, I.T., Meldau, S., 2015. The role of cis-zeatin-type cytokinins in plant growth regulation and mediating responses to environmental interactions. *J. Exp. Bot.* 66, 4873–4884.
- Schlüter, T., Leide, J., Conrad, K., 2011. Light promotes an increase of cytokinin oxidase/dehydrogenase activity during senescence of barley leaf segments. *J. Plant Physiol.* 168, 694–698.
- Schmülling, T., Werner, T., Riefler, M., Krupková, E., Bartrina, Y., Manns, I., 2003. Structure and function of cytokinin oxidase/dehydrogenase genes of maize, rice, *Arabidopsis* and other species. *J. Plant Res.* 116, 241–252.
- Šmečilová, M., Galuszka, P., Bilyeu, K.D., Jaworek, P., Kowalska, M., Šebela, M., Sedláčková, M., English, J.T., Frébort, I., 2009. Subcellular localization and biochemical comparison of cytosolic and secreted cytokinin dehydrogenase enzymes from maize. *J. Exp. Bot.* 60, 2701–2712.
- Song, J., Jiang, L., Jameson, P.E., 2012. Co-ordinate regulation of cytokinin gene family members during flag leaf and reproductive development in wheat. *BMC Plant Biol.* 12, 78.
- Vandenbusche, F., Habricot, Y., Condiff, A.S., Maldiney, R., Van Der Straeten, D., Ahmad, M., 2007. HY5 is a point of convergence between cryptochrome and cytokinin signalling pathways in *Arabidopsis thaliana*. *Plant J.* 49, 428–441.
- Vandesompele, J., De Preter, K., Pattyn, F., Poppe, B., Van Roy, N., De Paepe, A., Speleman, F., 2002. Accurate normalization of real-time quantitative RT-PCR data by geometric averaging of multiple internal control genes. *Genome Biol.* 3 research0034.I-0034.II.
- Vyroubalová, S., Václavíková, K., Turecková, V., Novák, O., Šmečilová, M., Hluska, T., Ohnoutková, L., Frébort, I., Galuszka, P., 2009. Characterization of new maize genes putatively involved in cytokinin metabolism and their expression during osmotic stress in relation to cytokinin levels. *Plant Physiol.* 151, 433–447.
- Wang, W., Hao, Q., Tian, F., Li, Q., Wang, W., 2016. The stay-green phenotype of wheat mutant *tasg1* is associated with altered cytokinin metabolism. *Plant Cell Rep.* 35, 585–599.
- Zatloukal, M., Gemrotová, M., Doležal, K., Havlíček, L., Spíchal, L., Strnad, M., 2008. Novel potent inhibitors of *A. thaliana* cytokinin oxidase/dehydrogenase. *Bioorgan. Med. Chem.* 16, 9268–9275.



# Whole transcriptome analysis of transgenic barley with altered cytokinin homeostasis and increased tolerance to drought stress

Petr Vojta<sup>1,2</sup>, Filip Kokáš<sup>1</sup>, Alexandra Husičková<sup>3</sup>, Jiří Grúz<sup>4</sup>, Veronique Bergougnoux<sup>1</sup>, Cintia F. Marchetti<sup>1</sup>, Eva Jiskrová<sup>1</sup>, Eliška Ježilová<sup>3</sup>, Václav Mik<sup>4</sup>, Yoshihisa Ikeda<sup>1</sup> and Petr Galuszka<sup>1</sup>

<sup>1</sup> Department of Molecular Biology, Centre of the Region Haná for Biotechnological and Agricultural Research, Faculty of Science, Palacký University in Olomouc, Šlechtitelů 27, 783 71 Olomouc, Czech Republic

<sup>2</sup> Institute of Molecular and Translational Medicine, Faculty of Medicine and Dentistry, Palacký University in Olomouc, Hněvotínská 1333/5, 779 00 Olomouc, Czech Republic

<sup>3</sup> Department of Biophysics, Centre of the Region Haná for Biotechnological and Agricultural Research, Faculty of Science, Palacký University in Olomouc, Šlechtitelů 27, 783 71 Olomouc, Czech Republic

<sup>4</sup> Department of Chemical Biology and Genetics, Centre of the Region Haná for Biotechnological and Agricultural Research, Faculty of Science, Palacký University in Olomouc, Šlechtitelů 27, 783 71 Olomouc, Czech Republic

Cytokinin plant hormones have been shown to play an important role in plant response to abiotic stresses. Herein, we expand upon the findings of Pospíšilová et al. [30] regarding preparation of novel transgenic barley lines overexpressing *cytokinin dehydrogenase 1* gene from *Arabidopsis* under the control of mild root-specific promoter of maize  $\beta$ -glycosidase. These lines showed drought-tolerant phenotype mainly due to alteration of root architecture and stronger lignification of root tissue. A detailed transcriptomic analysis of roots of transgenic plants subjected to revitalization after drought stress revealed attenuated response through the HvHK3 cytokinin receptor and up-regulation of two transcription factors implicated in stress responses and abscisic acid sensitivity. Increased expression of several genes involved in the phenylpropanoid pathway as well as of genes encoding *arogenate dehydratase/lyase* participating in phenylalanine synthesis was found in roots during revitalization. Although more precursors of lignin synthesis were present in roots after drought stress, final lignin accumulation did not change compared to that in plants grown under optimal conditions. Changes in transcriptome indicated a higher auxin turnover in transgenic roots. The same analysis in leaves revealed that genes encoding putative enzymes responsible for production of jasmonates and other volatile compounds were up-regulated. Although transgenic barley leaves showed lower chlorophyll content and down-regulation of genes encoding proteins involved in photosynthesis than did wild-type plants when cultivated under optimal conditions, they did show a tendency to return to initial photochemical activities faster than did wild-type leaves when re-watered after severe drought stress. In contrast to optimal conditions, comparative transcriptomic analysis of revitalized leaves displayed up-regulation of genes encoding enzymes and proteins involved in photosynthesis, and especially those encoded by the chloroplast genome. Taken together, our results indicate that the partial cytokinin insensitivity induced in barley overexpressing cytokinin dehydrogenase contributes to tolerance to drought stress.

Corresponding author: Galuszka, P. ([petr.galuszka@upol.cz](mailto:petr.galuszka@upol.cz))

## Introduction

Cytokinins (CKs) are plant hormones which together with auxins mainly influence plant morphology. Their role in other physiological processes, such as senescence and nutrient remobilization, is very well described [1]. Evidence, mostly from studies of *Arabidopsis* (*Arabidopsis thaliana*), suggests also an important role of CKs in the regulation of responses to environmental stresses [2]. CK-deficient *Arabidopsis* plants exhibited a strong stress-tolerant phenotype associated with increased cell membrane integrity and abscisic acid (ABA) hypersensitivity [3]. ABA's stress-related role consists mainly in induction of stomatal closure to prevent water losses under conditions of water limitation. Moreover, loss-of-function mutants of CK receptors and proteins involved in the CK-signaling pathway have been shown to be strongly tolerant to drought and salt stress because they up-regulated many stress-inducible genes [4,5]. Similarly, rice seedlings with knock-down proteins of the CK transduction pathway have been observed to be tolerant of osmotic stress but hypersensitive to salt stress [6]. Activated CK receptors negatively control osmotic stress responses and thus confirm that reduced CK status is a prerequisite for better drought tolerance.

On the other hand, increased drought tolerance or avoidance by stress-induced CK accumulation has been proven in several plant species [7–12]. A transgenic approach has exploited expression of the CK biosynthetic *isopentenyl transferase* (*IPT*) gene under a stress- and maturation-inducible promoter. Under drought-stress conditions, the transgenic plants maintained high photosynthetic activity in contrast to control plants due to the direct effect of CKs on delaying leaf senescence. The acquired drought tolerance was also due to CKs' effect on maintenance of nitrate acquisition from soil [13]. Thus, stress-induced CK synthesis in these transgenic plants promoted sink strengthening through the maintenance and coordination of N and C assimilation during water stress.

In abiotic stress responses, CKs can act in orchestration with other phytohormones. Auxin's role in drought tolerance has been demonstrated when increased activity of auxin conjugating enzyme, which reduces auxin maxima in leaves, led to the accumulation of late-embryogenesis abundant proteins responsible for the switch from plant growth to stress adaptation [14]. Auxin is able to induce the expression of genes encoding enzymes participating in biosynthesis of such stress-related hormones as ethylene [15]; vice versa, ethylene promotes local auxin biosynthesis and consequently reduces root cell elongation [16]. As CKs are known to affect production of both auxin and ethylene, coordinated regulation of hormonal biosynthetic pathways could play a crucial role in plants' adaptation to abiotic stresses [17]. Plants with stress-induced CK production showed up-regulation of brassinosteroid synthesis and signaling genes [11,18]. Brassinosteroids act synergistically with another group of plant hormones, gibberellins (GAs), due to shared components in their signaling pathways [19]. Transgenic *Arabidopsis* seedlings constitutively overexpressing GA-responsive genes exhibited improved tolerance to various abiotic stresses; stress tolerance was accompanied by biosynthesis of salicylic acid [20], another plant hormone mainly implicated in stress responses.

Plants exposed to drought stress show an alteration of CK content. Hormonal analysis of wild-type (WT) maize leaves subjected to drought showed a gradual decline in CK and GA contents

during stress [21]. A comprehensive study on maize seedlings exposed to salt and osmotic stress also demonstrated rapid decline in some CK forms due to enforced CK catabolism. During acclimatization, however, accelerated CK metabolism led to a moderate increase in active CK forms [22]. Higher accumulation of all CK forms was also determined in tobacco exposed to severe drought stress [23]. Hence, accumulation of active CKs among other processes might contribute to the mechanisms by which plants overcome stress status and avoid growth inhibition. Regarding stress signaling, CKs do not, due to the slow response of their biosynthetic genes to stress induction, have a direct function similar to ABA, which directly affects stomatal closure [22].

Maintenance of high photosynthetic capacity is an important prerequisite for preserving crop yield under adverse environmental conditions. Although increasing CK content by senescence-regulated expression of a CK biosynthetic gene is an efficient tool for prolonging leaf photosynthetic activity [24], engineered wheat plants with senescence-regulated CK production showed no differences in yield-related parameters [25]. Shoot growth inhibition and promotion of root growth have been regarded as advantageous for crop stability under stressful conditions and constitute an integral part of plant stress tolerance [26,27]. Accordingly, plants with reduced shoot-to-root ratios as a consequence of CK deficiency showed greater tolerance to or avoidance of drought stress [28,29]. Hence, down- and up-regulation of CK levels *in planta* can have a synergistically positive effect on enhanced tolerance to water deficit: in the first case, through alteration of plant morphology to a root architecture that is better adapted to withstand water deprivation, and, in the second case, through activation of photosynthetic processes and source–sink relations.

Recently, we prepared several barley transgenic lines overexpressing a cytokinin catabolic enzyme—cytokinin dehydrogenase 1 (CKX) from *Arabidopsis* targeted to various subcellular compartments. Transgenic barley exhibited greater tolerance to or avoidance of drought stress that most probably was due to higher lignification and changes in root morphology [30]. While focusing primarily on post-stress revitalization, the in-depth transcriptomic analysis of our transgenic barley lines aimed to clarify and describe in detail all processes that enable CK-deficient barley plants to cope better with drought.

## Material and methods

### *Plant material and cultivation*

Transgenic and WT plants of the spring barley cultivar Golden Promise were grown in an environmental chamber with a photoperiod of 15°C/16 hours light and 12°C/8 hours darkness. The light source was a combination of mercury tungsten lamps and sodium lamps providing an intensity of 300  $\mu\text{mol m}^{-2} \text{s}^{-1}$ . Plants were cultivated in a 2:1 mixture of soil and perlite (Perlit Ltd., Czech Republic). Soil composition was 1:1 professional substrate (peat type) for growing plants (Rašelina Soběslav, Czech Republic) and a muck-type arable soil from the Olomouc Region (Czech Republic).

### *Application of drought stress*

For transcriptomic analysis of the root system exposed to drought stress, plants were grown hydroponically in a modified Hoagland solution [31] within an environmental chamber under the same



conditions as given above. The experiment was performed in the following arrangement: 2/3 of each vessel was filled with two transgenic genotypes and 1/3 with WT plants. In total, 27 plants from each genotype were cultivated together in three vessels. Three plants were pooled per biological replicate. Drought stress was induced on plants 4 weeks old by pouring the solution out of the growth vessel after the plants had been temporarily removed. Plants were then returned to the vessel, where they were further kept for another 24 hours, after which the solution was poured back into the vessel. The entire root system was collected after 24 hours of stress and after 14 days of revitalization. The youngest fully expanded leaves were collected for analyzing chlorophyll content every 2nd or 3rd day.

In order to perform transcriptome analysis of the upper part, barley plants were cultivated in shallow trays (30 cm × 20 cm with a depth of 5 cm) filled with soil and watered on a daily basis. Drought stress was applied to 4-week-old plants by keeping them without watering for 4 days, after which regularly watering on a daily basis was resumed. Photosynthetic parameters and relative water content [32] were determined on the youngest fully expanded leaves. Samples were collected 12 hours after the last watering, the 4th day of the stress application, 12 hours after re-watering, and after 14 days of revitalization.

#### Real-time PCR analysis

Isolation of total RNA was performed using an RNAqueous Kit (Life Technologies, USA). Isolated RNA was then treated using a TURBO DNA-free Kit (Life Technologies) and purified using magnetic beads (Agencourt RNA-CLEAN XP, Beckman Coulter, USA). cDNA was obtained using a RevertAid First Strand cDNA Synthesis Kit (Fermentas, Lithuania). Real-time PCR was set up with cDNA as template in total volume of 10  $\mu$ L containing POWER SYBR Green PCR Master Mix (Life Technologies) and 300 nM of each primer. Reactions were run in the StepOnePlus™ Real-Time PCR System using the default program (Applied Biosystems, USA). Primers were designed using Primer Express 3.0 software (Supplemental Table S1).

The number of transcripts per ng of isolated total RNA was detected based on calibration curves made with genes cloned into the transformation vector. The relative quantification of most abundant endogenous genes involved in CK metabolism was made using the  $\Delta\Delta$ Ct method [33] with barley cyclophilin, actin, and elongation factor 1 (AK354091.1, AK248432.1, AK361008.1) analyzed as reference genes and then evaluated statistically using DataAssist v3.0 Software (Life Technologies). Each measurement consisted of four biological and two technical replicates.

#### RNA-seq analysis

Working with 2.5  $\mu$ g of total RNA from each sample, extracted as described above, Illumina® TruSeq® Stranded mRNA Sample Preparation Kit (Illumina, USA) was used for cDNA library preparation. Library concentration was assessed using a Kapa Library Quantification Kit (Kapa Biosystems, USA) and all libraries were pooled to a final 8 pM concentration for cluster generation and sequencing. The clusters were generated using an Illumina® TruSeq® SR Cluster Kit v3 cBot HS and sequenced on a HiSeq SR Flow Cell v3 with a HiSeq 2500 Sequencing System. Two independent libraries were prepared for each genotype at each time point from two biological replicates (3 pooled plants in each).

The reads generated by sequencing were mapped to the reference genome of *Hordeum vulgare* v.25 (Ensembl, UK) using the TopHat2 v.2.0.12 splice-read mapper [34] with default parameters. The reads mapped to the transcripts annotated in the reference genome were quantified by using HTSeq v.0.6.0 [35] with respect to the stranded library. The tests for differential gene expression were performed using the DESeq2 package [36] implemented in R (R Development Core Team, 2008). The technical replicates were first analyzed as two independent experiments, which yielded similar results (see Figure 4 in Ref [37]). Thereafter, technical replicates were merged into one technical replicate to obtain higher coverage of the reference transcriptome. Gene ontology (GO) annotation of the reference genome was improved using the Blast2GO v.3.0 program [38], nt database (b2g\_Jan15), the ncbi-blast+ v.2.2.28 program [39], as well as the UniProtKB (<http://www.uniprot.org/>, 02.2015) and PGSB (<http://pgsb.helmholtz-muenchen.de/plant/>, 31.07.2014) databases (see Figure 1 in Ref [37]). This additional GO annotation helped to increase the number of GO annotated genes to 17,885 (from a total of 26,074 predicted genes in barley).

#### Quantification of lignin and its precursor

Lignin quantification was carried out in protein-free cell wall fractions using the acetyl bromide method [40]. Cinnamic and benzoic acids were determined by an LC-MS method described previously [41]. Monolignols and aromatic amino acids were analyzed with a UHPLC-QTOF-MS system (Synapt G2-Si, Waters, UK) operating in positive ion mode. Coumaryl, coniferyl and sinapyl alcohols were quantified by detecting product ions of the corresponding  $[M-H_2O^+H]^+$  ions (i.e., 133 > 105.08, 163 > 131.06, and 193 > 105.08, respectively) while using  $^{13}C_6$ -isovanillic acid (157 > 114.05) as an internal standard. The relative levels of aromatic amino acids were estimated from peak area acquired in resolution MS mode. All compounds were identified and quantified based on authentic standards.

#### Measurement of chlorophyll content

Chlorophyll content was determined using a chlorophyll content meter (CCM-300, Opti-Sciences, Hudson, NH, USA) in plants 7–42 days old that were grown hydroponically under drought and control conditions. Measurement for each line consisted of at least 15 biological replicates and two technical replicates. Each transgenic genotype was grown together with the same number of WT barley plants in the same plastic vessel.

#### Chlorophyll fluorescence imaging

Chlorophyll fluorescence was monitored on the abaxial side of the youngest fully developed attached leaves using an imaging system (FluorCam 700 MF, Photon Systems Instruments, Czech Republic). All measurements were performed on at least four replicates. To measure fluorescence signal, short (microseconds in length) measuring flashes of red light placed 20 ms apart were applied and the signals detected during the measuring flash and just prior to the measuring flash were subtracted. The overall integral light intensity of the measuring flashes was low enough not to close the photosystem II reaction centers but still able to measure fluorescence. The minimum chlorophyll fluorescence yield ( $F_0$ ) was determined after 40 min of dark adaptation by application of

the measuring flashes only. A saturating pulse of 1.6 s (white light,  $2500 \mu\text{mol m}^{-2} \text{s}^{-1}$ ) was applied to determine the maximum chlorophyll fluorescence yield in a dark-adapted state ( $F_M$ ). The leaves were then exposed to red actinic light ( $200 \mu\text{mol m}^{-2} \text{s}^{-1}$ ) for 8 min. After 5 s, the actinic light was accompanied by a series of saturating pulses placed 30 s apart to estimate the maximum fluorescence yield during light adaptation ( $F'_M$ ). The non-photochemical quenching of chlorophyll fluorescence was calculated as  $(F_M - F'_M)/F'_M$  and the coefficient of photochemical quenching ( $q_P$ ) as  $(F'_M - F_t)/(F'_M - F'_0)$ , where  $F_t$  is the fluorescence yield measured just prior to application of the saturating pulse and  $F'_0$  is the minimal fluorescence for a light-adapted state calculated as  $F_0/((F_V/F_M) + (F_0/F'_M))$  [42].

#### Gas exchange parameters

Gas exchange parameters were measured on the youngest fully developed, attached leaves using an open gas-exchange system (Li-6400, LI-COR Biosciences Inc., Lincoln, NE, USA). Six to eight plants of each transgenic line were measured for each treatment (control, stress, and re-watering). The measurement was started after 3 min of adaptation to chamber conditions ( $380 \mu\text{mol CO}_2 \text{mol}^{-1}$ , 70% relative humidity,  $16^\circ\text{C}$ ). The rate of  $\text{CO}_2$  assimilation ( $A$ ,  $\text{mmol (CO}_2\text{) m}^{-2} \text{s}^{-1}$ ), stomatal conductance ( $g_s$ ,  $\text{mol (H}_2\text{O) m}^{-2} \text{s}^{-1}$ ), and transpiration rate ( $\text{mol (H}_2\text{O) m}^{-2} \text{s}^{-1}$ ) were measured every 30 s over 5 min. Intrinsic water-use efficiency ( $\text{mmol (CO}_2\text{) mol}^{-1} \text{(H}_2\text{O)}$ ) was calculated as the ratio of averaged values of  $A$  and  $g_s$ .

#### Water potential

The water potential was estimated on four leaves of each treatment and for each line using a Model 600 pressure chamber instrument from PMS Instrument Company (Albany, OR, USA).

#### Statistical analysis

Two-sample *t*-tests and ANOVA (Tukey and Bonferroni tests) at significance level 0.05 were performed using OriginPro 8.5.1 (OriginLab Corporation, Northampton, MA, USA). Some of the *t*-tests were carried out with STATISTICA 12 (StatSoft CR, Czech Republic).

### Results and discussion

Two genotypes of *AtCKX1*-overexpressing transgenic barley, which were not affected in their yield parameters, were selected for detailed transcriptomic analysis: one targeting expressed recombinant CKX protein to vacuoles (*vAtCKX1*) and the other with predicted cytosolic localization (*cAtCKX1*). The genotype expressing a secreted CKX to apoplast (*aAtCKX1*) was negatively affected in its yield parameters and was used only for the analysis of photosynthetic parameters. To study differences in transcriptomes, 28 single-read sequencing libraries were prepared and sequenced on an Illumina Hi-Seq 2500 system. The basic features of all sequenced libraries are summarized in Supplemental Table S2.

#### Photosynthetic parameters of transgenic plants under optimal conditions and drought stress

Heterologous expression of *AtCKX1* negatively affected chlorophyll content, which was estimated in the developmental stage

during which the highest expression of the transgene was detected [30]. In comparison to WT leaves of plants cultivated hydroponically, 25%, 11%, and 6% decreases were measured in 4- to 5-week-old leaves of *vAtCKX1*, *aAtCKX1*, and *cAtCKX1* plants, respectively (Fig. 1a). All transgenic genotypes maintained chlorophyll content around WT levels when exposed to two periods of drought stress and re-watering, and this was in contrast to their reduced levels observed under optimal conditions (Fig. 1b).

To examine changes in the photosynthetic apparatus, the chlorophyll fluorescence induction and gas exchange of leaves were examined in the plants cultivated in soil. Drought stress, detected as bending of the leaves, was accompanied by decreases in  $g_s$  and, consequently, decreases in transpiration rate and  $\text{CO}_2$  assimilation (Table 1). Lower accessibility of  $\text{CO}_2$  due to closed stomata led to lower usage of light excitations for photochemical reactions (i.e., a decrease in photochemical quenching and an induced increase in the regulated thermal dissipation of absorbed light) and a rise in the non-photochemical quenching of chlorophyll fluorescence (Table 1). Increases in non-photochemical quenching of chlorophyll fluorescence of light-adapted leaves is a known consequence of drought stress [43,44]. Such a response reflects the usage of absorbed excitation energy to regulate heat dissipation and serves as a protective mechanism against damage to photosystem II. As a consequence, drought stress induces a decrease in photochemical quenching [45] and reflects fewer photosystem II reaction centers being open for photosynthetic electron transport. Interestingly, both of these changes caused by water deficiency were least marked in the *cAtCKX1* and *aAtCKX1* genotypes despite the fact that they had lower  $g_s$  (Table 1).

The most notable changes were observed after 24 hours of re-watering: when plants had once again been watered, all measured parameters had a tendency to return to their initial values and the return of photochemical activities in all three transgenic lines was more noticeable in comparison to those for the WT plants (Table 1).

Gas exchange parameters did not differ between genotypes prior to stress treatment. Drought stress did, however, induce a more significant decrease in  $g_s$  in the transgenic *cAtCKX1* and *aAtCKX1* genotypes compared to WT. The strong decrease in  $g_s$  protects plants from unendurable loss of water through transpiration; on the other hand, it results in lower accessibility of  $\text{CO}_2$  for photosynthesis. It is noteworthy that although the *cAtCKX1* plants still had significantly reduced  $g_s$  after 24 hours of re-watering, their rate of  $\text{CO}_2$  assimilation had by that time completely recovered to its initial value. Our results indicate that *cAtCKX1* barley was the most effective in using water for photosynthesis (Table 1). While the water potential of WT plants after 24 hours of re-watering remained almost unchanged in comparison to stressed plants, all transgenic genotypes had significant increases in this value (Table 1). Transgenic plants with altered root morphology and stronger lignification therefore have greater ability to redistribute the necessary amount of water to the aerial parts during recovery from drought stress.

#### Effect of cytokinin deficiency on the aerial part of *vAtCKX1* plants under optimal conditions

The mild expression of *AtCKX1* under the control of  $\beta$ -glucosidase promoter had a positive effect on root system development

**(a)** Chlorophyll content in mg m<sup>-2</sup>

Plant age in days	<i>vAtCKX1</i>		WT		<i>cAtCKX1</i>		WT		<i>aAtCKX1</i>		WT	
	7	460 ± 98	436 ± 57	483 ± 70	485 ± 64	450 ± 34	485 ± 64	532 ± 37	518 ± 57	496 ± 51	496 ± 55	492 ± 47
9	475 ± 62	454 ± 77	N.D. ± N.D.	518 ± 57	532 ± 37	518 ± 57	496 ± 51	496 ± 55	492 ± 47	555 ± 43	476 ± 74	535 ± 33
11	415 ± 56	425 ± 56	N.D. ± N.D.	496 ± 55	496 ± 51	496 ± 55	492 ± 47	555 ± 43	476 ± 74	535 ± 33	462 ± 21	459 ± 38
14	481 ± 27	492 ± 28	643 ± 59	597 ± 66	492 ± 47	555 ± 43	476 ± 74	535 ± 33	462 ± 21	459 ± 38	597 ± 49	592 ± 45
16	560 ± 24	551 ± 26	529 ± 66	553 ± 36	476 ± 74	535 ± 33	462 ± 21	459 ± 38	597 ± 49	592 ± 45	505 ± 26	534 ± 45
18	627 ± 39	618 ± 38	529 ± 66	553 ± 36	462 ± 21	459 ± 38	597 ± 49	592 ± 45	505 ± 26	534 ± 45	603 ± 42	589 ± 39
21	687 ± 29	651 ± 61	N.D. ± N.D.	N.D. ± N.D.	597 ± 49	592 ± 45	505 ± 26	534 ± 45	603 ± 42	589 ± 39	608 ± 34	628 ± 34
23	682 ± 39	680 ± 50	567 ± 28	576 ± 31	603 ± 42	589 ± 39	608 ± 34	628 ± 34	547 ± 37	582 ± 44	476 ± 62	532 ± 43
25	544 ± 58	581 ± 44	666 ± 68	664 ± 38	547 ± 37	582 ± 44	476 ± 62	532 ± 43	550 ± 52	591 ± 68	575 ± 59	581 ± 71
28	461 ± 83	555 ± 46	689 ± 50	712 ± 54	550 ± 52	591 ± 68	575 ± 59	581 ± 71	550 ± 52	591 ± 68	575 ± 59	581 ± 71
30	451 ± 47	599 ± 62	675 ± 41	716 ± 35	550 ± 52	591 ± 68	575 ± 59	581 ± 71	550 ± 52	591 ± 68	575 ± 59	581 ± 71
35	389 ± 55	528 ± 61	783 ± 32	791 ± 33	550 ± 52	591 ± 68	575 ± 59	581 ± 71	550 ± 52	591 ± 68	575 ± 59	581 ± 71
39	502 ± 63	577 ± 71	773 ± 65	721 ± 37	550 ± 52	591 ± 68	575 ± 59	581 ± 71	550 ± 52	591 ± 68	575 ± 59	581 ± 71
42	536 ± 68	552 ± 74	736 ± 59	691 ± 61	550 ± 52	591 ± 68	575 ± 59	581 ± 71	550 ± 52	591 ± 68	575 ± 59	581 ± 71

**(b)**

Plant age in days	<i>vAtCKX1</i>		WT		<i>cAtCKX1</i>		WT		<i>aAtCKX1</i>		WT	
	2 hours long drought		2 hours long drought		2 hours long drought		2 hours long drought		2 hours long drought		2 hours long drought	
7	404 ± 96	395 ± 80	N.D. ± N.D.	N.D. ± N.D.	467 ± 30	435 ± 58	517 ± 44	483 ± 64	473 ± 53	422 ± 66	425 ± 62	413 ± 48
11	450 ± 31	430 ± 82	N.D. ± N.D.	N.D. ± N.D.	517 ± 44	483 ± 64	473 ± 53	422 ± 66	425 ± 62	413 ± 48	489 ± 71	508 ± 62
14	437 ± 33	442 ± 30	648 ± 67	550 ± 47	504 ± 40	472 ± 34	473 ± 53	422 ± 66	425 ± 62	413 ± 48	489 ± 71	508 ± 62
16	540 ± 46	562 ± 40	493 ± 81	494 ± 60	425 ± 62	413 ± 48	489 ± 71	508 ± 62	459 ± 28	453 ± 40	N.D. ± N.D.	N.D. ± N.D.
18	619 ± 46	587 ± 71	494 ± 81	494 ± 60	425 ± 62	413 ± 48	489 ± 71	508 ± 62	459 ± 28	453 ± 40	N.D. ± N.D.	N.D. ± N.D.
21	646 ± 37	664 ± 48	N.D. ± N.D.	N.D. ± N.D.	489 ± 71	508 ± 62	459 ± 28	453 ± 40	N.D. ± N.D.	N.D. ± N.D.	N.D. ± N.D.	N.D. ± N.D.
23	669 ± 38	687 ± 34	569 ± 69	517 ± 41	459 ± 28	453 ± 40	N.D. ± N.D.	N.D. ± N.D.	N.D. ± N.D.	N.D. ± N.D.	N.D. ± N.D.	N.D. ± N.D.
25	698 ± 34	696 ± 37	581 ± 47	572 ± 31	N.D. ± N.D.	N.D. ± N.D.	N.D. ± N.D.	N.D. ± N.D.	N.D. ± N.D.	N.D. ± N.D.	N.D. ± N.D.	N.D. ± N.D.
27	766 ± 38	713 ± 38	686 ± 49	648 ± 36	500 ± 39	488 ± 41	500 ± 39	488 ± 41	500 ± 39	488 ± 41	500 ± 39	488 ± 41
28	24 hours long drought		24 hours long drought		24 hours long drought		24 hours long drought		24 hours long drought		24 hours long drought	
29	Revitalization		Revitalization		Revitalization		Revitalization		Revitalization		Revitalization	
30	N.D. ± N.D.	N.D. ± N.D.	N.D. ± N.D.	N.D. ± N.D.	582 ± 60	680 ± 42	615 ± 48	663 ± 60	663 ± 64	675 ± 53	674 ± 47	721 ± 48
35	754 ± 41	722 ± 44	726 ± 78	741 ± 57	615 ± 48	663 ± 60	663 ± 64	675 ± 53	674 ± 47	721 ± 48	674 ± 47	721 ± 48
39	786 ± 61	751 ± 74	672 ± 57	660 ± 64	663 ± 64	675 ± 53	674 ± 47	721 ± 48	674 ± 47	721 ± 48	674 ± 47	721 ± 48
42	756 ± 74	801 ± 68	647 ± 90	686 ± 62	674 ± 47	721 ± 48	674 ± 47	721 ± 48	674 ± 47	721 ± 48	674 ± 47	721 ± 48

FIGURE 1

Chlorophyll content in mg m<sup>-2</sup> for WT, *vAtCKX1*, *cAtCKX1*, and *aAtCKX1* barley leaves. Plants were cultivated hydroponically (a) under optimal conditions (highlighted results indicate significant decreases in transgenic plants at chlorophyll level), and (b) under conditions of mild stress applied to 7-day-old seedlings and subsequent severe stress applied to 4-week-old plants with subsequent re-watering.

whereas the aerial part was not substantially affected [30]. The height of *vAtCKX1* plants was slightly reduced (Fig. 2a,d), while *cAtCKX1* plants exhibited no visible changes in their aerial part during the first 4 weeks of development. Differential expression examination revealed that approximately 400 genes were significantly affected in the 6-week-old aerial part in contrast to more than 2400 genes affected in the roots of hydroponically cultivated *vAtCKX1* plants [30]. In order to understand those mechanisms only regulated by the altered hormonal status during leaf development, we performed an in-depth transcriptomic analysis of *vAtCKX1* plants of the same age but cultivated in the soil. In contrast to hydroponically cultivated plants, approximately four times more genes were found to be affected by altered CK content. Of the total 26,067 annotated genes, 988 and 609 genes were

significantly down- or up-regulated, respectively (adjusted *P*-value ≤ 0.01; Supplemental Table S3). GO terms at level 6 of the most significantly affected genes from both sequencing experiments were compared and those 15 most affected and which overlap in the two environments are summarized in Table 2.

The four most negatively affected processes in leaves of *vAtCKX1* plants were linked to photosynthesis (Table 2). The fluorescence photosynthetic parameters, suggesting a decrease in energy transfer to the photosystem II core complexes (Table 1), together with lower chlorophyll content in non-stressed leaves (Fig. 1a), indicated that the photosynthetic apparatus and photosynthesis were slightly affected in transgenic plants. On the transcriptomic level, the effect was much more pronounced in those plants cultivated in the shallow soil (Table 2).

TABLE 1

**Transgenic and wild type (WT) barley plants grown in shallow soil tested for ability to recover after 4 days of drought stress. Plants were stressed by drought in the 4th week of growth. Physiological parameters were determined directly prior to stress, on the 3rd day of the stress period, and 24 hours after the stress period. Quenching characteristics of chlorophyll fluorescence determined after drought stress and during revitalization were calculated as percentages of their values prior to stress**

	WT	vAtCKX1	cAtCKX1	aAtCK1
<b>Prior to stress</b>				
CO <sub>2</sub> assimilation (mmol (CO <sub>2</sub> ) m <sup>-2</sup> s <sup>-1</sup> )	2.00 ± 0.70	2.60 ± 0.70	1.60 ± 0.90	2.10 ± 0.70
Stomatal conductance (mol (H <sub>2</sub> O) m <sup>-2</sup> s <sup>-1</sup> )	0.06 ± 0.03	0.08 ± 0.02	0.05 ± 0.02	0.04 ± 0.01
Transpiration rate (mol (H <sub>2</sub> O) m <sup>-2</sup> s <sup>-1</sup> )	0.30 ± 0.13	0.38 ± 0.09	0.24 ± 0.10	0.20 ± 0.05
Non-photochemical quenching	0.72 ± 0.12	0.85 ± 0.10	0.99 ± 0.08*	0.87 ± 0.13
Photochemical quenching	0.41 ± 0.06	0.38 ± 0.04	0.32 ± 0.03*	0.36 ± 0.05
<b>Drought stress</b>				
CO <sub>2</sub> assimilation (mmol (CO <sub>2</sub> ) m <sup>-2</sup> s <sup>-1</sup> )	1.30 ± 0.94	1.19 ± 1.13	-1.33 ± 0.77*	-1.77 ± 0.75*
Stomatal conductance (mol (H <sub>2</sub> O) m <sup>-2</sup> s <sup>-1</sup> )	0.036 ± 0.026	0.031 ± 0.019	0.005 ± 0.003*	0.005 ± 0.003*
Transpiration rate (mol (H <sub>2</sub> O) m <sup>-2</sup> s <sup>-1</sup> )	0.18 ± 0.13	0.16 ± 0.09	0.03 ± 0.02*	0.03 ± 0.01*
Non-photochemical quenching (%)	137 ± 23	171 ± 21	121 ± 16	102 ± 24
Photochemical quenching (%)	71 ± 12	57 ± 12	82 ± 15	76 ± 11
Water potential (MPa)	-1.11 ± 0.09	-1.25 ± 0.15	-1.69 ± 0.11*	-1.73 ± 0.04*
<b>Re-watering</b>				
CO <sub>2</sub> assimilation (mmol (CO <sub>2</sub> ) m <sup>-2</sup> s <sup>-1</sup> )	2.21 ± 0.47	1.43 ± 0.53*	1.31 ± 0.87*	1.03 ± 0.99*
Stomatal conductance (mol (H <sub>2</sub> O) m <sup>-2</sup> s <sup>-1</sup> )	0.09 ± 0.03	0.07 ± 0.02	0.04 ± 0.01*	0.05 ± 0.02*
Transpiration rate (mol (H <sub>2</sub> O) m <sup>-2</sup> s <sup>-1</sup> )	0.43 ± 0.11	0.36 ± 0.08	0.19 ± 0.07*	0.23 ± 0.09*
Non-photochemical quenching (%)	126 ± 18	101 ± 20	95 ± 16*	93 ± 5*
Photochemical quenching (%)	86 ± 9	104 ± 12*	108 ± 11*	103 ± 6*
Water potential (MPa)	-1.04 ± 0.21	-0.59 ± 0.02*	-0.59 ± 0.04*	-0.46 ± 0.07*
Relative water content (%)	78.38 ± 7.64	94.97 ± 1.02*	97.82 ± 2.06*	91.84 ± 5.05*

\*Significant difference between WT and transgenic tissue according to unpaired Student's *t*-test at  $P \leq 0.05$ .

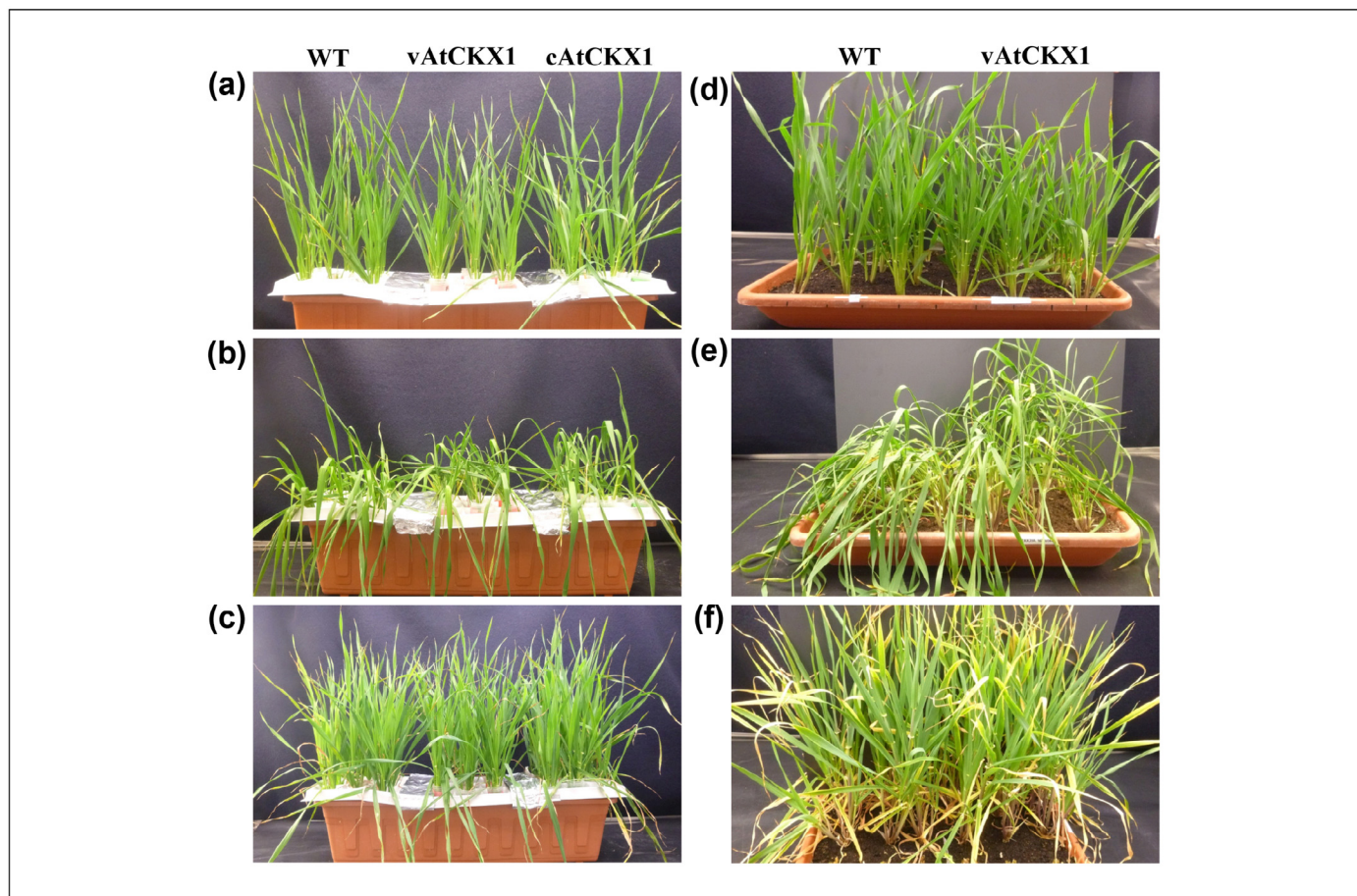
Three of four putative genes coding for prephenate/arogenate dehydratase, an enzyme participating in the final steps of the aromatic amino acid pathway that produces tyrosine and phenylalanine [46], were up-regulated in the leaves of vAtCKX1 plants. Phenylalanine is the primary substrate for the phenylpropanoid pathway that gives rise to lignin, flavonoids, and anthocyanins. Accordingly, the most up-regulated GO terms were GO:0009963 'Positive regulation of flavonoid biosynthetic process' and GO:0009718 'Anthocyanin-containing compound biosynthetic process.' Enforced production of phenylalanine thus might serve as a pool for the larger amount of flavonoids and anthocyanins in transgenic leaves, where these compounds participate in protection mechanisms against various stresses. However, four of eight genes encoding phenylalanine ammonia lyases, whose activity is considered a key switch between the phenylpropanoid pathway and primary aromatic amino acid metabolism [47], were significantly down-regulated. Nevertheless, all four genes, *MLOC\_4684*, *MLOC\_62322*, *MLOC\_79728* and *MLOC\_477*, were found to be up-regulated (by 3.6-, 3.0-, 2.7-, and 1.9-fold, respectively) in the roots of vAtCKX1 plants [30]. Hence, and inasmuch as the aromatic amino acid metabolism was not affected in vAtCKX1 transgenic roots, surplus phenylalanine might be translocated from leaves to roots, where it can supply enhanced lignin deposition.

The third most enriched process in vAtCKX1 leaves was linked to the activity of lipoxygenases, which enzymes participate in the release of volatile compounds, including jasmonates (JAs), from intracellular lipids [48]. These compounds are usually released during plant defense against various pathogens. As the result is based on two independent experiments in which two biological replicates were sequenced and compared to the respective WT

plants, it is not very likely that the observed lipoxygenase activation was merely a response to an undetected biotic stressor. In addition to plant defenses, JAs participate in several developmental processes such as trichome formation and leaf senescence [49]. Interestingly, JA-dependent formation of trichomes is accompanied by production of such secondary compounds as flavonoids, anthocyanins, and terpenoids [49,50]. Although there is not enough evidence to indicate cross-talk between JAs and CKs, it is predicted that their interaction might be antagonistic inasmuch as JAs strongly inhibit the CK-induced callus growth [51]. Nevertheless, the interplay of both phytohormone groups probably depends not only on the CK:JA ratio but also on other hormones [52]. In total, 12 of 55 and 8 of 39 genes categorized as GO:0009753 'Response to jasmonic acid' and GO:0010026 'Trichome differentiation,' respectively, were found to be significantly upregulated in the roots of two independent vAtCKX1 lines [30]. Hence, predicted JA production in the upper part of transgenic plants might affect mainly roots and their fine architecture. Volatile methyl JA can be translocated as a rapid chemical signal from shoot to root and function there as a gene expression inducer [53]. Nevertheless, enforced JA production directly in roots is also feasible inasmuch as GO:0016165 'Linoleate 13S-lipoxygenase activity' is among enriched terms in transgenic roots during revitalization (see below).

#### Whole transcriptome response of vAtCKX1 plants during revitalization after drought stress

In addition to optimal conditions, three other kinds of sequencing libraries were generated from the upper part of vAtCKX1 and WT plants cultivated in the shallow soil: the first from plants exposed

**FIGURE 2**

Photographs of transgenic and wild-type (WT) barley plants cultivated in hydroponic system (left) or shallow soil (right). (a,d) optimally watered 4-week-old plants, (b,e) plants suffering from severe drought stress, (c,f) regenerated plants 2 weeks after the application of drought stress.

to 4-day drought (Fig. 2e), the second from material 12 hours after re-watering, and the third from leaves having undergone 14-day revitalization (Fig. 2f). Unsurprisingly, only five genes were significantly altered (adjusted  $P$ -value  $\leq 0.05$ ) between stressed transgenic and WT leaves, thereby indicating that transcriptomes of both genotypes were strongly affected by the water deficit (Supplemental Table S3, see Supplemental Table S2 in Ref [37]). Twelve hours after re-watering, 10 and 9 genes were significantly up- and down-regulated, respectively, between *vAtCKX1* and WT leaves (Supplemental Table S3). Additionally, 5 of these 19 genes were not altered between the libraries made from optimally cultivated versus stressed leaves of either transgenic or WT leaves. Two putative *F-box-like proteins* (*MLOC\_75620*, *MLOC\_43997*), which have been shown to play an essential role in multiple phytohormone-signaling pathways [54], and one *receptor-like protein kinase* (*MLOC\_17138*) were detected among them. The protein *MLOC\_17138* contains in addition to the kinase domain, a pfam01657 domain associated with a role in salt stress response and antifungal activity.

Transgenic plants overexpressing *AtCKX1* exhibit better growth parameters (e.g., biomass production and yield) when encountering drought stress [30]. To understand processes attributed to the beneficial growth of *vAtCKX1* plants, a comparative transcriptomic analysis was carried out examining transgenic versus WT

leaves 2 weeks after revitalization from stress. Of the total 26,067 barley genes, 301 and 31 genes were significantly up- and down-regulated, respectively, in revitalized *vAtCKX1* leaves in contrast to WT (Supplemental Table S3). The enriched GO terms in up-regulated genes of *vAtCKX1* are summarized in Table 3A.

Products of many genes up-regulated by *vAtCKX1* participate as structural proteins or enzymes of the photosynthetic apparatus. Accordingly, the measured photosynthetic parameters of transgenic plants were better in the early stage of revitalization (Table 1), and chlorophyll content reached WT levels 2 weeks after re-watering (Fig. 1b), as compared to plants of the same age grown for their entire life span under optimal conditions. Interestingly, the most activated genes comprised those encoded by the barley chloroplast genome (indicated by the prefix EPIHVUG). In total, 14 of 112 translatable chloroplast genes were 2- to 3-fold up-regulated with high significance (adjusted  $P$ -value  $\leq 0.05$ ). Real-time PCR was performed on six selected genes to confirm the accuracy of the transcriptomic data (Supplemental Fig. S1). Chloroplasts are a known target of CK action. Indeed, exogenously applied CK is able directly to activate the expression of several chloroplast-encoded genes in detached barley leaves which accumulated also the stress hormone ABA [55]. Because it is not yet clear whether CK acts directly on chloroplast transcription, we can only speculate that the increase in chloroplast transcripts observed

TABLE 2

**The most affected gene ontology (GO) terms in the upper part of *vAtCKX1* plants cultivated hydroponically or in soil compared to wild-type plants. Percentages are shown of differentially expressed genes (adjusted *P*-value  $\leq 0.05$ ) at GO level 6 and higher from total number of genes with the same GO number. MF, molecular function; BP, biological process. Genes affected in both culture conditions are in bold. Genes in several GO terms are not listed because the term parsed to several other child terms**

GO number	Category	GO term	Total #	% of affected genes		Accession of affected genes in format MLOC_XXXXX
				Hydrop.	Soil	
<b>Up-regulated</b>						
GO:0004664	MF	Prephenate dehydratase activity	4	50.0	25.0	23316, 65725, 56414
GO:0008131	MF	Primary amine oxidase activity	6	16.7	50.0	<b>70980</b> , 4986, 17390
GO:0016165	MF	Linoleate 13S-lipoxygenase activity	16	31.3	18.8	<b>64972</b> , 54031, <b>55029</b> , 71275, 51884, 69572
GO:0005544	MF	Calcium-dependent phospholipid binding	10	20.0	20.0	54932, 40592, 55134, 15770
GO:0004834	MF	Tryptophan synthase activity	5	20.0	20.0	59863, 61188
GO:0009963	BP	Positive regulation of flavonoid biosynthetic process	9	11.1	22.2	81070, 54366, 19988
GO:0004034	MF	Aldose 1-epimerase activity	7	14.3	14.3	<b>5638</b>
GO:0005337	MF	Nucleoside transmembrane transporter activity	7	14.3	14.3	<b>55464</b>
GO:0009718	BP	Anthocyanin-containing compound biosynthetic process	11	18.2	9.1	61512, 65788, 64248
GO:0009407	BP	Toxin catabolic process	27	7.4	18.5	<b>17760</b> , 73593, <b>68101</b> , 57709, 72489
GO:0047262	MF	Polygalacturonate 4- $\alpha$ -galacturonosyltransferase activity	8	12.5	12.5	11661, 57229
GO:0031418	MF	L-Ascorbic acid binding	13	15.4	7.7	<b>77814</b> , 64248
GO:0004806	MF	Triglyceride lipase activity	41	9.8	12.2	<b>17298</b> , <b>18031</b> , <b>80878</b> , <b>80586</b> , 58940
GO:0006569	BP	Tryptophan catabolic process	14	14.3	7.1	12847, 57323, 69262
GO:0015996	BP	Chlorophyll catabolic process	33	3.3	15.2	80455, 34851, 55009, 21175, <b>64277</b>
<b>Down-regulated</b>						
GO:0008937	MF	Ferredoxin-NAD(P) reductase activity	4	25.0	50.0	7761, 53537, 40355
GO:0010027	BP	Thylakoid membrane organization	106	2.8	61.3	<b>58382</b> ; not listed
GO:0051667	BP	Establishment of plastid localization	63	4.8	55.6	Not listed
GO:0045548	MF	Phenylalanine ammonia lyase activity	7	28.6	28.6	79728, 62322, 477, 4684
GO:0009658	BP	Chloroplast organization	137	2.2	54.0	Not listed
GO:0019682	BP	Glyceraldehyde-3-phosphate metabolic process	202	1.5	51.5	Not listed
GO:0006720	BP	Isoprenoid metabolic process	237	1.3	46.0	Not listed
GO:0010310	BP	Regulation of hydrogen peroxide metabolic process	15	6.7	26.7	33774, 1518, 15501, 65632, 1340
GO:0030855	BP	Epithelial cell differentiation	7	14.3	14.3	38181, 54366
GO:0016054	BP	Organic acid catabolic process	153	3.9	14.4	Not listed
GO:0008544	BP	Epidermis development	9	11.1	11.1	38181, 54366
GO:0009699	BP	Phenylpropanoid biosynthetic process	22	9.1	9.1	4684, 477, 57736, 79728
GO:0070726	BP	Cell wall assembly	11	9.1	9.1	52864, 67760
GO:0032870	BP	Cellular response to hormone stimulus	205	8.8	5.7	Not listed
GO:0007166	BP	Cell surface receptor signaling pathway	30	3.3	10.0	63541, 17680, 44275, 72162

in revitalized *vAtCKX1* transgenic plants relays an accumulation of CK in leaves upon water stress. Our hypothesis is supported by the strong activation of endogenous *IPT* genes in *vAtCKX1* leaves at several developmental time points as a consequence of CK depletion [30]. Hence, increased local maxima of CKs, produced by *IPT* activity localized in chloroplasts, might trigger similar machinery as was described in CK-treated detached leaves to activate the chloroplast genome. The analysis of endogenous CK content in chloroplasts under these conditions would provide support for our hypothesis. It is noteworthy that none of the chloroplast-encoded genes were down-regulated in *vAtCKX1* plants cultivated under optimal conditions when as many nucleus-encoded genes participating in photosynthesis were down-regulated compared to those in WT plants (Table 2). Nevertheless, eight chloroplast-encoded genes were significantly up-regulated (Supplemental Fig. S1), indicating that the phenomenon is linked rather to CK imbalance than to activation by drought.

Among other interesting genes significantly up-regulated in revitalized *vAtCKX1* leaves were these coding for four putative aquaporins (*MLOC\_56278*, *MLOC\_71237*, *MLOC\_552*, *MLOC\_22808*), which are channel proteins facilitating the transport of water through plasma and intracellular membranes. The increased expression of several genes encoding barley aquaporins had already been observed in plants exposed to salinity stress [56]. Those authors had hypothesized that an increase in water channel activity would facilitate maintenance or recovery of growth during or after the stress period.

Two genes classified under the GO term 'phenylpropanoid catabolic process' encode putative laccases – aromatic compound: oxygen oxidoreductase (Table 3A), which might participate in lignin degradation or its polymerization. Nevertheless, in contrast to root tissue, significantly altered lignin content in the upper part of *vAtCKX1* plants was not determined in comparison to that in WT plants (Fig. 4a).

TABLE 3A

The most enriched GO terms in up-regulated genes (adjusted  $P$ -value  $\leq 0.05$ ) in the aerial part of *vAtCKX1* plants collected 2-weeks after re-watering. Percentages are shown of differentially expressed genes at GO level 6 and higher from total number of genes with the same GO number. MF, molecular function; BP, biological process; CC, cellular component.

GO number	Category	GO term	Total #	% of affected genes	Accession of affected genes in format MLOC_XXXXX or EPIHVUG000000XXXX
GO:0016984	MF	Ribulose-bisphosphate carboxylase activity	5	40.0	EPIHVUG00000010074, MLOC_21811
GO:0009765	BP	Photosynthesis, light harvesting	32	34.4	Not listed
GO:0030076	CC	Light-harvesting complex	8	25.0	EPIHVUG00000010021, MLOC_57061
GO:0009718	BP	Anthocyanin-containing compound biosynthetic process	10	20.0	MLOC_5324, 19814
GO:0016165	MF	Linoleate 13S-lipoxygenase activity	16	18.8	MLOC_37378, 51884, 71948
GO:0045259	CC	Proton-transporting ATP synthase complex	27	14.8	EPIHVUG00000010007, 10016, 10047, MLOC_26730
GO:0009767	BP	Photosynthetic electron transport chain	56	14.3	EPIHVUG00000010010, 10072, 10065, 10026, 10021, MLOC_52515, 22512, 39436
GO:0046271	BP	Phenylpropanoid catabolic process	20	10.0	MLOC_15203, 61189
GO:0052716	MF	Hydroquinone:oxygen oxidoreductase activity	20	10.0	MLOC_15203, 61189
GO:0009579	CC	Thylakoid	331	9.9	Not listed
GO:0016597	MF	Amino acid binding	31	9.7	MLOC_62844, 19879, 80634
GO:0004499	MF	<i>N,N</i> -Dimethylaniline monooxygenase activity	22	9.1	MLOC_11897, 11896
GO:0009637	BP	Response to blue light	48	8.3	MLOC_43394, 22512, 11312, 52515
GO:0055082	BP	Cellular chemical homeostasis	47	6.4	MLOC_22808, 65878, 69460
GO:0034754	BP	Cellular hormone metabolic process	38	5.3	MLOC_6666, 73942

Furthermore, genes significantly affected between non-stressed and revitalized leaves were evaluated separately for *vAtCKX1* and WT plants. Those from the transgenic plants that did not overlap with WT plants were further compared with genes differentially regulated between the two genotypes (i.e., the 301 up- and 31 down-regulated genes). Only seven up-regulated genes remained as being not developmentally dependent but genotype dependent. None of the down-regulated genes meet both criteria (Table 3B). Two genes coding for putative enzymes of the flavonoid biosynthesis pathway – chalcone isomerase and isoflavone 2'-hydroxylase – were found to be up-regulated in *vAtCKX1* plants. These two genes combine with two other genes found to be up-regulated in revitalized *vAtCKX1* leaves and participating in the regulation of

flavonoid metabolism (*chalcone isomerase*: MLOC\_5324; *zinc-finger (B-box) protein*: MLOC\_19814), indicating an enforced production of isoflavonoids and anthocyanins. Recently, an unambiguous positive effect of flavonoid and anthocyanin production in improving tolerance to drought stress has been shown [57]. Due to their antioxidative activity, the over-accumulation of flavonoids mitigates the negative effect of reactive oxygen species released under stress conditions. Peroxiredoxin (MLOC\_74367) belongs to a family of cysteine-dependent peroxidases which also participate in detoxification of plant cells by scavenging reactive oxygen species [58]. An orthologue of peroxiredoxin has been found among another 25 over-accumulated proteins in wheat seedlings of a cultivar that is drought-stress tolerant in comparison to a

TABLE 3B

Significantly up-regulated genes in *vAtCKX1* leaves 2 weeks after re-watering (adjusted  $P$ -value  $\leq 0.05$ ) which are not developmentally dependent and also significantly up-regulated between revitalized and non-stressed leaves of *vAtCKX1* genotype but not in wild-type plants (adjusted  $P$ -value  $\leq 0.001$ ); R2W, 2-week revitalization; NS, non-stressed

Gene number	Gene annotation	Mean expression (R2W)	Fold change	
			<i>vAtCKX1</i> (R2W) versus WT (R2W)	<i>vAtCKX1</i> (R2W) versus <i>vAtCKX1</i> (NS)
MLOC_8529	Nematode-resistance protein	1471	4.28	2.21
MLOC_14310	GDSL esterase/lipase	1163	2.51	2.62
MLOC_74636	tolB protein (WD40-like Beta Propeller)	185	2.38	3.60
MLOC_30661	Putative isoflavone 2'-hydroxylase	78	2.31	6.66
MLOC_70609	unknown protein located in chloroplast stroma	104	2.30	4.30
MLOC_74367	Peroxiredoxin (Thioredoxin-like fold)	2443	2.23	2.66
MLOC_80571	Chalcone isomerase	598	2.19	2.86

drought-sensitive one [59]. MLOC\_14310 belongs to a large family of GDSL-type esterase/lipases with hydrolytic activity toward triacylglycerols. Members of this family are involved in plant development, morphogenesis, secondary metabolite synthesis, and defense responses, and some members are activated by JAs. The closest rice orthologue of MLOC\_14310 (LOC\_Os01g46080) was found to be activated by desiccation stress in rice leaves [60]. Moreover, pepper GDSL lipase caused higher susceptibility to pathogens but increased tolerance to osmotic stress when over-expressed in Arabidopsis [61].

Taken together, the differential expression study in *vAtCKX1* and WT leaves before and after the stress period reveal several genes whose increased expression initiated by the CK imbalance may lead to better drought tolerance and/or faster growth after re-watering.

#### Response of *vAtCKX1* and *cAtCKX1* roots during stress and revitalization

Due to the impossibility of collecting root tissues from soil without causing mechanical stress, transcriptome of the root system was studied from plants grown hydroponically. Twelve sequencing libraries were generated from *vAtCKX1*, *cAtCKX1*, and WT roots collected at two time points: during the severe drought stress (Fig. 2b) and 2 weeks after revitalization (Fig. 2c). Similarly as in the aerial part, stress induced a strong response at the transcriptome level (see Supplemental Table S1 in Ref [37]). Between transgenic plants and WT plants, only a few genes were deregulated during the stress (Supplemental Table S4). Just seven genes were significantly up-regulated in both *vAtCKX1* and *cAtCKX1* genotypes, including, for example, putative *nicotianamine synthase* (MLOC\_71596) and *4-coumarate CoA ligase* (MLOC\_18901) involved in lignification. Fifty-seven genes were significantly down-regulated. The most strongly down-regulated gene in both lines was a putative *F-box-like protein* (MLOC\_75620; 12.6- and 5.3-fold), which was found also among the most strongly down-regulated genes in the early and late phases of leaf revitalization. The unambiguous and strong depletion of MLOC\_75620 transcripts in all transgenic samples indicates that this F-box protein might play a crucial role in regulating responses in CKX-over-expressing plants via cross-talk with other hormones. F-box proteins represent one of the largest superfamilies in plants, that is, involved in the process of ubiquitination and protein degradation. To date, only a limited number of F-box proteins have been functionally characterized. Most of them are involved in regulating hormone signaling pathways, where they degrade repressors or activators of auxin, GA, ethylene, and JA response [54].

Analysis of differentially expressed genes in revitalized 6-week-old roots (Supplemental Table S4) revealed that the gene encoding one of the cytokinin receptors (*HvHK3*; MLOC\_44452) was significantly down-regulated in both transgenic genotypes (Fig. 3a,c). The gene was also down-regulated in 6-week-old *vAtCKX1* and *cAtCKX1* roots cultivated under optimal conditions (see Figure 3B in Ref [30]), thus leading to the conclusion that cessation of CK perception via *HvHK3* is a developmental consequence rather than a response to stress. The addition of one *CKX* gene to the barley genome led to a hormonal imbalance which plants tend to buffer by regulation of endogenous CKX and IPTs, which are CK biosynthetic enzymes, in a very sensitive way [30]. Plant IPT genes

are generally very weakly expressed, and the enzyme's activity is regulated by farnesylation [62]. Significant up-regulation of two abundant endogenous CKX enzymes – *HvCKX4* and *HvCKX5* – was observed in both independent experiments with 6-week-old *AtCKX1*-overexpressing plants, while other *HvCKXs* were down-regulated or unchanged in comparison to WT plants. Although it is difficult to estimate the final CK homeostasis, one might expect a local minimum in CK content that leads to cessation in *HvHK3* transcription and CK perception through this receptor.

CK receptors belong to a small group of histidine kinases. The Arabidopsis genome encompasses three real CK receptors binding CKs (*AHK2*, *AHK3*, and *AHK4/CRE1*) and three others implicated in CK transduction cascade and osmosensing without the ability directly to bind CKs (*AHK1*, *CKI1*, and *CKI2*) [4]. In contrast to other genes participating in CK signal transduction, phosphotransfer proteins, and response regulators (RR, Fig. 3d), CK receptors show lineage-specific expansion between dicot and monocot species that implies their specific and evolutionarily old function among all green plants [63]. Thus, in the barley genome, *HvHK3* is an orthologue of *AHK3*, while the orthologue of *AHK2* is missing and *AHK4* has otherwise two duplicated orthologues (Fig. 3a). A similar representation of CK receptors was found in rice [63].

Interestingly, Arabidopsis knock-outs of *AHK3* and *AHK2* or double knock-out manifest strong drought-tolerance phenotype [4]. This is the first direct evidence demonstrating that CKs might be a negative regulator of the stress signaling pathway. Tran et al. explained the phenomenon by the up-regulation of many stress and ABA responsive genes in *ahk2/ahk3* double knock-out already under non-stress conditions. To check if the response of *AtCKX1*-overexpressing barley was similar, we blasted the barley orthologous genes closest to these significantly up-regulated genes in the Arabidopsis double knock-out (Supplemental Table S5). In total, 23 and 25 orthologues of the 40 genes presented in Tran et al. were also significantly up-regulated in *vAtCKX1* and *cAtCKX1* transgenic barley, respectively. Among them, we found several regulatory genes implicated in responses to stress, such as MLOC\_37104 (an orthologue of *ANAC055*), *NAC* (no apical meristem) transcription factor [64], and MLOC\_71611 (an orthologue of *AtMYC2*). Over-expression of both transcription factors in Arabidopsis led to drought-tolerance and increased sensitivity to ABA [65]. Both genes have been shown to be activated by JAs [66], the overproduction of which is expected in the upper part of *AtCKX1* transgenic plants. While it is interesting that both genes have relatively strong expression in barley and are more abundant in roots than in leaves, their action has been studied mainly in Arabidopsis leaves [64,65]. Hence, drought tolerance mediated via these two transcription factors might be universal for the entire plant body. Recently, rice plants overexpressing *OsNAC9*, the closest orthologue of MLOC\_37104, under the control of a root-specific promoter have been shown to be more drought tolerant during vegetative development due to their enlarged root diameter and aerenchyma formation [67].

Altered homeostasis of CKs in *AtCKX1*-overexpressing barley, which influences root system architecture, might anticipate changes in auxin levels, transport, and perception. There exist several groups of auxin response genes in plant genomes that react sensitively to auxin imbalance. Auxin early response genes are divided into two categories – the Aux/IAA and SAUR (small auxin



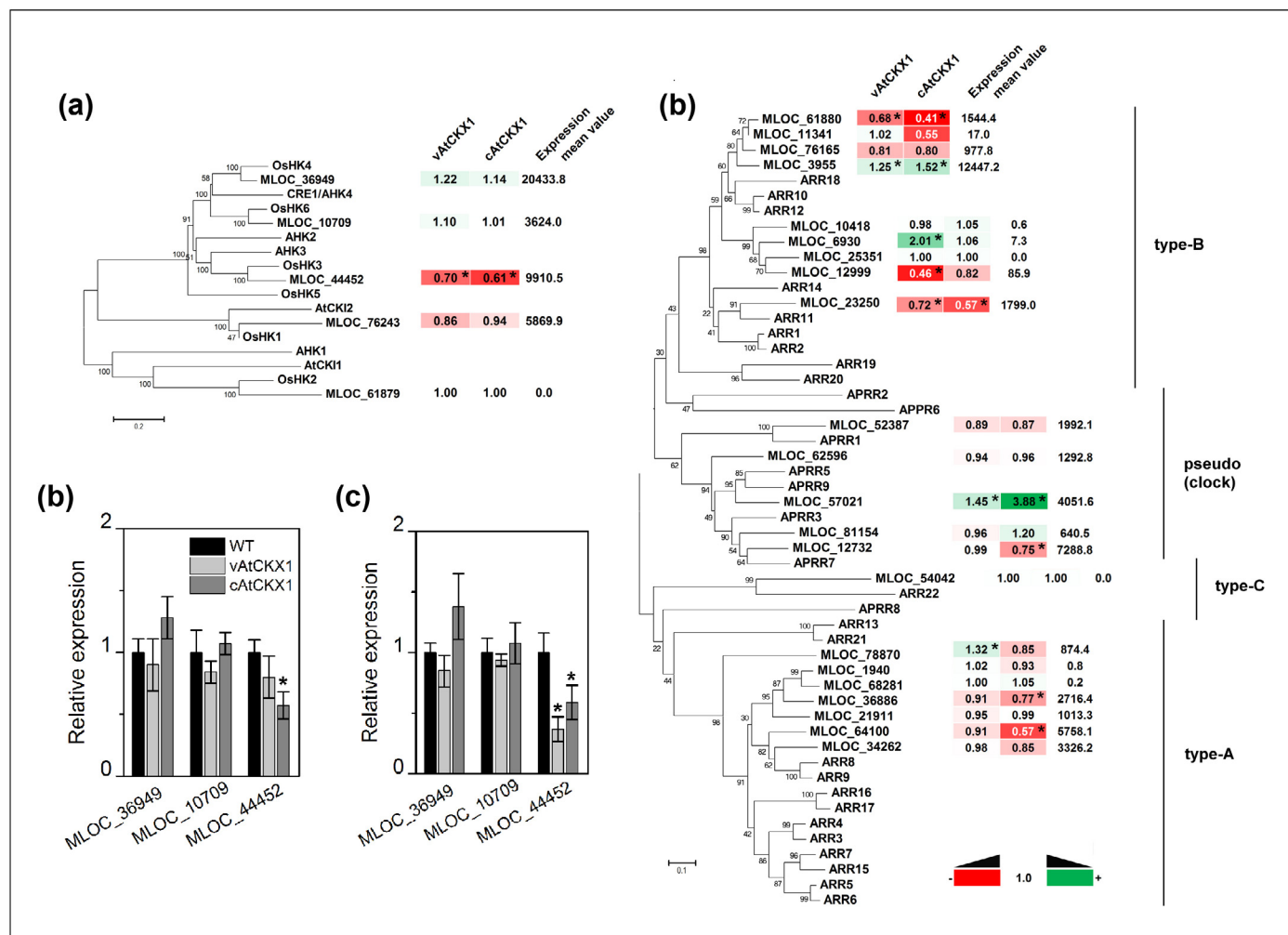


FIGURE 3

Cytokinin perception in *vAtCKX1* and *cAtCKX1* plants. (a) Phylogenetic relationship of barley, rice, and Arabidopsis histidine kinases implicated in CK perception. Expression relative to wild-type (WT) of all homologues found in the annotated barley genome are depicted in up- and down-regulation color code together with their mean expression values. Real-time PCR analysis of three CK receptors in roots cultivated (b) under optimal conditions or (c) 2 weeks after re-watering following the drought stress. (d) Phylogenetic relationship of all CK response regulators found in the barley genome and their Arabidopsis counterparts. Expression relative to WT plants is shown in the color code. Unrooted trees were generated using ClustalW by neighbor-joining method. \*Significant difference between WT and transgenic tissue according to unpaired Student's *t*-test at  $P \leq 0.05$ .

up RNA) – and all regulate plant physiology by modulating the interaction with auxin response elements of other transcription factors, such as a major group of auxin response factors (ARFs). Auxin action is influenced by its polar transport that is mediated by auxin efflux carriers (PINs). Its homeostasis is also regulated by *GH3* (*Gretchen Hagen3*) genes encoding mainly auxin–amino acid synthetases that form from surplus auxin its inactive conjugates [68]. *AtCKX1*/WT comparative data indicated that transgenic roots contain elevated levels of auxin, inasmuch as 3 of 12 predicted and expressed PIN transporters and 3 of 7 *GH3* genes were significantly up-regulated in *cAtCKX1* roots (Supplemental Table S6). Analysis of *vAtCKX1* roots showed a similar but slightly weaker tendency.

Many of the 48 significantly down-regulated genes in Arabidopsis *ahk2/ahk3* double knock-out with higher stress tolerance are auxin early responsive genes (*SAUR* and *IAA/AUX*). The dwarf phenotype of *ahk2/ahk3* plants was attributed to the observed down-regulation of auxin response [4]. Because *vAtCKX1* and

*cAtCKX1* plants were not substantially affected in their aerial part but had positively altered root system morphology, a different way of auxin response might be expected. In contrast to *ARF* and *GH3* genes, several *SAUR* and *IAA/AUX* genes exhibited lower expression in transgenic plants than in WT plants. Nevertheless, no straightforward comparison can be made between the auxin response of Arabidopsis *ahk2/ahk3* mutant and *AtCKX1*-overexpressing barley (Supplemental Tables S5 and S6). Particularly noteworthy was that two type-A *AtRR* genes were found among the down-regulated genes of the *ahk2/ahk3* mutant [4]. Two of seven *HvRR* genes were significantly down-regulated in *cAtCKX1* transgenic barley, thus implicating reduced CK sensing due to decreased CK content and/or silenced HvHK3 receptor (Fig. 3d). Taken together, the comparison of our transcriptomic data with the previous work of Tran et al. [4] suggests that the general mechanism of drought-stress tolerance relates in part to CK insensitivity, which can be acquired by receptor knock-out or CKX overexpression in all species across the plant kingdom.

*Up-regulation of genes in the phenylpropanoid biosynthesis pathway leads to higher lignification of AtCKX1 transgenic roots exposed to drought stress*

Our pilot whole-transcriptome characterization of *vAtCKX1* transgenic roots revealed strong up-regulation of many genes encoding proteins involved in the phenylpropanoid biosynthesis pathway [30]. Lignin content was quantified by the acetyl bromide method in protein-free cell wall samples prepared separately from whole root and leaf mass of hydroponically cultivated plants. Both transgenic genotypes showed systematic increase in total lignin content in roots from the 2nd week after germination (data not

shown). Approximately up to 20% higher lignin content was determined in roots of transgenic compared to WT plants cultivated under optimal conditions 6 weeks after germination, while lignin content in leaves was not significantly altered (Fig. 4a).

Analysis of lignin precursors in 4-week-old transgenic plants showed that *cAtCKX1* accumulated significantly greater amounts of cinnamates and monolignols than did WT tissue (Fig. 4b). Four-week-old roots of *vAtCKX1* genotype contained a larger amount of sinapyl alcohol, similarly as 2 weeks later, when grown under optimal conditions. The exposure to drought stress and the following revitalization resulted in more pronounced accumulation

Research Paper

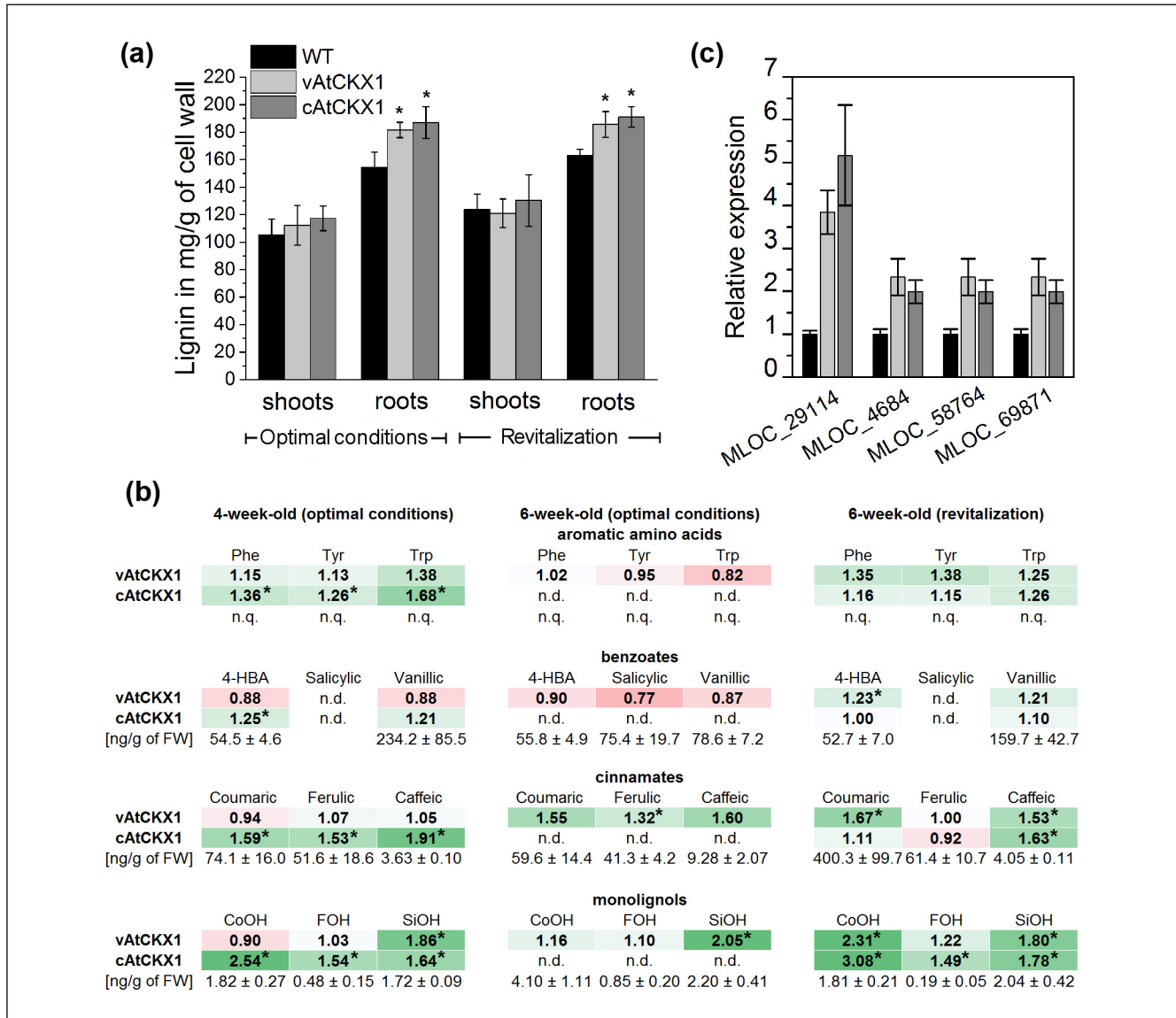


**FIGURE 4**

Lignin content and intermediates of the phenylpropanoid pathway in *vAtCKX1* and *cAtCKX1* transgenic barley. (a) Total lignin content of hydroponically cultivated plants under optimal conditions (6th week) and during 2-week revitalization (6th week); each value represents the mean of four biological replicates. (b) Quantification of aromatic amino acids, phenylpropanoid intermediates, and benzoic acids in roots of hydroponically cultivated plants (each in three biological replicates) collected during 4th and 6th weeks of growth under optimal conditions and 2nd week of revitalization after drought stress; n.q., not quantified due to lack of internal standard; n.d., not determined; Phe, phenylalanine; Tyr, tyrosine; Trp, tryptophan; 4-HBA, 4-hydroxybenzoic acid; CoOH, coumaryl alcohol; FOH, coniferyl alcohol; SiOH, sinapyl alcohol; \*significant difference between WT and transgenic tissue according to unpaired Student's *t*-test at  $P \leq 0.05$ . (c) Real-time PCR analysis of four selected genes encoding enzymes involved in the phenylpropanoid pathway in transgenic barley roots 2 weeks after re-watering following the drought stress; MLOC\_29114, cinnamoyl-CoA reductase; MLOC\_4684, phenylalanine ammonia lyase; MLOC\_58764, 4-coumarate:CoA ligase; MLOC\_69871, cinnamate 4-hydroxylase.

of all quantified intermediates of the phenylpropanoid pathway (Fig. 4b) as well as in higher lignin content of the root cell wall fraction in both transgenic genotypes compared to WT plants. However, lignification in transgenic roots having passed through severe stress was not greater than in the transgenic roots cultivated under optimal conditions (Fig. 4a). Measurement confirmed that decreased CK sensitivity has a positive impact on root lignification

but that the effect is not augmented by exposure to stress, even though more precursors are formed. Thus, the inability to produce more lignin after revitalization from stress may consist in limiting of specific peroxidases participating in monolignol polymerization. The most enriched GO terms in revitalized roots of both transgenic genotypes nicely corresponded to the observed increased amount of phenylpropanoid pathway intermediates and

TABLE 4

**The most affected gene ontology (GO) terms in the roots of *vAtCKX1* and *cAtCKX1* plants cultivated hydroponically 2 weeks after re-watering compared to wild-type plants. Percentages are shown of differentially expressed genes (adjusted *P*-value  $\leq 0.05$ ) at GO level 6 and higher from total number of genes with the same GO number. MF, molecular function; BP, biological process. Genes affected in both genotypes are in bold. Genes in several GO terms are not listed because the term parsed to several other child terms**

GO number	Category	GO term	Total #	% of affected genes		Accession of affected genes in format MLOC_XXXXX
				<i>vAtCKX1</i>	<i>cAtCKX1</i>	
<b>Up-regulated</b>						
GO:0008792	MF	Arginine decarboxylase activity	2	100.0	100.0	<b>58866, 39205</b>
GO:0047987	MF	Hydroperoxide dehydratase activity	2	100.0	100.0	<b>8106, 21933</b>
GO:0004664	MF	Prephenate dehydratase activity	4	75.0	100.0	23316, <b>65725, 56414, 60716</b>
GO:0009916	MF	Alternative oxidase activity	4	75.0	50.0	<b>34173, 82029, 53632</b>
GO:0045548	MF	Phenylalanine ammonia lyase activity	7	71.4	71.4	<b>79728, 62322, 4684, 19798, 67067</b>
GO:0003979	MF	UDP-glucose 6-dehydrogenase activity	3	66.7	100.0	<b>5287, 70967, 63077</b>
GO:0005345	MF	Purine nucleobase transmembrane transporter activity	3	66.7	66.7	<b>66246, 32910</b>
GO:0004470	MF	Malic enzyme activity	6	50.0	83.3	<b>11548, 75667, 35785, 64502, 51144</b>
GO:0009805	BP	Coumarin biosynthetic process	9	55.6	55.6	66898, 20110, 17364, 19988, 52497
GO:0009699	BP	Phenylpropanoid biosynthetic process	26	53.9	46.2	Not listed
GO:0016165	MF	Linoleate 13S-lipoxygenase activity	16	50.0	56.3	Not listed
GO:0052542	BP	Defense response by callose deposition	10	50.0	50.0	<b>57937, 51297, 42826, 17648, 59580</b>
GO:0006986	BP	Response to unfolded protein	25	40.0	40.0	Not listed
GO:0035967	BP	Cellular response to topologically incorrect protein	25	40.0	40.0	Not listed
GO:0042538	BP	Hyperosmotic salinity response	10	40.0	40.0	<b>69262, 52084, 42826, 2170</b>
GO:0004348	MF	Glucosylceramidase activity	5	40.0	40.0	<b>398, 53162, 13522</b>
GO:0010942	BP	Positive regulation of cell death	5	40.0	40.0	<b>12681, 75133</b>
GO:0003885	MF	D-Arabinono-1,4-lactone oxidase activity	9	33.3	44.4	<b>31769, 34835, 68610, 59091</b>
GO:0003978	MF	UDP-glucose 4-epimerase activity	6	33.3	33.3	<b>70713, 10406</b>
GO:0015020	MF	Glucuronosyltransferase activity	12	25.0	41.7	<b>4722, 54026, 65730, 8254, 56928</b>
<b>Down-regulated</b>						
GO:0004650	MF	Polygalacturonase activity	32	21.9	12.5	6444, 4738, 68357, 67885, <b>51158, 53562, 75889, 13213, 72199</b>
GO:0001666	BP	Response to hypoxia	13	7.7	23.1	<b>36714, 1340, 65221</b>
GO:0042886	BP	Amide transport	28	3.6	25.0	22335, 59508, 20029, 71333, 10510, <b>56891, 58935</b>
GO:0009735	BP	Response to cytokinin	13	7.7	15.4	<b>23250, 58762</b>
GO:0008375	MF	Acetylglucosaminyltransferase activity	36	2.8	19.4	38958, <b>37085, 65593, 74430, 5087, 63430, 60533</b>
GO:0016307	MF	Phosphatidylinositol phosphate kinase activity	18	5.6	16.7	<b>81640, 62872, 5875</b>
GO:0008509	MF	Anion transmembrane transporter activity	104	4.8	16.4	Not listed
GO:0042594	BP	Response to starvation	44	6.8	13.6	<b>56127, 7416, 44452, 16652, 4685, 57969</b>
GO:0005667	CC	Transcription factor complex	30	3.3	16.7	<b>76757, 67781, 7755, 36554, 62730</b>
GO:0045786	BP	Negative regulation of cell cycle	25	8.0	12.0	<b>57670, 65158, 62665</b>
GO:0031669	BP	Cellular response to nutrient levels	45	6.7	13.3	<b>56127, 7416, 44452, 16652, 4685, 57969</b>
GO:0042559	BP	Pteridine-containing compound biosynthetic process	15	6.7	13.3	<b>74131, 10075</b>
GO:0008643	BP	Carbohydrate transport	41	4.9	14.6	65088, 13612, 17903, 280, 63767, 67524, 10342, 59161
GO:0019901	MF	Protein kinase binding	36	5.6	13.9	46471, <b>57670, 66940, 51179</b>
GO:0010565	BP	Regulation of cellular ketone metabolic process	16	6.3	12.5	<b>36714, 14398</b>
GO:0004672	MF	Protein kinase activity	1099	4.3	14.5	Not listed
GO:0000272	BP	Polysaccharide catabolic process	43	7.0	11.6	40915, 54306, 59047, 49756, 4022
GO:0009751	BP	Response to salicylic acid	54	5.6	13.0	21464, 1340, <b>36714, 14398, 43518, 71936, 10787</b>
GO:0003950	MF	NAD+ ADP-ribosyltransferase activity	11	9.1	9.1	66554, 72444
GO:0009723	BP	Response to ethylene	35	8.6	8.6	44452, 53881, 64636

stronger lignification. Indeed, about half of the genes assigned as participating in the phenylpropanoid pathway were significantly up-regulated, as were 5 of 7 genes encoding phenylalanine ammonia lyases and all four genes encoding prephenate dehydratase. The up-regulation of the four selected genes was confirmed by real-time PCR (Fig. 4c). Lignin synthesis depends on precursors the same as those for benzoic acids. The levels of the three most abundant benzoic acids were reduced in the *vAtCKX1* roots cultivated under optimal conditions (Fig. 4b). Hence, a metabolic switch between lignin and benzoic acid production seems to be a downstream process of reduced CK status. Nevertheless, a more precise analysis of all possible products needs to be conducted in the future to elucidate all consequences of the observed dramatic regulation of genes involved in the phenylpropanoid pathway.

Among other up-regulated processes, we could identify also hydroperoxide dehydratase and linoleate 13S-lipoxygenase activity, which may stimulate the production of JAs or other volatile compounds, the biosynthesis of coumarin, and the response to hyperosmotic salinity (Table 4).

**Conclusions**

Here, we presented one of the first whole-transcriptome studies done on barley plants. Although a rough draft of the barley genome has been available for several years [69], its precise annotation and the classification of predicted genes into GO categories are still incomplete and in some aspects unsatisfying. For instance, the GO term ‘response to cytokinin’ counts only 13 putative genes and none of the type A-RR are included. Nevertheless, the

Research Paper

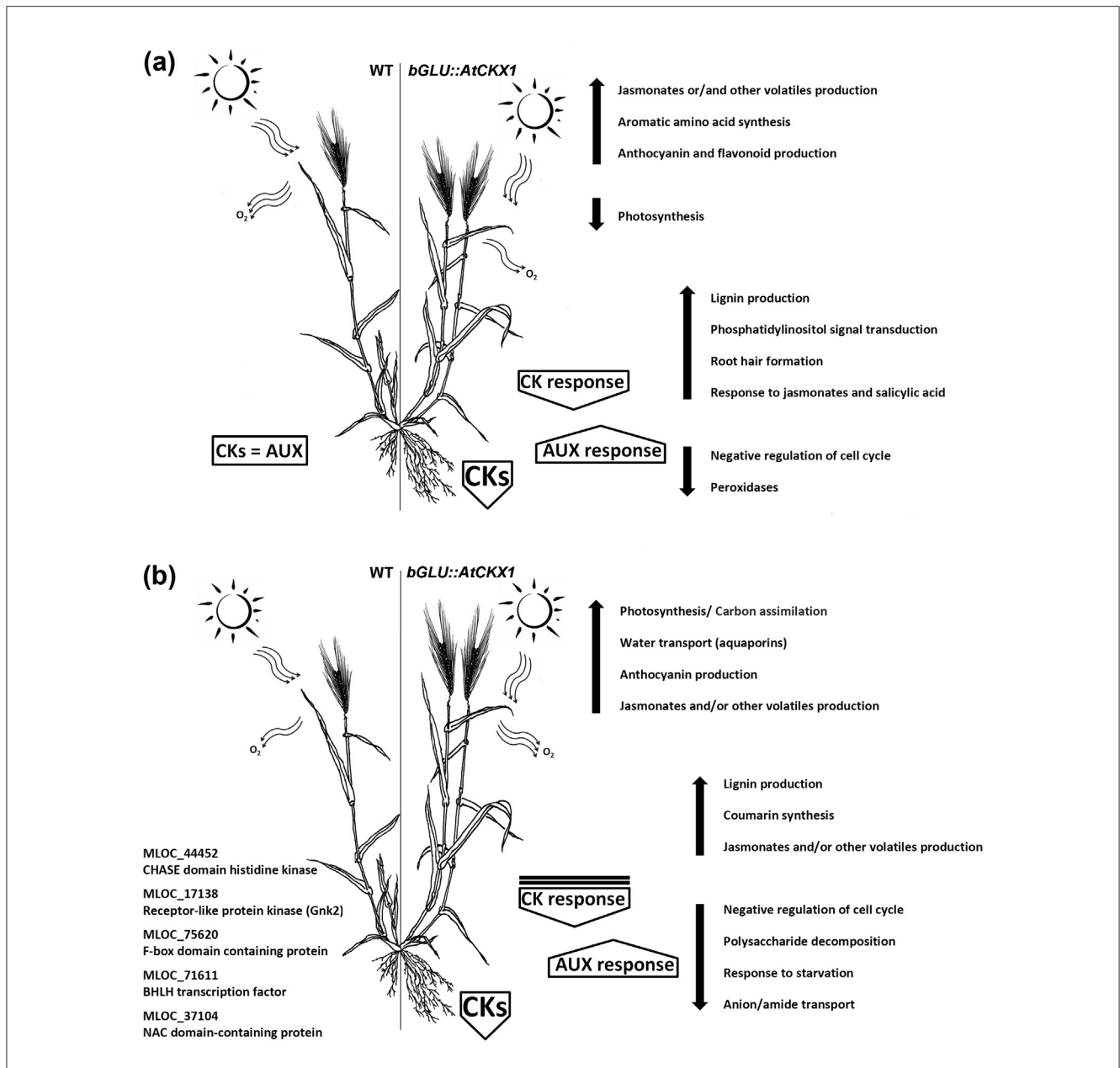


**FIGURE 5** Conceptual diagram of main physiological responses in transgenic barley overexpressing *CKX* gene under the control of mild root-specific promoter (a) under optimal conditions or (b) during revitalization after drought stress. Predicted key regulatory genes are listed.

challenging RNA-seq method enabled us to comprehensively inspect all processes occurring in plant tissue with CK imbalance and suggest a new context especially toward other phytohormones. In addition to the fact that the described transgenic plants showed better drought avoidance due to modified root morphology, probably as a consequence of an altered cytokinin-to-auxin ratio, partial CK insensitivity due to down-regulation of HvHK3 receptor expression influenced also other physiological processes leading to drought tolerance (Fig. 5). Up-regulation of four *aquaporin* genes might have contributed to the fact that all transgenic genotypes were able to increase water potential faster than were WT plants. The process of leaf revitalization is accompanied by up-regulation of genes implicated in photosynthesis, and especially those encoded by the chloroplast genome. This aspect leads to faster regeneration of transgenic plants that is observed as higher biomass accumulation. Altered CK status noticeably accelerates secondary metabolism derived from phenylalanine and leads to accumulation of intermediates of the phenylpropanoid pathway in the roots. In this manner, more lignin is deposited in the root tissue and formation of such other compounds as anthocyanins and flavonoids can be expected. The comparative transcriptomic analyses disclosed several genes that might play a crucial role in the drought-tolerant phenotype of *AtCKX1*-overexpressing barley plants. In addition to two transcription factors of the MYB and NAC families shown to increase sensitivity to ABA, the expression of a

putative F-box-like protein (MLOC\_75620) was strongly depleted in all transgenic tissues. This protein might be involved in ubiquitination of repressors or activators of other phytohormone transduction pathways and thus mediate cross-talk of CKs with auxins, GAs, or JAs. Enforced production of JAs or other volatile compounds might be another process attributed to *AtCKX1*-overexpression phenotype inasmuch as linoleate 13S-lipoxygenase activity is among the most enriched GO terms in both transgenic leaves as well as roots after re-watering. In conclusion, introduction of one CK-degradation enzyme into the barley genome under the control of a mild promoter resulted in a CK-insensitive phenotype that activates processes enabling plants to regenerate better after a water deficit (Fig. 5).

### Acknowledgements

The authors thank Hana Pospíšilová for providing plant material. This work was supported by the Czech Science Foundation (grant no. 14-12355S) as well as the Czech Ministry of Education, Youth and Sports through the National Programme for Sustainability I (project no. LO1204), and Mobility (project no. 7AMB15AR011) programs.

### Appendix A. Supplementary data

Supplementary data associated with this article can be found, in the online version, at <http://dx.doi.org/10.1016/j.nbt.2016.01.010>.

### References

- Zalabák D, Pospíšilová H, Šmehilová M, Mrázová K, Frébort I, Galuszka P. Genetic engineering of cytokinin metabolism: prospective way to improve agricultural traits of crop plants. *Biotechnol Adv* 2013;31:97–117.
- Ha S, Vankova R, Yamaguchi-Shinozaki K, Shinozaki K, Tran LSP. Cytokinins: metabolism and function in plant adaptation to environmental stresses. *Trends Plant Sci* 2012;17:172–9.
- Nishiyama R, Watanabe Y, Fujita Y, Le DT, Kojima M, Werner T, et al. Analysis of cytokinin mutants and regulation of cytokinin metabolic genes reveals important regulatory roles of cytokinins in drought, salt and abscisic acid responses, and abscisic acid biosynthesis. *Plant Cell* 2011; 23:2169–83.
- Tran LSP, Urao T, Qin F, Maruyama K, Kakimoto T, Shinozaki K, et al. Functional analysis of AHK1/ATHK1 and cytokinin receptor histidine kinases in response to abscisic acid, drought, and salt stress in Arabidopsis. *Proc Natl Acad Sci U S A* 2007;104:20623–28.
- Nishiyama R, Watanabe Y, Leyva-Gonzalez MA, Ha CV, Fujita Y, Tanaka M, et al. Arabidopsis AHP2, AHP3, and AHP5 histidine phosphotransfer proteins function as redundant negative regulators of drought stress response. *Proc Natl Acad Sci U S A* 2013;110:4840–5.
- Sun L, Zhang Q, Wu J, Zhang L, Jiao X, Zhang S, et al. Two rice authentic histidine phosphotransfer proteins, OsAHP1 and OsAHP2, mediate cytokinin signaling and stress responses in rice. *Plant Phys* 2014;165:335–45.
- Rivero RM, Kojima M, Gepstein A, Sakakibara H, Mittler R, Gepstein S, et al. Delayed leaf senescence induces extreme drought tolerance in a flowering plant. *Proc Natl Acad Sci U S A* 2007;104:19631–36.
- Zhang P, Wang WQ, Zhang GL, Kaminek M, Dobrev P, Xu J, et al. Senescence-inducible expression of isopentenyl transferase extends leaf life, increases drought stress resistance and alters cytokinin metabolism in cassava. *J Integr Plant Biol* 2010;52:653–69.
- Ghanem ME, Albacete A, Smigocki AC, Frébort I, Pospíšilová H, Martínez-Andújar C, et al. Root-synthesized cytokinins improve shoot growth and fruit yield in salinized tomato (*Solanum lycopersicum* L.) plants. *J Exp Bot* 2011; 62:125–40.
- Merewitz EB, Gianfagna T, Huang B. Photosynthesis, water use, and root viability under water stress as affected by expression of *SAG12-ipt* controlling cytokinin synthesis in *Agrostis stolonifera*. *J Exp Bot* 2011;62:383–95.
- Peleg Z, Reguera M, Tumimbang E, Walia H, Blumwald E. Cytokinin-mediated source/sink modifications improve drought tolerance and increase grain yield in rice under water-stress. *Plant Biotechnol J* 2011;9:747–58.
- Kuppu S, Mishra N, Hu R, Sun L, Zhu X, Shen G, et al. Water-deficit inducible expression of a cytokinin biosynthetic gene *IPT* improves drought tolerance in cotton. *PLoS ONE* 2013;8:e64190.
- Reguera M, Peleg Z, Abdel-Tawab YM, Tumimbang EB, Delatorre Ca, Blumwald E. Stress-induced cytokinin synthesis increases drought tolerance through the coordinated regulation of carbon and nitrogen assimilation in rice. *Plant Physiol* 2013;163:1609–22.
- Zhang SW, Li CH, Cao J, Zhang YC, Zhang SQ, Xia YF, et al. Altered architecture and enhanced drought tolerance in rice via the down-regulation of indole-3-acetic acid by *TLD1/OsGH3.13* activation. *Plant Physiol* 2009;151:1889–901.
- Tsuchisaka A, Theologis A. Unique and overlapping expression patterns among the Arabidopsis 1-amino-cyclopropane-1-carboxylate synthase gene family members. *Plant Physiol* 2004;136:2982–3000.
- Růžička K, Ljung K, Vanneste S, Podhorská R, Beeckman T, Friml J, et al. Ethylene regulates root growth through effects on auxin biosynthesis and transport-dependent auxin distribution. *Plant Cell* 2007;19:2197–212.
- Peleg Z, Blumwald E. Hormone balance and abiotic stress tolerance in crop plants. *Curr Opin Plant Biol* 2011;14:290–5.
- Rivero RM, Gimeno J, Van Deynze A, Walia H, Blumwald E. Enhanced cytokinin synthesis in tobacco plants expressing *P<sub>SARK</sub>::IPT* prevents the degradation of photosynthetic protein complexes during drought. *Plant Cell Physiol* 2010;51:1929–41.
- Wang L, Wang Z, Xu Y, Joo SH, Kim SK, Xue Z, et al. *Osgsri1* is involved in crosstalk between gibberellins and brassinosteroids in rice. *Plant J* 2009; 57:498–510.
- Alonso-Ramírez A, Rodríguez D, Reyes D, Jiménez JA, Nicolás G, López-Climent M, et al. Evidence for a role of gibberellins in salicylic acid-modulated early plant responses to abiotic stress in Arabidopsis seeds. *Plant Physiol* 2009;150:1335–44.
- Wang C, Yang A, Yin H, Zhang J. Influence of water stress on endogenous hormone contents and cell damage of maize seedlings. *J Integr Plant Biol* 2008;50:427–34.
- Vyroubalová Š, Václavíková K, Turečková V, Novák O, Šmehilová M, Hluska T, et al. Characterization of new maize genes putatively involved in cytokinin metabolism and their expression during osmotic stress in relation to cytokinin levels. *Plant Physiol* 2009;151:433–47.
- Havlová M, Dobrev P, Motyka V, Štorchová H, Libus J, Dobrá J, et al. The role of cytokinins in responses to water deficit in tobacco plants over-expressing *trans-zeatin O-glucosyltransferase* gene under *35S* or *SAG12* promoters. *Plant Cell Environ* 2008;31:341–53.
- Gan S, Amasino RM. Inhibition of leaf senescence by autoregulated production of cytokinin. *Science* 1995;270:1986–8.
- Sýkorová B, Kurešová G, Daskalova S, Trčková M, Hoyerová K, Raimanová I, et al. Senescence-induced ectopic expression of the *A. tumefaciens ipt* gene in wheat delays leaf senescence, increases cytokinin content, nitrate influx, and nitrate reductase activity, but does not affect grain yield. *J Exp Bot* 2008;59:377–87.

- [26] Sharp RE, LeNoble ME. ABA, ethylene and the control of shoot and root growth under water stress. *J Exp Bot* 2002;53:33–7.
- [27] Albacete AA, Martínez-Andújar C, Pérez-Alfocea F. Hormonal and metabolic regulation of source–sink relations under salinity and drought: from plant survival to crop yield stability. *Biotechnol Adv* 2014;32:12–30.
- [28] Werner T, Nehnevajova E, Köllmer I, Novák O, Strnad M, Krämer U, et al. Root-specific reduction of cytokinin causes enhanced root growth, drought tolerance, and leaf mineral enrichment in *Arabidopsis* and tobacco. *Plant Cell* 2010;22:3905–20.
- [29] Macková H, Hronková M, Dobrá J, Turečková V, Novák O, Lubovská Z, et al. Enhanced drought and heat stress tolerance of tobacco plants with ectopically enhanced cytokinin oxidase/dehydrogenase gene expression. *J Exp Bot* 2013;64:2805–15.
- [30] Pospíšilová H, Jiskrová E, Vojta P, Mrázová K, Kokáš P, Majeská Čudejková M, et al. Transgenic barley overexpressing a cytokinin dehydrogenase gene shows greater tolerance to drought stress. *New Biotechnol* 2016;33:692–705.
- [31] Vlamis J, Williams DE. Ion competition in manganese uptake by barley plants. *Plant Physiol* 1962;37:650–5.
- [32] Turner NC, Abbo S, Berger JD, Chaturvedi SK, French RJ, Ludwig C, et al. Osmotic adjustment in chickpea (*Cicer arietinum* L.) results in no yield benefit under terminal drought. *J Exp Bot* 2007;58:187–94.
- [33] Livak KJ, Schmittgen TD. Analysis of relative gene expression data using real-time quantitative PCR and the 2<sup>-ΔΔCT</sup> method. *Methods* 2001;25:402–8.
- [34] Kim D, Pertea G, Trapnell C, Pimentel H, Kelley R, Salzberg SL. TopHat2: accurate alignment of transcriptomes in the presence of insertions, deletions and gene fusions. *Genome Biol* 2013;14:R36.
- [35] Anders S, Pyl PT, Huber W. HTSeq – a Python framework to work with high-throughput sequencing data. *Bioinformatics* 2014;31:166–9.
- [36] Love MI, Huber W, Anders S. Moderated estimation of fold change and dispersion for RNA-Seq data with DESeq2. *Genome Biol* 2014;15:550.
- [37] Kokáš P, Vojta P, Galuszka P. Comparative transcriptome analysis of barley (*Hordeum vulgare*) exposed to drought and subsequent re-watering. *Data Brief* 2016 [submitted for publication].
- [38] Conesa A, Götz S, García-Gómez JM, Terol J, Talón M, Robles M. Blast2GO: a universal tool for annotation, visualization and analysis in functional genomics research. *Bioinformatics* 2005;21:3674–6.
- [39] Camacho C, Coulouris G, Avagyan V, Ma N, Papadopoulos J, Bealer K, et al. BLAST+: architecture and applications. *BMC Bioinform* 2009;10:421.
- [40] Moreira-Vilar FC, Siqueira-Soares RDC, Finger-Teixeira A, De Oliveira DM, Ferro AP, Da Rocha GJ, et al. The acetyl bromide method is faster, simpler and presents best recovery of lignin in different herbaceous tissues than klason and thioglycolic acid methods. *PLoS ONE* 2014;9:e110000.
- [41] Gruz J, Novák O, Strnad M. Rapid analysis of phenolic acids in beverages by UPLC–MS/MS. *Food Chem* 2008;111:789–94.
- [42] Oxborough K, Baker NR. Resolving chlorophyll *a* fluorescence images of photosynthetic efficiency into photochemical and non-photochemical components – calculation of *qP* and *Fv'/Fm'* without measuring *Fo'*. *Photosynth Res* 1997;54:135–42.
- [43] Hassan IA. Effects of water stress and high temperature on gas exchange and chlorophyll fluorescence in *Triticum aestivum* L.. *Photosynthetica* 2006;44:312–5.
- [44] Roostaei M, Mohammadi SA, Amri A, Majidi E, Nachit M, Haghparast R. Chlorophyll fluorescence parameters and drought tolerance in a mapping population of winter bread wheat in the highlands of Iran. *Russ J Plant Physiol* 2011;58:351–8.
- [45] Robredo A, Pérez-López U, Miranda-Apodaca J, Lacuesta M, Mena-Petite A, Muñoz-Rueda A. Elevated CO<sub>2</sub> reduces the drought effect on nitrogen metabolism in barley plants during drought and subsequent recovery. *Environ Exp Bot* 2011;71:399–408.
- [46] Rippert P, Matringe M. Molecular and biochemical characterization of an *Arabidopsis thaliana* arogenate dehydrogenase with two highly similar and active protein domains. *Plant Mol Biol* 2002;48:361–8.
- [47] Cass CL, Peraldi A, Dowd PF, Mottiar Y, Santoro N, Karlen SD, et al. Effects of PHENYLALANINE AMMONIA LYASE (PAL) knockdown on cell wall composition, biomass digestibility, and biotic and abiotic stress responses in *Brachypodium*. *J Exp Bot* 2015;66:4317–35.
- [48] Feussner I, Wasternack C. The lipoxygenase pathway. *Annu Rev Plant Biol* 2002;53:275–97.
- [49] Wasternack C. Action of jasmonates in plant stress responses and development – applied aspects. *Biotechnol Adv* 2014;32:31–9.
- [50] Tian D, Tooker J, Peiffer M, Chung SH, Felton GW. Role of trichomes in defense against herbivores: comparison of herbivore response to woolly and hairless trichome mutants in tomato (*Solanum lycopersicum*). *Planta* 2012;236:1053–66.
- [51] Ueda J, Kato J. Identification of jasmonic acid and abscisic acid as senescence-promoting substances from *Cleyera ochracea* DC. *Agric Biol Chem* 1982;46:1975–6.
- [52] O'Brien JA, Benková E. Cytokinin cross-talking during biotic and abiotic stress responses. *Front Plant Sci* 2013;4:451.
- [53] Baldwin IT, Schemelz EA, Ohnmeiss TE. Wound-induced changes in root and shoot jasmonic acid pools correlate with induced nicotine synthesis in *Nicotiana sylvestris* ssp. *spagazzini* and *comes*. *J Chem Ecol* 1994;20:2139–57.
- [54] Moon J, Parry G, Estelle M. The ubiquitin–proteasome pathway and plant development. *Plant Cell* 2004;16:3181–95.
- [55] Zubo YO, Yamburenko MV, Selivankina SY, Shakirova FM, Avalbaev AM, Kudryakova NV, et al. Cytokinin stimulates chloroplast transcription in detached barley leaves. *Plant Physiol* 2008;148:1082–93.
- [56] Wei W, Alexandersson E, Gollmack D, Miller AJ, Kjellbom PO, Fricke W. HvPIP1;6, a barley (*Hordeum vulgare* L.) plasma membrane water channel particularly expressed in growing compared with non-growing leaf tissues. *Plant Cell Physiol* 2007;48:1132–47.
- [57] Nakabayashi R, Yonekura-Sakakibara K, Urano K, Suzuki M, Yamada Y, Nishizawa T, et al. Enhancement of oxidative and drought tolerance in *Arabidopsis* by overaccumulation of antioxidant flavonoids. *Plant J* 2014;77:367–79.
- [58] Cha JY, Barman DN, Kim MG, Kim WY. Stress defense mechanisms of NADPH-dependent thioredoxin reductases (NTRs) in plants. *Plant Signal Behav* 2015;10:e1017698.
- [59] Cheng Z, Dong K, Ge P, Bian Y, Dong L, Deng X, et al. Identification of leaf proteins differentially accumulated between wheat cultivars distinct in their levels of drought tolerance. *PLoS ONE* 2015;10:e0125302.
- [60] Jiang Y, Chen R, Dong J, Xu Z, Gao X. Analysis of GDSL lipase (GLIP) family genes in rice (*Oryza sativa*). *Plant Omics* 2012;5:351–8.
- [61] Hong JK, Choi HW, Hwang IS, Kim DS, Kim NH, Choi DS, et al. Function of a novel GDSL-type pepper lipase gene, *CaGLIP1*, in disease susceptibility and abiotic stress tolerance. *Planta* 2008;227:539–58.
- [62] Galichet A, Hoyerová K, Kamínková M, Gruitsem V. Farnesylation directs AtIPT3 subcellular localization and modulates cytokinin biosynthesis in *Arabidopsis*. *Plant Physiol* 2008;146:1155–64.
- [63] Tsai YC, Weir NR, Hill K, Zhang W, Kim HJ, Shiu SH, et al. Characterization of genes involved in cytokinin signaling and metabolism from rice. *Plant Physiol* 2012;158:1666–84.
- [64] Tran LSP, Nakashima K, Sakuma Y, Simpson SD, Fujita Y, Maruyama K, et al. Isolation and functional analysis of *Arabidopsis* stress-inducible NAC transcription factors that bind to a drought-responsive *cis*-element in the *early responsive to dehydration stress 1* promoter. *Plant Cell* 2004;16:2481–98.
- [65] Abe H, Urao T, Ito T, Seki M, Shinozaki K, Yamaguchi-Shinozaki K. *Arabidopsis* AtMYC2 (bHLH) and AtMYB2 (MYB) function as transcriptional activators in abscisic acid signaling. *Society* 2003;15:63–78.
- [66] Bu Q, Jiang H, Li CB, Zhai Q, Zhang J, Wu X, et al. Role of the *Arabidopsis thaliana* NAC transcription factors ANAC019 and ANAC055 in regulating jasmonic acid-signaled defense responses. *Cell Res* 2008;18:756–67.
- [67] Redillas MCFR, Jeong JS, Kim YS, Jung H, Bang SW, Choi YD, et al. The overexpression of OsNAC9 alters the root architecture of rice plants enhancing drought resistance and grain yield under field conditions. *Plant Biotechnol J* 2012;10:792–805.
- [68] McSteen P. Auxin and monocot development. *Cold Spring Harb Perspect Biol* 2010;2:a001479.
- [69] Mayer KFX, Waugh R, Langridge P, Close TJ, Wise RP, et al. A physical, genetic and functional sequence assembly of the barley genome. *Nature* 2012;491:711–6.

## Down-regulation of catalase activity contributes to senescence induction in wheat leaves exposed to shading stress

H.F. CAUSIN<sup>1\*</sup>, C.F. MARCHETTI<sup>1</sup>, L.B. PENA<sup>2</sup>, S.M. GALLEGGO<sup>2</sup>, and A.J. BARNEIX<sup>3</sup>

*Facultad de Ciencias Exactas y Naturales, Universidad de Buenos Aires, C1428EHA Ciudad Autónoma de Buenos Aires, Argentina<sup>1</sup>*

*Facultad de Farmacia y Bioquímica, Universidad de Buenos Aires, C1113AAC Ciudad Autónoma de Buenos Aires, Argentina<sup>2</sup>*

*Instituto de Suelos, CIRN-INTA, N. Repetto y de los Reseros, 1686 Castelar, Buenos Aires, Argentina<sup>3</sup>*

### Abstract

In shaded wheat (*Triticum aestivum* L.) leaves, the suppression of blue radiation (BR) triggers senescence. This phenomenon is correlated to an increase in oxidative stress symptoms and a decrease of catalase (CAT) activity, among other traits. Previous data suggest that the radiation signal transduction pathway may involve changes in  $\text{Ca}^{2+}$  and  $\text{H}_2\text{O}_2$  homeostasis. For better a understanding of the interaction among the spectral composition of radiation,  $\text{Ca}^{2+}$  availability, and the antioxidant metabolism in the regulation of shade-induced senescence, detached wheat leaves were placed in a growth chamber and exposed to either blue (B, high BR transmittance) and/or green (G, very low BR transmittance) *Lee*<sup>®</sup> filters in the absence or presence of 0.8 mM verapamil (a  $\text{Ca}^{2+}$  channels blocker), 4.0 mM EGTA (a  $\text{Ca}^{2+}$  chelator), or 8.0 mM 3-amino-1,2,4-triazole (a CAT inhibitor). At defined time points, the leaf samples were analyzed for changes in chlorophyll content, specific activities of CAT, ascorbate peroxidase (APX), and guaiacol peroxidase (POX), CAT isozymes, and gene expression of *CAT1*, *CAT2*, and two senescence markers (*TaSAG1* and *TaSAG3*). BR transmittance decreased the chlorophyll degradation rate and *SAG* genes expression either in leaves continuously exposed under the B filter, as well as in leaves previously exposed under the G filter. The effect of BR was associated with the maintenance of a high CAT (but not APX and POX) activity, and it was suppressed either in the presence of 3-AT or when  $\text{Ca}^{2+}$  availability was decreased. BR altered the CAT activity both at the transcriptional and at the post-transcriptional level. Nevertheless, different responses of CAT isozymes and CAT genes expression profiles to specific treatment combinations indicate that they differed in their regulatory pathways.

*Additional key words:* antioxidants, blue radiation, calcium, gene expression, *Triticum aestivum*

### Introduction

Senescence is a physiological process during which leaves experience major changes in their morphology and metabolism (Gepstein 2004, Keskitalo *et al.* 2005, Lim *et al.* 2007, Love *et al.* 2008). Even though it is a genetically controlled process, many exogenous factors can prompt it. Leaves beneath a dense canopy experience a marked reduction of the photon flux density (PFD) as well as of the red (660 nm) and blue (400 - 450 nm)

wavelengths due to chlorophyll and other pigments absorption, and it has been shown that changes in either PFD or spectral composition can induce leaf senescence in an independent way (reviewed in Causin and Barneix 2007). Although a decrease in the red to far red ratio was shown to trigger leaf senescence in different dicotyledonous species (Guamét *et al.* 1989, Rouseaux *et al.* 1996, 1997, Yang *et al.* 2012), we have recently

---

Submitted 20 May 2014, last revision 7 August 2014, accepted 12 August 2014.

*Abbreviations:* APX - ascorbate peroxidase; 3-AT - 3-amino-1,2,4-triazole; BR - blue radiation; CAT - catalase; EGTA - ethyleneglycol-bis-( $\beta$ -amino-ethylether)-N,N,N',N'-tetraacetic acid; PFD - photon flux density; POX - guaiacol peroxidase; PVPP - polyvinylpyrrolidone.

*Acknowledgements:* We thank Dr. Ezequiel Petrillo for his valuable help in the determination of *TaSAG* genes expression. The present work was supported by CONICET (PIP 11220080101142), and the University of Buenos Aires (UBACyT 20020100200214 and UBACyT 20020100100059).

\* Corresponding author; fax: (+54) 11 45763300, e-mail: ssvhfc@gmail.com

demonstrated that in leaves of wheat, chlorophyll and soluble protein degradation rates under shade conditions are only slightly affected by changes in the red to far red ratio, but they significantly increase when blue wavelengths are suppressed (Causin *et al.* 2006, Causin and Barneix 2007, Causin *et al.* 2009, see also Fig. 1 Suppl.). Among other factors, the development of senescence symptoms is correlated with changes in the content of H<sub>2</sub>O<sub>2</sub> and other indicators of oxidative stress, or with a decrease of catalase (CAT, EC 1.11.1.6) activity. These results led us to hypothesize that in wheat leaves, blue radiation (BR) suppression would act as a stress signal that initiates senescence, and that oxidative processes are an important component of this phenomenon. Even though the pathway of the BR signal perception and transduction remains to be elucidated, previous work suggested that changes in Ca<sup>2+</sup> availability associated to BR signaling pathways are involved in the regulation of this process (Causin *et al.* 2006).

Plants possess both enzymatic and non-enzymatic systems to counteract oxidative stress and among them, the CAT activity plays a central role in stress defense (Willekens *et al.* 1997). Plant CATs are heme-containing enzymes usually present in multiple isoforms. In Angiosperms studied so far, CATs are encoded by a small family of genes showing complex spatial and temporal patterns of expression (Luna *et al.* 2004, Smykowski *et al.* 2010, Mhamdi *et al.* 2012). The active enzyme is believed to be a homo- or hetero-tetramer made up of four subunits of about 60 kDa each. An adequate CAT activity is essential for the removal of H<sub>2</sub>O<sub>2</sub> produced by photorespiration (Noctor *et al.* 2000), but also appears to be critical for maintaining the redox

## Materials and methods

**Plant growth and experiments:** Wheat (*Triticum aestivum* L., cv. INTA Oasis) caryopses were surface sterilized in 10 % (v/v) H<sub>2</sub>O<sub>2</sub> for 12 min, germinated on wet tissue paper, after 24 h transplanted to plastic pots containing a mixture of sand : *Agrolite* : *Vermiculite* (2:1:1), and grown in a greenhouse at a natural (12 - 13 h depending on the time of the year) photoperiod. Pots were periodically irrigated with tap water and, after a week, fertilized as indicated in Causin *et al.* (2006). To study the effect of radiation spectral quality on leaf senescence under shading conditions, four fully expanded leaf blades (usually the third ones) of 26-d-old plants were excised and incubated for different times in plastic boxes (3 - 4 independent replicates per treatment conditions) whose lids were covered with *Lee Filters* (Andover, UK), green #089 (which simulates the transmittance spectrum of a green leaf) or blue #075, hereafter referred as treatment G or B, respectively. These filters were chosen because, even though they differed in the percent transmission of blue wavelengths,

they decreased the photosynthetically active photon flux density (PPFD) to a similar extent and supplied a similar proportion of red (R = 660 nm) to far-red (FR = 730 nm) radiation (Causin *et al.* 2006, Fig. 1 Suppl. ). Where indicated, boxes without added filters were used as non-shaded controls (Ctr). The incubations were performed in a chamber supplied with an equal number of white (*Sylvania F27W T8/LD/54*) and blue + red radiation (*Sylvania GroLux F30W T12*) fluorescent tubes (an 18-h photoperiod), at day/night temperatures of 26 ± 2/17 ± 2 °C, and a relative humidity of 60/70 %. Average values for PFD were 192 ± 3 (non-shaded Ctr), 38 ± 2 (treatment G), and 37 ± 3 (treatment B) μmol m<sup>-2</sup> s<sup>-1</sup>. The measurements of PFD were performed with a *LI-190* quantum sensor (*LI-COR*, Lincoln, NE, USA) attached to a *CAVA-RAD* data logger (Cavadevices, Argentine). Depending on the experiment, the excised leaves were incubated on distilled water or on aqueous solutions containing either 4.0 mM ethyleneglycol-bis-(β-amino-ethylether)-N,N,N',N'-tetraacetic acid (EGTA; an

balance in the cell and for the prevention of oxidative damage under different stress conditions (Willekens *et al.* 1997, Orendi *et al.* 2001, Procházková *et al.* 2001, Luna *et al.* 2004, Vandenabeele *et al.* 2004, Azpillicueta *et al.* 2008, Pena *et al.* 2011). The presence of a Ca<sup>2+</sup>/calmodulin binding motif as well as an antioxidant responsive element (ARE) in the promoter of plant *CAT* genes probably underlies this important protective role (Polidoros and Scandalios 1999, Yang and Poovaiah 2002). In wheat, two *CAT* isoforms account for most of the enzyme activity present in the leaves, and two genes (*CAT1* and *CAT2*) have been demonstrated to encode *CAT* subunits (Luna *et al.* 2004, Yang *et al.* 2006). In wheat leaves, the expression of both genes is modulated by PFD, and the *CAT1* expression shows characteristics of circadian control (Luna *et al.* 2004). CATs are mostly PFD-sensitive. At moderate to high PFD, the prosthetic heme sensitizes their inactivation by BR in the presence of O<sub>2</sub> (Shang and Feierabend 1999). However, in rye leaves, BR was shown to be most effective in activating *CAT1* mRNA expression (Schmidt *et al.* 2006), which indicates that changes in both PFD and spectral composition may exert complex effects on the activity of *CAT* isozymes. To our knowledge, no information is available on how changes in spectral composition affect the activity and gene expression of *CAT* isoforms during shade induced senescence.

In the present work we studied the effect of changes in PFD and spectral composition on *CAT* activity and *CAT* genes expression profiles in wheat leaves exposed to a shading stress and analyzed the role of Ca<sup>2+</sup> ions as well as *CAT* suppression in the regulation of the senescence rate.



apoplastic Ca<sup>2+</sup> chelator), 0.8 mM verapamil (a Ca<sup>2+</sup> channels blocker), or 8.0 mM 3-amino-1,2,4 triazole (3-AT; a CAT inhibitor) which were added from appropriate stock solutions at specified time intervals. The solutions were supplied with 5 mm<sup>3</sup> dm<sup>-3</sup> Tween 20 to increase tissue contact with the medium. Leaves were sampled at different time intervals, briefly rinsed in distilled water, blotted dry and immediately ground with liquid N<sub>2</sub>. Tissue samples were kept at -70 °C for the further analysis. When indicated, the same procedure was performed with samples of leaves detached prior to beginning radiation treatments (T<sub>0</sub>). All the experiments were repeated at least twice. Whenever possible, data from different experiments were averaged, otherwise data from one representative experiment are presented.

**Chlorophyll content and enzyme activities:** Chlorophyll *a+b* content was measured either in N,N-dimethylformamide extracts (10 mg of leaf fresh mass per 4 cm<sup>3</sup>) according to Porra (2002) or with a SPAD Chlorophyll Meter 502 (Konica Minolta, Tokyo, Japan), depending on the experiment. On average, eight measurements per leaf blade and three to five leaves were measured per treatment.

Catalase, ascorbate peroxidase (APX, EC 1.11.1.11), and guaiacol peroxidase (POX, EC 1.11.1.7) activities were assayed in crude homogenates obtained by grinding a 0.1 g leaf sample with 1.2 cm<sup>3</sup> of an extraction buffer [50 mM potassium phosphate, pH 7.6, containing 1.0 mM ethylenediaminetetraacetic acid (disodium salt), 1.0 mM ascorbic acid, 1.0 mM dithiothreitol, 0.5 mM phenylmethylsulfonyl fluoride, and 0.15 % (v/v) Triton X100] in the presence of 20 - 25 mg polyvinylpyrrolidone. The homogenates were centrifuged (18 000 g, 25 min), the supernatants collected and centrifuged for a second time (19 500 g, 10 min) prior to enzyme assays. All procedures were performed at 4 °C. Reaction buffers were either 50 mM potassium phosphate, pH 7.0 (for CAT and APX assays) or 150 mM potassium phosphate, pH 6.1 (for POX assay). CAT activity was measured according to Aebi (1984). For calculations, the slope of the initial (20 s) decrease in absorbance due to H<sub>2</sub>O<sub>2</sub> consumption was taken into account. One unit was the amount of enzyme that decomposed 1 μmol of H<sub>2</sub>O<sub>2</sub> per min in 1 cm<sup>3</sup> of reaction mixture at pH 7.0 and 25 °C. APX and POX activities were assayed following the procedures described in Procházková *et al.* (2001). CAT isozymes were separated on 9 % (m/v) non-denaturing polyacrylamide gels (15 μg of protein from crude extracts per lane), at 4 °C (3 h, 150 V). After electrophoresis, CAT isoforms were visualized according to Woodbury *et al.* (1971). Densitometric analysis of zymograms was performed on scanned images of the gels using the Image J free software (Image J 1.47v. NIH, Bethesda, USA) and their content was expressed as relative units. Protein content in the crude extracts was determined with the method of Bradford (1976).

#### **Analysis of CAT1 and CAT2 expression by RT-PCR:**

Total RNA was isolated from 100 mg of frozen, powdered leaves by the addition of 1 cm<sup>3</sup> of a TRIzol® reagent according to the manufacturer's protocol (Molecular Research Center Inc., Cincinnati, USA). RNA content was determined using NanoDrop 2000 (Thermo Scientific, Waltham, USA). RNA (1 μg) was treated with DNase I (Promega, Madison, USA) and then converted to cDNA with oligo-dT 15 (Invitrogen, Carlsbad, USA) using RevertAid™ M-MuLV reverse transcriptase (Invitrogen). The primers and accession numbers (GeneBank ID) used were: wheat CAT1 (E16461) F 5'-ACTACGACGGGCTCATG-3' and R 5'-GCCCTGAAGCAGATTTCT-3', wheat CAT2 (X94352), F 5'-CCTTAATCAGCAGGGATG-3' and R 5'-AGATAGAACACGCGGAG -3'. PCR conditions were: 5 mm<sup>3</sup> of cDNA diluted 1/40 per reaction, and annealing at 95 °C for 3 min, 35 cycles of 95 °C for 30 s, 52 °C for 30 s, 72 °C for 40 s, and a final extension at 72 °C for 10 min. PCR reactions were performed using a programmable Thermocycler T 18 (Ivema, Buenos Aires, Argentina). The PCR-amplified products were fractionated by electrophoresis on a 1.5 % (m/v) agarose gel and stained with ethidium bromide. Fragments of wheat *actin* and *tubulin* genes were amplified as internal standards. The primers and accession numbers used were: *actin* (AB181991) F 5'-GGATCGGTGGCTCTATTT TG-3' and R 5'-TGTACCCCTTATTCCTCTGAGG-3', *tubulin* (*Tubb5*, U76896) F 5'-TTCCTGCACTGG TACACGGG-3' and R 5'-AGCCATCAGAAATAGCC CCG-3'. Gels were photographed with a digital imaging system (FOTODYNE, Hartland, USA) and analyzed with a Gel-Pro analyzer (Exon-Intron, Loganville, USA). Each expression profile presented is representative of at least three biological replicates.

#### **Analysis of TaSAG genes expression by real-time quantitative (RT-qPCR):**

Two leaf senescence-associated gene homologs were used as developmental markers (Kajimura *et al.* 2010). Reverse transcription reactions were performed using 2 μg of purified total RNA (see above) and using oligo-dT according to the M-MLV reverse transcriptase protocol (Life Technologies, Carlsbad, USA). RT-qPCR reactions were performed using an Eppendorf Master cycler Realplex machine. The primers and accession numbers used were: *TaSAG1* (CJ637025) F 5'-GTTGCCATTGAAGCGTTG-3' and R 5'-CACTCC TGTCGAATATAGC-3', *TaSAG3* (CJ683824) F 5'-TATACAGCAGTAGATTCCAAGAG-3' and R 5'-CACGCCATAGAAGAACC-3'. The reaction mixture contained 5 mm<sup>3</sup> of cDNA diluted 1/30, 20 μM specific primers, 0.75 U of Taq DNA polymerase (Life Technologies), 3 mM MgCl<sub>2</sub>, 10 mM dNTP, 0.025 mm<sup>3</sup> of SYBR Green (Roche, Mannheim, Germany) in a final volume of 25 mm<sup>3</sup>. Wheat β-tubulin (*Tubb2*, U76745) was used as internal standard with the following primers sequences: F 5'-CAATGTCAAGTCCAGCG

TCT-3' and R 5'-AGGTCGTTTCATGTTGCTCTC-3'. PCR conditions were: 95 °C for 2 min, 40 cycles of 95 °C for 15 s, 68 °C for 35 s, 95 °C for 15 s, 60 °C for 15 s, and 95 °C for 15 s. We completed each run with a melting curve to confirm the specificity of amplification.

**Statistical analyses:** Within each experiment, data from each sampling were analyzed separately with conventional one-way or two-way *ANOVA* (*Statistica*,

## Results

A high BR transmission in the shading treatments consistently decreased the senescence rate of excised leaves, although the efficiency was higher in treatments with a longer exposure to the B filter (Fig. 1A, compare treatments B, GB<sub>30</sub>, and GB<sub>54</sub>). In all cases, the senescence retardant effect of BR was accompanied by the maintenance of a higher CAT activity than in the treatment G (Fig. 1B).

To further analyze the role of CAT activity as well as the influence of Ca<sup>2+</sup> ions on this process, an experiment was conducted where leaves firstly exposed under the G filter for 52 h were then exposed under the filter B in the absence (treatment GB) or presence of the CAT inhibitor 3-AT (treatment GB<sub>3AT</sub>), the Ca<sup>2+</sup> chelator EGTA (treatment GB<sub>EGTA</sub>), or the Ca<sup>2+</sup> channel blocker verapamil (treatment GB<sub>VP</sub>). Leaves continuously exposed to filter B or G were used as controls. The senescence retardant effect of BR was consistently suppressed when leaves were exposed to GB<sub>AT</sub>, GB<sub>EGTA</sub>, or GB<sub>VP</sub> (Fig. 2A). The analysis of CAT activity confirmed that BR is an important cue for its stimulation (compare treatments B, G, and GB in Fig. 2B). As for chlorophyll degradation, the presence of either 3-AT or EGTA (but not verapamil) markedly inhibited the CAT stimulatory effect of BR (Fig. 2B). The fact that only a minor effect was exerted by verapamil (Fig. 2B, the treatment GB<sub>VP</sub>) suggests that this Ca<sup>2+</sup> channel blocker could alter the senescence rate by interfering with BR-regulated processes other than CAT activity. The activities of APX and POX increased with time in all the experimental conditions (Fig. 2C,D). Nevertheless, as opposed to CAT, the activities of these peroxidases were either not stimulated (POX), or rather inhibited (APX) by BR. Moreover, after 80 h, the activity of APX and, to a lesser extent, POX was up-regulated in those conditions where the senescence rate decreased with respect to the treatment B (Fig. 2C,D, the treatments G, GB<sub>3AT</sub>, GB<sub>EGTA</sub>, and GB<sub>VP</sub>).

The expressions of *TaSAG1* and *TaSAG3* slightly increased with time in the treatment B, but they were significantly higher than at T<sub>0</sub> in leaves exposed under the G filter for 52 and 80 h (Fig. 3). At 80 h, the expressions of both genes were down-regulated to almost initial levels in the treatment GB indicating that BR not only

*Stat Soft Inc.*, Tulsa, USA), depending on the experimental design. The model included radiation treatment and, where appropriate, pharmacological treatments as fixed factors. When necessary, data were log transformed to meet *ANOVA* assumptions. Post-hoc comparisons for significant main effects or interaction terms were performed using the Tukey HSD test. A given effect was assumed significant at *P* < 0.05, unless otherwise stated.

prevented chlorophyll degradation, but acted as overall senescence retardant signal when supplied to the shade stressed leaves. As for chlorophyll degradation, the effect of BR on *TaSAG* genes expression was also consistently suppressed when either the Ca<sup>2+</sup> availability or CAT activity was negatively affected (Fig. 3, the treatments GB<sub>3AT</sub>, GB<sub>EGTA</sub>, and GB<sub>VP</sub>).

In order to better understand the role of radiation spectral composition in the regulation of CAT activity, we performed CAT zymograms, and analyzed *CAT1* and *CAT2* expression profiles. Native PAGE of crude extracts revealed the presence of two CAT isoforms, although

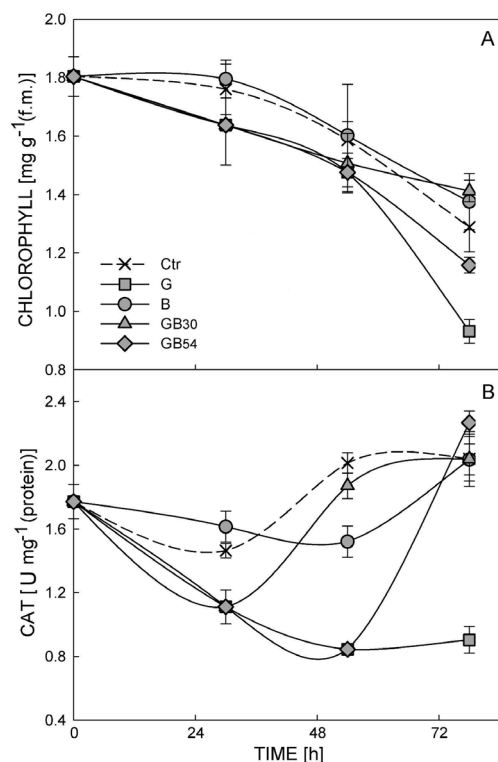


Fig. 1. The chlorophyll content (A) and CAT specific activity (B) in excised wheat leaves floated on distilled water and exposed to white radiation (control, Ctr) or shaded under the green (G) or blue (B) filter. A set of leaves from the treatment G were changed to the B after either 30 h (treatment GB<sub>30</sub>) or 54 h (treatment GB<sub>54</sub>). Data are means  $\pm$  SD (*n* = 4).

CAT2 was the prominent enzyme (Fig. 4). Even though the activity of both the isoforms declined when BR was suppressed, or in the presence of either 3-AT or EGTA,

the densitometric measurements indicate that the minor isoform, CAT1, was more sensitive than CAT2 (Fig. 4). As for the total CAT activity, verapamil did not

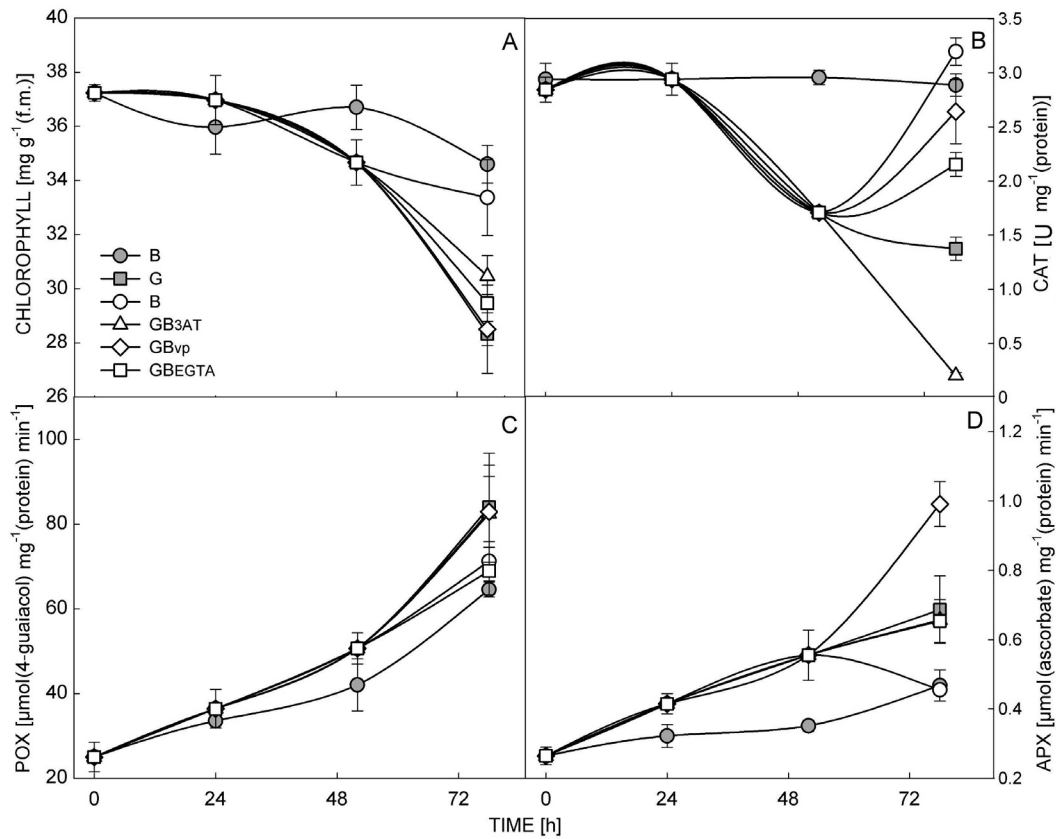


Fig. 2. The chlorophyll content (A), CAT specific activity (B), POX specific activity (C), and APX specific activity (D), in excised wheat leaves exposed under the G filter and after 52 h under the B filter in the absence (treatment GB) or presence of 8.0 mM 3-AT (treatment GB<sub>3AT</sub>), 4.0 mM EGTA (treatment GB<sub>EGTA</sub>), or 0.8 mM verapamil (treatment GB<sub>vp</sub>). Leaves continuously exposed to the filter B or G without pharmacological treatments were used as controls. Means  $\pm$  SD ( $n = 4$ ).

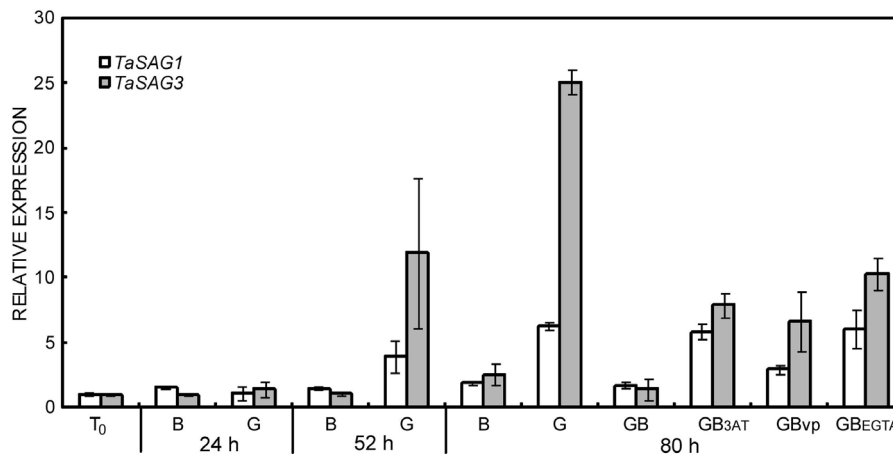


Fig. 3. Relative abundances of *TaSAG1* and *TaSAG3* transcripts at 0, 24, 52, and 80 h in excised wheat leaves exposed under the G filter and after 52 h under the B filter in the absence (treatment GB), or presence of 8.0 mM 3-AT (treatment GB<sub>3AT</sub>), 4.0 mM EGTA (treatment GB<sub>EGTA</sub>), or 0.8 mM verapamil (treatment GB<sub>vp</sub>). Leaves continuously exposed to the filter B or G without pharmacological treatments were used as controls. Data were normalized considering the expression at T<sub>0</sub> = 1. Means  $\pm$  SD ( $n = 3$ ).

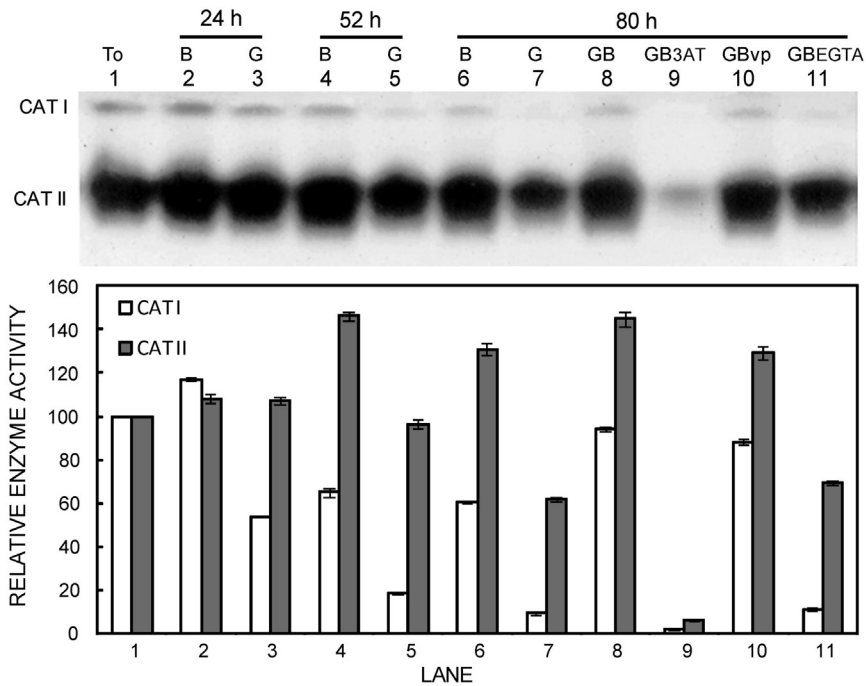


Fig. 4. Activities of CAT isoforms at 0, 24, 52, and 80 h in excised wheat leaves exposed under the G filter and after 52 h under the B filter in the absence (treatment GB), or presence of 8.0 mM 3-AT (treatment GB<sub>3AT</sub>), 4.0 mM EGTA (treatment GB<sub>EGTA</sub>), or 0.8 mM verapamil (treatment GB<sub>VP</sub>). Leaves continuously exposed to the filter B or G without pharmacological treatments were used as controls. Values from the densitometric analysis represent means  $\pm$  SD ( $n = 3$ ). Data were normalized considering density units at  $T_0 = 100$  %. Note that the picture was inverted (“negative image”) to better visualize CAT I bands.

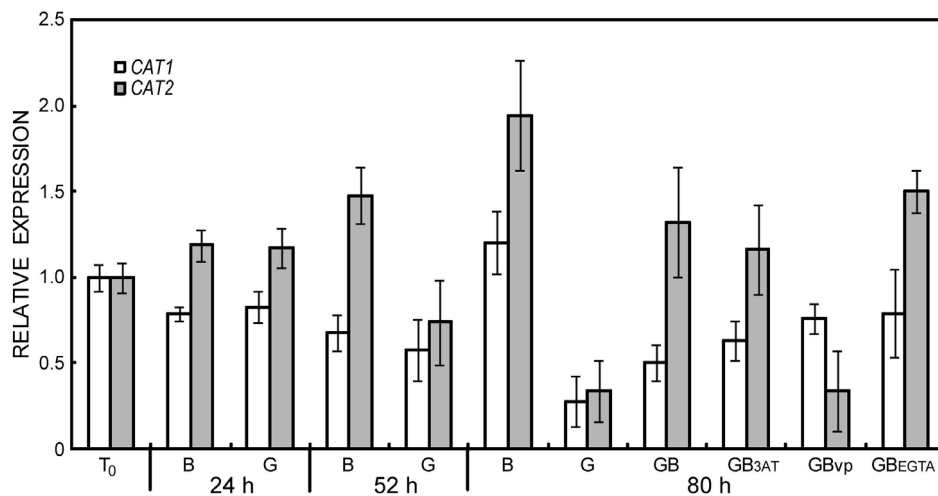


Fig. 5. Relative abundances of *CAT1* and *CAT2* transcripts at 0, 24, 52, and 80 h in excised wheat leaves exposed under the G filter and after 52 h under the B filter in the absence (treatment GB), or presence of 8.0 mM 3-AT (treatment GB<sub>3AT</sub>), 4.0 mM EGTA (treatment GB<sub>EGTA</sub>), or 0.8 mM verapamil (treatment GB<sub>VP</sub>). Leaves continuously exposed to the filter B or G without pharmacological treatments were used as controls. Data were normalized considering the expression levels at  $T_0 = 1$ . Means  $\pm$  SD ( $n = 3$ ).

significantly suppress the effect of BR on any isoform.

As CAT activity is down-regulated during the night (see Fig. 2 Suppl.), the analysis of *CAT* genes expression was performed on leaves sampled 5 to 6 h after the initiation of the photoperiod. The *CAT1* relative

expression decreased with time to a similar extent in both the G- and B-treatments during the first 52 h (Fig. 5). At 80 h, the *CAT1* expression increased to the initial level in leaves exposed to the treatment B, whereas it attained about 30 % of the  $T_0$ -expression in leaves shaded under

the filter G (Fig. 5). In leaves under the GB treatment, a partial (statistically significant) recovery of *CAT1* expression was obtained (Fig. 5). Interestingly, this stimulatory effect of BR was independent of the three pharmacological treatments tested. In contrast to *CAT1*, the *CAT2* expression increased with time in leaves continuously exposed to the B filter, whereas it

significantly decreased after the 52 and 80 h exposures to the G filter (Fig. 5). As for *CAT1*, the expression of *CAT2* consistently increased at 80 h in leaves from the GB treatment. Although this increment was also independent on the presence of 3-AT or EGTA, verapamil suppressed the stimulatory effect of BR (Fig. 5).

## Discussion

Data from the present work support previous evidence indicating that changes in BR transmittance have a central role in the regulation of the senescence rate in wheat leaves exposed to shading (Causin *et al.* 2006, Causin and Barneix 2007). This was confirmed not only by the analysis of chlorophyll degradation rate, but also at the molecular level as indicated by the changes in the expression profiles of two senescence markers (*TaSAG1* and *TaSAG3*).

Under our experimental conditions, the senescence retardant effect of BR was systematically accompanied by the maintenance of a high CAT activity but not by APX or POX activities. Moreover, the effect of BR was suppressed in the presence of 3-AT even when the activities of APX and POX were stimulated. This is consistent with our hypothesis that the increment of senescence symptoms is associated to CAT rather than peroxidases down-regulation. CAT activity has been shown to play a central role in the prevention of cellular damage and the maintenance of the redox balance under different abiotic stresses as well as during senescence (Willekens *et al.* 1997, Corpas *et al.* 2001, Srivalli and Khanna-Chopra, 2001, Yang *et al.* 2006). Although different reports showed that the down-regulation of CAT activity causes serious disorders in leaves exposed to high PFD (*e.g.*, Willekens *et al.* 1997, Vandenabeele *et al.* 2004), our results suggest that a decrease in CAT activity could also play an important role in the increment of senescence rate in the shade stressed leaves.

Changes in  $\text{Ca}^{2+}$  content have been implicated in the regulation of CAT activity (Yang and Poovaiah 2002, Jiang and Zhang 2003). Different environmental signals can trigger rapid and transient increases in cytosolic  $\text{Ca}^{2+}$ , which in turn may increase the production of  $\text{O}_2^-$  and  $\text{H}_2\text{O}_2$ , through the stimulation of plasma membrane NADPH-oxidases among other mechanisms (Yang and Poovaiah 2002). Particularly, there is ample evidence that BR may alter  $\text{Ca}^{2+}$  homeostasis, and that many physiological processes regulated by BR depend either on changes in cytosolic  $\text{Ca}^{2+}$  and/or on specific  $\text{Ca}^{2+}$ -binding proteins as secondary messengers (Shinkle and Jones 1988, Elzenga *et al.* 1997, Baum *et al.* 1999, Guo *et al.* 2001, Folta *et al.* 2003, Stoelzle *et al.* 2003, Dodd *et al.* 2010). Some plant CATs have been shown to bind calmodulin which in turn increases their catalytic activity (Yang and Poovaiah 2002). Even though there is no

direct evidence that this is also true for wheat CATs, the fact that the stimulatory effect of BR on the CAT activity was suppressed by the presence of EGTA indicates that  $\text{Ca}^{2+}$  was involved in the signaling process. It has been suggested that the alteration of  $\text{Ca}^{2+}$  pools by BR may be mediated by the activation of  $\text{Ca}^{2+}$ -permeable voltage-gated channels (Stoelzle *et al.* 2003, Dodd *et al.* 2010). Verapamil is well known antagonist of plant hyperpolarization-activated  $\text{Ca}^{2+}$  channels (Demidchik *et al.* 2002, Shang *et al.* 2005), and it was shown to suppress some BR-mediated physiological responses (*e.g.*, Elzenga *et al.* 1997, Shimazaki *et al.* 1997). In our experimental conditions, verapamil exerted only a minor negative effect on either overall as well as CAT-isozymes activities suggesting that (an)other  $\text{Ca}^{2+}$  channel type(s) might be involved in the control of  $\text{Ca}^{2+}$  fluxes regulating this enzyme. Nevertheless, the fact that both the chlorophyll degradation rate as well as *SAG* genes expression increased in the presence of verapamil indicates that  $\text{Ca}^{2+}$  fluxes through voltage-gated channels contributed to the regulation of the overall senescence process by BR. This is in agreement with data reported by Huang *et al.* (1990) and Huang and Kao (1992), who found that failure to maintain the normal transmembrane flux of  $\text{Ca}^{2+}$ , including through verapamil-sensitive channels, markedly affects dark-induced senescence in detached leaves of certain crops like rice and maize.

Apart from stimulating the CAT specific activity, BR also increased the *CAT1* and *CAT2* expressions. Nevertheless, the control pathways involved seemed to differ between them. In fact, while the *CAT2* expression increased with time in leaves exposed to BR, the *CAT1* expression was particularly stimulated by BR at the later senescent stages. This may in part explain why a high CAT activity could be attained in leaves from the treatment G when they were changed to the B treatment at 52 - 54 h after the excision. On the other hand, although the presence of verapamil partially increased the *CAT1* expression, it suppressed the stimulatory effect exerted by BR on the *CAT2* expression. Interestingly, EGTA did not decrease the expression of both the *CAT* genes in the GB treated leaves, which suggests that, in our experimental conditions, the alteration of apoplastic  $\text{Ca}^{2+}$  availability by EGTA affected the enzyme activity mainly at the post-transcription level. The existence of differences in the radiation-regulated pathways among

*CAT* genes has been reported in other plants. For example, Acevedo *et al.* (1996) found that etiolated leaves of barley have greater amounts of *CAT1* mRNA compared with green leaves, whereas mRNA homologous to maize *CAT2* was induced by irradiance suggesting that barley contains radiation-inducible and radiation-repressible *CAT* genes. In *Arabidopsis thaliana*, mutational disruption of a BR photoreceptor, cryptochrome I, alters the pattern of the dark-expression of *CAT3* mRNA but not *CAT2* mRNA suggesting that in this species, the synthesis of the different *CAT* subunits are regulated by distinct cues (Zhong *et al.* 1997). Recently, Smykowski *et al.* (2010) identified G-box binding factor 1 (GBF1) as DNA-binding protein of the *CAT2* promoter which could be involved in the onset of senescence during bolting time in *A. thaliana* plants, most likely *via* the regulation of intracellular H<sub>2</sub>O<sub>2</sub> content.

Interestingly, GBF1 belongs to the group G of bZIP transcription factors which have been related to UV and BR signaling in different plant species (Jakoby *et al.* 2002).

In conclusion, changes in BR perception could be among the first cues triggering the signaling pathway regulating senescence rate in wheat leaves exposed to shading. When BR transmission was not suppressed, the development of senescence symptoms was delayed. This effect was in part associated to a stimulation of *CAT* activity which in turn had an important role in the control of the senescence rate by maintaining the homeostasis of endogenous H<sub>2</sub>O<sub>2</sub> content (*e.g.*, Causin *et al.* 2009). The alteration of Ca<sup>2+</sup> fluxes through verapamil-sensitive and -insensitive channels could be involved in the regulation of *CAT* isozymes and senescence rate by BR.

## References

- Aebi, H.: Catalase *in vitro*. - Methods Enzymol. **105**: 121-126, 1984.
- Acevedo, A., Skadsen, R.W., Scandalios, J.G.: Two barley catalase genes respond differentially to light. - Physiol. Plant. **96**: 369-374, 1996.
- Azpillicueta, C.E., Pena, L.B., Tomaro, M.L., Gallego, S.M.: Modifications in catalase activity and expression in developing sunflower seedlings under cadmium stress. - Redox Rep. **13**: 40-46, 2008.
- Baum, G., Long, C., Jenkins, G.I., Trewavas, A.J.: Stimulation of the blue light phototropic receptor NPH1 causes a transient increase in cytosolic Ca<sup>2+</sup>. - Proc. nat. Acad. Sci. USA **96**: 13554-13559, 1999.
- Bradford, M.M.: A rapid and sensitive method for the quantification of microgram quantities of proteins utilizing the principle of protein-dye binding. - Anal. Biochem. **72**: 248-254, 1976.
- Causin, H.F., Barneix, A.J.: The role of oxidative metabolism in the regulation of leaf senescence by the light environment. - Int. J. Plant Develop. Biol. **1**: 239-244, 2007.
- Causin, H.F., Jauregui, R.N., Barneix, A.J.: The effect of light spectral quality on leaf senescence and oxidative stress in wheat. - Plant Sci. **171**: 24-33, 2006.
- Causin, H.F., Roberts, I.N., Criado, M.V., Gallego, S.M., Pena, L.B., Ríos, M. del C., Barneix, A.J.: Changes in hydrogen peroxide homeostasis and cytokinin levels contribute to the regulation of shade-induced senescence in wheat leaves. - Plant Sci. **177**: 698-704, 2009.
- Corpas, F.J., Barroso, J.B., Del Río, L.A.: Peroxisomes as a source of reactive oxygen species and nitric oxide signal molecules in plant cells. - Trends Plant Sci. **6**: 145-150, 2001.
- Demidchik, V., Bowen, H.C., Maathuis, F.J.M., Shabala, S.N., Tester, M.A., White, P.J., Davies, J.M.: *Arabidopsis thaliana* root non-selective cation channels mediate calcium uptake and are involved in growth. - Plant J. **32**: 799-808, 2002.
- Dodd, A.N., Kudla, J., Sanders, D.: The language of calcium signaling. - Annu. Rev. Plant Biol. **61**: 593-620, 2010.
- Elzenga, J.T.M., Staal, M., Prins, H.B.A.: Calcium-calmodulin signalling is involved in light-induced acidification by epidermal leaf cells of pea, *Pisum sativum* L. - J. exp. Bot. **48**: 2055-2060, 1997.
- Folta, K.M., Lieg, E.J., Durham, T., Spalding, E.P.: Primary inhibition of hypocotyl growth and phototropism depend differently on phototropin-mediated increases in cytoplasmic calcium induced by blue light. - Plant Physiol. **133**: 1464-1470, 2003.
- Gepstein, S.: Leaf senescence - not just a 'wear and tear' phenomenon. - Genome Biol. **5**: 212, 2004.
- Guimét, J.J., Willemoes, J.G., Montaldi, E.R.: Modulation of progressive leaf senescence by red:far-red ratio of incident light. - Bot. Gaz. **150**: 148-151, 1989.
- Guo, H., Mockler, T., Duong, H., Lin, C.: SUB1, an *Arabidopsis* Ca<sup>2+</sup>-binding protein involved in cryptochrome and phytochrome coaction. - Science **291**: 487-490, 2001.
- Huang, Y., Chen, C.T., Kao, C.H.: Senescence of rice leaves XXIV. Involvement of calcium and calmodulin in the regulation of senescence. - Plant Cell Physiol. **31**: 1015-1520, 1990.
- Huang, Y., Kao, C.H.: The importance of transmembrane flux of Ca<sup>2+</sup> in regulating dark-induced senescence of detached corn leaves. - Bot. Bull. Acad. sin. **33**: 17-21, 1992.
- Jakoby, M., Weisshaar, B., Dröge-Laser, W., Vicente-Carbajosa, J., Tiedemann, J., Kroj, T., Parcy, F.: bZIP transcription factors in *Arabidopsis*. - Trends Plant Sci. **7**: 106-111, 2002.
- Jiang, M., Zhang, J.: Cross-talk between calcium and reactive oxygen species originated from NADPH oxidase in abscisic acid-induced antioxidant defense in leaves of maize seedlings. - Plant Cell Environ. **26**: 929-939, 2003.
- Kajimura, T., Mizuno, N., Takumi, S.: Utility of leaf senescence-associated gene homologs as developmental markers in common wheat. - Plant Physiol. Biochem. **48**: 851-859, 2010.
- Keskitalo, J., Bergquist, G., Gardeström, P., Jansson, S.: A cellular timetable of autumn senescence. - Plant Physiol. **139**: 1635-1648, 2005.
- Lim, P.O., Kim, H.J., Nam, H.G.: Leaf senescence. - Annu. Rev. Plant Biol. **58**: 115-136, 2007.

- Love, A.J., Milner, J.L., Sadanandom, A.: Timing is everything: regulatory overlap in plant cell death. - *Trends Plant Sci.* **13**: 589-595, 2008.
- Luna, C.M., Pastori, G.M., Driscoll, S., Groten, K., Bernard, S., Foyer, C.H.: Drought controls on H<sub>2</sub>O<sub>2</sub> accumulation, catalase (CAT) activity and *CAT* gene expression in wheat. - *J. exp. Bot.* **56**: 417-423, 2004.
- Mhamdi, A., Noctor, G., Baker, A.: Plant catalases: peroxisomal redox guardians. - *Arch. Biochem. Biophys.* **525**: 181-194, 2012.
- Noctor, G., Veljovic-Jovanovic, S., Foyer, C.: Peroxide processing in photosynthesis: antioxidant coupling and redox signalling. - *Phil. trans. roy. Soc. London B* **355**: 1465-1475, 2000.
- Orendi, G., Zimmermann, P., Baar, C., Zentgraf, U.: Loss of stress-induced expression of catalase 3 during leaf senescence in *Arabidopsis thaliana* is restricted to oxidative stress. - *Plant Sci.* **161**: 301-314, 2001.
- Pena, L.B., Azpilicueta, C.E., Gallego, S.M.: Sunflower cotyledons cope with copper stress by inducing catalase subunits less sensitive to oxidation. - *J. Trace Element med. Biol.* **25**: 125-129, 2011.
- Polidoros, A.N., Scandalios, J.G.: Role of hydrogen peroxide and different classes of antioxidants in the regulation of catalase and glutathione S-transferase gene expression in maize (*Zea mays* L.). - *Physiol. Plant.* **106**: 112-120, 1999.
- Porra, R.J.: The chequered history of the development and use of simultaneous equations for the accurate determination of chlorophylls *a* and *b*. - *Photosynth. Res.* **73**: 149-156, 2002.
- Procházková, D., Sairam, R.K., Srivastava, G.C., Singh, D.V.: Oxidative stress and antioxidant activity as the basis of senescence in maize leaves. - *Plant Sci.* **161**: 765-771, 2001.
- Rousseaux, M.C., Hall, A.J., Sánchez, R.A.: Far-red enrichment and photosynthetically active radiation level influence leaf senescence in field-grown sunflower. - *Physiol. Plant.* **96**: 217-224, 1996.
- Rousseaux, M.C., Ballaré, C.L., Jordan, E.T., Vierstra, R.D.: Directed overexpression of *PHYA* locally suppresses stem elongation and leaf senescence responses to far-red radiation. - *Plant Cell Environ.* **20**: 1551-1558, 1997.
- Schmidt, M., Grief, J., Feierabend, J.: Mode of translational activation of the catalase (*CAT1*) mRNA of rye leaves (*Secale cereale* L.) and its control through blue light and reactive oxygen. - *Planta* **223**: 835-846, 2006.
- Shang, W., Feierabend, J.: Dependence of catalase photoinactivation in rye leaves in light intensity and quality and characterization of a chloroplast-mediated inactivation in red light. - *Photosynth. Res.* **59**: 201-213, 1999.
- Shang, Z., Ma, L., Zhang, H., He, R., Wang, X., Cui, S.: Ca<sup>2+</sup> influx into lily pollen grains through a hyperpolarization-activated Ca<sup>2+</sup>-permeable channel which can be regulated by extracellular CaM. - *Plant Cell Physiol.* **46**: 598-608, 2005.
- Shimazaki, K., Misumi, T., Ayako, S.: Inhibition of the stomatal blue light response by verapamil at high concentration. - *Plant Cell Physiol.* **38**: 747-750, 1997.
- Shinkle, J.R., Jones, R.J.: Inhibition of stem elongation in *Cucumis* seedlings by blue light requires calcium. - *Plant Physiol.* **86**: 960-966, 1988.
- Smykowski, A., Zimmermann, P., Zentgraf, U.: G-box Binding Factor 1 reduces *CATALASE 2* expression and regulates the onset of leaf senescence in *Arabidopsis*. - *Plant Physiol.* **153**: 1321-1331, 2010.
- Srivalli, B., Khanna-Chopra, R.: Induction of new isoforms of superoxide dismutase and catalase enzymes in the flag leaf of wheat during monocarpic senescence. - *Biochem. biophys. Res. Commun.* **288**: 1037-1042, 2001.
- Stoelzle, S., Kagawa, T., Wada, M., Rainer, H., Dietrich, P.: Blue light activates calcium-permeable channels in *Arabidopsis* mesophyll cells via the phototropin signaling pathway. - *Proc. nat. Acad. Sci. USA* **100**: 1456-1466, 2003.
- Vandenabeele, S., Vanderauwera, S., Vuylsteke, M., Rombauts, S., Langebartels, C., Seidlitz, H.K., Zabeau, M., Van Montagu, M., Inzé, D., Van Breusegem, F.: Catalase deficiency drastically affects gene expression induced by high light in *Arabidopsis thaliana*. - *Plant J.* **39**: 45-58, 2004.
- Willekens, H., Chamnongpol, S., Davey, M., Schraudner, M., Langebartels, C., Van Montagu, M., Inzé, D., Van Camp, W.: Catalase is a sink for H<sub>2</sub>O<sub>2</sub> and is indispensable for stress defence in C3 plants. - *EMBO J.* **16**: 4806-4816, 1997.
- Woodbury, W., Spencer, A.K., Stahmann, M.A.: An improved procedure using ferricyanide for detecting catalase isozymes. - *Anal. Biochem.* **44**: 301-305, 1971.
- Yang, T., Poovaiah, B.W.: Hydrogen peroxide homeostasis: activation of plant catalase by calcium/calmodulin. - *Proc. nat. Acad. Sci. USA* **99**: 4097-5002, 2002.
- Yang, W.L., Liu, J.M., Chen, F., Liu, Q., Gong, Y.D., Zhao, N.M.: Identification of *Festuca arundinacea* Schreb *Cat1* catalase gene and analysis of its expression under abiotic stresses. - *J. integr. Plant. Biol.* **48**: 334-340, 2006.
- Yang, Z.Q., Li, Y.X., Jiang, X.D., Zhu, J., Zhang, J.B.: Effects of different red to far-red radiation ratios on the senescence of greenhouse *Chrysanthemum* leaves. - *Afr. J. agr. Res.* **7**: 1919-1925, 2012.
- Zhong, H.H., Resnick, A.S., Straume, M., Robertson McClung, C.: Effects of synergistic signaling by phytochrome A and cryptochrome1 on circadian clock-regulated catalase expression. - *Plant Cell* **9**: 947-955, 1997.